# Shear Strength of Clay and Silt Embankments

Teruhisa Masada, Ph.D.
ORITE, Ohio University

for the
Ohio Department of Transportation
Office of Research and Development

and the
U.S. Department of Transportation
Federal Highway Administration

State Job Number 134319 (0)

September 2009

Ohio Research Institute for Transportation and the Environment (ORITE)

| 1. Report No.<br>**FHWA/OH-2009/7** | 2. Government Accession No. | 3. Recipient's Catalog No. |
|---|---|---|
| 4. Title and Subtitle<br>**Shear Strength of Clay and Silt Embankments** | | 5. Report Date<br>**September 2009** |
| | | 6. Performing Organization Code |
| 7. Author(s)<br>**Dr. Teruhisa Masada** | | 8. Performing Organization Report |
| 9. Performing Organization Name and Address<br>**Ohio Research Institute for Transportation and the Environment**<br>**141 Stocker Center**<br>**Ohio University**<br>**Athens OH 45701-2979** | | 10. Work Unit No. (TRAIS) |
| | | 11. Contract or Grant No.<br>**134319** |
| 12. Sponsoring Agency Name and Address<br>**Ohio Department of Transportation**<br>**1980 West Broad St.**<br>**Columbus OH 43223** | | 13. Type of Report and Period Covered<br>**Technical Report** |
| | | 14. Sponsoring Agency Code |

15. Supplementary Notes

Prepared in cooperation with the Ohio Department of Transportation (ODOT) and the U.S. Department of Transportation, Federal Highway Administration

16. Abstract

Highway embankment is one of the most common large-scale geotechnical facilities constructed in Ohio. In the past, the design of these embankments was largely based on soil shear strength properties that had been estimated from previously published empirical correlations and/or crude soil test results. This is because either the actual soil fill material is not available for testing at the time of embankment design or detailed shear strength determination of soil samples in the laboratory tends to be time-consuming and expensive. Structural stability of these embankments is vital to the state economy and public safety. There is a strong need to conduct a study to examine whether the empirical correlations are truly applicable to Ohio soils and to develop comprehensive geotechnical guidelines concerning the shear strength properties of cohesive soils typically used in Ohio.

In this study, soil samples from nine highway embankment sites scattered across Ohio were tested both in the field and laboratory to establish comprehensive geotechnical properties of cohesive soil fills, which represent a wide range of geological features existing in the state. The large volume of soil data produced in the study was then analyzed to evaluate reliability of the empirical correlations and derive statistically strong correlations for shear strength properties of cohesive soil fill materials found in Ohio. Based on the outcome of these analyses, multi-level guidelines are proposed by the author for estimating shear strength properties of Ohio cohesive soils more confidently.

| 17. Key Words | 18. Distribution Statement |
|---|---|
| shear strength, embankment, highway, soils, cohesive, slope stability, trixial test, statistical analysis, geotechnical guidelines | No Restrictions. This document is available to the public through the National Technical Information Service, Springfield, Virginia 22161 |

| 19. Security Classif. (of this report) | 20. Security Classif. (of this page) | 21. No. of Pages | 22. Price |
|---|---|---|---|
| Unclassified | Unclassified | 300+ | |

**Form DOT F 1700.7 (8-72)** **Reproduction of completed pages authorized**

# SI* (MODERN METRIC) CONVERSION FACTORS

## APPROXIMATE CONVERSIONS TO SI UNITS

| Symbol | When You Know | Multiply By | To Find | Symbol |
|---|---|---|---|---|
| **LENGTH** | | | | |
| in | inches | 25.4 | millimetres | mm |
| ft | feet | 0.305 | metres | m |
| yd | yards | 0.914 | metres | m |
| mi | miles | 1.61 | kilometres | km |
| **AREA** | | | | |
| $in^2$ | square inches | 645.2 | millimetres squared | $mm^2$ |
| $ft^2$ | square feet | 0.093 | metres squared | $m^2$ |
| $yd^2$ | square yards | 0.836 | metres squared | $m^2$ |
| ac | acres | 0.405 | hectares | ha |
| $mi^2$ | square miles | 2.59 | kilometres squared | $km^2$ |
| **VOLUME** | | | | |
| fl oz | fluid ounces | 29.57 | millilitres | mL |
| gal | gallons | 3.785 | litres | L |
| $ft^3$ | cubic feet | 0.028 | metres cubed | $m^3$ |
| $yd^3$ | cubic yards | 0.765 | metres cubed | $m^3$ |

NOTE: Volumes greater than 1000 L shall be shown in $m^3$.

| | | | | |
|---|---|---|---|---|
| **MASS** | | | | |
| oz | ounces | 28.35 | grams | g |
| lb | pounds | 0.454 | kilograms | kg |
| T | short tons (2000 lb) | 0.907 | megagrams | Mg |
| **TEMPERATURE (exact)** | | | | |
| °F | Fahrenheit temperature | 5(F-32)/9 | Celcius temperature | °C |

## APPROXIMATE CONVERSIONS FROM SI UNITS

| Symbol | When You Know | Multiply By | To Find | Symbol |
|---|---|---|---|---|
| **LENGTH** | | | | |
| mm | millimetres | 0.039 | inches | in |
| m | metres | 3.28 | feet | ft |
| m | metres | 1.09 | yards | yd |
| km | kilometres | 0.621 | miles | mi |
| **AREA** | | | | |
| $mm^2$ | millimetres squared | 0.0016 | square inches | $in^2$ |
| $m^2$ | metres squared | 10.764 | square feet | $ft^2$ |
| ha | hectares | 2.47 | acres | ac |
| $km^2$ | kilometres squared | 0.386 | square miles | $mi^2$ |
| **VOLUME** | | | | |
| mL | millilitres | 0.034 | fluid ounces | fl oz |
| L | litres | 0.264 | gallons | gal |
| $m^3$ | metres cubed | 35.315 | cubic feet | $ft^3$ |
| $m^3$ | metres cubed | 1.308 | cubic yards | $yd^3$ |
| **MASS** | | | | |
| g | grams | 0.035 | ounces | oz |
| kg | kilograms | 2.205 | pounds | lb |
| Mg | megagrams | 1.102 | short tons (2000 lb) | T |
| **TEMPERATURE (exact)** | | | | |
| °C | Celcius temperature | 1.8C + 32 | Fahrenheit temperature | °F |

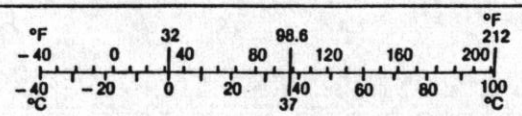


* SI is the symbol for the International System of Measurement

(Revised April 1989)

# Shear Strength of Clay and Silt Embankments

**Final Report**

Prepared in cooperation with the
Ohio Department of Transportation
and the
U.S. Department of Transportation, Federal Highway Administration

by

Teruhisa Masada, Ph.D. (Professor of Civil Engineering)

Leading Research Agency: Ohio Research Institute for Transportation and the Environment
Russ College of Engineering and Technology
Ohio University
Athens, Ohio 45701-2979

and

Sub-Contractor: BBC & M Engineering Inc.
6190 Enterprise Ct.
Dublin, Ohio 43016-7297



September 2009

# Acknowledgements

The author would like to acknowledge the support of the Ohio Department of Transportation (ODOT) technical liaison, Gene Geiger and Steve Sommers (both from the Office of Geotechnical Engineering) as well as the ODOT Director of R & D Office Monique Evans. The author is also grateful to his graduate research assistants Jeffrey Holko and Xiao Han, who spent long hours performing triaxial compression tests and statistical data analysis.

## TABLE OF CONTENTS

## LIST OF TABLES

**CHAPTER 5: EVALUATION OF EMPIRICAL CORRELATIONS, STATISTICAL ANALYSIS, AND GEOTECHNICAL GUIDELINES**

## LIST OF FIGURES

Page No.

# CHAPTER 1: INTRODUCTION

## 1.1 Background

Highway embankments constitute some of the most common geotechnical facilities being built by civil engineers. The design and construction of highway embankments is of great importance to transportation costs and safety. When the embankment is not properly designed and/or constructed, problems such as slope instability and excessive settlement can arise. Also, very conservatively designed embankments can lead to significant budgetary waste for the highway departments/agencies. The problems of highway embankments are generally controlled by five key factors: (1) the embankment soil's shear strength, (2) the soil's moist unit weight, (3) the height of the embankment, (4) the angle of the embankment slope, and (5) the pore pressures in the soil.

Das (2002) defines the shear strength of soil as "the internal resistance per unit area that the soil mass can offer to resist failure and sliding along any plane inside it." There are two important shear strength parameters for soils, the angle of internal friction and cohesion. The angle of internal friction indicates the degree of friction and interlocking existing among soil particles, and the cohesion represents the ionic attraction and chemical cementation between soil particles. Both of these parameters can be determined in a geotechnical laboratory by performing appropriate shear strength tests. Also, there are a few test methods that can be performed in the field to estimate shear strength properties of in-situ soils.

In Ohio, highway embankments are typically built using silty and clayey soils found at/near the construction site. In some areas of Ohio, the embankments are also

constructed largely using weathered shale material. It has been known that some cohesive soils found in Ohio have low to medium shear strengths and also that weathered shale material may undergo further weathering over time. These factors require the embankment design engineers in Ohio to carefully study the on-site fill materials and specify their engineering properties carefully, so that slope stability failure and other problems will not occur. However, in reality detailed investigations of engineering properties of fill material are rarely conducted due to cost and time constraints. Instead, highway embankment engineers in Ohio consult outside sources such as Design Manual 7.2 by U.S. Dept. of Navy (1982), which present correlations between shear strength properties and in-situ or laboratory index test results, to estimate shear strength properties of embankment fill materials. In some embankment projects, unconfined compression strength tests may be performed on relatively undisturbed samples of the fill material to determine strength properties of the soils. These practices can lead to either very conservative or improper designing of the embankments, since the outside sources examined soils from completely different regions of the country or world. There is a need to develop reliable shear strength correlations for embankment fill materials found in Ohio.

## 1.2 Objectives of Study

The study described in this report had six objectives. They are listed below:

- Conduct a literature review to document information relevant to the design and construction of highway embankments in Ohio;
- Identify a total of nine highway embankment sites in Ohio, which can supply

representative samples of major soil fill types existing in Ohio;

- Perform field soil testing and sampling at the selected highway embankment sites in Ohio;
- Obtain detailed engineering properties of soil samples recovered from the highway embankment sites by performing standard index property and shear strength tests in the laboratory;
- Perform a variety of statistical analysis on the field and laboratory test data accumulated for the highway embankment soil fill samples to develop reliable correlations between shear strength properties and in-situ soil test data and between shear strength properties and index properties; and
- Based on the findings of the current study, develop a set of geotechnical guidelines concerning shear strength properties of Ohio embankment soils.

## 1.3 Outline of Report

Chapter 1 laid out background information for and objectives of the current project. The background information described the current state of practice in Ohio and problems associated with it.

Chapter 2 presents results of a literature review conducted as part of the study, which are relevant to both highway embankment stability and the types of soil commonly found in Ohio. This information is essential for locating several highway embankment sites that represent all of soil types typically used to construct highway embankments in Ohio. Journal and textbook articles related to the standard penetration test (SPT) and triaxial compression test are discussed in Chapter 2. Some useful empirical correlations

related to soil shear strength are also identified and presented in this chapter.

Chapter 3 focuses on the research methodology utilized in the current study. The current study consisted of four phases – 1) preliminary work (literature review); 2) field soil testing & sampling; 3) laboratory soil testing; and 4) statistical data analysis. This chapter describes in general the methodology used in each of these phases.

The aim of Chapter 4 is to present all the field and laboratory test results obtained in the study. The results are presented for each embankment site and include those from the standard penetration test (SPT), the laboratory soil index tests, and the laboratory soil shear strength tests. The index properties consist of specific gravity, natural moisture content, Atterberg limits (liquid limits, plastic limits), grain size distribution, and AASHTO/ODOT soil classification. The shear strength tests refer to the unconfined compression and triaxial compression tests. The last part of Chapter 4 discusses briefly geographical and profile distribution of different soil types and differences in basic properties among the soils encountered in the study.

Chapter 5 presents the results of a variety of statistical analysis performed on the state-wide geotechnical data assembled in the study. The chapter first evaluates those empirical correlations presented earlier in Chapter 2, in light of the study data. Next, it describes a few different simpler statistical approaches (linear regression, nonlinear regression, multi-variable regression) that were carried out to analyze the geotechnical data. It then presents results from more comprehensive statistical analyses conducted with the aid of computer software package SPSS. In each part, statistically strong correlations are clearly delineated for each major soil type encountered. At the end of this chapter geotechnical guidelines are proposed for highway embankment soil fill

materials in Ohio, which are based on the results of the empirical correlations evaluated and statistical data analyses performed.

Chapter 6 provides a summary of and conclusions drawn from all phases of the current project. Chapter 7 offers plans that can be implemented easily by ODOT to take full advantage of the findings made in the current study and improve the way highway embankment structures can be designed in the future. Finally, a few appendix sections follow the bibliography. This was necessary to provide essential supplementary materials.

# CHAPTER 2: LITERATURE REVIEW

The current research project is related to soil shear strength, highway embankment stability, standard penetration test (SPT), empirical correlations, Ohio regional geology, and statistical analysis of geotechnical data. The aim of this chapter is to present both general information and research findings on these relevant topics, which were assembled through an extensive literature review conducted.

## 2.1 General

### 2.1.1 Shear Strength of Soil

The basic definition of soil shear strength was given in Chapter 1. Also mentioned were two important shear strength parameters, the angle of internal friction and cohesion. Shear strength of soil is a function of the normal stress applied, the angle of internal friction, and the cohesion. The angle of internal friction describes the inter-particle friction and the degree of the particle interlocking. This property depends on soil mineral type, soil particle texture/shape/gradation, void ratio, and normal stress. The frictional component of the soil shear strength cannot exist without any normal stress acting on the soil mass. The cohesion describes soil particle bonding caused by electrostatic attractions, covalent link, and/or chemical cementation. So, with normal stress, the angle of internal friction, and cohesion, the following equation, known as the Mohr-Coulomb theory, can be used to find the shear strength of soil under a certain condition:

$$\tau_f = c + \sigma (\tan \phi) \quad (2.1)$$

where $\tau_f$ = shear strength; c = cohesion; $\sigma$ = normal stress applied; and $\phi$ = angle of internal friction.

This equation can be plotted on an x-y graph with shear stress on the ordinate and normal stress on the abscissa. This is known as a shear failure envelope and is shown in Figure 2.1. Here, the cohesion and the friction angle are represented by the intercept and the slop of the linear curve, respectively. In reality, the shear failure envelope may not be perfectly linear. The degree of electrostatic attraction and cementation of cohesive particles in the soil can cause a slight concave downward curve to form instead.

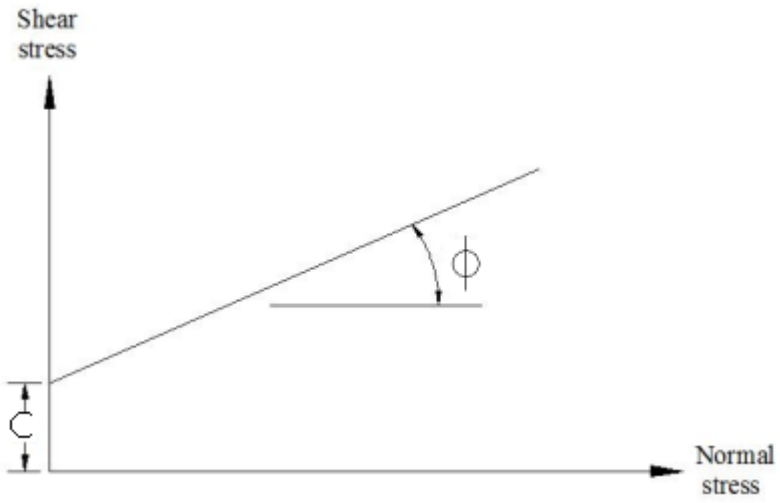


**Figure 2.1:** Shear Failure Envelope for Soil

### 2.1.2 Pore Water Pressure in Soil

Saturated soils have water filling all of their void spaces. This leads to the concept of effective and normal stress. When a column of saturated soil is subjected to load, the total stress is carried by both the soil particles and the pore water. The equation

given below describes this:

$$\sigma = \sigma' + u \tag{2.2}$$

where $\sigma$ = total stress; $\sigma'$ = effective stress; and u = pore water pressure.

The effective stress concept can be explained by the soil particles acting as a connected skeleton to support the load. Therefore, the effective stress is often directly proportional to the total stress. Also, the shear failure envelope formula, Equation 2.1, can be addressed in terms of effective stresses for saturated soils:

$$\tau_f' = c' + \sigma'(\tan \phi') \tag{2.3}$$

where $c'$ = effective-stress cohesion; and $\phi'$ = effective-stress angle of internal friction.

In the field, however, soil may be only partially saturated. Bishop et. al (1960) gave the following equation to describe the shear strength of unsaturated soils:

$$\sigma' = \sigma - u_a - \chi\,(u_a - u_w) \tag{2.4}$$

where $u_a$ = pore air pressure; $\chi$ = degree of saturation; and $u_w$ = pore water pressure.

Going back to Equation 2.3 and adding new variables, the shear strength at failure for unsaturated soil can be written as:

$$\tau_f = c' + [\sigma - u_a + \chi\,(u_a - u_w)]\,(\tan \phi') \tag{2.5}$$

For soil that is completely dry ($\chi = 0$), soil that is 50% saturated, and soil that is 100% saturated, the following three equations result, respectively:

$$\tau_f = c' + (\sigma - u_a) (\tan \phi') \quad (2.6)$$

$$\tau_f = c' + (\sigma - 0.5u_a - 0.5u_w) (\tan \phi') \quad (2.7)$$

$$\tau_f = c' + (\sigma - u_w) (\tan \phi') \quad (2.8)$$

Typically, $u_a$ is less than 0 and $u_w$ is greater than 0. Experiments done by Casagrande and Hirschfeld (1960) revealed that unsaturated soil has greater shear strength than the same soil in a saturated condition. In some cases the unsaturated state may be temporary, and the soil may become eventually saturated due to surface precipitation and subsurface drainage events. Therefore, it is conservative to design highway embankments using the shear strength of saturated soils.

### 2.1.3 Consolidation

As mentioned before, saturated soil will have part of its support coming from the soil skeleton and part of it from the pore water pressure. When loads are applied to clay that has low hydraulic conductivity, the pore pressure will increase greatly. Gradually, the pore water pressure will dissipate and in turn the effective stress will increase, resulting in a volume reduction. This can happen over a period of days, months, or years, depending on the type of soil and the corresponding drainage paths (Das 2002).

This leads to a discussion on the overconsolidation ratio (OCR) for soils. The equation for OCR is given below:

$$OCR = \frac{\sigma_c'}{\sigma'} \quad (2.9)$$

where $\sigma_c'$ = the highest past overburden stress for a soil; and $\sigma'$ = the current overburden stress for a soil.

Essentially, if the current overburden stress for a soil is the highest stress it has ever been subjected to, then the OCR will be 1. Soils under this condition are referred to as normally consolidated. Soils with an OCR above 1 are overconsolidated. This means they have been subjected to greater stresses than the current overburden one (Das 2002). The consolidation of soils and their past stress histories are important for triaxial compression testing.

### 2.1.4 Stability of Highway Embankments

As it was mentioned in Chapter 1, the five factors that influence stability of an embankment are – (1) shear strength of the soil used, (2) the unit weight, (3) the embankment height, (4) the slope steepness, and (5) the pore pressures within the soil. With this in mind, failure generally occurs in two ways, which are the concerns of geotechnical design engineers. The first case is by the physical sliding action of the embankment slope. This can occur either locally (shallow failure) in a confined segment of the slope or more globally through the toe of the embankment (toe circle failure). The second case is by shear failure deep within the base layer. This is called the base failure and typically occurs when the subsurface soils are softer. This type of failure happens most frequently in the short-term period after construction when excess pore pressures are still existent. Figure 2.2 diagrams each of these cases.

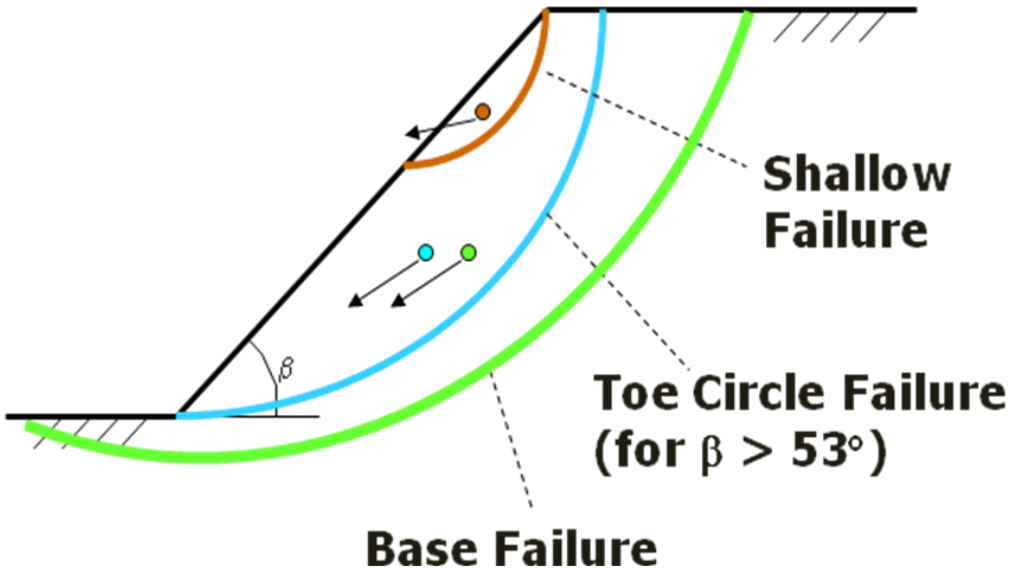


**Figure 2.2:** Different Slope Failure Cases for Embankment

Another concern when building road embankments stems from the use of rock fragments. This could occur in an unglaciated region and can pose long-term stability problems due to gradual weathering of the rock fragments (i.e. shale).

### 2.1.5 Soil Classification

Soils are classified into groups based upon their engineering behavior. Soil engineers currently use two systems, the United Soil Classification System (USCS) and the American Association of State Highway and Transportation Officials (AASHTO) system.

The USCS first groups soils based on whether they are gravels and sands or silts and clays. Next, further sieve analysis is done on the gravels and sands to get a more detailed classification until a group name is given for the soil. There are a total of 36 group names for gravels and sands under the USCS. For silts and clays, the first divider

is the liquid limit value. Next, the plasticity index and further sieve analysis is done to classify the silts into one of 35 group names.

The AASHTO system is different. Soils are divided into seven groups initially based upon sieve analysis. The groups A-1, A-2, and A-3 contain mostly granular materials. Groups A-4, A-5, A-6, and A-7-6 contain mostly silty and clayey materials. Liquid limit and plasticity index values are then used to further classify the soils. A group index number can also be used with the silty and clayey groups of soils. This number is based upon the percent of soil going through the No. 200 sieve, the liquid limit, and the plasticity index. Table 2.1 outlines these fine grained soil classifications.

**Table 2.1:** AASHTO Classifications for Fine-Grained Materials

| Group Classification | A-4 | A-5 | A-6 | A-7-6 |
|---|---|---|---|---|
| Percentage Passing Sieve #200 (%) | 36 min. | 36 min. | 36 min. | 36 min. |
| Liquid Limit (%) | 40 max. | 41 min. | 40 max. | 41 min. |
| Plasticity Index (%) | 10 max. | 10 max. | 11 min. | 11 min. |

A-4 soils and A-6 soils can be broken down further into the categories of A-4a, A-4b, A-6a, and A-6b. A-4a soils are A-4 soils that have between 36 and 49 percent of their particles passing through the No. 200 sieve. A-4b soils are A-4 soils that contain a minimum of 50 percent of its particles passing through the No. 200 sieve. A-4a soils contain mostly sands and silts while A-4b soils contain mostly silt. A-6a soils are A-6 soils that have a plasticity index range of 11 – 15. A-6b soils are A-6 soils that have a plasticity index greater than 15. According to ODOT (2006), the maximum dry unit weight may be typically close to 120 pcf (18.9 $kN/m^3$) for A-4 soils, 110 pcf (17.3 $kN/m^3$) for A-6 soils, and 110 pcf (17.3 $kN/m^3$) for A-7-6 soils.

## 2.2 Review of Literature in Ohio

### 2.2.1 Glaciers

Glaciers covered all of Ohio except for the eastern and southeastern portions of the state. The unglaciated portion is shown as "Soils in Sandstone and Shale," from the Ohio's Soil Regions map. Many of the deposits found in northern and western Ohio contain rock fragments that originated from Canada because of the glaciers. Portions of the state that were subjected to glaciers characterize two types of drift. The first, stratified glacial drift, is seen by layers in the soil. Geological features such as kames, eskers, and outwash plains, display this layered characteristic. The second drift, known as nonstratified, results from the four documented glacial events which occurred in Ohio. Glaciers picked up bedrock and soils along their path and deposited them when they melted in random patterns. Sand and gravel are found in these areas.

### 2.2.2 Soil and Bedrock

The soil found throughout Ohio formed over thousands of years. Bedrock, glaciers, streams, relief, climate, and biota were all contributing factors. Because of this, soil types differ throughout the state. In Figure 2.3, Ohio's seven soil regions can be seen. Lake deposit soils tend to be A-4 when looked at using the AASHTO Classification System. These are seen throughout northern and northeast Ohio. A-7-6 soils, which contain silt and clay, are found throughout central and western Ohio in the glacial till. A-6 soils are found in the eastern and southeastern portion of the state, the unglaciated region. They contain silts, clays, and rock fragments. These soil deposits in Ohio are shown in Figure 2.4.

Western Ohio bedrock contains mostly limestone and dolomite. Some calcareous shale can be found also. Eastern Ohio is mostly sandstone and silaceous shale.

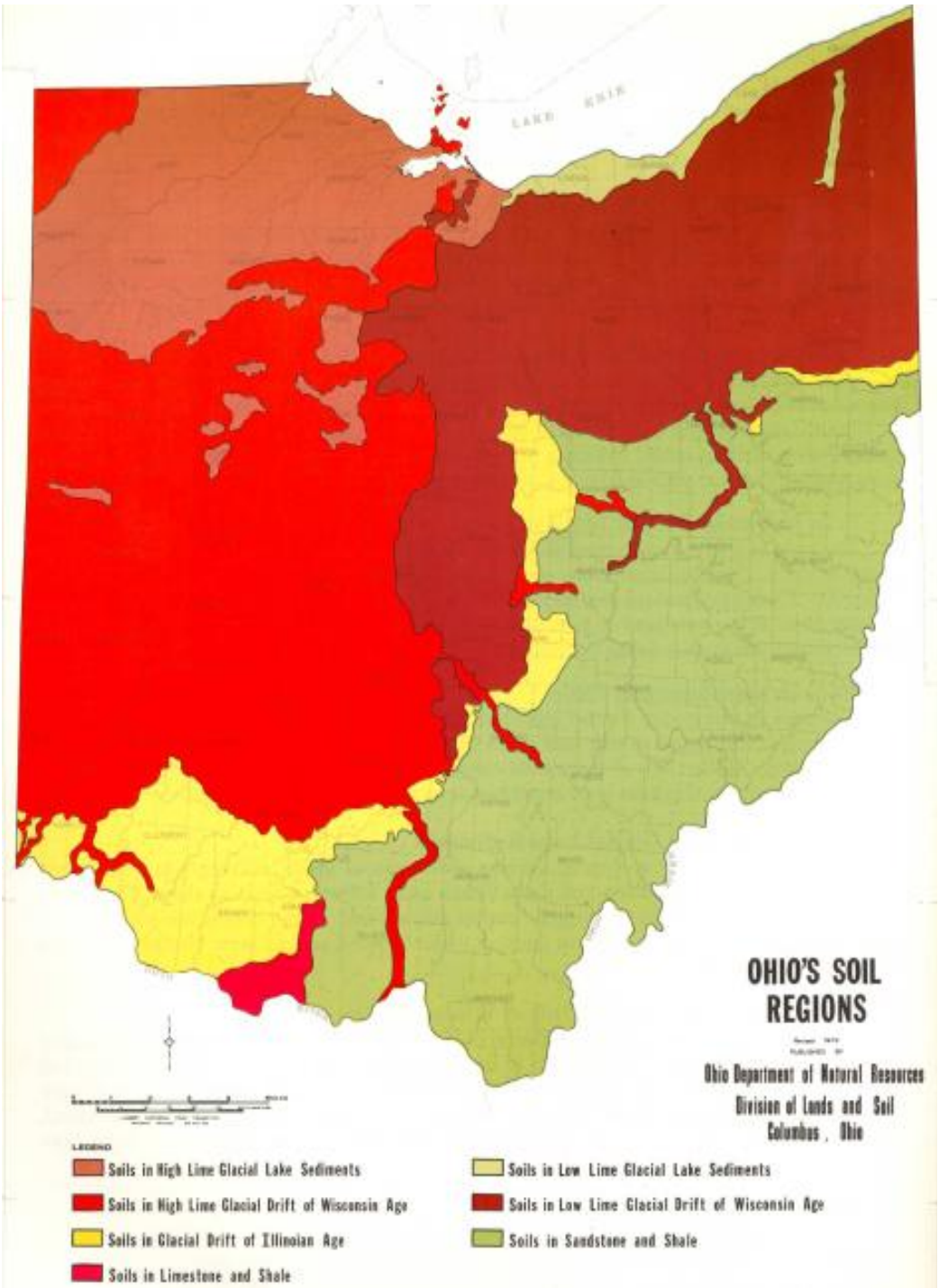


**Figure 2.3:** Ohio's Soil Regions (Source: Johnson 1975)

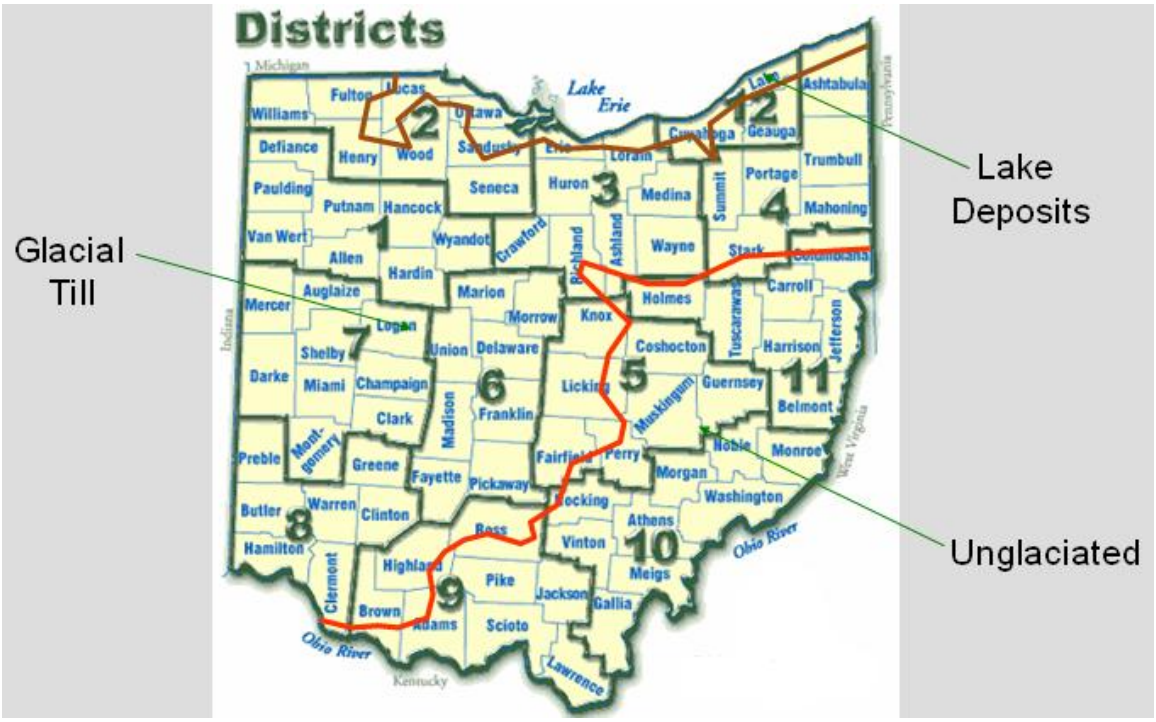


**Figure 2.4:** Soil Deposits in Ohio

## 2.3 Standard Penetration Test (SPT)

### 2.3.1 SPT-General

The SPT is the oldest and most commonly used test method for subsurface exploration. The general process consists of augering a hole in the ground and then hammering a hollow tube through the soil at the bottom. The hammering is done using a large truck with a drill rig attached to the back. The resistance given off by the soil during hammering provides engineers valuable information on the characteristics of the soil. This section will describe in detail the SPT.

### 2.3.2 SPT Equipment

As mentioned earlier, the SPT is performed by using a drill rig attached to the

back of a large truck. Figure 2.5 shows this. An eight inch hole is created in the ground using augers attached to the rig. Then, a split-spoon sampler is attached to the rig after removing the augers. Augers in use and a split-spoon sampler are shown in Figures 2.6 and 2.7, respectively. In some testing procedures, investigators will want to bring up soil specimens wider than those found in the split-spoon sampler. In this case, a Shelby tube will be attached to the drill rig and pushed into the soil. A Shelby tube is a hollow steel tube about 30 inches (762 mm) long and 3 inches (76 mm) wide. It brings to the surface undisturbed specimens that can be used for laboratory testing.

**Figure 2.5:** SPT Drill Rig Mounted on Back of Truck

**Figure 2.6:** Augering into Soil

**Figure 2.7:** Split-Spoon Sampler (detached from the drill rig with soil sample inside)

### 2.3.3 SPT Procedure

Once a hole has been augered into the ground and the split-spoon sampler is attached to the rig, a hammer is dropped onto steel rods connected to the sampler. Throughout the years, three types of hammers have been used: the donut hammer, the safety hammer, and the automatic hammer. In the procedure, the 140-pound (623-N) hammer is dropped 30 inches (0.76 m) onto the steel rods. This process is done until the sampler moves 18 inches (0.46 m) through the ground. The blows from the hammer it takes to move the sampler through each 6 inch (152 mm) interval are recorded. The blow counts from the bottom two 6 inch (152 mm) intervals are then added together, giving the raw SPT-N value.

Despite the available hammers, the automatic hammer has become the most commonly used in recent years for reasons of safety and efficiency, as Drumright et al.

(1996) points out. Their study concluded that the automatic hammer transferred about 50% more energy to the sampler than the safety hammer. The automatic hammer also reduces the probability of human error involved in the process since the rig does all of the work.

### 2.3.4 SPT Energy Corrections

As mentioned in the previous section, different hammers transfer different amounts of energy to the split-spoon sampler even if they each drop 140 pounds (623 N) over 30 inches (0.76 m). Therefore, it is important to correct SPT-N values to a "standard" measurement. This standard measurement is the 60% free-fall energy value ($N_{60}$). Essentially, this is 60% of the energy that would theoretically be transferred by the hammer.

In most cases, however, the transfer energy is somewhere between 60 and 100%. Therefore, the following series of equations is used to convert raw SPT-N values to $N_{60}$:

$$EMX = \int F(t) \cdot V(t)\, dt \qquad (2.10)$$

where $F(t)$ = force measured at time $t$; and $V(t)$ = velocity measured at time $t$.

The value of Equation 2.10 is then put into the numerator for Equation 2.11, given below:

$$\text{Energy transfer ratio (ETR)} = EMX / (\text{Theoretical SPT Hammer Energy}) \qquad (2.11)$$

where Theoretical SPT Hammer Energy = 0.35 kip-ft (0.47 kN-m).

Finally, the energy transfer ratio can be used to find $N_{60}$ in Equation 2.12. This process will be described more in detail in Chapter 3 and Appendix A.

$$N_{60} = \frac{ETR}{60} * (\text{raw SPT-N value}) \quad (2.12)$$

### 2.3.5 Normalization of SPT-N Values

In addition to energy transfer corrections, raw SPT-N values are also normalized using a variety of methods. Using the current overburden stress, the $N_{60}$ value is normalized to an overburden stress of 13.9 psi (95.8 kPa). This process will convert the $N_{60}$ value to the fully corrected N-value or $(N_{60})_1$ value as:

$$(N_{60})_1 = C_N * N_{60} \quad (2.13)$$

where $C_N$ = depth (or overburden pressure) correction

There are five different normalization factors presented in this section. The first is Peck et al. (1974):

$$C_N = 0.77 \log \frac{20}{\sigma_0'} \quad (2.14)$$

where $\sigma_0'$ = effective overburden stress (tsf).

The second method is given as Terzaghi et al. (1996):

$$C_N = \sqrt{\frac{100}{\sigma_0'}} \tag{2.15}$$

The third method is given as Bazaraa (1967):

$$C_N = \frac{4}{1 + 2\sigma_0'} \qquad \text{for } \sigma_0' \leq 1.5 \text{ ksf (71.8 kPa)} \tag{2.16}$$

$$C_N = \frac{4}{3.25 + 0.5\sigma_0'} \qquad \text{for } \sigma_0' > 1.5 \text{ ksf (71.8 kPa)} \tag{2.17}$$

where $\sigma_0'$ = effective overburden stress (ksf).

The fourth correction factor is given as Seed et al. (1975):

$$C_N = 1 - 1.25 \log \frac{\sigma_0'}{2000} \tag{2.18}$$

Finally, the fifth correction factor is given as Skempton (1986):

$$C_N = \frac{2}{1 + (\frac{\sigma_0'}{2000})} \tag{2.19}$$

where $\sigma_0'$ = effective overburden stress (psf).

### 2.3.6 Static Forces and Stresses in SPT

To understand the static forces and stresses involved in the SPT, one must

understand how each component works in the process. It can begin by looking at a simple equation, presented by Schmertmann (1979):

$$F + W' = F_e + ( F_o + F_i ) \qquad (2.20)$$

where F = the force transferred from the hammer to the sampler; W' = the weight of the rods and sampler; $F_e$ = the reaction force given by the ground onto the bottom surface to the sampler; $F_o$ = the frictional reaction force on the outside of the sampler; and $F_i$ = the frictional reaction force on the inside of the sampler.

A diagram of a split-spoon sampler used in a SPT and the forces acting on it is shown in Figure 2.8.

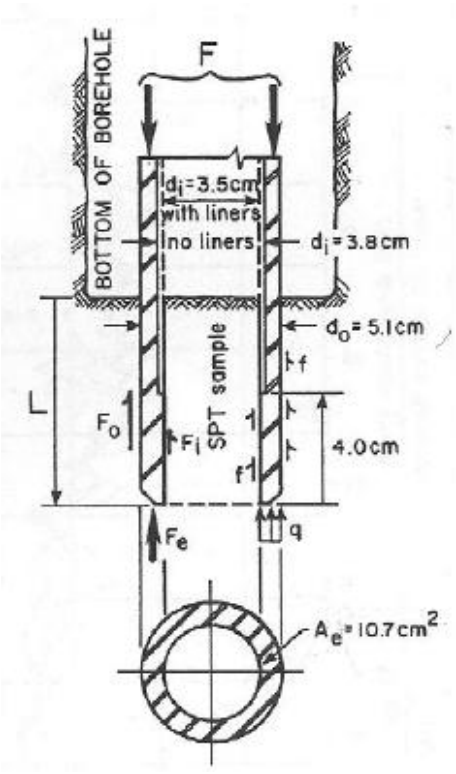


**Figure 2.8:** Forces and Stresses Acting on Split-Spoon Sampler (Ref.: Schmertmann 1979)

Next, to better understand the process, some variables will be added to Equation 2.20. An assumption is made that the unit friction acting inside and outside of the sampler is the same and will be designated with the variable *f*. The unit bearing pressure acting on the bottom of the sampler will be designated as *q*. Also, the standard split-spoon sampler's base area is 10.7 $cm^2$. Using these three new values, Equation 2.20 can be changed to the following (Schmertmann 1979):

$$F + W' = 10.7\, q + (\, d_i + d_o\,)\, \pi\, L f \qquad (2.21)$$

where $d_i$ = inside diameter of the sampler; $d_o$ = outside diameter of the sampler; and L = the depth of the sampler into the ground.

Next, in Equation 2.21, *q*, the unit bearing pressure on the bottom of the sampler, will be replaced with the product: $C_1 q_c$. Also, *f*, the unit frictional force on the sampler will be replaced with the product: $C_2 f_c$. $C_1$ and $C_2$ are constants with no units. $q_c$ and $f_c$ are both in units of force per area. With these assumptions, Schmertmann (1979) gives the following equation:

$$F + W' = C_1\, q_c\, A_e + (\, d_i + d_o\,)\, \pi\, L\, C_2 f_c \qquad (2.22)$$

Now, with the introduction of another variable, the friction ratio, $R_f$, which is equal to $f_c/q_c$, Schmertmann (1979) gives this equation:

$$F + W' = [C_1\, A_e + (d_i + d_o)\, \pi\, L\, C_2\, R_f\,]\, q_c \qquad (2.23)$$

The left side of this equation contains the two components that will push the sampler into the ground (hammer energy and weight of equipment). The right side contains the reaction forces. As the sampler is pushed into the ground, L is the only variable on the right side (reaction force side) that changes. Likewise, as the sampler is pushed into the ground, the left side of the equation must change too. Since the weight of the equipment is fixed, then F must increase. Also, as mentioned before, the blow count over a six inch interval is the result of the SPT. As the sampler is pushed further into the ground, more force is used and the blow count is increased. Therefore, this equation (Equation 2.24), given by Schmertmann (1979) is logical, since $F_{avg}$ (the average force used through the six inch interval) and $\Delta L$ (the length of sample pushed into the ground) are directly proportional to an increase in blow count:

$$\Delta N \sim F_{avg} \cdot \Delta L \tag{2.24}$$

Finally, a comparison will be made between the blow counts experienced in the three intervals: (0 inches – 6 inches or 152 mm), (6 inches or 152 mm – 12 inches or 305 mm), and (12 inches or 305 mm – 18 inches or 457 mm). If it is assumed that the average depth of the sampler while testing the top interval is 3 inches (76 mm), while testing the middle interval is 9 inches (229 mm), and while testing the bottom interval is 15 inches (381 mm), each of these values can be put into Equations 2.25 – 2.27. Also, replacing F on the left side of Equations 2.25 – 2.27 with $\Delta N$ (since they are directly proportional), the following three relations can be made (Schmertmann 1979).

$$\frac{\Delta N_{0-6}}{\Delta N_{12-18}} = \frac{[(10.7C_1 + 2.052C_2R_f)q_c - W'}{[(10.7C_1 + 10.26C_2R_f)q_c - W'} \tag{2.25}$$

$$\frac{\Delta N_{6-12}}{\Delta N_{12-18}} = \frac{[(10.7C_1 + 6.156C_2R_f)q_c - W'}{[(10.7C_1 + 10.26C_2R_f)q_c - W'} \tag{2.26}$$

$$\frac{\Delta N_{12-18}}{\Delta N_{12-18}} = \frac{[(10.7C_1 + 10.26C_2R_f)q_c - W'}{[(10.7C_1 + 10.26C_2R_f)q_c - W'} = 1 \tag{2.27}$$

Essentially, under the assumption the soil being testing throughout the entire 18 inch (457 mm) interval has the same frictional and bearing capacity characteristics, the blow counts will increase with each lower interval. The reason they will increase is because more soil is adhering and rubbing against the inside and outside of the split-spoon sampler, even though that soil may be from a higher up interval. While testing the bottom interval, the soil from the top and middle intervals is affecting the sampler. The sampler is only affected by the soil in the top interval when this section is being tested. This explains, why, in many SPTs, the bottom 6 inch (152 mm) interval is highest even if the soil is very consistent.

## 2.4 Empirical SPT Correlations

Currently, there are a few correlations involving SPT-N values and friction angles. The first one given is between corrected SPT-N values and unconfined compressive strength for cohesive soils. This is shown in Table 2.2.

Essentially, as the soil gets harder, it takes more blows to push the sampler 12 inches (305 mm). Likewise, the harder and better interlocking between soil particles there is, a higher unconfined compressive strength will arise. The next set of correlations,

given by Dept. of Navy (1982) in Table 2.3, uses the unconfined compressive strength again, but also factors in the plasticity of the soil.

**Table 2.2:** SPT-$(N_{60})_1$ vs. Unconfined Compressive Strength by Terzaghi

| SPT-$(N_{60})_1$ | Stiffness | Strength (psi) |
|---|---|---|
| < 2 | very soft | < 3.6 |
| 2 - 4 | soft | 3.6 – 7.3 |
| 4 - 8 | medium soft | 7.3 – 14.5 |
| 8 - 15 | stiff | 14.5 - 29 |
| 15 - 30 | very stiff | 29 - 58 |
| > 30 | hard | > 58 |

*[Reference]* Terzaghi et al. (1996)

**Table 2.3:** SPT-$(N_{60})_1$ vs. Unconfined Compressive Strength by Dept. of Navy

| SPT-$(N_{60})_1$ | $q_u$ (psi) of clays (low plasticity) & clayey silts | $q_u$ (psi) of clays (medium plasticity) | $q_u$ (psi) of clays (high plasticity) |
|---|---|---|---|
| 5 | 5.2 | 10.4 | 17.4 |
| 10 | 10.4 | 20.8 | 34.7 |
| 15 | 15.6 | 31.3 | 52.1 |
| 20 | 20.8 | 41.7 | 69.4 |
| 25 | 26.0 | 52.1 | 86.8 |
| 30 | 31.2 | 62.5 | 104.1 |

*[Reference]* Dept. of Navy (1982)

As previously seen in the Terzaghi correlations, an increase in SPT-N value leads to an increase in unconfined compressive strength. Also, the higher the plasticity of a soil, the larger the increase in strength typically is. The last correlation given is between the effective angle of internal friction and the plasticity index. This is shown in Table 2.4. The general trend is a decreasing effective friction angle with an increasing plasticity index. Figure 2.9 shows the values of Table 2.4 in an x-y plot. Finally, a correlation between the undrained shear strength of clay and the energy corrected SPT-N value is given in the following equation from Stroud (1975):

$$s_u = f_1 \, p_a \, N_{60} \tag{2.28}$$

where $f_1 = 0.045$; and $p_a = 14.7$ psi (101 kPa).

This equation can only be used if the plasticity index is greater than 40.

**Table 2.4:** Effective Friction Angle vs Plasticity Index by Terzaghi

| Plasticity Index | $\phi'$ (degrees) |
|---|---|
| 10 | 33.3 |
| 20 | 30.8 |
| 30 | 29.2 |
| 40 | 27.1 |
| 50 | 25.6 |
| 60 | 24.6 |
| 70 | 23.8 |
| 80 | 23.1 |

*[Note]* The actual $\phi'$ value may be off by at least $\pm$ 3 degrees.

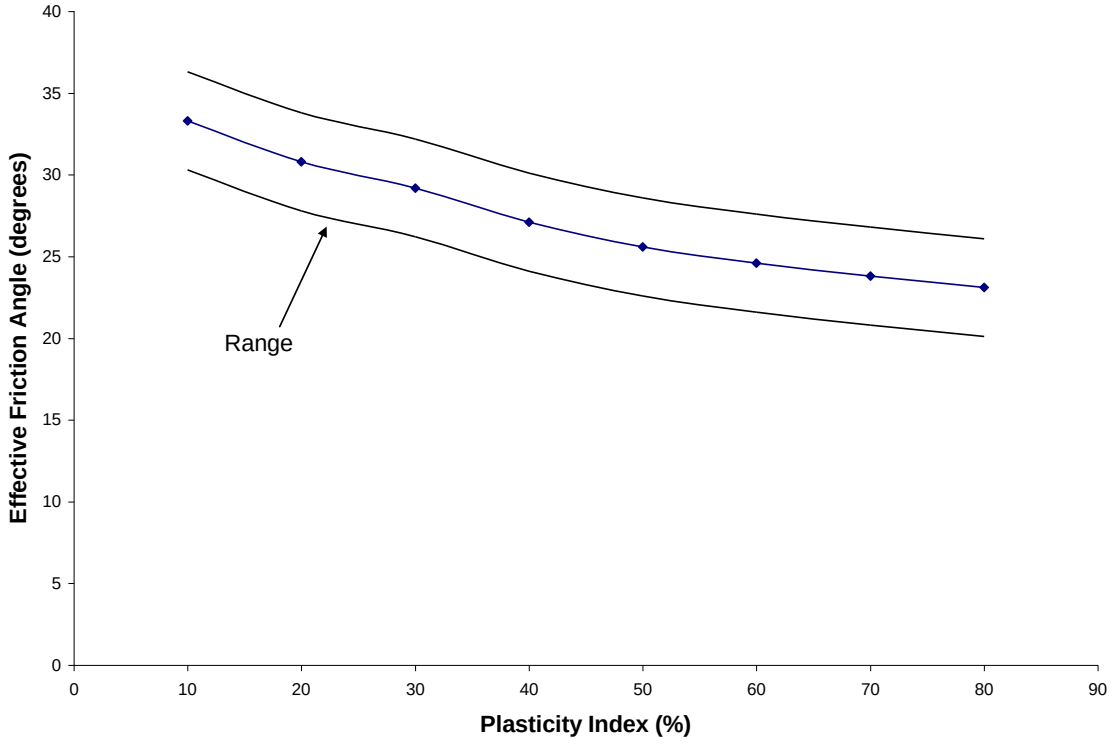


**Figure 2.9:** Terzaghi's Correlation Between $\phi$' and Plasticity Index

## 2.5 Triaxial Compression Test

The triaxial compression test is a well-established realistic test method for obtaining shear strength parameters of soil specimens. There are three variations of triaxial compression tests available to geotechnical engineers and researchers. They vary in both scope and procedure.

### 2.5.1 Test Set-up and Equipment

The test begins by extracting a soil sample from a standard Shelby tube. The specimen is then encased in a thin rubber membrane and placed on top of the bottom platen. Another platen is then placed on top of the specimen. There are drainage lines built into both platens. These drainage lines allow the specimen to undergo saturation and consolidation stages.

### 2.5.2 Back Pressure Saturation

In a triaxial compression test, saturation of the specimen is achieved by back-pressuring water through the drainage lines. As the specimen is surrounded by a rubber membrane on its sides and solid platens at the top and bottom, water is pushed in to fill the void spaces inside the soil specimen. Saturation can be checked by finding the specimen's B-value. This is found by closing the drainage valves and increasing the confining pressure and recording the corresponding increase in pore pressure. This ratio is known as the pore water parameter B:

$$B = \Delta u / \Delta \sigma_3 \tag{2.29}$$

where $\Delta u$ = increase in pore pressure; and $\Delta\sigma_3$ = increase in confining pressure.

If this value is over 0.95, then it can be assumed that the specimen has reached full saturation.

### 2.5.3 Consolidated-Drained (C-D) Test

In this test, the specimen is extracted, saturated, and then put through a consolidation process. Consolidation is done by opening drainage lines and removing any back pressure. Then, a confining pressure acts on the specimen, causing all of the pore pressures to be removed. After this, an axial stress slowly compresses the specimen with drainage valves open. Bishop et al. (1960) pointed out that this prevents any excess pore pressures from developing, which is important, since this test looks at the long term stability of soil when dissipation has already occurred. These tests do take a long time to carry out, however, which is why they are not used very frequently.

### 2.5.4 Consolidated-Undrained (C-U) Test

The C-U test differs from the C-D test in a few ways. First, during consolidation, there is a back pressure being applied to the specimen through the drainage lines. This is typically done for a 24 hour period. Also, because there is back pressure applied, the pore pressure in the specimen will not reduce to zero. So, after consolidation is completed, the drainage lines are closed off and an axial stress is applied to the specimen. The axial stress is applied by a strain rate that is determined from consolidation data. This type of test typically lasts for a few hours to almost one day. During the loading, a

pressure transducer connected to the bottom specimen ends can provide the pore water pressure readings.

Three different C-U tests are done on the same type of soil, each at different confining pressure level. This will give three different Mohr's circles on a shear stress-axial stress diagram. Using these total-stress Mohr's circles, the $\phi$ angle can be found as shown below in Figure 2.10. This was shown previously in Figure 2.1. The Mohr's circles can be also drawn in terms of the effective stresses, which will allow the $\phi'$ angle to be measured in a similar manner. Bishop et al. (1960) also point out that for normally consolidated silts and clays, cohesion is approximately zero. This is why it is important the effective consolidation stress be higher than the highest past overburden stress. The effective consolidation stress will be discussed more in Chapter 3.

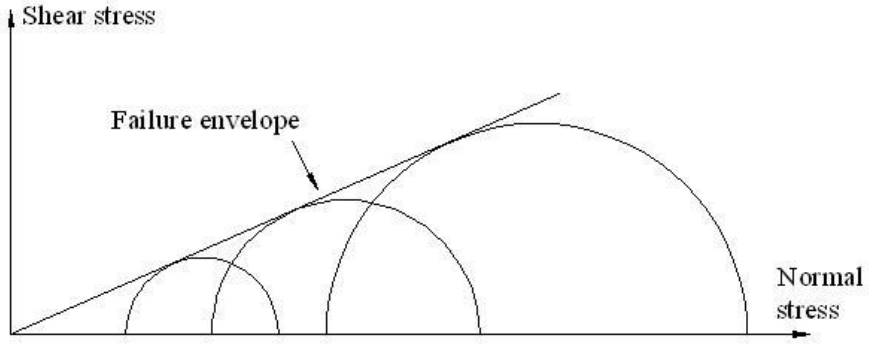


**Figure 2.10:** Mohr's Circles Created for Three C-U Triaxial Tests

There is also another method to find the angle of internal friction for a soil without drawing Mohr's circles as in Figure 2.7. It is done by using a p-q or p′-q′ diagram. To construct a p-q diagram, the total major ($\sigma_{1fail}$) and total minor ($\sigma_{3fail}$) principal stresses at failure are put into the following equations:

$$p = 0.5\ (\sigma_{1fail} + \sigma_{3fail}) \quad (2.30)$$

$$q = 0.5\ (\sigma_{1fail} - \sigma_{3fail}) \quad (2.31)$$

Then, they are plotted on an x-y graph with p on the abscissa and q on the ordinate. The same procedure can be used for effective stresses. Figure 2.11 shows an example of a p-q diagram. In this diagram, the angle between the best-fit line and the abscissa can be referred to as $\alpha$. And, the intercept on the q-axis is defined as *m*. The angle of internal friction and cohesion can be found by the following equations:

$$\phi = \sin^{-1}(\tan \alpha) \quad (2.32)$$

$$c = m/\cos \phi \quad (2.33)$$

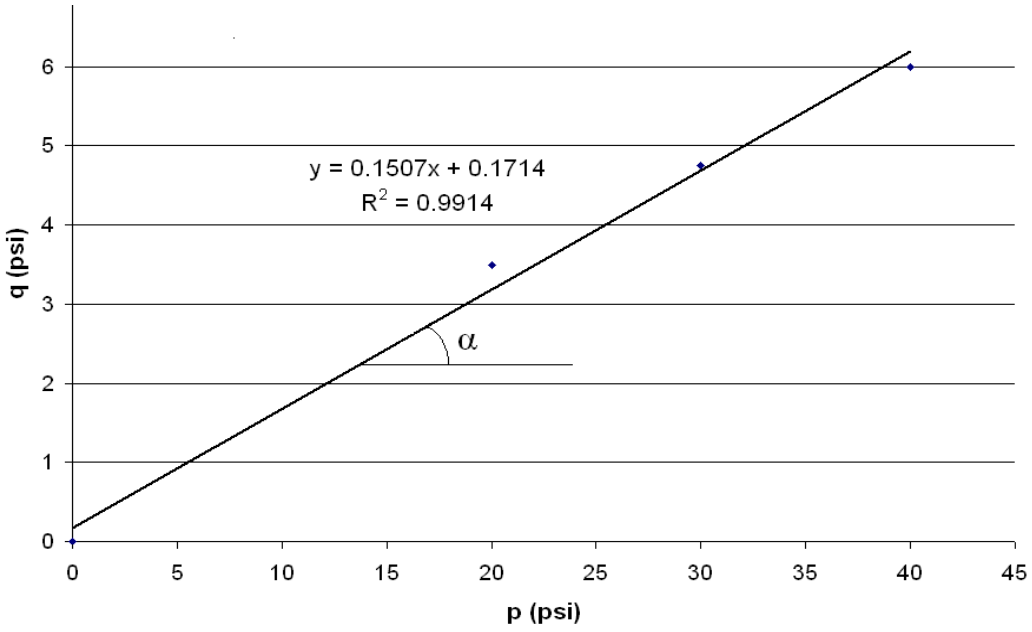


**Figure 2.11:** Example of a p-q Diagram

Similarly, the C-U test data can be analyzed in terms of effective stresses to determine the effective-stress shear strength parameters ($c'$, $\phi'$) as:

$$p' = 0.5\ (\sigma'_{1fail} + \sigma'_{3fail}) \quad (2.34)$$

$$q' = 0.5\ (\sigma'_{1fail} - \sigma'_{3fail}) \quad (2.35)$$

$$\phi' = \sin^{-1}(\tan \alpha') \quad (2.36)$$

$$c' = m'/\cos \phi' \quad (2.37)$$

where $\tan \alpha'$ = slope of the linear curve ($p'$-$q'$ diagram); and $m'$= intercept ($p'$-$q'$ diagram).

### 2.5.5 Unconsolidated-Undrained (U-U) Test

This is the third type of triaxial compression test in use. It is typically used on undisturbed samples of clay and silt to measure the existing strength of natural strata (Bishop et al. 1960). After back pressure saturation is complete, the drainage lines are closed off to the specimen and loading begins. Deviator stress is applied until the specimen fails, at which point the test is over. This type of test is done very fast. Also, in a U-U test, the shear strength is independent of the confining pressure. Because of this, the total stress Mohr's circles will produce an angle of internal friction of zero.

## 2.6 Unconfined Compression Test

The unconfined compression (UC) test is similar to the triaxial compression test except for the lack of a confining pressure. It is performed using a soil specimen of similar size. The specimen is placed between two loading platens and then stress is

applied to compress the soil. Since there is no confining pressure and no membrane around the specimen, only cohesive soils can be used for this. During a test, a stress-strain curve will be created. The highest stress applied on this curve is defined as the unconfined compressive strength ($q_u$). Plotting this on a Mohr's circle diagram is shown below in Figure 2.12. The undrained shear strength of the soil, entirely dictated by undrained cohesion ($c_u$), is simply the unconfined compression strength divided in half.

$$c_u = \frac{q_u}{2} \tag{2.38}$$

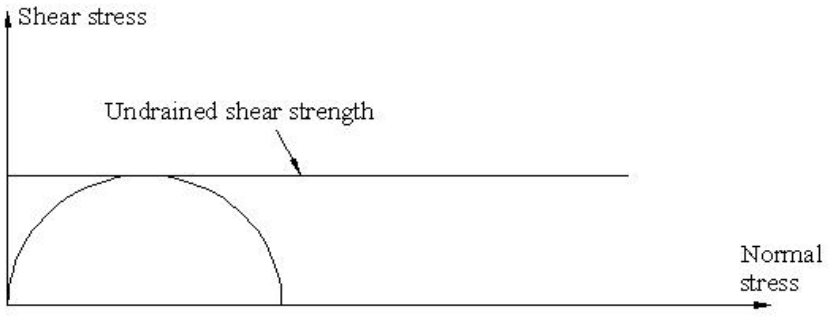


**Figure 2.12:** Mohr's Circle for Unconfined Compression Strength Test

## 2.7 Additional Information on Soil Shear Strengths

During the triaxial compression test, specimen is considered to have failed when any of the following conditions is observed:

- Deviatoric stress reaches a peak and then declines by 20%
- Axial strain goes 5% beyond the strain level corresponding to a peak in the deviatoric stress

- Axial strain reaches 15%.

During the triaxial compression test, saturated soil exhibits no volume change and positive or negative excess pore water pressure when undrained and some volume change and no buildup of excess pore water pressure when drained. The pore water pressure at failure tends to be positive for normally consolidated clays and negative for overconsolidated clays. This is seen in the following equation involving the pore water pressure parameter A:

$$u_f = \sigma_3 + A(\sigma_{1f} - \sigma_3) \tag{2.39}$$

Shear strength parameters derived from undrained tests can be used to address short-term stability of embankment slopes, while those based on drained tests are useful for long-term stability of embankment slopes. Cohesion is essentially zero for cohesionless (granular, silty) soils and normally consolidated clays. Well compacted clayey soils behave somewhat similar to slightly overconsolidated clays. They possess small cohesion in addition to friction angle.

## 2.8 Statistical Analysis of Geotechnical Data

Researchers have been compiling and analyzing geotechnical data for many years to provide supporting evidences for new theories, develop new useful empirical correlations, or validate existing theories/relationships. Several different mathematical functions (or models) were applied to best represent the correlations existing among

geotechnical data.

Linear functions were used to represent the relationships between the plasticity index and the liquid limit in the plasticity chart (Casagrande 1932), between the plasticity index and % clay (Skempton 1953), between the specific discharge and the hydraulic gradient for clean sands in the laminar flow domain (Darcy 1856), and between the shear strength and normal stress in the Mohr-Coulomb failure criterion. Terzaghi et al. (1996) examined the relationship between the effective angle of friction and the plasticity index for a wide range of fine-grained soils and summarized the results by a nonlinear function. Semi-log functions were relied upon to describe the relationships between the moisture content and the blows by the falling cup device (for the determination of liquid limit) and between the void ratio and effective stress for clays. Duncan (1980) utilized a hyperbolic function to express the initial tangent modulus of soil in terms of the deviatoric stress and axial strain. Recently, Masada et al. (2006) analyzed a set of laboratory resilient modulus test data obtained for fine-grained soils in Ohio and concluded that a hyperbolic function can describe the correlation between the resilient modulus and deviatoric stress well. Other functions (ex. exponential) were also utilized by geotechnical researchers in the past to describe, for example, the relationship between the specific discharge and the hydraulic gradient for granular soils in the turbulent flow domain and the relationship between effective friction angle and the SPT-$N_{60}$ for granular soils (Schmertmann 1975).

# CHAPTER 3: RESEARCH METHODOLOGY

## 3.1 General

The current research work was performed jointly by the ORITE and a private geotechnical consulting firm, BBCM Engineering, Inc. (Dublin, OH). The ORITE was the leading institution, and BBCM served as a subcontractor. This arrangement was necessary, since the ORITE does not possess any capability to perform augering, SPT, and Shelby tube sampling. Also, the joint venture between the academic unit and the industry was encouraged by the sponsor of the project (Ohio Department of Transportation) for maximizing benefits of the research to the engineering community.

The project consisted of four phases --- preparations phase, field testing/sampling phase, laboratory soil testing phase, and data analysis phase. This chapter describes general methodology employed in each phase and roles played by each member of the research team (ORITE, BBCM).

## 3.2 Site Selection Criteria

A set of criteria was established in the preparations phase to select a total of nine (9) sites in Ohio, which can represent a range of highway embankment soils typically encountered in Ohio. The criteria were:

Criterion #1: Embankment fill height over 25 ft (7.6 m)

Criterion #2: Site location on major highway

Criterion #3: Site estimated to consist of desired soil type(s)

Criterion #4: Site location highly recommended by ODOT district geotechnical engineers or subcontractor

Criterion #5: Site location in unique geographical and/or geological area within the state

Criterion #6: A lack of gravel size particles and rock fragments

Criterion #7: No guardrails close to the pavement edge

Criterion #8: Relatively large and level grassed median area

The first three criteria were proposed during the initial meeting between the Ohio Department of Transportation and the ORITE. Criterion #5 was added by the ORITE researchers after studying geological maps of Ohio. The last four criteria were devised by the subcontractor (BBCM) to minimize potential problems during the planned field soil testing/sampling work.

It was decided during the initial meeting that the embankment age will not be an issue. It was also decided early on that any of the sites selected should not have a history of slope instability or other problems. This was to ensure safe access to the site, reliable SPT results, and high quality soil samples. Any embankment site chosen for the project should have an overall height of at least 25 ft (7.6 m), so that a relatively large volume of SPT results can be collected within the embankment soil fill. SPT should not be performed into the foundation soil layers. The sites should be located mostly on major highways such as Interstate highways and U.S. routes, due to their relative importance over lower class roadways.

As part of the preparations phase, the ORITE contacted the ODOT district

geotechnical engineer in each ODOT district to briefly describe the research project and request for a few recommended highway embankment sites in the region. Also, geotechnical engineers at BBCM, who have supervised subsurface exploration work at numerous locations in Ohio, were consulted to come up with a list of recommended highway embankment sites. Any sites recommended highly by the ODOT geotechnical engineers and/or BBCM geotechnical engineers received a serious consideration in the current project.

According to ODOT, the three major soil types (in terms of the AASHTO classification system) found in Ohio are A-4, A-6, and A-7-6. Therefore, the sites selected for the project must consist of these major soil types. The sites should be spread throughout the state, covering the northeastern, northwestern, central, southeastern, and southwestern regions. As it was presented in Chapter 2, geological setting in the state of Ohio is divided into glaciated and unglaciated regions. The ODOT Districts 5, 9, 10, and 11 are mostly in the unglaciated region, while other ODOT Districts are in the glaciated plains. It has been found in the past that silty A-4 soils (lake deposits) are abundant in the area surrounding the shorelines of Lake Erie. Clayey A-7-6 soils have been found in the northwestern portion of the state (ODOT Districts 1 and 2). A-6 soils, which are silty clay with possible rock fragments, can be found in the unglaciated eastern and southeastern parts of the state. Based on these reports, it may be ideal to have two sites in the A-4 soils (lake deposits) zone, at least three sites in the unglaciated region, and three or four sites in the glaciated region.

## 3.3 Subsurface Exploration Protocol

All the subsurface exploration work in this project was conducted by the subcontractor (BBCM Engineering), with the ORITE researchers involved as decision makers. During the initial meeting, it was decided that a dedicated truck-mounted drilling rig equipped with a calibrated automatic hammer should be assigned to the project, along with dedicated crew, to minimize undesirable equipment-to-equipment or human-factor variability during the SPT.

### 3.3.1 SPT Hammer Calibration

The automatic hammer attached to the BBCM drilling rig identified for the project was calibrated by GRL Engineers, Inc. (Cleveland, Ohio), prior to the field work at the first site. The calibration testing was done by hammering the sampler into the ground according to the normal SPT procedure. AWJ rods were used to connect the automatic hammer to the split barrel sampler. Hammering was done at depths of 1, 4.5, 9, 14, and 19 ft (0.3, 1.4, 2.7, 4.3, and 5.8 m) with corresponding AWJ rod lengths of 6, 9, 14, 19, and 24 ft (1.8, 2.7, 4.3, 5.8, and 7.3 m), respectively. As mentioned in Chapter 2, the SPT was done by dropping a 140-lb (623-N) hammer over 30 inches (0.76 m). Assuming no frictional losses, this operation should produce 0.35 kip-ft (0.47 kN-m) of free-fall energy.

GRL Engineers used a PAK model Pile Driving Analyzer to measure the strain and acceleration exerted on the sampler. The analyzer converted the strain and acceleration measurements into force and velocity, so that the results could be easily interpreted. The average energy transferred from the hammer to the sampler was 0.290,

0.277, 0.277, 0.290, and 0.295 kip-ft (0.39, 0.38, 0.38, 0.39, and 0.40 kN-m), for the depths of 1, 4.5, 9, 14, and 19 ft (0.3, 1.4, 2.7, 4.3, and 5.8 m), respectively. Dividing each of the above energy values by 0.35 kip-ft (0.47 kN-m) gives the transfer ratio at each depth. The average energy transfer ratio for the five depths resulted at 0.817 (81.7%). This means that about 81.7% of the free-fall energy generated by dropping the hammer weight was transferred to the sampler as it was pushed into the ground. The calibration test report by GRL Engineers is included in Appendix A.

### 3.3.2 SPT Protocol and Soil Sampling

The ORITE researchers decided to have at each field site a continuous SPT performed through embankment soil fill to the depth of 25 ft (7.6 m). This was necessary to collect comprehensive subsurface soil profile data, which can be used to establish detailed soil boring logs and aid in selecting the depth ranges for soil sampling. In a typical geotechnical project, SPT is performed at 5 ft (1.5 m) intervals. A standard split-spoon sampler, with a retainer, inside liners, and sampling length of 18 inches (457 mm), was used during the SPT. The hammering was done automatically for the depth ranges of 1.0 to 2.5, 2.5 to 4.0, 4.0 to 5.5, 5.5 to 7.0, 7.0 to 8.5, 8.5 to 10.0, 10.0 to 11.5, 11.5 to 13.0, 13.0 to 14.5, 14.5 to 16.0, 16.0 to 17.5, 17.5 to 19.0, 19.0 to 20.5, 20.5 to 22.0, 22.0 to 23.5, and 23.5 to 25.0 ft (0.3 to 0.8, 0.8 to 1.2, 1.2 to 1.7, 1.7 to 2.1, 2.1 to 2.6, 2.6 to 3.0, 3.0 to 3.5, 3.5 to 4.0, 4.0 to 4.4, 4.4 to 4.9, 4.9 to 5.3. 5.3 to 5.8, 5.8 to 6.2, 6.2 to 6.7, 6.7 to 7.2, 7.2 to 7.6 m).

During the SPT, the BBCM drill team kept a soil boring log. The blow counts over each 18-inch (457-mm) penetration interval were recorded. Whenever the sampler

was brought to the ground surface after each SPT, it was split-open to reveal the types and thicknesses of soil layers present at the tested depth range. While logging the soils, a hand penetrometer tip was pushed against each soil layer to record the estimated bearing capacity value in tons per square foot (tsf). Soil samples were broken up into sections and placed into separate sealed glass jars for transportation and later inspections in the laboratory.

Once the continuous SPT was performed, the depth vs. raw SPT blow counts data was quickly analyzed by the ORITE team. Since the main objective of the current project was to correlate SPT N-values to other soil properties, it is desirable to find three depth ranges that differ from each other in terms of SPT-N values. For example, depths at which the SPT-N value was approximately equal to 10, 20, and 30 might be suitable for obtaining Shelby tube samples. Here, it is better to rely on the SPT-N values corrected for the overburden soil pressure effect. Several different correction methods were described for the SPT-N value in Chapter 2.

To complete the field work at any site, four soil sampling holes were placed about 3 ft (0.9 m) away from the location of the continuous SPT. The short offset distance was necessary to stay close to the soil conditions encountered during the continuous SPTs. This arrangement would assure reliable input data when seeking correlations between the SPT-N values and the other soil properties. Figure 3.1 shows the ideal Shelby tube sampling plan to be executed in the field.

The procedure for pushing three Shelby tube samples in each soil sampling hole was as follows. First, the hole was located according to the plan shown in Figure 3.1 Next, the hole was augered with continuous-flight augers to the shallowest depth at which

soil sampling was planned. At that point, the BBCM drill team cleaned out the bottom of the hole, attached a Shelby tube to the tip of the AWJ rods, and pushed the Shelby tube hydraulically 2 ft (0.61 m) into the ground. It was preferable that the Shelby tube be pushed 2 ft (0.61 m) into the ground. However, this did not always happen since some

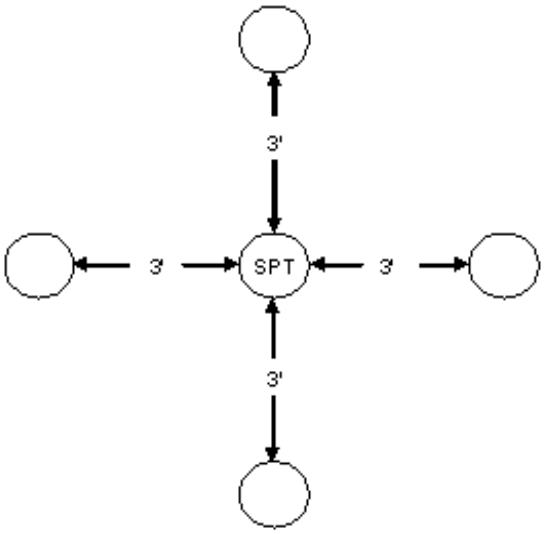


**Figure 3.1:** Shelby Tubes Sampling Plan

soils gave a great deal of resistance to the Shelby tube penetration. If this was the case, then the drill team pushed the tube as deep as possible. After the first Shelby tube was recovered to the ground surface, removed from the rods, and labeled properly (along with its actual soil sample length), the hole was augered down to the middle sampling depth. Here, the second Shelby tube was pushed hydraulically. Next, augering continued down to the final depth, where the third Shelby tube captured a relatively undisturbed soil sample.

The Shelby tube sampling procedure described above was repeated precisely in the three remaining holes. When soil sampling efforts were not successful (low sample recovery, crushing of Shelby tube) at one of the four hole locations, an alternative hole

was randomly located near the initial continuous SPT hole to progress through the soil sampling program. Since there were three tubes obtained per hole, a total of twelve Shelby tubes were recovered. At the end of the soil sampling work, both ends of each Shelby tube were sealed with wax and tight plastic caps. Nine of the tubes (three tubes at each sampling depth) were transported to the ORITE laboratory at Ohio University. The remaining three tubes were kept by BBCM and taken to their soils laboratory. It was important that each Shelby tube retained by the ORITE team had a soil recovery length of 10 inches or more. This was because at least one good triaxial test specimen had to be trimmed out of the soil inside each tube to perform a C-U triaxial test. A triaxial compression test specimen should have a length of approximately 6 inches (152 mm). Here, the actual recovery should be much more than 6 inches (152 mm), since the sample ends were usually uneven and somewhat disturbed from trimming. With this requirement met, three C-U triaxial tests could be performed at each soil sampling depth. Each tube taken by BBCM also had to have a soil recovery length of at least 10 inches (254 mm), so that they could secure a 6-inch (152-mm) length soil specimen for unconfined compression strength test and use the rest for index property tests.

### 3.4 Laboratory Soil Testing Protocol

In the current research project, a wide variety of laboratory soil tests was performed by BBCM and the ORITE for soil samples recovered from each highway embankment site. The joint efforts were necessary to complete a large number of tests within a reasonable amount of time. The ORITE research team performed C-U triaxial compression tests, while BBCM focused mainly on index property tests.

### 3.4.1 Soil Index Property Testing

The soil index property tests, as mentioned in Chapter 2, included the specific gravity test, natural moisture content test, liquid limit test, plastic limit test, mechanical sieve analysis, and hydrometer test. A laboratory technician at BBCM measured the specific gravity of selected soil samples according to the ASTM D-854 method. Split spoon sampler soil samples, broken up and sealed in jars, were used to determine the natural moisture content of the soils found at each field site. Liquid limit and plastic limit tests were both performed according to the ASTM D-4318 protocol. The falling cup method was used to determine the liquid limit. Figure 3.2 shows the liquid limit test equipment. Once the Atterberg limits were found, they provided the plasticity index.

Grain size analysis consisted of the mechanical sieve analysis and the hydrometer test. The mechanical sieve analysis was performed according to the ASTM D-422 method. The main outcome of this test was the grain size distribution curve, which provided percent gravel, percent sand, percent fines (silt + clay), and key particle sizes ($D_{60}$, $D_{30}$, and $D_{10}$). The hydrometer test was conducted by following the ASTM D-421 test method. This test provided further breakdowns of the fines into silt and clay size particles. The results from the Atterberg limit and grain size analysis tests were then combined together to arrive at the AASHTO soil classification designation for each soil sample tested. For soils classified as either A-4 or A-6, the additional steps proposed by ODOT were applied to group them into A-4*a*, A-4*b*, A-6*a*, or A-6*b*. The soil index property test reports issued by BBCM are included in Appendix C.

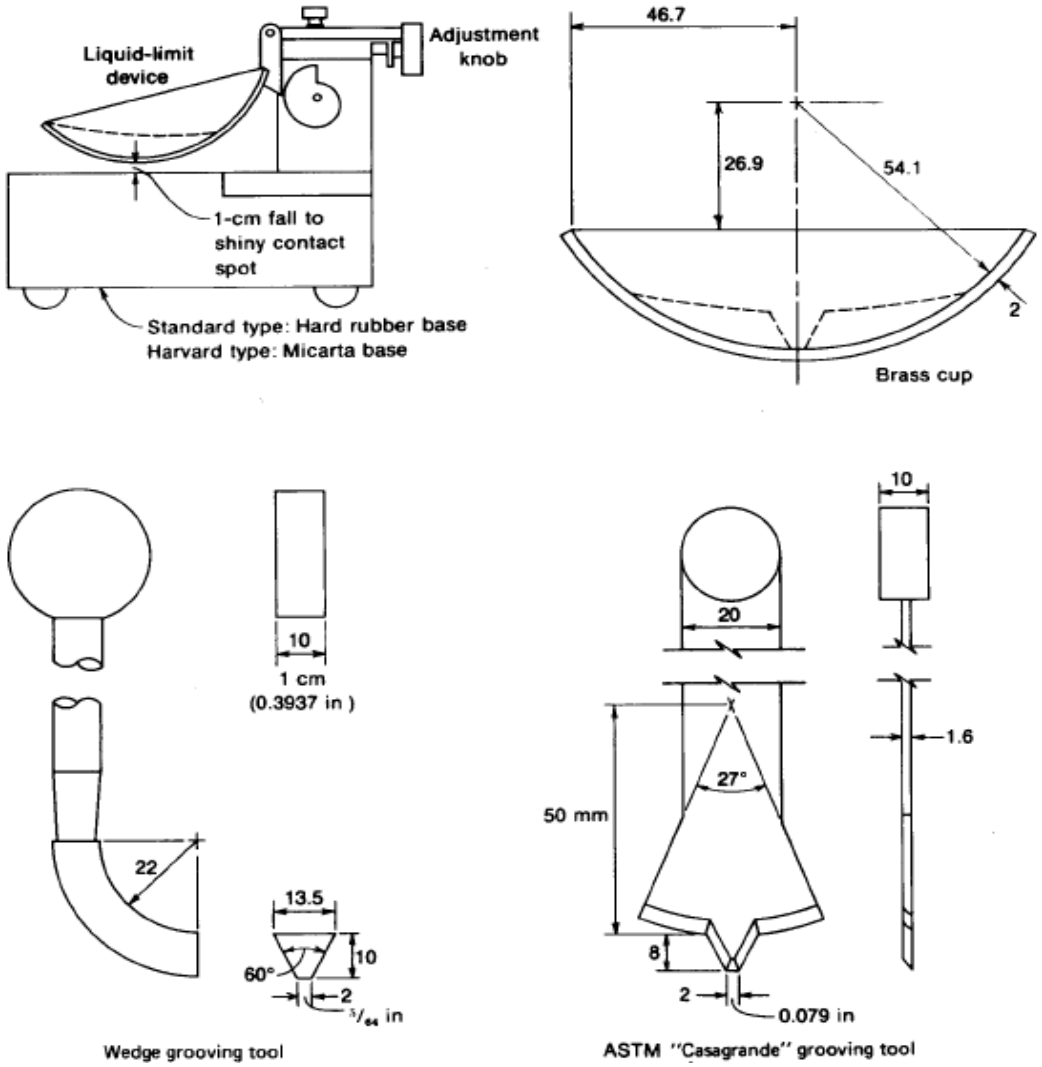


**Figure 3.2:** Liquid Limit Testing Equipment (Source: Bowles 1992)

### 3.4.2 Unconfined Compression Strength Test

In addition to the index property tests, BBCM performed unconfined compression tests on Shelby tube specimens recovered from each highway embankment site. The unconfined compression test was performed according to the ASTM D-2166 method. Figure 3.3 shows an unconfined compression test machine typically used by soil testing laboratories. Each test was performed in a strain-controlled mode. The loading rate

typically ranged between 0.056 and 0.060 inches (1.42 and 1.52 mm) per minute. The test produced load vs. displacement data until a sign of specimen failure was observed. The raw data was then converted into stress vs. strain plots, with unconfined compression strength (undrained shear strength) and strain at failure delineated on each plot. The additional data obtained during each unconfined compression test included moist and dry unit weights, moisture content, degree of saturation, and void ratio. The unconfined compression test results issued by BBCM can be found in Appendix D.


**Figure 3.3:** Unconfined Compression Test Machine

### 3.4.3 C-U Triaxial Compression Test

Accurate determination of shear strength properties of embankment soils

commonly encountered in Ohio constituted one of the most important tasks identified in the current research project. The ORITE research team performed all the consolidated-undrained (C-U) triaxial compression tests in the project, using the Shelby tube soil samples recovered from all the highway embankment sites. The following sections provide details on the triaxial test equipment and test procedures.

#### 3.4.3.1 C-U Triaxial Test Equipment

The triaxial compression test system housed in the ORITE laboratory comprised of many state-of-the-art pieces of equipment to permit a careful and high-precision C-U test to be carried out by trained laboratory personnel. The important system components are listed below:

Vacuum Pump — This was used to pull air out of the soil specimen and deair the water used to fill the chamber interior and saturate the soil specimen.

Water Tank — This cylinder shaped tank was used to hold the deaired water.

Load Frame — This device pressed a loading piston downward against the platen sitting on top of soil specimen to load it axially.

Test Cell — This cylinder shaped cell held the soil specimen and pressurized water around it. The top plate allowed a loading piston to penetrate into the cell. The bottom assembly connected pressure transducers and drainage/saturation lines to the soil specimen or chamber water.

Sensors (a) Linear Position Sensor (LPS): This sensor measured the axial displacement of the soil specimen during the test.

(b) Load Cell: This sensor measured the reaction force on the soil specimen as it is compressed.

(c) Pore Pressure Transducer: This sensor measured the pore wtaer pressure within the soil specimen.

(d) Cell Pressure Transducer: This sensor measured the confining pressure surrounding the soil specimen.

Panel This multi-functional unit contained a vacuum regulator and pressure regulator. Three large burettes mounted on the panel held pressurized water and were connected to the cell water and soil specimen ends. It controlled the confining pressure and back pressure during testing. Also, the panel has tubes connecting it to a tap water and air pressure supply.

Others (a) Network Module: This device regulates the flow of commands and data between the computer and the sensors on the load frame.

(b) PC: A standard IBM-compatible PC ran special software prepared by the manufacturer of the triaxial test system, so that the sensor readings acquisition and test management will be automatic once the soil specimen is conditioned in the test cell.

Figure 3.4 shows a photograph of the main test setup and the equipment used. Only system components not shown in the photograph are the vacuum pump, water tank, network module, and PC.

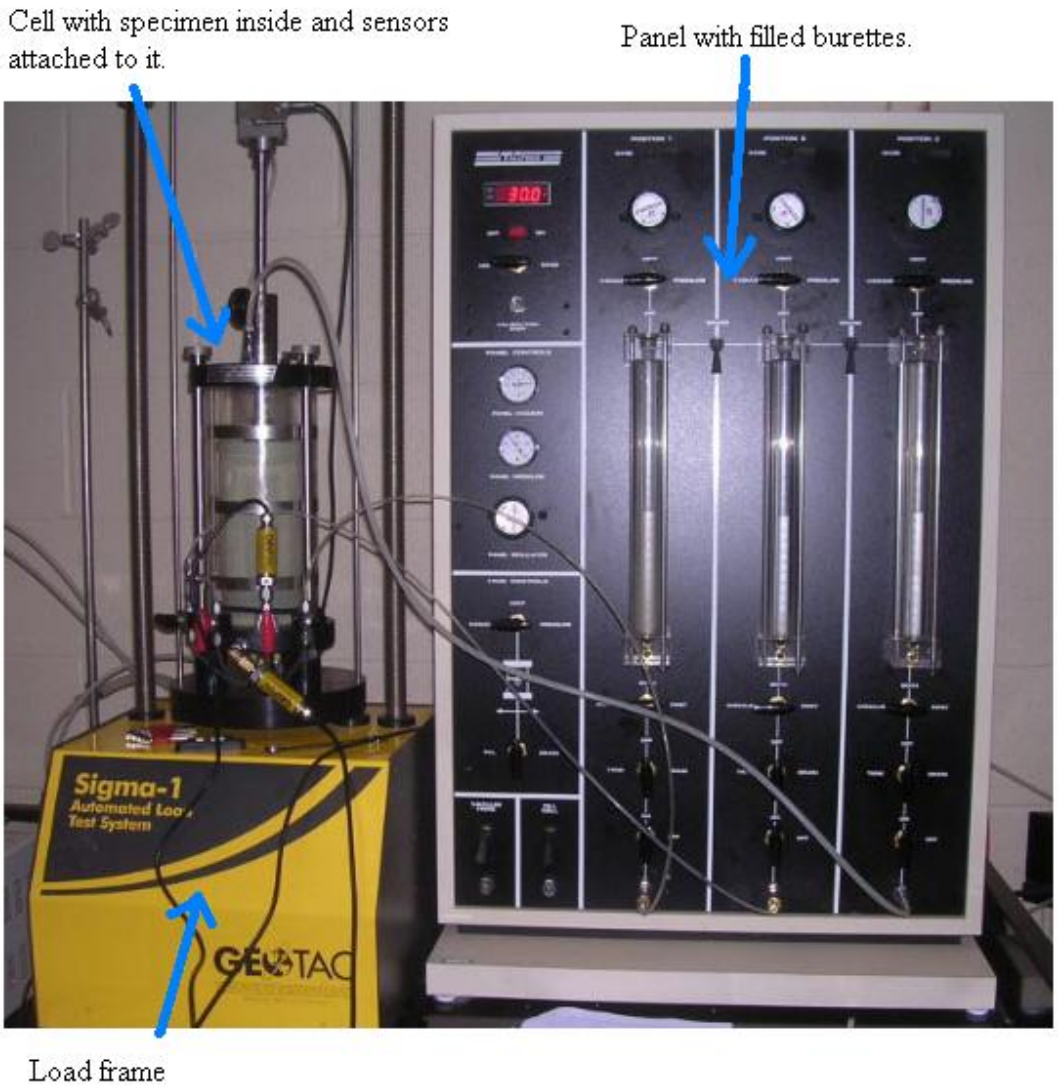


**Figure 3.4:** Triaxial Compression Test System

### 3.4.3.2 C-U Triaxial Test Procedure

The C-U triaxial compression test procedure followed the guidelines set fourth by ASTM Standard D-4767. The guidelines, however, were fairly general in their descriptions. Major efforts were made to translate some of the specifications outlined in the ASTM test protocol into practical steps applicable to the actual test equipment being used in the laboratory. The following list maps out the steps taken in running the C-U

test:

Step 1: Water tank is filled with tap water up to about 1 inch below the top. A vacuum pressure of 13 psi (90 kPa) is applied to the water tank for 4 hours to remove most of the dissolved air present in the tap water.

Step 2: The specimen extraction process is initiated by cutting the Shelby tube into an approximate 6 inch (152 mm) length section, using a circular blade saw. The ASTM guidelines require the actual soil specimen length to be between 5.6 and 7.0 inches (152 and 178 mm). They also require the diameter of the test specimen to be close to 2.8 inches (71 mm). This requirement was met by using standard-size Shelby tubes (inside diameter 2.8 inches or 71 mm). The Shelby tube section is mounted on a hydraulic jacking device. The soil specimen is extracted out of the tube (in the direction the soil entered into the tube in the field) by slowly advancing the hydraulic piston. Care is needed to prevent bending or fracturing of the soil specimen during the extraction process.

Step 3: If the specimen does not have smooth and flat end surfaces, it may be placed sideway on a special curved block to slice off thin uneven sections. The average specimen diameter and length are obtained with a caliper. The specimen is weighed on an electronic scale, so that the initial moist unit weight is known. A small amount of soil remaining inside the tube or trimmed from uneven ends is placed into laboratory oven for determining the initial (natural) moisture content of the soil.

Step 4: The soil specimen is placed on the bottom platen attached to the base assembly of the triaxial test cell. The top platen is then placed on top of the soil specimen. The specimen is enveloped fully with a thin rubber membrane. The ends of the membrane stretching over the top and bottom platens are sealed using rubber O-rings. The test cell is assembled by placing the plexiglass cylinder cell wall around the soil specimen and the top assembly over the cell wall. Flexible tubings coming from the panel are attached to the base assembly ports. The space between the specimen and the cell wall is filled with the de-aired water by applying positive pressure to the water in the water tank. The cell should be being filled until excess water flows out of the tube connected to the top assembly.

Step 5: Pressurized water is forced into the bottom of the soil specimen, while applying a negative air pressure (vacuum) to the top of the soil specimen. This is done to remove air out of the specimen during the initial specimen saturation stage. This step is continued until water starts flowing out of the top end of the soil specimen.

Step 6: The full saturation process is initiated by applying back pressure to the top and bottom ends of the soil specimen. Care must be taken to make sure that the chamber water pressure is larger than the backwater pressure by 2.0 psi or 13.8 kPa (set the chamber pressure at 32.0 psi or 221 kPa and the backwater pressure at 30.0 psi or 207 kPa). The specimen needs to be continuously subjected to this

state for a period of time until a B-value of 0.95 is reached. This is done by monitoring the pore water pressure reading frequently. A B-value check is made by closing off valves connected to the top and bottom ends of the soil specimen and increasing the chamber pressure by 10.0 psi (69 kPa). The pore water pressure reading increases gradually in response to this raised chamber pressure. The B-value is determined by dividing the change taking place in the pore water pressure (over 2 minutes) by the increase in the chamber pressure.

Step 7: Once the specimen is fully saturated, the consolidation process can be started. The confining pressure is increased so that the difference between the confining pressure and back pressure matches the desired effective consolidation pressure. The effective consolidation pressure should be equal to or higher than the estimated overburden pressure that existed in the field. This is to assure that the soil specimen will not exhibit overconsolidated behaviors during the test. The specimen is left in this state for 24 hours. The burette water level readings and the pore water pressure reading must be recorded at specified times. Also, the axial compression experienced by the specimen can be measured using a caliper. These data can be used to verify the completion of the consolidation process and determine the loading rate for the triaxial test based on the $t_{50}$ value. The ASTM D-4767 states that the loading rate should be set by dividing a default rate of at 4% per minute by ten times the $t_{50}$ value ($10*t_{50}$), so that pore water pressure can achieve equilibrium during each increment of the triaxial test.

Step 8: After consolidating the soil specimen, the drainage paths in and out of the specimen are all closed off. The loading piston is carefully brought down, so that its tip is in contact with the center depression on the top platen. At this time, the PC can be accessed to go into the computer software and set the loading rate to the value specified in the previous step. The loading process can now begin. During the shear load test, the computer records automatically all of the sensor readings frequently and update key graphical plots on the computer screen. The actual test duration will depend on the loading rate, maximum axial strain selected, and actual behaviors of the soil specimen. According to ASTM D-4767, the test is to be terminated at 15% axial strain, a 20% decrease in the deviatoric stress, or 5% additional strain beyond a peak in the deviatoric stress.

Step 9: Shortly after the triaxial test, the test cell can be fully drained. The cell is disassemble carefully to remove the soil specimen. Photograph and sketch of the final conditions of the test specimen are taken to observe the failure mode. If a shear plane is visible, its inclination angle can be measured using a protractor. The final moisture content of the soil is determined by placing the entire specimen in the laboratory oven.

This completes the general protocol for running the C-U triaxial compression test.

### 3.5 Statistical Analysis Protocol

The main objective of the current research work was to develop for highway

embankment soils commonly found in Ohio reliable correlations between shear strength properties and in-situ soil test data and between shear strength properties and index properties. This was done by first performing detailed analysis of each triaxial test data, grouping the triaxial and all of the other test data (including the original and corrected SPT-N values) according to the AASHTO soil types, and performing a variety of statistical analyses on the assembled data using computer software.

Data produced by each C-U triaxial test were processed to produce p-q and p′-q′ diagrams. A linear curve was fit to the data points on each diagram, providing an equation and $r^2$ value. The constants in the equations (m, $\alpha$, m′, and $\alpha'$) were converted to actual shear strength parameters ($c_u$, $\phi$, c′, and $\phi'$).

Before getting into the comprehensive statistical analysis, the data produced in the project were first used to examine the previously published correlation between plasticity index (PI) and effective friction angle ($\phi'$) by Terzaghi and between unconfined compression strength and SPT-N value by Department of Navy. This was important, because many practicing geotechnical engineers in Ohio had relied on these published relationships to estimate shear strength properties of Ohio soils for their highway embankment design work.

For each data set grouped for a specific AASHTO soil type, single-variable or X-Y correlations were sought along several different paths, which are listed below, and shown again in Figure 3.5:

Path 1 - Correlations between SPT-N values and index properties

Path 2 – Correlations between triaxial test results and index properties

Path 3 – Correlations between triaxial test results and unconfined compression strength

Path 4 – Correlations between unconfined compression strength and SPT-N values

Path 5 – Correlations between unconfined compression strength and index properties

Path 6 – Correlations between triaxial test results and SPT-N values

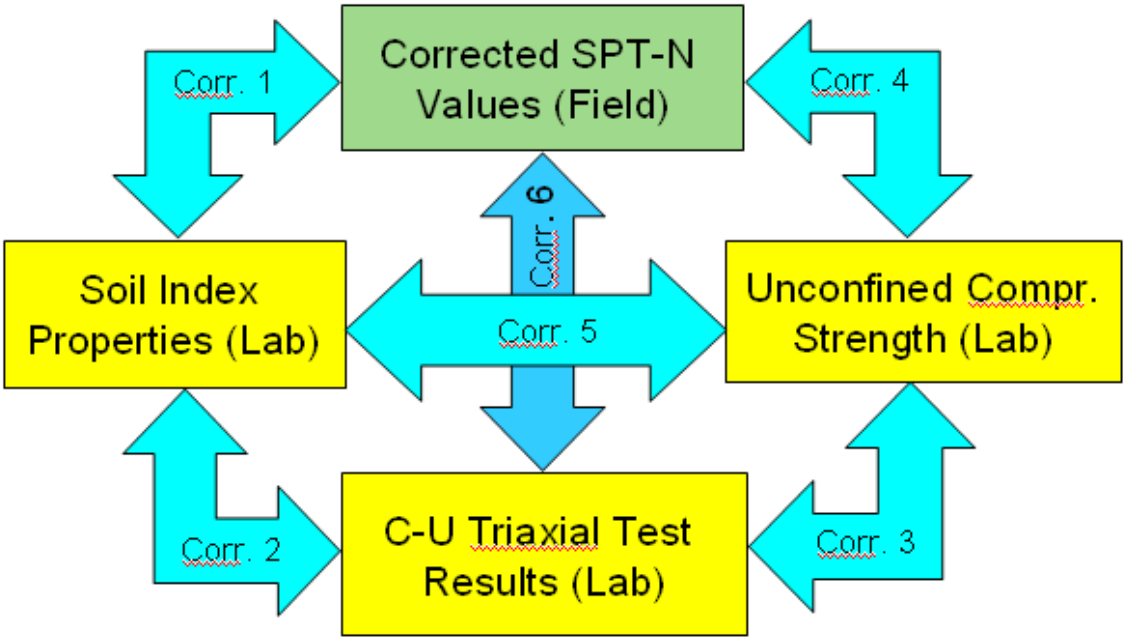


**Figure 3.5:** Correlation Paths Identified for Project

With the aid of computer software, many mathematical models (such as linear, 2nd degree polynomial, logarithmic, power, exponential, hyperbolic, and reciprocal) could be easily applied to the data set to identify the best model and strongest correlations that appear to exist for the shear strength characteristics of major highway embankment soils in Ohio.

Once the single-variable correlations are exhausted, next multi-variable correlations can be explored within each data set. Two types of multi-variable correlations (linear, nonlinear) were investigated. For each type, incremental forward,

backward, and stepwise schemes were adopted to yield the best correlation cases.

Statistical analysis was also extended to examine the presence of any regional differences. For example, if A-6 soils were encountered both in northern and southern Ohio, their data were analyzed first together and then separately. For soils classified as AASHTO A-4 or A-6, additional statistical analysis was carried out to determine if any distinctions exist between their sub-classifications (i.e., between A-4a and A-4b, between A-6a and A-6b). Further details on the analytical phase and the results of the statistical data analysis can be both found in Chapter 5.

# CHAPTER 4: RESEARCH DATA AND RESULTS

## 4.1 Introduction

The data for the current research project was mainly produced during the field subsurface exploration and laboratory soil testing phases. In this chapter, the results from these two major activities will be presented in detail for the nine highway embankment sites explored successfully in Ohio.

The results will be presented in three separate sections. The first section will focus on the subsurface exploration work. The second section will provide the soil index properties determined at the BBCM soil laboratory. The third section will present soil shear strength test data, which include unconfined compression test results by BBCM and consolidated-undrained (C-U) triaxial test results by the ORITE. Each section will have a number of subsections organized according to the sites. The order of the sites presented in this chapter will be – (Site 1) Interstate 275 site in Hamilton County or HAM-275; (Site 2) U.S. Route 35 site in Fayette County or FAY-35; (Site 3) State Route 2 site in Lake County or LAK-2; (Site 4) U.S. Route 33 site in Athens County or ATH-33; (Site 5) Interstate 71 site in Morrow County or MRW-71; (Site 6) State Route 2 site in Erie County or ERI-2; (Site 7) Interstate 75 in Hancock County or HAN-75; (Site 8) Interstate 70 site in Muskingum County or MUS-70; and (Site 9) Interstate 77 site in Noble County or NOB-77. A brief description and a photograph taken, and a set of field exploration data will constitute the site data presentation. There was actually one more site, located on USR 35 in Jackson County (JAC-35). But, no information will be presented for the tenth site, since the subsurface exploration work did not encounter any cohesive soil fill materials.

## 4.2 Embankment Sites Selected

The nine sites selected for the field testing/sampling phase of the current project are listed in Section 4.1. Figure 4.1 shows general locations of these sites in the State of Ohio.


**Figure 4.1:** General Locations of Highway Embankment Sites in Ohio

These sites covered a wide variety of geographical locations, geological settings, and ODOT districts. The nine sites represented seven different ODOT districts (Districts 1, 3, 5, 6, 8, 10, and 12). Three sites (ERI-2, HAN-75, and LAK-2) are located in the northern Ohio. Four of the nine sites (FAY-35, MRW-71, MUS-70, and NOB-77) are found in the central Ohio. The remaining two sites (ATH-33 and HAM-275) exist in the

southern part of Ohio. Two of the nine sites (ERI-2 and LAK-2) are located in the lake deposit area. Four sites (FAY-35, HAM-275, HAN-75, and MRW-71) are situated in the glaciated region of the state, while three sites (ATH-33, MUS-70, and NOB-77) are found in the unglaciated region.

## 4.3 Subsurface Exploration Work

### 4.3.1 Calibration Test Result for SPT Automatic Hammer

The automatic hammer attached to the BBCM drilling rig identified for the current study was calibrated by GRL Engineers, Inc. (Cleveland, Ohio), prior to the field work at the first site. GRL Engineers used a PAK model Pile Driving Analyzer to measure the strain and acceleration exerted on the sampler. According to GRL report, the average energy transfer ratio was 0.817. This means that 81.7% of the free-fall energy generated by the automatic SPT hammer weight was transferred to the sampler as it was pushed into the ground.

### 4.3.2 Subsurface Exploration Data for I-275 Site in Hamilton County

The first highway embankment site is found in the southwestern part of Ohio, near the Ohio River. The site selected was located alongside Interstate Highway 275, about 10 miles northwest of downtown Cincinnati, in Hamilton County. A photograph showing a general view of the site is given in Figure 4.2. This site was recommended for the current project by the ODOT geotechnical engineer serving ODOT District 8.

**Figure 4.2:** Highway Embankment Site No. 1 on I-275 (Hamilton County)

Standard penetration tests (SPT) were performed continuously down to a depth of 19 ft, using an automatic SPT hammer attached to the BBCM drilling rig. The planned maximum depth of 25 ft (7.6 m) could not be reached due to weathered shale found from the depth of 16.5 ft (5.0 m). This was surprising to the field team, because the plan drawings obtained from the ODOT did not indicate the bedrock to be located at such a shallow depth. During the filed work, the split-spoon barrel brought samples of relatively uniform silty clay soil to the ground surface. No water table was encountered during the field work. The original (or uncorrected) SPT-N values are tabulated against depth in Table 4.1. The SPT-N value showed a general trend of increasing steadily with depth.

**Table 4.1:** Uncorrected SPT-N Values at Site No. 1 (Hamilton County)

| Depth Range (ft) | Uncorrected SPT-N Value (blows/ft) |
|---|---|
| 1.0 - 2.5 | 7 |
| 2.5 - 4.0 | 7 |
| 4.0 - 5.5 | 13 |
| 5.5 - 7.0 | 24 |
| 7.0 - 8.5 | 22 |
| 8.5 - 10.0 | 31 |
| 10.0 - 11.5 | 20 |
| 11.5 - 13.0 | 29 |
| 13.0 - 14.5 | 37 |
| 14.5 - 16.0 | 29 |
| 16.0 - 17.5 | 30 |
| 17.5 - 19.0 | 45 |

[Note] 1 ft = 0.3 m.

Based on the original SPT blow counts, it was decided that Shelby tubes would be pushed at the depth ranges of 2.5 to 4.5, 4.5 to 6.5, and 10.0 to 12.0 ft (0.76 to 1.37, 1.37 to 1.98, and 1.89 to 3.66 m). As it was mentioned earlier, correlations with N values is a major objective of this project. Therefore, selecting a wide array of values is most desirable. Here, values of 7, 13, and 20 can be used for making correlations since they correspond to the soil that will be brought up by the Shelby tubes.

As it was discussed in Chapter 3, the plan shown in Figure 3.1 represented the ideal pattern in which Shelby tube soil samples should be recovered at this site. However, when Hole A was drilled, a large amount of gravel was recovered. This forced a change in the plan. The modified Shelby tube sampling plan, shown in Figure 4.3, was then adapted and executed to produce all twelve tube samples.

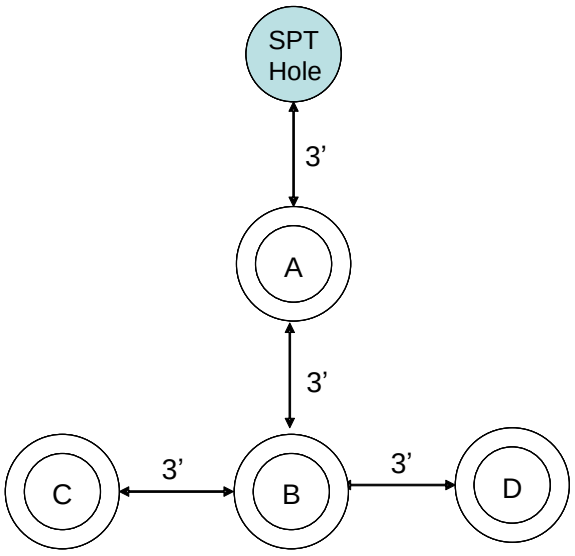


**Figure 4.3:** Modified Shelby Tube Sampling Plan at Site No. 1

After extracting all twelve Shelby tubes, the ORITE personnel inspected each tube and selected nine of them to go to the ORITE laboratory. The soil recovery and notes on each tube kept by ORITE is included in Appendix B as Table B.2.

After the field testing was completed, a series of corrections were done to the original SPT-N values. The first correction made was for the energy transfer to the automatic hammer attached to the SPT truck. This correction was already discussed back in Chapter 2. Also, details on the automatic hammer calibration are given in Appendix A. Next, five more corrections were performed. These are the Peck, Terzaghi, Bazaraa, Seed et. al, and Skempton corrections. These correction methods were also given in Chapter 2. Table 4.2 presents the corrected SPT-N values from the I-275 site. According to the table, the correction method by Seed et al. produced values closest to the overall average. A summary of the corrected SPT-N values for this site is given above in Appendix B as Tables B.1.

**Table 4.2:** Hamilton County Site SPT-$(N_{60})_1$ Values

| Depth (ft) | Original SPT-N | Energy Correction Only | Peck | Terzaghi | Bazaraa | Seed et al. | Skempton | **Avg.** |
|---|---|---|---|---|---|---|---|---|
| 2.5-4.0 | 7 | 10 | 16 | 26 | 24 | 20 | 18 | **20** |
| 4.0-5.5 | 13 | 18 | 26 | 38 | 37 | 32 | 29 | **32** |
| 10-11.5 | 20 | 27 | 32 | 37 | 33 | 35 | 35 | **34** |

[Note] The value 'Avg.' is simply the rounded average of the five previous columns (Peck, Terzaghi, Bazaraa, Seed et. al., and Skempton.

### 4.3.3 Subsurface Exploration Data for USR 35 Site in Fayette County

The second highway embankment site can be found in the central-southwestern part of Ohio in Fayette County. This site, near Jeffersonville, was located on the old USR 35 embankment about 100 ft (30 m) away from a bridge abutment. The abutment supported a bridge that went over the new USR 35. Figure 4.4 shows the general view of the site. This site was identified as one of the potential sites, while searching for a site in the central region of Ohio. It was recommended strongly by BBCM based on their prior drilling in this area.

Standard penetration tests (SPT) were conducted to a depth of 25 ft (7.6 m). During the filed work, the split-spoon barrel brought samples of hard silt with clay and sand to the ground surface. No water table was encountered during the field work. The original (or uncorrected) SPT-N values are tabulated against depth in Table 4.3. The SPT-N value fluctuated mostly between 10 and 25 in the top 20-ft (6.1-m) depth, increased with depth from the depth of 20 to 23 ft (6.1 to 7.0 m), and declined to 20 at the maximum depth of 25 ft (7.6 m).

**Figure 4.4:** Highway Embankment Site No. 2 on USR 35 (Fayette County)

Based on the SPT-N values, it was decided to utilize Shelby tubes at depth ranges of 5.5 to 7.5, 8.5 to 10.5, and 14.5 to 16.5 ft (1.7 to 2.3, 2.6 to 3.2, and 4.4 to 5.0 m). At these depths, the original SPT-N values were 18, 23, and 10. The original plan for the Shelby tube sampling was shown previously in Figure 3.1. While pushing the tubes, Holes A and B produced good recovery at each depth. However, Hole C gave very little recovery at the depth range of 8.5 to 10.5 ft (2.6 to 3.2 m) and no recovery at the 14.5 to 16.5 ft (4.4 to 5.0 m) range. This led the field team to modify the plan to the one illustrated in Figure 4.5, by adding the fifth sampling hole (Hole E). This hole was located far from Hole C to avoid more problems with soil in that area. Holes D and E gave moderate recoveries at each depth range.

**Table 4.3:** Uncorrected SPT-N Values at Site No. 2 (Fayette County)

| Depth Range (ft) | Uncorrected SPT-N Value (blows/ft) |
|---|---|
| 1.0 - 2.5 | 18 |
| 2.5 - 4.0 | 14 |
| 4.0 - 5.5 | 21 |
| 5.5 - 7.0 | 18 |
| 7.0 - 8.5 | 21 |
| 8.5 - 10.0 | 23 |
| 10.0 - 11.5 | 21 |
| 11.5 - 13.0 | 13 |
| 13.0 - 14.5 | 14 |
| 14.5 - 16.0 | 10 |
| 16.0 - 17.5 | 21 |
| 17.5 - 19.0 | 16 |
| 19.0 - 20.5 | 23 |
| 20.5 - 22.0 | 32 |
| 22.0 - 23.5 | 43 |
| 23.5 - 25.0 | 20 |

[Note] 1 ft = 0.3 m.

In total, fifteen Shelby tubes were recovered at the second site. Nine of the tubes with good sample recovery were kept by the ORITE. The soil recovery and notes on each tube are included in Appendix B as Table B.4. After field testing was complete, a series of corrections were applied to the original SPT-N values. This was done in a similar manner to the ones for the first (Hamilton County) site. Table 4.4 presents the corrected SPT-N values from the Fayette County site. A summary of the corrected SPT-N values for this site is given in Appendix B as Tables B.3.

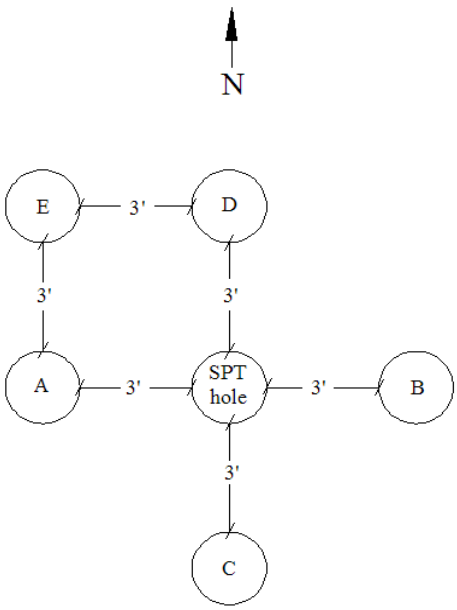


**Figure 4.5:** Actual Shelby Tube Sampling Plan at Site No. 2

**Table 4.4:** Fayette County Site SPT-$(N_{60})_1$ Values

| Depth (ft) | Original SPT-N | Energy Correction Only | Peck | Terzaghi | Bazaraa | Seed et. al. | Skempton | **Avg.** |
|---|---|---|---|---|---|---|---|---|
| 5.5-7.0 | 18 | 25 | 34 | 45 | 43 | 40 | 37 | **40** |
| 8.5-10.0 | 23 | 31 | 39 | 45 | 42 | 43 | 42 | **42** |
| 14.5-16.0 | 10 | 14 | 15 | 13 | 14 | 14 | 14 | **14** |

### 4.3.4 Subsurface Exploration Data for SR 2 Site in Lake County

The third highway embankment site can be found in northeast Ohio, along Lake Erie, in Lake County. The site was located on an embankment supporting two bridges carrying State Route 2 over State Route 615. No site photographs are available for this site. This site was placed in this region with an intention of examining A-4 soils that are abundant along the shores of Lake Erie.

Standard penetration tests (SPT) were performed continuously down to a depth of 25 ft (7.6 m), as planned. During the filed work, the split-spoon barrel brought samples

of hard silt and clay to the ground surface. No water table was encountered during the field work. The uncorrected SPT-N value at each depth range is listed in Table 4.5. The raw SPT-N values fluctuated between 10 and 30 without exhibiting any clear trend with depth.

**Table 4.5:** Uncorrected SPT-N Values at Site No. 3 (Lake County)

| Depth Range (ft) | Uncorrected SPT-N Value (blows/ft) |
|---|---|
| 1.0 - 2.5 | 10 |
| 2.5 - 4.0 | 17 |
| 4.0 - 5.5 | 25 |
| 5.5 - 7.0 | 30 |
| 7.0 - 8.5 | 21 |
| 8.5 - 10.0 | 12 |
| 10.0 - 11.5 | 13 |
| 11.5 - 13.0 | 28 |
| 13.0 - 14.5 | 9 |
| 14.5 - 16.0 | 16 |
| 16.0 - 17.5 | 12 |
| 17.5 - 19.0 | 18 |
| 19.0 - 20.5 | 14 |
| 20.5 - 22.0 | 22 |
| 22.0 - 23.5 | 13 |
| 23.5 - 25.0 | 28 |

[Note] 1 ft = 0.3 m.

Based on the original SPT blow counts, it was decided to obtain Shelby tube samples at depth ranges of 1.0 to 3.0, 4.0 to 6.0, 14.0 to 16.0 ft (0.3 to 0.9, 1.2 to 1.8, and 4.3 to 4.9 m). At these depths, the uncorrected SPT-N values were 10, 25, and 16, respectively. Shelby tube soil sampling work went according to the plan (illustrated in Figure 3.1) with very few problems and good recovery for each tube. Nine of the twelve total tubes were retained by the ORITE. The recovery and notes on these tubes are included in Appendix B in Table B.6. After the completion of the field work, corrections were applied to the original SPT-N values. The new, corrected SPT N-values for the

Lake County site are shown below in Table 4.6. A summary of the fully corrected SPT-N values for this site is given in Appendix B as Tables B.5.

**Table 4.6:** Lake County Site SPT-$(N_{60})_1$ Values

| Depth (ft) | Original SPT-N | Energy Correction Only | Peck | Terzaghi | Bazaraa | Seed et. al. | Skempton | **Avg.** |
|---|---|---|---|---|---|---|---|---|
| 1.0-2.5 | 10 | 14 | 26 | 56 | 44 | 34 | 26 | **37** |
| 4.0-5.5 | 25 | 34 | 50 | 69 | 68 | 60 | 54 | **60** |
| 14.5-16.0 | 16 | 22 | 23 | 23 | 21 | 23 | 23 | **23** |

### 4.3.5 Subsurface Exploration Data for USR 33 Site in Athens County

The fourth highway embankment site was located along U.S. Route 33 in Athens County. It was on top of a large embankment, approximately five miles south of Athens on a two-lane portion of the road. Figure 4.6 provides a general view of the site location. This site was identified jointly with the ODOT District 10 Office in an attempt to examine typical embankment materials in the unglaciated region of Ohio.

Field work at this site started with a continuous SPT to a depth of 25 ft (7.6 m), as usual. This went forward with no problems. A few different types of soil (or different mixtures of clays and silts) were encountered during the subsurface exploration work. No water table was encountered during the field work. The uncorrected SPT-N values recorded at this site are tabulated against depth in Table 4.7. The raw SPT-N values fluctuated between 15 and 45 without exhibiting any clear trend with depth.

**Figure 4.6:** Highway Embankment Site No. 4 on USR 33 (Athens County)

**Table 4.7:** Uncorrected SPT-N Values at Site No. 4 (Athens County)

| Depth Range (ft) | Uncorrected SPT-N Value (blows/ft) |
|---|---|
| 1.0 - 2.5 | 27 |
| 2.5 - 4.0 | 40 |
| 4.0 - 5.5 | 16 |
| 5.5 - 7.0 | 33 |
| 7.0 - 8.5 | 16 |
| 8.5 - 10.0 | 17 |
| 10.0 - 11.5 | 25 |
| 11.5 - 13.0 | 19 |
| 13.0 - 14.5 | 20 |
| 14.5 - 16.0 | 40 |
| 16.0 - 17.5 | 45 |
| 17.5 - 19.0 | 36 |
| 19.0 - 20.5 | 21 |
| 20.5 - 22.0 | 32 |
| 22.0 - 23.5 | 21 |
| 23.5 - 25.0 | 32 |

[Note] 1 ft = 0.3 m.

Based on the SPT blow counts, it was decided that Shelby tubes be pushed at depth ranges of 4.5 to 6.5, 8.0 to 10.0, and 19.0 to 21.0 ft (1.4 to 2.0, 2.4 to 3.0, and 5.8 to 6.4 m). This gave the uncorrected SPT-N values of 33, 17, and 21, respectively. At this site, Shelby tube pushing went according to plan (illustrated in Figure 3.1), with no problems. Nine of the Shelby tubes were retained by the ORITE, and the remaining three were taken by BBCM. The recovery and notes on the nine tubes are included in Appendix B in Table B.8. Corrections were made to the original SPT-N values similar to the other field sites. They are shown in Table 4.8. A summary of the fully corrected SPT-N values is given in Table B.7 in Appendix B.

**Table 4.8:** Athens County Site SPT-$(N_{60})_1$ Values

| Depth (ft) | Original SPT-N | Energy Correction Only | Peck | Terzaghi | Bazaraa | Seed et al. | Skempton | **Avg.** |
|---|---|---|---|---|---|---|---|---|
| 5.5-7.0 | 33 | 45 | 62 | 80 | 77 | 72 | 68 | **72** |
| 8.5-10.0 | 17 | 23 | 28 | 33 | 30 | 32 | 31 | **31** |
| 19.0-20.5 | 21 | 29 | 27 | 27 | 26 | 27 | 27 | **27** |

### 4.3.6 Subsurface Exploration Data for I-71 Site in Morrow County

The fifth highway embankment site was located in the median of Interstate Highway 71 in Morrow County, about 60 miles (97 km) north of Columbus. The field operation took place on an embankment about 30 feet (9.1 m) high. The embankment supported two bridges for I-71 as it traveled over a small creek and local road at the bottom of a valley. The general view of the site is seen in a photograph inserted here as Figure 4.7.

At this location, a continuous SPT was done to a depth of 25 ft (7.6 m). During the filed work, the split-spoon barrel brought samples of hard silt and clay to the ground

surface. No water table was encountered during the field work. The uncorrected SPT-N values obtained at this site are given in Table 4.9. Although the blow counts oscillated, they exhibited a general trend of increasing with depth.

**Figure 4.7:** Highway Embankment Site No. 5 on I-71 (Morrow County)

**Table 4.9:** Uncorrected SPT-N Values at Site No. 5 (Morrow County)

| Depth Range (ft) | Uncorrected SPT-N Value (blows/ft) |
|---|---|
| 1.0 - 2.5 | 11 |
| 2.5 - 4.0 | 10 |
| 4.0 - 5.5 | 9 |
| 5.5 - 7.0 | 13 |
| 7.0 - 8.5 | 14 |
| 8.5 - 10.0 | 16 |
| 10.0 - 11.5 | 9 |
| 11.5 - 13.0 | 21 |
| 13.0 - 14.5 | 17 |
| 14.5 - 16.0 | 25 |
| 16.0 - 17.5 | 15 |
| 17.5 - 19.0 | 31 |
| 19.0 - 20.5 | 16 |
| 20.5 - 22.0 | 30 |
| 22.0 - 23.5 | 16 |
| 23.5 - 25.0 | 35 |

[Note] 1 ft = 0.3 m.

After analyzing the above data, the ORITE team decided to push Shelby tubes at depth ranges of 10.0 to 12.0, 13.0 to 15.0, and 17.5 to 19.5 ft (3.0 to 3.7, 4.0 to 4.6, and 5.3 to 5.9 m). This gave the uncorrected SPT-N values of 9, 17, and 31, respectively. The original soil sampling plan, shown in Figure 3.1, had to be modified. The SPT truck was setup in the median of the freeway, in the center of the drainage path. There had also been substantial rain in the area the past few days. The soil was saturated at the surface, and it was very difficult for the truck to move around. Figure 4.8 shows the modified pattern.

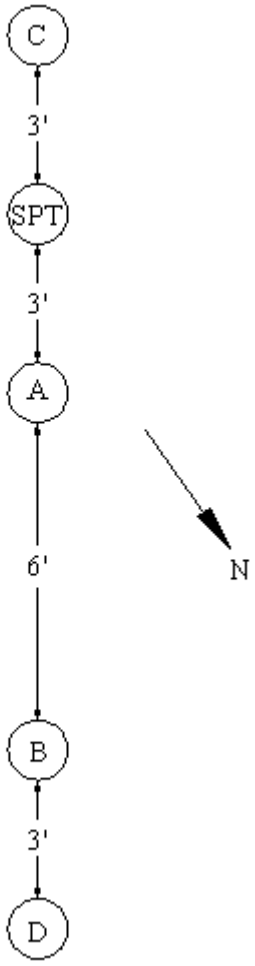


**Figure 4.8:** Actual Shelby Tube Sampling Plan at Site No. 5

A total of twelve tubes were pushed with ORITE taking nine of them. Details on the tubes taken by ORITE are given in Appendix B in Table B.10. Corrections, as done with the previous field sites, were also done with this site. The corrected SPT-N values are shown below in Table 4.10. A summary of the fully corrected SPT-N values is given in Table B.9 in Appendix B.

**Table 4.10:** Morrow County Site SPT-$(N_{60})_1$ Values

| Depth (ft) | Original SPT-N | Energy Correction Only | Peck | Terzaghi | Bazaraa | Seed et al. | Skempton | **Avg.** |
|---|---|---|---|---|---|---|---|---|
| 10-12 | 9 | 12 | 14 | 16 | 14 | 15 | 15 | **15** |
| 13-15 | 17 | 23 | 24 | 26 | 22 | 25 | 25 | **25** |
| 17.5-19.5 | 31 | 42 | 40 | 40 | 38 | 39 | 39 | **40** |

### 4.3.7 Subsurface Exploration Data for SR 2 Site in Erie County

The sixth highway embankment site was located on State Route 2, about 210 ft (64 m) south of the Edison Bridge south abutment, in Erie County. At this location, a continuous SPT was done in the median section of the highway to a depth of 25 ft (7.6 m). During the filed work, the split-spoon barrel brought samples of hard silt and clay to the ground surface. No water table was encountered during the field work. The uncorrected SPT-N values obtained at this site are given in Table 4.11. Although the blow counts oscillated, they exhibited a general trend of increasing with depth. A total of twelve Shelby tubes were pushed according to the plan shown in Figure 3.1, with ORITE taking nine of them. Details on the tubes taken by ORITE are given in Appendix B in Table B.12. Corrections, as done with the previous field sites, were also done with this site. The corrected SPT-N values are shown below in Table 4.12 and Table B.11 (in Appendix B).

**Table 4.11:** Uncorrected SPT-N Values at Site No. 6 (Erie County)

| Depth Range (ft) | Uncorrected SPT-N Value (blows/ft) |
|---|---|
| 1.0 - 2.5 | NA |
| 2.5 - 4.0 | 7 |
| 4.0 - 5.5 | 8 |
| 5.5 - 7.0 | 12 |
| 7.0 - 8.5 | 6 |
| 8.5 - 10.0 | 8 |
| 10.0 - 11.5 | 11 |
| 11.5 - 13.0 | 14 |
| 13.0 - 14.5 | 11 |
| 14.5 - 16.0 | 17 |
| 16.0 - 17.5 | 20 |
| 17.5 - 19.0 | 14 |
| 19.0 - 20.5 | 14 |
| 20.5 - 22.0 | 24 |
| 22.0 - 23.5 | 18 |
| 23.5 - 25.0 | 39 |

[Note] 1 ft = 0.3 m.

**Table 4.12:** Erie County Site SPT-$(N_{60})_1$ Values

| Depth (ft) | Original SPT-N | Energy Correction Only | Peck | Terzaghi | Bazaraa | Seed et al. | Skempton | **Avg.** |
|---|---|---|---|---|---|---|---|---|
| 2.5-4.5 | 7 | 10 | 16 | 28 | 25 | 10 | 17 | **21** |
| 5.5-7.5 | 12 | 16 | 23 | 32 | 31 | 28 | 26 | **28** |
| 11.5-13.5 | 14 | 19 | 23 | 26 | 20 | 25 | 24 | **23** |

### 4.3.8 Subsurface Exploration Data for Interstate 75 Site in Hancock County

The seventh highway embankment site was located about 0.5 miles (0.8 km) north of Exit 142 (Bluffton Exit) on Interstate 75 in Hancock County. The site was situated more than 200 ft (61 m) away from any bridge abutments. At this location, a continuous SPT was done in the area outside the northbound lanes of the highway to a depth of 25 ft (7.6 m). The uncorrected SPT-N values obtained at this site are given in Table 4.13.

**Table 4.13:** Uncorrected SPT-N Values at Site No. 7 (Hancock County)

| Depth Range (ft) | Uncorrected SPT-N Value (blows/ft) |
|---|---|
| 1.0 - 2.5 | 19 |
| 2.5 - 4.0 | 13 |
| 4.0 - 5.5 | 14 |
| 5.5 - 7.0 | 16 |
| 7.0 - 8.5 | 15 |
| 8.5 - 10.0 | 23 |
| 10.0 - 11.5 | 9 |
| 11.5 - 13.0 | 20 |
| 13.0 - 14.5 | 12 |
| 14.5 - 16.0 | 25 |
| 16.0 - 17.5 | 17 |
| 17.5 - 19.0 | 33 |
| 19.0 - 20.5 | 10 |
| 20.5 - 22.0 | 21 |
| 22.0 - 23.5 | 21 |
| 23.5 - 25.0 | 25 |

[Note] 1 ft = 0.3 m.

The soil coming up to the surface appeared to be uniform and of A-6 or A-7-6 type material. A decision was then made to push Shelby tubes at depths of 5.5, 10.0, and 16.0 ft (1.7, 3.0, and 4.9 m) below the ground surface. A total of twelve Shelby tubes were recovered, as usual. The original soil sampling plan, shown in Figure 3.1, was executed smoothly. Details on the tubes taken by ORITE are given in Appendix B in Table B.14. Corrections, as done with the previous field sites, were also done with this site. The corrected SPT-N values are shown below in Table 4.14. A summary of the fully corrected SPT-N values is given in Tables B.13 (in Appendix B).

**Table 4.14:** Hancock County Site SPT-$(N_{60})_1$ Values

| Depth (ft) | Original SPT-N | Energy Correction Only | Peck | Terzaghi | Bazaraa | Seed et al. | Skempton | **Avg.** |
|---|---|---|---|---|---|---|---|---|
| 5.5-7.5 | 16 | 22 | 29 | 37 | 36 | 34 | 32 | **34** |
| 10.0-11.5 | 9 | 12 | 14 | 16 | 14 | 15 | 15 | **15** |
| 16.0-17.5 | 17 | 23 | 23 | 23 | 22 | 23 | 23 | **23** |

### 4.3.9 Subsurface Exploration Data for Interstate 70 Site in Muskingum County

The eighth highway embankment site was located in the grassed median section of Interstate 70 in Muskingum County. This site can be found just west of Exit 153, near Zanesville, Ohio. During the initial SPT work conducted at least 100 ft or 30 m away (to the east) from a nearby bridge abutment wall, dense (stiff) sand was commonly encountered. A decision was then made to move the SPT hole location another 100 ft (30 m) away from the bridge abutment. The same sand was detected even in the second SPT hole. However, a layer of clayey soil was found from 9.5 to 11 ft (2.9 to 3.4 m) below the ground surface. The uncorrected SPT-N values obtained at this site are given in Table 4.15.


**Figure 4.9:** Highway Embankment Site No. 8 on I-70 (Muskingum County)

**Table 4.15:** Uncorrected SPT-N Values at Site No. 8 (Muskingum County)

| Depth Range (ft) | Uncorrected SPT-N Value (blows/ft) |
|---|---|
| 1.0 - 2.5 | 15 |
| 2.5 - 4.0 | 17 |
| 4.0 - 5.5 | 20 |
| 5.5 - 7.0 | 42 |
| 7.0 - 8.5 | 36 |
| 8.5 - 10.0 | 13 |
| 10.0 - 11.5 | 19 |
| 11.5 - 13.0 | 48 |
| 13.0 - 14.5 | 46 |
| 14.5 - 16.0 | 53 |
| 16.0 - 17.5 | 38 |
| 17.5 - 19.0 | 53 |
| 19.0 - 20.5 | 44 |
| 20.5 - 22.0 | 49 |
| 22.0 - 23.5 | 42 |
| 23.5 - 25.0 | 61 |

[Note] 1 ft = 0.3 m.

**Table 4.16:** Muskingum County Site SPT-$(N_{60})_1$ Values

| Depth (ft) | Original SPT-N | Energy Correction Only | Peck | Terzaghi | Bazaraa | Seed et al. | Skempton | **Avg.** |
|---|---|---|---|---|---|---|---|---|
| 8.5-10.0 | 13 | 18 | 21 | 24 | 21 | 23 | 22 | **22** |
| 10.0-11.5 | 19 | 26 | 29 | 32 | 28 | 31 | 31 | **30** |

Only five Shelby tube soil samples were recovered from within the thickness of the clay soil layer. The original soil sampling plan, shown in Figure 3.1, was executed smoothly. Three of these tubes were transported to the ORITE laboratory. Details on the tubes taken by ORITE are given in Appendix B in Table B.16. Corrections, as done with the previous field sites, were also done with this site. The corrected SPT-N values are shown below in Table 4.14. A summary of the fully corrected SPT-N values is given in Table B.15 (in Appendix B).

### 4.3.10 Subsurface Exploration Data for Interstate 77 Site in Noble County

The ninth highway embankment site was located in the grassed median section of Interstate 77 in Noble County, about 2,850 ft (0.87 km) north of the CR 13 overpass bridge. The location of this site was chosen carefully to allow testing and sampling of highly weathered shale fill material. It is not uncommon for highway sections to be built on weathered shale especially in ODOT Districts 10. After going through the top soil layer, weathered shale resembling reddish brown silty clay was encountered consistently. The uncorrected SPT-N values obtained at this site are given in Table 4.17. At the depth of 17 ft (5.2 m), some rock fragments were detected, which raised the blow count. No water table was encountered during the field work.

**Figure 4.10:** Highway Embankment Site No. 9 on I-77 (Noble County)

**Table 4.17:** Uncorrected SPT-N Values at Site No. 9 (Noble County)

| Depth Range (ft) | Uncorrected SPT-N Value (blows/ft) |
|---|---|
| 1.0 – 2.5 | 11 |
| 2.5 – 4.0 | 10 |
| 4.0 – 5.5 | 14 |
| 5.5 – 7.0 | 15 |
| 7.0 – 8.5 | 9 |
| 8.5 – 10.0 | 15 |
| 10.0 – 11.5 | 17 |
| 11.5 – 13.0 | 18 |
| 13.0 – 14.5 | 14 |
| 14.5 – 16.0 | 22 |
| 16.0 – 17.5 | 44 |
| 17.5 – 19.0 | 33 |
| 19.0 – 20.5 | 12 |
| 20.5 – 22.0 | 20 |
| 22.0 – 23.5 | 26 |
| 23.5 – 25.0 | 26 |

[Note] 1 ft = 0.3 m.

Based on the SPT-N value data, three depths of 4 ft, 7 ft, and 10 ft (1.2, 2.1, and 3.0 m) were chosen for obtaining relatively undisturbed soil samples. Table 4.18 lists the fully corrected SPT-N values at the soil sampling depths. Figure 4.11 below shows general locations of four soil sampling holes with respect to the continuous SPT hole. Although the material seemed fairly stiff, the soil sampling work went smoothly with a good recovery recorded for each tube. The fifth hole (Hole E) was added to procure an additional sample at the depth of 7 ft (2.1 m). For, soil recovery was very poor at the mid-depth in Hole C.

**Table 4.18:** Noble County Site SPT-$(N_{60})_1$ Values

| Depth (ft) | Original SPT-N | Energy Correction Only | Peck | Terzaghi | Bazaraa | Seed et al. | Skempton | **Avg.** |
|---|---|---|---|---|---|---|---|---|
| 4.0-5.5 | 14 | 19 | 27 | 37 | 36 | 32 | 30 | **32** |
| 7.0-8.5 | 9 | 12 | 15 | 18 | 17 | 17 | 16 | **17** |
| 10.0-11.5 | 17 | 23 | 26 | 28 | 24 | 28 | 27 | **27** |

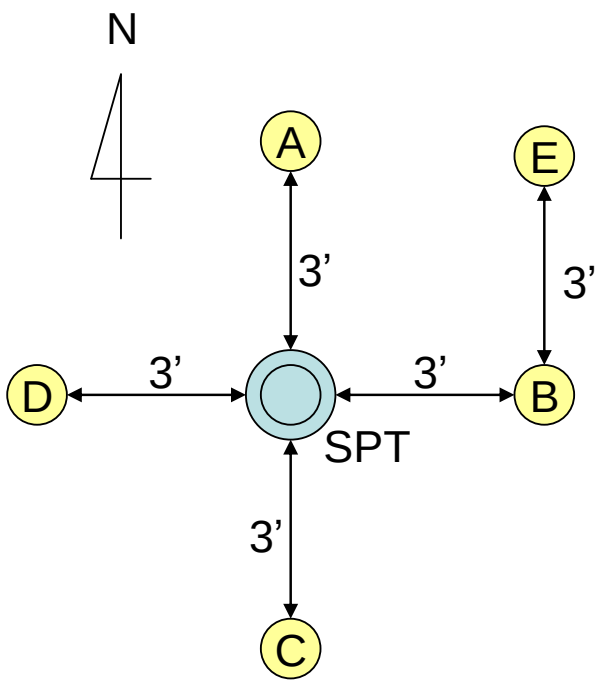


**Figure 4.11:** Actual Shelby Tube Sampling Plan at Site No. 9

A summary information on the fully corrected SPT-N values and the Shelby tubes taken (by ORITE) can be found in Appendix B (see Tables B.17 & B.18).

## 4.4 Laboratory Index Properties and Sieve Analyses

Index properties of soils encountered in the current project were determined using the Shelby tube samples obtained in the field. The index properties included a wide range of properties such as natural moisture content, unit weights (dry, moist), Atterberg limits (plastic limit, liquid limit, plasticity index), specific gravity, and grain size characteristics (percentages of gravel, sand, silt, and clay). These results will be presented for each site in the following subsections.

### 4.4.1 Soil Index Properties for Site No. 1 (Hamilton County)

Four sets of index property testing were performed by BBCM on the soil samples recovered from the first (Hamilton County) site. Two sets were done on Shelby tube soil samples taken in the depth range of 2.5 to 4.5 ft (0.76 to 1.4 m), one set was done on a Shelby tube sample from the depth range of 4.5 to 6.5 feet (1.4 to 2.0 m), and one more set was done on a Shelby tube sample from the depth range of 10.0 to 12.0 ft (3.0 to 3.7 m). The results of the index and grain size analysis tests are summarized below in Tables 4.19 and 4.20.

**Table 4.19:** Index Properties of Soils at Site No. 1 (Hamilton County)

| Depth of Soil (ft) | Natural *w* (%) | Moist Unit Wt (pcf) | Dry Unit Wt (pcf) | Specific Gravity | Liquid Limit | Plastic Limit | Plasticity Index |
|---|---|---|---|---|---|---|---|
| 2.75 | 15.7 | 130.4 | 112.7 | 2.74 | 41 | 19 | 22 |
| 3.25 | 22.0 | 127.4 | 104.4 | N/A | 58 | 21 | 37 |
| 4.75 | 17.6 | 126.7 | 107.8 | N/A | 50 | 20 | 30 |
| 10.25 | 15.4 | 128.9 | 111.7 | 2.66 | 43 | 22 | 21 |

[Note] 1 ft = 0.3 m; and 1 pcf = 0.157 kN/m$^3$.

**Table 4.20:** Sieve Analysis Results for Site No. 1 (Hamilton County)

| Depth of Soil (ft) | % Gravel | % Sand | % Silt | % Clay | AASHTO Soil Class. |
|---|---|---|---|---|---|
| 2.75 | 11 | 14 | 30 | 46 | A-7-6 |
| 3.25 | 10 | 13 | 26 | 51 | A-7-6 |
| 4.75 | 7 | 11 | 34 | 48 | A-7-6 |
| 10.25 | 6 | 12 | 30 | 51 | A-7-6 |

### 4.4.2 Soil Index Properties for Site No. 2 (Fayette County)

Four sets of index property testing were performed by BBCM on the soil samples recovered from the Fayette County site. One set was done on a Shelby tube sample taken from the depth range of 5.5 to 7.5 ft (1.7 to 2.3 m), two sets on two separate Shelby tubes in the depth range of 8.5 to 10.5 ft (2.6 to 3.2 m), and one set was done on a Shelby tube

sample taken in the depth range of 14.5 to 16.5 ft (4.4 to 5.0 m). As it was mentioned earlier, a total of five Shelby tubes sampling holes were created at this site. This allowed for an extra tube being available at each soil sampling depth. Hence, two tubes were tested at the mid-depth range. The results of the index and sieve analysis tests are summarized in Tables 4.21 and 4.22.

**Table 4.21:** Index Properties of Soils at Site No. 2 (Fayette County)

| Depth of Soil (ft) | Natural *w* (%) | Moist Unit Wt (pcf) | Dry Unit Wt (pcf) | Specific Gravity | Liquid Limit | Plastic Limit | Plasticity Index |
|---|---|---|---|---|---|---|---|
| 5.75 | 15.3 | 131.0 | 113.6 | 2.68 | 32 | 17 | 15 |
| 8.75 | 8.8 | 138.4 | 127.2 | N/A | 20 | 14 | 6 |
| 8.8 | 9.1 | 140.7 | 129.0 | N/A | 21 | 13 | 8 |
| 14.75 | 9.2 | 142.2 | 130.3 | 2.65 | 21 | 13 | 8 |

[Note] 1 ft = 0.3 m; and 1 pcf = 0.157 kN/m$^3$.

**Table 4.22:** Sieve Analysis Results for Site No. 2 (Fayette County)

| Depth of Soil (ft) | % Gravel | % Sand | % Silt | % Clay | AASHTO Soil Class. |
|---|---|---|---|---|---|
| 5.75 | 6 | 24 | 40 | 30 | A-6a |
| 8.75 | 10 | 26 | 45 | 19 | A-4a |
| 8.8 | 15 | 27 | 39 | 19 | A-4a |
| 14.75 | 16 | 28 | 38 | 18 | A-4a |

### 4.4.3 Soil Index Properties for Site No. 3 (Lake County)

Five sets of index testing were done by BBCM on the soil samples recovered from the Lake County site. One set was done on a Shelby tube sample obtained in the depth range of 1.0 to 3.0 ft (0.3 to 0.9 m), two on two separate Shelby tube samples taken in the depth range of 4.0 to 6.0 ft (1.2 to 1.8 m), and two on a Shelby tube sample from the depth range of 14.0 to 16.0 ft (4.3 to 4.9 m). The results of the index and grain size analysis tests are summarized in Tables 4.23 and 4.24.

**Table 4.23:** Index Properties of Soils at Site No. 3 (Lake County)

| Depth of Soil (ft) | Natural *w* (%) | Moist Unit Wt (pcf) | Dry Unit Wt (pcf) | Specific Gravity | Liquid Limit | Plastic Limit | Plasticity Index |
|---|---|---|---|---|---|---|---|
| 1.75 | 14.0 | 140.0 | 122.8 | 2.76 | 29 | 18 | 11 |
| 4.25 | 12.0 | 138.9 | 123.9 | N/A | 28 | 18 | 10 |
| 4.75 | 12.5 | 140.9 | 125.2 | N/A | 29 | 19 | 10 |
| 14.25 | 11.5 | 139.3 | 124.9 | 2.60 | 26 | 16 | 10 |
| 14.75 | 13.1 | 141.8 | 125.3 | N/A | 25 | 18 | 7 |

[Note] 1 ft = 0.3 m; and 1 pcf = 0.157 kN/m$^3$.

**Table 4.24:** Sieve Analysis Results for Site No. 3 (Lake County)

| Depth of Soil (ft) | % Gravel | % Sand | % Silt | % Clay | AASHTO Soil Class. |
|---|---|---|---|---|---|
| 1.75 | 7 | 23 | 37 | 33 | A-6a |
| 4.25 | 5 | 27 | 35 | 33 | A-4a |
| 4.75 | 4 | 23 | 37 | 36 | A-4a |
| 14.25 | 9 | 23 | 38 | 31 | A-4a |
| 14.75 | 8 | 24 | 37 | 30 | A-4a |

### 4.4.4 Soil Index Properties for Site No. 4 (Athens County)

Five sets of index tests and sieve analyses were done by BBCM on the Athens County site. One set was done on a Shelby tube in the depth range of 4.5 to 6.5 ft (1.4 to 2.0 m), one was done on a Shelby tube in the depth range of 8.0 to 10.0 ft (2.4 to 3.0 m), and three were done on a Shelby tube in the depth range of 19.0 to 21.0 ft (5.8 to 6.4 m). The soil varied greatly throughout the tube at the lowest depth. This is why three tests were done on it. The results of the index and mechanical sieve analysis tests are summarized in Tables 4.25 and 4.26.

**Table 4.25:** Index Properties of Soils at Site No. 4 (Athens County)

| Depth of Soil (ft) | Natural *w* (%) | Moist Unit Wt (pcf) | Dry Unit Wt (pcf) | Specific Gravity | Liquid Limit | Plastic Limit | Plasticity Index |
|---|---|---|---|---|---|---|---|
| 5.25 | 12.7 | 134.9 | 119.7 | 2.72 | 29 | 18 | 11 |
| 8.25 | 12.0 | 122.4 | 109.2 | N/A | 29 | 18 | 11 |
| 19.25 | 15.2 | 121.7 | 105.7 | 2.68 | 39 | 23 | 16 |
| 19.75 | 14.8 | 133.8 | 116.5 | N/A | 38 | 22 | 16 |
| 20.25 | 22.0 | 128.2 | 105.1 | N/A | 45 | 21 | 24 |

[Note] 1 ft = 0.3 m; and 1 pcf = 0.157 kN/m$^3$.

**Table 4.26:** Sieve Analysis Results for Site No. 4 (Athens County)

| Depth of Soil (ft) | % Gravel | % Sand | % Silt | % Clay | AASHTO Soil Class. |
|---|---|---|---|---|---|
| 5.25 | 4 | 26 | 37 | 33 | A-6a |
| 8.25 | 5 | 23 | 40 | 32 | A-6a |
| 19.25 | 8 | 15 | 45 | 32 | A-6b |
| 19.75 | 12 | 22 | 40 | 25 | A-6b |
| 20.25 | 1 | 23 | 32 | 44 | A-7-6 |

### 4.4.5 Soil Index Properties for Site No. 5 (Morrow County)

Four sets of index tests and sieve analyses were done by BBCM on the Morrow County site. Two sets were done on a Shelby tube in the depth range of 10.0 to 12.0 ft (3.0 to 3.7 m), one was done on a Shelby tube in the depth range of 13.0 to 15.0 ft (4.0 to 4.6 m), and one was done on a Shelby tube in the depth range of 17.5 to 19.5 ft (5.3 to 5.9 m). The results of the index and grain size analysis tests are shown below in Tables 4.27 and 4.28.

**Table 4.27:** Index Properties of Soils at Site No. 5 (Morrow County)

| Depth of Soil (ft) | Natural *w* (%) | Moist Unit Wt (pcf) | Dry Unit Wt (pcf) | Specific Gravity | Liquid Limit | Plastic Limit | Plasticity Index |
|---|---|---|---|---|---|---|---|
| 10.25 | 14.0 | 134.7 | 118.2 | 2.68 | 24 | 16 | 8 |
| 10.75 | 11.4 | 142.7 | 128.2 | N/A | 28 | 15 | 13 |
| 13.25 | 14.8 | 128.0 | 111.4 | N/A | 30 | 17 | 13 |
| 17.75 | 16.0 | 127.5 | 110.0 | 2.64 | 30 | 18 | 12 |

[Note] 1 ft = 0.3 m; and 1 pcf = 0.157 kN/m$^3$.

**Table 4.28:** Sieve Analysis Results for Site No. 5 (Morrow County)

| Depth of Soil (ft) | % Gravel | % Sand | % Silt | % Clay | AASHTO Soil Class. |
|---|---|---|---|---|---|
| 10.25 | 10 | 28 | 39 | 23 | A-4a |
| 10.75 | 8 | 27 | 40 | 25 | A-6a |
| 13.25 | 3 | 23 | 47 | 27 | A-6a |
| 17.75 | 8 | 24 | 44 | 25 | A-6a |

### 4.4.6 Soil Index Properties for Site No. 6 (Erie County)

Five sets of index tests and sieve analyses were done by BBCM on the Erie County site. Two sets were done on a Shelby tube in the depth range of 2.5 to 4.5 ft (0.8 to 1.4 m), two were done on a Shelby tube in the depth range of 5.5 to 7.5 ft (1.5 to 2.3 m), and one was done on a Shelby tube in the depth range of 11.5 to 13.5 ft (3.5 to 4.1 m). The results of the index and grain size analysis tests are shown below in Tables 4.29 and 4.30.

**Table 4.29:** Index Properties of Soils at Site No. 6 (Erie County)

| Depth of Soil (ft) | Natural *w* (%) | Moist Unit Wt (pcf) | Dry Unit Wt (pcf) | Specific Gravity | Liquid Limit | Plastic Limit | Plasticity Index |
|---|---|---|---|---|---|---|---|
| 2.95 | 25.4 | 122.9 | 98.0 | 2.68 | 49 | 22 | 27 |
| 3.50 | 26.0 | 123.1 | 97.7 | 2.68 | 60 | 24 | 36 |
| 6.50 | 24.6 | 125.8 | 101.0 | 2.68 | 48 | 22 | 26 |
| 7.15 | 28.1 | 124.4 | 97.1 | 2.68 | 55 | 23 | 22 |
| 11.75 | 25.7 | 122.7 | 97.6 | 2.71 | 61 | 24 | 37 |

[Note] 1 ft = 0.3 m; and 1 pcf = 0.157 kN/m$^3$.

**Table 4.30:** Sieve Analysis Results for Site No. 6 (Erie County)

| Depth of Soil (ft) | % Gravel | % Sand | % Silt | % Clay | AASHTO Soil Class. |
|---|---|---|---|---|---|
| 2.95 | 1 | 3 | 38 | 58 | A-7-6 |
| 3.50 | 1 | 3 | 34 | 62 | A-7-6 |
| 6.50 | 0 | 2 | 46 | 52 | A-7-6 |
| 7.15 | 0 | 2 | 36 | 61 | A-7-6 |
| 11.75 | 1 | 3 | 30 | 66 | A-7-6 |

### 4.4.7 Soil Index Properties for Site No. 7 (Hancock County)

Five sets of index tests and sieve analyses were done by BBCM on the Hancock County site. Two sets were done on a Shelby tube in the depth range of 5.5 to 7.0 ft (1.7 to 2.1 m), two were done on a Shelby tube in the depth range of 10.0 to 11.5 ft (3.0 to 3.5 m), and one was done on a Shelby tube in the depth range of 16.0 to 17.5 ft (4.9 to 5.3

m). The results of the index and sieve analysis tests are shown below in Tables 4.31 and 4.32.

**Table 4.31:** Index Properties of Soils at Site No. 7 (Hancock County)

| Depth of Soil (ft) | Natural *w* (%) | Moist Unit Wt (pcf) | Dry Unit Wt (pcf) | Specific Gravity | Liquid Limit | Plastic Limit | Plasticity Index |
|---|---|---|---|---|---|---|---|
| 6.55 | 20.0 | 132.1 | 110.1 | 2.69 | 41 | 19 | 22 |
| 7.00 | 21.4 | 130.1 | 107.2 | 2.69 | 45 | 21 | 24 |
| 10.95 | 21.6 | 127.8 | 105.1 | 2.69 | 47 | 22 | 25 |
| 11.05 | 20.1 | 130.7 | 108.8 | 2.69 | 38 | 20 | 18 |
| 17.45 | 18.5 | 131.9 | 111.3 | 2.68 | 39 | 19 | 20 |

[Note] 1 ft = 0.3 m; and 1 pcf = 0.157 kN/m$^3$.

**Table 4.32:** Sieve Analysis Results for Site No. 7 (Hancock County)

| Depth of Soil (ft) | % Gravel | % Sand | % Silt | % Clay | AASHTO Soil Class. |
|---|---|---|---|---|---|
| 6.55 | 2 | 19 | 32 | 46 | A-7-6 |
| 7.00 | 3 | 16 | 33 | 48 | A-7-6 |
| 10.95 | 1 | 16 | 32 | 50 | A-7-6 |
| 11.05 | 1 | 19 | 36 | 44 | A-6b |
| 17.45 | 3 | 17 | 34 | 47 | A-6b |

### 4.4.8 Soil Index Properties for Site No. 8 (Muskingum County)

Two sets of index tests and sieve analyses were done by BBCM on the Muskingum County site. They were done on a Shelby tube in the depth range of 9.5 to 11.5 ft (2.9 to 3.5 m), due to a lack of cohesive soil fill encountered at this site. The results of the index and grain size analysis tests are shown below in Tables 4.33 and 4.34.

**Table 4.33:** Index Properties of Soils at Site No. 8 (Muskingum County)

| Depth of Soil (ft) | Natural *w* (%) | Moist Unit Wt (pcf) | Dry Unit Wt (pcf) | Specific Gravity | Liquid Limit | Plastic Limit | Plasticity Index |
|---|---|---|---|---|---|---|---|
| 9.75 | 14.9 | 136.8 | 119.1 | 2.70 | 29 | 19 | 10 |
| 10.25 | 13.9 | 138.3 | 121.4 | 2.69 | 30 | 19 | 11 |

[Note] 1 ft = 0.3 m; and 1 pcf = 0.157 kN/m$^3$.

**Table 4.34:** Sieve Analysis Results for Site No. 8 (Muskingum County)

| Depth of Soil (ft) | % Gravel | % Sand | % Silt | % Clay | AASHTO Soil Class. |
|---|---|---|---|---|---|
| 9.75 | 8 | 22 | 50 | 20 | A-4b |
| 10.25 | 10 | 29 | 42 | 19 | A-6a |

### 4.4.9 Soil Index Properties for Site No. 9 (Noble County)

Three sets of index tests and sieve analyses were done by BBCM on the Noble County site. One set was done on a Shelby tube in the depth range of 4.0 to 6.0 ft (1.2 to 1.8 m), one was done on a Shelby tube in the depth range of 7.0 to 9.0 ft (2.1 to 2.7 m), and one was done on a Shelby tube in the depth range of 10.0 to 12.0 ft (3.0 to 3.7 m). The results of the index and sieve analysis tests are shown below in Tables 4.35 and 4.36.

**Table 4.35:** Index Properties of Soils at Site No. 9 (Noble County)

| Depth of Soil (ft) | Natural *w* (%) | Moist Unit Wt (pcf) | Dry Unit Wt (pcf) | Specific Gravity | Liquid Limit | Plastic Limit | Plasticity Index |
|---|---|---|---|---|---|---|---|
| 4.25 | 14.0 | 141.9 | 124.5 | 2.73 | 37 | 21 | 16 |
| 7.25 | 13.5 | 139.8 | 123.2 | 2.73 | 39 | 22 | 17 |
| 10.25 | 12.5 | 142.7 | 126.8 | 2.79 | 36 | 21 | 15 |

[Note] 1 ft = 0.3 m; and 1 pcf = 0.157 kN/m$^3$.

**Table 4.36:** Sieve Analysis Results for Site No. 9 (Noble County)

| Depth of Soil (ft) | % Gravel | % Sand | % Silt | % Clay | AASHTO Soil Class. |
|---|---|---|---|---|---|
| 4.25 | 13 | 11 | 48 | 28 | A-6b |
| 7.25 | 7 | 17 | 46 | 30 | A-6b |
| 10.25 | 12 | 15 | 43 | 30 | A-6a |

## 4.5 Soil Shear Strength Properties

In this section, the shear strength properties for the soils obtained at each site will be given. This includes data from the unconfined compression and C-U triaxial compression tests.

### 4.5.1 Shear Strength Properties for Site No. 1 (Hamilton County)

Four unconfined compression tests were performed by BBCM on the soil samples taken from this site. Two were done on Shelby tubes from the highest depth range, one from the middle depth range, and one on the lowest depth range. Table 4.37 summarizes the test results.

A total of eight C-U triaxial compression tests were done on the Shelby tube samples taken at this site. Three were done at the highest depth range, three were done at the middle depth range, and two were done at the lowest depth range. Specimen depth, $t_{50}$, $\phi$ angles, and effective consolidation stress for each specimen are given in Table 4.38. Six of the specimens tested went to 15% axial strain without failure. Two of them were tested to less strain – Specimen A-1 (2.5 – 3.0 ft or 0.76 – 0.91 m depth) to 13.39%; and Specimen A-1 (3.1 – 3.6 ft or 0.94 – 1.1 m depth) to 10.2%. Large rocks (larger than 1/6 of the diameter of the specimen) were also found in some of the specimens that could have affected the results.

Soil recovery was poor at the lowest depth range for this site. That is why only two tests were done there. In addition, a variety of plots are in Appendix C related to the data just given. Figures C.1 through C.8 give stress-strain curves for each specimen, and Figures C.9 through C.14 give p'-q' and p-q plots for each depth range.

**Table 4.37:** Unconfined Compression Test Results for Site No. 1 (Hamilton County)

| Avg. Depth of Specimen (ft) | Moisture Content (%) | Dry Unit Weight (pcf) | Unconfined Comp. Strength (psi) | Strain at Failure (%) |
|---|---|---|---|---|
| 2.75 | 15.7 | 112.7 | 24.8 | 7.4 |
| 3.25 | 22.0 | 104.4 | 30.6 | 7.1 |
| 4.75 | 17.6 | 107.8 | 18.7 | 7.3 |
| 10.25 | 15.4 | 111.7 | 46.9 | 5.9 |

[Note] 1 ft = 0.3 m; 1 pcf = 0.157 kN/m$^3$; and 1 psi = 6.895 kPa.

**Table 4.38:** C-U Triaxial Compression Test Results (Hamilton County)

| Specimen (Depth) | $t_{50}$ (min) | $\phi$ (degrees) | $\phi'$ (degrees) | Effective Consolidation Pressure (psi) |
|---|---|---|---|---|
| A-1 (2.5' - 3.0') | 20.0 | 11.1 | 30.8 | 5.0 |
| A-1 (3.1' - 3.6') | 35.0 | 10.6 | 28.0 | 15.0 |
| D-1 (2.5' - 3.0') | 18.0 | 11.5 | 25.3 | 30.0 |
| A-2 (5.1' - 5.6') | 30.0 | 13.7 | 29.2 | 7.5 |
| C-2 (4.9' - 5.4') | 15.0 | 10.5 | 27.9 | 15.0 |
| D-2 (4.6' - 5.1') | 12.0 | 10.4 | 24.5 | 30.0 |
| A-3 (10.3' - 10.8') | 24.0 | 12.6 | 26.4 | 12.5 |
| D-3 (10.2' - 10.6') | 30.0 | 14.9 | 26.8 | 20.0 |

[Note] 1 ft = 0.3 m; and 1 psi = 6.895 kPa.

### 4.5.2 Shear Strength Properties for Site No. 2 (Fayette County)

Four unconfined compression tests were performed on soil from this site by BBCM. One was done on a Shelby tube from the highest depth range, two were done from the middle depth range, and one on the lowest depth range. Table 4.39 summarizes the test data.

**Table 4.39:** Unconfined Compression Test Results for Site No. 2 (Fayette County)

| Ave. Depth of Specimen (ft) | Moisture Content (%) | Dry Unit Weight (pcf) | Unconfined Comp. Strength (psi) | Strain at Failure (%) |
|---|---|---|---|---|
| 5.75 | 15.3 | 113.6 | 36.6 | 6.8 |
| 8.75 | 8.8 | 127.2 | 47.2 | 5.9 |
| 8.80 | 9.1 | 129.0 | 41.0 | 7.1 |
| 14.75 | 9.2 | 130.3 | 45.1 | 4.6 |

[Note] 1 ft = 0.3 m; 1 pcf = 0.157 kN/m$^3$; and 1 psi = 6.895 kPa.

A total of nine C-U triaxial compression tests were performed on the relatively undisturbed soil samples taken from this site. Four were done at the highest depth range, three were done at the middle depth range, and two were done at the lowest depth range. Specimen depth, $t_{50}$, $\phi$ angles, and effective consolidation stress for each specimen are

given Table 4.40. Every C-U triaxial test specimen went all the way to 15% axial strain without showing any failure characteristics. Rocks were also found in some of the specimens after testing.

**Table 4.40:** C-U Triaxial Compression Test Results for Site No. 2 (Fayette County)

| Specimen (Depth) | $t_{50}$ (min) | $\phi$ (degrees) | $\phi'$ (degrees) | Effective Consolidation Pressure (psi) |
|---|---|---|---|---|
| A-1 (5.7' - 6.2') | 3.7 | 20.8 | 37.8 | 7.5 |
| D-1 (6.6' - 7.1') | 10.2 | 17.1 | 32.9 | 15.0 |
| E-1 (6.3' - 6.7') | 30.5 | 18.6 | 30.5 | 22.5 |
| E-1 (5.5' - 6.0') | 10.1 | 18.0 | 36.8 | 30.0 |
| A-2 (9.2' - 9.7') | 1.3 | 32.5 | 34.7 | 15.0 |
| D-2 (9.2' - 9.7') | 1.1 | 31.3 | 34.8 | 22.5 |
| E-2 (9.2' - 9.7') | 3.4 | 33.1 | 33.6 | 30.0 |
| B-3 (14.7' - 15.2') | 1.8 | 21.9 | 33.5 | 18.0 |
| B-3 (15.4' - 15.8') | 3.6 | 26.6 | 34.2 | 24.0 |

[Note] 1 ft = 0.3 m; and 1 psi = 6.895 kPa.

Soil recovery was again poor at the lowest depth range for this site also. That is why only two tests were done there. In addition, a variety of plots are in Appendix C related to the data just given. Figures C.15 through C.23 give stress-strain curves for each specimen, and Figures C.24 through C.29 give p'-q' and p-q plots for each depth range.

### 4.5.3 Shear Strength Properties for Site No. 3 (Lake County)

Five unconfined compression tests were performed on the relatively undisturbed soil samples recovered from this site by BBCM. One was done on a Shelby tube from the highest depth range, two were done from the middle depth range, and two were done on the lowest depth range. Table 4.41 summarizes the test results.

**Table 4.41:** Unconfined Compression Test Results for Site No. 3 (Lake County)

| Ave. Depth of Specimen (ft) | Moisture Content (%) | Dry Unit Weight (pcf) | Unconfined Comp. Strength (psi) | Strain at Failure (%) |
|---|---|---|---|---|
| 1.75 | 14.0 | 122.8 | 57.3 | 7.1 |
| 4.25 | 12.0 | 123.9 | 79.0 | 7.2 |
| 4.75 | 12.5 | 125.2 | 71.3 | 5.5 |
| 14.25 | 11.5 | 124.9 | 30.2 | 12.3 |
| 14.75 | 13.1 | 125.3 | 46.1 | 16.9 |

[Note] 1 ft = 0.3 m; 1 pcf = 0.157 kN/m$^3$; and 1 psi = 6.895 kPa.

A total of nine C-U triaxial compression tests were conducted on the Shelby tube soil samples recovered from this site. Three were done at the highest depth range, three were done at the middle depth range, and three were done at the lowest depth range. Specimen depth, $t_{50}$, internal friction angles, and effective consolidation stress for each specimen are given in Table 4.42. Every specimen at this site was loaded to a 15% axial strain without exhibiting any failure conditions. Very few rocks were found in the specimens after testing also.

**Table 4.42:** C-U Triaxial Compression Test Results for Site No. 3 (Lake County)

| Specimen (Depth) | $t_{50}$ (min) | $\phi$ (degrees) | $\phi'$ (degrees) | Effective Consolidation Pressure (psi) |
|---|---|---|---|---|
| A-1 (1.6' - 2.1') | 8.0 | 18.8 | 31.9 | 5.0 |
| A-1 (1.0' - 1.5') | 10.5 | 26.9 | 31.4 | 15.0 |
| D-1 (1.1' - 1.6') | 9.0 | 25.5 | 30.8 | 30.0 |
| A-2 (4.1' - 4.6') | 2.2 | 20.3 | 37.4 | 7.5 |
| D-2 (4.0' - 4.5') | 2.1 | 21.4 | 37.1 | 15.0 |
| D-2 (4.7' - 5.2') | 10.1 | 26.0 | 28.8 | 30.0 |
| C-3 (14.7’ - 15.2’) | 10.2 | 21.6 | 30.6 | 18.0 |
| A-3 (14.6' - 15.1') | 4.1 | 21.5 | 30.8 | 24.0 |
| D-3 (14.6' - 15.1') | 7.2 | 29.1 | 30.2 | 30.0 |

[Note] 1 ft = 0.3 m; and 1 psi = 6.895 kPa.

In addition, a variety of plots are in Appendix C related to the data just given. Figures C.30 through C.38 give stress-strain curves for each specimen, and Figures C.39 through C.44 give p'-q' and p-q plots for each depth range.

### 4.5.4 Shear Strength Properties for Site No. 4 (Athens County)

Five unconfined compression tests were performed on soil from this site by BBCM. One was done on a Shelby tube from the highest depth range, one was done from the middle depth range, and three were done at the lowest depth range. Table 4.43 summarizes the test results.

A total of nine C-U triaxial compression tests were conducted on the relatively undisturbed soil samples coming from this site. Three were done at each depth range. Specimen depth, $t_{50}$, $\phi$ angles, and effective consolidation stress for each specimen are given in Table 4.44. Eight of the nine specimens were tested to 15% axial strain without showing any signs of failure. Specimen B-3 (20.0 – 20.5 ft or 6.1 – 6.2 m depth) failed at 12.72% strain. A few small rocks and shale fragments were found after testing, but they were not large enough to affect the results. Also, it should be mentioned that two tests were done with soil from different tubes. The first specimen listed in Table 4.44 is given as A-1 (5.9 – 6.1 ft or 1.8 – 1.9 m) and B-1 (6.1 – 6.4 ft or 1.9 – 2.0 m). Here, because there was not enough soil in each of the tubes to make a specimen of proper height, two smaller sections were placed on top of each other. The same procedure was done with the specimen listed as B-2 (9.4 – 9.5 ft or 2.8 – 2.9 m) and D-2 (9.6 – 10.0 ft or 2.9 – 3.0 m). In addition, a variety of plots related to the data just given are in Appendix C. Figures C.45 through C.53 give stress-strain curves for each specimen, and Figures C.54 through

C.59 give p'-q' and p-q plots for each depth range.

**Table 4.43:** Unconfined Compression Strength Test Results for Site No. 4 (Athens County)

| Ave. Depth of Specimen (ft) | Moisture Content (%) | Dry Unit Weight (pcf) | Unconfined Comp. Strength (psi) | Strain at Failure (%) |
|---|---|---|---|---|
| 5.25 | 12.7 | 119.7 | 38.0 | 2.1 |
| 8.25 | 12.0 | 109.2 | 25.8 | 1.3 |
| 19.25 | 15.2 | 105.7 | 15.0 | 2.1 |
| 19.75 | 14.8 | 116.5 | 31.5 | 3.8 |
| 20.25 | 22.0 | 105.1 | 41.8 | 7.0 |

[Note] 1 ft = 0.3 m; and 1 psi = 6.895 kPa.

**Table 4.44:** C-U Triaxial Compression Test Results for Site No. 4 (Athens County)

| Specimen (Depth) | $t_{50}$ (min) | $\phi$ (degrees) | $\phi'$ (degrees) | Effective Consolidation Pressure (psi) |
|---|---|---|---|---|
| A-1 (5.9' – 6.1') & B-1 (6.1' – 6.4') | 6.0 | 23.2 | 34.8 | 7.5 |
| B-1 (5.5' - 6.0') | 7.4 | 24.3 | 34.8 | 15.0 |
| D-1 (5.9' – 6.4') | 7.5 | 23.9 | 33.9 | 30.0 |
| B-2 (8.8' - 9.3') | 3.2 | 25.9 | 34.1 | 15.0 |
| D-2 (9.0' - 9.5') | 4.0 | 19.1 | 33.7 | 22.5 |
| B-2 (9.4' – 9.5') & D-2 (9.6' – 10.0') | 2.9 | 22.2 | 31.4 | 30.0 |
| A-3 (20.0' - 20.5') | 50.0 | 17.6 | 27.4 | 22.0 |
| B-3 (20.0' - 20.5') | 25.0 | 15.0 | 25.4 | 30.0 |
| D-3 (20.0' - 20.5') | 53.0 | 18.8 | 27.6 | 40.0 |

### 4.5.5 Shear Strength Properties from Site No. 5 (Morrow County)

Four unconfined compression tests were performed on soil from this site by BBCM. Two were done on a Shelby tube from the highest depth range, one was done from the middle depth range, and one was done at the lowest depth range. Table 4.45 summarizes the test results.

**Table 4.45:** Unconfined Compression Strength Test Results for Site No. 5 (Morrow County)

| Ave. Depth of Specimen (ft) | Moisture Content (%) | Dry Unit Weight (pcf) | Unconfined Comp. Strength (psi) | Strain at Failure (%) |
|---|---|---|---|---|
| 10.25 | 14.0 | 118.2 | 20.3 | 8.4 |
| 10.75 | 11.4 | 128.2 | 47.8 | 8.2 |
| 13.25 | 14.8 | 111.4 | 19.1 | 9.1 |
| 17.75 | 16.0 | 110.0 | 20.8 | 9.4 |

[Note] 1 ft = 0.3 m; 1 pcf = 0.157 kN/m$^3$; and 1 psi = 6.895 kPa.

A total of nine C-U triaxial compression tests were performed on the Shelby tube soil samples taken from this site. Three were done at the top depth range, three were done at the middle depth range, and three were done at the lowest depth range. Specimen depth, $t_{50}$, and $\phi$ angles for each specimen are given in Table 4.46. All of the specimens were tested to 15% axial strain without reaching any failure conditions. There were also a few small rocks found in some of the samples, but they likely did not affect the final results. In addition, a variety of plots related to the data just given are in Appendix C. Figures C.60 through C.68 give stress-strain curves for each specimen, and Figures C.69 through C.74 give p'-q' and p-q plots for each depth range.

**Table 4.46:** C-U Triaxial Compression Test Results for Site No. 5 (Morrow County)

| Specimen (Depth) | $t_{50}$ (min) | $\phi$ (degrees) | $\phi'$ (degrees) | Effective Consolidation Pressure (psi) |
|---|---|---|---|---|
| B-1 (10.5' - 11.0') | 2.7 | 22.3 | 34.4 | 15.0 |
| C-1 (10.5' - 11.0') | 5.0 | 20.9 | 33.7 | 22.5 |
| D-1 (10.5' - 11.0') | 9.0 | 17.7 | 33.2 | 30.0 |
| D-2 (13.3' -13.8') | 5.1 | 25.4 | 33.8 | 15.0 |
| C-2 (13.8' - 14.3') | 5.3 | 25.1 | 32.7 | 22.5 |
| C-2 (13.3' - 13.7') | 4.0 | 21.1 | 32.7 | 30.0 |
| B-3 (17.9' - 18.4') | 6.8 | 23.1 | 34.1 | 20.0 |
| D-3 (18.2' - 18.6') | 3.1 | 20.0 | 36.9 | 30.0 |
| C-3 (17.6' - 18.1') | 4.7 | 15.1 | 31.8 | 35.0 |

[Note] 1 ft = 0.3 m; and 1 psi = 6.895 kPa.

### 4.5.6 Shear Strength Properties from Site No. 6 (Erie County)

Five unconfined compression tests were performed by BBCM on soil samples recovered from this site. Two were done on a Shelby tube from the highest depth range, two were done from the middle depth range, and one was done at the lowest depth range. Table 4.47 summarizes the test results.

A total of nine C-U triaxial compression tests were conducted on the Shelby tube samples recovered from this site. Three were done at the top depth range, three were done at the middle depth range, and three were done at the lowest depth range. Specimen depth, $t_{50}$, and $\phi$ angles for each specimen are given in Table 4.48. All of the specimens were tested to 15% axial strain without reaching any clear failure conditions. These soil specimens contained no gravel size particles and/or rock fragments.

In addition, a variety of plots related to the data just given are in Appendix C. Figures C.75 through C.84 give stress-strain curves for each specimen, and Figures C.85 through C.90 give p'-q' and p-q plots for each depth range.

**Table 4.47:** Unconfined Compression Strength Test Results for Site No. 6 (Erie County)

| Ave. Depth of Specimen (ft) | Moisture Content (%) | Dry Unit Weight (pcf) | Unconfined Comp. Strength (psi) | Strain at Failure (%) |
|---|---|---|---|---|
| 2.95 | 25.4 | 98.0 | 21.3 | 13.0 |
| 3.50 | 26.0 | 97.7 | 18.9 | 16.1 |
| 6.50 | 24.6 | 101.0 | 24.3 | 6.6 |
| 7.15 | 28.1 | 97.1 | 21.2 | 7.8 |
| 11.80 | 25.7 | 97.6 | 16.9 | 8.5 |

[Note] 1 ft = 0.3 m; 1 pcf = 0.157 kN/m$^3$; and 1 psi = 6.895 kPa.

**Table 4.48:** C-U Triaxial Compression Test Results for Site No. 6 (Erie County)

| Specimen (Depth) | $t_{50}$ (min) | $\phi$ (degrees) | $\phi'$ (degrees) | Effective Consolidation Pressure (psi) |
|---|---|---|---|---|
| B-1 (2.7' - 3.2') | 72.0 | 13.5 | 26.7 | 29.5 |
| B-1 (3.0' - 3.5') | 45.0 | 10.6 | 26.6 | 15.2 |
| D-1 (3.25' - 3.75') | 10.2 | 9.2 | 35.6 | 5.2 |
| D-2 (6.25' -6.75') | 20.0 | 10.9 | 25.6 | 20.0 |
| D-2 (6.8' - 7.3') | 75.0 | 9.2 | 28.1 | 10.2 |
| B-2 (6.9' - 7.4') | 110.0 | 11.7 | 25.5 | 29.9 |
| B-3 (11.55' - 12.05') | 23.0 | 12.9 | 26.6 | 15.0 |
| C-3 (11.55' - 12.05') | 30.0 | 12.8 | 27.2 | 22.3 |
| D-3 (12.9' - 13.4') | 79.0 | 12.1 | 26.9 | 27.2 |

[Note] 1 ft = 0.3 m; and 1 psi = 6.895 kPa.

### 4.5.7 Shear Strength Properties from Site No. 7 (Hancock County)

Five unconfined compression tests were performed by BBCM on soil samples recovered from this site. One was done on a Shelby tube from the highest depth range, three were done from the middle depth range, and one was done at the lowest depth range. Table 4.49 summarizes the test results. The first two specimens listed in the table did not exhibit any peak in the compressive stress when loaded to 20% axial strain.

**Table 4.49:** Unconfined Compression Strength Test Results for Site No. 7 (Hancock County)

| Ave. Depth of Specimen (ft) | Moisture Content (%) | Dry Unit Weight (pcf) | Unconfined Comp. Strength (psi) | Strain at Failure (%) |
|---|---|---|---|---|
| 6.55 | 20.0 | 110.1 | 24.6 | 20.0 |
| 10.95 | 21.4 | 107.2 | 39.4 | 20.0 |
| 10.95 | 21.6 | 105.1 | 34.4 | 8.3 |
| 11.05 | 20.1 | 108.8 | 35.9 | 11.9 |
| 17.45 | 18.5 | 111.3 | 61.2 | 10.2 |

[Note] 1 ft = 0.3 m; 1 pcf = 0.157 kN/m$^3$; and 1 psi = 6.895 kPa.

A total of eight C-U triaxial compression tests were performed on the Shelby tube soil samples obtained from this site. Three were done at the top depth range, two were

done at the middle depth range, and three were done at the lowest depth range. Specimen depth, $t_{50}$, and $\phi$ angles for each specimen are given in Table 4.50. All of the specimens were tested to 15% axial strain without reaching any clear failure conditions. These soil specimens contained no gravel size particles and/or rock fragments.

**Table 4.50:** C-U Triaxial Compression Test Results for Site No. 7 (Hancock County)

| Specimen (Depth) | $t_{50}$ (min) | $\phi$ (degrees) | $\phi'$ (degrees) | Effective Consolidation Pressure (psi) |
|---|---|---|---|---|
| D-1 (6.3' - 6.8') | 60.0 | 14.0 | 26.2 | 25.0 |
| C-1 (6.5' - 7.0') | 46.0 | 15.2 | 27.6 | 17.1 |
| A-1 (6.75' - 7.25') | 19.0 | 16.4 | 28.0 | 10.0 |
| A-2 (10.7' -11.2') | 40.0 | 14.7 | 28.2 | 11.9 |
| B-2 (10.7' - 11.2') | 36.0 | 12.5 | 26.5 | 18.9 |
| A-3 (17.2' - 17.7') | 9.0 | 20.0 | 29.1 | 15.1 |
| B-3 (17.2' - 17.7') | 9.3 | 20.7 | 30.2 | 22.3 |
| D-3 (17.4' - 17.9') | 10.0 | 20.7 | 28.3 | 31.3 |

[Note] 1 ft = 0.3 m; and 1 psi = 6.895 kPa.

In addition, a variety of plots related to the data just given are in Appendix C. Figures C.91 through C.99 give stress-strain curves for each specimen, and Figures C.100 through C.105 give p'-q' and p-q plots for each depth range.

### 4.5.8 Shear Strength Properties from Site No. 8 (Muskingum County)

Only three unconfined compression tests were performed by BBCM on soil samples recovered from this site. They were all done in the depth range where a cohesive soil layer was found. Table 4.51 summarizes the test results.

**Table 4.51:** Unconfined Compression Strength Test Results for Site No. 8 (Muskingum County)

| Ave. Depth of Specimen (ft) | Moisture Content (%) | Dry Unit Weight (pcf) | Unconfined Comp. Strength (psi) | Strain at Failure (%) |
|---|---|---|---|---|
| 9.50 | 14.9 | 119.1 | 30.3 | 11.2 |
| 9.75 | 15.9 | 117.2 | 48.9 | 10.9 |
| 10.25 | 13.9 | 121.4 | 28.0 | 8.1 |

[Note] 1 ft = 0.3 m; 1 pcf = 0.157 kN/m$^3$; and 1 psi = 6.895 kPa.

A total of five C-U triaxial compression tests were performed on the soils taken from this site. All five tests were done for the depth range, in which a cohesive soil layer was encountered in the field. Specimen depth, $t_{50}$, and $\phi$ angles for each specimen are given in Table 4.52. All of the specimens were tested to 15% axial strain without reaching any clear failure conditions. These soil specimens each contained a few small gravel size particles.

**Table 4.52:** C-U Triaxial Compression Test Results for Site No. 8 (Muskingum County)

| Specimen (Depth) | $t_{50}$ (min) | $\phi$ (degrees) | $\phi'$ (degrees) | Effective Consolidation Pressure (psi) |
|---|---|---|---|---|
| B-1 (9.5' - 10.0') | 9.0 | 19.0 | 34.7 | 15.2 |
| C-1 (9.5' - 10.5') | 4.0 | 24.1 | 36.4 | 20.2 |
| A-1 (10.0' -10.5') | 8.0 | 14.4 | 35.8 | 12.6 |
| B-1 (10.0' - 10.5') | 7.0 | 20.0 | 33.9 | 20.4 |
| C-1 (10.0' – 10.5') | 5.0 | 22.8 | 34.6 | 16.6 |

In addition, a variety of plots related to the data just given are in Appendix C. Figures C.106 through C.110 give stress-strain curves for each specimen, and Figures C.111 through C.114 give p'-q' and p-q plots for each depth range.

### 4.5.9 Shear Strength Properties from Site No. 9 (Noble County)

Five unconfined compression tests were performed by BBCM on soil samples recovered from this site. Two were done on a Shelby tube from the highest depth range, one was done from the middle depth range, and two were done at the lowest depth range. Table 4.53 summarizes the test results.

**Table 4.53:** Unconfined Compression Strength Test Results for Site No. 9 (Noble County)

| Ave. Depth of Specimen (ft) | Moisture Content (%) | Dry Unit Weight (pcf) | Unconfined Comp. Strength (psi) | Strain at Failure (%) |
|---|---|---|---|---|
| 4.25 | 14.0 | 124.5 | 20.2 | 2.5 |
| 4.75 | 15.2 | 117.3 | 18.4 | 3.0 |
| 7.25 | 13.5 | 123.2 | 21.2 | 1.5 |
| 10.25 | 12.5 | 123.8 | 20.8 | 3.0 |
| 10.50 | 12.5 | 126.8 | 30.3 | 2.6 |

[Note] 1 ft = 0.3 m; 1 pcf = 0.157 kN/m$^3$; and 1 psi = 6.895 kPa.

A total of nine C-U triaxial compression tests were performed on the soil samples recovered from this site. Three were done at the top depth range, three were done at the middle depth range, and three were done at the lowest depth range. Specimen depth, $t_{50}$, and $\phi$ angles for each specimen are given in Table 4.54. All of the specimens were tested to 15% axial strain without reaching any clear failure conditions. These soil specimens often contained a few small size rock fragments.

In addition, a variety of plots related to the data just given are in Appendix C. Figures C.115 through C.125 give stress-strain curves for each specimen, and Figures C.126 through C.131 give p'-q' and p-q plots for each depth range.

**Table 4.54:** C-U Triaxial Compression Test Results for Site No. 9 (Noble County)

| Specimen (Depth) | $t_{50}$ (min) | $\phi$ (degrees) | $\phi'$ (degrees) | Effective Consolidation Pressure (psi) |
|---|---|---|---|---|
| B-1 (6.3' - 6.8') | 3.0 | 12.0 | 33.6 | 12.0 |
| C-1 (6.5' - 7.0') | 20.0 | 13.3 | 30.6 | 20.0 |
| B-1 (6.75' - 7.25') | 10.0 | 13.8 | 31.0 | 25.3 |
| A-2 (10.7' -11.2') | 2.0 | 15.2 | 33.2 | 12.7 |
| D-2 (10.7' - 11.2') | 4.5 | 14.5 | 31.9 | 19.9 |
| E-1 (10.8' - 11.3') | 17.0 | 13.3 | 29.6 | 25.5 |
| B-3 (17.2' - 17.7') | 4.3 | 9.6 | 31.4 | 12.9 |
| C-3 (17.2' - 17.7') | 3.5 | 14.7 | 32.1 | 20.2 |
| D-3 (17.4' - 17.9') | 3.0 | 14.3 | 32.7 | 25.2 |

[Note] 1 ft = 0.3 m; and 1 psi = 6.895 kPa.

## 4.6 Shear Strength Parameters for Different Soil Types

In the previous section, total-stress and effective-stress angles of internal friction were determined for each soil specimen. Now they can be combined to address shear strength properties for each soil type. Also, the C-U triaxial test data was revisited to determine short-term (undrained) and long-term (drained) cohesion properties.

**Table 4.55:** Effective-Stress Friction Angle for Each Soil Type Encountered

| Soil Type | Drained (or Long-Term) Angle of Internal Friction $\phi'$ (degrees) | | | | | | |
|---|---|---|---|---|---|---|---|
| | Value 1 | Value 2 | Value 3 | Value 4 | Value 5 | Value 6 | Value 7 |
| A-4a | 34.7 | 34.8 | 33.6 | 33.5 | 34.2 | 37.4 | 37.1 |
| A-4b | 34.7 | 36.4 | --- | --- | --- | --- | --- |
| A-6a | 37.8 | 32.9 | 30.5 | 36.8 | 31.9 | 31.4 | 30.8 |
| A-6b | 29.1 | 30.2 | 28.3 | 33.6 | 30.6 | 24.4 | 31.0 |
| A-7-6 | 30.8 | 28.0 | 25.3 | 29.2 | 27.9 | 24.5 | 26.4 |

| Soil Type | Drained (or Long-Term) Angle of Internal Friction $\phi'$ (degrees) | | | | | | |
|---|---|---|---|---|---|---|---|
| | Value 8 | Value 9 | Value 10 | Value 11 | Value 12 | Value 13 | Value 14 |
| A-4a | 28.8 | 30.6 | 30.8 | 30.2 | 33.8 | 32.7 | 34.1 |
| A-6a | 34.8 | 33.9 | 34.1 | 33.7 | 31.4 | 34.4 | 33.7 |
| A-6b | 33.2 | 31.9 | 29.6 | --- | --- | --- | --- |
| A-7-6 | 26.8 | 27.4 | 25.4 | 27.6 | 26.8 | 26.7 | 26.6 |

| Soil Type | Drained (or Long-Term) Angle of Internal Friction $\phi'$ (degrees) | | | | | | |
|---|---|---|---|---|---|---|---|
| | Value 15 | Value 16 | Value 17 | Value 18 | Value 19 | Value 20 | Value 21 |
| A-4a | 36.9 | 31.8 | --- | --- | --- | --- | --- |
| A-6a | 33.2 | 35.8 | 33.9 | 34.6 | 31.4 | 32.1 | 32.7 |
| A-7-6 | 35.6 | 25.6 | 28.1 | 25.5 | 26.6 | 27.2 | 26.9 |

| Soil Type | Drained (or Long-Term) Angle of Internal Friction $\phi'$ (degrees) | | | | | | |
|---|---|---|---|---|---|---|---|
| | Value 22 | Value 23 | Value 24 | Value 25 | Value 26 | Range | Average |
| A-4a | --- | --- | --- | --- | --- | 28.8-37.4 | 33.4 |
| A-4b | --- | --- | --- | --- | --- | 34.7-36.4 | 35.6 |
| A-6a | --- | --- | --- | --- | --- | 30.5-37.8 | 33.4 |
| A-6b | --- | --- | --- | --- | --- | 24.4-33.6 | 30.2 |
| A-7-6 | 26.2 | 27.6 | 28.0 | 28.2 | 26.5 | 24.5-35.6 | 27.4 |

**Table 4.56:** Undrained (or Short-Term) Cohesions Based on C-U Test Results

| Soil Type | Undrained (or Short-Term) Cohesion (psi) | | | | | | |
|---|---|---|---|---|---|---|---|
| | Value 1 | Value 2 | Value 3 | Value 4 | Value 5 | Value 6 | Average |
| A-4a | 14.63 | 4.82 | 12.80 | 15.99 | --- | --- | 12.06 |
| A-6a | 12.48 | 7.09 | 12.48 | 11.90 | 15.42 | --- | 11.87 |
| A-6b | 9.53 | 4.39 | 12.73 | --- | --- | --- | 8.88 |
| A-7-6 | 5.37 | 9.19 | 1.58 | 2.60 | 2.86 | 13.03 | 5.77 |

[Note] 1 psi = 6.895 kPa.

**Table 4.57:** Undrained (or Short-Term) Cohesions Based on UC Test Results

| Soil Type | Undrained (or Short-Term) Cohesion $c_u$ (psi) | | | | | | |
|---|---|---|---|---|---|---|---|
| | Value 1 | Value 2 | Value 3 | Value 4 | Value 5 | Value 6 | Value 7 |
| A-4a | 20.50 | 22.55 | 39.50 | 35.65 | 15.10 | 23.05 | 9.55 |
| A-4b | 15.15 | 24.45 | --- | --- | --- | --- | --- |
| A-6a | 18.30 | 28.65 | 19.00 | 12.90 | 23.90 | 14.00 | 10.40 |
| A-6b | 17.95 | 30.60 | 10.10 | 9.20 | 10.60 | --- | --- |
| A-7-6 | 12.40 | 15.30 | 12.40 | 9.35 | 23.45 | 20.90 | 10.65 |

| Soil Type | Undrained (or Short-Term) Cohesion $c_u$ (psi) | | | | | | |
|---|---|---|---|---|---|---|---|
| | Value 8 | Value 9 | Value 10 | Value 11 | Value 12 | Value 13 | Average |
| A-4a | 10.40 | --- | --- | --- | --- | --- | 22.04 |
| A-4b | --- | --- | --- | --- | --- | --- | 19.80 |
| A-6a | 15.15 | --- | --- | --- | --- | --- | 17.79 |
| A-6b | --- | --- | --- | --- | --- | --- | 15.69 |
| A-7-6 | 9.45 | 12.15 | 10.60 | 8.45 | 12.30 | 19.70 | 13.62 |

**Table 4.58:** Drained (or Long-Term) Cohesions Based on C-U Triaxial Test Results

| Soil Type | Long-Term Cohesion c′ (psi) | | | | | |
|---|---|---|---|---|---|---|
| | Value 1 | Value 2 | Value 3 | Value 4 | Value 5 | Average |
| A-4a | 6.05 | 8.20 | 1.03 | 4.41 | --- | 4.92 |
| A-6a | 6.15 | 0.89 | 1.80 | 4.82 | --- | 3.42 |
| A-6b | 2.97 | 1.98 | 8.66 | --- | --- | 4.54 |
| A-7-6 | 2.76 | 4.65 | 1.35 | 1.25 | 6.45 | 3.29 |

[Note] 1 psi = 6.895 kPa.

# CHAPTER 5: EVALUATION OF EMPIRICAL CORRELATIONS, STATISTICAL ANALYSIS, AND GEOTECHNICAL GUIDELINES

This chapter first evaluates the empirical correlations presented in Chapter 2 in light of the data collected in the current study. Then, meaningful correlations between the different soil properties are sought using various linear and nonlinear mathematical models and multi-variable regression analysis method. Appendix E present statistically strong correlation plots for shear strength properties of Ohio cohesive soils. In addition, differences between soil type subsets or regions in Ohio are assessed using a T-test technique. Based on the outcome of these data analyses, preliminary guidelines are recommended for estimating shear strength properties of embankment soils encountered in Ohio.

## 5.1 Evaluations of Empirical Correlations

### 5.1.1 SPT-N vs. Unconfined Compression Strength by Terzaghi

The first empirical correlation to be evaluated is the one between the fully corrected SPT-N value and unconfined compression strength proposed by Terzaghi (1996). This correlation was previously presented in Table 2.2. In Table 5.1, the unconfined compressive strengths of A-4 soils measured for four sites (FAY-35, LAK-2, MRW-71, and MUS-70) are entered into the chart prepared by Terzaghi, along with the corresponding $(N_{60})_1$ values. All of the unconfined compression strength data obtained for Site 2 (FAY-35) and Site 5 (MRW-71) reside outside the range reported by Terzaghi. In contrast, all of the strength measurements from Site 3 (LAK-2) and Site 8 (MUS-70) conform to the ranges cited by Terzaghi. Overall, slightly more than half (54.5%) of the data points reside within the range given by Terzaghi.

**Table 5.1:** Evaluation of Terzaghi's Correlation for A-4 Soils

| SPT $(N_{60})_1$ | Unconfined Compressive Strength (psi) | | |
|---|---|---|---|
| | Terzaghi | Values Within Range | Values Outside Range |
| < 2 | < 3.6 | --- | --- |
| 2 - 4 | 3.6-7.3 | --- | --- |
| 4 – 8 | 7.3 – 14.5 | --- | --- |
| 8 – 15 | 14.5 – 29 | 20.3 | 45.1 |
| 15 – 30 | 29 – 58 | 30.2, 30.3, 46.1, 48.9 | 19.1 |
| > 30 | > 58 | 71.3, 79.0 | 20.8, 25.2, 41.0 |

[Note] 1 psi = 6.895 kPa.

Next, the unconfined compression strengths of A-6 soils are compared to Terzaghi's empirical SPT-$(N_{60})_1$ vs. unconfined compression strength relation for seven sites (FAY-35, LAK-2, ATH-33, MRW-71, HAN-75, MUS-70, and NOB-77), as shown in Table 5.2. All the measured values for Site 2 (FAY-35), Site 3 (LAK-2), Site 4 (ATH-33), and Site 5 (MRW-71) are falling out of Terzaghi's range. In contrast, all of the strength measurements from Site 7 (HAN-75) and Site 8 (MUS-70) conform to the ranges cited by Terzaghi. Only one of the five measured unconfined compression strength values are staying within the range reported by Terzaghi for A-6 soils recovered from Site 9 (NOB-77). Overall, only about a quarter (28.6%) of the data points reside within the range given by Terzaghi.

**Table 5.2:** Evaluation of Terzaghi's Correlation for A-6 Soils

| SPT $(N_{60})_1$ | Unconfined Compressive Strength (psi) | | |
|---|---|---|---|
| | Terzaghi | Values Within Range | Values Outside Range |
| < 2 | < 3.6 | --- | --- |
| 2 - 4 | 3.6-7.3 | --- | --- |
| 4 – 8 | 7.3 – 14.5 | --- | --- |
| 8 – 15 | 14.5 – 29 | --- | 47.8 |
| 15 – 30 | 29 – 58 | 28.0, 30.3, 35.9 | 18.4, 20.8, 21.2, 25.8, 61.2 |
| > 30 | > 58 | 61.2 | 20.2, 36.6, 38.0, 57.3 |

Finally, the unconfined compression strengths of A-7-6 soil samples encountered at four sites (HAM-75, ATH-33, ERI-2, and HAN-75) are applied to the empirical correlation of Terzaghi, as seen in Table 5.3. Only one of the four measured unconfined compression test values are staying within the range reported by Terzaghi for A-7-6 soils recovered from Site 1 (HAM-75). The value of 41.8 psi (288 kPa) coming from the Site 4 (ATH-33) is conforming to the Terzaghi's guideline. On the contrary, five of the six measurements obtained for Site 6 (ERI-2) are within the Terzaghi's range. None of the data from Site 7 (HAN-75) is falling within the range reported by Terzaghi. It is noted here that unconfined compression strengths of all of the data points are falling within the range specified by Terzaghi for cases where the SPT $(N_{60})_1$ value ranges between 8 and 15. It is also noted that unconfined compression strength of every data point is outside the range specified by Terzaghi for cases where the SPT $(N_{60})_1$ value is above 30. Overall, about half (53.8%) of the data points reside within the range given by Terzaghi.

**Table 5.3:** Evaluation of Terzaghi's Data for A-7-6 Soils

| SPT $(N_{60})_1$ | Unconfined Compressive Strength (psi) | | |
|---|---|---|---|
| | Terzaghi | Values Within Range | Values Outside Range |
| < 2 | < 3.6 | --- | --- |
| 2 - 4 | 3.6-7.3 | --- | --- |
| 4 – 8 | 7.3 – 14.5 | --- | --- |
| 8 – 15 | 14.5 – 29 | 18.9, 21.2, 21.3, 24.3 | --- |
| 15 – 30 | 29 – 58 | 30.6, 39.4, 41.8 | 16.9, 18.7, 24.8 |
| > 30 | > 58 | --- | 24.6, 39.4, 46.9 |

[Note] 1 psi = 6.895 kPa.

The results presented in Tables 5.1 through 5.3 indicate that the empirical correlation between the SPT-$(N_{60})_1$ and unconfined compression strength published by Terzaghi is not well suited to the highway embankment soils encountered in Ohio.

### 5.1.2 SPT-N vs. Unconfined Compression by Dept. of Navy

The next correlation to be assessed is also concerned with the link between the SPT-$(N_{60})_1$ and the unconfined compression strength. It was presented by the Dept. of Navy (1982), as summarized in Table 2.3. The correlation here involves the lower and upper bounds, depending on the value of liquid limit. The lower bound is given by the values in Table 2.3 listed as 'low plasticity'. The upper bound is given by the values in Table 2.3 listed as 'high plasticity'. The actual unconfined compression strengths measured during the current study can be plotted into the correlation chart. Figure 5.1 shows this for all three soil types (A-4, A-6, and A-7-6).

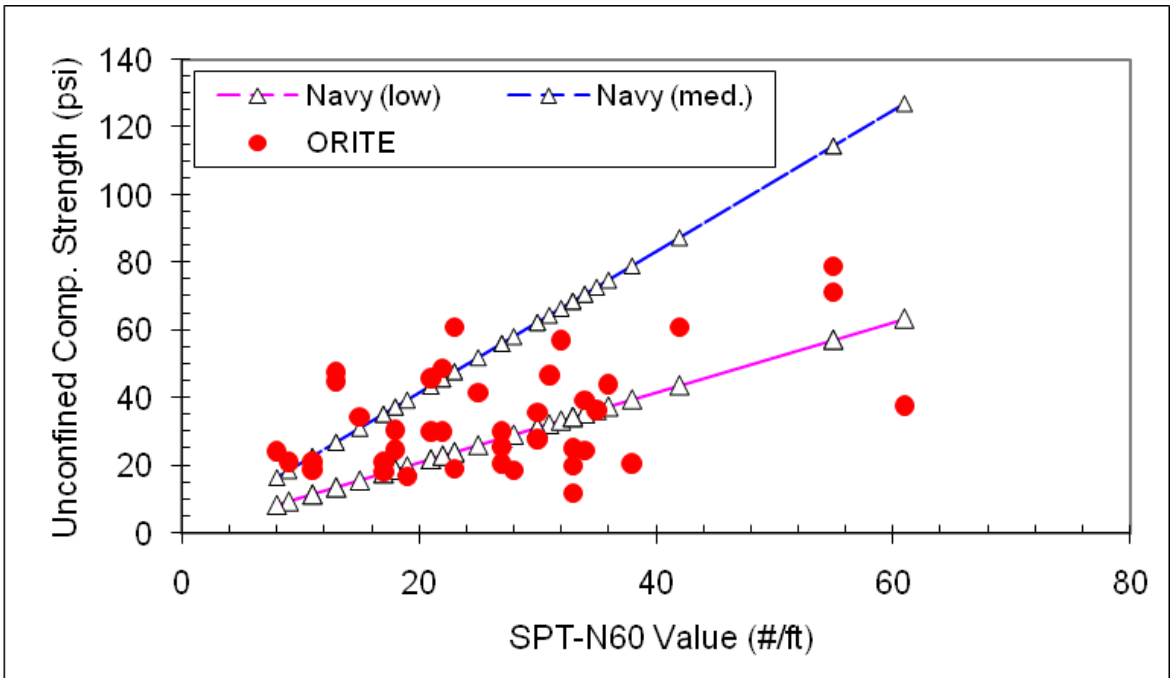


**Figure 5.1:** Evaluation of Dept. of Navy $q_u$ vs. SPT-$(N_{60})_1$ Plot for All Soil Types
[Note] 1 psi = 6.895 kPa.

A total of thirty-eight data points are shown in Figure 5.1. Nineteen of these points fall in the zone between the upper and lower bound curves given by the Dept. of

Navy (1982). This means that exactly half (50.0%) of the measured SPT and unconfined compression data for all three major Ohio soil types follow the empirical correlations reported by the Dept. of Navy. Among the nineteen data points located outside the range specified by the Dept. of Navy, ten data points (about 52.6%) reside below the lower bound curve and nine data points (47.4%) reside above the upper bound curve.

To evaluate the Navy's empirical correlation further, the data compiled for each major soil type are entered into the correlation chart. Figure 5.2 shows a plot of unconfined compressive strength against $(N_{60})_1$ for A-4 soil samples. There are ten data points shown in the plot. Five (50.0%) of these points are located between the lower and upper bound curves. Out of the remaining five data points, two (40.0%) of them are found below the lower bound curve and three (60.0%) are above the upper bound curve.

Figure 5.3 shows a similar plot of unconfined compressive strength against $(N_{60})_1$ for A-6 soils analyzed in the current study. The figure contains a total of fourteen data points. Out of these data points, seven (50.0%) are located inside the zone specified by the Dept. of Navy. Among the remaining half of the data points, five (71.4%) are seen below the lower bound curve and two (28.6%) reside above the upper bound curve. Figure 5.3 includes eight data points of A-6a soils and six data points of A-6b soils. In case of A-6a soils, three (37.5%) data points fall within the zone specified by the Dept. of Navy. Out of the five data points located outside the zone, four (80.0%) are found below the lower bound curve and only one point (20.0%) exists above the upper bound curve. In case of A-6b soils, four (66.7%) data points fall within the zone specified by the Dept. of Navy. Out of the two data points located outside the zone, one point (50.0%) is found below the lower bound curve and one point (50.0%) exists above the upper bound curve.

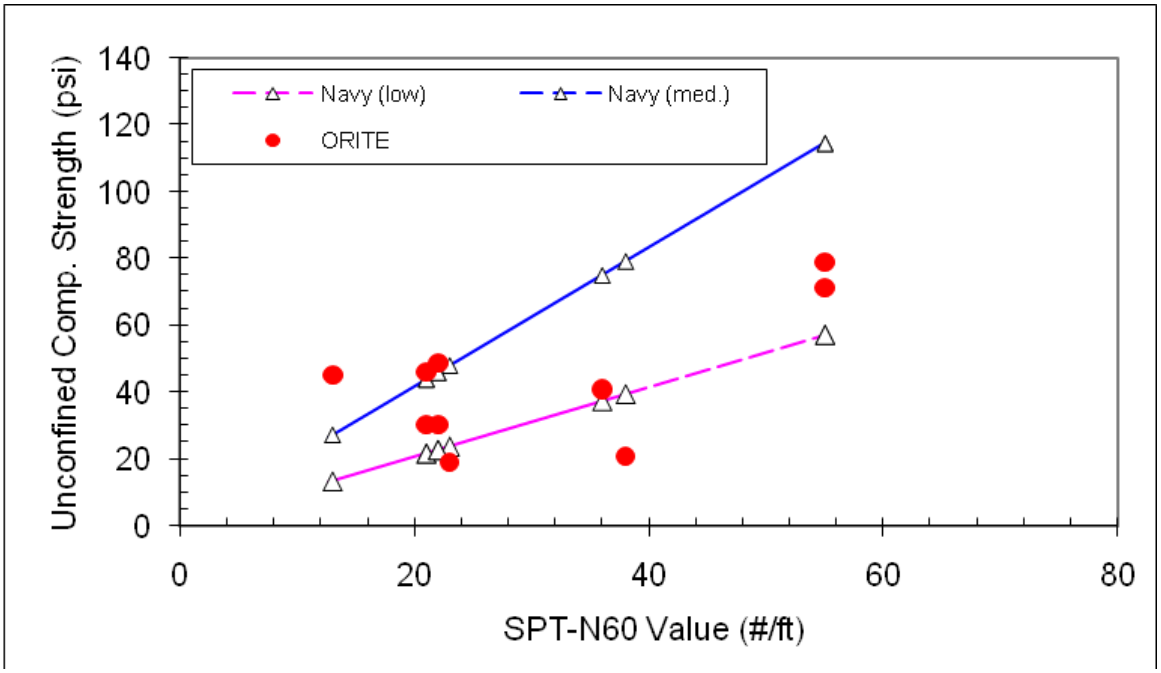


**Figure 5.2:** Evaluation of Dept. of Navy Correlation Plot for A-4 Soils

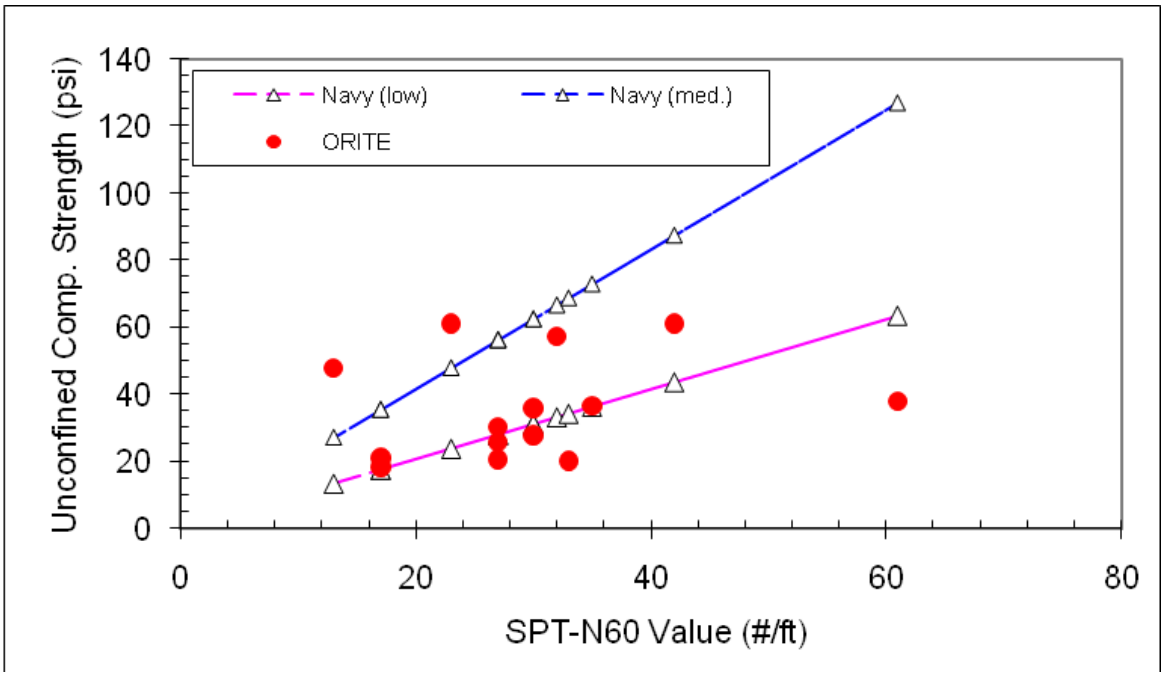


**Figure 5.3:** Evaluation of Dept. of Navy (1982) Data for A-6 Soils

[Note] 1 psi = 6.895 kPa.

Finally, in Figure 5.4, the unconfined compression strength vs. SPT-$(N_{60})_1$ data compiled for A-7-6 soils is compared with the empirical correlations established by the Dept. of Navy (1982). A total of fourteen data exists in the plot. Seven (50.0%) of the data points in Figure 5.4 are staying within the bounds given by the Dept. of Navy. Among the remaining seven data points, three (42.9%) are located below the lower bound curve and four data points are (57.1%) are found above the upper bound curve.

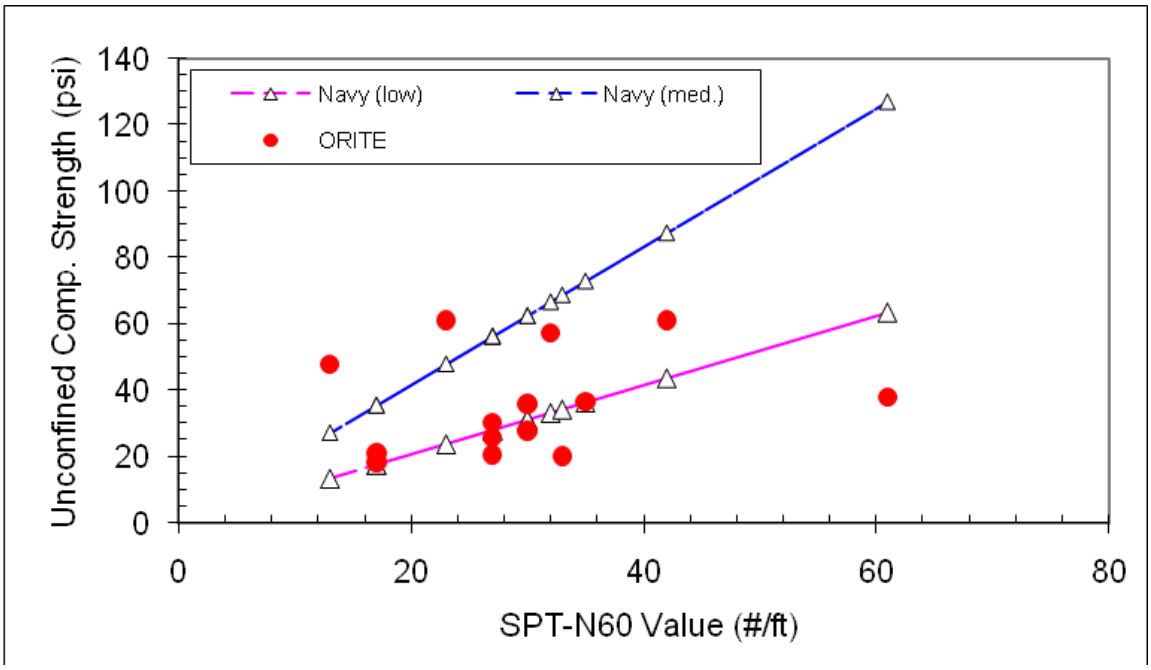


**Figure 5.4:** Evaluation of Dept. of Navy (1982) Data for A-7-6 Soils

[Note] 1 psi = 6.895 kPa.

In summary, although the amount of data may be still somewhat lacking, the results presented above indicate that the empirical SPT-$(N_{60})_1$ vs. unconfined compression strength correlation reported by the Dept. of Navy (1982) is reliable only in 50% of the cases involving the cohesive soils found in Ohio.

### 5.1.3 Effective Friction Angle vs. Plasticity Index by Terzaghi

The third empirical correlation to be tested here is the one between the effective friction angle and the plasticity index. This was established previously by Terzaghi, as shown in Table 2.4 and Figure 2.9. All of the data produced in the current study are added to Figure 2.9 to see how well engineering properties of the Ohio embankment soils obey to the Terzaghi's empirical relationship. This is shown in Figure 5.5 for all three major soil types (A-4, A-6, and A-7-6) encountered in the study.

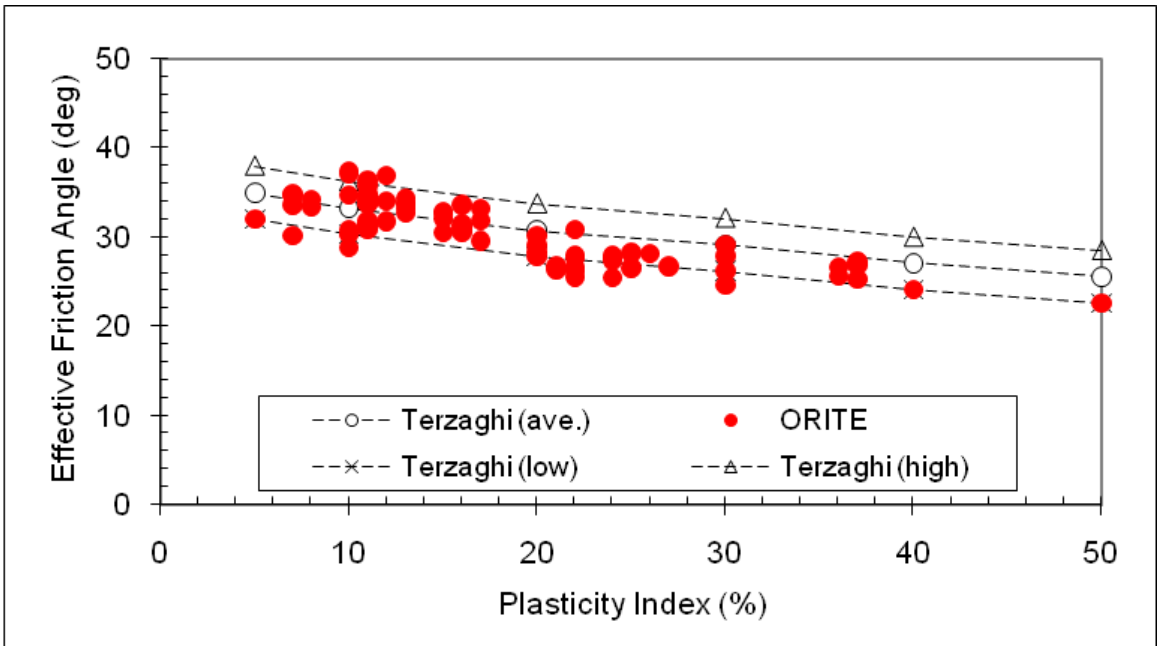


**Figure 5.5:** Comparison of Terzaghi & ORITE Data (All Soil Types)

Figure 5.5 contain a total of seventy three data points. Looking at the results summarized in Figure 5.5, it is noted that fifty six (76.7%) of the data points produced in this study land inside the correlation band reported by Terzaghi. This means that seventeen data points (23.3%) are falling outside the band. The correlation band is 6°

deep, with the upper bound and lower bound curves located at $\pm$ 3° of the central curve. Most of the data points located outside the band seem to be positioned within $\pm$ 5° of the central curve. Out of the points falling outside the range, five data points (29.4%) exist above the upper bound curve and fourteen (70.6%) are located below the lower bound curve.

Statistically speaking, the standard deviation between the measured $\phi'$ values and the Terzaghi's average $\phi'$ values is 2.51. More than half (63.5%) of the measured values reside within the Terzaghi's average value $\pm$ 1$\sigma$ (standard deviation). Most (96.0%) of the measured values reside within the Terzaghi's average value $\pm$ 2$\sigma$ (standard deviation).

The results shown in Figure 5.5 can be also broken down further into each major soil type to examine which soil type conform to the Terzaghi's $\phi'$-PI correlation more closely than others. Figure 5.6 shows such a plot for the A-4 soil samples tested in the current study. The A-4 soil data points crowd the upper left portion of the plot, where the plasticity index values range from 7 to 13. Out of nineteen data points appearing in the plot, thirteen (68.4%) are landing inside the correlation band set by Terzaghi. This means that six data points (31.6%) did not conform to the Terzaghi's correlation pattern. Out of these outliers, three (50.0%) reside above the upper bound curve and three are below the lower bound curve.

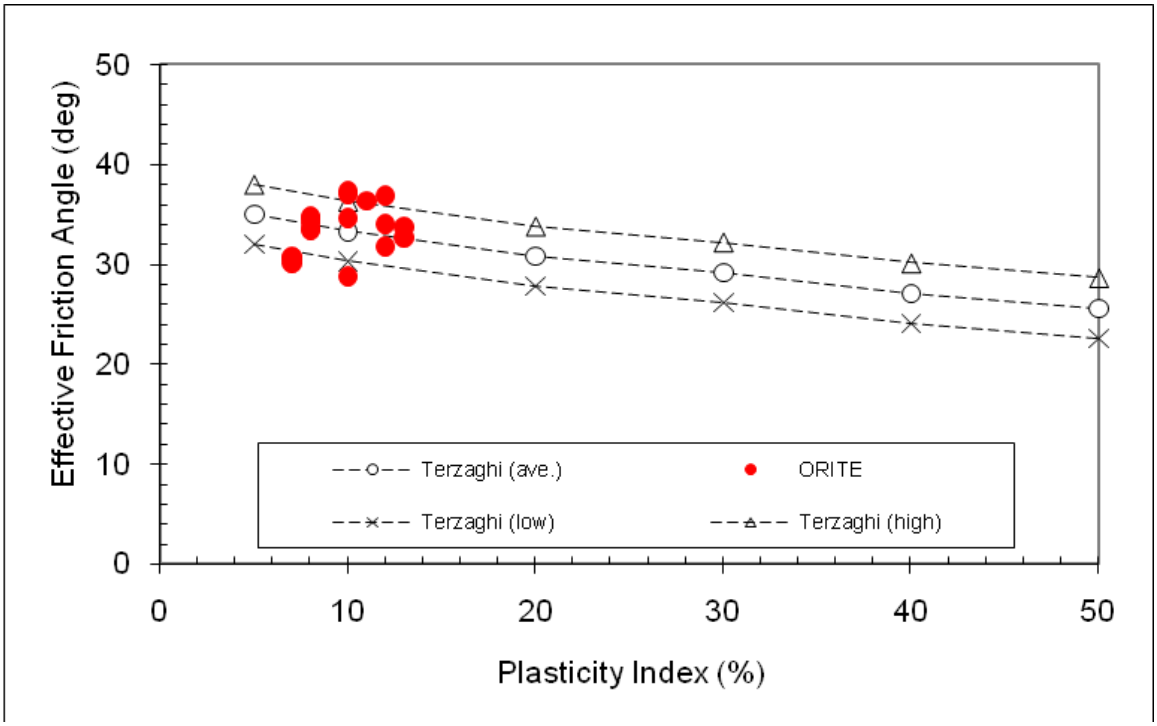


**Figure 5.6:** Comparison of Terzaghi & ORITE Data (A-4 Soils)

In Figure 5.7 the measured properties of the A-6a soil samples are plotted in terms of the effective friction angle against the plasticity index. The figure has a total of twenty two data points. Out of these data points, twenty data points (90.9%) are falling inside the band. The remaining two data points, which are located outside the band, are both found above the upper bound curve. None are seen below the lower bound curve. Figure 5.8 present a similar graphical plot for the A-6b soils tested in the current study. Here, there are nine data points involved. Out of these, none ended up outside the band.

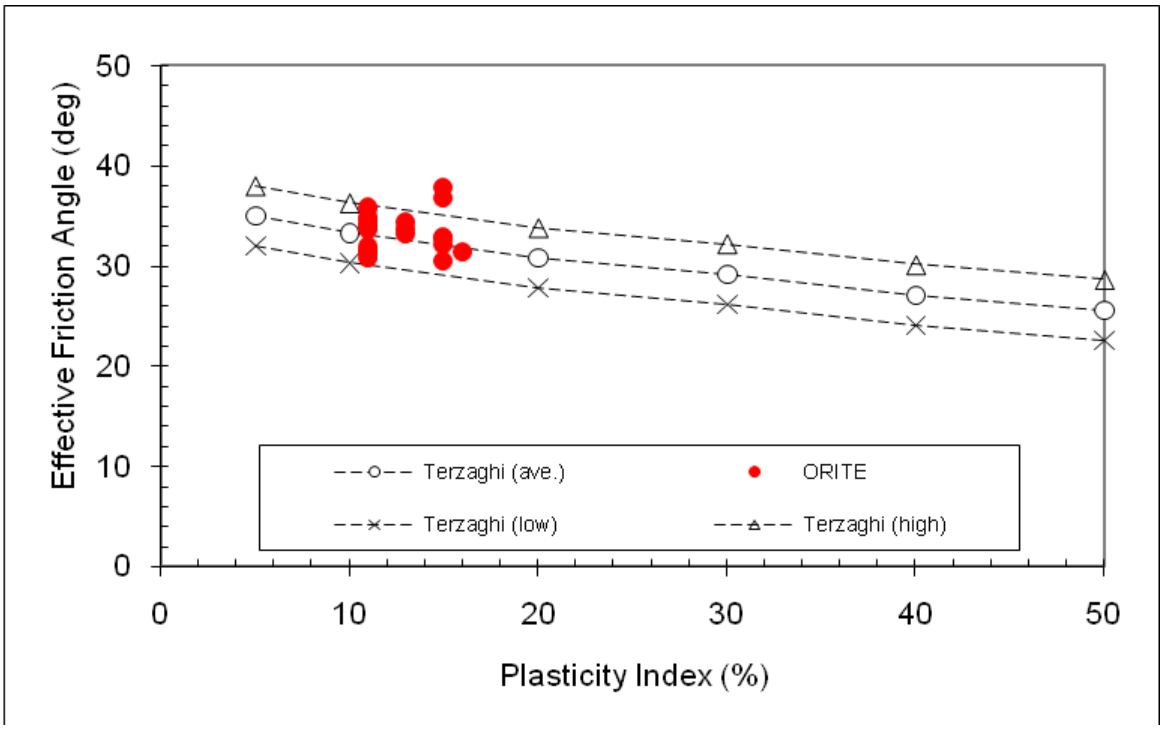


**Figure 5.7:** Comparison of Terzaghi & ORITE Data (A-6a Soils)

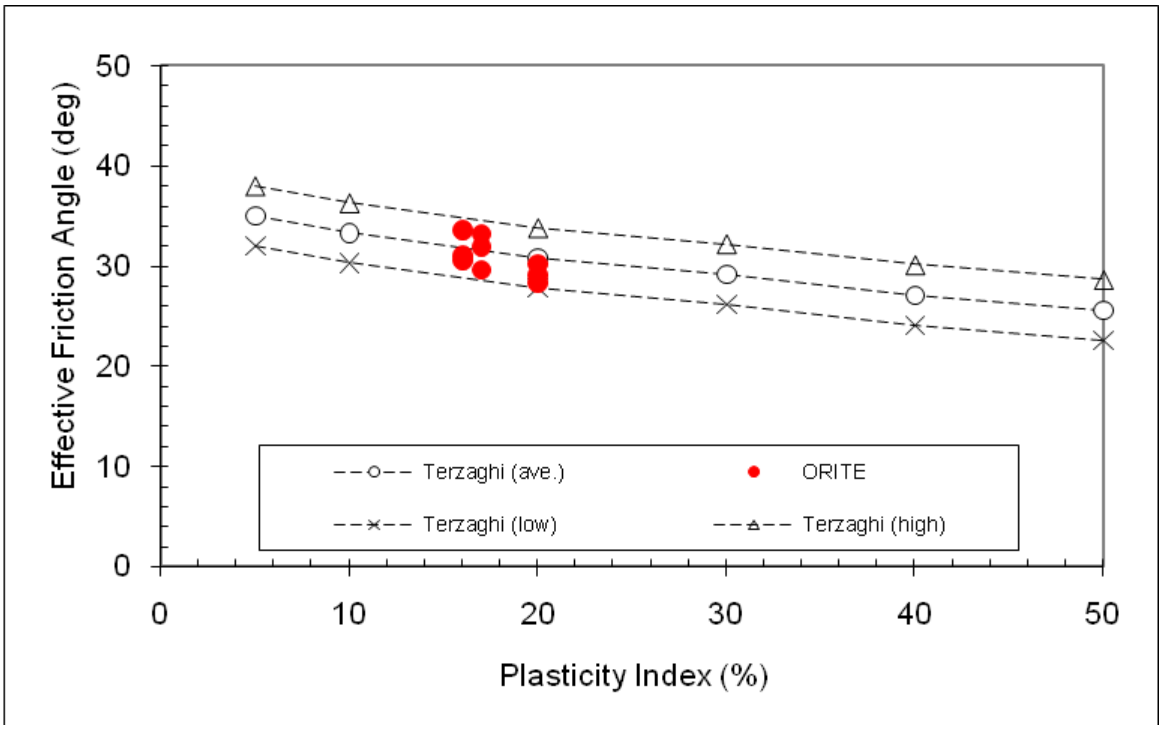


**Figure 5.8:** Comparison of Terzaghi & ORITE Data (A-6b Soils)

Finally, in Figure 5.9, the measured properties of the A-7-6 soil samples are plotted over the Terzaghi's empirical correlation chart. Here, a total of twenty three data points are presented graphically. Out of these cases, fourteen (60.9%) are landing inside the band reported by Terzaghi. Most of the outside data points are within 5° below the central curve. None of the outside points are detected near the upper bound curve.

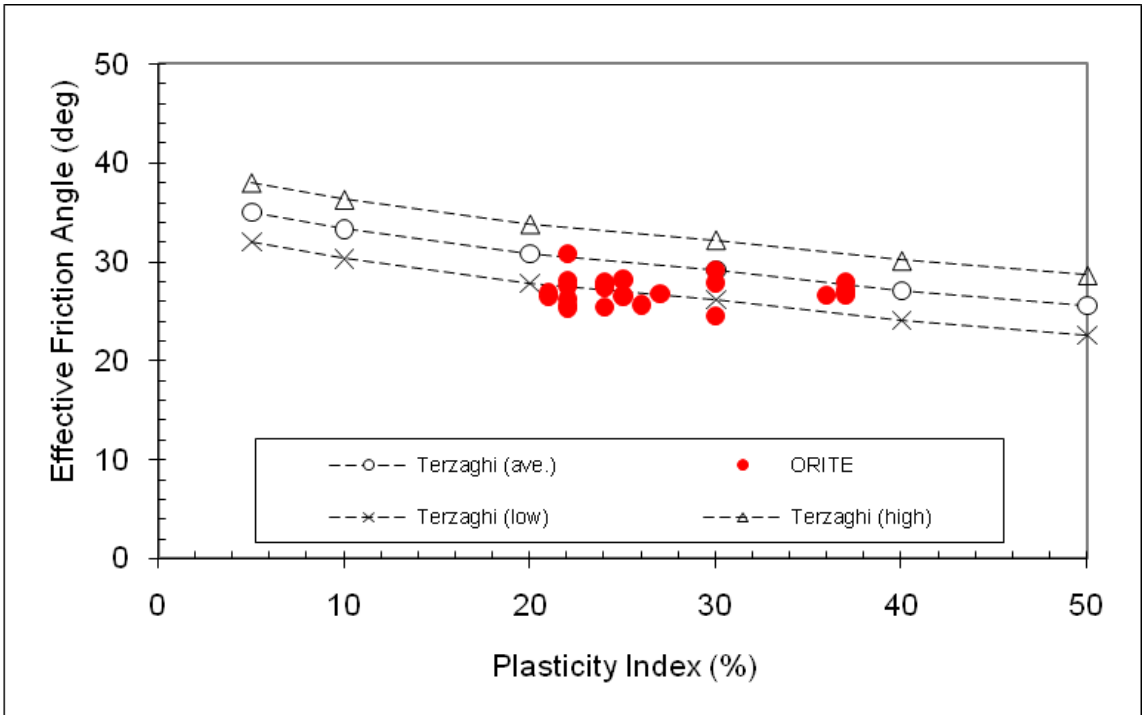


**Figure 5.9:** Comparison of Terzaghi & ORITE Data (A-7-6 Soils)

In summary, it can be stated that the empirical $\phi'$-PI correlation established by Terzaghi appear to be fairly reliable for most of the cohesive soils encountered in the current study. This statement is especially true for A-4 and A-6 soils. In case of A-7-6 soils found in Ohio, the actual $\phi'$-PI correlation tends to center about the lower bound curve set by Terzaghi.

### 5.1.4 Soil Type vs. Effective Friction Angle by Dept. of Navy

The last empirical correlation that can be evaluated here involves the soil type and effective friction angle, as reported by Dept. of Navy (1982). This correlation is shown in Table 5.4, along with the range and average effective angle of internal friction determined for each major soil type in the current study.

**Table 5.4:** Comparison of Dept. of Navy and ORITE Data

| Soil Type | $\phi'$ (degrees) – Dept. of Navy (1982) | $\phi'$ (degrees) – ORITE Value |
|---|---|---|
| A-4 | 32 | Range 28.8-37.4 (Ave. 33.6) |
| A-6 | 28 | Range 28.3-37.8 (Ave. 32.7) |
| A-7-6 | Range 19-28 (Ave. 25) | Range 24.5-35.6 (Ave. 27.4) |

According to this table, the average measured $\phi'$ value and the Dept. of Navy (1982) $\phi'$ value are fairly close to each other for A-4 soil. For A-6 soils, the average measured $\phi'$ value is higher than the $\phi'$ value listed by the Dept. of Navy. For A-7-6 soil, the average measured $\phi'$ value is slightly below the upper bound of the range reported by the Dept. of Navy.

## 5.2 Single-Variable Linear Regression Analysis

In Section 3.5, it was stated that many mathematical models (such as linear, 2$^{nd}$ degree polynomial, logarithmic, power, exponential, hyperbolic, and reciprocal) would be applied to the data set to identify the best model and strongest correlations that appear to exist for the shear strength characteristics of major highway embankment soils found in Ohio.

Single-variable linear regression analysis was performed for the soils tested. As

mentioned in Chapter 3, six paths of correlations were formulated. These paths were illustrated in Figure 3.5. They are described again in Table 5.5.

The following equation was applied in all of the linear regression analyses:

$$y = mx + b \tag{5.1}$$

**Table 5.5:** Correlation Paths for Single-Variable Data Analysis

| Path | Dependent Variable vs. Independent Variable |
|---|---|
| 1 | Corrected SPT-N Values vs. Laboratory Soil Index Properties |
| 2 | Laboratory Triaxial Test Results vs. Laboratory Soil Index Properties |
| 3 | Unconfined Compressive Strength vs. Laboratory Triaxial Test Results |
| 4 | Corrected SPT-N Values vs. Unconfined Compressive Strength |
| 5 | Unconfined Compressive Strength vs. Laboratory Soil Index Properties |
| 6 | Corrected SPT-N Values vs. Laboratory Triaxial Test Results |

With all the variables involved and the mathematical functions enlisted, the analysis along the six paths illustrated in Figure 3.5 created more than one hundred cases for each soil type. Among the variables, both the natural moisture content and % compaction were ties to the unconfined compression (UC) tests conducted in the project. There are two versions of the dry unit weight (one measured for the unconfined compression test and another measured during the C-U triaxial test). % compaction was computed for each UC test specimen using the maximum dry unit values listed previously in Section 2.1.5. Units used for some of the variables include psi for the unconfined compression strength ($q_u$), degrees for friction angle ($\phi$) and effective-stress friction angle ($\phi'$), psi for cohesion ($c_u$) and effective-stress cohesion ($c'$), pcf for dry unit weight ($\gamma_d$), and minutes for 50% consolidation time ($t_{50}$). Throughout this chapter, the correlations will be listed with the strongest one at the top of the table and getting weaker

as they go down. Any correlation with the coefficient of determination ($R^2$) value equal to 0.8 or above will be viewed as a statistically strong (meaningful) correlation.

### 5.2.1 A-4a Soils

Table 5.6 summarizes the results of the linear regression analysis performed for SPT-$(N_1)_{60}$ measured in A-4a soils. None of the correlations listed in the table yielded the $R^2$ value higher than 0.80.

**Table 5.6:** Single-Variable Linear Correlations for SPT-$(N_{60})_1$ of A-4a Soils

| Dependent Variable y | Independent Variable x | $R^2$ | Equation |
|---|---|---|---|
| SPT-$(N_{60})_1$ | Unconf. Compr. Strength ($q_u$) | 0.354 | y = 0.402x + 16.24 |
| SPT-$(N_{60})_1$ | % Clay | 0.201 | y = 2.000x – 25.00 |
| SPT-$(N_{60})_1$ | Plastic Limit (PL) | 0.125 | y = 2.109x – 2.547 |
| SPT-$(N_{60})_1$ | Effective Friction Angle ($\phi'$) | 0.116 | y = 1.918x – 31.98 |
| SPT-$(N_{60})_1$ | Liquid Limit (LL) | 0.112 | y = 1.196x + 0.728 |
| SPT-$(N_{60})_1$ | Final Moisture Content (C-U Test) | 0.091 | y = 1.211x + 15.13 |
| SPT-$(N_{60})_1$ | % Gravel | 0.086 | y = -0.841x + 39.38 |
| SPT-$(N_{60})_1$ | % Silt | 0.072 | y = - 0.870x + 67.07 |
| SPT-$(N_{60})_1$ | Plasticity Index (PI) | 0.043 | y = 1.249x + 19.86 |
| SPT-$(N_{60})_1$ | Dry Unit Weight (C-U Test) | 0.033 | y = -0.401x + 83.49 |
| SPT-$(N_{60})_1$ | Specific Gravity ($G_s$) | 0.020 | y = 74.76x – 168.6 |
| SPT-$(N_{60})_1$ | Friction Angle ($\phi$) | 0.007 | y = -0.234x + 37.78 |
| SPT-$(N_{60})_1$ | Natural Moisture Content ($w$) | 0.005 | y = 0.386x + 27.21 |
| SPT-$(N_{60})_1$ | Dry Unit Weight (UC Test) | 0.004 | y = -0.099x + 44.07 |
| SPT-$(N_{60})_1$ | % Sand | 0.003 | y = 0.416x + 21.60 |
| SPT-$(N_{60})_1$ | % Compaction | 0.003 | y = -0.115x + 43.67 |
| SPT-$(N_{60})_1$ | Time for 50% Consolidation ($t_{50}$) | 0.003 | y = -0.256x + 33.20 |

[Note] C-U = Consolidated-Undrained Triaxial; and UC = Unconfined Compression.

Tables 5.7 through 5.11 present similar regression analysis results for unconfined compression strength, effective stress friction angle, internal friction angle, cohesion, and effective stress (or long-term) cohesion of A-4a soils, respectively. No strong linear

correlations are surfacing for the unconfined compression strength and effective stress friction angle possessed by the A-4a soils (see Tables 5.7 and 5.8). No statistically significant results are seen for the cohesion and effective stress cohesion of the A-4a soils (see Tables 5.10 and 5.11). Only two statistically strong ($r^2 \geq 0.8$) correlations surfaced here for A-4a soils. The first one is a linear correlation between the internal friction angle and the dry unit weight measured during the C-U triaxial compression tests ($R^2 = 0.837$). The second one is a correlation between the effective-stress cohesion and effective-stress friction angle ($R^2 = 0.912$). No results can be compiled for the A-4b soils due to a lack of data points available.

**Table 5.7:** Single-Variable Linear Correlations for Unconfined Compression Strength of A-4a Soils

| Dependent Variable y | Independent Variable x | $R^2$ | Equation |
|---|---|---|---|
| Unconf. Compr. Strength | % Clay | 0.701 | y = 5.523x – 118.2 |
| Unconf. Compr. Strength | % Silt | 0.657 | y = -3.894x + 196.0 |
| Unconf. Compr. Strength | % Compaction | 0.375 | y = 1.822x – 144.7 |
| Unconf. Compr. Strength | Dry Unit Weight (UC Test) | 0.374 | y = 1.515x – 144.3 |
| Unconf. Compr. Strength | % Sand | 0.268 | y = 5.485x – 98.44 |
| Unconf. Compr. Strength | Natural Moisture Content (*w*) | 0.256 | y = 3.943x + 88.94 |
| Unconf. Compr. Strength | Plasticity Index (PI) | 0.149 | y = -3.431x + 72.84 |
| Unconf. Compr. Strength | Specific Gravity ($G_s$) | 0.101 | y = 246.7x – 622.6 |
| Unconf. Compr. Strength | Final Moisture Content (C-U Test) | 0.070 | y = -1.565x + 61.22 |
| Unconf. Compr. Strength | Liquid Limit (LL) | 0.049 | y = -1.172x + 70.01 |
| Unconf. Compr. Strength | Effective Friction Angle ($\phi'$) | 0.044 | y = 1.743x – 18.86 |
| Unconf. Compr. Strength | Dry Unit Weight (C-U Test) | 0.043 | y = 0.681x – 48.02 |
| Unconf. Compr. Strength | Time for 50% Consolidation ($t_{50}$) | 0.015 | y = -0.900x + 43.36 |
| Unconf. Compr. Strength | Internal Friction Angle ($\phi$) | 0.007 | y = -0.234x + 37.78 |
| Unconf. Compr. Strength | % Gravel | 0.002 | y = 0.173x + 37.83 |
| Unconf. Compr. Strength | Plastic Limit (PL) | 0.0002 | y = 0.117x + 37.42 |

[Note] C-U = Consolidated-Undrained Triaxial; and UC = Unconfined Compression.

**Table 5.8:** Single-Variable Linear Correlations for Effective-Stress Friction Angle of A-4a Soils

| Dependent Variable y | Independent Variable x | $R^2$ | Equation |
|---|---|---|---|
| Eff. Friction Angle ϕ' | Time for 50% Consolidation ($t_{50}$) | 0.559 | y = -0.665x + 36.37 |
| Eff. Friction Angle ϕ' | % Sand | 0.293 | y = 0.688x + 16.12 |
| Eff. Friction Angle ϕ' | Plastic Limit (PL) | 0.062 | y = -0.264x + 37.73 |
| Eff. Friction Angle ϕ' | Plasticity Index (PI) | 0.051 | y = 0.240x + 31.06 |
| Eff. Friction Angle ϕ' | Unconf. Compr. Strength ($q_u$) | 0.044 | y = 0.025x + 32.41 |
| Eff. Friction Angle ϕ' | % Clay | 0.043 | y = -0.163x + 38.05 |
| Eff. Friction Angle ϕ' | Specific Gravity ($G_s$) | 0.038 | y = -18.11x + 82.00 |
| Eff. Friction Angle ϕ' | Final Moisture Content (C-U Test) | 0.024 | y = -0.110x + 34.93 |
| Eff. Friction Angle ϕ' | % Gravel | 0.021 | y = 0.074x + 32.75 |
| Eff. Friction Angle ϕ' | Natural Moisture Content (*w*) | 0.021 | y = -0.136x + 35.11 |
| Eff. Friction Angle ϕ' | Dry Unit Weight (C-U Test) | 0.012 | y = 0.042x + 27.95 |
| Eff. Friction Angle ϕ' | Dry Unit Weight (UC Test) | 0.004 | y = -0.020x + 35.76 |
| Eff. Friction Angle ϕ' | % Compaction | 0.004 | y = -0.022x + 35.66 |
| Eff. Friction Angle ϕ' | Internal Friction Angle (ϕ) | 0.003 | y = -0.027x + 34.04 |
| Eff. Friction Angle ϕ' | Liquid Limit (LL) | 0.0002 | y = -0.010x + 33.65 |
| Eff. Friction Angle ϕ' | % Silt | 1E-06 | y = -0.0006x + 33.42 |

**Table 5.9:** Single-Variable Linear Correlations for Friction Angle of A-4a Soils

| Dependent Variable | Independent Variable | $R^2$ | Equation |
|---|---|---|---|
| Friction Angle ϕ | Dry Unit Weight (C-U Test) | **0.837** | y = 0.718x – 67.79 |
| Friction Angle ϕ | Final Moisture Content (C-U Test) | 0.484 | y = -0.991x + 38.27 |
| Friction Angle ϕ | Natural Moisture Content (*w*) | 0.413 | y = -1.202x + 39.54 |
| Friction Angle ϕ | Liquid Limit (LL) | 0.396 | y = -0.798x + 45.30 |
| Friction Angle ϕ | Plastic Limit (PL) | 0.386 | y = -1.316x + 46.01 |
| Friction Angle ϕ | Dry Unit Weight (UC Test) | 0.288 | y = 0.319x – 14.26 |
| Friction Angle ϕ | % Compaction | 0.286 | y = 0.382x – 14.14 |
| Friction Angle ϕ | % Gravel | 0.239 | y = 0.496x + 20.10 |
| Friction Angle ϕ | Specific Gravity ($G_s$) | 0.196 | y = 82.22x – 196.2 |
| Friction Angle ϕ | Plasticity Index (PI) | 0.188 | y = -0.923x + 33.43 |
| Friction Angle ϕ | % Sand | 0.101 | y = 0.808x + 4.133 |
| Friction Angle ϕ | % Silt | 0.033 | y = -0.208x + 32.81 |
| Friction Angle ϕ | Unconf. Compr. Strength ($q_u$) | 0.016 | y = 0.030x + 23.24 |
| Friction Angle ϕ | Time for 50% Consolidation ($t_{50}$) | 0.015 | y = -0.218x + 25.39 |
| Friction Angle ϕ | Effective Friction Angle (ϕ') | 0.003 | y = -0.107x + 27.98 |
| Friction Angle ϕ | % Clay | 6E-05 | y = -0.013x + 24.78 |

[Note] C-U = Consolidated-Undrained Triaxial; and UC = Unconfined Compression.

**Table 5.10:** Single-Variable Linear Correlations for Cohesion of A-4a Soils

| Dependent Variable | Independent Variable | $R^2$ | Equation |
|---|---|---|---|
| Cohesion $c_u$ | % Clay | 0.701 | y = 2.762x – 59.12 |
| Cohesion $c_u$ | % Silt | 0.657 | y = -1.947x + 98.01 |
| Cohesion $c_u$ | % Compaction | 0.375 | y = 0.911x – 72.35 |
| Cohesion $c_u$ | Dry Unit Weight (UC Test) | 0.374 | y = 0.757x – 72.14 |
| Cohesion $c_u$ | % Sand | 0.268 | y = 2.743x – 49.22 |
| Cohesion $c_u$ | Natural Moisture Content (*w*) | 0.256 | y = -1.971x + 44.47 |
| Cohesion $c_u$ | Plasticity Index (PI) | 0.149 | y = -1.716x + 36.42 |
| Cohesion $c_u$ | Specific Gravity ($G_s$) | 0.101 | y = 123.3x – 311.3 |
| Cohesion $c_u$ | Final Moisture Content (C-U Test) | 0.070 | y = -0.783x + 30.61 |
| Cohesion $c_u$ | Liquid Limit (LL) | 0.049 | y = -0.586x + 35.01 |
| Cohesion $c_u$ | Effective Friction Angle ($\phi'$) | 0.044 | y = 0.871x – 9.431 |
| Cohesion $c_u$ | Internal Friction Angle ($\phi$) | 0.016 | y = 0.261x + 13.30 |
| Cohesion $c_u$ | Time for 50% Consolidation ($t_{50}$) | 0.015 | y = -0.450x + 21.68 |
| Cohesion $c_u$ | % Gravel | 0.002 | y = 0.086x + 18.92 |
| Cohesion $c_u$ | Plastic Limit (PL) | 0.0002 | y = 0.058x + 18.71 |

**Table 5.11:** Single-Variable Linear Correlations for Effective-Stress Cohesion of A-4a Soils

| Dependent Variable | Independent Variable | $R^2$ | Equation |
|---|---|---|---|
| Cohesion $c'$ | Effective Friction Angle ($\phi'$) | **0.912** | y = 1.583x – 47.47 |
| Cohesion $c'$ | Unconf. Compr. Strength ($q_u$) | 0.461 | y = 0.085x + 1.264 |
| Cohesion $c'$ | Time for 50% Consolidation ($t_{50}$) | 0.410 | y = -0.903x + 9.146 |
| Cohesion $c'$ | % Sand | 0.339 | y = 0.994x – 19.85 |
| Cohesion $c'$ | Natural Moisture Content (*w*) | 0.151 | y = -0.491x + 10.96 |
| Cohesion $c'$ | % Clay | 0.140 | y = 0.341x – 5.147 |
| Cohesion $c'$ | Plasticity Index (PI) | 0.107 | y = 0.375x + 1.355 |
| Cohesion $c'$ | Plastic Limit (PL) | 0.033 | y = -0.223x + 8.632 |
| Cohesion $c'$ | % Silt | 0.024 | y = -0.093x + 8.631 |
| Cohesion $c'$ | Dry Unit Weight (C-U Test) | 0.022 | y = 0.086x – 6.326 |
| Cohesion $c'$ | Internal Friction Angle ($\phi$) | 0.014 | y = 0.076x + 2.947 |
| Cohesion $c'$ | % Compaction | 0.014 | y = 0.056x – 0.804 |
| Cohesion $c'$ | Dry Unit Weight (UC Test) | 0.013 | y = 0.045x – 0.706 |
| Cohesion $c'$ | Liquid Limit (LL) | 0.011 | y = 0.081x + 2.808 |
| Cohesion $c'$ | % Gravel | 9E(-5) | y = -0.005x + 4.964 |
| Cohesion $c'$ | Specific Gravity ($G_s$) | 4E(-16) | y = 1.891x – 0.183 |
| Cohesion $c'$ | Final Moisture Content (C-U Test) | 0.000 | y = 0.038x + 4.411 |

[Note] C-U = Consolidated-Undrained Triaxial; and UC = Unconfined Compression.

### 5.2.2 A-6a Soils

Single-variable linear regression analysis was also performed for the A-6*a* soil data along each correlation path. Tables 5.12 through 5.17 present the entire outcome. Only one statistically meaningful outcome can be seen among the results. The linear correlation between the effective-stress cohesion and % silt has a $R^2$ value of 0.929 (see Table 5.17). Beyond this, the next best result, found in Table 5.16, exists between the cohesion and effective stress friction angle, which were both derived from the C-U triaxial test data. This linear correlation has the coefficient of determination $R^2$ of 0.6215. Overall, the outcomes reported here indicate that a single-variable linear function is not suitable for expressing correlations that exist between various properties possessed by the A-6a soils found in Ohio.

**Table 5.12:** Single-Variable Linear Correlations for SPT-$(N_{60})_1$ of A-6a Soils

| Dependent Variable y | Independent Variable x | $R^2$ | Equation |
|---|---|---|---|
| SPT-$(N_{60})_1$ | % Silt | 0.293 | y = -3.574x + 174.5 |
| SPT-$(N_{60})_1$ | % Gravel | 0.244 | y = -2.264x + 49.25 |
| SPT-$(N_{60})_1$ | % Clay | 0.202 | y = 1.252x – 3.663 |
| SPT-$(N_{60})_1$ | Final Moisture Content (C-U Test) | 0.123 | y = 2.365x – 5.638 |
| SPT-$(N_{60})_1$ | Friction Angle ($\phi$) | 0.091 | y = 0.927x + 13.69 |
| SPT-$(N_{60})_1$ | Natural Moisture Content (*w*) | 0.083 | y = 2.910x – 6.184 |
| SPT-$(N_{60})_1$ | Dry Unit Weight (UC Test) | 0.078 | y = -0.590x + 103.0 |
| SPT-$(N_{60})_1$ | % Compaction | 0.078 | y = -0.652x + 103.3 |
| SPT-$(N_{60})_1$ | Dry Unit Weight (C-U Test) | 0.069 | y = -0.680x + 115.7 |
| SPT-$(N_{60})_1$ | Plasticity Index (PI) | 0.067 | y = -1.817x + 55.15 |
| SPT-$(N_{60})_1$ | Plastic Limit (PL) | 0.050 | y = 1.776x + 0.380 |
| SPT-$(N_{60})_1$ | Effective Friction Angle ($\phi'$) | 0.037 | y = 1.373x – 13.70 |
| SPT-$(N_{60})_1$ | Time for 50% Consol. ($t_{50}$) | 0.024 | y = 0.368x + 29.56 |
| SPT-$(N_{60})_1$ | % Sand | 0.009 | y = 0.339x + 24.12 |
| SPT-$(N_{60})_1$ | Liquid Limit (LL) | 0.003 | y = 0.102x + 29.42 |
| SPT-$(N_{60})_1$ | Unconf. Compr. Strength ($q_u$) | 0.002 | y = -0.064x + 34.66 |
| SPT-$(N_{60})_1$ | Specific Gravity ($G_s$) | 1E(-5) | y = 1.109x + 29.250 |

[Note] C-U = Consolidated-Undrained Triaxial; and UC = Unconfined Compression.

**Table 5.13:** Single-Variable Linear Correlations for Unconfined Compression Strength of A-6a Soils

| Dependent Variable y | Independent Variable x | $R^2$ | Equation |
|---|---|---|---|
| Unconf. Compr. Strength | % Silt | 0.451 | y = -3.637x + 182.0 |
| Unconf. Compr. Strength | Final Moisture Content ($w_f$) | 0.331 | y = -3.176x + 88.10 |
| Unconf. Compr. Strength | Dry Unit Weight (C-U Test) | 0.302 | y = 1.160x – 105.2 |
| Unconf. Compr. Strength | Plastic Limit (PL) | 0.285 | y = -3.464x + 99.41 |
| Unconf. Compr. Strength | Friction Angle ($\phi$) | 0.188 | y = 1.093x + 15.30 |
| Unconf. Compr. Strength | Dry Unit Weight (UC Test) | 0.175 | y = 0.727x – 49.89 |
| Unconf. Compr. Strength | % Compaction | 0.173 | y = 0.797x – 49.65 |
| Unconf. Compr. Strength | % Clay | 0.095 | y = 0.705x + 16.95 |
| Unconf. Compr. Strength | % Gravel | 0.075 | y = -1.033x + 44.95 |
| Unconf. Compr. Strength | Time for 50% Consol. ($t_{50}$) | 0.046 | y = 0.414x + 34.15 |
| Unconf. Compr. Strength | Effective Friction Angle ($\phi'$) | 0.042 | y = -1.193x + 77.17 |
| Unconf. Compr. Strength | Plasticity Index (PI) | 0.035 | y = -1.078x + 50.77 |
| Unconf. Compr. Strength | % Sand | 0.030 | y = 0.499x + 25.22 |
| Unconf. Compr. Strength | Liquid Limit (LL) | 0.027 | y = 0.253x + 30.16 |
| Unconf. Compr. Strength | Specific Gravity ($G_s$) | 0.013 | y = 33.70x – 54.44 |
| Unconf. Compr. Strength | Natural Moisture Content ($w$) | 0.008 | y = 0.740x + 27.41 |

**Table 5.14:** Single-Variable Linear Correlations for Effective-Stress Friction Angle of A-6a Soils

| Dependent Variable y | Independent Variable x | $R^2$ | Equation |
|---|---|---|---|
| Eff. Friction Angle $\phi$' | Specific Gravity ($G_s$) | 0.273 | y = -26.55x + 105.6 |
| Eff. Friction Angle $\phi$' | % Sand | 0.188 | y = 0.212x + 28.38 |
| Eff. Friction Angle $\phi$' | Time for 50% Consol. ($t_{50}$) | 0.114 | y = -0.112x + 34.30 |
| Eff. Friction Angle $\phi$' | Liquid Limit (LL) | 0.083 | y = -0.075x + 35.58 |
| Eff. Friction Angle $\phi$' | % Clay | 0.063 | y = -0.099x + 36.32 |
| Eff. Friction Angle $\phi$' | Plastic Limit (PL) | 0.052 | y = -0.254x + 38.05 |
| Eff. Friction Angle $\phi$' | % Gravel | 0.048 | y = -0.142x + 34.54 |
| Eff. Friction Angle $\phi$' | Unconf. Compr. Strength ($q_u$) | 0.042 | y = -0.035x + 34.79 |
| Eff. Friction Angle $\phi$' | Dry Unit Weight (UC Test) | 0.026 | y = -0.048x + 39.32 |
| Eff. Friction Angle $\phi$' | % Compaction | 0.026 | y = -0.053x + 39.30 |
| Eff. Friction Angle $\phi$' | Final Moisture Content ($w$) | 0.022 | y = 0.142x + 31.20 |
| Eff. Friction Angle $\phi$' | Natural Moisture Content (w) | 0.020 | y = 0.203x + 30.79 |
| Eff. Friction Angle $\phi$' | % Silt | 0.007 | y = 0.079x + 30.32 |
| Eff. Friction Angle $\phi$' | Dry Unit Weight (C-U Test) | 0.006 | y = 0.029x + 29.86 |
| Eff. Friction Angle $\phi$' | Friction Angle ($\phi$) | 0.005 | y = 0.032x + 32.82 |
| Eff. Friction Angle $\phi$' | Plasticity Index (PI) | 0.000 | y = -0.013x + 33.65 |

[Note] C-U = Consolidated-Undrained Triaxial; and UC = Unconfined Compression.

**Table 5.15:** Single-Variable Linear Correlations for Friction Angle of A-6a Soils

| Dependent Variable | Independent Variable | $R^2$ | Equation |
|---|---|---|---|
| Friction Angle $\phi$ | % Gravel | 0.500 | y = -1.055x + 27.94 |
| Friction Angle $\phi$ | % Silt | 0.461 | y = -1.462x + 78.28 |
| Friction Angle $\phi$ | Plasticity Index (PI) | 0.451 | y = -1.536x + 39.38 |
| Friction Angle $\phi$ | % Sand | 0.190 | y = 0.491x + 8.235 |
| Friction Angle $\phi$ | Unconf. Compr. Strength ($q_u$) | 0.188 | y = 0.172x + 13.60 |
| Friction Angle $\phi$ | Dry Unit Weight (C-U Test) | 0.175 | y = 0.351x – 23.10 |
| Friction Angle $\phi$ | Plastic Limit (PL) | 0.171 | y = -1.067x + 39.19 |
| Friction Angle $\phi$ | % Clay | 0.133 | y = 0.332x + 10.51 |
| Friction Angle $\phi$ | Specific Gravity ($G_s$) | 0.076 | y = -32.43x + 108.2 |
| Friction Angle $\phi$ | % Compaction | 0.047 | y = -0.165x + 38.03 |
| Friction Angle $\phi$ | Dry Unit Weight (UC Test) | 0.046 | y = -0.148x + 37.83 |
| Friction Angle $\phi$ | Liquid Limit (LL) | 0.020 | y = -0.087x + 22.46 |
| Friction Angle $\phi$ | Final Moisture Content (C-U Test) | 0.005 | y = 0.168x + 17.33 |
| Friction Angle $\phi$ | Effective Friction Angle ($\phi'$) | 0.005 | y = 0.171x + 14.29 |
| Friction Angle $\phi$ | Natural Moisture Content ($w$) | 0.001 | y = -0.142x + 21.92 |
| Friction Angle $\phi$ | Time for 50% Consolidation ($t_{50}$) | 0.000 | y = -0.016x + 20.15 |

**Table 5.16:** Single-Variable Linear Correlations for Cohesion of A-6a Soils

| Dependent Variable | Independent Variable | $R^2$ | Equation |
|---|---|---|---|
| Cohesion $c_u$ | Effective Friction Angle ($\phi'$) | 0.622 | y = 1.822x – 49.05 |
| Cohesion $c_u$ | Specific Gravity ($G_s$) | 0.619 | y = -78.00x + 223.4 |
| Cohesion $c_u$ | % Clay | 0.558 | y = -0.668x + 32.33 |
| Cohesion $c_u$ | % Sand | 0.577 | y = 1.258x – 19.08 |
| Cohesion $c_u$ | Plastic Limit (PL) | 0.514 | y = -1.654x + 40.32 |
| Cohesion $c_u$ | % Silt | 0.402 | y = 1.161x – 33.16 |
| Cohesion $c_u$ | Internal Friction Angle ($\phi$) | 0.315 | y = -0.748x + 28.16 |
| Cohesion $c_u$ | Natural Moisture Content ($w$) | 0.240 | y = -0.936x + 24.114 |
| Cohesion $c_u$ | Unconf. Compr. Strength ($q_u$) | 0.166 | y = -0.102x + 16.10 |
| Cohesion $c_u$ | Plasticity Index (PI) | 0.196 | y = 0.743x + 2.804 |
| Cohesion $c_u$ | Time for 50% Consolidation ($t_{50}$) | 0.060 | y = -0.189x + 13.34 |
| Cohesion $c_u$ | % Compaction | 0.016 | y = 0.056x + 5.803 |
| Cohesion $c_u$ | Dry Unit Weight (UC Test) | 0.016 | y = 0.051x + 5.873 |
| Cohesion $c_u$ | Liquid Limit (LL) | 0.009 | y = -0.188x + 17.40 |
| Cohesion $c_u$ | % Gravel | 0.003 | y = 0.107x + 11.23 |
| Cohesion $c_u$ | Final Moisture Content (C-U Test) | 0.003 | y = 0.071x + 10.74 |

[Note] C-U = Consolidated-Undrained Triaxial; and UC = Unconfined Compression.

**Table 5.17:** Single-Variable Linear Correlations for Effective-Stress Cohesion of A-6a Soils

| Dependent Variable | Independent Variable | $R^2$ | Equation |
|---|---|---|---|
| Cohesion c′ | % Silt | **0.929** | y = 1.380x – 49.71 |
| Cohesion c′ | Specific Gravity ($G_s$) | **0.881** | y = -68.14x + 188.4 |
| Cohesion c′ | % Clay | **0.834** | y = -1.601x + 54.66 |
| Cohesion c′ | Internal Friction Angle ($\phi$) | 0.778 | y = -0.901x + 23.37 |
| Cohesion c′ | Dry Unit Weight (C-U Test) | 0.759 | y = -0.686x + 87.57 |
| Cohesion c′ | Dry Unit Weight (UC Test) | 0.749 | y = -0.352x + 44.37 |
| Cohesion c′ | % Compaction | 0.748 | y = -0.389x + 44.56 |
| Cohesion c′ | Final Moisture Content (C-U Test) | 0.632 | y = 1.096x – 14.78 |
| Cohesion c′ | Plasticity Index (PI) | 0.540 | y = 0.911x – 7.525 |
| Cohesion c′ | Plastic Limit (PL) | 0.540 | y = -3.646x + 68.14 |
| Cohesion c′ | Liquid Limit (LL) | 0.540 | y = 1.215x – 32.74 |
| Cohesion c′ | Unconf. Compr. Strength ($q_u$) | 0.511 | y = -0.135x + 8.749 |
| Cohesion c′ | Effective Friction Angle ($\phi'$) | 0.283 | y = 0.887x – 26.18 |
| Cohesion c′ | Natural Moisture Content ($w$) | 0.068 | y = 0.445x – 2.605 |
| Cohesion c′ | Time for 50% Consolidation ($t_{50}$) | 0.056 | y = 0.137x + 2.274 |
| Cohesion c′ | % Sand | 0.040 | y = -0.351x + 11.85 |
| Cohesion c′ | % Gravel | 0.005 | y = -0.140x + 4.185 |

[Note] C-U = Consolidated-Undrained Triaxial; and UC = Unconfined Compression.

### 5.2.3 A-6b Soils

A set of single-variable linear regression was also performed for the A-6b soil data along each correlation path. Tables 5.18 through 5.23 present the results. Unlike the previous cases with the A-4a and A-6a soil data, some strong correlations are emerging for the unconfined compression strength, friction angle, and cohesion possessed by this soil type. There are seventeen statistically strong cases here, with seven of them having the $R^2$ value above 0.9. Among numerous index properties, plasticity index (PI), specific gravity ($G_s$), % silt, and % clay appeared more frequently as key independent variables.

**Table 5.18:** Single-Variable Linear Correlations for SPT-$(N_{60})_1$ of A-6b Soils

| Dependent Variable | Independent Variable x | $R^2$ | Equation |
|---|---|---|---|
| SPT-$(N_{60})_1$ | % Gravel | 0.556 | y = 1.432x + 10.86 |
| SPT-$(N_{60})_1$ | Plastic Limit (PL) | 0.463 | y = -5.268x + 137.8 |
| SPT-$(N_{60})_1$ | Unconf. Compr. Strength ($q_u$) | 0.218 | y = 0.231x + 21.48 |
| SPT-$(N_{60})_1$ | Specific Gravity ($G_s$) | 0.206 | y = -175.7x + 505.9 |
| SPT-$(N_{60})_1$ | % Silt | 0.172 | y = -0.572x + 53.67 |
| SPT-$(N_{60})_1$ | % Compaction | 0.163 | y = -0.673x + 100.4 |
| SPT-$(N_{60})_1$ | Natural Moisture Content (*w*) | 0.150 | y = 1.430x + 6.494 |
| SPT-$(N_{60})_1$ | Liquid Limit (LL) | 0.123 | y = -3.339x + 156.6 |
| SPT-$(N_{60})_1$ | % Clay | 0.109 | y = 0.354x + 16.48 |
| SPT-$(N_{60})_1$ | Effective Friction Angle ($\phi'$) | 0.097 | y = -1.795x + 83.92 |
| SPT-$(N_{60})_1$ | Friction Angle ($\phi$) | 0.087 | y = 0.766x + 17.23 |
| SPT-$(N_{60})_1$ | Plasticity Index (PI) | 0.079 | y = 1.547x + 1.939 |
| SPT-$(N_{60})_1$ | Time for 50% Consolid. ($t_{50}$) | 0.064 | y = 0.084x + 26.00 |
| SPT-$(N_{60})_1$ | Dry Unit Weight (UC Test) | 0.063 | y = -0.355x + 71.26 |
| SPT-$(N_{60})_1$ | Dry Unit Weight (C-U Test) | 0.044 | y = -0.292x + 61.91 |
| SPT-$(N_{60})_1$ | % Sand | 0.01 | y = -0.295x + 33.39 |
| SPT-$(N_{60})_1$ | Final Moisture Content (C-U Test) | 8E(-6) | y = 0.009x + 28.81 |

**Table 5.19:** Single-Variable Linear Correlations for Unconfined Compression Strength of A-6b Soils

| Dependent Variable | Independent Variable x | $R^2$ | Equation |
|---|---|---|---|
| Unconf. Compr. Strength | Plasticity Index (PI) | **0.938** | y = 10.75x – 155.8 |
| Unconf. Compr. Strength | Specific Gravity ($G_s$) | **0.930** | y = -752.6x + 2074. |
| Unconf. Compr. Strength | % Silt | **0.902** | y = -2.638x + 146.0 |
| Unconf. Compr. Strength | % Clay | **0.877** | y = 2.026x – 39.19 |
| Unconf. Compr. Strength | Plastic Limit (PL) | **0.864** | y = -14.50x + 332.1 |
| Unconf. Compr. Strength | Friction Angle ($\phi$) | **0.857** | y = 4.841x – 41.83 |
| Unconf. Compr. Strength | Dry Unit Weight (UC Test) | 0.692 | y = -2.362x + 313.0 |
| Unconf. Compr. Strength | % Compaction | 0.690 | y = -2.593x + 312.4 |
| Unconf. Compr. Strength | Natural Moisture Content (*w*) | 0.689 | y = 6.163x – 64.56 |
| Unconf. Compr. Strength | % Gravel | 0.472 | y = 2.660x – 1.029 |
| Unconf. Compr. Strength | % Sand | 0.384 | y = 3.573x – 19.14 |
| Unconf. Compr. Strength | Liquid Limit (LL) | 0.281 | y = 10.16x – 355.2 |
| Unconf. Compr. Strength | Effective Friction Angle ($\phi'$) | 0.097 | y = -1.795x + 83.92 |
| Unconf. Compr. Strength | Time for 50% Consolid. ($t_{50}$) | 0.064 | y = 0.084x + 26.00 |
| Unconf. Compr. Strength | Dry Unit Weight (C-U Test) | 0.057 | y = 0.674x – 43.44 |
| Unconf. Compr. Strength | Final Moisture Content (C-U Test) | 0.027 | y = -1.165x + 54.70 |

[Note] C-U = Consolidated-Undrained Triaxial; and UC = Unconfined Compression.

**Table 5.20:** Single-Variable Linear Correlations for Effective-Stress Friction Angle of A-6b Soils

| Dependent Variable y | Independent Variable x | $R^2$ | Equation |
|---|---|---|---|
| Eff. Friction Angle ϕ' | % Silt | 0.546 | y = 0.191x + 22.58 |
| Eff. Friction Angle ϕ' | Unconf. Compr. Strength ($q_u$) | 0.485 | y = -0.061x + 32.90 |
| Eff. Friction Angle ϕ' | Specific Gravity ($G_s$) | 0.464 | y = 49x – 102.1 |
| Eff. Friction Angle ϕ' | Plasticity Index (PI) | 0.451 | y = -0.669x + 42.65 |
| Eff. Friction Angle ϕ' | Friction Angle (ϕ) | 0.422 | y = -0.333x + 36.14 |
| Eff. Friction Angle ϕ' | % Sand | 0.410 | y = -0.377x + 36.28 |
| Eff. Friction Angle ϕ' | Plastic Limit (PL) | 0.398 | y = 0.857x + 13.11 |
| Eff. Friction Angle ϕ' | % Clay | 0.387 | y = -0.126x + 35.30 |
| Eff. Friction Angle ϕ' | Natural Moisture Content (*w*) | 0.338 | y = -0.457x + 37.93 |
| Eff. Friction Angle ϕ' | % Gravel | 0.321 | y = -0.207x + 33.32 |
| Eff. Friction Angle ϕ' | Dry Unit Weight (UC Test) | 0.289 | y = 0.156x + 12.26 |
| Eff. Friction Angle ϕ' | % Compaction | 0.287 | y = 0.171x + 12.31 |
| Eff. Friction Angle ϕ' | Liquid Limit (LL) | 0.141 | y = -0.675x + 56.70 |
| Eff. Friction Angle ϕ' | Final Moisture Content (C-U Test) | 0.043 | y = 0.151x + 28.02 |
| Eff. Friction Angle ϕ' | Time for 50% Consolid. ($t_{50}$) | 0.030 | y = 0.261x + 24.43 |
| Eff. Friction Angle ϕ' | Dry Unit Weight (C-U Test) | 0.000 | y = 0.003x + 30.46 |

**Table 5.21:** Single-Variable Linear Correlations for Friction Angle of A-6b Soils

| Dependent Variable | Independent Variable | $R^2$ | Equation |
|---|---|---|---|
| Friction Angle ϕ | % Clay | **0.922** | y = 0.419x + 0.812 |
| Friction Angle ϕ | Plasticity Index (PI) | **0.919** | y = 2.042x – 20.37 |
| Friction Angle ϕ | Dry Unit Weight (UC Test) | **0.902** | y = -0.590x + 85.99 |
| Friction Angle ϕ | % Compaction | **0.901** | y = -0.649x + 85.98 |
| Friction Angle ϕ | Natural Moisture Content (*w*) | **0.868** | y = 1.598x – 9.209 |
| Friction Angle ϕ | Specific Gravity ($G_s$) | **0.865** | y = -145.9x + 411.4 |
| Friction Angle ϕ | Unconf. Compr. Strength ($q_u$) | **0.857** | y = 0.177x + 9.598 |
| Friction Angle ϕ | % Silt | **0.831** | y = -0.514x + 37.77 |
| Friction Angle ϕ | Plastic Limit (PL) | 0.624 | y = -2.391x + 64.86 |
| Friction Angle ϕ | % Sand | 0.502 | y = 0.874x + 3.030 |
| Friction Angle ϕ | Liquid Limit (LL) | 0.483 | y = 2.55x – 82.05 |
| Friction Angle ϕ | % Gravel | 0.258 | y = 0.416x + 10.32 |
| Friction Angle ϕ | Dry Unit Weight (C-U Test) | 0.099 | y = 0.168x – 3.666 |
| Friction Angle ϕ | Effective Friction Angle (ϕ') | 0.097 | y = -1.795x + 83.92 |
| Friction Angle ϕ | Time for 50% Consolid. ($t_{50}$) | 0.064 | y = 0.084x + 26.00 |
| Friction Angle ϕ | Final Moisture Content (C-U Test) | 0.041 | y = -0.271x + 20.53 |

[Note] C-U = Consolidated-Undrained Triaxial; and UC = Unconfined Compression.

**Table 5.22:** Single-Variable Linear Correlations for Cohesion of A-6b Soils

| Dependent Variable | Independent Variable | $R^2$ | Equation |
|---|---|---|---|
| Cohesion $c_u$ | Time for 50% Consolidation ($t_{50}$) | **0.890** | y = -0.308x + 13.79 |
| Cohesion $c_u$ | Final Moisture Content (C-U Test) | **0.872** | y = -4.691x + 97.70 |
| Cohesion $c_u$ | Liquid Limit (LL) | **0.855** | y = 3.370x – 120.3 |
| Cohesion $c_u$ | % Sand | 0.621 | y = 1.071x – 6.582 |
| Cohesion $c_u$ | % Gravel | 0.270 | y = -0.393x + 13.59 |
| Cohesion $c_u$ | % Compaction | 0.135 | y = -0.247x + 35.66 |
| Cohesion $c_u$ | Plasticity Index (PI) | 0.135 | y = 0.742x – 4.231 |
| Cohesion $c_u$ | Internal Friction Angle ($\phi$) | 0.134 | y = 0.362x + 3.204 |
| Cohesion $c_u$ | Dry Unit Weight (UC Test) | 0.133 | y = -0.223x + 35.47 |
| Cohesion $c_u$ | % Clay | 0.086 | y = 0.122x + 4.563 |
| Cohesion $c_u$ | Plastic Limit (PL) | 0.040 | y = 0.547x – 2.424 |
| Cohesion $c_u$ | Effective Friction Angle ($\phi'$) | 0.036 | y = -0.561x + 26.18 |
| Cohesion $c_u$ | % Silt | 0.031 | y = -0.093x + 12.90 |
| Cohesion $c_u$ | Natural Moisture Content ($w$) | 0.022 | y = 0.239x + 5.171 |
| Cohesion $c_u$ | Unconf. Compr. Strength ($q_u$) | 0.018 | y = 0.023x + 8.072 |
| Cohesion $c_u$ | Specific Gravity ($G_s$) | 0.018 | y = -19.40x + 61.52 |

**Table 5.23:** Single-Variable Linear Correlations for Effective-Stress Cohesion of A-6b Soils

| Dependent Variable | Independent Variable | $R^2$ | Equation |
|---|---|---|---|
| Cohesion $c'$ | Dry Unit Weight (C-U Test) | 0.778 | y = 0.543x – 57.55 |
| Cohesion $c'$ | % Gravel | 0.765 | y = -0.566x + 11.33 |
| Cohesion $c'$ | Plastic Limit (PL) | 0.434 | y = 1.555x – 27.60 |
| Cohesion $c'$ | Time for 50% Consolidation ($t_{50}$) | 0.427 | y = -0.183x + 7.450 |
| Cohesion $c'$ | Final Moisture Content (C-U Test) | 0.400 | y = -2.724x + 56.12 |
| Cohesion $c'$ | Liquid Limit (LL) | 0.377 | y = 1.917x – 68.96 |
| Cohesion $c'$ | % Sand | 0.143 | y = 0.440x – 1.829 |
| Cohesion $c'$ | Specific Gravity ($G_s$) | 0.141 | y = 47.00x – 122.9 |
| Cohesion $c'$ | Unconf. Compr. Strength ($q_u$) | 0.140 | y = -0.057x + 6.473 |
| Cohesion $c'$ | Natural Moisture Content ($w$) | 0.132 | y = -0.508x + 12.43 |
| Cohesion $c'$ | % Silt | 0.113 | y = 0.153x – 2.090 |
| Cohesion $c'$ | Effective Friction Angle ($\phi'$) | 0.104 | y = 0.823x – 20.83 |
| Cohesion $c'$ | % Clay | 0.048 | y = -0.077x + 7.297 |
| Cohesion $c'$ | Dry Unit Weight (UC Test) | 0.021 | y = 0.076x – 4.525 |
| Cohesion $c'$ | Plasticity Index (PI) | 0.020 | y = -0.247x + 8.905 |
| Cohesion $c'$ | Internal Friction Angle ($\phi$) | 0.020 | y = -0.122x + 6.458 |
| Cohesion $c'$ | % Compaction | 0.020 | y = 0.082x – 4.382 |

[Note] C-U = Consolidated-Undrained Triaxial; and UC = Unconfined Compression.

### 5.2.4 A-7-6 Soils

A comprehensive single-variable linear regression analysis was carried out using the project data compiled for the A-7-6 soils. Results are presented in Tables 5.24 through 5.29. Similar to the analysis performed for the A-6a soils, no statistically strong correlations are surfacing from the analysis. The best result is seen in Table 5.24 between the SPT-$(N_{60})_1$ value and dry unit weight of the soil specimen measured before each C-U triaxial test. This linear correlation has the coefficient of determination $R^2$ of 0.628. These outcomes point out that a single-variable linear function is not suitable for expressing correlations that exist between various properties possessed by the A-7-6 soils found in Ohio.

**Table 5.24:** Single-Variable Linear Correlations for SPT-$(N_{60})_1$ of A-7-6 Soils

| Dependent Variable | Independent Variable x | $R^2$ | Equation |
|---|---|---|---|
| SPT-$(N_{60})_1$ | Dry Unit Weight (C-U Test) | 0.628 | y = 0.96x – 84.21 |
| SPT-$(N_{60})_1$ | Final Moisture Content (C-U Test) | 0.487 | y = -1.974x + 67.50 |
| SPT-$(N_{60})_1$ | Dry Unit Weight (UC Test) | 0.472 | y = 1.043x – 88.05 |
| SPT-$(N_{60})_1$ | % Compaction | 0.450 | y = 1.114x – 84.95 |
| SPT-$(N_{60})_1$ | Natural Moisture Content (*w*) | 0.424 | y = -1.357x + 50.47 |
| SPT-$(N_{60})_1$ | % Sand | 0.410 | y = 0.741x + 12.77 |
| SPT-$(N_{60})_1$ | % Silt | 0.391 | y = -0.353x + 35.96 |
| SPT-$(N_{60})_1$ | % Clay | 0.324 | y = -0.634x + 54.38 |
| SPT-$(N_{60})_1$ | Plastic Limit (PL) | 0.317 | y = -2.793x + 81.23 |
| SPT-$(N_{60})_1$ | Liquid Limit (LL) | 0.275 | y = -0.624x + 52.00 |
| SPT-$(N_{60})_1$ | Internal Friction Angle ($\phi$) | 0.274 | y = 1.778x – 1.941 |
| SPT-$(N_{60})_1$ | Unconf. Compression Strength ($q_u$) | 0.153 | y = 0.319x + 12.11 |
| SPT-$(N_{60})_1$ | % Gravel | 0.092 | y = 0.714x + 18.62 |
| SPT-$(N_{60})_1$ | Plasticity Index (PI) | 0.090 | y = -0.427x + 32.68 |
| SPT-$(N_{60})_1$ | Time for 50% Consolidation ($t_{50}$) | 0.077 | y = -0.095x + 24.74 |
| SPT-$(N_{60})_1$ | Effective Friction Angle ($\phi'$) | 0.021 | y = -0.571x + 36.65 |
| SPT-$(N_{60})_1$ | Specific Gravity ($G_s$) | 0.001 | y = -17.59x + 68.43 |

[Note] C-U = Consolidated-Undrained Triaxial; and UC = Unconfined Compression.

**Table 5.25:** Single-Variable Linear Correlations for Unconfined Compression Strength of A-7-6 Soils

| Dependent Variable | Independent Variable x | $R^2$ | Equation |
|---|---|---|---|
| Unconf. Compr. Strength | % Sand | 0.458 | y = 0.959x + 17.14 |
| Unconf. Compr. Strength | Internal Friction Angle ($\phi$) | 0.408 | y = 2.652x – 6.428 |
| Unconf. Compr. Strength | % Silt | 0.407 | y = -0.441x + 46.46 |
| Unconf. Compr. Strength | Liquid Limit (LL) | 0.347 | y = -0.858x + 70.40 |
| Unconf. Compr. Strength | % Clay | 0.319 | y = -0.770x + 68.30 |
| Unconf. Compr. Strength | Plasticity Index (PI) | 0.317 | y = -0.979x + 54.53 |
| Unconf. Compr. Strength | Dry Unit Weight (C-U Test) | 0.315 | y = 0.831x – 63.31 |
| Unconf. Compr. Strength | % Compaction | 0.252 | y = 1.019x – 69.18 |
| Unconf. Compr. Strength | Dry Unit Weight (UC Test) | 0.246 | y = 0.921x – 68.56 |
| Unconf. Compr. Strength | Final Moisture Content (C-U Test) | 0.167 | y = -1.415x + 61.10 |
| Unconf. Compr. Strength | Natural Moisture Content ($w$) | 0.157 | y = -1.012x + 49.75 |
| Unconf. Compr. Strength | Specific Gravity ($G_s$) | 0.070 | y = -129.5x + 377.1 |
| Unconf. Compr. Strength | Plastic Limit (PL) | 0.034 | y = -1.126x + 52.07 |
| Unconf. Compr. Strength | Time for 50% Consolidation ($t_{50}$) | 0.016 | y = -0.054x + 29.91 |
| Unconf. Compr. Strength | Effective Friction Angle ($\phi'$) | 0.016 | y = -0.614x + 44.60 |
| Unconf. Compr. Strength | % Gravel | 0.000 | y = 0.087x + 27.48 |

**Table 5.26:** Single-Variable Linear Correlations for Effective-Stress Friction Angle of A-7-6 Soils

| Dependent Variable y | Independent Variable x | $R^2$ | Equation |
|---|---|---|---|
| Eff. Friction Angle $\phi'$ | Plasticity Index (PI) | 0.059 | y = 0.088x + 24.96 |
| Eff. Friction Angle $\phi'$ | Time for 50% Consolidation ($t_{50}$) | 0.054 | y = -0.020x + 28.18 |
| Eff. Friction Angle $\phi'$ | Dry Unit Weight (C-U Test) | 0.049 | y = -0.069x + 34.94 |
| Eff. Friction Angle $\phi'$ | Liquid Limit (LL) | 0.040 | y = 0.061x + 24.31 |
| Eff. Friction Angle $\phi'$ | Final Moisture Content (C-U Test) | 0.035 | y = 0.135x + 24.18 |
| Eff. Friction Angle $\phi'$ | Internal Friction Angle ($\phi$) | 0.031 | y = -0.154x + 29.37 |
| Eff. Friction Angle $\phi'$ | % Clay | 0.017 | y = 0.037x + 25.41 |
| Eff. Friction Angle $\phi'$ | Plastic Limit (PL) | 0.016 | y = 0.161x + 23.90 |
| Eff. Friction Angle $\phi'$ | Unconf. Compr. Strength ($q_u$) | 0.016 | y = -0.027x + 28.13 |
| Eff. Friction Angle $\phi'$ | % Silt | 0.011 | y = 0.015x + 26.73 |
| Eff. Friction Angle $\phi'$ | % Sand | 0.010 | y = -0.029x + 27.71 |
| Eff. Friction Angle $\phi'$ | % Compaction | 0.009 | y = -0.041x + 31.29 |
| Eff. Friction Angle $\phi'$ | Dry Unit Weight (UC Test) | 0.008 | y = -0.035x + 31.09 |
| Eff. Friction Angle $\phi'$ | Natural Moisture Content ($w$) | 0.005 | y = 0.040x + 26.50 |
| Eff. Friction Angle $\phi'$ | % Gravel | 0.003 | y = 0.034x + 27.26 |
| Eff. Friction Angle $\phi'$ | Specific Gravity ($G_s$) | 0.002 | y = 5.037x + 13.80 |

[Note] C-U = Consolidated-Undrained Triaxial; and UC = Unconfined Compression.

**Table 5.27:** Single-Variable Linear Correlations for Friction Angle of A-7-6 Soils

| Dependent Variable | Independent Variable | $R^2$ | Equation |
|---|---|---|---|
| *Friction Angle $\phi$* | *% Sand* | *0.480* | *y = 0.236x + 10.27* |
| Friction Angle $\phi$ | Unconf. Compr. Strength ($q_u$) | 0.408 | y = 0.153x + 8.620 |
| Friction Angle $\phi$ | Final Moisture Content (C-U Test) | 0.302 | y = -0.458x + 23.69 |
| Friction Angle $\phi$ | Dry Unit Weight (C-U Test) | 0.266 | y = 0.184x – 7.293 |
| Friction Angle $\phi$ | Liquid Limit (LL) | 0.237 | y = -0.170x + 21.38 |
| Friction Angle $\phi$ | % Clay | 0.223 | y = -0.155x + 21.06 |
| Friction Angle $\phi$ | % Silt | 0.163 | y = -0.067x + 15.74 |
| Friction Angle $\phi$ | Plasticity Index (PI) | 0.141 | y = -0.157x + 17.19 |
| Friction Angle $\phi$ | Dry Unit Weight (UC Test) | 0.088 | y = 0.133x – 1.032 |
| Friction Angle $\phi$ | % Compaction | 0.085 | y = 0.142x – 0.695 |
| Friction Angle $\phi$ | Plastic Limit (PL) | 0.059 | y = -0.357x + 20.59 |
| Friction Angle $\phi$ | % Gravel | 0.056 | y = -0.163x + 13.43 |
| Friction Angle $\phi$ | Natural Moisture Content (*w*) | 0.031 | y = -0.108x + 15.26 |
| Friction Angle $\phi$ | Effective Friction Angle ($\phi'$) | 0.031 | y = -0.204x + 18.48 |
| Friction Angle $\phi$ | Specific Gravity ($G_s$) | 0.011 | y = -12.44x + 46.44 |
| Friction Angle $\phi$ | Time for 50% Consolidation ($t_{50}$) | 0.011 | y = 0.010x + 12.47 |

**Table 5.28:** Single-Variable Linear Correlations for Cohesion of A-7-6 Soils

| Dependent Variable | Independent Variable | $R^2$ | Equation |
|---|---|---|---|
| Cohesion $c_u$ | Plastic Limit (PL) | 0.480 | y = -1.946x + 46.76 |
| Cohesion $c_u$ | % Compaction | 0.435 | y = 0.605x – 51.85 |
| Cohesion $c_u$ | Dry Unit Weight (UC Test) | 0.433 | y = 0.550x – 51.79 |
| Cohesion $c_u$ | Final Moisture Content (C-U Test) | 0.337 | y = -0.906x + 27.29 |
| Cohesion $c_u$ | Natural Moisture Content (*w*) | 0.331 | y = -0.654x + 20.01 |
| Cohesion $c_u$ | Liquid Limit (LL) | 0.278 | y = -0.457x + 28.09 |
| Cohesion $c_u$ | % Silt | 0.234 | y = -0.151x + 11.96 |
| Cohesion $c_u$ | % Clay | 0.166 | y = -0.270x + 19.48 |
| Cohesion $c_u$ | Time for 50% Consolidation ($t_{50}$) | 0.158 | y = -0.103x + 9.857 |
| Cohesion $c_u$ | % Gravel | 0.095 | y = 0.326x + 4.577 |
| Cohesion $c_u$ | % Sand | 0.076 | y = 0.149x + 4.012 |
| Cohesion $c_u$ | Plasticity Index (PI) | 0.033 | y = -0.198x + 11.05 |
| Cohesion $c_u$ | Unconf. Compr. Strength ($q_u$) | 0.032 | y = -0.094x + 8.275 |
| Cohesion $c_u$ | Effective Friction Angle ($\phi'$) | 0.019 | y = -0.531x + 20.40 |
| Cohesion $c_u$ | Internal Friction Angle ($\phi$) | 0.015 | y = 0.201x + 3.199 |
| Cohesion $c_u$ | Specific Gravity ($G_s$) | 0.004 | y = 13.30x – 30.10 |

[Note] C-U = Consolidated-Undrained Triaxial; and UC = Unconfined Compression.

**Table 5.29:** Single-Variable Linear Correlations for Effective-Stress Cohesion of A-7-6 Soils

| Dependent Variable | Independent Variable | $R^2$ | Equation |
|---|---|---|---|
| Cohesion c′ | % Sand | 0.781 | y = 0.286x + 0.557 |
| Cohesion c′ | Internal Friction Angle (ϕ) | 0.754 | y = 1.037x – 9.051 |
| Cohesion c′ | Final Moisture Content (C-U Test) | 0.753 | y = -0.635x + 18.62 |
| Cohesion c′ | Dry Unit Weight (C-U Test) | 0.731 | y = 0.256x – 24.44 |
| Cohesion c′ | Liquid Limit (LL) | 0.693 | y = -0.345x + 20.43 |
| Cohesion c′ | % Clay | 0.689 | y = -0.281x + 17.99 |
| Cohesion c′ | Plastic Limit (PL) | 0.640 | y = -1.004x + 24.44 |
| Cohesion c′ | Dry Unit Weight (UC Test) | 0.602 | y = 0.289x – 27.02 |
| Cohesion c′ | % Compaction | 0.601 | y = 0.317x – 26.94 |
| Cohesion c′ | % Silt | 0.567 | y = -0.110x + 8.000 |
| Cohesion c′ | Natural Moisture Content (*w*) | 0.434 | y = -0.334x + 10.56 |
| Cohesion c′ | Unconf. Compr. Strength ($q_u$) | 0.251 | y = 0.242x – 2.368 |
| Cohesion c′ | Time for 50% Consolidation ($t_{50}$) | 0.200 | y = -0.051x + 5.320 |
| Cohesion c′ | Plasticity Index (PI) | 0.122 | y = -0.178x + 8.150 |
| Cohesion c′ | Effective Friction Angle (ϕ') | 0.091 | y = -0.554x + 18.66 |
| Cohesion c′ | Specific Gravity ($G_s$) | 0.014 | y = 10.81x – 25.88 |
| Cohesion c′ | % Gravel | 0.002 | y = -0.025x + 3.933 |

[Note] C-U = Consolidated-Undrained Triaxial; and UC = Unconfined Compression.

### 5.3.4 All Four Soil Types Combined

Finally, the data compiled for all four soil types (A-4a, A-6a, A-6b, and A-7-6) were analyzed by the single-variable linear regression approach. Results are summarized in Tables 5.30 through 5.35. No statistically strong correlations can be detected anywhere. The case with the highest $R^2$ value (of 0.659) involved friction angle as the dependable variable and dry unit weight as the independent variable. This is understandable, considering the fact that hardly any positive results came out of three out of the four soil types.

**Table 5.30:** Single-Variable Linear Correlations for SPT-$(N_{60})_1$ of All Soil Types

| Dependent Variable y | Independent Variable x | $R^2$ | Equation |
|---|---|---|---|
| SPT-$(N_{60})_1$ | Unconf. Compr. Strength ($q_u$) | 0.118 | y = 0.266x + 21.64 |
| SPT-$(N_{60})_1$ | % Silt | 0.115 | y = -0.993x + 71.89 |
| SPT-$(N_{60})_1$ | % Clay | 0.071 | y = 0.555x + 14.74 |
| SPT-$(N_{60})_1$ | Effective Friction Angle ($\phi'$) | 0.050 | y = 1.258x – 9.975 |
| SPT-$(N_{60})_1$ | % Gravel | 0.034 | y = -0.517x + 36.18 |
| SPT-$(N_{60})_1$ | Final Moisture Content (C-U) | 0.028 | y = 0.662x + 20.97 |
| SPT-$(N_{60})_1$ | Dry Unit Weight (UC Test) | 0.027 | y = -0.296x + 67.08 |
| SPT-$(N_{60})_1$ | % Compaction | 0.027 | y = -0.296x + 62.87 |
| SPT-$(N_{60})_1$ | Friction Angle ($\phi$) | 0.025 | y = 0.373x + 23.84 |
| SPT-$(N_{60})_1$ | % Sand | 0.012 | y = 0.269x + 25.48 |
| SPT-$(N_{60})_1$ | Natural Moisture Content ($w$) | 0.012 | y = 0.588x + 23.51 |
| SPT-$(N_{60})_1$ | Dry Unit Weight (C-U Test) | 0.008 | y = -0.146x + 49.51 |
| SPT-$(N_{60})_1$ | Plastic Limit (PL) | 0.007 | y = 0.453x + 23.32 |
| SPT-$(N_{60})_1$ | Plasticity Index (PI) | 0.004 | y = -0.248x + 34.65 |
| SPT-$(N_{60})_1$ | Time for 50% Consol. ($t_{50}$) | 0.001 | y = 0.041x + 30.96 |
| SPT-$(N_{60})_1$ | Specific Gravity ($G_s$) | 0.000 | y = -5.283x + 45.79 |
| SPT-$(N_{60})_1$ | Liquid Limit (LL) | 0.000 | y = 0.032x + 30.54 |

**Table 5.31:** Single-Variable Linear Correlations for Unconfined Compression Strength of All Soil Types

| Dependent Variable y | Independent Variable x | $R^2$ | Equation |
|---|---|---|---|
| Unconf. Compr. Strength | % Silt | 0.271 | y = -0.853x + 69.07 |
| Unconf. Compr. Strength | Friction Angle ($\phi$) | 0.235 | y = 1.249x + 11.39 |
| Unconf. Compr. Strength | % Sand | 0.228 | y = 0.908x + 17.04 |
| Unconf. Compr. Strength | Dry Unit Weight (C-U Test) | 0.206 | y = 0.699x – 48.85 |
| Unconf. Compr. Strength | Final Moisture Content (C-U) | 0.189 | y = -1.385x + 59.50 |
| Unconf. Compr. Strength | Dry Unit Weight (UC Test) | 0.158 | y = 0.614x – 36.67 |
| Unconf. Compr. Strength | Plastic Limit (PL) | 0.154 | y = -2.174x + 75.65 |
| Unconf. Compr. Strength | Plasticity Index (PI) | 0.141 | y = -0.695x + 46.13 |
| Unconf. Compr. Strength | Liquid Limit (LL) | 0.117 | y = -0.439x + 49.82 |
| Unconf. Compr. Strength | Natural Moisture Content ($w$) | 0.106 | y = -1.009x + 50.33 |
| Unconf. Compr. Strength | % Compaction | 0.106 | y = 0.599x – 27.42 |
| Unconf. Compr. Strength | Time for 50% Consol. ($t_{50}$) | 0.069 | y = -0.173x + 36.77 |
| Unconf. Compr. Strength | Effective Friction Angle ($\phi'$) | 0.038 | y = 0.868x + 7.099 |
| Unconf. Compr. Strength | % Gravel | 0.032 | y = 0.565x + 30.17 |
| Unconf. Compr. Strength | % Clay | 0.022 | y = -0.180x + 40.69 |
| Unconf. Compr. Strength | Specific Gravity ($G_s$) | 0.002 | y = -23.09x + 96.32 |

[Note] C-U = Consolidated-Undrained Triaxial; and UC = Unconfined Compression.

**Table 5.32:** Single-Variable Linear Correlations for Effective-Stress Friction Angle of All Soil Types

| Dependent Variable y | Independent Variable x | $R^2$ | Equation |
|---|---|---|---|
| Eff. Friction Angle ϕ' | % Clay | 0.533 | y = -0.201x + 38.63 |
| Eff. Friction Angle ϕ' | Liquid Limit (LL) | 0.487 | y = -0.202x + 38.36 |
| Eff. Friction Angle ϕ' | Plasticity Index (PI) | 0.445 | y = -0.278x + 35.95 |
| Eff. Friction Angle ϕ' | Time for 50% Consol. ($t_{50}$) | 0.444 | y = -0.108x + 33.02 |
| Eff. Friction Angle ϕ' | Natural Moisture Content (*w*) | 0.434 | y = -0.462x + 38.57 |
| Eff. Friction Angle ϕ' | % Sand | 0.407 | y = 0.275x + 25.90 |
| Eff. Friction Angle ϕ' | Final Moisture Content (C-U) | 0.386 | y = -0.450x + 39.35 |
| Eff. Friction Angle ϕ' | Plastic Limit (PL) | 0.350 | y = -0.740x + 45.24 |
| Eff. Friction Angle ϕ' | Dry Unit Weight (C-U Test) | 0.330 | y = 0.204x + 6.840 |
| Eff. Friction Angle ϕ' | Dry Unit Weight (UC Test) | 0.326 | y = 0.200x + 8.002 |
| Eff. Friction Angle ϕ' | Friction Angle (ϕ) | 0.279 | y = 0.310x + 25.41 |
| Eff. Friction Angle ϕ' | % Compaction | 0.194 | y = 0.185x + 12.10 |
| Eff. Friction Angle ϕ' | % Gravel | 0.071 | y = 0.192x + 29.85 |
| Eff. Friction Angle ϕ' | Unconf. Compr. Strength ($q_u$) | 0.038 | y = 0.044x + 29.52 |
| Eff. Friction Angle ϕ' | Specific Gravity ($G_s$) | 3E(-5) | y = 0.620x + 29.37 |
| Eff. Friction Angle ϕ' | % Silt | 0.000 | y = -0.009x + 31.43 |

**Table 5.33:** Single-Variable Linear Correlations for Friction Angle of All Soil Types

| Dependent Variable | Independent Variable | $R^2$ | Equation |
|---|---|---|---|
| Friction Angle ϕ | Dry Unit Weight (C-U Test) | 0.659 | y = 0.486x – 39.49 |
| Friction Angle ϕ | Plastic Limit (PL) | 0.608 | y = -1.676x + 50.16 |
| Friction Angle ϕ | % Sand | 0.559 | y = 0.552x + 7.740 |
| Friction Angle ϕ | Final Moisture Content (C-U) | 0.556 | y = -0.923x + 35.08 |
| Friction Angle ϕ | Plasticity Index (PI) | 0.519 | y = -0.517x + 27.10 |
| Friction Angle ϕ | Liquid Limit (LL) | 0.513 | y = -0.356x + 30.92 |
| Friction Angle ϕ | Natural Moisture Content (*w*) | 0.380 | y = -0.744x + 30.08 |
| Friction Angle ϕ | % Clay | 0.300 | y = -0.259x + 27.72 |
| Friction Angle ϕ | Effective Friction Angle (ϕ′) | 0.279 | y = 0.898x – 9.782 |
| Friction Angle ϕ | Dry Unit Weight (UC Test) | 0.270 | y = 0.312x – 17.94 |
| Friction Angle ϕ | Time for 50% Consol. ($t_{50}$) | 0.247 | y = -0.129x + 20.40 |
| Friction Angle ϕ | Unconf. Compr. Strength ($q_u$) | 0.235 | y = 0.188x + 11.60 |
| Friction Angle ϕ | % Silt | 0.079 | y = -0.179x + 25.41 |
| Friction Angle ϕ | % Compaction | 0.075 | y = 0.195x – 2.067 |
| Friction Angle ϕ | % Gravel | 0.043 | y = 0.259x + 16.42 |
| Friction Angle ϕ | Specific Gravity ($G_s$) | 0.016 | y = -24.29x + 83.64 |

[Note] C-U = Consolidated-Undrained Triaxial; and UC = Unconfined Compression.

**Table 5.34:** Single-Variable Linear Correlations for Cohesion of All Soil Types

| Dependent Variable | Independent Variable | $R^2$ | Equation |
|---|---|---|---|
| Cohesion $c_u$ | Plastic Limit (PL) | 0.491 | y = -1.281x + 33.64 |
| Cohesion $c_u$ | Dry Unit Weight (C-U Test) | 0.481 | y = 0.332x – 30.06 |
| Cohesion $c_u$ | Final Moisture Content (C-U Test) | 0.453 | y = -0.678x + 21.93 |
| Cohesion $c_u$ | Time for 50% Consol. ($t_{50}$) | 0.444 | y = -0.169x + 12.61 |
| Cohesion $c_u$ | Liquid Limit (LL) | 0.417 | y = -0.299x + 20.33 |
| Cohesion $c_u$ | % Clay | 0.408 | y = -0.274x + 19.80 |
| Cohesion $c_u$ | Natural Moisture Content ($w$) | 0.403 | y = -0.612x + 19.30 |
| Cohesion $c_u$ | % Sand | 0.348 | y = 0.357x + 2.704 |
| Cohesion $c_u$ | Friction Angle ($\phi$) | 0.324 | y = 0.437x + 1.219 |
| Cohesion $c_u$ | Plasticity Index (PI) | 0.303 | y = -0.337x + 15.23 |
| Cohesion $c_u$ | Effective Friction Angle ($\phi'$) | 0.281 | y = 0.862x – 17.31 |
| Cohesion $c_u$ | Dry Unit Weight (UC Test) | 0.225 | y = 0.231x – 17.24 |
| Cohesion $c_u$ | % Compaction | 0.144 | y = 0.228x – 13.99 |
| Cohesion $c_u$ | % Silt | 0.042 | y = -0.112x + 13.93 |
| Cohesion $c_u$ | % Gravel | 0.015 | y = 0.122x + 8.913 |
| Cohesion $c_u$ | Specific Gravity ($G_s$) | 0.004 | y = -13.96x + 47.14 |
| Cohesion $c_u$ | Unconf. Compr. Strength ($q_u$) | 0.002 | y = -0.013x + 9.872 |

**Table 5.35:** Single-Variable Linear Correlations for Effective-Stress Cohesion of All Soil Types

| Dependent Variable | Independent Variable | $R^2$ | Equation |
|---|---|---|---|
| Cohesion $c'$ | Dry Unit Weight (C-U Test) | 0.129 | y = 0.091x – 6.858 |
| Cohesion $c'$ | Natural Moisture Content ($w$) | 0.125 | y = -0.187x + 6.987 |
| Cohesion $c'$ | % Sand | 0.117 | y = 0.110x + 1.978 |
| Cohesion $c'$ | Time for 50% Consol. ($t_{50}$) | 0.117 | y = -0.047x + 4.837 |
| Cohesion $c'$ | Effective Friction Angle ($\phi'$) | 0.103 | y = 0.292x – 5.123 |
| Cohesion $c'$ | % Clay | 0.096 | y = -0.071x + 6.718 |
| Cohesion $c'$ | Final Moisture Content (C-U Test) | 0.072 | y = -0.145x + 6.675 |
| Cohesion $c'$ | Plastic Limit (PL) | 0.055 | y = -0.239x + 8.531 |
| Cohesion $c'$ | Dry Unit Weight (UC Test) | 0.054 | y = 0.063x – 3.317 |
| Cohesion $c'$ | % Silt | 0.053 | y = -0.066x + 6.700 |
| Cohesion $c'$ | Liquid Limit (LL) | 0.047 | y = -0.053x + 5.932 |
| Cohesion $c'$ | Plasticity Index (PI) | 0.023 | y = -0.049x + 4.818 |
| Cohesion $c'$ | Specific Gravity ($G_s$) | 0.021 | y = -15.90x + 46.98 |
| Cohesion $c'$ | Friction Angle ($\phi$) | 0.021 | y = 0.057x + 2.893 |
| Cohesion $c'$ | % Compaction | 0.021 | y = 0.050x – 1.217 |
| Cohesion $c'$ | Unconf. Compr. Strength ($q_u$) | 0.019 | y = 0.021x + 3.243 |
| Cohesion $c'$ | % Gravel | 0.002 | y = -0.043x + 10.25 |

[Note] C-U = Consolidated-Undrained Triaxial; and UC = Unconfined Compression.

## 5.3 Single-Variable Nonlinear Regression Analysis

With the outcome of the linear regression analysis rather disappointing, nonlinear regression analyses were performed extensively on the geotechnical data compiled in the current study to uncover additional single-variable correlations useful to geotechnical engineers in Ohio. These analyses applied six different nonlinear models. The models were the exponential, logarithmic, power, hyperbolic, reciprocal, and second-degree polynomial. These are defined in the equations below:

| | | |
|---|---|---|
| $y = a_0 + a_1x + a_2x^2$ | $2^{nd}$ Degree Polynomial | (5.2) |
| $y = b\ x^m$ | Power | (5.3) |
| $y = b\ e^{mx}$ | Exponential | (5.4) |
| $y = b + Ln(x)$ | Logarithmic | (5.5) |
| $y = b + m\left(\frac{1}{x}\right)$ | Reciprocal | (5.6) |
| $y = \frac{b + mx}{x}$ | Hyperbolic | (5.7) |

The nonlinear regression model was applied to all of the variables identified along the correlation paths for each different soil type. With all the variables involved and the nonlinear functions enlisted above, the analysis created more than one hundred cases for each soil type. Among the variables, both the natural moisture content and % compaction were ties to the unconfined compression tests conducted in the project. There are two versions of the dry unit weight (one measured for the unconfined compression test and another measured during the C-U triaxial test). Units specified for the variables include

psi for the unconfined compression strength ($q_u$), degrees for friction angle ($\phi$) and effective-stress friction angle ($\phi'$), psi for cohesion ($c_u$) and effective-stress cohesion ($c'$) pcf for dry unit weight ($\gamma_d$), and minutes for 50% consolidation time ($t_{50}$).

### 5.3.1 A-4a Soils

Tables 5.36 through 5.41 present strongest nonlinear correlations identified for the SPT-$(N_{60})_1$, unconfined compression strength, effective-stress friction angle, angle of internal friction, cohesion, and effective-stress cohesion possessed by A-4a soils. Due to a lack of data, no analytical results are available for A-4b soils. The tables list results with the $R^2$ value above 0.50 or 0.60. All statistically strong correlations are marked with the $R^2$ values ($\geq$ 0.8) in bold to stand out. A large number (twenty-eight) of statistically strong correlations were discovered during the analysis, with most of them associated with either the friction angle, effective-stress friction angle, or effective-stress cohesion. Among the mathematical models, the hyperbolic function appears to have the best ability to describe the basic correlations existing for the A-4a soils. In some cases, other mathematical functions (power, exponential, logarithmic, reciprocal) also yielded good correlations. Cautions are recommended for any strong correlations identified through the polynomial function, because the 2$^{nd}$ degree polynomial tends to produce an imaginary peak over the range of independent variable. Out of the long list of the index and state properties employed in the analysis, % silt, % clay, dry unit weight ($\gamma_d$), and effective-stress friction angle ($\phi'$) surfaced as key independent variables.

**Table 5.36:** Single-Variable Nonlinear Regression Results for SPT-$(N_{60})_1$ of A-4a Soils

| Independent Variable x | Function | $R^2$ | Correlation Equation |
|---|---|---|---|
| Unconf. Compr. Strength ($q_u$) | Hyperbolic | **0.821** | $(N_{60})_1 = (60.84x - 973.2)/x$ |
| Plasticity Index (PI) | Polynomial | 0.661 | $(N_{60})_1 = -3.258x^2 + 66.58x - 291.1$ |
| Time for 50% Consolid. ($t_{50}$) | Hyperbolic | 0.616 | $(N_{60})_1 = (35.00x - 14.99)/x$ |
| Unconf. Compr. Strength ($q_u$) | Polynomial | 0.597 | $(N_{60})_1 = 0.018x^2 - 1.310x + 48.75$ |
| % Clay | Polynomial | 0.574 | $(N_{60})_1 = 0.820x^2 - 47.18x + 703.4$ |
| Effective Friction Angle ($\phi'$) | Polynomial | 0.564 | $(N_{60})_1 = 1.383x^2 - 90.33x + 1498.2$ |

**Table 5.37:** Single-Variable Nonlinear Regression Results for Unconfined Compression Strength of A-4a Soils

| Independent Variable x | Function | $R^2$ | Correlation Equation |
|---|---|---|---|
| % Silt | Power | **0.805** | $q_u = 3E08x^{-4.356}$ |
| % Silt | Exponential | 0.794 | $q_u = 2411.6e^{-0.105x}$ |
| % Clay | Hyperbolic | 0.793 | $q_u = (213.2x - 4912.0)/x$ |
| % Silt | Polynomial | 0.770 | $q_u = 0.550x^2 - 49.32x + 1124.7$ |
| % Clay | Polynomial | 0.701 | $q_u = 0.018x^2 + 4.434x - 102.1$ |
| % Clay | Log | 0.697 | $q_u = 163.6Ln(x) - 508.0$ |
| % Silt | Reciprocal | 0.695 | $q_u = 6718.0/x - 129.3$ |
| % Clay | Reciprocal | 0.688 | $q_u = -4775.0/x + 208.4$ |
| % Silt | Log | 0.677 | $q_u = -162.4Ln(x) + 638.4$ |
| Plasticity Index (PI) | Polynomial | 0.671 | $q_u = -4.430x^2 + 85.38x - 349.9$ |
| % Clay | Power | 0.635 | $q_u = 9E-05x^{3.8426}$ |
| % Clay | Exponential | 0.629 | $q_u = 0.8844e^{0.1288x}$ |
| % Silt | Hyperbolic | 0.605 | $q_u = (-121.1x + 6391.0)/x$ |

**Table 5.38:** Single-Variable Nonlinear Regression Results for Effective-Stress Friction Angle of A-4a Soils

| Independent Variable x | Function | $R^2$ | Correlation Equation |
|---|---|---|---|
| Time for 50% Consolid. ($t_{50}$) | Hyperbolic | **0.988** | $\phi' = (28.95x + 15.10)/x$ |
| Unconf. Compr. Strength ($q_u$) | Hyperbolic | **0.964** | $\phi' = (35.47x - 72.07)/x$ |
| Plasticity Index (PI) | Hyperbolic | **0.923** | $\phi' = (35.13x - 15.82)/x$ |
| Final Moisture Content (C-U Test) | Hyperbolic | **0.893** | $\phi' = (32.07x + 17.19)/x$ |
| Friction Angle ($\phi$) | Hyperbolic | **0.887** | $\phi' = (32.92x + 10.74)/x$ |
| Natural Moisture Content | Hyperbolic | **0.876** | $\phi' = (32.33x + 12.46)/x$ |
| % Sand | Hyperbolic | 0.788 | $\phi' = (50.88x - 436.9)/x$ |
| Liquid Limit (LL) | Hyperbolic | 0.787 | $\phi' = (33.56x - 4.635)/x$ |
| % Gravel | Hyperbolic | 0.759 | $\phi' = (-1487x + 530.8)/x$ |
| Plastic Limit (PL) | Hyperbolic | 0.712 | $\phi' = (29.26x + 66.43)/x$ |
| % Silt | Hyperbolic | 0.704 | $\phi' = (33.62x - 9.341)/x$ |

**Table 5.39:** Single-Variable Nonlinear Regression Results for Friction Angle of A-4a Soils

| Independent Variable x | Function | $R^2$ | Correlation Equation |
|---|---|---|---|
| Time for 50% Consolid. ($t_{50}$) | Hyperbolic | **0.923** | $\phi = (24.19x - 0.556)/x$ |
| Dry Unit Weight (C-U Test) | Hyperbolic | **0.882** | $\phi = (116.5x - 11800.0)/x$ |
| Dry Unit Weight (C-U Test) | Power | **0.858** | $\phi = 2E(-7)x^{3.8525}$ |
| Unconf. Compr. Strength ($q_u$) | Hyperbolic | **0.855** | $\phi = (23.26x + 57.19)/x$ |
| Dry Unit Weight (C-U Test) | Exponential | **0.855** | $\phi = 0.5039e^{0.0301x}$ |
| Dry Unit Weight (C-U Test) | Polynomial | **0.838** | $\phi = 0.0037x^2 - 0.237x - 6.747$ |
| Dry Unit Weight (C-U Test) | Log | **0.833** | $\phi = 91.63Ln(x) - 420.3$ |
| Dry Unit Weight (C-U Test) | Reciprocal | **0.828** | $\phi = -11634.0/x + 115.2$ |
| % Gravel | Hyperbolic | 0.618 | $\phi = (1260.0x + 425.5)/x$ |

[Note] C-U = Consolidated-Undrained Triaxial.

**Table 5.40:** Single-Variable Nonlinear Regression Results for Cohesion of A-4a Soils

| Independent Variable x | Function | $R^2$ | Correlation Equation |
|---|---|---|---|
| % Silt | Power | **0.805** | $c_u = 2E(+8)x^{-4.356}$ |
| % Silt | Exponential | 0.794 | $c_u = 1205.8e^{-0.105x}$ |
| % Clay | Hyperbolic | 0.793 | $c_u = (106.6x - 2456.2)/x$ |
| % Gravel | Hyperbolic | 0.771 | $c_u = (21.22x - 11.58)/x$ |
| % Silt | Polynomial | 0.770 | $c_u = 0.275x^2 - 24.66x + 562.3$ |
| % Clay | Polynomial | 0.701 | $c_u = 0.009x^2 + 2.217x - 51.06$ |
| % Clay | Log | 0.697 | $c_u = 81.80Ln(x) - 254.02$ |
| % Silt | Reciprocal | 0.696 | $c_u = 3359.2/x - 64.67$ |
| % Clay | Reciprocal | 0.688 | $c_u = -2387.6/x + 104.22$ |
| % Silt | Log | 0.677 | $c_u = -81.18Ln(x) + 319.2$ |
| Plasticity Index (PI) | Polynomial | 0.671 | $c_u = -2.215x^2 + 42.69x - 174.9$ |
| % Clay | Power | 0.635 | $c_u = 5E(-5)x^{3.8426}$ |
| % Clay | Exponential | 0.629 | $c_u = 0.442e^{0.1288x}$ |

**Table 5.41:** Single-Variable Nonlinear Regression Results for Effective-Stress Cohesion of A-4a Soils

| Independent Variable x | Function | $R^2$ | Correlation Equation |
|---|---|---|---|
| Effective Friction Angle ($\phi'$) | Power | **0.976** | $c' = 1E(-24)x^{16.13}$ |
| Effective Friction Angle ($\phi'$) | Exponential | **0.974** | $c' = 3E(-7)e^{0.497x}$ |
| Dry Unit Weight (C-U Test) | Polynomial | **0.965** | $c' = 0.545x^2 - 143.6x + 9461.0$ |
| Plasticity Index (PI) | Polynomial | **0.955** | $c' = -0.641x^2 + 13.28x - 60.08$ |
| % Clay | Polynomial | **0.951** | $c' = 0.456x^2 - 27.39x + 412.4$ |
| Effective Friction Angle ($\phi'$) | Polynomial | **0.926** | $c' = 0.210x^2 - 12.10x + 174.1$ |
| Effective Friction Angle ($\phi'$) | Hyperbolic | **0.910** | $c' = (55.50x - 1670.0)/x$ |
| Effective Friction Angle ($\phi'$) | Log | **0.909** | $c' = 51.24Ln(x) - 174.3$ |
| Effective Friction Angle ($\phi'$) | Reciprocal | **0.905** | $c' = -1656.0/x + 55.07$ |

**Table 5.41:** Single-Variable Nonlinear Regression Results for Effective-Stress Cohesion of A-4a Soils (cont'd)

| Independent Variable x | Function | $R^2$ | Correlation Equation |
|---|---|---|---|
| Unconf. Compr. Strength ($q_u$) | Hyperbolic | **0.877** | $c' = (10.38x - 197.6)/x$ |
| Friction Angle ($\phi$) | Polynomial | **0.867** | $c' = 0.424x^2 - 23.83x + 330.2$ |
| Final Moisture Content (C-U Test) | Polynomial | 0.784 | $c' = 1.004x^2 - 25.15x + 157.5$ |
| Time for 50% Consolid. ($t_{50}$) | Polynomial | 0.738 | $c' = -0.441x^2 + 3.061x + 1.786$ |
| % Gravel | Hyperbolic | 0.666 | $c' = (5.808x - 6.904)/x$ |

[Note] UC = Unconfined Compression.

### 5.3.2 A-6a Soils

Next, results of a series of single-variable nonlinear regression analysis are summarized for A-6a soils in Tables 5.42 through 5.47. Forty-three statistically strong correlations emerged during the analysis, with most of them associated with effective-stress friction angle and effective-stress cohesion. Among the mathematical models, the hyperbolic function proved to have the best ability to describe the basic correlations existing for the A-6a soils. Other mathematical functions (polynomial, power, exponential, reciprocal, log) also yielded some strong correlations. However, cautions are recommended for any strong correlations identified through the polynomial function, because the 2$^{nd}$ degree polynomial tends to produce an imaginary peak over the range of independent variable. Out of the long list of index and state properties, the time for 50% consolidation ($t_{50}$), measured during each C-U triaxial compression test, surfaced as the most important independent variables.

**Table 5.42:** Single-Variable Nonlinear Regression Results for SPT-$(N_{60})_1$ of A-6a Soils

| Independent Variable x | Function | $R^2$ | Correlation Equation |
|---|---|---|---|
| Time for 50% Consol. ($t_{50}$) | Hyperbolic | **0.845** | $(N_{60})_1 = (35.80x - 14.37)/x$ |
| Dry Unit Weight (UC Test) | Polynomial | 0.584 | $(N_{60})_1 = -0.268x^2 + 63.02x - 3661.0$ |
| % Compaction | Polynomial | 0.583 | $(N_{60})_1 = -0.326x^2 + 69.68x - 3680.0$ |
| % Gravel | Polynomial | 0.522 | $(N_{60})_1 = 0.724x^2 - 14.97x + 97.85$ |

**Table 5.43:** Single-Variable Nonlinear Regression Results for Unconfined Compression Strength of A-6a Soils

| Independent Variable x | Function | $R^2$ | Correlation Equation |
|---|---|---|---|
| Time for 50% Consol. ($t_{50}$) | Hyperbolic | **0.890** | $q_u = (39.27x - 2.316)/x$ |
| Friction Angle ($\phi$) | Hyperbolic | 0.548 | $q_u = (55.63x - 348.9)/x$ |

**Table 5.44:** Single-Variable Nonlinear Regression Results for Effective-Stress Friction Angle of A-6a Soils

| Independent Variable x | Function | $R^2$ | Correlation Equation |
|---|---|---|---|
| Time for 50% Consolid. ($t_{50}$) | Hyperbolic | **0.992** | $\phi' = (30.37x + 19.34)/x$ |
| % Gravel | Hyperbolic | **0.979** | $\phi' = (31.86x + 10.93)/x$ |
| Unconf. Compr. Strength ($q_u$) | Hyperbolic | **0.960** | $\phi' = (31.00x + 87.93)/x$ |
| Liquid Limit (LL) | Hyperbolic | **0.945** | $\phi' = (32.21x + 31.35)/x$ |
| Friction Angle ($\phi$) | Hyperbolic | **0.935** | $\phi' = (33.28x + 4.509)/x$ |
| % Sand | Hyperbolic | **0.927** | $\phi' = (38.13x - 108.5)/x$ |
| % Clay | Hyperbolic | **0.881** | $\phi' = (31.19x + 63.35)/x$ |
| Plasticity Index (PI) | Hyperbolic | **0.857** | $\phi' = (33.11x + 4.525)/x$ |
| Final Moisture Content (C-U Test) | Hyperbolic | **0.844** | $\phi' = (35.56x - 32.81)/x$ |
| Natural Moisture Content ($w$) | Hyperbolic | 0.765 | $\phi' = (36.57x - 40.53)/x$ |
| Plastic Limit (PL) | Hyperbolic | 0.686 | $\phi' = (28.51x + 88.43)/x$ |

[Note] C-U = Consolidated-Undrained Triaxial.

**Table 5.45:** Single-Variable Nonlinear Regression Results for Friction Angle of A-6a Soils

| Independent Variable x | Function | $R^2$ | Correlation Equation |
|---|---|---|---|
| Time for 50% Consolid. ($t_{50}$) | Hyperbolic | **0.930** | $\phi = (18.85x + 8.170)/x$ |
| Unconf. Compr. Strength ($q_u$) | Hyperbolic | **0.828** | $\phi = (27.17x - 245.7)/x$ |
| % Clay | Hyperbolic | 0.599 | $\phi = (29.67x - 269.2)/x$ |
| % Sand | Hyperbolic | 0.586 | $\phi = (27.79x - 179.0)/x$ |
| % Gravel | Exponential | 0.564 | $\phi = 31.40e^{-0.06x}$ |
| % Gravel | Polynomial | 0.542 | $\phi = -0.091x^2 + 0.554x + 21.79$ |
| Specific Gravity ($G_s$) | Polynomial | 0.534 | $\phi = -2778.x^2 + 15169x - 20678$ |
| Plasticity Index (PI) | Polynomial | 0.504 | $\phi = -0.555x^2 + 12.98x - 53.48$ |

**Table 5.46:** Single-Variable Nonlinear Regression Results for Cohesion of A-6a Soils

| Independent Variable x | Function | $R^2$ | Correlation Equation |
|---|---|---|---|
| Effective Friction Angle ($\phi'$) | Polynomial | **0.860** | $c_u = -1.258x^2 + 84.78x - 1414.0$ |
| Specific Gravity ($G_s$) | Polynomial | **0.823** | $c_u = -1846.0x^2 + 9975.0x - 13459.0$ |
| Time for 50% Consolid. ($t_{50}$) | Hyperbolic | 0.758 | $c_u = (10.88x + 5.359)/x$ |
| % Sand | Hyperbolic | 0.748 | $c_u = (43.56x - 776.1)/x$ |
| Natural Moisture Content ($w$) | Polynomial | 0.736 | $c_u = 1.251x^2 - 34.37x + 245.0$ |
| Effective Friction Angle ($\phi'$) | Power | 0.709 | $c_u = 5E(-9)x^{6.162}$ |
| Effective Friction Angle ($\phi'$) | Exponential | 0.698 | $c_u = 0.023e^{0.185x}$ |
| Effective Friction Angle ($\phi'$) | Hyperbolic | 0.692 | $c_u = (70.03x - 1942.3)/x$ |
| Specific Gravity ($G_s$) | Exponential | 0.688 | $c_u = 2E(+10)e^{-7.91x}$ |
| Specific Gravity ($G_s$) | Power | 0.684 | $c_u = 2E(+10)x^{-21.40}$ |
| Effective Friction Angle ($\phi'$) | Reciprocal | 0.642 | $c_u = -2006.0/x + 71.94$ |
| Effective Friction Angle ($\phi'$) | Log | 0.631 | $c_u = 60.49Ln(x) - 200.4$ |
| Unconf. Compr. Strength ($q_u$) | Polynomial | 0.616 | $c_u = -0.016x^2 + 1.278x - 10.90$ |
| Specific Gravity ($G_s$) | Log | 0.615 | $c_u = -211.0Ln(x) + 223.1$ |
| Specific Gravity ($G_s$) | Reciprocal | 0.612 | $c_u = 574.9/x - 200.1$ |

**Table 5.47:** Single-Variable Nonlinear Regression Results for Effective-Stress Cohesion of A-6a Soils

| Independent Variable x | Function | $R^2$ | Correlation Equation |
|---|---|---|---|
| Natural Moisture Content ($w$) | Polynomial | **1.000** | $c' = 1.819x^2 - 49.27x + 334.1$ |
| Time for 50% Consolid. ($t_{50}$) | Polynomial | **0.979** | $c' = 0.165x^2 - 2.701x + 12.15$ |
| % Clay | Polynomial | **0.977** | $c' = -0.936x^2 + 57.40x - 873.1$ |
| Friction Angle ($\phi$) | Polynomial | **0.965** | $c' = -0.416x^2 + 16.73x - 160.9$ |
| Specific Gravity ($G_s$) | Power | **0.951** | $c' = 4E(+30)x^{-69.5}$ |
| Specific Gravity ($G_s$) | Exponential | **0.950** | $c' = 4E(+30)e^{-25.5x}$ |
| Specific Gravity ($G_s$) | Polynomial | **0.948** | $c' = 785.2x^2 - 4342.0x + 6003.0$ |

**Table 5.47:** Single-Variable Nonlinear Regression Results for Effective-Stress Cohesion of A-6a Soils (cont'd)

| Independent Variable x | Function | $R^2$ | Correlation Equation |
|---|---|---|---|
| % Silt | Hyperbolic | **0.935** | $c' = (56.54x - 2042.0)/x$ |
| % Gravel | Polynomial | **0.934** | $c' = -2.070x^2 + 22.63x - 55.84$ |
| % Silt | Log | **0.929** | $c' = 53.10\text{Ln}(x) - 190.4$ |
| % Silt | Reciprocal | **0.929** | $c' = -2042.0/x + 56.54$ |
| Specific Gravity ($G_s$) | Reciprocal | **0.885** | $c' = 505.7/x - 182.8$ |
| % Silt | Power | **0.884** | $c' = 6E(-30)x^{18.71}$ |
| % Silt | Exponential | **0.884** | $c' = 2E(-8)e^{0.486x}$ |
| % Compaction | Polynomial | **0.883** | $c' = -0.052x^2 + 10.61x - 534.1$ |
| Dry Unit Weight (UC Test) | Polynomial | **0.883** | $c' = -0.042x^2 + 9.505x - 526.1$ |
| Specific Gravity ($G_s$) | Log | **0.883** | $c' = -185.0\text{Ln}(x) + 188.8$ |
| Specific Gravity ($G_s$) | Hyperbolic | **0.881** | $c' = (-182.0x + 503.3)/x$ |
| Dry Unit Weight (C-U Test) | Power | **0.834** | $c' = 2E(+67)x^{-32.0}$ |
| Dry Unit Weight (C-U Test) | Exponential | **0.834** | $c' = 2E(+14)e^{-0.26x}$ |
| Dry Unit Weight (UC Test) | Exponential | **0.830** | $c' = 2E(+7)e^{-0.13x}$ |
| % Compaction | Exponential | **0.829** | $c' = 2E(+7)e^{-0.14x}$ |
| % Clay | Log | **0.827** | $c' = -50.1\text{Ln}(x) + 177.2$ |
| Dry Unit Weight (UC Test) | Power | **0.819** | $c' = 2E(+32)x^{-15.4}$ |
| % Clay | Reciprocal | **0.819** | $c' = 1570.0/x - 45.73$ |
| % Compaction | Power | **0.818** | $c' = 6E(+31)x^{-15.4}$ |
| Final Moisture Content (C-U) | Exponential | **0.809** | $c' = 0.001e^{0.448x}$ |
| Final Moisture Content (C-U) | Power | **0.807** | $c' = 5E(-9)x^{7.145}$ |

### 5.3.3 A-6b Soils

Tables 5.48 through 5.53 present strongest nonlinear correlations identified for the SPT-$(N_{60})_1$, unconfined compression strength, effective-stress friction angle, angle of internal friction, cohesion, and effective-stress cohesion possessed by the A-6b soils. Tables 5.48 and 5.50 list results having the $R^2$ value above 0.50 or 0.60. Other tables present results with the $R^2$ value higher than 0.80. More than one hundred statistically strong correlations were discovered during the analysis, with some of them having the $R^2$ value rounded off to 1.00. Among the mathematical models, the hyperbolic function appeared to have the best ability to describe the basic correlations existing for the A-6b soils. Other mathematical functions (polynomial, power, exponential, logarithmic,

reciprocal) also yielded good results. Cautions are recommended for any strong correlations identified through the polynomial function, because the 2nd degree polynomial tends to produce an imaginary peak for the dependent variable. % silt, % clay, plasticity index (PI), dry unit weight ($\gamma_d$), time for 50% consolidation ($t_{50}$), and specific gravity ($G_s$) surfaced as key independent variables.

**Table 5.48:** Single-Variable Nonlinear Regression Results for SPT-$(N_{60})_1$ of A-6b Soils

| Independent Variable x | Function | $R^2$ | Correlation Equation |
|---|---|---|---|
| Time for 50% Consol. ($t_{50}$) | Hyperbolic | **0.988** | $(N_{60})_1 = (33.32x - 48.37)/x$ |
| Unconf. Compr. Strength ($q_u$) | Hyperbolic | **0.840** | $(N_{60})_1 = (40.25x - 291.9)/x$ |
| % Gravel | Hyperbolic | **0.826** | $(N_{60})_1 = (41.74x - 130.2)/x$ |
| % Gravel | Power | 0.653 | $(N_{60})_1 = 6.651x^{0.580}$ |
| Plastic Limit (PL) | Polynomial | 0.649 | $(N_{60})_1 = -3.889x^2 + 153.7x - 1482.0$ |
| % Gravel | Polynomial | 0.630 | $(N_{60})_1 = -0.125x^2 + 4.332x - 3.002$ |
| % Gravel | Exponential | 0.612 | $(N_{60})_1 = 13.47e^{0.056x}$ |
| % Clay | Hyperbolic | 0.587 | $(N_{60})_1 = (45.36x - 553.9)/x$ |
| % Gravel | Log | 0.586 | $(N_{60})_1 = 14.66Ln(x) - 6.872$ |
| Friction Angle ($\phi$) | Hyperbolic | 0.561 | $(N_{60})_1 = (46.45x - 258.2)/x$ |
| % Clay | Polynomial | 0.560 | $(N_{60})_1 = 0.232x^2 - 17.1x + 327.4$ |
| % Gravel | Reciprocal | 0.533 | $(N_{60})_1 = -114.3/x + 40.23$ |
| Plasticity Index (PI) | Polynomial | 0.502 | $(N_{60})_1 = 3.677x^2 - 131.2x + 1189.0$ |

**Table 5.49:** Single-Variable Nonlinear Regression Results for Unconfined Compression Strength of A-6b Soils

| Independent Variable x | Function | $R^2$ | Correlation Equation |
|---|---|---|---|
| Specific Gravity ($G_s$) | Polynomial | **0.998** | $q_u = 42764x^2 - 23217x + 31513$ |
| Plastic Limit (PL) | Polynomial | **0.997** | $q_u = 6.632x^2 - 285.7x + 3095.0$ |
| Plasticity Index (PI) | Polynomial | **0.985** | $q_u = 2.472x^2 - 78.53x + 643.0$ |
| Friction Angle ($\phi$) | Polynomial | **0.979** | $q_u = 0.639x^2 - 15.77x + 115.7$ |
| % Clay | Polynomial | **0.974** | $q_u = 0.217x^2 - 14.33x + 252.1$ |
| Specific Gravity ($G_s$) | Power | **0.965** | $q_u = 1E(+26)x^{-56.6}$ |
| Specific Gravity ($G_s$) | Exponential | **0.964** | $q_u = 1E(+26)e^{-20.9x}$ |
| % Silt | Power | **0.958** | $q_u = 3E(+6)x^{-3.03}$ |
| % Silt | Polynomial | **0.953** | $q_u = 0.269x^2 - 24.88x + 593.0$ |
| % Silt | Exponential | **0.950** | $q_u = 689.6e^{-0.07x}$ |
| Plasticity Index (PI) | Hyperbolic | **0.946** | $q_u = (234.8x - 3515.0)/x$ |
| Plasticity Index (PI) | Exponential | **0.933** | $q_u = 0.168e^{0.293x}$ |
| Specific Gravity ($G_s$) | Log | **0.931** | $q_u = -2037Ln(x) + 2065.0$ |
| Specific Gravity ($G_s$) | Reciprocal | **0.931** | $q_u = 5512.0/x - 1999.0$ |

**Table 5.49:** Single-Variable Nonlinear Regression Results for Unconfined Compression Strength of A-6b Soils (cont'd)

| Independent Variable x | Function | $R^2$ | Correlation Equation |
|---|---|---|---|
| Specific Gravity ($G_s$) | Hyperbolic | **0.929** | $q_u = (-1997.0x + 5507.0)/x$ |
| Plasticity Index (PI) | Log | **0.925** | $q_u = 192.0Ln(x) - 516.4$ |
| % Silt | Reciprocal | **0.924** | $q_u = 4410.0/x - 72.55$ |
| Plasticity Index (PI) | Power | **0.923** | $q_u = 9E(-06)x^{5.242}$ |
| % Silt | Log | **0.914** | $q_u = -108.0Ln(x) + 439.2$ |
| Time for 50% Consol. ($t_{50}$) | Hyperbolic | **0.913** | $q_u = (19.06x + 106.1)/x$ |
| Plasticity Index (PI) | Reciprocal | **0.911** | $q_u = -3408.0/x + 228.6$ |
| % Clay | Hyperbolic | **0.909** | $q_u = (115.1x - 2785.0)/x$ |
| % Clay | Exponential | **0.905** | $q_u = 3.901e^{0.056x}$ |
| Friction Angle ($\phi$) | Hyperbolic | **0.899** | $q_u = (119.5x - 1273.0)/x$ |
| Plastic Limit (PL) | Reciprocal | **0.890** | $q_u = 6119.0/x - 264.6$ |
| Plastic Limit (PL) | Power | **0.887** | $q_u = 2E(+12)x^{-8.19}$ |
| % Clay | Power | **0.880** | $q_u = 0.020x^{2.039}$ |
| Plastic Limit (PL) | Log | **0.878** | $q_u = -298.0Ln(x) + 935.4$ |
| Plastic Limit (PL) | Exponential | **0.875** | $q_u = 10839.0e^{-0.39x}$ |
| % Silt | Hyperbolic | **0.864** | $q_u = (-70.26x + 4313.0)/x$ |
| % Clay | Log | **0.851** | $q_u = 73.4Ln(x) - 227.4$ |
| Friction Angle ($\phi$) | Exponential | **0.848** | $q_u = 3.799e^{0.130x}$ |
| Plastic Limit (PL) | Hyperbolic | **0.848** | $q_u = (-256.0x + 5941.0)/x$ |
| % Clay | Reciprocal | **0.822** | $q_u = -2595.0/x + 109.6$ |

**Table 5.50:** Single-Variable Nonlinear Regression Results for Effective-Stress Friction Angle of A-6b Soils

| Independent Variable x | Function | $R^2$ | Correlation Equation |
|---|---|---|---|
| Time for 50% Consolid. ($t_{50}$) | Hyperbolic | **0.998** | $\phi' = (29.75x + 6.659)/x$ |
| Unconf. Compr. Strength ($q_u$) | Hyperbolic | **0.995** | $\phi' = (27.98x + 73.62)/x$ |
| % Gravel | Hyperbolic | **0.980** | $\phi' = (28.48x + 23.77)/x$ |
| % Clay | Hyperbolic | **0.956** | $\phi' = (25.56x + 178.1)/x$ |
| % Silt | Hyperbolic | **0.956** | $\phi' = (38.48x - 321.6)/x$ |
| Friction Angle ($\phi$) | Hyperbolic | **0.946** | $\phi' = (24.88x + 91.21)/x$ |
| % Sand | Hyperbolic | **0.938** | $\phi' = (25.55x + 73.14)/x$ |
| % Compaction | Hyperbolic | **0.938** | $\phi' = (-15.44x + 2159.0)/x$ |
| Final Moisture Content (C-U Test) | Hyperbolic | **0.873** | $\phi' = (34.89x - 74.34)/x$ |
| Natural Moisture Content ($w$) | Hyperbolic | **0.847** | $\phi' = (22.83x + 121.9)/x$ |
| Plastic Limit (PL) | Hyperbolic | **0.823** | $\phi' = (47.87x - 350.8)/x$ |
| Dry Unit Weight (UC Test) | Hyperbolic | 0.736 | $\phi' = (48.72x - 2124.0)/x$ |
| Plasticity Index (PI) | Hyperbolic | 0.675 | $\phi' = (18.31x + 219.3)/x$ |
| Natural Moisture Content ($w$) | Polynomial | 0.621 | $\phi' = -0.527x^2 + 16.58x - 96.99$ |
| % Silt | Polynomial | 0.620 | $\phi' = 0.030x^2 - 2.281x + 72.00$ |
| Unconf. Compr. Strength ($q_u$) | Polynomial | 0.620 | $\phi' = 0.019x^2 - 1.649x + 57.00$ |

**Table 5.51:** Single-Variable Nonlinear Regression Results for Friction Angle of A-6b Soils

| Independent Variable x | Function | $R^2$ | Correlation Equation |
|---|---|---|---|
| Unconf. Compr. Strength ($q_u$) | Hyperbolic | **0.995** | $\phi = (24.05x - 220.0)/x$ |
| % Clay | Hyperbolic | **0.988** | $\phi = (32.42x - 563.5)/x$ |
| Time for 50% Consolid. ($t_{50}$) | Hyperbolic | **0.983** | $\phi = (9.685x + 49.67.0)/x$ |
| Plasticity Index (PI) | Hyperbolic | **0.966** | $\phi = (53.46x - 660.9)/x$ |
| Natural Moisture Content ($w$) | Hyperbolic | **0.955** | $\phi = (42.59x - 411.5)/x$ |
| % Clay | Polynomial | **0.925** | $\phi = -0.007x^2 + 0.981x - 9.239$ |
| % Clay | Log | **0.925** | $\phi = 15.51Ln(x) - 39.27$ |
| % Clay | Reciprocal | **0.924** | $\phi = -560.0/x + 32.31$ |
| Plasticity Index (PI) | Polynomial | **0.919** | $\phi = 0.002x^2 + 1.941x - 19.47$ |
| Plastic Limit (PL) | Polynomial | **0.919** | $\phi = 2.038x^2 - 85.63x + 911.5$ |
| Plasticity Index (PI) | Log | **0.919** | $\phi = 36.751Ln(x) - 89.67$ |
| Plasticity Index (PI) | Reciprocal | **0.917** | $\phi = -658.0/x + 53.29$ |
| Dry Unit Weight (UC Test) | Polynomial | **0.910** | $\phi = 0.024x^2 - 6.269x + 419.8$ |
| Effective Friction Angle ($\phi'$) | Polynomial | **0.910** | $\phi = 0.029x^2 - 7.044x + 427.8$ |
| Dry Unit Weight (UC Test) | Reciprocal | **0.905** | $\phi = 8197.0/x - 53.36$ |
| Effective Friction Angle ($\phi'$) | Reciprocal | **0.904** | $\phi = 7453.0/x - 53.37$ |
| Dry Unit Weight (UC Test) | Log | **0.903** | $\phi = -69.6Ln(x) + 348.3$ |
| Effective Friction Angle ($\phi'$) | Log | **0.903** | $\phi = -69.6Ln(x) + 341.7$ |
| Natural Moisture Content ($w$) | Polynomial | **0.883** | $\phi = 0.273x^2 - 7.229x + 60.71$ |
| % Silt | Polynomial | **0.876** | $\phi = 0.052x^2 - 4.798x + 123.4$ |
| Time for 50% Consolid. ($t_{50}$) | Polynomial | **0.873** | $\phi = 0.015x^2 - 1.042x + 28.10$ |
| % Clay | Power | **0.871** | $\phi = 0.494x^{0.968}$ |
| Plasticity Index (PI) | Power | **0.870** | $\phi = 0.021x^{2.298}$ |
| Plasticity Index (PI) | Exponential | **0.868** | $\phi = 1.606e^{0.127x}$ |
| Specific Gravity ($G_s$) | Polynomial | **0.865** | $\phi = -145.9x + 411.4$ |
| Specific Gravity ($G_s$) | Log | **0.865** | $\phi = -394.Ln(x) + 409.5$ |
| Specific Gravity ($G_s$) | Reciprocal | **0.865** | $\phi = 1067./x - 377.8$ |
| % Clay | Exponential | **0.864** | $\phi = 6.048e^{0.026x}$ |
| Natural Moisture Content ($w$) | Log | **0.861** | $\phi = 25.52Ln(x) - 54.15$ |
| % Gravel | Polynomial | **0.860** | $\phi = 0.170x^2 - 3.329x + 27.32$ |
| Dry Unit Weight (UC Test) | Power | **0.856** | $\phi = 2E(+10)x^{-4.35}$ |
| Effective Friction Angle ($\phi'$) | Power | **0.856** | $\phi = 1E(+10)x^{-4.35}$ |
| Dry Unit Weight (UC Test) | Exponential | **0.856** | $\phi = 1245.0e^{-0.03x}$ |
| Effective Friction Angle ($\phi'$) | Exponential | **0.855** | $\phi = 1245.0e^{-0.04x}$ |
| Natural Moisture Content ($w$) | Reciprocal | **0.853** | $\phi = -403.7/x + 42.08$ |
| Specific Gravity ($G_s$) | Hyperbolic | **0.852** | $\phi = (-377.8x + 1067.0)/x$ |
| Unconf. Compr. Strength ($q_u$) | Log | **0.848** | $\phi = 6.504Ln(x) - 6.355$ |
| % Silt | Reciprocal | **0.847** | $\phi = 849.5/x - 4.608$ |

**Table 5.51:** Single-Variable Nonlinear Regression Results for Friction Angle of A-6b Soils (cont'd)

| Independent Variable x | Function | $R^2$ | Correlation Equation |
|---|---|---|---|
| % Silt | Log | **0.840** | $\phi = -21.0\text{Ln}(x) + 94.49$ |
| Dry Unit Weight (UC Test) | Hyperbolic | **0.836** | $\phi = (-53.16x + 8172.0)/x$ |
| Effective Friction Angle ($\phi'$) | Hyperbolic | **0.835** | $\phi = (-53.15x + 7429.0)/x$ |
| Unconf. Compr. Strength ($q_u$) | Reciprocal | **0.831** | $\phi = -213.8/x + 23.82$ |
| % Gravel | Hyperbolic | **0.806** | $\phi = (21.80x - 69.90)/x$ |

[Note] UC = Unconfined Compression.

**Table 5.52:** Single-Variable Nonlinear Regression Results for Cohesion of A-6b Soils

| Independent Variable x | Function | $R^2$ | Correlation Equation |
|---|---|---|---|
| Plasticity Index (PI) | Polynomial | **1.000** | $c_u = -2.351x^2 + 85.94x - 768.7$ |
| % Gravel | Polynomial | **1.000** | $c_u = 0.225x^2 - 5.468x + 37.43$ |
| % Clay | Polynomial | **1.000** | $c_u = -0.142x^2 + 10.96x - 190.8$ |
| % Silt | Polynomial | **1.000** | $c_u = -0.906x^2 + 73.94x - 1457.0$ |
| % Sand | Polynomial | **1.000** | $c_u = -0.640x^2 + 18.78x - 124.7$ |
| Plastic Limit (PL) | Polynomial | **1.000** | $c_u = 3.636x^2 - 148.0x + 1509.0$ |
| Dry Unit Weight (UC Test) | Polynomial | **1.000** | $c_u = -0.217x^2 + 50.92x - 2962.0$ |
| Natural Moisture Content ($w$) | Polynomial | **1.000** | $c_u = -26.63x^2 + 866.8x - 6910.0$ |
| Final Moisture Content (C-U) | Polynomial | **1.000** | $c_u = 51.97x^2 - 1997.x + 19180.0$ |
| Unconf. Compr. Strength ($q_u$) | Polynomial | **1.000** | $c_u = -2.907x^2 + 236.8x - 3592.0$ |
| Time for 50% Consolid. ($t_{50}$) | Polynomial | **1.000** | $c_u = 0.095x^2 - 4.043x + 38.54$ |
| Friction Angle ($\phi$) | Polynomial | **1.000** | $c_u = -0.566x^2 + 19.19x - 146.0$ |
| Effective Friction Angle ($\phi'$) | Polynomial | **1.000** | $c_u = -21.13x^2 + 1285x - 19514.0$ |
| % Compaction | Polynomial | **1.000** | $c_u = -0.261x^2 + 55.59x - 2940.0$ |
| Dry Unit Weight (C-U Test) | Polynomial | **1.000** | $c_u = -0.006x^2 + 2.207x - 157.8$ |
| Dry Unit Weight (C-U Test) | Reciprocal | **1.000** | $c_u = -9277.0/x + 90.17$ |
| Dry Unit Weight (C-U Test) | Hyperbolic | **1.000** | $c_u = (90.16x - 9276.0)/x$ |
| Dry Unit Weight (C-U Test) | Log | **0.999** | $c_u = 81.67\text{Ln}(x) - 378.0$ |
| Dry Unit Weight (C-U Test) | Power | **0.980** | $c_u = 1\text{E}(-21)x^{10.58}$ |
| Time for 50% Consolid. ($t_{50}$) | Power | **0.974** | $c_u = 52.14x^{-0.72}$ |
| Time for 50% Consolid. ($t_{50}$) | Reciprocal | **0.957** | $c_u = 81.56/x + 1.555$ |
| Time for 50% Consolid. ($t_{50}$) | Exponential | **0.954** | $c_u = 15.76e^{-0.04x}$ |
| Final Moisture Content (C-U) | Power | **0.942** | $c_u = 3\text{E}(+16)x^{-12.2}$ |
| Final Moisture Content (C-U) | Exponential | **0.942** | $c_u = 1\text{E}(+6)e^{-0.63x}$ |
| Liquid Limit (LL) | Power | **0.930** | $c_u = 2\text{E}(-27)x^{17.47}$ |
| Liquid Limit (LL) | Exponential | **0.930** | $c_u = 2\text{E}(-7)e^{0.459x}$ |
| Time for 50% Consolid. ($t_{50}$) | Log | **0.920** | $c_u = -5.39\text{Ln}(x) + 22.71$ |
| Time for 50% Consolid. ($t_{50}$) | Hyperbolic | **0.909** | $c_u = (1.837x + 78.06)/x$ |
| Unconf. Compr. Strength ($q_u$) | Hyperbolic | **0.887** | $c_u = (10.01x - 29.28)/x$ |
| Final Moisture Content (C-U) | Reciprocal | **0.873** | $c_u = 1723.0/x - 82.26$ |

[Note] C-U = Consolidated-Undrained Triaxial; and UC = Unconfined Compression.

**Table 5.52:** Single-Variable Nonlinear Regression Results for Cohesion of A-6b Soils (cont'd)

| Independent Variable x | Function | $R^2$ | Correlation Equation |
|---|---|---|---|
| Final Moisture Content (C-U) | Log | **0.872** | $c_u = -89.9Ln(x) + 273.3$ |
| Liquid Limit (LL) | Hyperbolic | **0.863** | $c_u = (135.8x - 4862.0)/x$ |
| Final Moisture Content (C-U) | Hyperbolic | **0.860** | $c_u = (-82.13x + 1721.0)/x$ |
| Liquid Limit (LL) | Log | **0.855** | $c_u = 128.0Ln(x) - 457.9$ |
| Liquid Limit (LL) | Reciprocal | **0.855** | $c_u = -4862.0/x + 135.8$ |

[Note] C-U = Consolidated-Undrained Triaxial; and UC = Unconfined Compression.

**Table 5.53:** Single-Variable Nonlinear Regression Results for Effective-Stress Cohesion of A-6b Soils

| Independent Variable x | Function | $R^2$ | Correlation Equation |
|---|---|---|---|
| Dry Unit Weight (C-U Test) | Polynomial | **1.000** | $c' = 0.090x^2 - 19.95x + 1106.0$ |
| % Compaction | Polynomial | **1.000** | $c' = -0.238x^2 + 50.99x - 2717.0$ |
| Effective Friction Angle ($\phi'$) | Polynomial | **1.000** | $c' = -17.45x^2 + 1062.0x - 16154.0$ |
| Friction Angle ($\phi$) | Polynomial | **1.000** | $c' = -0.516x^2 + 17.03x - 129.4$ |
| Time for 50% Consolid. ($t_{50}$) | Polynomial | **1.000** | $c' = 0.186x^2 - 7.470x + 55.74$ |
| Unconf. Compr. Strength ($q_u$) | Polynomial | **1.000** | $c' = -2.330x^2 + 189.7x - 2880.0$ |
| Final Moisture Content (C-U) | Polynomial | **1.000** | $c' = 96.29x^2 - 3695.0x + 35410.0$ |
| Plastic Limit (PL) | Polynomial | **1.000** | $c' = 2.391x^2 - 96.16x + 966.6$ |
| % Silt | Polynomial | **1.000** | $c' = -0.742x^2 + 60.82x - 1206.0$ |
| % Sand | Polynomial | **1.000** | $c' = -0.825x^2 + 23.26x - 154.1$ |
| % Clay | Polynomial | **1.000** | $c' = -0.124x^2 + 9.403x - 163.5$ |
| % Gravel | Polynomial | **1.000** | $c' = 0.109x^2 - 3.030x + 22.90$ |
| Plasticity Index (PI) | Polynomial | **1.000** | $c' = -2.144x^2 + 77.43x - 688.1$ |
| % Gravel | Reciprocal | **0.915** | $c' = 59.72/x - 1.483$ |
| Dry Unit Weight (C-U Test) | Exponential | **0.876** | $c' = 3E(-6)e^{0.121x}$ |
| Dry Unit Weight (C-U Test) | Power | **0.867** | $c' = 2E(-28)x^{13.78}$ |
| % Gravel | Log | **0.856** | $c' = -6.17Ln(x) + 19.32$ |

### 5.3.4 A-7-6 Soils

Next, results of a series of single-variable nonlinear regression analysis are summarized for A-7-6 soils in Tables 5.54 through 5.59. Over twenty statistically strong correlations surfaced by the end of the analysis. Among the mathematical models, the hyperbolic function proved to have the best ability to describe the basic correlations existing for the A-6a soils. In one case, another mathematical function (polynomial) also

yielded a good correlation. Cautions are recommended for any strong correlations identified through the polynomial function, because the 2nd degree polynomial tends to produce an imaginary peak over the range of independent variable. Out of the long list of index and state properties, % gravel and % sand appears to serve as the most important independent variables.

**Table 5.54:** Single-Variable Nonlinear Regression Results for SPT-$(N_{60})_1$ of A-7-6 Soils

| Independent Variable x | Function | $R^2$ | Correlation Equation |
|---|---|---|---|
| % Gravel | Hyperbolic | **0.885** | $(N_{60})_1 = (21.51x + 7.240)/x$ |
| % Sand | Hyperbolic | **0.853** | $(N_{60})_1 = (27.75x - 36.66)/x$ |
| Unconf. Compr. Strength ($q_u$) | Hyperbolic | 0.724 | $(N_{60})_1 = (33.16x - 304.8)/x$ |
| Dry Unit Weight (C-U Test) | Hyperbolic | 0.704 | $(N_{60})_1 = (125.1x - 11367)/x$ |
| Dry Unit Weight (C-U Test) | Power | 0.662 | $(N_{60})_1 = 5E(-11)x^{5.680}$ |
| Dry Unit Weight (C-U Test) | Exponential | 0.653 | $(N_{60})_1 = 0.067e^{0.051x}$ |
| Dry Unit Weight (C-U Test) | Polynomial | 0.652 | $(N_{60})_1 = -0.026x^2 + 6.869x - 407.0$ |
| Dry Unit Weight (C-U Test) | Reciprocal | 0.640 | $(N_{60})_1 = -11547/x + 126.8$ |
| Dry Unit Weight (C-U Test) | Log | 0.635 | $(N_{60})_1 = 105.5Ln(x) - 474.5$ |
| % Gravel | Polynomial | 0.603 | $(N_{60})_1 = -0.630x^2 + 7.197x + 11.96$ |
| Friction Angle ($\phi$) | Hyperbolic | 0.595 | $(N_{60})_1 = (45.07x - 299.8)/x$ |
| % Sand | Power | 0.552 | $(N_{60})_1 = 8.858x^{0.370}$ |
| Dry Unit Weight (UC Test) | Hyperbolic | 0.545 | $(N_{60})_1 = (128.3x - 11190.0)/x$ |
| % Compaction | Hyperbolic | 0.524 | $(N_{60})_1 = (125.0x - 9864.0)/x$ |
| % Sand | Reciprocal | 0.522 | $(N_{60})_1 = -37.12/x + 27.80$ |
| Final Moisture Content (C-U) | Exponential | 0.512 | $(N_{60})_1 = 237.4e^{-0.10x}$ |
| Dry Unit Weight (UC Test) | Polynomial | 0.501 | $(N_{60})_1 = -0.061x^2 + 13.91x - 756.8$ |

**Table 5.55:** Single-Variable Nonlinear Regression Results for Unconfined Compression Strength of A-7-6 Soils

| Independent Variable x | Function | $R^2$ | Correlation Equation |
|---|---|---|---|
| % Sand | Hyperbolic | **0.864** | $q_u = (39.35x - 78.89)/x$ |
| % Gravel | Hyperbolic | **0.835** | $q_u = (26.49x + 5.36)/x$ |
| Friction Angle ($\phi$) | Hyperbolic | 0.699 | $q_u = (66.62x - 485.0)/x$ |
| Time for 50% Consolid. ($t_{50}$) | Hyperbolic | 0.635 | $q_u = (20.31x + 260.0)/x$ |
| % Sand | Exponential | 0.500 | $q_u = 17.80e^{0.034x}$ |

**Table 5.56:** Single-Variable Nonlinear Regression Results for Effective-Stress Friction Angle of A-7-6 Soils

| Independent Variable x | Function | $R^2$ | Correlation Equation |
|---|---|---|---|
| Time for 50% Consolid. ($t_{50}$) | Hyperbolic | **0.994** | $\phi' = (26.14x + 36.55)/x$ |
| % Sand | Hyperbolic | **0.991** | $\phi' = (26.91x + 3.683)/x$ |
| % Gravel | Hyperbolic | **0.989** | $\phi' = (27.72x - 0.708)/x$ |
| Unconf. Compr. Strength ($q_u$) | Hyperbolic | **0.971** | $\phi' = (26.44x + 23.32)/x$ |
| % Silt | Hyperbolic | **0.930** | $\phi' = (28.24x - 33.18)/x$ |
| Friction Angle ($\phi$) | Hyperbolic | **0.894** | $\phi' = (26.12x + 15.28)/x$ |
| Plasticity Index (PI) | Hyperbolic | **0.876** | $\phi' = (30.24x - 75.15)/x$ |
| Liquid Limit (LL) | Hyperbolic | 0.779 | $\phi' = (30.89x - 171.4)/x$ |
| % Clay | Hyperbolic | 0.767 | $\phi' = (29.48x - 108.3)/x$ |
| Final Moisture Content (C-U Test) | Hyperbolic | 0.736 | $\phi' = (32.16x - 111.3)/x$ |
| Plastic Limit (PL) | Hyperbolic | 0.547 | $\phi' = (31.33x - 84.79)/x$ |

**Table 5.57:** Single-Variable Nonlinear Regression Results for Friction Angle of A-7-6 Soils

| Independent Variable x | Function | $R^2$ | Correlation Equation |
|---|---|---|---|
| % Gravel | Hyperbolic | **0.972** | $\phi = (11.20x + 3.578)/x$ |
| % Sand | Hyperbolic | **0.935** | $\phi = (16.39x - 26.58)/x$ |
| Unconf. Compr. Strength ($q_u$) | Hyperbolic | **0.901** | $\phi = (18.21x - 131.7)/x$ |
| Time for 50% Consolid. ($t_{50}$) | Hyperbolic | **0.877** | $\phi = (12.24x + 31.71)/x$ |
| % Silt | Hyperbolic | 0.720 | $\phi = (9.40x + 133.5)/x$ |
| % Sand | Polynomial | 0.583 | $\phi = 0.017x^2 - 0.170x + 11.70$ |

**Table 5.58:** Single-Variable Nonlinear Regression Results for Cohesion of A-7-6 Soils

| Independent Variable x | Function | $R^2$ | Correlation Equation |
|---|---|---|---|
| Friction Angle ($\phi$) | Polynomial | **0.895** | $c_u = -1.256x^2 + 34.87x - 226.9$ |
| % Gravel | Hyperbolic | **0.827** | $c_u = (6.293x + 2.951)/x$ |
| % Gravel | Reciprocal | 0.778 | $c_u = -8.495/x + 8.929$ |
| Plastic Limit (PL) | Polynomial | 0.638 | $cu = 1.405x^2 - 62.17x + 688.8$ |
| % Gravel | Polynomial | 0.544 | $c_u = -0.291x^2 + 3.412x + 1.539$ |
| % Sand | Polynomial | 0.536 | $c_u = -0.059x^2 + 1.564x - 0.971$ |

**Table 5.59:** Single-Variable Nonlinear Regression Results for Effective-Stress Cohesion of A-7-6 Soils

| Independent Variable x | Function | $R^2$ | Correlation Equation |
|---|---|---|---|
| Final Moisture Content (C-U Test) | Exponential | **0.899** | $c' = 628.5e^{-0.22x}$ |
| Final Moisture Content (C-U Test) | Power | **0.897** | $c' = 1E(+8)x^{-5.48}$ |
| Friction Angle ($\phi$) | Hyperbolic | **0.890** | $c' = (17.73x - 168.9)/x$ |
| Friction Angle ($\phi$) | Polynomial | **0.882** | $c' = -0.597x^2 + 16.63x - 108.4$ |
| Unconf. Compr. Strength ($q_u$) | Polynomial | **0.876** | $c' = 0.145x^2 - 6.767x + 79.38$ |
| Dry Unit Weight (C-U Test) | Power | **0.859** | $c' = 3E(-20)x^{9.810}$ |
| % Sand | Exponential | **0.853** | $c' = 1.058e^{0.097x}$ |
| % Sand | Power | **0.851** | $c' = 0.707x^{0.687}$ |
| % Clay | Power | **0.837** | $c' = 5E(+9)x^{-5.39}$ |
| % Sand | Hyperbolic | **0.834** | $c' = (6.138x - 16.21)/x$ |
| % Clay | Exponential | **0.830** | $c' = 515.5e^{-0.10x}$ |

### 5.3.5 All Cohesive Soil Types Combined

Once again, the data of all four cohesive soil types tested was combined for the nonlinear single independent variable analysis. Table 5.60 presents the top sixteen (with nine of them being very strong) nonlinear correlations identified for the effective-stress friction angles of all four soil types encountered. Table 5.61 shows other strong single-variable nonlinear regression models that surfaced during the analysis for all the soil types. Among of the index and state properties, the time for 50% consolidation ($t_{50}$), measured during each C-U triaxial compression test, surfaced as the most important independent variable. No strong correlations surfaced for cohesion ($c_u$) or effective-stress cohesion ($c'$).

**Table 5.60:** Top Sixteen Nonlinear Regression Models for All Four Soil Types

| Independent Variable x | Function | $R^2$ | Correlation Equation |
|---|---|---|---|
| Time for 50% Consolid. ($t_{50}$) | Hyperbolic | **0.996** | $\phi' = (26.23x + 37.59)/x$ |
| % Gravel | Hyperbolic | **0.976** | $\phi' = (31.95x - 0.876)/x$ |
| % Sand | Hyperbolic | **0.960** | $\phi' = (35.30x - 61.84)/x$ |
| Friction Angle ($\phi$) | Hyperbolic | **0.950** | $\phi' = (36.95x - 96.21)/x$ |
| Plasticity Index (PI) | Hyperbolic | **0.940** | $\phi' = (24.91x + 88.90)/x$ |
| Unconfined Compressive Strength ($q_u$) | Hyperbolic | **0.939** | $\phi' = (33.36x - 68.46)/x$ |
| % Clay | Hyperbolic | **0.891** | $\phi' = (22.30x + 297.7)/x$ |
| Liquid Limit (LL) | Hyperbolic | **0.879** | $\phi' = (22.24x + 253.6)/x$ |
| Natural Moisture Content (UC Test) | Hyperbolic | **0.853** | $\phi' = (22.13x + 133.7)/x$ |
| Final Moisture Content (C-U Test) | Hyperbolic | 0.779 | $\phi' = (22.38x + 149.5)/x$ |
| % Silt | Hyperbolic | 0.759 | $\phi' = (27.86x + 130.1)/x$ |
| Dry Unit Weight (UC Test) | Hyperbolic | 0.732 | $\phi' = (53.45x - 2553.0)/x$ |
| Dry Unit Weight (C-U Test) | Hyperbolic | 0.724 | $\phi' = (55.15x - 2836.0)/x$ |
| % Compaction | Hyperbolic | 0.639 | $\phi' = (49.85x - 1910.0)/x$ |
| Time for 50% Consolid. ($t_{50}$) | Power | 0.633 | $\phi' = 37.62x^{-0.08}$ |
| Time for 50% Consolid. ($t_{50}$) | Log | 0.628 | $\phi' = -2.53\text{Ln}(x) + 36.89$ |

**Table 5.61:** Additional Nonlinear Regression Models for All Four Soil Types

(a) Dependent Variable y = SPT-$(N_{60})_1$

| Independent Variable x | Function | $R^2$ | Correlation Equation |
|---|---|---|---|
| Time for 50% Consolid. ($t_{50}$) | Hyperbolic | **0.961** | $y = (33.07x - 7.872)/x$ |

(b) Dependent Variable y = Unconfined Compression Strength ($q_u$)

| Independent Variable x | Function | $R^2$ | Correlation Equation |
|---|---|---|---|
| Time for 50% Consolid. ($t_{50}$) | Hyperbolic | **0.810** | $y = (22.54x + 116.8)/x$ |

(c) Dependent Variable y = Friction Angle ($\phi$)

| Independent Variable x | Function | $R^2$ | Correlation Equation |
|---|---|---|---|
| Time for 50% Consolid. ($t_{50}$) | Hyperbolic | **0.922** | $y = (11.69x + 51.05)/x$ |
| Unconf. Compr. Strength ($q_u$) | Hyperbolic | **0.832** | $y = (25.71x - 217.8)/x$ |
| % Sand | Hyperbolic | **0.817** | $y = (26.05x - 114.2)/x$ |

## 5.4 Multi-Variable Linear Regression Analysis

Until now, linear and nonlinear correlations were explored between a dependent variable and a single independent variable. There were some moderately strong to very strong correlations emerging from these relatively simple regression analyses. But,

numerous very weak correlations were produced during the single-variable regression analysis. The next logical step is to look at correlations between a dependent variable and two or more independent variables. General form of the linear multi-variable regression model is given below:

$$y = a_0 + a_1x_1 + a_2x_2 + a_3x_3 + \ldots \quad (5.8)$$

where $a_0$, $a_1$, $a_2$, $a_3$ , … = linear regression model coefficients.

This section presents results of the multi-variable linear and nonlinear regression analyses performed for each major soil type and all three soil types combined. A powerful computer software package SPSS (version 17.0) was utilized to perform these advanced analyses efficiently and comprehensively. SPSS has been one of the most powerful and popular statistical packages for many decades. The use of this software was necessary due to the fact that the data amassed in the current study involved different soil types and many variables coming from the field and laboratory tests. All possible cases must be investigated, and there are over eighty cases that can be addressed here.

The linear regression analysis features included in SPSS allow the user to apply any one of the three available schemes – forward selection, backward elimination, and stepwise selection. In the forward selection scheme, the linear model starts out with no variables in the linear equation. It will search for the first variable out of a pool of all independent variables so that the selected variable has the largest positive or negative correlation with the dependent variable. The software performs the F test against a criterion to decide whether to select the variable or not. Next, the software will search for

the second variable out of the pool of remaining independent variables so as to strengthen the correlation further. This process can continue on to keep adding more independent variables. The forward selection process can be terminated abruptly at any stage if there are no variables that can meet the F statistic criterion. In the backward elimination scheme, the model starts out with all independent variables in the linear equation. It will then drop the variables one by one so as to strengthen the correlation. The F-test is performed in each step to justify the elimination. The process can be terminated at any time if it fails to find variables that can meet the elimination criterion. Finally, the stepwise selection scheme takes advantages of both approaches described above. The stepwise selection process will first add two variables to the regression equation in the same way FS selects its first two variables. Then, it will examine if the first variable should drop out or not by performing the F test. Next, the stepwise selection will pick up the third variable. It will then examine to see if any of the variables already in the equation should stay or not. The process will go on until either no more variables can be added or dropped.

The correlations established in the previous section are those between dependent variable and single independent variable. To explore stronger and more reasonable correlations, the effective approach, displayed in this section, is to consider multiple independent variables. Since the combination of independent variables is more than thousands, it is more efficient to analyze the integration of all independent variables by SPSS. The analytical schemes ultimately utilized are stepwise selection and backward elimination. This is because the forward and stepwise selection methods always yielded identical results in any analysis case.

Tables 5.62 through 5.66 present the results of the linear multi-variable regression analysis for each soil type as well as all four soil types combined. The results are qualified if their ultimate $R^2$ value is greater than 0.80. The satisfying correlations revealed in this section are arranged by the order of dependent variables, which are SPT-$(N_{60})_1$ value, unconfined compression stress, friction angle, effective-stress friction angle, cohesion and effective-stress cohesion.

Table 5.62 shows that a total of eight statistically strong multi-variable linear regression models are identified for the A-4a soils tested in the current study. The number of independent variables needed for a reliable regression model is ranging from three to eight. Among the variables, % clay, % sand, and % compaction appear more frequently in these multi-variable regression models. The analysis was successful, for at least one satisfying model emerged for each dependent variable. The lowest $R^2$ value is 0.909. No results are available for the A-4b soil type, due to a lack of the data.

Table 5.63 shows that a total of seven statistically strong multi-variable linear regression models are identified for the A-6a soils tested in the current study. The number of independent variables needed for a reliable regression model is ranging from three to seven. Among the variables, % compaction, natural moisture content, specific gravity, and % silt appear more frequently in these multi-variable regression models. The analysis was less successful, for no satisfying model emerged for the effective-stress friction angle possessed by this soil type. The $R^2$ value is all equal to 1.000.

Table 5.64 shows that a total of ten statistically strong multi-variable linear regression models are identified for the A-6b soils tested in the current study. The number of independent variables needed for reliable regression models is ranging from

only two to seven. Among the variables, % compaction, fully corrected SPT-N value, time for 50% consolidation, % gravel, and % sand appear more frequently in these multi-variable regression models. The analysis was successful, for at least one satisfying model emerged for each dependent variable. The $R^2$ value is 1.000 for most of the models.

**Table 5.62:** Multi-Variable Linear Regression Models for A-4a Soils

| Dependent Variable | Independent Variables | $R^2$ | Correlation Equation |
|---|---|---|---|
| SPT-$(N_{60})_1$ | $G_s$, %Gravel, %Clay, %Sand, PL, %Compaction | **1.000** | $(N_{60})_1$ = -2168.608 + 960.817($G_s$) +15.822(%G) + 16.132(%C) + 6.539(%S) + 5.813(PL) - 12.229(%Comp) |
| Unconfined Compress. Strength | SPT-$(N_{60})_1$, %Clay, %Sand | **0.985** | $q_u$ = -225.762 + 0.380$(N_{60})_1$ + 4.575(%C) + 4.872(%S) |
| Unconfined Compress. Strength | %Clay, %Sand, PL, $w_f$, $\phi$, $\phi'$, %Compaction | **0.988** | $q_u$ = -337.145 + 5.754(%C) + 12.774(%S) + 3.031(PL) + 1.049($w_f$) + 1.541($\phi$) - 1.381($\phi'$) - 1.628(%Comp) |
| Friction Angle | %Clay, %Sand, PL, $w_f$, $q_u$, $t_{50}$, $\phi'$, %Compaction | **0.954** | $\phi$ = 165.295 - 2.738(%C) - 6.981(%S) - 2.149(PL) - 0.629($w_f$) + 0.480($q_u$) + 0.507($t_{50}$) + 1.264($\phi'$) + 0.924(%Comp) |
| Effective Friction Angle | %Clay, %Sand, PL, $q_u$, $t_{50}$, $\phi$, %Compaction | **0.909** | $\phi'$ = -31.176 + 0.916(%C) +2.989(%S) + 0.956(PL) - 0.146($q_u$) - 0.353($t_{50}$) + 0.331($\phi$) - 0.525(%Comp) |
| Cohesion | SPT-$(N_{60})_1$, %Clay, $t_{50}$ | **1.000** | $c_u$ = 49.308 - 0.095$(N_{60})_1$ - 1.16(%C) + 0.043($t_{50}$) |
| Cohesion | %Clay, $\phi'$, %Compaction | **1.000** | $c_u$ = 77.770 - 1.418(%C) - 0.599($\phi'$) - 0.040(%Comp) |
| Effective Cohesion | %Clay, $\phi'$, %Compaction | **1.000** | $c'$= -51.949 + 0.280(%C) + 1.546($\phi'$) - 0.025(%Comp) |

[Note] %G = % Gravel; %C = % Clay; %S = % Sand; PL = Plastic Limit; %Comp = % Compaction (based on standard Proctor max. dry unit weight); $w_f$ = Final Moisture Content (measured at the end of C-U triaxial test); $q_u$ = Unconfined Compression Strength (in psi); and $t_{50}$ = Time for 50% Consolidation (in minutes).

**Table 5.63:** Multi-Variable Linear Regression Models for A-6a Soils

| Dependent Variable | Independent Variables | $R^2$ | Correlation Equation |
|---|---|---|---|
| SPT-$(N_{60})_1$ | $G_s$, %Gravel, %Silt, PL, *w*, $q_u$, %Compaction | **1.000** | $(N_{60})_1 = -559.743 + 193.570(G_s) - 5.523(\%G) - 5.477(\%M) - 0.913(PL) + 8.113(w) - 2.003(q_u) + 2.835(\%Comp)$ |
| SPT-$(N_{60})_1$ | %Gravel, %Silt, PL, LL, *w*, $q_u$, %Compaction | **1.000** | $(N_{60})_1 = -68.756 - 4.501(\%G) - 6.201(\%M) + 2.733(PL) + 0.234(LL) + 6.393(w) - 1.637(q_u) + 2.778(\%Comp)$ |
| Unconfined Compress. Strength | SPT-$(N_{60})_1$, $G_s$, PI, %Gravel, %Silt, *w*, %Compaction | **1.000** | $q_u = -239.466 - 0.527(N_{60})_1 + 80.669(G_s) + 0.114(PI) - 2.826(\%G) - 2.975(\%M) + 3.976(w) + 1.469(\%Comp)$ |
| Unconfined Compress. Strength | SPT-$(N_{60})_1$, %Gravel, %Silt, PL, LL, *w*, %Compaction | **1.000** | $q_u = -42.013 - 0.611(N_{60})_1 - 2.750(\%G) - 3.789(\%M) + 1.670(PL) + 0.143(LL) + 3.906(w) + 1.697(\%Comp)$ |
| Cohesion | %Gravel, %Clay, LL, $\phi$ | **1.000** | $c_u = 60.979 - 1.795(\%G) - 1.288(\%C) - 0.002(LL) + 0.051(\phi)$ |
| Cohesion | SPT-$(N_{60})_1$, PI, *w*, %Compaction | **1.000** | $c_u = 20.492 + 0.077(N_{60})_1 + 1.962(PI) - 2.337(w) - 0.042(\%Comp)$ |
| Effective Cohesion | %Sand, *w*, %Compaction | **1.000** | $c' = 34.361 + 0.255(\%S) + 0.888(w) - 0.464(\%Comp)$ |

[Note] $G_s$ = Specific Gravity; %G = % Gravel; %M = % Silt; *w* = Natural Moisture Content (measured during unconfined compression test); $q_u$ = Unconfined Compression Strength (in psi); %Comp = % Compaction (based on standard Proctor maximum dry unit weight); PI = Plasticity Index; and %S = % Sand.

**Table 5.64:** Multi-Variable Linear Regression Models for A-6b Soils

| Dependent Variable | Independent Variables | $R^2$ | Correlation Equation |
|---|---|---|---|
| SPT-$(N_{60})$ | %Gravel, %Sand, $w_f$, $t_{50}$, $\phi$, $\phi'$, %Compaction | **1.000** | $(N_{60})_1 = -29.538 - 0.589(\%G) - 5.833(\%S) - 4.796(w_f) + 1.032(t_{50}) + 6.532(\phi) + 3.242(\phi') + 0.216(\%Comp)$ |
| Unconfined Compress. Strength | $G_s$, %Silt, $w$ | **1.000** | $q_u = 2402.086 - 862.857(G_s) - 0.214(\%M) - 1.143(w)$ |
| Unconfined Compress. Strength | %Gravel, %Sand, %Compaction | **1.000** | $q_u = 204.568 + 1.843(\%G) + 1.611(\%S) - 1.997(\%Comp)$ |
| Friction Angle | SPT-$(N_{60})_1$, %Gravel, %Sand, $w_f$, $t_{50}$, $\phi'$, %Compaction | **1.000** | $\phi = 4.522 + 0.153(N_{60})_1 + 0.090(\%G) + 0.893(\%S) + 0.734(w_f) - 0.158(t_{50}) - 0.496(\phi') - 0.033(\%Comp)$ |
| Effective Friction Angle | PI, $t_{50}$ | **0.869** | $\phi' = 43.337 - 0.599(PI) - 0.189(t_{50})$ |
| Effective Friction Angle | SPT-$(N_{60})_1$, %Gravel, %Sand, $w_f$, $t_{50}$, $\phi$, %Compaction | **1.000** | $\phi' = 9.110 + 0.308(N_{60})_1 + 0.182(\%G) + 1.799(\%S) + 1.479(w_f) - 0.318(t_{50}) - 2.015(\phi) - 0.067(\%Comp)$ |
| Cohesion | $w_f$, $t_{50}$ | **1.000** | $c_u = -1076.189 + 60.898(w_f) - 4.270(t_{50})$ |
| Cohesion | SPT-$(N_{60})_1$, %Compaction | **1.000** | $c_u = 98.455 - 0.387(N_{60})_1 - 0.718(\%Comp)$ |
| Effective Cohesion | SPT-$(N_{60})_1$, $w$ | **1.000** | $c' = 0.965 - 0.413(N_{60})_1 + 1.046(w)$ |
| Effective Cohesion | SPT-$(N_{60})_1$, %Compaction | **1.000** | $c' = 52.875 - 0.352(N_{60})_1 - 0.347(\%Comp)$ |

[Note] %G = % Gravel; %S = % Sand; $w_f$ = Final Moisture Content (measured at the end of C-U triaxial test); $t_{50}$ = Time for 50% Consolidation (in minutes); %Comp = % Compaction (based on standard Proctor maximum dry unit weight); $G_s$ = Specific Gravity; %M = % Silt; $w$ = Natural Moisture Content (measured during each unconfined compression test); and PI = Plasticity Index.

Table 5.65 shows that a total of seven statistically strong multi-variable linear regression models are identified for the A-7-6 soils tested in the current study. The number of independent variables needed for reliable regression models is ranging from

only two to eleven. Among the variables, % compaction, fully corrected SPT-N value, unconfined compression strength, and specific gravity appear more frequently in these multi-variable regression models. The analysis was less than successful, for no satisfying model emerged for the effective-stress friction angle. The lowest $R^2$ value is 0.858.

**Table 5.65:** Multi-Variable Linear Regression Models for A-7-6 Soils

| Dependent Variable | Independent Variables | $R^2$ | Correlation Equation |
|---|---|---|---|
| SPT-$(N_{60})_1$ | PI,$G_s$, %Gravel, %Silt, %Sand, PL, LL, $\gamma_d$, $w$, $q_u$, %Compaction | **0.989** | $(N_{60})_1 = 266.112 + 0.391(PI) - 162.730(G_s) - 2.997(\%G) + 3.234(\%M) - 0.565(\%S) - 33.120(PL) + 5.914(LL) - 9.414(\gamma_d) - 2.363(w) + 3.486(q_u) + 14.941(\%Comp)$ |
| Unconfined Compress. Strength | SPT-$(N_{60})_1$, PI, $G_s$, %Gravel, %Silt, %Sand, PL, LL, $\gamma_d$, $w$, %Compaction | **0.999** | $q_u = -71.183 + 0.272(N_{60})_1 - 0.114(PI) + 43.838(G_s) + 0.853(\%G) - 0.920(\%M) + 0.179(\%S) + 9.455(PL) - 1.675(LL) + 2.759(\gamma_d) + 0.665(w) - 4.323(\%Comp)$ |
| Friction Angle | SPT-$(N_{60})_1$, $G_s$, %Silt, PL, LL, $\gamma_d$, $q_u$, $t_{50}$, %Compaction | **0.858** | $\phi = -207.728 + 0.401(N_{60})_1 + 124.361(G_s) - 0.902(\%M) + 8.512(PL) - 1.760(LL) + 2.854(\gamma_d) - 0.754(q_u) + 0.024(t_{50}) - 4.829(\%Comp)$ |
| Cohesion | SPT-$(N_{60})_1$, $q_u$ | **0.872** | $c_u = 3.556 + 0.473(N_{60})_1 - 0.295(q_u)$ |
| Cohesion | PI, $G_s$, $\phi$, $\phi'$, %Compaction | **1.000** | $c_u = 497.741 - 0.390(PI) - 245.297(G_s) - 0.961(\phi) + 1.515(\phi') + 1.585(\%Comp)$ |
| Effective Cohesion | SPT-$(N_{60})_1$, %Clay, %Sand, $\phi$ | **1.000** | $c' = -2.649 + 0.185(N_{60})_1 + 0.002(\%C) + 0.014(\%S) + 0.163(\phi)$ |
| Effective Cohesion | $q_u$, $\phi$, $\phi'$, %Compaction | **1.000** | $c' = -18.586 - 0.206(q_u) + 1.027(\phi) - 0.250(\phi') + 0.225(\%Comp)$ |

[Note] PI = Plasticity Index; $G_s$ = Specific Gravity; %G = % Gravel; %M = % Silt; %S = % Sand; PL = Plastic Limit; LL = Liquid Limit; $\gamma_d$ = Dry Unit Weight (in pcf); $w$ = Natural Moisture Content (measured during each unconfined compression test); $w_f$ = Final Moisture Content (measured at the end of C-U triaxial test); %Comp = % Compaction (based on standard Proctor maximum dry unit weight); $q_u$ = Unconfined Compression Strength (in psi); and $t_{50}$ = Time for 50% Consolidation (in minutes).

Finally, Table 5.66 shows that a total of four statistically strong multi-variable linear regression models are identified for all the soil types (A-4, A-6, and A-7-6) tested

in the current study. The number of independent variables needed for reliable regression models is ranging from seven to seventeen. Among the variables, % clay, % sand, % compaction, plasticity index, and plastic limit appear more frequently in these multi-variable regression models. The analysis was successful, for at least one satisfying model emerged for each shear strength parameter. The lowest $R^2$ value is 0.795, which is very close to the minimum acceptable value of 0.800.

**Table 5.66:** Multi-Variable Linear Regression Models for All Soil Types

| Dependent Variable | Independent Variables | $R^2$ | Correlation Equation |
|---|---|---|---|
| Friction Angle | PI, %Clay, %Silt, %Sand, PL, $w_f$, %Compaction | 0.795 | $\phi = 32.324 - 0.350(PI) + 0.283(\%C) + 0.117(\%M) + 0.380(\%S) - 0.492(PL) - 0.517(w_f) - 0.115(\%Comp)$ |
| Cohesion | SPT-$(N_{60})_1$, PI, $G_s$, %Gravel, %Clay, %Silt, %Sand, PL, LL, $\gamma_d$, $w$, $w_f$, $q_u$, $t_{50}$, $\phi$, $\phi'$, %Compaction | **1.000** | $c_u = 805.708 - 0.400(N_{60})_1 - 0.099(PI) - 431.512(G_s) - 4.818(\%G) - 5.728(\%C) - 4.304(\%M) - 9.302(\%S) - 7.193(PL) + 1.765(LL) + 2.840(\gamma_d) + 8.928(w) + 13.764(w_f) + 0.339(q_u) - 1.869(t_{50}) + 9.247(\phi) + 1.223(\phi') + 1.368(\%Comp)$ |
| Effective Cohesion | SPT-$(N_{60})_1$, PI, $G_s$, %Gravel, %Clay, %Sand, PL, LL, $\gamma_d$, $w$, $q_u$, $t_{50}$, $\phi$ | **0.995** | $c' = 153.883 - 0.217(N_{60})_1 - 0.336(PI) - 96.823(G_s) + 0.316(\%G) - 0.861(\%C) + 1.642(\%S) + 2.123(PL) + 2.786(LL) - 0.195(\gamma_d) - 2.257(w) + 0.195(q_u) - 0.422(t_{50}) + 1.481(\phi)$ |
| Effective Cohesion | SPT-$(N_{60})_1$, PI, $G_s$, %Gravel, %Clay, %Silt, PL, LL, $\gamma_d$, $w$, $q_u$, $t_{50}$, $\phi$, $\phi'$, %Compaction | **1.000** | $c' = 204.186 - 0.347(N_{60})_1 - 0.512(PI) - 137.863(G_s) - 0.079(\%G) - 1.516(\%C) - 1.177(\%M) + 3.549(PL) + 3.248(LL) - 0.156(\gamma_d) - 1.219(w) + 0.187(q_u) + 0.475(t_{50}) + 3.051(\phi) + 2.444(\phi') + 0.019(\%Comp)$ |

[Note] PI = Plasticity Index ; %C = % Clay; %M = % Silt; %S = % Sand; PL = Plastic Limit; $w_f$ = Final Moisture Content (measured at the end of C-U triaxial test); %Comp = % Compaction (based on standard Proctor maximum dry unit weight); $t_{50}$ = Time for 50% Consolidation (in minutes); $G_s$ = Specific Gravity; %G = % Gravel; LL = Liquid Limit; $\gamma_d$ = Dry Unit Weight (in pcf); $w$ = Natural Moisture Content (measured during each unconfined compression test); $q_u$ = Unconfined Compression Strength (in psi); and $t_{50}$ = Time for 50% Consolidation (in minutes).

## 5.5 Multi-Variable Nonlinear Regression Analysis

As the final stage of the comprehensive statistical analysis, the data compiled in the current study was analyzed by the multi-variable nonlinear regression model available in SPSS. The single-variable regression analyses carried out earlier produced more strong correlations with the nonlinear models than with the linear model. General form of the nonlinear multi-variable regression model is given below:

$$y = a_0 (x_1)^{a1} (x_2)^{a2} (x_3)^{a3} \ \ldots \qquad (5.9)$$

where $a_0$, $a_1$, $a_2$, $a_3$ , … = nonlinear regression model coefficients.

No automated schemes (such as the forward selection, backward elimination) are possible with the nonlinear analysis. Thus, the above model was applied to each successful case that surfaced during the previous multi-variable linear regression analysis. It was hoped that a few holes observed among the results of the multi-variable linear regression analysis would be filled during the nonlinear regression analysis.

Table 5.67 shows a total of five statistically strong nonlinear regression models identified for the A-4a soils. The number of independent variables needed for reliable regression models is three to eight. The analysis is considered reasonably successful, although it produced a less number of strong models than the linear regression did. The $R^2$ value is ranging from 0.893 to 0.982 in the list.

**Table 5.67:** Multi-Variable Nonlinear Regression Models for A-4a Soils

| Dependent Variable | Independent Variables | $R^2$ | Correlation Equation |
|---|---|---|---|
| SPT-$(N_{60})_1$ | $G_s$, %Gravel, %Clay, %Sand, PL, %Compaction | **0.893** | $(N_{60})_1 = 2.370*10^{13}*(G_s)^{65.182}*(\%G)^{2.498}*(\%C)^{13.067}*(\%S)^{2.453}*(PL)^{-1.834}*(\%Comp)^{-31.049}$ |
| Unconfined Compress. Strength | SPT-$(N_{60})_1$, %Clay, %Sand | **0.962** | $q_u = 9.148*10^{-9}*(N_{60})_1^{0.110}*(\%C)^{3.487}*(\%S)^{3.118}$ |
| Unconfined Compress. Strength | %Clay, %Sand, PL, $w_f$, $\phi$, $\phi'$, %Compaction | **0.982** | $q_u = 8.780*10^{-9}*(\%C)^{3.817}*(\%S)^{7.125}*(PL)^{0.937}*(w_f)^{0.091}*(\phi)^{0.878}*(\phi')^{-1.727}*(\%Comp)^{-2.861}$ |
| Friction Angle | %Clay, %Sand, PL, $w_f$, $q_u$, $t_{50}$, $\phi'$, %Compaction | **0.970** | $\phi = 995514.958*(\%C)^{-2.015}*(\%S)^{-7.239}*(PL)^{-1.483}*(w_f)^{-0.481}*(q_u)^{0.670}*(t_{50})^{0.147}*(\phi')^{2.777}*(\%Comp)^{2.711}$ |
| Effective Friction Angle | %Clay, %Sand, PL, $q_u$, $t_{50}$, $\phi$, %Compaction | **0.936** | $\phi' = 0.973*(\%C)^{0.455}*(\%S)^{1.900}*(PL)^{0.407}*(q_u)^{-0.133}*(t_{50})^{-0.049}*(\phi)^{0.202}*(\%Comp)^{-1.159}$ |

[Note] $G_s$ = Specific Gravity; %G = % Gravel; %C = % Clay; %S = % Sand; PL = Plastic Limit; %Comp = % Compaction (based on standard Proctor maximum dry unit weight); $q_u$ = Unconfined Compression Strength (in psi); $w_f$ = Final Moisture Content (measured at the end of each C-U triaxial test); and $t_{50}$ = Time for 50% Consolidation (in minutes).

Table 5.68 lists four statistically strong nonlinear regression models identified for the A-6a soils. The number of independent variables needed for reliable regression models is three to eight. The analysis is considered not so successful, for the nonlinear analysis failed to fill the void (no strong model for effective-stress friction angle) left by the linear analysis. The $R^2$ values are all high (ranging from 0.998 to 1.000) in the table.

Table 5.69 presents only two statistically strong nonlinear regression models that surfaced during the analysis for the A-6b soils. The number of independent variables in these models is only two or three. The $R^2$ values are again high in the table. No judgment for the success of the results shown here is necessary, since the linear regression analysis carried out earlier was satisfactory (see Table 5.64).

**Table 5.68:** Multi-Variable Nonlinear Regression Models for A-6a Soils

| Dependent Variable | Independent Variables | $R^2$ | Correlation Equation |
|---|---|---|---|
| SPT-$(N_{60})_1$ | $G_s$, %Gravel, %Silt, PL, *w*, $q_u$, %Compaction | **1.000** | $(N_{60})_1 = 4.884*10^{-13}*(G_s)^{4.217} * (\%G)^{-1.293}*(\%M)^{-2.101}*(PL)^{1.682} *(w)^{3.052}*(q_u)^{-1.054}*(\%Comp)^{6.149}$ |
| SPT-$(N_{60})_1$ | %Gravel, %Silt, PL, LL, *w*, $q_u$, %Compaction | **1.000** | $(N_{60})_1 = 1.625*10^{-11}*(\%G)^{-1.215} * (\%M)^{-2.459}*(PL)^{2.196}*(LL)^{0.056} *(w)^{2.875}*(q_u)^{-0.983}*(\%Comp)^{6.237}$ |
| Unconfined Compress. Strength | SPT-$(N_{60})_1$, $G_s$, PI, %Gravel, %Silt, *w*, %Compaction | **0.998** | $q_u = 6.387*10^{-10}*(N_{60})_1^{-0.641} *(G_s)^{8.440}* (PI)^{-0.101}*(\%G)^{-0.846} *(\%M)^{-1.623}* (w)^{2.435}*(\%Comp)^{4.284}$ |
| Unconfined Compress. Strength | SPT-$(N_{60})_1$, %Gravel, %Silt, PL, LL, *w*, %Compaction | **1.000** | $q_u = 7.555*10^{-9}*(N_{60})_1^{-0.891} *(\%G)^{-0.999}* (\%M)^{-2.945}*(PL)^{1.769} *(LL)^{0.064}* (w)^{2.606}*(\%Comp)^{5.559}$ |

[Note] $G_s$ = Specific Gravity; %G = % Gravel; %M = % Silt; PL = Plastic Limit; *w* = Natural Moisture Content (measured during each unconfined compression test); $q_u$ = Unconfined Compression Strength (in psi); %Comp = % Compaction (based on standard Proctor maximum dry unit weight); LL = Liquid Limit; and PI = Plasticity Index.

**Table 5.69:** Multi-Variable Nonlinear Regression Models for A-6b Soil Type

| Dependent Variable | Independent Variables | $R^2$ | Correlation Equation |
|---|---|---|---|
| Unconfined Compress. Strength | $G_s$, %Silt, *w* | **1.000** | $q_u = 67.623*(G_s)^{26.046}*(\%M)^{-6.049}*(w)^{-1.532}$ |
| Effective Friction Angle | PI, $t_{50}$ | **0.935** | $\phi' = 75.261*(PI)^{-0.275}*(t_{50})^{-0.050}$ |

[Note] $t_{50}$ = Time for 50% Consolidation (in minutes).

Table 5.70 lists the only one statistically strong nonlinear regression model identified for the A-7-6 soils. This is a demanding model, as the number of independent variables in this reliable model is eleven. No judgment for the success of the results shown here is necessary, since the linear regression analysis carried out earlier was satisfactory (see Table 5.65). The $R^2$ value is again very high.

Finally, the multi-variable nonlinear regression analysis returned only one statistically strong regression model when it was applied to the entire project data involving all of the soil types (A-4, A-6, and A-7-6). The number of independent variables needed for this relatively reliable model is seven. The analysis is considered unsuccessful, for the nonlinear analysis failed to fill the void (no strong model for effective-stress friction angle) left by the linear analysis.

**Table 5.70:** Multi-Variable Nonlinear Regression Models for A-7-6 Soils

| Dependent Variable | Independent Variables | $R^2$ | Correlation Equation |
|---|---|---|---|
| Unconfined Compress. Strength | SPT-$(N_{60})_1$, PI, $G_s$, %Gravel, %Silt, %Sand, PL, LL, $\gamma_d$, w, %Compaction | **0.908** | $q_u = 5.416*10^{-7}*(N_{60})_1^{0.033}*(PI)^{-1.038}*(G_s)^{-0.797}*(\%G)^{-2.909E-8}*(\%M)^{0.264}*(\%S)^{0.323}*(PL)^{3.092}*(LL)^{0.766}*(\gamma_d)^{0.990}*(w)^{0.208}*(\%Comp)^{0.964}$ |

[Note] $\gamma_d$ = Dry Unit weight (in pcf).

**Table 5.71:** Multi-Variable Nonlinear Regression Models for All Soil Types

| Dependent Variable | Independent Variables | $R^2$ | Correlation Equation |
|---|---|---|---|
| Friction Angle | PI, %Clay, %Silt, %Sand, PL, $w_f$, %Compaction | **0.817** | $\phi = 0.695*(PI)^{-0.354}*(\%C)^{0.829}*(\%M)^{0.892}*(\%S)^{0.513}*(PL)^{-0.345}*(w_f)^{-0.260}*(\%Comp)^{-0.371}$ |

[Note] PI = Plasticity Index; %C = % Clay; %M = % Silt; %S = % Sand; PL = Plastic Limit; $w_f$ = Final Moisture Content (measured at the end of each C-U triaxial test); and %Comp = % Compaction (based on standard Proctor maximum dry unit weight).

## 5.6 Revised Multi-Variable Linear Regression Analysis

Earlier efforts to find reliable prediction models for shear strength parameter values possessed by the cohesive soils of Ohio through the multi-variable linear regression analysis included independent variables that are nearly impossible to obtain unless embankment structures are already in existence. These variables included fully corrected

SPT-N value SPT-$(N_{60})_1$, unconfined compression strength ($q_u$), time for 50% consolidation ($t_{50}$), and internal friction angle ($\phi$). With this in consideration, the data assembled in the current study was analyzed again by the multi-variable linear regression analysis option available in SPSS. During the revised analysis, the variables mentioned above are removed from the list of independent variables. Table 5.72 through 5.75 present the results for A-4a, A-6a, A-6b, and A-7-6 soil types, respectively. Symbols appearing in the correlation equations have been defined previously. During this reanalysis, no statistically strong models surfaced when the entire data was treated as one set of data (or when all soil types were combined together).

**Table 5.72:** Revised Multi-Variable Linear Regression Models for A-4a Soils

| Dependent Variable | Independent Variables | $R^2$ | Correlation Equation |
|---|---|---|---|
| SPT-$(N_{60})_1$ | $G_s$, *w*, PI, %Clay, %Silt, %Sand, | **1.000** | $(N_{60})_1 = 1370.435 + 28.454(PI) + 129.616(G_s) - 13.655(\%C) - 20.890(\%M) - 22.391(\%S) - 13.633(w)$ |
| SPT-$(N_{60})_1$ | $G_s$, %Gravel, %Clay, %Sand, PL, %Compaction | **1.000** | $(N_{60})_1 = -2168.608 + 960.817(G_s) + 15.822(\%G) + 16.132(\%C) + 6.539(\%S) + 5.813(PL) - 12.229(\%Comp)$ |
| Unconfined Compress. Strength | %Clay, %Sand, LL | **0.953** | $q_u = -332.785 + 5.208(\%C) + 7.306(\%S) + 1.53(LL)$ |
| Unconfined Compress. Strength | $G_s$, %Gravel, %Clay, %Sand, %Compaction | **0.970** | $q_u = -638.239 + 212.659(G_s) + 4.197(\%G) + 10.411(\%C) + 6.955(\%S) - 3.973(\%Comp)$ |
| Effective Friction Angle | $G_s$, %Sand, $\gamma_d$ | **0.810** | $\phi' = -57.709 + 33.074(G_s) + 1.873(\%S) - 0.369(\gamma_d)$ |
| Effective Friction Angle | $G_s$, %Sand, %Compaction | **0.809** | $\phi' = -57.281 + 32.89(G_s) + 1.878(\%S) - 0.443(\%Comp)$ |
| Cohesion | %Clay, %Sand, %Compaction | **1.000** | $c_u = 62.494 - 1.496(\%C) - 1.1(\%S) + 0.207(\%Comp)$ |
| Effective Cohesion | %Gravel, %Sand, LL | **1.000** | $c' = -110.941 + 1.03(\%G) + 2.106(\%S) + 2.128(LL)$ |
| Effective Cohesion | %Clay, %Sand, %Compaction | **1.000** | $c' = -12.544 + 0.481(\%C) + 2.837(\%S) - 0.66(\%Comp)$ |

**Table 5.73:** Revised Multi-Variable Linear Regression Models for A-6a Soils

| Dependent Variable | Independent Variables | $R^2$ | Correlation Equation |
|---|---|---|---|
| SPT-$(N_{60})_1$ | PI, $G_s$, %Silt, PL, LL, w, %Compaction | **1.000** | $(N_{60})_1 = 2107.777 + 0.097(PI) - 857.641(G_s) - 9.418(\%M) + 18.956(PL) + 1.247(LL) - 1.32(w) + 2.508(\%Comp)$ |
| SPT-$(N_{60})_1$ | PI, %Gravel, %Silt, PL, LL, w, %Compaction | **1.000** | $(N_{60})_1 = 84.221 + 12.917(PI) - 7.897(\%G) - 7.592(\%M) + 11.863(PL) - 2.674(LL) - 5.753(w) + 0.774(\%Comp)$ |
| Unconfined Compress. Strength | $G_s$, PI, %Sand, PL, LL, *w*, %Compaction | **1.000** | $q_u = -338.124 + 168.105(G_s) - 3.611(PI) - 1.02(\%S) - 7.417(PL) + 0.228(LL) + 5.495(w) + 0.847(\%Comp)$ |
| Unconfined Compress. Strength | PI, %Gravel, %Silt, PL, LL, *w*, %Compaction | **1.000** | $q_u = -93.476 - 7.893(PI) - 2.075(\%G) - 0.85(\%M) - 5.579(PL) + 1.777(LL) + 7.422(w) + 1.224(\%Comp)$ |
| Cohesion | $G_s$, %Sand, LL, *w* | **1.000** | $c_u = 232.891 - 81.412(G_s) + 0.727(\%S) - 0.633(LL) + 0.037(w)$ |
| Cohesion | PI, %Gravel, *w*, %Compaction | **1.000** | $c_u = 9.948 + 1.918(PI) - 1.041(\%G) - 1.949(w) + 0.095(\%Comp)$ |
| Effective Cohesion | %Sand, *w*, %Compaction | **1.000** | $c' = 34.361 + 0.255(\%S) + 0.888(w) - 0.464(\%Comp)$ |

**Table 5.74:** Revised Multi-Variable Linear Regression Models for A-6b Soils

| Dependent Variable | Independent Variables | $R^2$ | Correlation Equation |
|---|---|---|---|
| Unconfined Compress. Strength | PI, $G_s$, %Clay, PL | **1.000** | $q_u = -6.156 + 9.989(PI) + 16.667(G_s) - 0.7(\%C) - 7.589(PL)$ |
| Unconfined Compress. Strength | %Sand, PL, LL, %Compaction | **1.000** | $q_u = -38.999 - 0.039(\%S) - 15.33(PL) + 8.615(LL) + 0.555(\%Comp)$ |
| Friction Angle | %Gravel, %Sand, %Compact | **0.929** | $\phi = 67.712 + 0.09(\%G) + 0.252(\%S) - 0.524(\%Comp)$ |
| Cohesion | PL, LL | **1.000** | $c_u = -152.567 + 3.637(PL) + 1.067(LL)$ |
| Cohesion | %Gravel, %Compaction | **1.000** | $c_u = 97.618 - 0.882(\%G) - 0.722(\%Comp)$ |
| Effective Cohesion | %Gravel, *w* | **1.000** | $c' = -0.576 - 0.944(\%G) + 1.059(w)$ |
| Effective Cohesion | %Gravel, %Compaction | **1.000** | $c' = 52.112 - 0.804(\%G) - 0.351(\%Comp)$ |

**Table 5.75:** Revised Multiple Variable Linear Regression Models for A-7-6 Soils

| Dependent Variable | Independent Variables | $R^2$ | Correlation Equation |
|---|---|---|---|
| SPT-$(N_{60})_1$ | PI,$G_s$, %Gravel, %Clay, %Silt, %Sand, PL, LL, $\gamma_d$, *w*, %Compaction | **0.834** | $(N_{60})_1$ = 479.726 - 0.112(PI) - 160.565($G_s$) - 1.08(%G) + 1.36(%C) - 0.082(%M) + 1.184(%S) -5.172(PL) + 0.94(LL) + 4.194($\gamma_d$) - 2.036(*w*)- 4.518(%Comp) |
| Unconfined Compress. Strength | $G_s$, %Silt, PL, LL, $\gamma_d$, %Compaction | **0.980** | $q_u$ = - 87.002 + 55.792($G_s$) -1.042(%M) + 8.878(PL)-1.524(LL) + 4.459($\gamma_d$) - 6.029(%Comp) |
| Unconfined Compress. Strength | %Gravel, %Clay, %Silt, %Sand, PL, LL, $\gamma_d$, %Compaction | **0.989** | $q_u$ = 87.779 + 0.523(%G) + 0.44(%C) - 0.984(%M) + 0.48(%S) + 8.015(PL) - 1.619(LL) + 3.831($\gamma_d$) - 5.692(%Comp) |
| Cohesion | %Silt, PL | **0.804** | $c_u$ = 127.646 + 0.58(%M) - 6.915(PL) |
| Cohesion | $G_s$, %Clay, %Sand, PI, %Compaction | **1.000** | $c_u$ = 304.328 - 0.074(PI) - 192.832($G_s$) + 0.62(%C) -0.043(%S) + 2.025(%Comp) |
| Effective Cohesion | PI, %Sand, $G_s$, %Compaction | **1.000** | c′= 158.752 + 0.026(PI) - 73.936($G_s$) + 0.101(%S) + 0.445(%Comp) |

## 5.7 t-Tests Between Soil Type Subsets

One of the fundamental questions identified for the current project early on was whether any noticeable differences exit in terms of shear strength properties between soil type subsets. Here, A-4a and A-4b soils can be considered subsets of AASHTO A-4 soil type. In a similar manner, A-6a and A-6b soils can be considered subsets of AASHTO A-6 soil type. In addition, A-7-6 soils in the northern region of Ohio and A-7-6 soils in the southern region of Ohio can be regarded as subsets of AASHTO A-7-6 soil type.

In the field of engineering statistics, there is a standard method for detecting differences between two sample populations. The method is referred as the standard t-test for two means ($\mu_1$, $\mu_2$) having unknown variances. The null hypothesis is to be tested here is that the means of two populations are the same: $H_0$: $\mu_1 - \mu_2 = 0$, and

the test statistics is given by: $$t = \frac{\bar{x}_1 - \bar{x}_2}{s_p \sqrt{1/n_1 + 1/n_2}}$$

where $\bar{x}_1$, $\bar{x}_2$ = means of two population samples; $s_p^2$ = pooled variance; $s_p^2 = \frac{s_1^2 (n_1 - 1) + s_2^2 (n_2 - 1)}{n_1 + n_2 - 2}$; $s_1^2$ = variance in population 1 = $\frac{n_1 \sum_{i=1}^{n1} x_{1i}^2 - \left( \sum_{i=1}^{n1} x_{1i} \right)^2}{n_1 (n_1 - 1)}$; $s_1^2$ = variance in population 1 = $\frac{n_2 \sum_{i=1}^{n2} x_{2i}^2 - \left( \sum_{i=1}^{n2} x_{2i} \right)^2}{n_2 (n_2 - 1)}$; and $n_1$, $n_2$ = number of samples in population 1, 2.

According to the statistics textbook (Walpole & Myers, 1989), the above null hypothesis is accepted (i.e., the means of two populations are considered the same) if:

$$-t_{\alpha/2,\, n1 + n2 - 2} < t < t_{\alpha/2,\, n1 + n2 - 2} \qquad (5.10)$$

where $\alpha$ = level of significance (ex. 0.05).

Table 5.76 below lists critical t-statistics values at different degrees of freedom. Table 5.77 summarizes the t-test results for A-4a and A-4b soil subsets. The numbers of data points were seventeen for A-4a soils and only two for A-4b soils. Table 5.78 summarizes the t-test results for A-6a and A-6b soil subsets. The numbers of data points were twenty-two for A-6a soils and nine for A-6b soils.

**Table 5.76:** Critical Values of t-Distribution at $\alpha$ of 0.05

| $\upsilon$ | $t_{\alpha/2,\upsilon}$ | $\upsilon$ | $t_{\alpha/2,\upsilon}$ | $\upsilon$ | $t_{\alpha/2,\upsilon}$ |
|---|---|---|---|---|---|
| 1 | 3.078 | 11 | 1.363 | 21 | 1.323 |
| 2 | 1.886 | 12 | 1.356 | 22 | 1.321 |
| 3 | 1.638 | 13 | 1.350 | 23 | 1.319 |
| 4 | 1.533 | 14 | 1.345 | 24 | 1.318 |
| 5 | 1.476 | 15 | 1.341 | 25 | 1.316 |
| 6 | 1.440 | 16 | 1.337 | 26 | 1.315 |
| 7 | 1.415 | 17 | 1.333 | 27 | 1.314 |
| 8 | 1.397 | 18 | 1.330 | 28 | 1.313 |
| 9 | 1.383 | 19 | 1.328 | 29 | 1.311 |
| 10 | 1.372 | 20 | 1.325 | $+\infty$ | 1.282 |

[Note] $\upsilon$ (deg. of freedom) = $n_1 + n_2 - 2$.

**Table 5.77:** Summary of t-Test Results for A-4a and A-4b Soil Subsets

| Type | $G_s$ | LL | PL | PI | %G | %S | %M |
|---|---|---|---|---|---|---|---|
| A-4a | 2.68 | 26.2 | 16.4 | 9.8 | 8.7 | 25.1 | 40.2 |
| A-4b | 2.70 | 29.5 | 19.0 | 10.5 | 0.0 | 17.0 | 59.0 |
| $S_p$ | 0.026 | 3.76 | 2.25 | 2.24 | 4.7 | 1.87 | 4.14 |
| t value | -0.086 | -1.18 | -1.54 | -0.438 | 2.48 | 5.79 | -6.07 |
| t critical | 1.333 | 1.333 | 1.333 | 1.333 | 1.333 | 1.333 | 1.333 |
| Hypothesis | Accept | Accept | Reject | Accept | Reject | Reject | Reject |

| Type | %C | $\gamma_d$ (pcf) | %Comp | $q_u$ (psi) | $(N_{60})_1$ | $t_{50}$ (min.) | $\phi'$ (deg.) |
|---|---|---|---|---|---|---|---|
| A-4a | 25.9 | 121.2 | 101.0 | 39.3 | 32.1 | 4.5 | 33.4 |
| A-4b | 24.0 | 117.2 | 97.7 | 48.9 | 22.0 | 6.5 | 35.6 |
| $S_p$ | 5.75 | 8.02 | 6.68 | 19.90 | 13.40 | 2.81 | 2.40 |
| t value | 0.451 | 0.670 | 0.670 | -0.644 | 1.000 | -0.962 | -1.200 |
| t critical | 1.333 | 1.333 | 1.333 | 1.333 | 1.333 | 1.333 | 1.333 |
| Hypothesis | Accept | Accept | Accept | Accept | Accept | Accept | Accept |

[Note] 1 pcf = 0.157 kN/m$^3$; and 1 psi = 6.895 kPa.

**Table 5.78:** Summary of t-Test Results for A-6a and A-6b Soil Subsets

| Type | $G_s$ | LL | PL | PI | %G | %S | %M |
|---|---|---|---|---|---|---|---|
| A-6a | 2.71 | 30.41 | 17.95 | 12.45 | 7.50 | 24.00 | 39.82 |
| A-6b | 2.71 | 38.33 | 20.67 | 17.67 | 7.33 | 14.44 | 43.11 |
| $S_p$ | 0.0387 | 4.944 | 2.635 | 3.154 | 13.04 | 13.78 | 25.52 |
| t value | 0.050 | -4.051 | -2.601 | -4.176 | 0.0323 | 1.753 | -0.326 |
| t critical | 1.311 | 1.311 | 1.311 | 1.311 | 1.333 | 1.311 | 1.311 |
| Hypothesis | Accept | Reject | Reject | Reject | Accept | Reject | Accept |

| Type | %C | $\gamma_d$ (pcf) | %Comp | $q_u$ (psi) | $(N_{60})_1$ | $t_{50}$ (min.) | $\phi'$ (deg.) |
|---|---|---|---|---|---|---|---|
| A-4a | 28.68 | 119.80 | 108.91 | 37.20 | 32.27 | 7.30 | 33.48 |
| A-4b | 35.44 | 119.01 | 108.19 | 33.89 | 28.56 | 9.20 | 30.83 |
| $S_p$ | 45.79 | 39.94 | 33.01 | 243.9 | 163.9 | 34.47 | 3.514 |
| t value | -0.373 | 0.050 | 0.0552 | 0.0344 | 0.0573 | -0.1396 | 1.905 |
| t critical | 1.311 | 1.311 | 1.311 | 1.311 | 1.311 | 1.311 | 1.311 |
| Hypothesis | Accept | Accept | Accept | Accept | Accept | Accept | Reject |

[Note] 1 pcf = 0.157 kN/m$^3$; and 1 psi = 6.895 kPa.

Table 5.79 summarizes the t-test results for A-7-6 (north) and A-7-6 (south) soil subsets. The numbers of data points were almost well balanced with fourteen for northern A-7-6 soils and eleven for A-7-6 southern A-7-6 soils.

**Table 5.79:** Summary of T-Test Results for A-7-6 Soil Subsets

| Type | $G_s$ | LL | PL | PI | %G | %S | %M |
|---|---|---|---|---|---|---|---|
| A-7-6 N | 2.69 | 52.2 | 22.4 | 29.9 | 1.07 | 7.86 | 33.9 |
| A-7-6 S | 2.70 | 46.5 | 20.5 | 25.9 | 6.18 | 15.2 | 31.3 |
| $S_p$ | 0.0205 | 6.64 | 1.47 | 5.63 | 2.58 | 6.45 | 3.56 |
| t value | -1.65 | 2.15 | 3.05 | 1.74 | -4.92 | -2.82 | 1.85 |
| t critical | 1.319 | 1.319 | 1.319 | 1.319 | 1.319 | 1.319 | 1.319 |
| Hypothesis | Reject | Reject | Reject | Reject | Reject | Reject | Reject |

| Type | %C | $\gamma_d$ (pcf) | %Comp | $q_u$ (psi) | $(N_{60})_1$ | $t_{50}$ (min.) | $\phi'$ (deg.) |
|---|---|---|---|---|---|---|---|
| A-7-6 N | 57.1 | 102.0 | 92.3 | 24.6 | 17.9 | 47.5 | 27.5 |
| A-7-6 S | 47.4 | 108.0 | 98.5 | 32.3 | 25.0 | 28.4 | 27.2 |
| $S_p$ | 5.99 | 4.47 | 4.07 | 10.0 | 7.83 | 23.08 | 2.22 |
| t value | 4.05 | -3.80 | -3.80 | -1.92 | -2.26 | 2.06 | 0.35 |
| t critical | 1.319 | 1.319 | 1.319 | 1.319 | 1.319 | 1.319 | 1.319 |
| Hypothesis | Reject | Reject | Reject | Reject | Reject | Reject | Accept |

It was not possible to perform the t-test on soil cohesion ($c_u$ and $c'$) values due to a much smaller data points they had. It is interesting to note here that Table 5.73 shows that the A-4a and A-4b soils are statistically indistinguishable, except in a few fundamental properties. On the contrary, according to Table 5.74 shear strength

properties are slightly different between A-6a and A-6b soils. Table 5.75 indicates that A-7-6 soils found in the northern and southern regions of the state share many different basic properties but are nearly identical in terms of their shear strength parameters.

## 5.7 Geotechnical Guidelines

The outcome of the empirical correlations evaluated in light of the current project data and the comprehensive statistical analysis of the data presented throughout this chapter can be combined to formulate a set of guidelines that geotechnical engineers can apply to estimate more confidently shear strength properties of highway embankment soils commonly encountered in Ohio. The guidelines presented in this section address both short-term and long-term shear strength parameters. The guidelines are established at multiple levels to allow varying degrees of sophistication involved in the estimation process. A-6 soil type includes highly weathered shale often encountered in the southeastern region of Ohio.

Short-Term Shear Strength Parameters ($c_u$, $\phi$) of Ohio Embankment Soils

Level 1: Set $\phi = 0°$. Use the following default short-term (or undrained) cohesion for each soil type found in Ohio:

A-4 Soils ……. $c_u$ = 9 to 20 psi (average 14.5 psi)

$c_u$ = 62 to 138 kPa (average 100 kPa)

A-6 Soils ……. $c_u$ = 9 to 18 psi (average 13.5 psi)

$c_u$ = 62 to 124 kPa (average 93 kPa)

A-7-6 Soils ……. $c_u$ = 9 to 14 psi (average 11.5 psi)

$c_u$ = 62 to 97 kPa (average 80 kPa)

Level 2: Set $\phi = 0°$. Use any of the following single-variable regression formulas to estimate the undrained cohesion for each soil type found in Ohio. Or, a few different formulas may be simultaneously applied to compute the average value of short-term cohesion.

A-4a Soils: $c_u$ (psi) = 2.762(%C) – 59.12 ….. $R^2 = 0.701$

$c_u$ (psi) = [106.6(%C) – 2456.2]/(%C) ….. $R^2 = 0.793$

$c_u$ (psi) = 2E(+8) $(\%M)^{-4.356}$ ….. $R^2 = 0.805$

A-6a Soils: $c_u$ (psi) = - 1846.0$(G_s)^2$ + 9975.0$(G_s)$ – 13459.0 ….. $R^2 = 0.823$

A-6b Soils: $c_u$ (psi) = - 0.308$(t_{50})$ + 13.79 ….. $R^2 = 0.890$

$c_u$ (psi) = - 5.390 Ln$(t_{50})$ + 22.71 ….. $R^2 = 0.920$

$c_u$ (psi) = [1.837$(t_{50})$ + 78.06]/$t_{50}$ ….. $R^2 = 0.909$

$c_u$ (psi) = 52.14$(t_{50})^{-0.72}$ ….. $R^2 = 0.974$

$c_u$ (psi) = 3.370(LL) – 120.30 ….. $R^2 = 0.855$

$c_u$ (psi) = [135.8(LL) – 4862.0]/LL ….. $R^2 = 0.863$

$c_u$ (psi) = - 9277.0/$(\gamma_d)$ + 90.17 ….. $R^2 = 1.000$

$c_u$ (psi) = [10.01$(q_u)$ – 29.28]/$q_u$ ….. $R^2 = 0.887$

A-7-6 Soils: $c_u$ (psi) = [6.293(%G) + 2.951]/(%G) ….. $R^2 = 0.827$

Level 3: Set $\phi = 0°$. Use any of the following regression formulas to estimate the undrained cohesion for each soil type found in Ohio:

A-4a Soils: $c_u$ (psi) = 62.494 – 1.496(%C) – 1.10(%S) + 0.207(%Comp) ….. $R^2 = 1.000$

$c_u$ (psi) = 49.308 – 0.095$(N_{60})_1$ – 1.16(%C) + 0.043($t_{50}$) ….. $R^2$ = 1.000

$c_u$ (psi) = 77.770 – 1.418(%C) – 0.599($\phi'$) – 0.040(%Comp) ….. $R^2$ = 1.0

A-6-a Soils: $c_u$ (psi) = 232.891 – 81.412($G_s$) + 0.727(%S) – 0.633(LL) + 0.037($w$) ….. $R^2$ = 1.000

$c_u$ (psi) = 9.948 + 1.918(PI) – 1.041(%G) – 1.949($w$) + 0.095(%Comp) ….. $R^2$ = 1.000

$c_u$ (psi) = 60.979 – 1.795(%G) – 1.288(%C) - 0.002(LL) + 0.051($\phi$) ….. $R^2$ = 1.000

$c_u$ (psi) = 20.492 + 0.077$(N_{60})_1$ + 1.962(PI) – 2.337($w$) - 0.042(% Comp) ….. $R^2$ = 1.000

A-6b Soils: $c_u$ (psi) = – 152.567 + 3.636(PL) + 1.067(LL) ….. $R^2$ = 1.000

$c_u$ (psi) = 97.618 – 0.882(%G) – 0.722(%Comp) ….. $R^2$ = 1.000

$c_u$ (psi) = 98.455 – 0.387$(N_{60})_1$ – 0.718(%Comp) ….. $R^2$ = 1.000

A-7-6 Soils: $c_u$ (psi) = 127.646 + 0.580(%M) – 6.915(PL) ….. $R^2$ = 0.804

$c_u$ (psi) = 304.328 – 0.074(PI) – 192.832($G_s$) + 0.62(%C) – 0.043(%S) + 2.025(%Comp) ….. $R^2$ = 1.000

$c_u$ (psi) = 3.556 + 0.473$(N_{60})_1$ – 0.295($q_u$) ….. $R^2$ = 0.872

Long-Term Shear Strength Parameters ($c'$, $\phi'$) of Ohio Embankment Soils

Level 1: Use the following default $\phi'$ values for each of the three major embankment soil types found in Ohio:

A-4a & A-4b Soils ……. $\phi'$ = 33°

A-6a Soils ……. $\phi'$ = 32°

A-6b Soils ……. $\phi' = 30°$

A-7-6 Soils ……. $\phi' = 27°$

In addition, use the following default long-term cohesion for each soil type:

A-4a & A-4b Soils ……. $c' = 4$ psi (28 kPa)

A-6a Soils ……. $c' = 3$ psi (21 kPa)

A-6b Soils ……. $c' = 4$ psi (28 kPa)

A-7-6 Soils ……..…. $c' = 3$ psi (21 kPa)

Level 2: Determine plasticity index (PI) of the soil. Estimate the long-tern friction angle of any major embankment soil type (A-4a, A-6a, A-6b, A-7-6) using the empirical $\phi'$ vs. PI correlation chart established by Terzaghi (1996). For A-4 and A-6 soils, use the average value resulting from the chart. For A-7-6 soils, lower the average $\phi'$ value by 3°.

Next, estimate the long-term cohesion by using any of the single-variable regression formulas below. Or, a few different formulas may be simultaneously applied to compute the average value of long-term cohesion.

A-4a Soils: $c'$ (psi) = $1.583(\phi') - 47.47$ ….. $R^2 = 0.912$

$c'$ (psi) = $[10.38(q_u) - 197.6]/q_u$ ….. $R^2 = 0.877$

A-6a Soils: $c'$ (psi) = $1.38(\%M) - 49.71$ ….. $R^2 = 0.929$

$c'$ (psi) = $[56.54(\%M) - 2042.0]/(\%M)$ ….. $R^2 = 0.935$

$c'$ (psi) = $53.1\ \mathrm{Ln}(\%M) - 190.4$ ….. $R^2 = 0.929$

$c'$ (psi) = $-\ 50.1\ \mathrm{Ln}(\%C) + 177.2$ ….. $R^2 = 0.827$

$c'$ (psi) = $1570.0/(\%C) - 45.73$ ….. $R^2 = 0.819$

$c'$ (psi) = 505.7/($G_s$) – 182.8 ….. $R^2$ = 0.885

$c'$ (psi) = 4E(+30)($G_s$) $^{-69.5}$ ….. $R^2$ = 0.951

$c'$ (psi) = 2E(+7) exp{-0.14(%Comp)} ….. $R^2$ = 0.829

A-6b Soils: $c'$ (psi) = 59.72/(%G) – 1.483 ….. $R^2$ = 0.915

$c'$ (psi) = - 6.17 Ln(%G) + 19.32 ….. $R^2$ = 0.867

$c'$ (psi) = 0.543($\gamma_d$) – 57.55 ….. $R^2$ = 0.778

A-7-6 Soils: $c'$ (psi) = 0.286(%S) + 0.557 ….. $R^2$ = 0.781

$c'$ (psi) = 3E(-20)($\gamma_d$)$^{9.810}$ ….. $R^2$ = 0.859

$c'$ (psi) = 0.707(%S)$^{0.687}$ ….. $R^2$ = 0.851

$c'$ (psi) = 5E(+9)(%C)$^{-5.39}$ ….. $R^2$ = 0.837

Level 2 (alternative): Estimate both the long-term friction angle by using any of the single-variable regression formulas below. Or, a few different formulas may be simultaneously applied to compute the average value of long-term (or drained) angle of friction.

Long-term (or drained) cohesion is obtained from the single-variable regression models listed above.

A-4a Soils: $\phi'$ (deg.) = [35.13(PI) – 15.82]/PI ….. $R^2$ = 0.923

$\phi'$ (deg.) = [28.95($t_{50}$) + 15.10]/$t_{50}$ ….. $R^2$ = 0.988

$\phi'$ (deg.) = [35.47($q_u$) – 72.07]/$q_u$ ….. $R^2$ = 0.964

A-6a Soils: $\phi'$ (deg.) = [32.21(LL) + 31.35]/LL ….. $R^2$ = 0.945

$\phi'$ (deg.) = [33.11(PI) + 4.525]/PI ….. $R^2$ = 0.857

$\phi'$ (deg.) = [31.86(%G) + 10.93]/(%G) ….. $R^2$ = 0.979

$\phi'$ (deg.) = [38.13(%S) – 108.5]/(%S) ….. $R^2 = 0.927$

$\phi'$ (deg.) = [31.19(%C) + 63.35]/(%C) ….. $R^2 = 0.881$

$\phi'$ (deg.) = [30.37($t_{50}$) + 19.34]/$t_{50}$ ….. $R^2 = 0.992$

$\phi'$ (deg.) = [31.00($q_u$) + 87.93]/$q_u$ ….. $R^2 = 0.960$

A-6b Soils: $\phi'$ (deg.) = [47.87(PL) – 350.8]/PL ….. $R^2 = 0.823$

$\phi'$ (deg.) = [28.48(%G) + 23.77]/(%G) ….. $R^2 = 0.980$

$\phi'$ (deg.) = [25.55(%S) + 73.14]/(%S) ….. $R^2 = 0.938$

$\phi'$ (deg.) = [38.48(%M) – 321.6]/(%M) ….. $R^2 = 0.956$

$\phi'$ (deg.) = [25.56(%C) + 178.1]/(%C) ….. $R^2 = 0.956$

$\phi'$ (deg.) = [- 15.44(%Comp) + 2159.0]/(%Comp) ….. $R^2 = 0.938$

$\phi'$ (deg.) = [29.75($t_{50}$) + 6.659]/$t_{50}$ ….. $R^2 = 0.998$

$\phi'$ (deg.) = [27.98($q_u$) + 73.62]/$q_u$ ….. $R^2 = 0.995$

A-7-6 Soils: $\phi'$ (deg.) = [30.24(PI) – 75.15]/PI ….. $R^2 = 0.876$

$\phi'$ (deg.) = [27.72(%G) – 0.708]/(%G) ….. $R^2 = 0.989$

$\phi'$ (deg.) = [26.91(%S) + 3.683]/(%S) ….. $R^2 = 0.991$

$\phi'$ (deg.) = [28.24(%M) – 33.18]/(%M) ….. $R^2 = 0.930$

$\phi'$ (deg.) = [26.14($t_{50}$) + 36.55]/$t_{50}$ ….. $R^2 = 0.994$

$\phi'$ (deg.) = [26.44($q_u$) + 23.32]/$q_u$ ….. $R^2 = 0.971$

All Above Soil Types Combined:

$\phi'$ (deg.) = [31.95(%G) – 0.876]/(%G) ….. $R^2 = 0.976$

$\phi'$ (deg.) = [35.30(%S) – 61.84]/(%S) ….. $R^2 = 0.960$

$\phi'$ (deg.) = [22.30(%C) + 297.7]/(%C) ….. $R^2 = 0.891$

$\phi'$ (deg.) = [22.24(LL) + 253.6]/LL ….. $R^2 = 0.879$

$\phi'$ (deg.) = [24.91(PI) + 88.90]/PI ….. $R^2 = 0.940$

$\phi'$ (deg.) = [33.36($q_u$) – 68.46]/$q_u$ ….. $R^2 = 0.939$

$\phi'$ (deg.) = [26.23($t_{50}$) + 37.59]/$t_{50}$ ….. $R^2 = 0.996$

Level 3: Estimate both the long-term cohesion and friction angle by using any of the following multi-variable regression formulas:

A-4a Soils: $\phi'$ (deg.) = - 57.709 + 33.074($G_s$) + 1.873(%S) – 0.369($\gamma_d$)

….. $R^2 = 0.810$

$\phi'$ (deg.) = - 57.281 + 32.89($G_s$) + 1.878(%S) – 0.443(%Comp)

….. $R^2 = 0.809$

$\phi'$ (deg.) = - 31.176 + 0.916(%C) + 2.989(%S) + 0.956(PL)

- 0.146($q_u$) – 0.353($t_{50}$) + 0.331($\phi$) – 0.525(%Comp)

….. $R^2 = 0.909$

where $\phi$ (deg.) = 0.718($\gamma_d$) – 67.79; $\phi$ (deg.) = [24.19($t_{50}$) – 0.556]/$t_{50}$; $\phi$ (deg.) = [23.26($q_u$) + 57.19]/$q_u$; or $\phi$ (deg.) = [116.5($\gamma_d$) – 11800.0]/ $\gamma_d$

$c'$ (psi) = - 110.941 + 1.03(%G) + 2.106(%S) + 2.128(LL)

….. $R^2 = 1.000$

$c'$ (psi) = - 12.544 + 0.481(%C) + 2.837(%S) + 0.66(%Comp)

….. $R^2 = 1.000$

$c'$ (psi) = -51.949 + 0.280(%C) + 1.546($\phi'$) – 0.025(%Comp)

….. $R^2 = 1.000$

A-6a Soils: $c'$ (psi) = 34.361 + 0.255(%S) + 0.888($w$) – 0.464(%Comp)

….. $R^2 = 1.000$

A-6b Soils: $\phi'$ (deg.) = 43.337 – 0.599(PI) – 0.189($t_{50}$) ….. $R^2 = 0.869$

$\phi'$ (deg.) = 75.261$(PI)^{-0.275}(t_{50})^{-0.050}$ ….. $R^2 = 0.935$

$c'$ (psi) = - 0.576 – 0.944(%G) + 1.059($w$) … $R^2 = 1.000$

$c'$ (psi) = 52.112 – 0.804(%G) – 0.351(%Comp) ….. $R^2 = 1.000$

$c'$ (psi) = 0.965 – 0.413$(N_{60})_1$ + 1.046($w$) ….. $R^2 = 1.000$

$c'$ (psi) = 52.875 – 0.352$(N_{60})_1$ – 0.347(%Comp) ….. $R^2 = 1.000$

A-7-6 Soils: No regression formula available for $\phi'$. Go to Level 2 for $\phi'$.

$c'$ (psi) = 158.752 + 0.026(PI) – 73.936($G_s$) + 0.101(%S)

+ 0.445(%Comp) ….. $R^2 = 1.000$

$c'$ (psi) = -2.649 + 0.185$(N_{60})_1$ + 0.002(%C) + 0.014(%S) +

0.163($\phi$) ….. $R^2 = 1.000$

$c'$ (psi) = -18.586 – 0.206($q_u$) + 1.027($\phi$) – 0.250($\phi'$) + 0.225(%

Comp) ….. $R^2 = 1.000$

where $\phi$ (deg.) = [11.20(%G) + 3.578]/(%G); = [16.39(%S) – 26.58]/(%S); = [18.21($q_u$) + 31.71]/$q_u$; or = [12.24($t_{50}$) + 31.71]/$t_{50}$

Symbols appearing in the above regression equations are defined below: $G_s$ = specific gravity; %G = % gravel (by mass); %S = % sand (by mass); %M = % silt (by mass); %C = % clay (by mass); %Comp = % compaction (based on standard Proctor maximum dry unit weight, see the note on the next page); LL = liquid limit (%); PL = plastic limit (%); PI = plasticity index (%); $w$ = natural moisture content (%); ; $\gamma_d$ = Dry Unit Weight (lb/ft$^3$); SPT-$(N_{60})_1$ = SPT-N value fully corrected to energy ratio and

overburden stress level (blows/ft); $t_{50}$ = time for 50% Consolidation (minutes); $q_u$ = unconfined compression strength ($lb/in^2$); $\phi$ = internal friction angle (degrees); and $\phi'$ = effective-stress or drained friction angle (degrees); c = short-term or undrained cohesion ($lb/in^2$); c′ = long-term or drained cohesion ($lb/in^2$); and Ln(x) = natural log of x.

Note 1: % Compaction is based on the following standard Proctor maximum dry unit weight values – A-4 soils (120 pcf or 18.9 $kN/m^3$), A-6 soils (110 pcf or 17.3 $kN/m^3$), and A-7-6 soils (110 pcf or 17.3 $kN/m^3$).

Note 2: Unit conversions are – 1 ft = 0.305 m; 1 $lb/ft^3$ = 0.1572 $kN/m^3$; and 1 psi = 6.895 $kN/m^2$.

# CHAPTER 6: SUMMARY AND CONCLUSIONS

## 6.1 Summary

Highway embankments constitute some of the most common geotechnical facilities being built by civil engineers. The design, construction, and field performance of these embankments are of great importance to transportation costs and safety. When the embankment is not properly designed and/or constructed, serious problems such as slope instability and excessive settlement can arise. Very conservatively designed embankments can lead to significant budgetary waste for the highway departments/agencies.

In Ohio, highway embankments are typically built using silty and clayey soils found at/near the construction sites. In some areas of Ohio, the embankments are also constructed often using weathered shale material. It has been known that some cohesive soils found in Ohio have low to medium shear strengths and weathered shale can undergo further weathering over time. These factors require the embankment design engineers in Ohio to study the on-site fill materials and specify their engineering properties carefully, so that slope stability failure and other problems will not occur. However, in reality detailed investigations of engineering properties of fill material are rarely conducted due to cost and time constraints. Instead, highway embankment engineers in Ohio consult outside sources such as Design Manual 7.2 by U.S. Dept. of Navy (1982), which present correlations between shear strength properties and in-situ or laboratory index test results, to estimate shear strength properties of embankment fill materials. In some embankment projects, unconfined compression strength tests may be performed on relatively undisturbed samples of the fill material to determine strength properties of the soils.

These practices can lead to either very conservative or improper designing of the embankments, since the outside sources examined soils from completely different regions of the country or world. There is a need to develop reliable shear strength correlations for embankment fill materials found in Ohio.

The study described in this report had six objectives. They are listed below:

- Conduct a literature review to document information relevant to the design and construction of highway embankments in Ohio;
- Identify a total of nine highway embankment sites in Ohio, which can supply representative samples of major soil fill types existing in Ohio;
- Perform field soil testing and sampling at the selected highway embankment sites in Ohio;
- Obtain detailed engineering properties of soil samples recovered from the highway embankment sites by conducting standard index property and shear strength tests in the laboratory;
- Perform a variety of statistical analysis on the field and laboratory test data accumulated for the highway embankment soil fill samples to develop reliable correlations between shear strength properties and in-situ soil test data and between shear strength properties and index properties; and
- Based on the findings of the current study, develop a set of geotechnical guidelines concerning shear strength properties of Ohio embankment fill soils.

In order to meet the above objectives, various tasks were conceived and executed by the leading research institute (ORITE) researcher with assistance from a subcontractor (BBCM Engineering). Task 1 consisted of a review of literature related to soil shear

strength and highway embankment stability. Information on the geological features and types of soil found in Ohio was presented, since this information would be valuable for locating several highway embankment sites that represent all of the major embankment soil types typically encountered in Ohio. Under Task 1 journal articles related to the standard penetration test (SPT) and triaxial compression test are also reviewed and summarized. Also, soil shear strength-related empirical correlations were identified as part of this initial task. These included the fully corrected SPT-N value $(N_{60})_1$ vs. unconfined compression strength ($q_u$) correlation by Terzaghi, SPT-$(N_{60})_1$ vs. $q_u$ correlation by Department of Navy, plasticity index (PI) vs. effective-stress friction angle ($\phi'$) chart by Terzaghi, and default cohesion and friction angle values for AASHTO soil types by Department of Navy.

Task 2 of the current study focused on the subsurface exploration work conducted at each highway embankment site. A set of clear site selection criteria was first set up to screen potential highway embankment sites. A total of nine sites spanning across Ohio were identified. A systematic subsurface exploration work was established to conduct a continuous SPT to a depth of 25 ft (7.6 m). and collect twelve Shelby tube samples at three depth ranges. Prior to the initiation of the field work, a mobile drill rig, equipped with a automatic SPT hammer, was calibrated to measure its actual energy delivery ratio. Throughout the field testing/sampling phase, the calibrated drill rig was operated by the same two crew to eliminate equipment-to-equipment and human-related variations. At the end of Task 3, data was produced to present all the field test results obtained for the soils encountered at the selected highway embankment sites.

Under Task 3 of the study, soil samples recovered from the highway embankment

sites were tested in the laboratory to characterize their geotechnical properties. The subcontractor (BBC & M Engineering) performed index property tests (natural moisture content, specific gravity, grain size analysis, liquid limit, plastic limit, and soil classification) as well as unconfined compression strength test. The leading research institute (ORITE) performed all of the consolidated-undrained (C-U) triaxial compression tests. All the tests were conducted according to the current test standards. The test programs at these laboratories were coordinated closely to examine engineering properties of the soils taken from the same depth ranges. At the end of this task, a large volume of data was produced.

Task 4 was concerned with various analyses of the geotechnical data produced in the study. First, the empirical correlations identified during Task 1 were evaluated in light of the project data. Secondly, single-variable linear and nonlinear regression analyses were carried out for each soil type data as well as the entire project data in an effort to create simple correlations that can be used to estimate shear strength properties of Ohio embankment soils. The third part of this task dealt with multi-variable linear and nonlinear regression analyses to produce more comprehensive prediction models for the embankment fill soils typically found in Ohio. These analyses were conducted with the aid of computer software package SPSS. At the end of this final task, a set of geotechnical guidelines was proposed for highway embankment fill materials in Ohio, by taking full advantage of the proven empirical correlations and reliable results yielded from the statistical analyses.

## 6.2 Conclusions

This section summarizes key findings and conclusions reached under each task of the study. They are summarized below in the order of the tasks performed.

### 6.2.1 Literature Review

Factors that influence stability of an embankment are – 1) shear strength of the fill soil; 2) unit weight of the fill soil; 3) embankment height; 4) embankment slope steepness; and 5) pore pressures within the fill soil. Soil fill embankment failure generally occurs in two ways. The first case is by the physical sliding action of the embankment slope. This can occur either locally (shallow failure) in a confined segment of the slope or more globally through the toe of the embankment (toe circle failure). The second case is by shear failure deep within the base layer. This is called the base failure and typically occurs when the subsoils underneath the embankment are soft. This type of failure happens most frequently in the short-term period after construction when excess pore pressures are still existent.

The soils found throughout Ohio formed over thousands of years. Bedrock, glaciers, streams, relief, climate, and biota were all contributing factors. Because of this, different soil types are detected throughout the state. Lake deposit soils tend to be A-4 when looked at using the AASHTO Classification System. These are seen throughout the northern and northeastern Ohio. A-7-6 soils, which contain silt and clay, are found throughout central and southwestern Ohio in the glacial till. A-6 residual soils are found in the eastern and southeastern portion of the state, the unglaciated region. They contain silts, clays, and rock fragments.

The underlining theory for soil shear strength is the Mohr-Coulomb theory. This theory can be expressed in either total stresses or effective stresses. The theory contains two parameters that dictate soil shear strength – the angle of internal friction and cohesion. The angle of internal friction describes the inter-particle friction and the degree of the particle interlocking. This property depends on soil mineral type, soil particle texture/shape/gradation, void ratio, and normal stress. The frictional component of the soil shear strength cannot exist without any normal stress acting on the soil mass. The cohesion describes soil particle bonding caused by electrostatic attractions, covalent link, and/or chemical cementation. Cohesion is zero for granular soils and normally consolidated clays. For the short-term analysis of soil embankment slopes, undrained cohesion ($c_u$) is an important shear strength parameter. Both effective-stress angle of friction ($\phi'$) and effective-stress cohesion ($c'$) are needed for the long-term stability of embankment slopes. A few standard laboratory test methods are available for measuring soil shear strength parameters. Among them, triaxial compression test method is regarded as the most advanced and realistic test method.

Soils making up highway embankment structures are normally unsaturated. Experimental evidences show that unsaturated soil has greater shear strength than the same soil in a saturated condition. However, the unsaturated state may not always exist. At many embankment sites soils do become saturated periodically, due to surface precipitation and subsurface drainage events. Therefore, it is sound to design highway embankments using the shear strength of saturated soils (to address worst site conditions).

### 6.2.2 Field and Laboratory Test Results

A total of nine embankment sites were selected for the field phase of the current study. The sites are listed here as – Site 1 = Interstate 275 site in Hamilton County or HAM-275; Site No. 2 = U.S. Route 35 site in Fayette County or FAY-35; Site No. 3 = State Route 2 site in Lake County or LAK-2; Site No. 4 = U.S. Route 33 site in Athens County or ATH-33; Site No. 5 = Interstate 71 site in Morrow County or MRW-71; Site No. 6 = State Route 2 site in Erie County or ERI-2; Site No. 7 = Interstate 75 in Hancock County or HAN-75; Site No. 8 = Interstate 70 site in Muskingum County or MUS-70; and Site No. 9 = Interstate 77 site in Noble County or NOB-77. These sites covered a wide variety of geographical locations, geological settings, and ODOT districts. The nine sites represented seven different ODOT districts. Three sites (ERI-2, HAN-75, and LAK-2) are located in the northern Ohio. Four of the nine sites (FAY-35, MRW-71, MUS-70, and NOB-77) are found in the central Ohio. The remaining two sites (ATH-33 and HAM-275) exist in the southern part of Ohio. Two of the nine sites (ERI-2 and LAK-2) are located in the lake deposit area. Four sites (FAY-35, HAM-275, HAN-75, and MRW-71) are situated in the glaciated region of the state, while three sites (ATH-33, MUS-70, and NOB-77) are found in the unglaciated region.

The automatic hammer attached to the BBCM drilling rig identified for the current study was calibrated by GRL Engineers, Inc. (Cleveland, Ohio), prior to the field work at the first site. GRL Engineers used a PAK model Pile Driving Analyzer to measure the strain and acceleration exerted on the sampler. According to GRL report, the average energy transfer ratio was 0.817. This means that 81.7% of the free-fall energy generated by the automatic SPT hammer weight was transferred to the sampler as it was

pushed into the ground. For normalizing the raw SPT-N values, the correction method proposed by Seed et al. (1975) is recommended over other methods by Bazaraa, Peck, Skempton, and Terzaghi. This is because the average of all the corrected N values tends to be closest to the value given by the Seed method.

During the subsurface exploration work, A-4a soils were encountered at three sites (FAY-35, LAK-2, MRW-71), A-4b soils at only one site (MUS-70), A-6a soils at six sites (ATH-33, FAY-35, LAK-2, MRW-71, MUS-70, NOB-77), A-6b soils at two sites (HAN-75, NOB-77), and A-7-6 soils at four sites (ATH-33, ERI-2, HAM-275, HAN-75). Thus, it may be stated that A-6a soils are widespread throughout Ohio. In contrast, A-4a and A-6b soils are rather rare in Ohio. The fully corrected SPT-N value or $(N_{60})_1$ ranged from 20 to 61 at Site No. 1 (HAM-275), from 14 to 68 at Site No. 2 (FAY-35), from 13 to 64 at Site No. 3 (LAK-2), from 25 to 115 at Site No. 4 (ATH-33), from 15 to 40 at Site No. 5 (MRW-71), from 13 to 49 at Site No. 6 (ERI-2), from 12 to 70 at Site No. 7 (HAN-75), from 22 to 87 at Site No. 8 (MUS-70), and from 17 to 57 at Site No. 9 (NOB-77).

### 6.2.3 Empirical Correlations

The empirical correlation between the SPT-$(N_{60})_1$ and unconfined compression strength published by Terzaghi is not well suited to the highway embankment soils encountered in Ohio. The percentage of the current project data that conformed to the Terzaghi's correlation was 54.5% for A-4 soils, 28.6% for A-6 soils, and 53.8% for A-7-6 soils.

Similarly, the correlation between the SPT-$(N_{60})_1$ and unconfined compression strength published by the Department of Navy was not highly reliable for embankment

fill soils in Ohio. Exactly half (50.0%) of the measured SPT and unconfined compression data conformed to the correlation chart established by the Dept. of Navy. Among the nineteen data points located outside the range specified by the Dept. of Navy, ten data points (about 53%) reside below the lower bound curve and nine data points (47%) reside above the upper bound curve.

The data produced during the current study was superimposed on top of the plasticity index (PI) vs. effective-stress friction angle ($\phi'$) chart developed by Terzaghi. Out of seventy three data points, fifty six (76.7%) of the data points landed inside the correlation band reported by Terzaghi. The correlation band is 6° deep. Statistically speaking, the standard deviation between the measured $\phi'$ values and the Terzaghi's average $\phi'$ values is 2.51. More than half (63.5%) of the measured values reside within the Terzaghi's average value $\pm \sigma$ (standard deviation). Most (96.0%) of the measured values reside within the Terzaghi's average value $\pm 2\sigma$ (standard deviation). Only negative observation that can be made here is that the data points belonging to A-7-6 soil type centered around the lower bound curve set up by Terzaghi. These observations point out that the PI vs. $\phi'$ chart developed by Terzaghi is applicable to A-4 and A-6 embankment soil fills found Ohio. A minor adjustment is necessary only for A-7-6 soils.

Lastly, the average $\phi'$ value recommended for each cohesive soil type by the Department of Navy was evaluated. For A-4 soils, the average $\phi'$ value (33.6°) measured in the current study was very close to the value (32°) by the Department of Navy. For A-6 soils, the average $\phi'$ value (32.7°) obtained in the study was higher than what was suggested (28°) by the Department of Navy. For A-7-6 soils, the average value (27.4°) produced by the current study corresponded to the upper bound of the range (19°-28°)

reported by the Department of Navy.

### 6.2.4 Statistical Analyses

Due to a lack of data available, no statistical analysis of geotechnical data was feasible for A-4b soil found at Site 7 (MUS-70). The single-variable linear regression analysis yielded only a few statistically strong correlations for A-4a, A-6a, and A-7-6 soils. In contrast, the analysis produced many good results for A-6b soil type. For this soil type, plasticity index (PI), specific gravity ($G_s$), % silt, and % clay proved to be key predictors.

The single-variable nonlinear regression analysis was more successful than the linear version of the same analysis in finding statistically strong correlations for each cohesive soil type. Many of these good results were based on the hyperbolic function. Among the long list of independent variables, % silt, % clay, time for 50% consolidation ($t_{50}$), and dry unit weight ($\gamma_d$) proved to be primary predictors of shear strength properties of cohesive soils in Ohio.

The multi-variable linear regression analysis was executed by SPSS in a fully automated mode. It utilized three different schemes (forward selection, backward elimination, and stepwise selection) to maximize its ability to locate the best linear models. The analysis was successful only with the A-4a soil data. For other soil types, the multi-variable linear regression analysis yielded rather disappointing outcome, for it came up with no statistically strong models for all of the shear strength parameters. Among the long list of independent variables, % compaction, % sand, specific gravity ($G_s$), and fully corrected SPT-N value $(N_{60})_1$ often emerged as key variables in the multi-

variable regression models. The multi-variable nonlinear regression analysis was carried out in a limited scope by SPSS. It did not produce any additional insightful models. After performing the multi-variable nonlinear regression analysis, the multi-variable linear regression analysis was ran again because of some difficult-to-obtain independent variables (ex. fully corrected SPT-N value, unconfined compression strength $q_u$, time for 50% consolidation $t_{50}$, internal friction angle $\phi$, …) being involved in the earlier SPSS analyses. The revised multi-variable linear regression analysis produced some reliable prediction models for shear strength properties of the Ohio cohesive soils. Here, % compaction, % sand, % gravel, and specific gravity emerged as important predictors of cohesive soil shear strength properties.

A series of t-tests were made to compare the average geotechnical properties possessed by similar soil type subsets. It was noted that A-4a and A-4b soils in Ohio are statistically indistinguishable, except in a few fundamental properties. On the contrary, shear strength properties are slightly different between A-6a and A-6b soils examined in the study. A-7-6 soils found in the northern and southern Ohio regions share many different basic properties but are nearly identical in terms of their shear strength properties. Additional data are helpful to verify these conclusions reached by the t-tests.

### 6.2.5 Geotechnical Guidelines

The outcomes of the empirical correlations evaluated in light of the current project data and the comprehensive statistical analysis of the geotechnical data were combined to formulate a set of guidelines that geotechnical engineers can apply to estimate more confidently shear strength properties of highway embankment soils

commonly encountered in Ohio. The guidelines address both short-term and long-term shear strength parameters and are multiple leveled to allow varying degrees of sophistication for the estimation process. At Level 1, default shear strength parameter values are listed for each major cohesive soil type. At Level 2, statistically strong correlations that emerged during the single-variable linear and nonlinear regression analysis are incorporated to allow more site- or project-specific estimation of soil shear strength properties. At Level 3, statistically strong models that surfaced during the multi-variable regression analysis were brought in to provide the most comprehensive prediction tools.

# CHAPTER 7: IMPLEMENTATIONS

Based on the findings made during the current study, the following implementation plans are recommended to ODOT:

- A mobile rig equipped with automatic SPT hammer should be utilized for any future highway embankment-related subsurface exploration work in Ohio. The SPT hammer system should be calibrated prior to each major site work so that its energy delivery ratio is precisely known.
- For normalizing original SPT-N values, the correction method proposed by Seed et al. (1975) should be applied.
- For any new highway embankment construction project, consider the Level 1 approaches described under the geotechnical guidelines as minimal measures to estimate shear strength parameter values.
- For any future highway embankment construction project, for which the main borrow area has been identified, representative soil samples taken from the borrow area should be tested in the laboratory to determine their index properties (grain size distribution, specific gravity, liquid limit, plastic limit, plasticity index, and AASHTO/ODOT soil type). Once these properties are determined, the Level 2 or Level 3 approaches described under the geotechnical guidelines can be applied to derive site-specific shear strength parameter values.
- For select highway embankment projects in which the existing embankment

structure will be modified (ex. roadway widening), additional geotechnical data such as SPT-N values (recorded in the field) and unconfined compression strength or time for 50% consolidation (measured in the laboratory on relatively undisturbed Shelby tube samples) available from the existing embankment section can be utilized to estimate shear strength parameter values using the multi-variable regression equations available at Level 3 of the geotechnical guidelines.

# BIBLIOGRAPHY

American Standards for Testing and Materials (2004). "Standard Test Method for Consolidated Undrained Triaxial Compression Test for Cohesive Soils." Designation D 4767, West Conshohocken, Pennsylvania, pp. 887-899.

Bazaraa, A. R. S. S. (1967). "Use of the Standard Penetration Test for Estimating Settlements of Shallow Foundations on Sand." Ph.D. Dissertation, Civil Engineering Department, University of Illinois, Urbana-Champaign, Illinois.

Bishop, A. W., Bjerrum, L. (1960). "The Relevance of the Triaxial Test to the Solution of Stability Problems," Proceedings, American Society of Civil Engineers, Research Conference on Shear Strength of Cohesive Soils, Boulder, Colorado, pp. 437-501.

Bowles, J. E. (1992). *Engineering Properties of Soils and Their Measurements*, 4th Edition, McGraw-Hill Inc., New York, New York, 241 pp.

Casagrande, A. (1932). "The Structure of Clay and Its Importance in Foundation Engineering." Proceedings, Contributions to Soil Mechanics, Boston Society of Civil Engineers, Boston, Massachusetts, pp. 72-112.

Casagrande, A., and Hirschfeld, R. C. (1960). "Stress Deformation and Strength Characteristics of Clay Compacted to a Constant Dry Unit Weight." Proceedings,

Research Conference on Shear Strength of Cohesive Soils, American Society of Civil Engineers, pp. 359-417.

Das, B. M. (2002). *Principles of Geotechnical Engineering*, 5th Edition, Brooks/Cole, Pacific Grove, California, pp. 268, 311 pp.

Department of Navy (1982). *Soil Mechanics Design Manual*, NAVFACDM-7.1, Alexandria, Virginia.

Drumright, E. E.. Pfingsten, C. W., Lukas, R. G. (1996). "Influence of Hammer Type on SPT Results." Journal of Geotechnical Engineering, American Society of Civil Engineers, Vol. 122, No. 7, pp. 598.

Duncan, J. M., Byrne, P., Wong, K. S., and Mabry, P. (1980). "Strength, Stress-Strain and Bulk Modulus Parameters for Finite Element Analysis of Stresses and Movements in Soil Masses." Report No. UCB/GT/80-01, College of Engineering, University of California at Berkeley, California.

Johnson, G. O. (1975). *Engineering Characteristics of Ohio Soil Series*, Vol. 1, Ohio Department of Transportation, Columbus, Ohio, pp. 1-12.

Kenny, T. C. (1958). "Discussion for Geotechnical Properties of Glacial Lake Clays by T. H. Wu." Journal of the Soil Mechanics Division, American Society of Civil Engineers,

Vol. 84, No. SM3, pp. 67-79.

Ohio Department of Transportation (ODOT) (2006). Construction Inspection Manual of Procedures. Columbus, Ohio.

Masada, T., Sargand, S. M., and Liao, Y. (2006). "Resilient Modulus Prediction Model for Fine-Grained Soils in Ohio: Preliminary Study." Proceedings, International Conference on Perpetual Pavements, Columbus, Ohio.

Peck, R. B., Hanson, W. E., and Thornburn, T. H. (1974). Foundation Engineering, 2nd Edition, John Wiley & Sons, Inc., New York, New York.

Schmertmann, J. H. (1975). "Measurement of In-Situ Strength." Proceedings, Conference on In-Situ Measurement of Soil Properties, American Society of Civil Engineers, pp. 55-138.

Schmertmann, J. H. (1979). "Statics of SPT," Journal of the Geotechnical Engineering Division. American Society of Civil Engineers, Vol. 105, No. GT5, pp. 655-657.

Seed, H. B., Arango, I., and Chan, C. K. (1975). "Evaluation of Soil Liquefaction Potential During Earthquakes." Report No. EERC 75-28, Earthquake Engineering Research Center, University of California, Berkeley, California.

Skempton, A. W. (1953). "The Colloidal Activity of Clay." Proceedings, Third International Conference on Soil Mechanics and Foundation Engineering, London, England, Vol. 1, pp. 57-61.

Skempton, A. W. (1986). "Standard Penetration Test Procedures and Effect in Sands of Overburden Pressure, Relative Density, Particle Size, Aging, and Overconsolidation." Geotechnique, Vol. 36, No. 3, pp. 425-447.

Stroud, M. A., and Butler, F. G. (1975). "Standard Penetration Test and Engineering Properties of Glacial Materials." Proceedings, Symposium on Engineering Properties of Glacial Materials, Midlands Geotechnical Society, Birmingham, England, pp. 117-128.

Terzaghi, K, Peck R. B., and Mesri, G. (1996). *Soil Mechanics in Engineering Practice,* 2nd Edition, John Wiley & Sons, Inc., New York, New York, 549 pp.

Wu, T. H. (1958). "Geotechnical Properties of Glacial Lake Clays." Journal of the Soil Mechanics Division, American Society of Civil Engineers, Vol. 84, No. SM3, pp. 1732-1 to 1732-35.

# Appendix A: SPT Equipment Calibration Test Data

Below is a short report from GRL on SPT equipment calibration.

February 28, 2007

Mr. Dan Furgason
BBC & M Engineering, Inc.
6190 Enterprise Court
Dublin OH 43016

Re: SPT Energy Calibration
ATV #550 and Truck #55 GRL Job No. 075017

Dear Mr. Furgason:

This report summarizes the results from the Standard Penetration Test (SPT) energy measurements performed on 2 SPT rigs. The field work associated with the energy measurements summarized in this report was performed on February 19, 2007.

The purpose in collecting the SPT energy measurements was to compute the energy transfer efficiency for 2 different automatic SPT hammers. To meet this objective, a PAK Model, Pile Driving Analyzer (PDA)® was used to acquire and process the dynamic test data. Additional information regarding the testing equipment and analytical procedures is provided in Appendix A.

***Test Sequence***

Using instrumented AWJ and NWJ rods, energy measurements were made at various sample depths for each drill rig. The drill rigs were identified as ATV #550 and Truck #55. Both rigs utilized CME automatic hammers. Dynamic measurements were obtained for sample depths between 1 and 25.5 feet. Each sample depth consisted of energy measurements over 18 inches of driving.

***Energy Transfer Measurements***

A PAK model Pile Driving Analyzer was used to take measurements of strain and acceleration. The strain and acceleration signals were conditioned and converted to force and velocities by the PDA. The PDA interprets the measured dynamic data according to the Case Method equations. Force and velocity records from the PDA were also viewed graphically on an LCD screen to evaluate data quality. All force and velocity records were also digitally stored for subsequent analysis.

The maximum energy transferred to the rod (EMX) was calculated by integrating both the force and velocity records over time as follows:

$$EMX = \int F(t)V(t)dt$$

Where: $F(t)$ = the force at time $t$
$V(t)$ = the velocity at time $t$

The energy transfer ratio or efficiency is computed from dividing EMX by the theoretical SPT hammer energy of 0.35 kip-ft (computed from the product of the hammer weight, assumed to be 0.14 kips, and the fall height, assumed to be 2.5 ft). The SPT N values can then be corrected for a nominal 60% transfer efficiency, $N_{60}$, as follows:

$$N_{60} = (e_m / 60)\, N_m$$

Where: $e_m$ = the measured transfer ratio (ETR)
$N_m$ = the measured SPT "N" value

***Conclusions***

Table 1 presents a summary of the average transferred energy and the energy transfer ratio for each drill rig at each sample depth calculated using the *EMX* equation. Included in Table 1 are also average values of the hammer operating rate, maximum impact force and maximum velocity of the rod. The overall performance, which represents the average of data from all sample depths for each rig/rod type is also shown. Complete information, including the maximum, minimum and standard deviation for each sampling depth, is included in Appendix B.

As indicated in Table 1, the average energy transfer ratio (ETR) from individual sample depths ranged from 80.1 to 86.6% for ATV #550 and 78.8 to 84.4% for Truck #55. The overall transfer ratio (for all sampling depths) was 83% for ATV #550 and 81% for Truck #55.

We appreciate the opportunity to be of assistance to you. Please do not hesitate to contact us if you have any questions regarding this report, or if we may be of further service.

Sincerely,
GRL Engineers, Inc.

Digitally signed by C. Michael Morgano, M. S., P.E.
DN: cn=C. Michael Morgano, M.S., P.E., o=GRL Engineers, Inc., ou=Cleveland Office Manager, email=cmm@pile.com, c=US
Date: 2007.02.28 17:56:31 -05'00'

C. Michael Morgano, P.E.

Benjamin A. White

## APPENDIX B: SUBSURFACE EXPLORATION DATA

### Site No. 1 (I 275 in Hamilton County or HAM-275)

**Table B.1:** Variations of SPT-N Value with Depth (HAM-275)

| Depth Range (ft) | SPT-N Value | | Depth Range (ft) | SPT-N Value | |
|---|---|---|---|---|---|
| | Uncorrected | Corrected | | Uncorrected | Corrected |
| 1.0 – 2.5 | 7 | 26 | 10.0 – 11.5 | 20 | 34 |
| 2.5 – 4.0 | 7 | 20 | 11.5 – 13.0 | 29 | 46 |
| 4.0 – 5.5 | 13 | 33 | 13.0 – 14.5 | 37 | 56 |
| 5.5 – 7.0 | 24 | 53 | 14.5 – 16.0 | 29 | 42 |
| 7.0 – 8.5 | 22 | 44 | 16.0 – 17.5 | 30 | 42 |
| 8.5 – 10.0 | 31 | 57 | 17.5 – 19.0 | 45 | 61 |

**Table B.2:** Basic Information on Shelby Tube Samples Taken by ORITE (HAM-275)

| Tube | Depth (ft) | Recovery (in) | Note |
|---|---|---|---|
| A-1 | 2.5 – 3.8 | 15.6 | Bottom end is slightly crushed. |
| A-2 | 4.5 – 5.6 | 13.2 | Tube appears to be in good shape. |
| A-3 | 10.0 – 11.0 | 12.0 | Tube appears to be in good shape. |
| B-1 | 2.5 – 3.9 | 16.8 | Tube appears to be in good shape. |
| C-2 | 4.5 – 5.4 | 10.8 | Tube appears to be in good shape. |
| C-3 | 10.0 – 11.1 | 13.2 | Tube is slightly pushed inward along one side. |
| D-1 | 2.5 – 3.8 | 15.6 | Tube appears to be in good shape. |
| D-2 | 4.5 – 5.4 | 10.8 | Tube appears to be in good shape. |
| D-3 | 10.0 – 10.9 | 10.8 | Tube appears to be in good shape. |

### Site No. 2 (USR 35 in Fayette County or FAY-35)

**Table B.3:** Variations of SPT N-Value with Depth (FAY-35)

| Depth Range (ft) | SPT-N Value | | Depth Range (ft) | SPT-N Value | |
|---|---|---|---|---|---|
| | Uncorrected | Corrected | | Uncorrected | Corrected |
| 1.0 – 2.5 | 18 | 68 | 13.0 – 14.5 | 14 | 21 |
| 2.5 – 4.0 | 14 | 41 | 14.5 – 16.0 | 10 | 14 |
| 4.0 – 5.5 | 21 | 52 | 16.0 – 17.5 | 21 | 29 |
| 5.5 – 7.0 | 18 | 40 | 17.5 – 19.0 | 16 | 21 |
| 7.0 – 8.5 | 21 | 42 | 19.0 – 20.5 | 23 | 29 |
| 8.5 – 10.0 | 23 | 42 | 20.5 – 22.0 | 32 | 39 |
| 10.0 – 11.5 | 21 | 35 | 22.0 – 23.5 | 43 | 50 |
| 11.5 – 13.0 | 13 | 20 | 23.5 – 25.0 | 20 | 23 |

[Note] 1 ft = 0.3 m; and 1 in = 25 mm.

**Table B.4:** Basic Information on Shelby Tube Samples Taken by ORITE (FAY-35)

| Tube | Depth (ft) | Recovery (in) | Note |
|---|---|---|---|
| A-1 | 5.5 – 6.4 | 10.8 | Tube appears to be in good shape. |
| B-1 | 5.5 – 6.3 | 9.6 | Slight elliptical shape at the bottom |
| D-1 | 5.5 – 7.2 | 20.4 | Elliptical shape over the bottom 6” |
| E-1 | 5.5 – 7.0 | 18.0 | Tube appears to be in good shape. |
| A-2 | 8.5 – 9.9 | 16.8 | Tube appears to be in good shape. |
| D-2 | 8.5 – 9.7 | 14.4 | Tube appears to be in good shape. |
| E-2 | 8.5 – 9.9 | 16.8 | Tube appears to be in good shape. |
| B-3 | 14.5 – 16.0 | 18.0 | Tube appears to be in good shape. |
| D-3 | 14.5 – 16.0 | 18.0 | Tube appears to be in good shape. |

**Site No. 3 (SR 2 in Lake County or LAK-2)**

**Table B.5:** Variations of SPT-N Value with Depth (LAK-2)

| Depth Range (ft) | SPT-N Value | | Depth Range (ft) | SPT-N Value | |
|---|---|---|---|---|---|
| | Uncorrected | Corrected | | Uncorrected | Corrected |
| 1.0 – 2.5 | 10 | 37 | 13.0 – 14.5 | 9 | 13 |
| 2.5 – 4.0 | 17 | 48 | 14.5 – 16.0 | 16 | 23 |
| 4.0 – 5.5 | 25 | 60 | 16.0 – 17.5 | 12 | 16 |
| 5.5 – 7.0 | 30 | 64 | 17.5 – 19.0 | 18 | 23 |
| 7.0 – 8.5 | 21 | 41 | 19.0 – 20.5 | 14 | 18 |
| 8.5 – 10.0 | 12 | 21 | 20.5 – 22.0 | 22 | 27 |
| 10.0 – 11.5 | 13 | 21 | 22.0 – 23.5 | 13 | 15 |
| 11.5 – 13.0 | 28 | 43 | 23.5 – 25.0 | 28 | 32 |

**Table B.6:** Basic Information on Shelby Tube Samples Taken by ORITE (LAK-2)

| Tube | Depth (ft) | Recovery (in) | Note |
|---|---|---|---|
| A-1 | 1.0 – 2.7 | 20.4 | Tube appears to be in good shape. |
| A-2 | 4.0 – 5.4 | 16.8 | Tube appears to be in good shape. |
| A-3 | 14.0 – 15.6 | 19.2 | Tube appears to be in good shape. |
| B-1 | 1.0 – 1.8 | 9.6 | Bottom end is deformed badly. |
| B-3 | 14.0 – 15.6 | 19.2 | Tube appears to be in good shape. |
| C-2 | 4.0 – 4.6 | 7.2 | Tube appears to be in good shape. |
| D-1 | 1.0 – 2.1 | 13.2 | Tube appears to be in good shape. |
| D-2 | 4.0 – 5.2 | 14.4 | Tube appears to be in good shape. |
| D-3 | 14.0 – 15.4 | 16.8 | Tube appears to be in good shape. |

[Note] 1 ft = 0.3 m; and 1 in = 25 mm.

**Site No. 4 (SR 33 in Athens County or ATH-33)**

**Table B.7:** Variations of SPT-N Value with Depth (ATH-33)

| Depth Range (ft) | SPT-N Value | | Depth Range (ft) | SPT-N Value | |
|---|---|---|---|---|---|
| | Uncorrected | Corrected | | Uncorrected | Corrected |
| 1.0 – 2.5 | 27 | 101 | 13.0 – 14.5 | 20 | 30 |
| 2.5 – 4.0 | 40 | 115 | 14.5 – 16.0 | 40 | 57 |
| 4.0 – 5.5 | 16 | 39 | 16.0 – 17.5 | 45 | 62 |
| 5.5 – 7.0 | 33 | 72 | 17.5 – 19.0 | 36 | 48 |
| 7.0 – 8.5 | 16 | 32 | 19.0 – 20.5 | 21 | 27 |
| 8.5 – 10.0 | 17 | 31 | 20.5 – 22.0 | 32 | 39 |
| 10.0 – 11.5 | 25 | 42 | 22.0 – 23.5 | 21 | 25 |
| 11.5 – 13.0 | 19 | 30 | 23.5 – 25.0 | 32 | 37 |

**Table B.8:** Basic Information on Shelby Tube Samples Taken by ORITE (ATH-33)

| Depth range (ft) | Tube | Recovery (in) | Note |
|---|---|---|---|
| 4.5 – 6.5 | A-1 | 20.4 | Tube appears to be in good shape. |
| | B-1 | 24.0 | Tube appears to be in good shape. |
| | D-1 | 24.0 | Tube appears to be in good shape. |
| 8.5 – 10.5 | A-2 | 10.8 | Oval shaped at the bottom. |
| | B-2 | 20.4 | Oval shaped at the bottom |
| | D-2 | 24.0 | Tube appears to be in good shape. |
| 19.0 – 21.0 | A-3 | 22.2 | Tube appears to be in good shape. |
| | B-3 | 24.0 | Tube appears to be in good shape. |
| | D-3 | 24.0 | Tube appears to be in good shape. |

**Site No. 5 (I 71 in Morrow County or MRW-71)**

**Table B.9:** Variations of SPT-N Value with Depth (MRW-71)

| Depth Range (ft) | SPT-N Value | | Depth Range (ft) | SPT-N Value | |
|---|---|---|---|---|---|
| | Uncorrected | Corrected | | Uncorrected | Corrected |
| 1.0 – 2.5 | 11 | 40 | 13.0 – 14.5 | 17 | 25 |
| 2.5 – 4.0 | 10 | 28 | 14.5 – 16.0 | 25 | 35 |
| 4.0 – 5.5 | 9 | 21 | 16.0 – 17.5 | 15 | 20 |
| 5.5 – 7.0 | 13 | 27 | 17.5 – 19.0 | 31 | 40 |
| 7.0 – 8.5 | 14 | 27 | 19.0 – 20.5 | 16 | 20 |
| 8.5 – 10.0 | 16 | 28 | 20.5 – 22.0 | 30 | 36 |
| 10.0 – 11.5 | 9 | 15 | 22.0 – 23.5 | 16 | 18 |
| 11.5 – 13.0 | 21 | 32 | 23.5 – 25.0 | 35 | 39 |

[Note] 1 ft = 0.3 m; and 1 in = 25 mm.

**Table B.10:** Basic Information on Shelby Tube Samples Taken by ORITE (MRW-71)

| Depth range (ft) | Tube | Recovery (in) | Note |
|---|---|---|---|
| 10.0 – 11.5 | D-1 | 19.2 | Tube appears to be in good shape. |
| | B-1 | 19.2 | Tube appears to be in good shape. |
| | C-1 | 14.4 | Tube appears to be in good shape. |
| 13.0 – 14.5 | D-2 | 10.8 | Tube appears to be in good shape. |
| | B-2 | 10.8 | Tube appears to be in good shape. |
| | C-2 | 15.6 | Tube appears to be in good shape. |
| 17.5 – 19.0 | D-3 | 14.4 | Tube appears to be in good shape. |
| | B-3 | 12.0 | Tube appears to be in good shape. |
| | C-3 | 7.2 | Very small recovery but usable. |

**Site No. 6 (SR 2 in Erie County or ERI-2)**

**Table B.11:** Variations of SPT-N Value with Depth (ERI-2)

| Depth Range (ft) | SPT-N Value | | Depth Range (ft) | SPT-N Value | |
|---|---|---|---|---|---|
| | Uncorrected | Corrected | | Uncorrected | Corrected |
| 1.0 – 2.5 | 7 | 21 | 13.0 – 14.5 | 17 | 26 |
| 2.5 – 4.0 | 8 | 21 | 14.5 – 16.0 | 20 | 30 |
| 4.0 – 5.5 | 12 | 28 | 16.0 – 17.5 | 14 | 20 |
| 5.5 – 7.0 | 6 | 13 | 17.5 – 19.0 | 14 | 19 |
| 7.0 – 8.5 | 8 | 16 | 19.0 – 20.5 | 24 | 32 |
| 8.5 – 10.0 | 11 | 20 | 20.5 – 22.0 | 18 | 23 |
| 10.0 – 11.5 | 14 | 23 | 22.0 – 23.5 | 39 | 49 |
| 11.5 – 13.0 | 11 | 18 | 23.5 – 25.0 | NA | NA |

**Table B.12:** Basic Information on Shelby Tube Samples Taken by ORITE (ERI-2)

| Depth range (ft) | Tube | Recovery (in) | Note |
|---|---|---|---|
| 10.0 – 11.5 | A-1 | 22.0 | Tube appears to be in good shape. |
| | B-1 | 22.0 | Tube appears to be in good shape. |
| | D-1 | 23.0 | Tube appears to be in good shape. |
| 13.0 – 14.5 | A-2 | 21.0 | Tube appears to be in good shape. |
| | B-2 | 23.0 | Tube appears to be in good shape. |
| | D-2 | 22.0 | Tube appears to be in good shape. |
| 17.5 – 19.0 | D-3 | 20.0 | Tube appears to be in good shape. |
| | B-3 | 21.0 | Tube appears to be in good shape. |
| | C-3 | 20.0 | Tube appears to be in good shape. |

[Note] 1 ft = 0.3 m; and 1 in = 25 mm.

**Site No. 7 (I 75 in Hancock County or HAN-75)**

**Table B.13.** Variations of SPT-N Value with Depth (HAN-75)

| Depth Range (ft) | SPT-N Value | | Depth Range (ft) | SPT-N Value | |
|---|---|---|---|---|---|
| | Uncorrected | Corrected | | Uncorrected | Corrected |
| 1.0 – 2.5 | 19 | 70 | 13.0 – 14.5 | 12 | 17 |
| 2.5 – 4.0 | 13 | 36 | 14.5 – 16.0 | 25 | 35 |
| 4.0 – 5.5 | 14 | 33 | 16.0 – 17.5 | 17 | 23 |
| 5.5 – 7.0 | 16 | 34 | 17.5 – 19.0 | 33 | 42 |
| 7.0 – 8.5 | 15 | 29 | 19.0 – 20.5 | 10 | 12 |
| 8.5 – 10.0 | 23 | 40 | 20.5 – 22.0 | 21 | 25 |
| 10.0 – 11.5 | 9 | 15 | 22.0 – 23.5 | 21 | 24 |
| 11.5 – 13.0 | 20 | 30 | 23.5 – 25.0 | 32 | 36 |

**Table B.14:** Basic Information on Shelby Tube Samples Taken by ORITE (HAN-75)

| Depth range (ft) | Tube | Recovery (in) | Note |
|---|---|---|---|
| 5.5 – 7.0 | A-1 | 18.0 | Tube appears to be in good shape. |
| | C-1 | 21.6 | Tube appears to be in good shape. |
| | D-1 | 16.8 | Tube appears to be in good shape. |
| 10.0 – 11.5 | A-2 | 15.6 | Tube appears to be in good shape. |
| | B-2 | 22.8 | Tube appears to be in good shape. |
| | D-2 | 16.8 | Tube appears to be in good shape. |
| 16.0 – 17.5 | A-3 | 21.6 | Tube appears to be in good shape. |
| | B-3 | 21.6 | Tube appears to be in good shape. |
| | C-3 | 24.0 | Tube appears to be in good shape. |

**Site No. 8 (I 70 in Muskingum County or MUS-70)**

**Table B.15:** Variations of SPT-N Value with Depth (MUS-70)

| Depth Range (ft) | SPT-N Value | | Depth Range (ft) | SPT-N Value | |
|---|---|---|---|---|---|
| | Uncorrected | Corrected | | Uncorrected | Corrected |
| 1.0 – 2.5 | 15 | 54 | 13.0 – 14.5 | 46 | 66 |
| 2.5 – 4.0 | 17 | 47 | 14.5 – 16.0 | 53 | 72 |
| 4.0 – 5.5 | 20 | 47 | 16.0 – 17.5 | 38 | 50 |
| 5.5 – 7.0 | 42 | 87 | 17.5 – 19.0 | 53 | 67 |
| 7.0 – 8.5 | 36 | 67 | 19.0 – 20.5 | 44 | 53 |
| 8.5 – 10.0 | 13 | 22 | 20.5 – 22.0 | 49 | 57 |
| 10.0 – 11.5 | 19 | 30 | 22.0 – 23.5 | 42 | 47 |
| 11.5 – 13.0 | 48 | 72 | 23.5 – 25.0 | 61 | 67 |

[Note] 1 ft = 0.3 m; and 1 in = 25 mm.

**Table B.16:** Basic Information on Shelby Tube Samples Taken (MUS-70)

| Depth range (ft) | Tube | Recovery (in) | Note |
|---|---|---|---|
| 9.5 – 11.5 | A | 21 | Silty Clay Sample; Retained by OU-ORITE |
| | B | 21 | Silty Clay Sample; Retained by OU-ORITE |
| | C | 21 | Silty Clay Sample; Retained by OU-ORITE |
| | D | 21 | Silty Clay Sample; Went to BBC & M |
| | E | 21 | Silty Clay Sample; Went to BBC & M |

**Site No. 9 (I 77 in Noble County or NOB-77)**

**Table B.17:** Variations of SPT-N Value with Depth (NOB-77)

| Depth Range (ft) | SPT-N Value | | Depth Range (ft) | Uncorrected N Value | |
|---|---|---|---|---|---|
| | Uncorrected | Corrected | | Uncorrected | Corrected |
| 1.0 – 2.5 | 11 | 40 | 13.0 – 14.5 | 14 | 20 |
| 2.5 – 4.0 | 10 | 27 | 14.5 – 16.0 | 22 | 30 |
| 4.0 – 5.5 | 14 | 32 | 16.0 – 17.5 | 44 | 57 |
| 5.5 – 7.0 | 15 | 31 | 17.5 – 19.0 | 22 | 27 |
| 7.0 – 8.5 | 9 | 17 | 19.0 – 20.5 | 12 | 14 |
| 8.5 – 10.0 | 15 | 25 | 20.5 – 22.0 | 20 | 23 |
| 10.0 – 11.5 | 17 | 27 | 22.0 – 23.5 | 26 | 29 |
| 11.5 – 13.0 | 18 | 27 | 23.5 – 25.0 | 26 | 28 |

**Table B.18:** Basic Information on Shelby Tube Samples Taken (NOB-77)

| Depth range (ft) | Tube | Recovery (in) | Note |
|---|---|---|---|
| 4.0 – 6.0 | A-1 | 22 to 23 | Weathered Shale; Retained by BBC & M |
| | B-1 | 22 to 23 | Weathered Shale; Retained by OU-ORITE |
| | C-1 | 22 to 23 | Weathered Shale; Retained by OU-ORITE |
| | D-1 | 22 to 23 | Weathered Shale; Retained by OU-ORITE |
| 7.0 – 9.0 | A-2 | 22 to 23 | Weathered Shale; Retained by OU-ORITE |
| | B-2 | 22 to 23 | Weathered Shale; Retained by BBC & M |
| | C-2 | Very poor | Weathered Shale; Discarded |
| | D-2 | 21 to 22 | Weathered Shale; Retained by OU-ORITE |
| | E-2 | 22 to 23 | Weathered Shale; Retained by OU-ORITE |
| 10.0 – 12.0 | A-3 | 22 to 23 | Weathered Shale; Retained by BBC & M |
| | B-3 | 21 to 22 | Weathered Shale; Retained by OU-ORITE |
| | C-3 | 18 to 19 | Weathered Shale; Retained by OU-ORITE |
| | D-3 | 12 to 13 | Weathered Shale; Retained by OU-ORITE |

[Note] 1 ft = 0.3 m; and 1 in = 25 mm.

# APPENDIX C: TRIAXIAL COMPRESSION TEST PLOTS

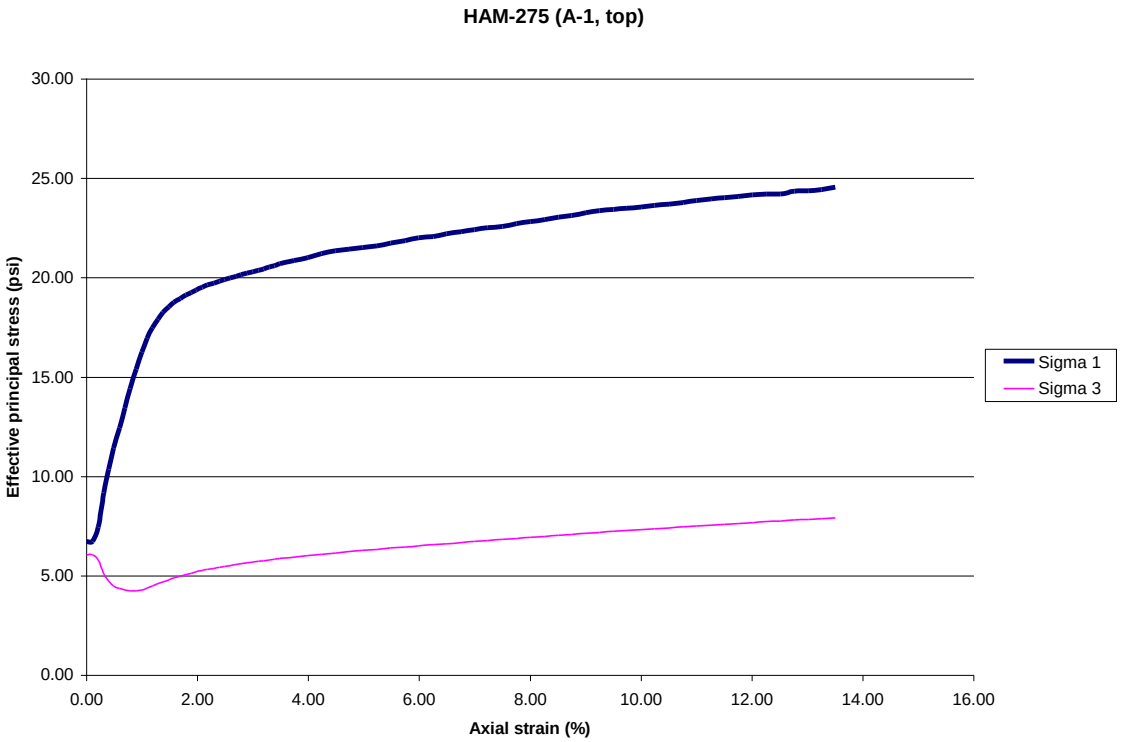


**Figure C.1:** Specimen A-1 (2.5' – 3.0' Depth) – Site No. 1

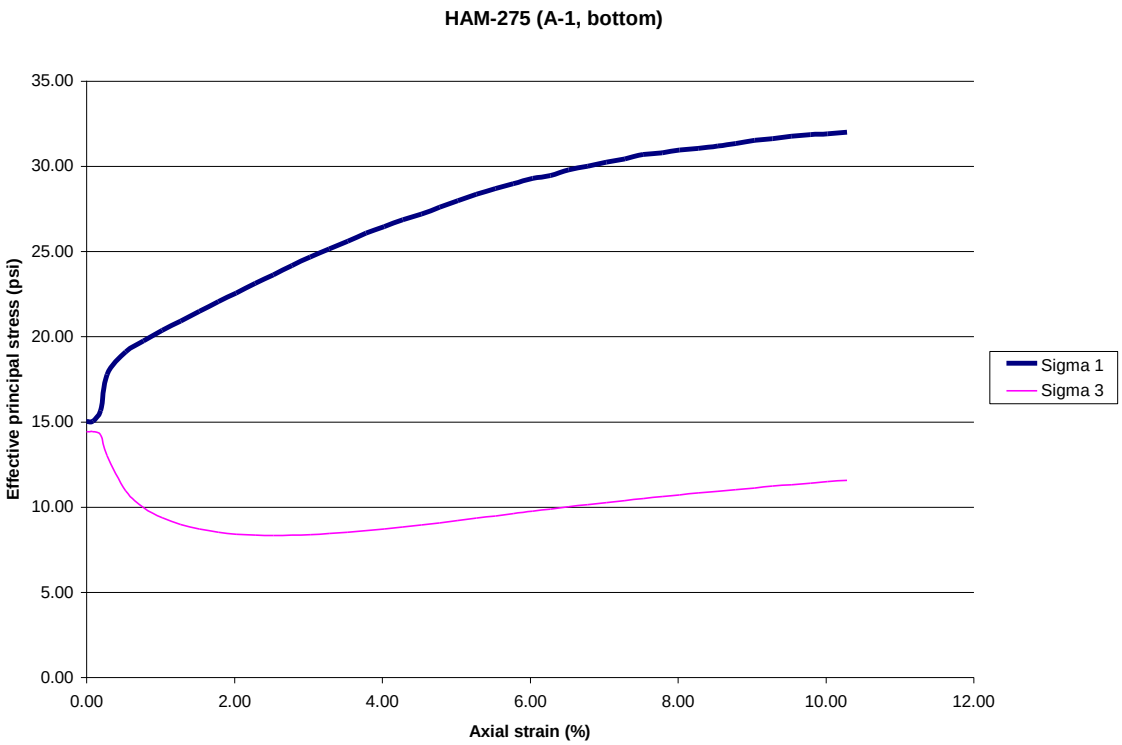


**Figure C.2:** Specimen A-1 (3.1' – 3.6' Depth) – Site No. 1

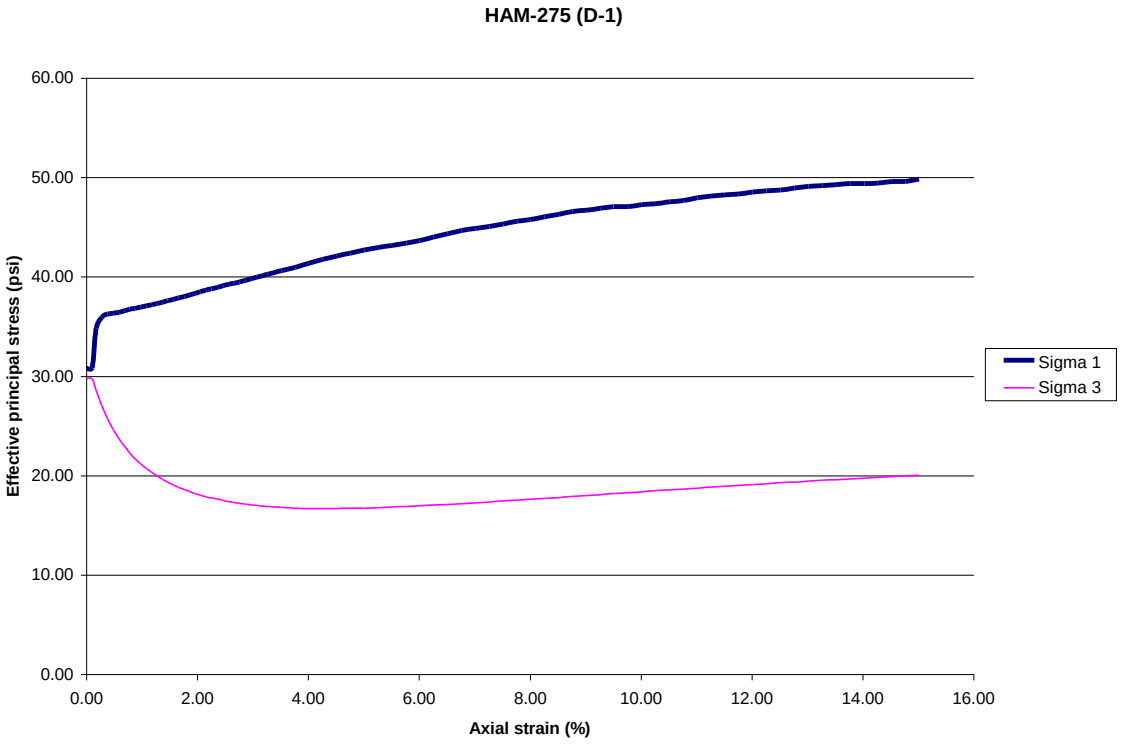


**Figure C.3:** Specimen D-1 (2.5' – 3.0' Depth) – Site No. 1

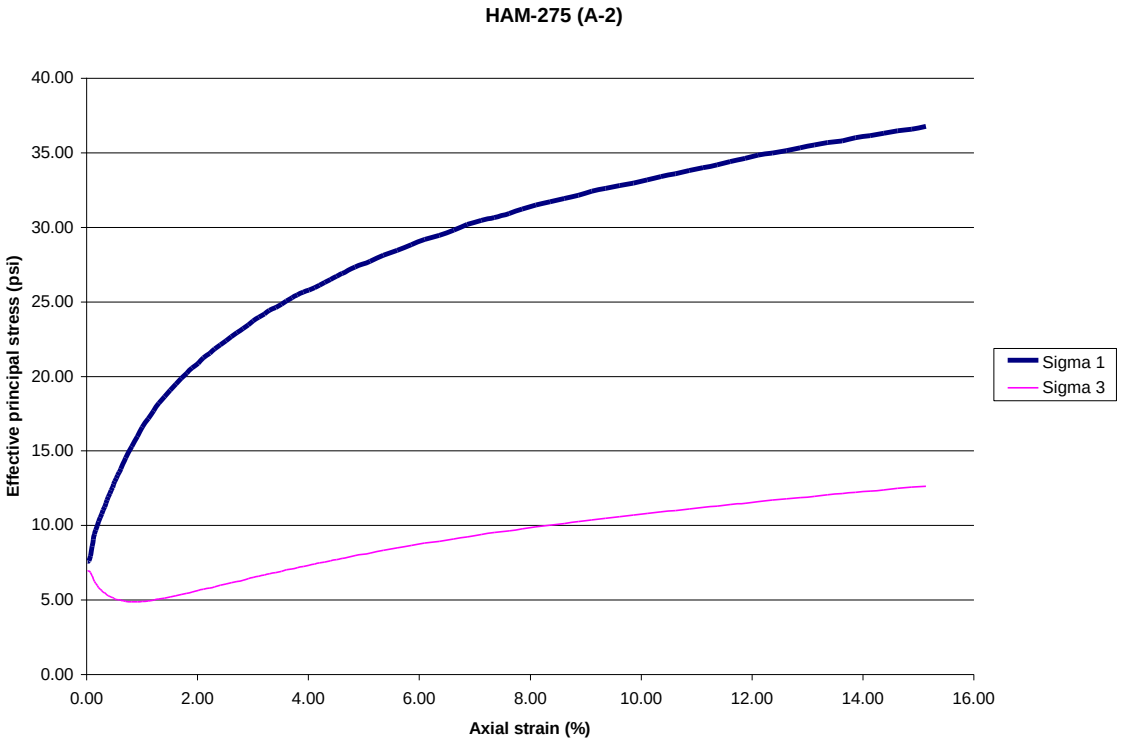


**Figure C.4:** Specimen A-2 (5.1' – 5.6' Depth) – Site No. 1

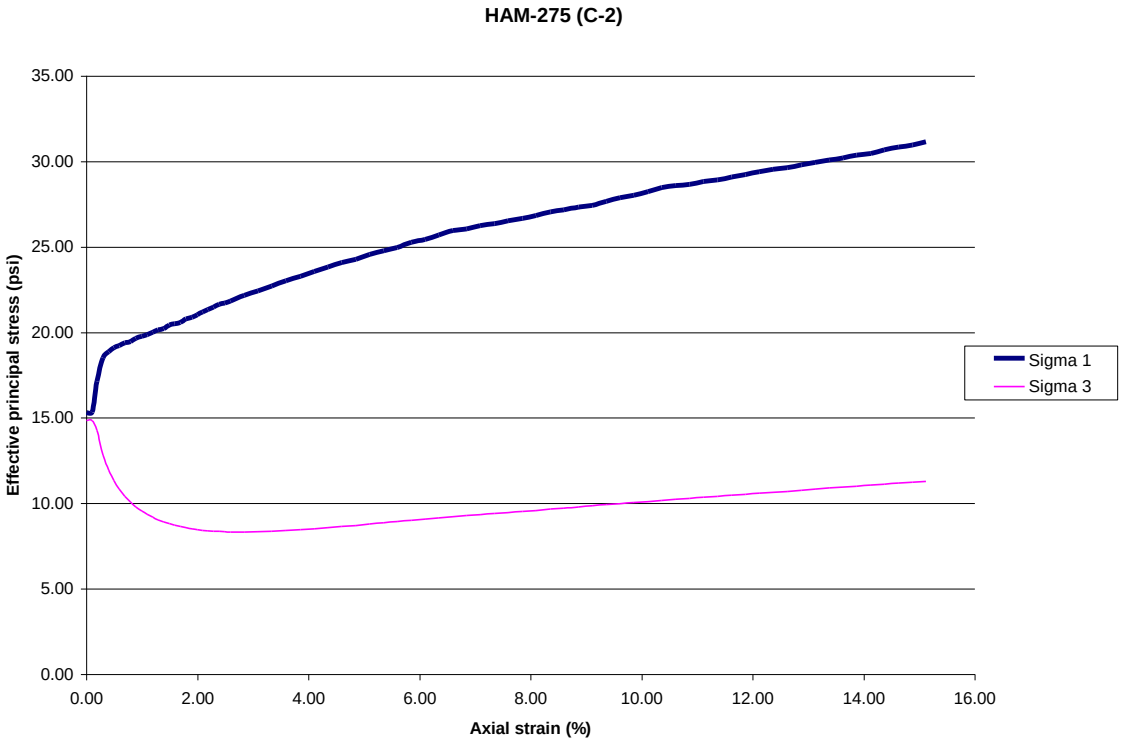


**Figure C.5:** Specimen C-2 (4.9' – 5.4' Depth) – Site No. 1

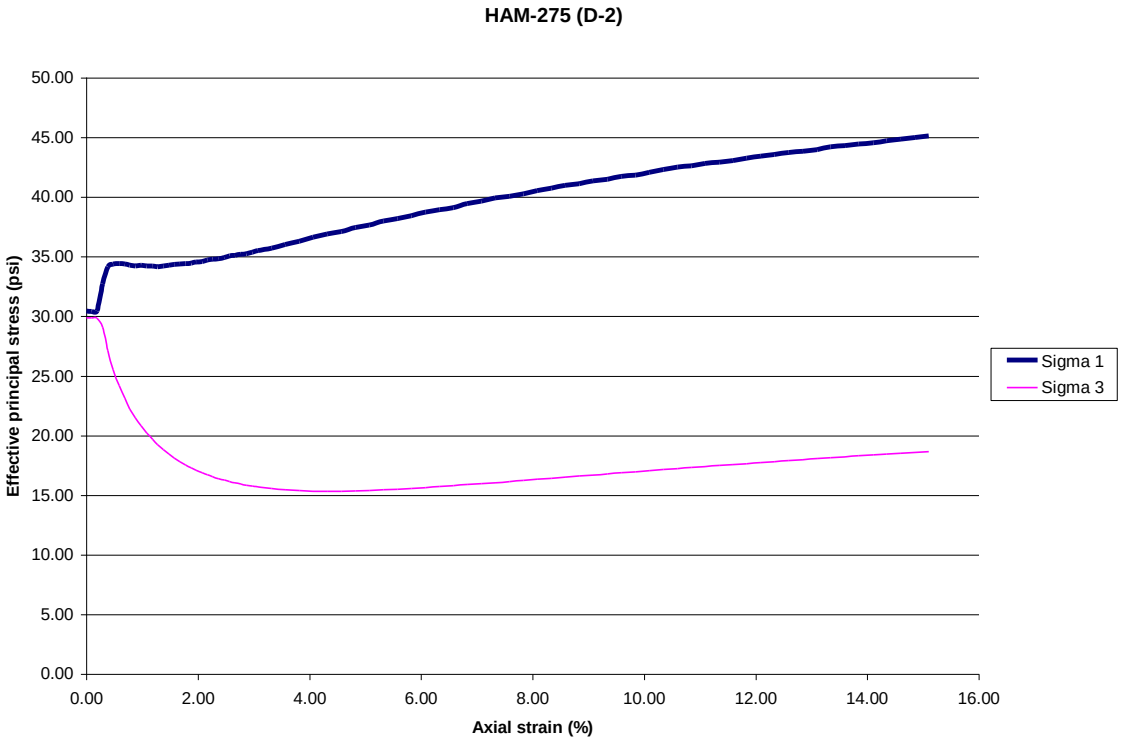


**Figure C.6:** Specimen D-2 (4.6' – 5.1' Depth) – Site No. 1

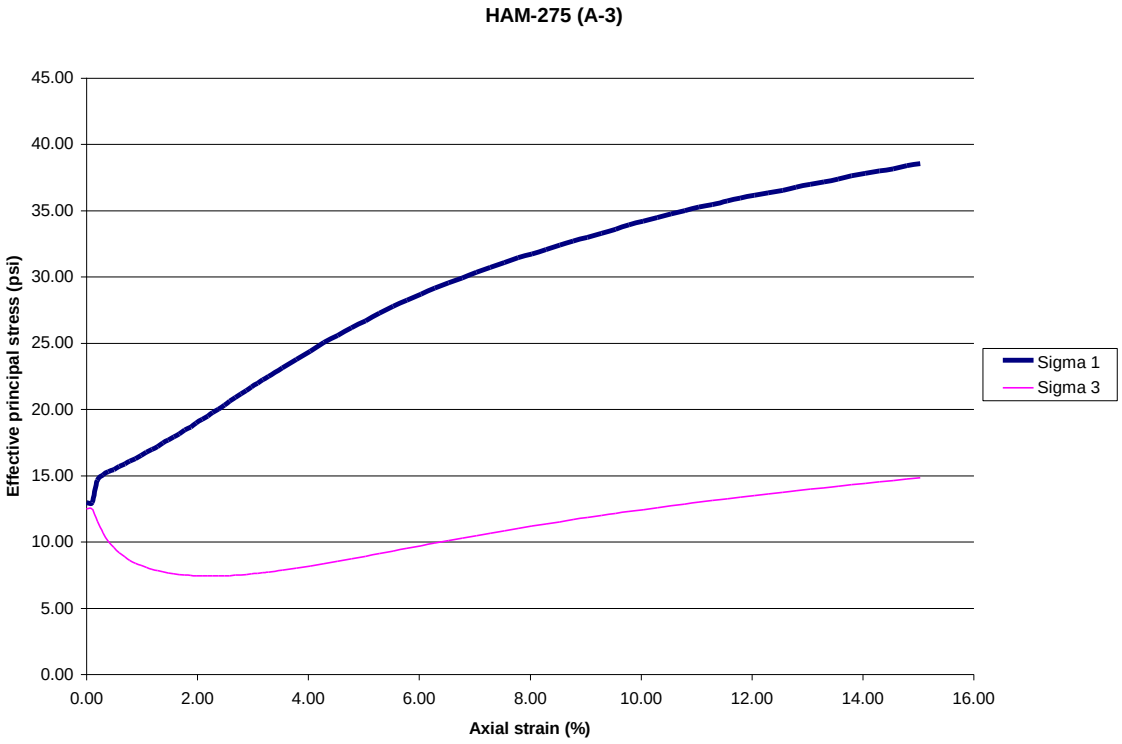


**Figure C.7:** Specimen A-3 (10.3' – 10.8' Depth) – Site No. 1

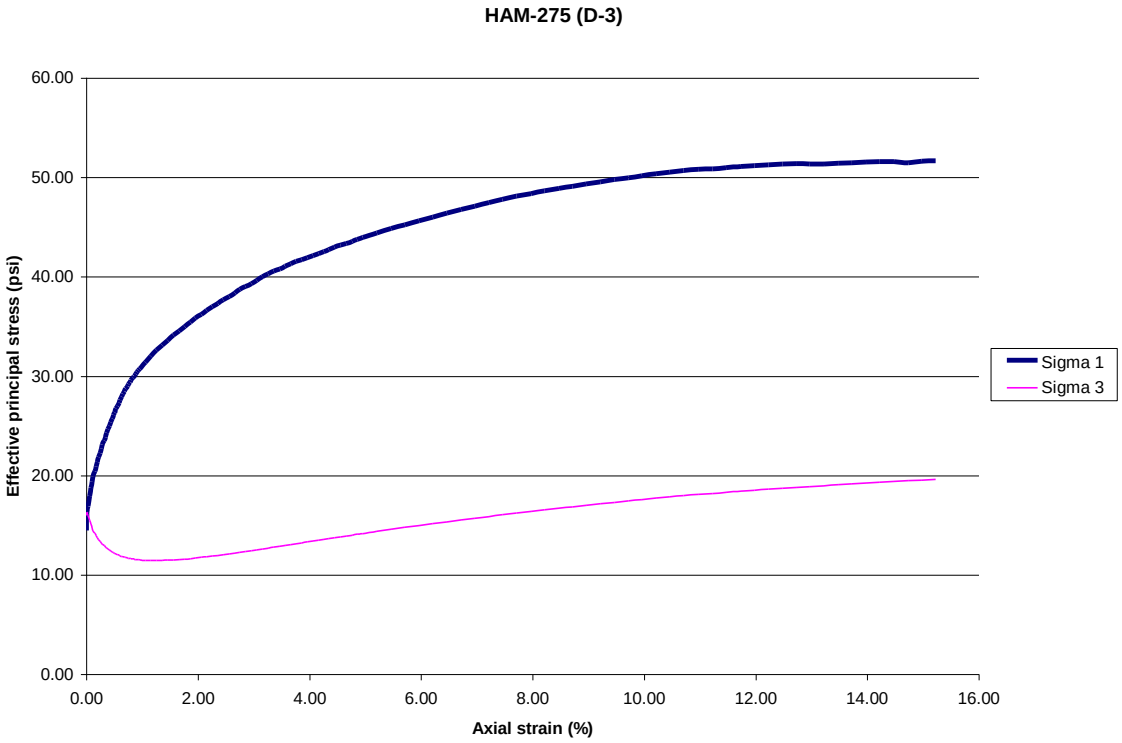


**Figure C.8:** Specimen D-3 (10.2' – 10.6' Depth) – Site No. 1

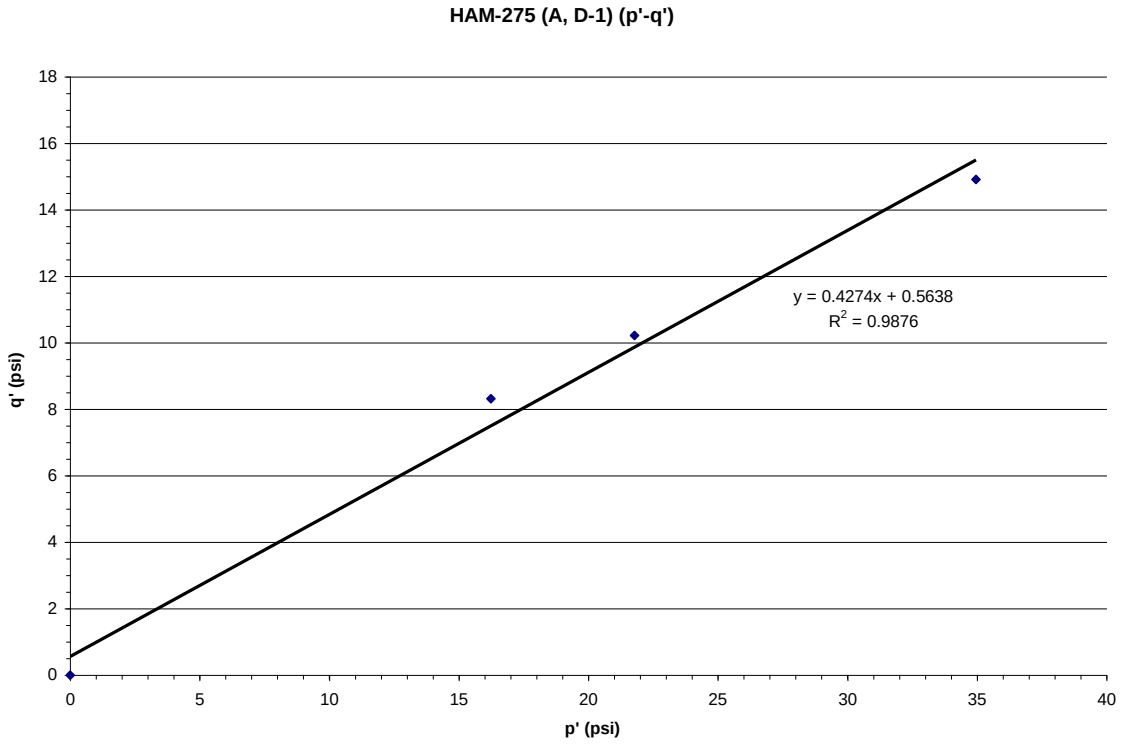


**Figure C.9:** p'-q' Diagram for the Highest Depth Range – Site No. 1

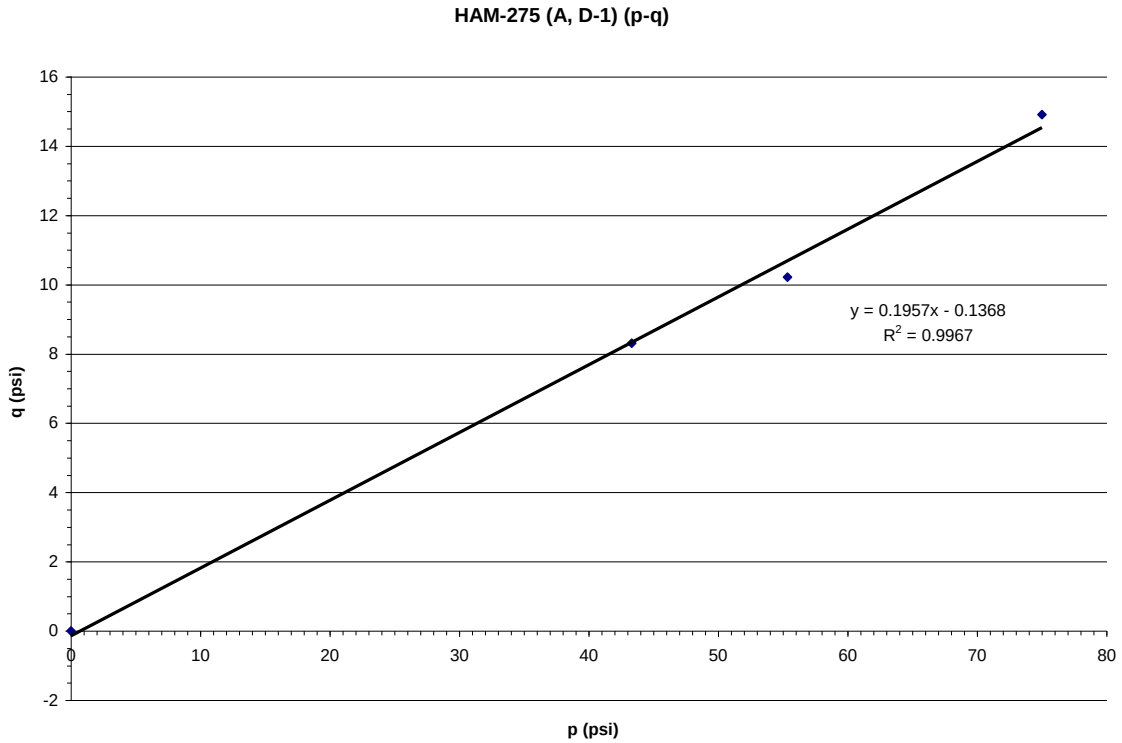


**Figure C.10:** p–q Diagram for the Highest Depth Range – Site No. 1

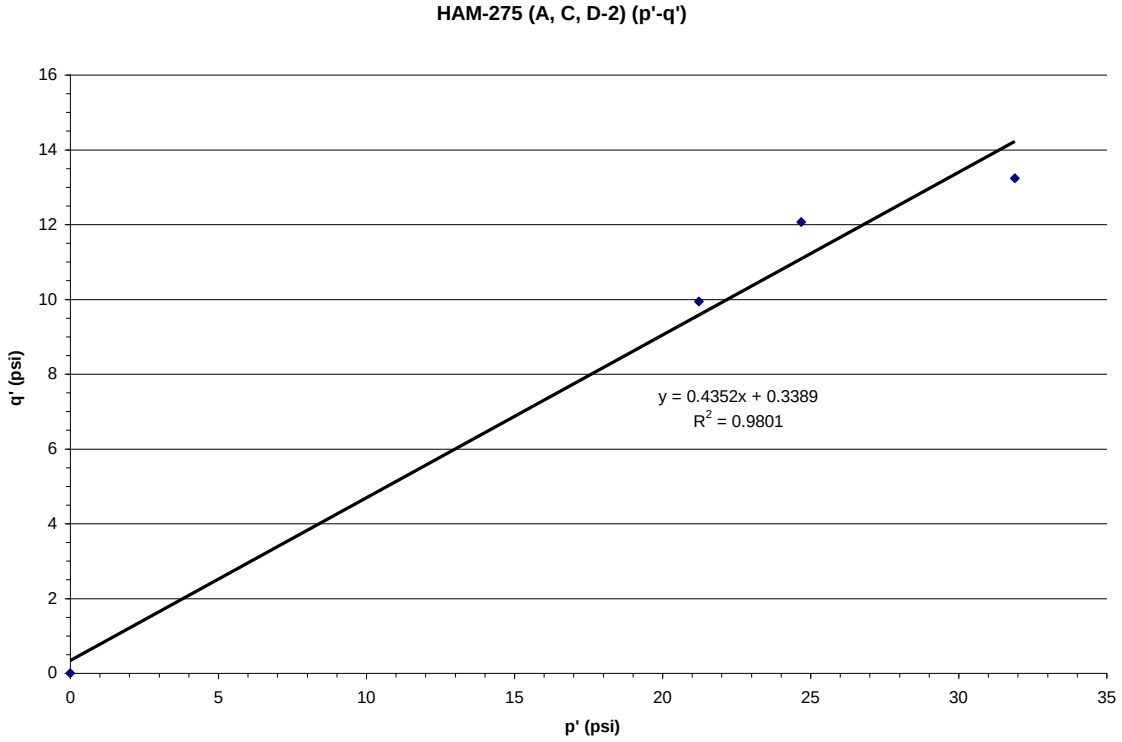


**Figure C.11:** p'-q' Diagram for the Middle Depth Range – Site No. 1

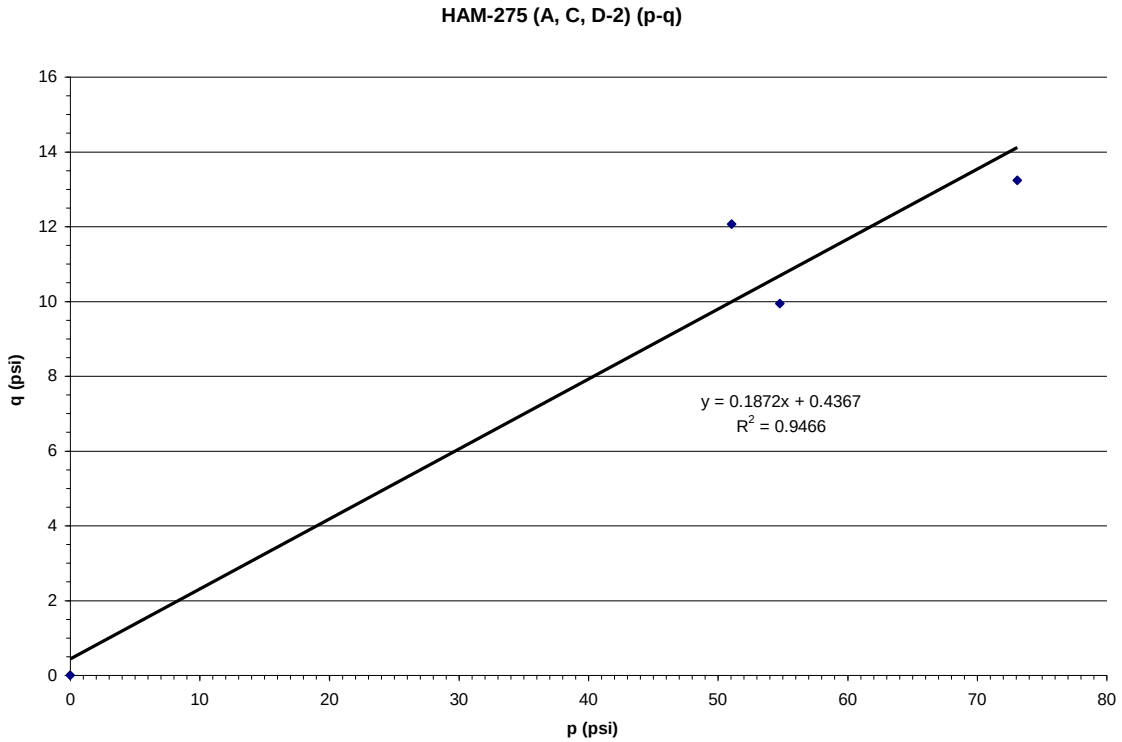


**Figure C.12:** p-q Diagram for the Middle Depth Range – Site No. 1

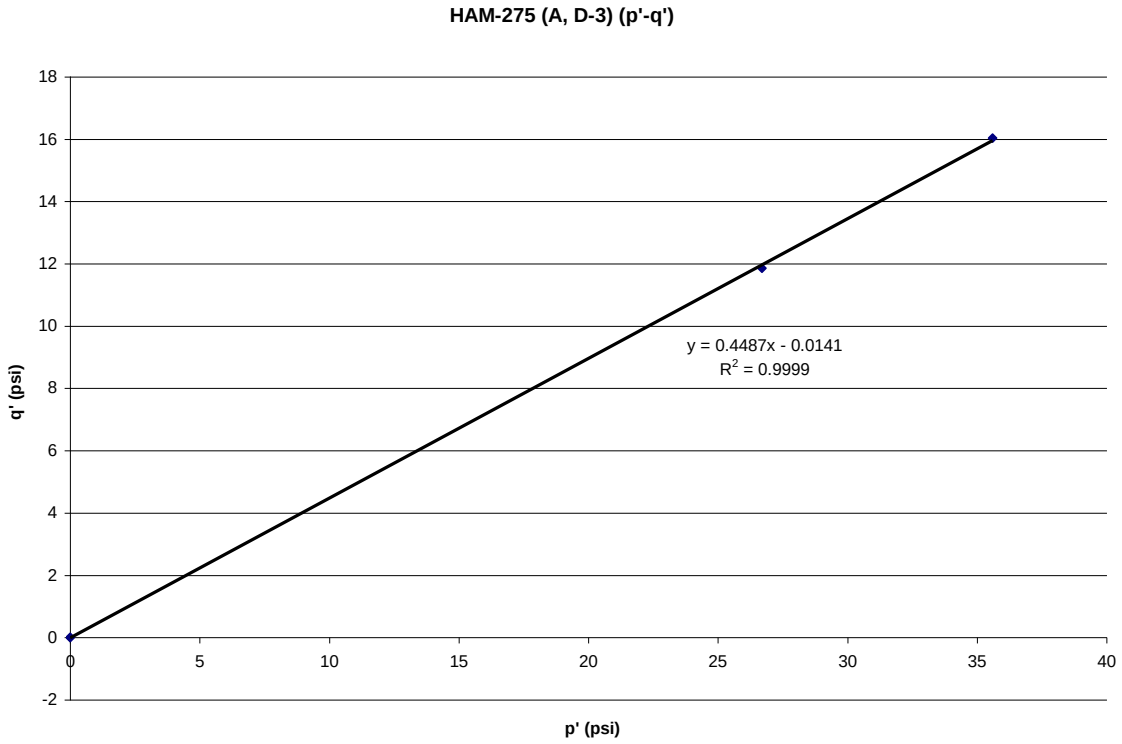


**Figure C.13:** p'-q' Diagram for the Lowest Depth Range – Site No. 1

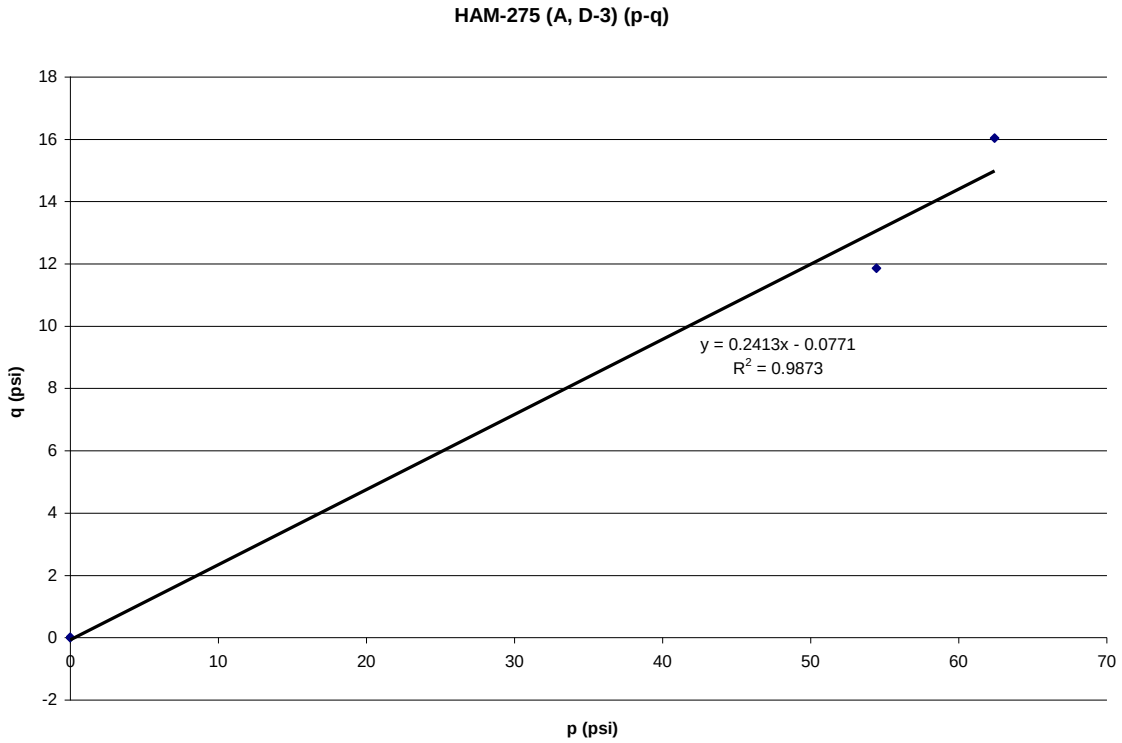


**Figure C.14:** p-q Diagram for the Lowest Depth Range – Site No. 1

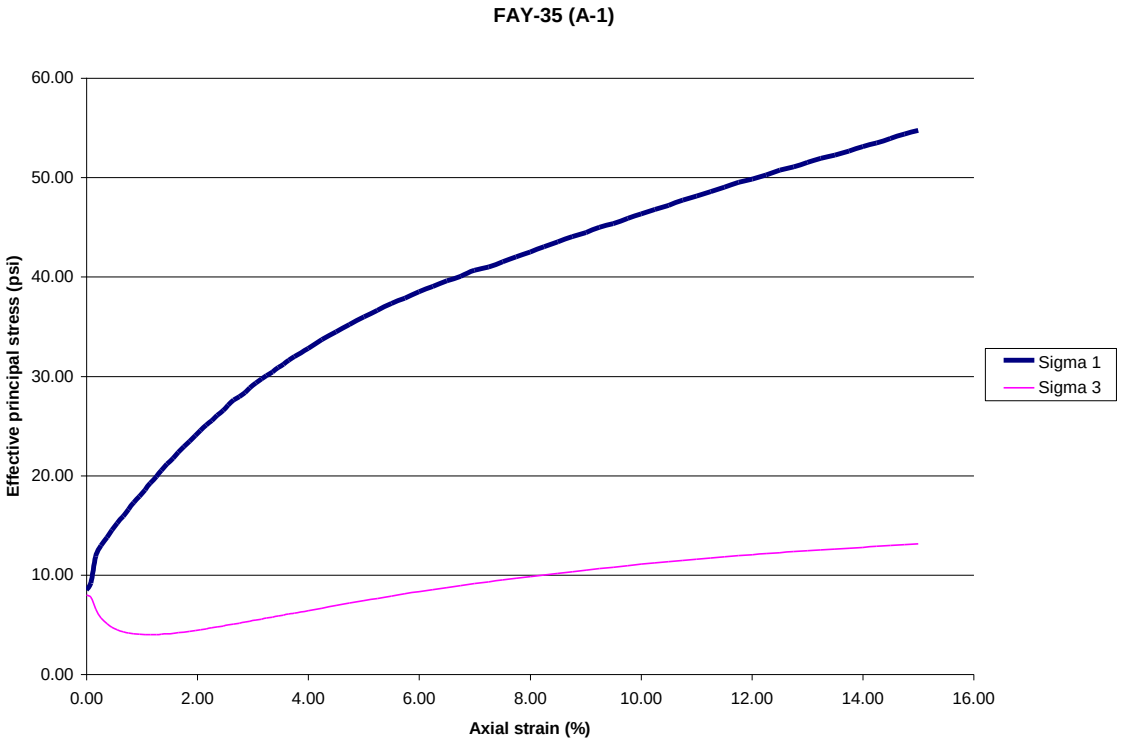


**Figure C.15:** Specimen A-1 (5.7' – 6.2' Depth) – Site No. 2

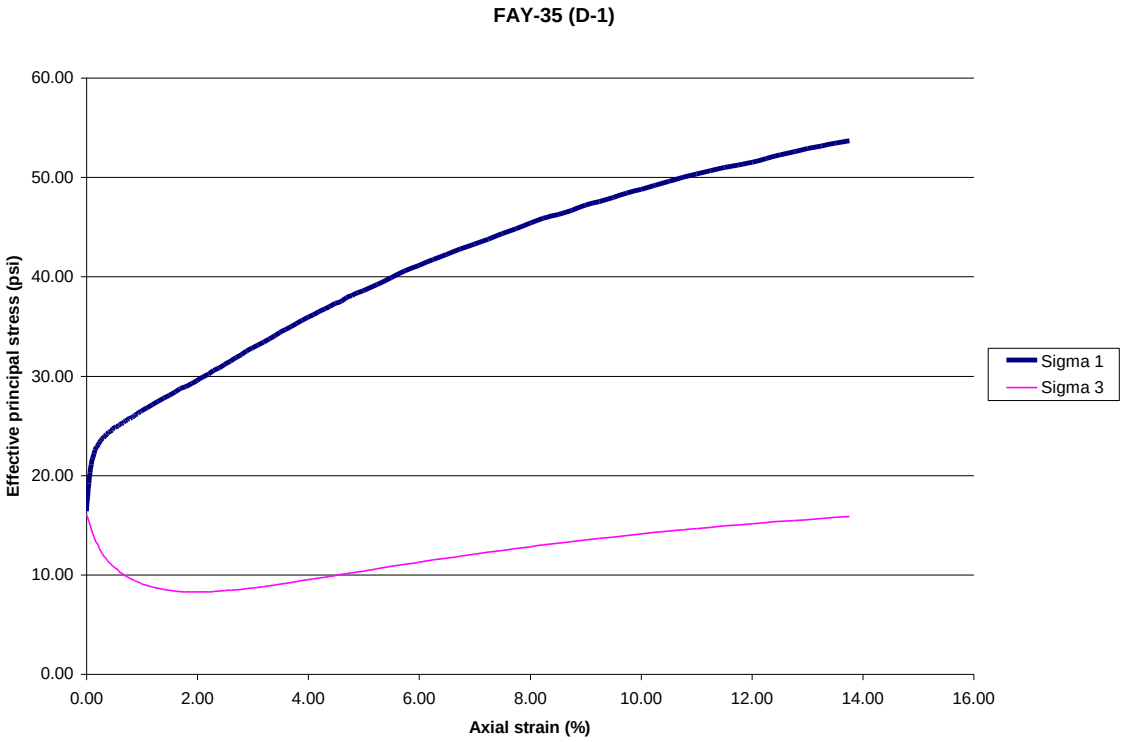


**Figure C.16:** Specimen D-1 (6.6' – 7.1' Depth) – Site No. 2

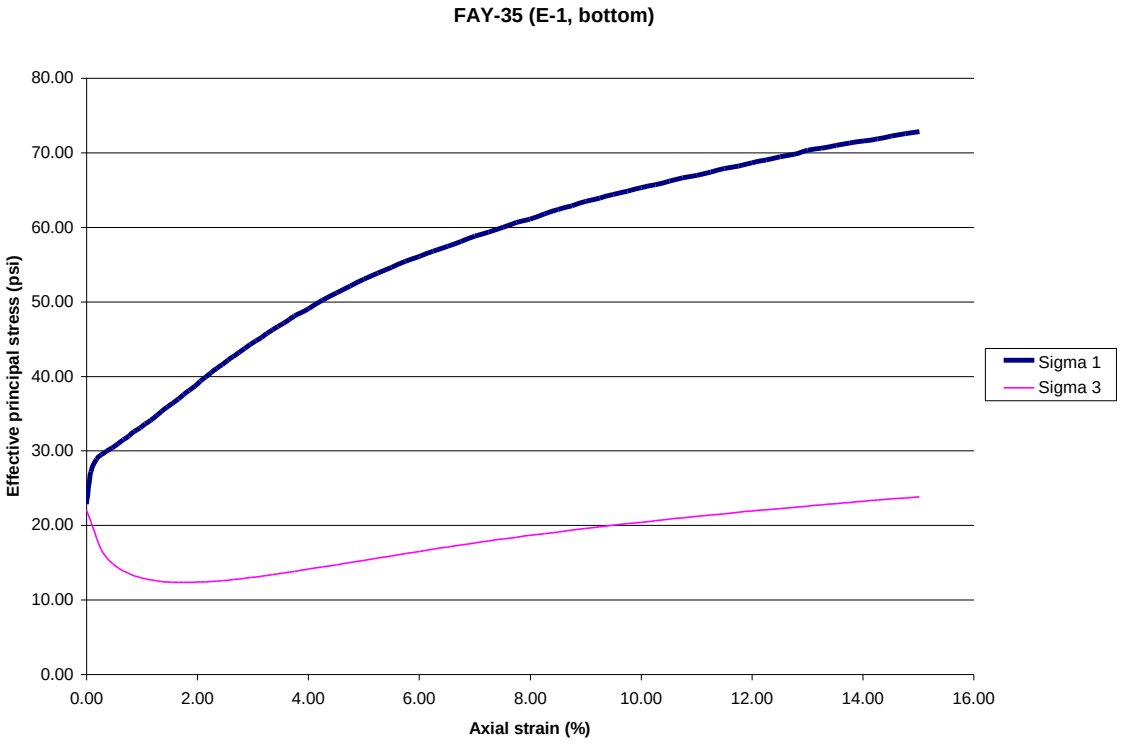


**Figure C.17:** Specimen E-1 (6.3' – 6.7' Depth) – Site No. 2

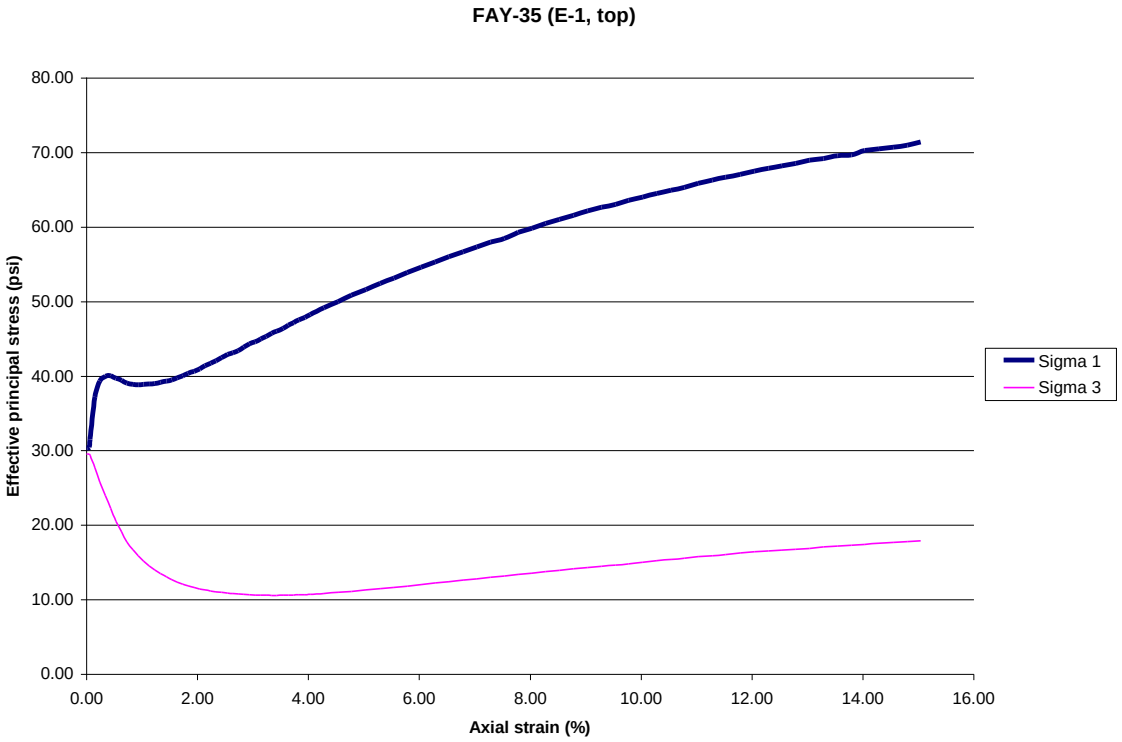


**Figure C.18:** Specimen E-1 (5.5' – 6.0' Depth) – Site No. 2

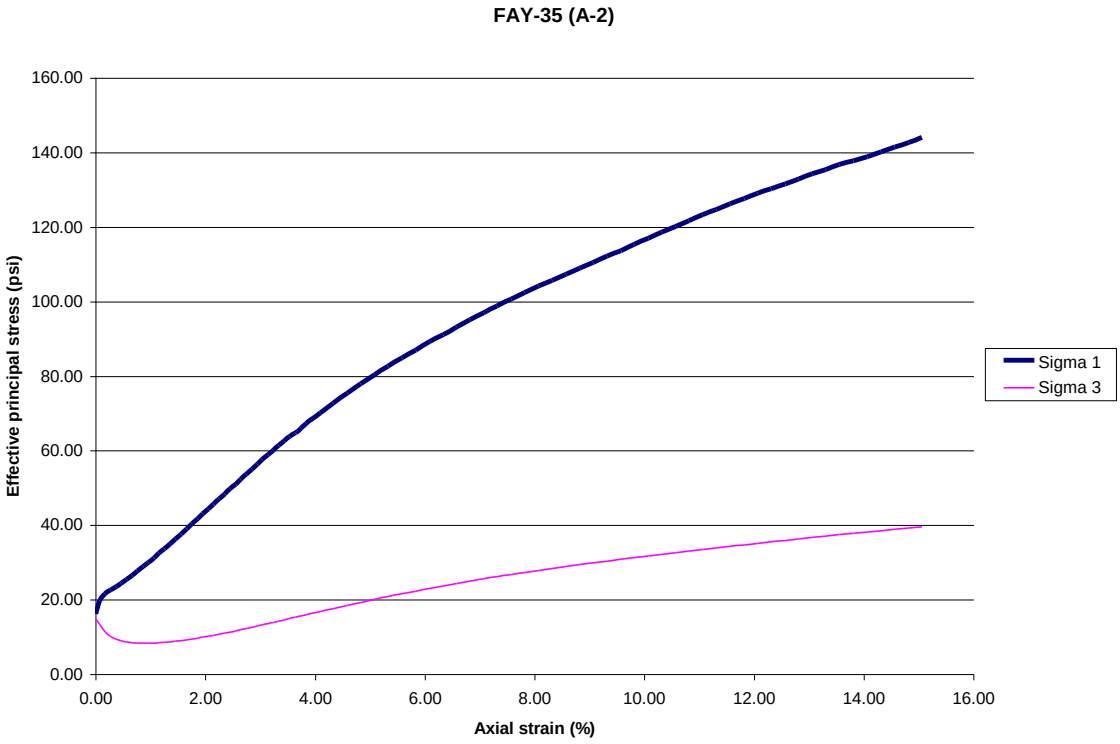


**Figure C.19:** Specimen A-2 (9.2' – 9.7' Depth) – Site No. 2

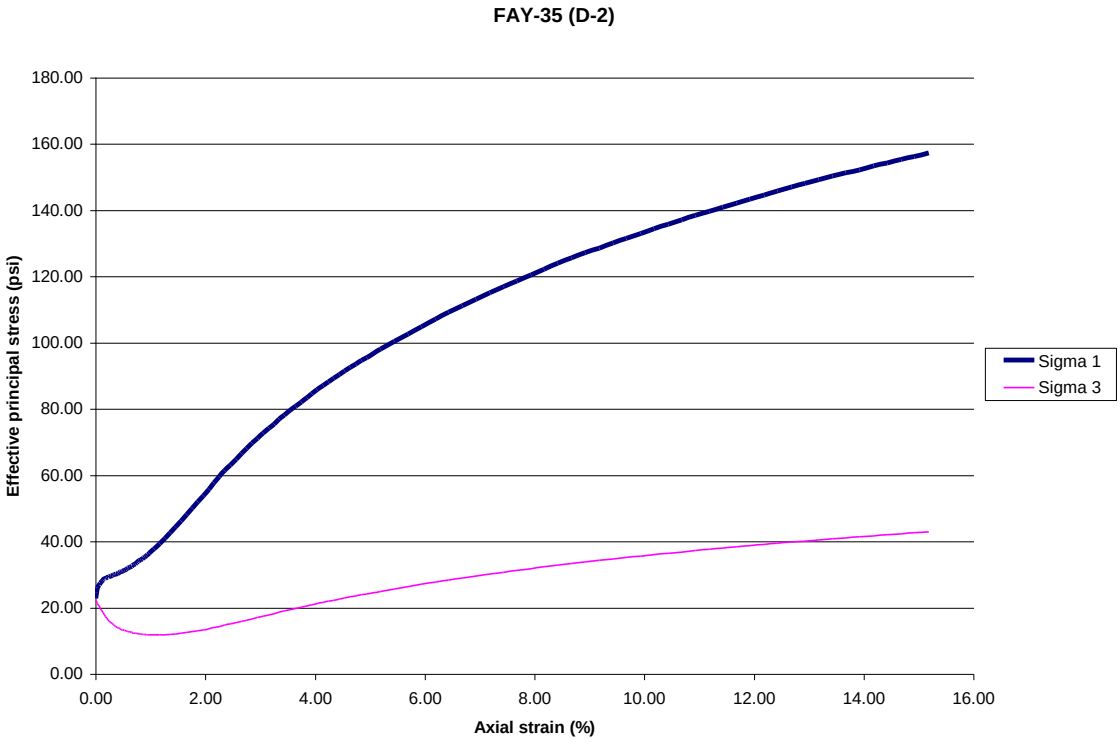


**Figure C.20:** Specimen D-2 (9.2' – 9.7' Depth) – Site No. 2

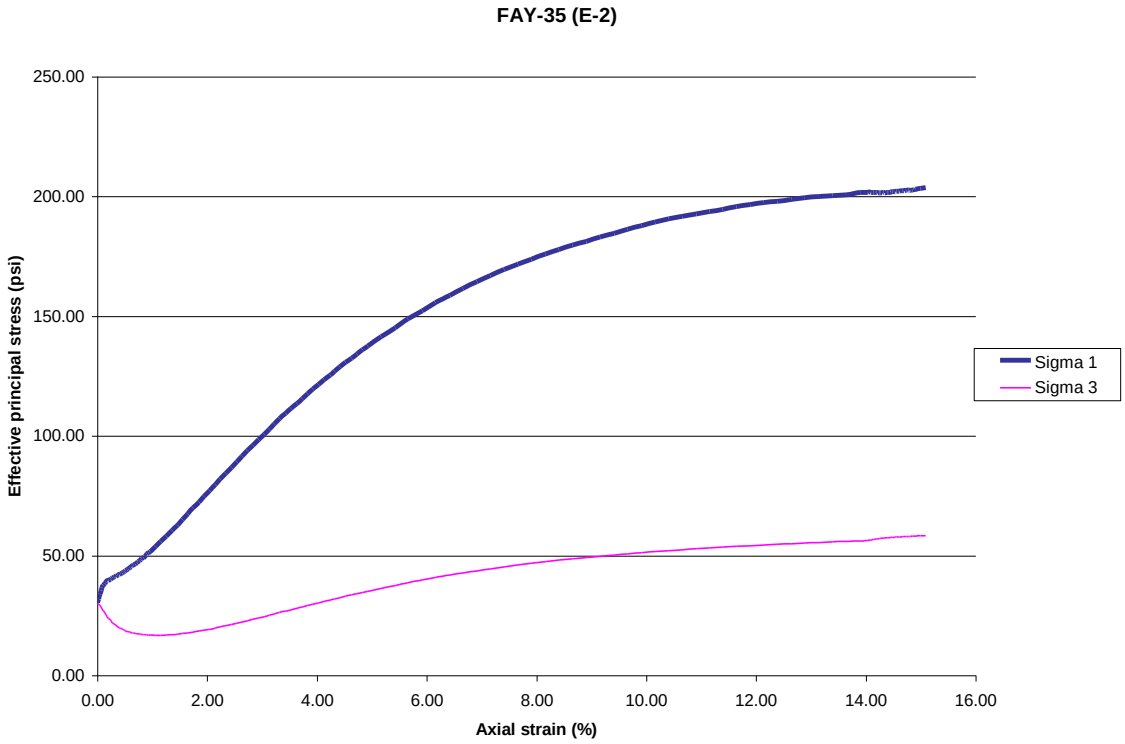


**Figure C.21:** Specimen E-2 (9.2' – 9.7' Depth) – Site No. 2

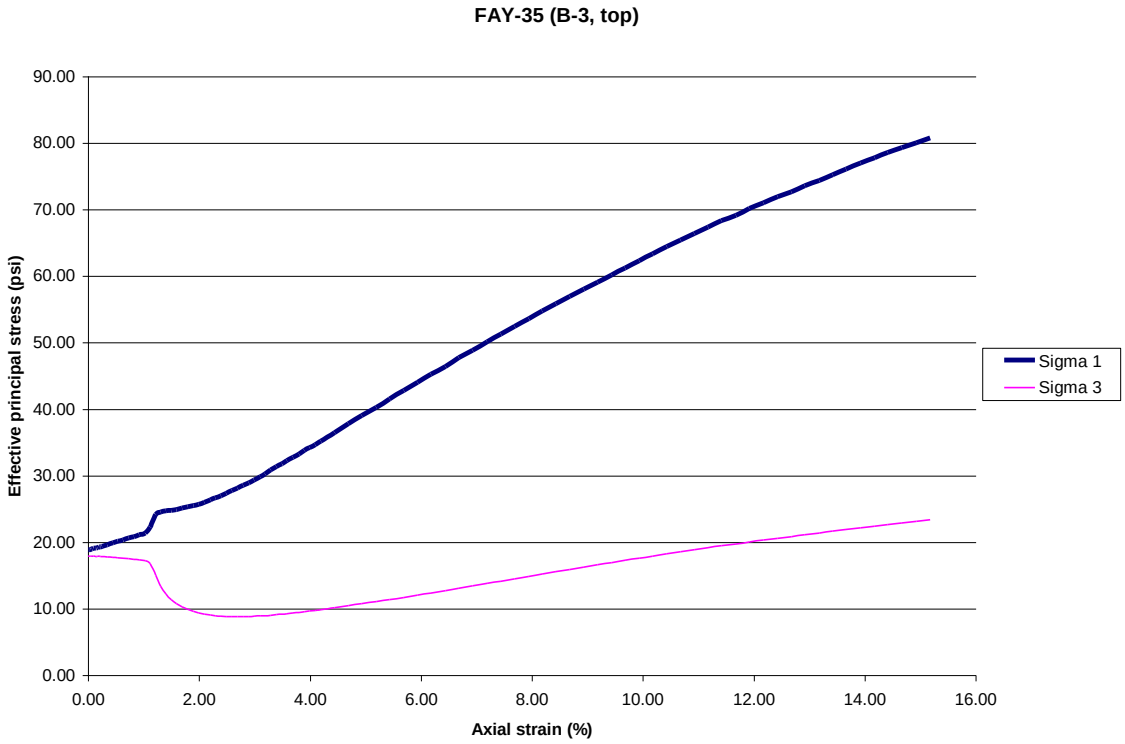


**Figure C.22:** Specimen B-3 (14.7' – 15.2' Depth) – Site No. 2

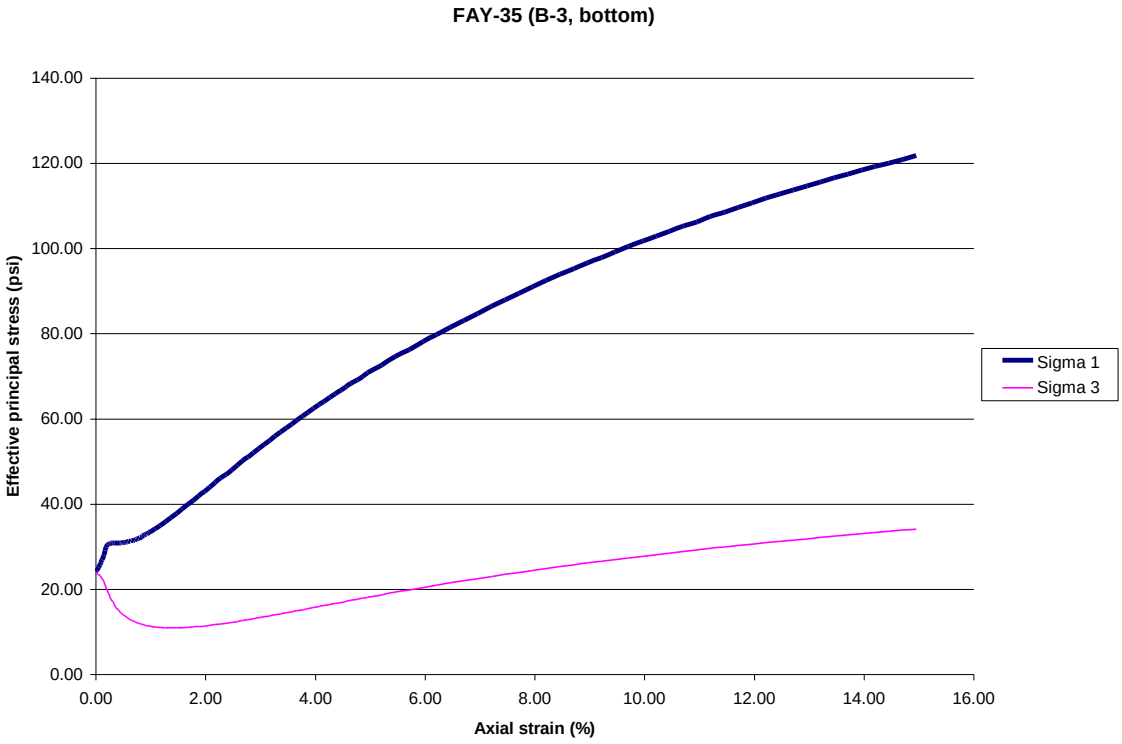


**Figure C.23:** Specimen B-3 (15.4' – 15.8' Depth) – Site No. 2

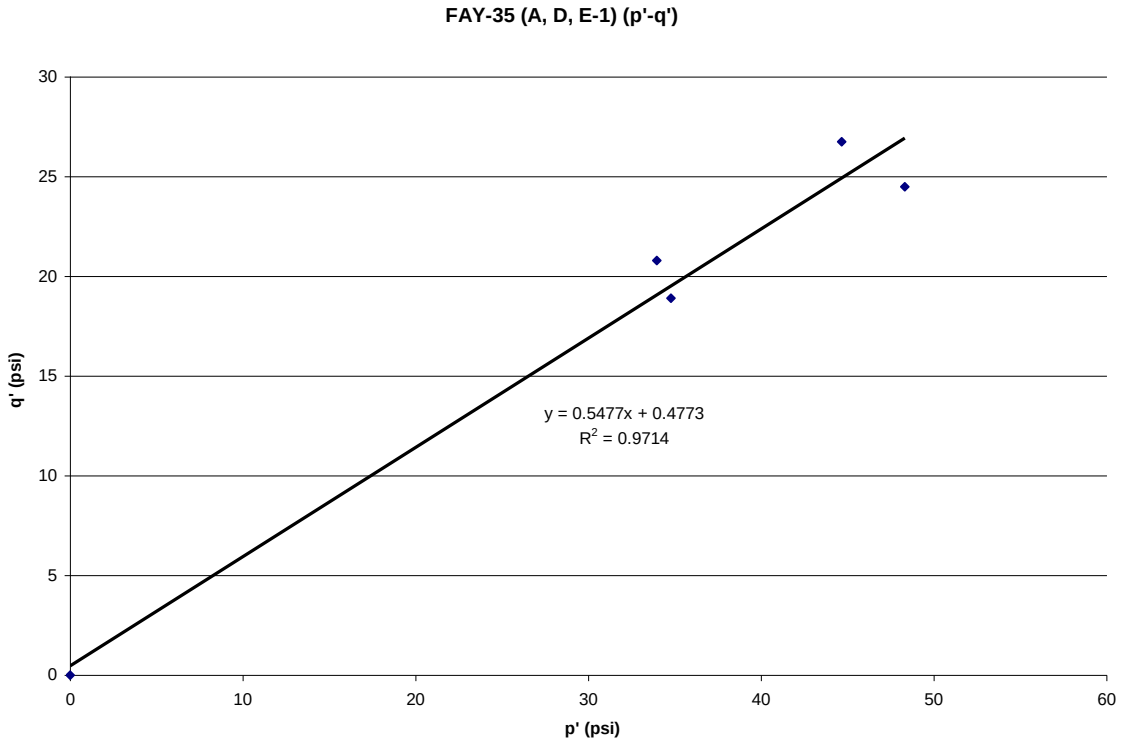


**Figure C.24:** p'-q' Diagram for the Highest Depth Range – Site No. 2

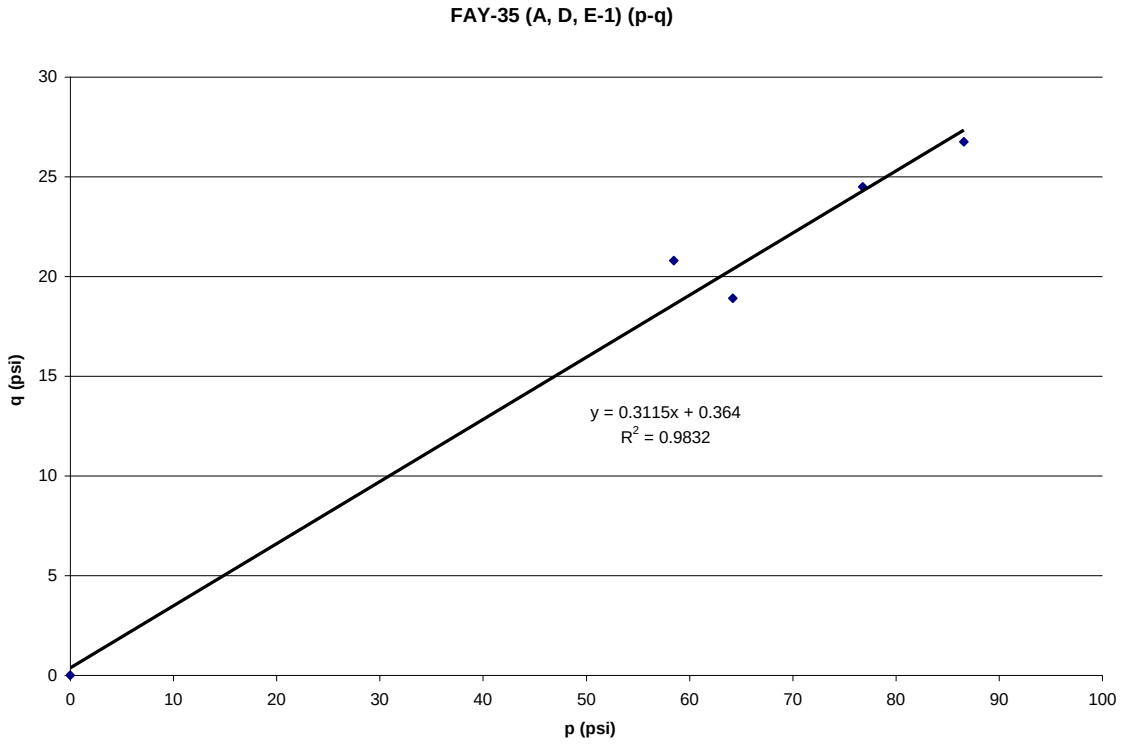


**Figure C.25:** p-q Diagram for the Highest Depth Range – Site No. 2

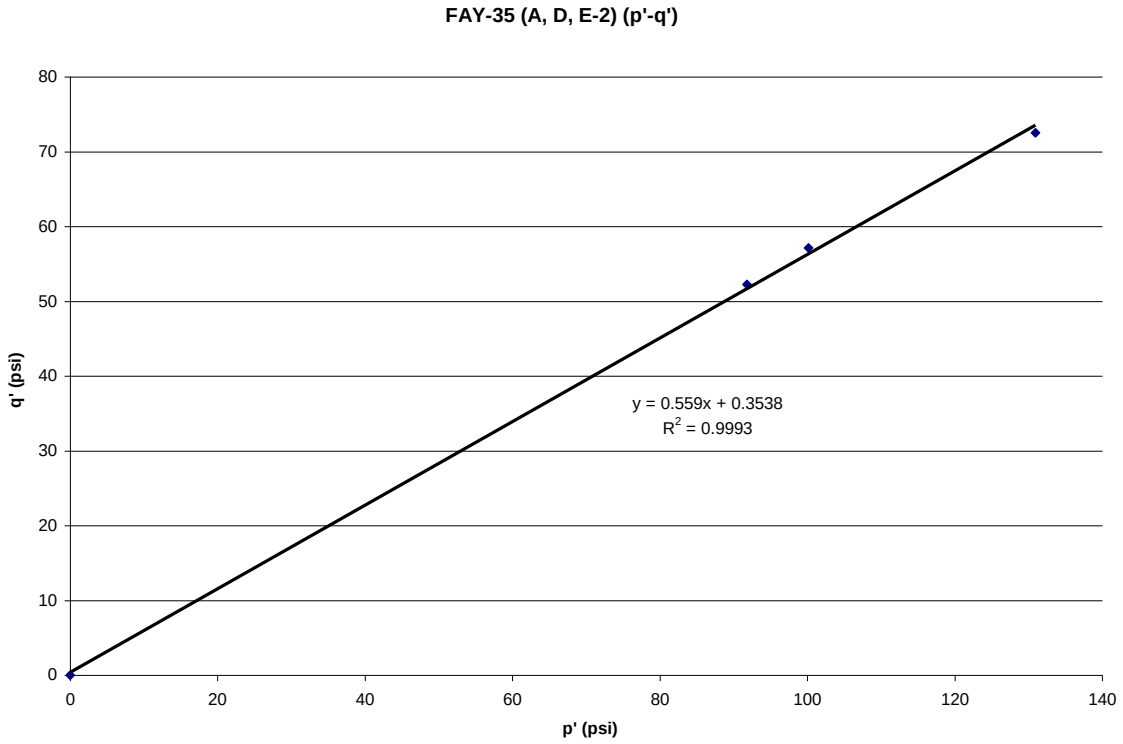


**Figure C.26:** p'-q' Diagram for the Middle Depth Range – Site No. 2

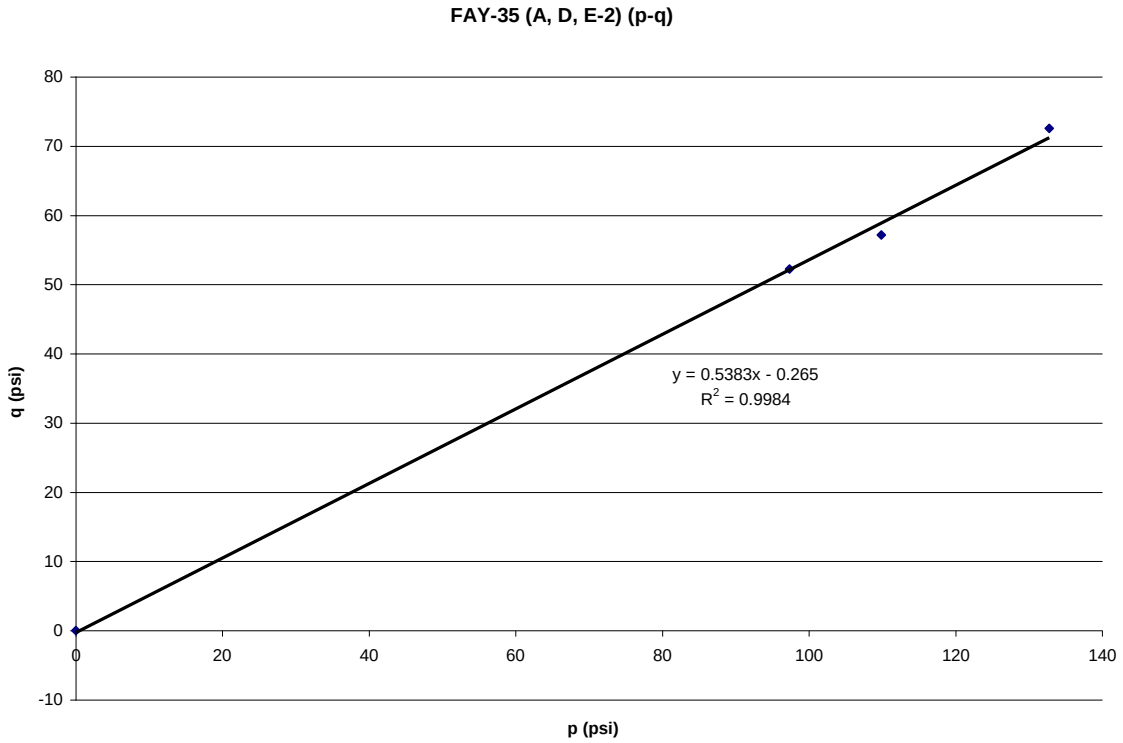


**Figure C.27:** p-q Diagram for the Middle Depth Range – Site No. 2

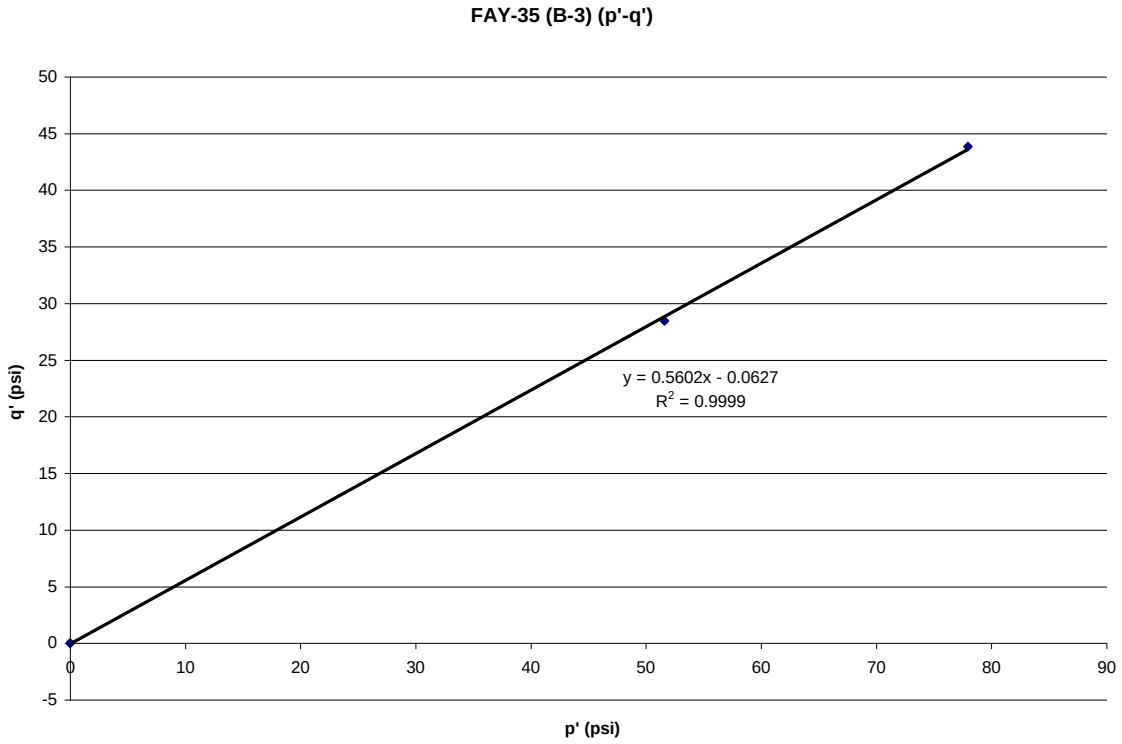


**Figure C.28:** p'-q' Diagram for the Lowest Depth Range – Site No. 2

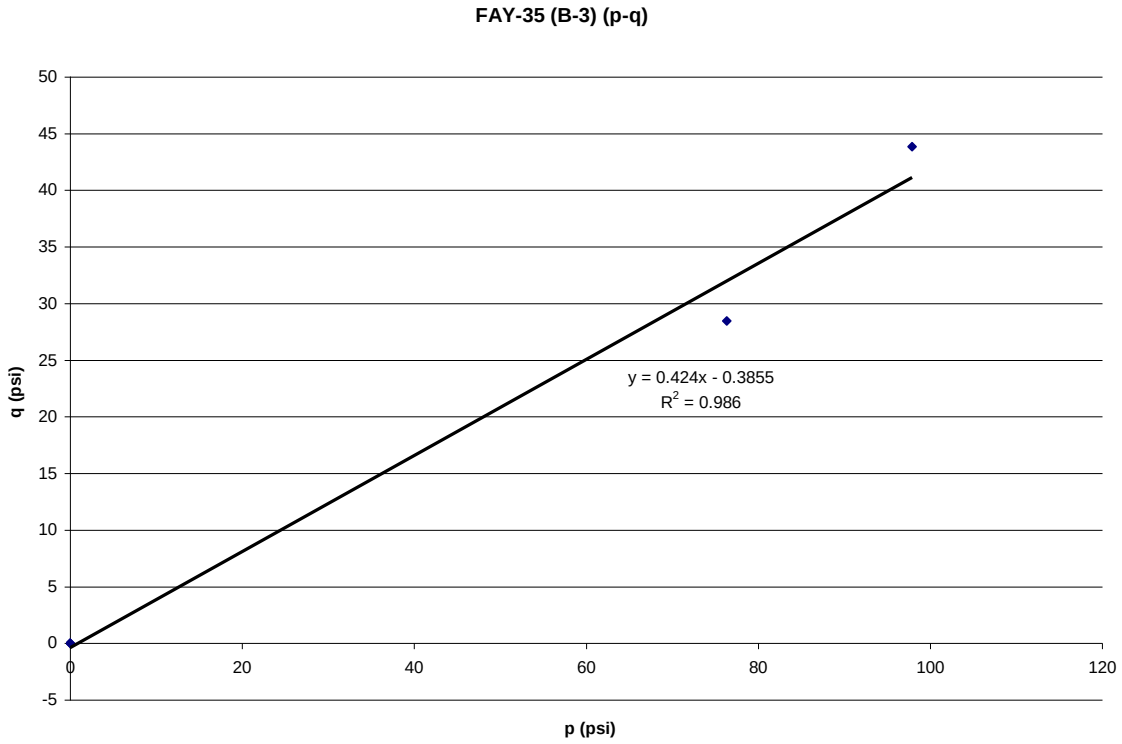


**Figure C.29:** p-q Diagram for the Lowest Depth Range – Site No. 2

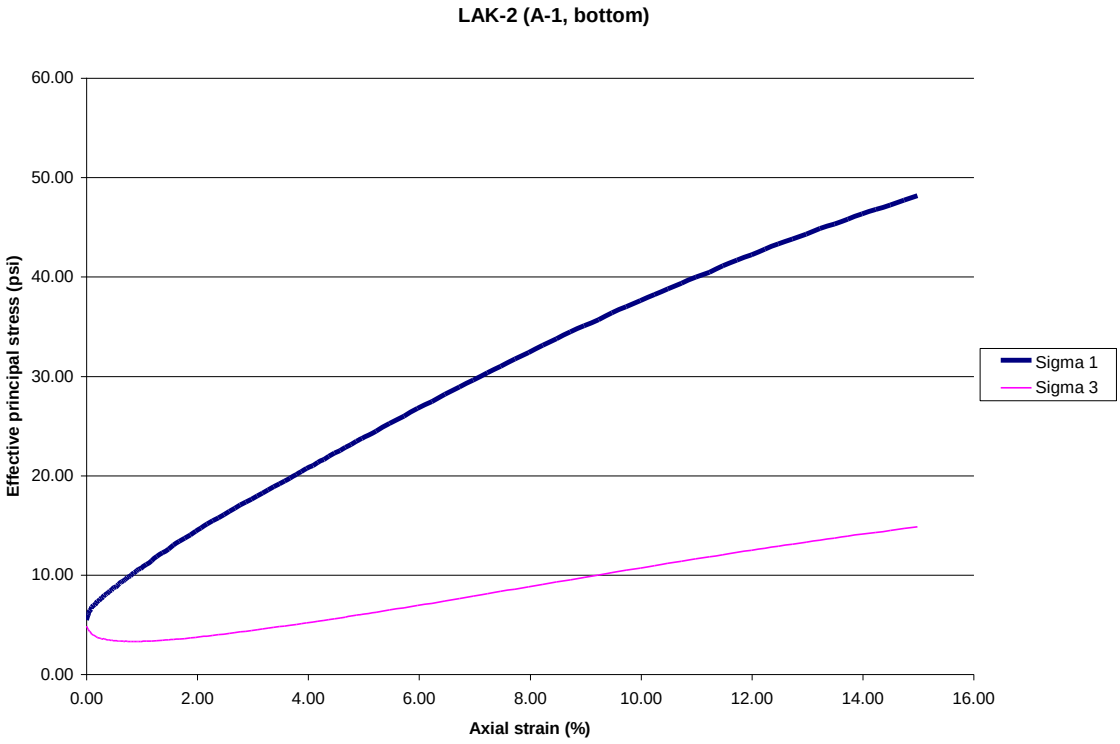


**Figure C.30:** Specimen A-1 (1.6' – 2.1' Depth) – Site No. 3

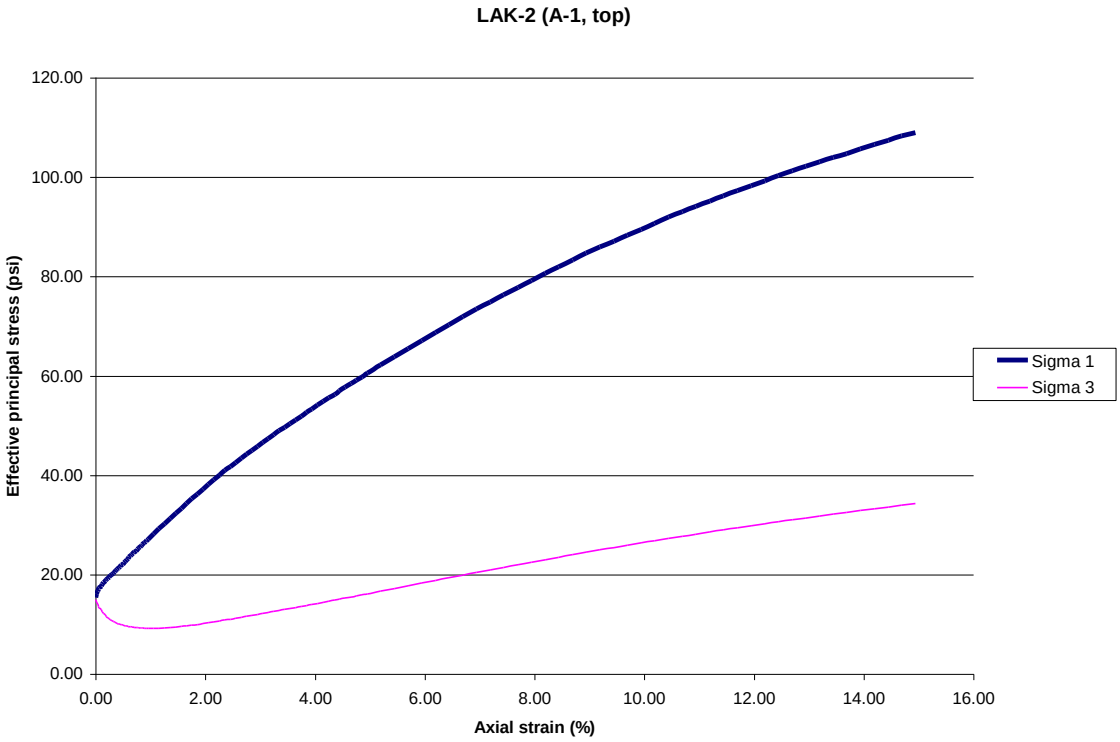


**Figure C.31:** Specimen A-1 (1.0' – 1.5' Depth) – Site No. 3

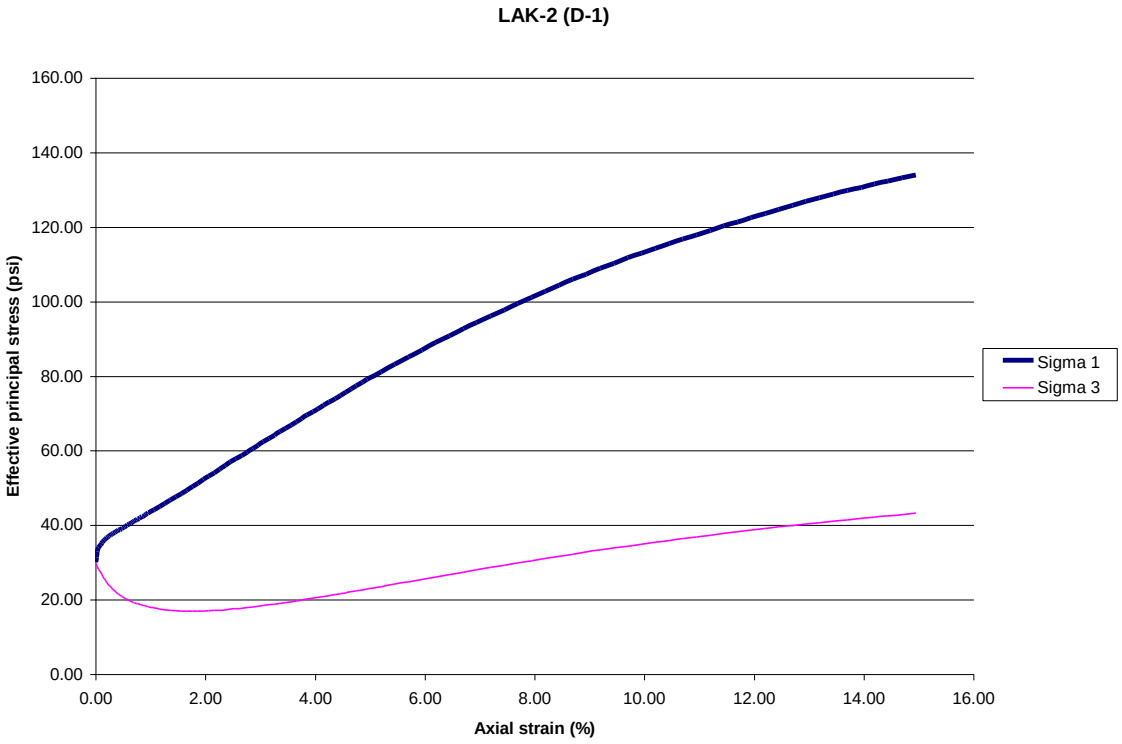


**Figure C.32:** Specimen D-1 (1.1' – 1.6' Depth) – Site No. 3

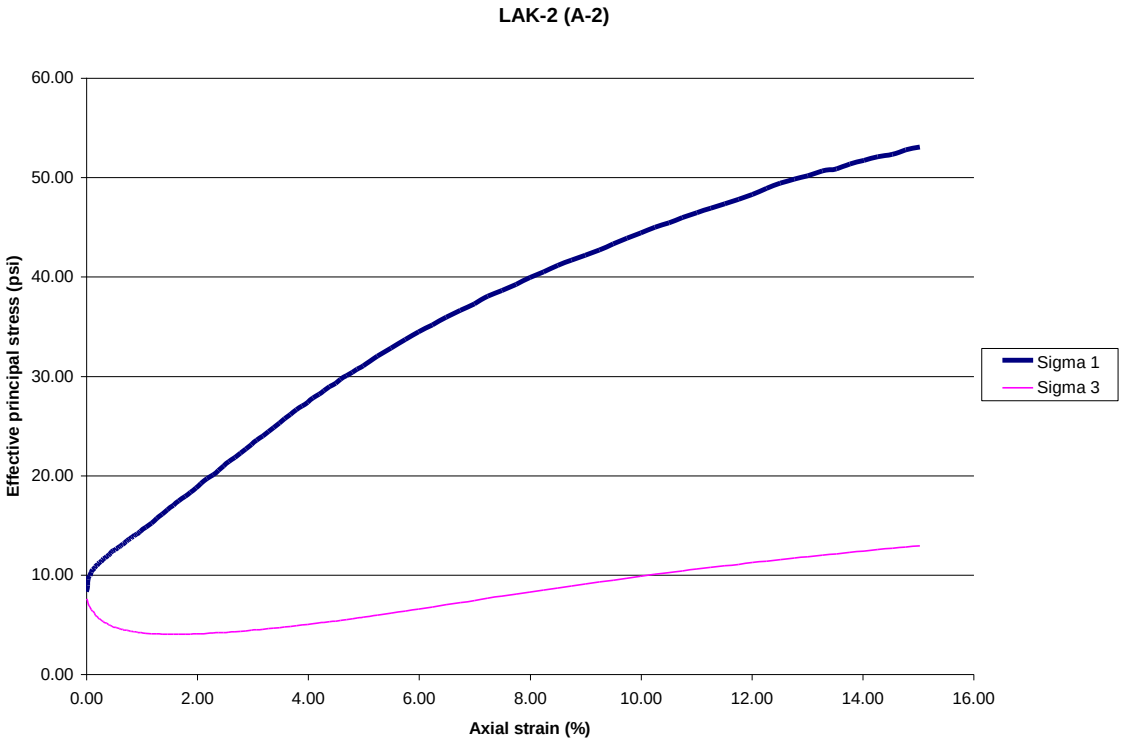


**Figure C.33:** Specimen A-2 (4.1' – 4.6' Depth) – Site No. 3

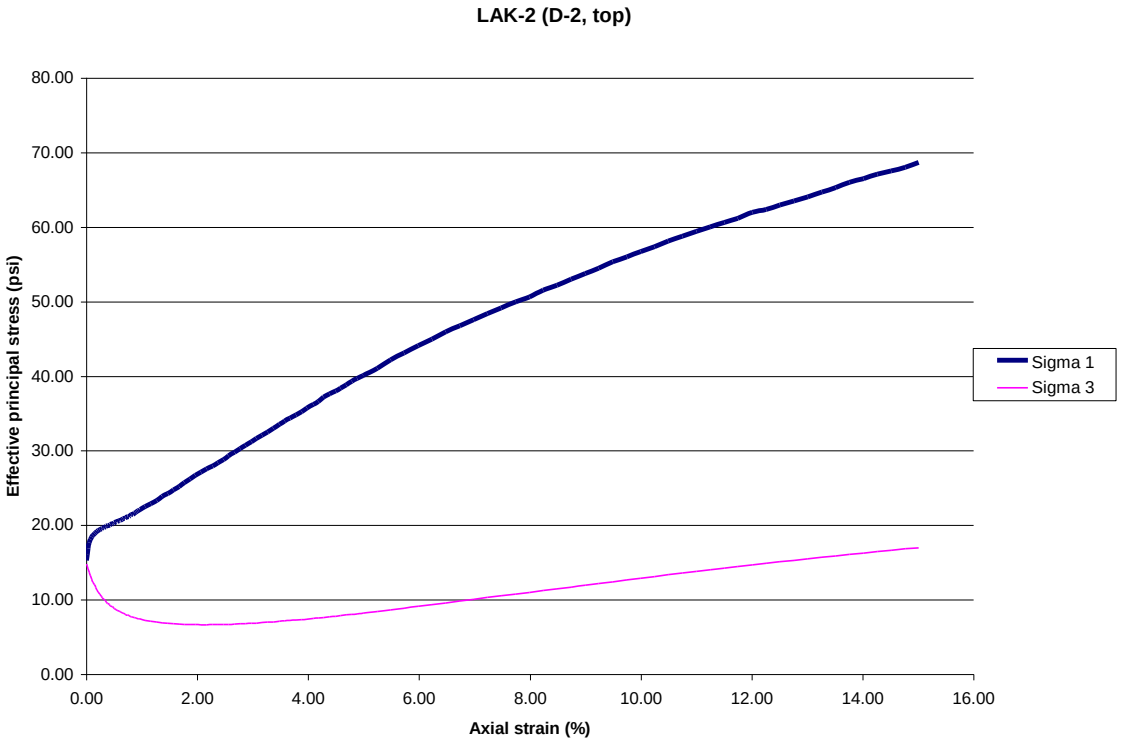


**Figure C.34:** Specimen D-2 (4.0' – 4.5' Depth) – Site No. 3

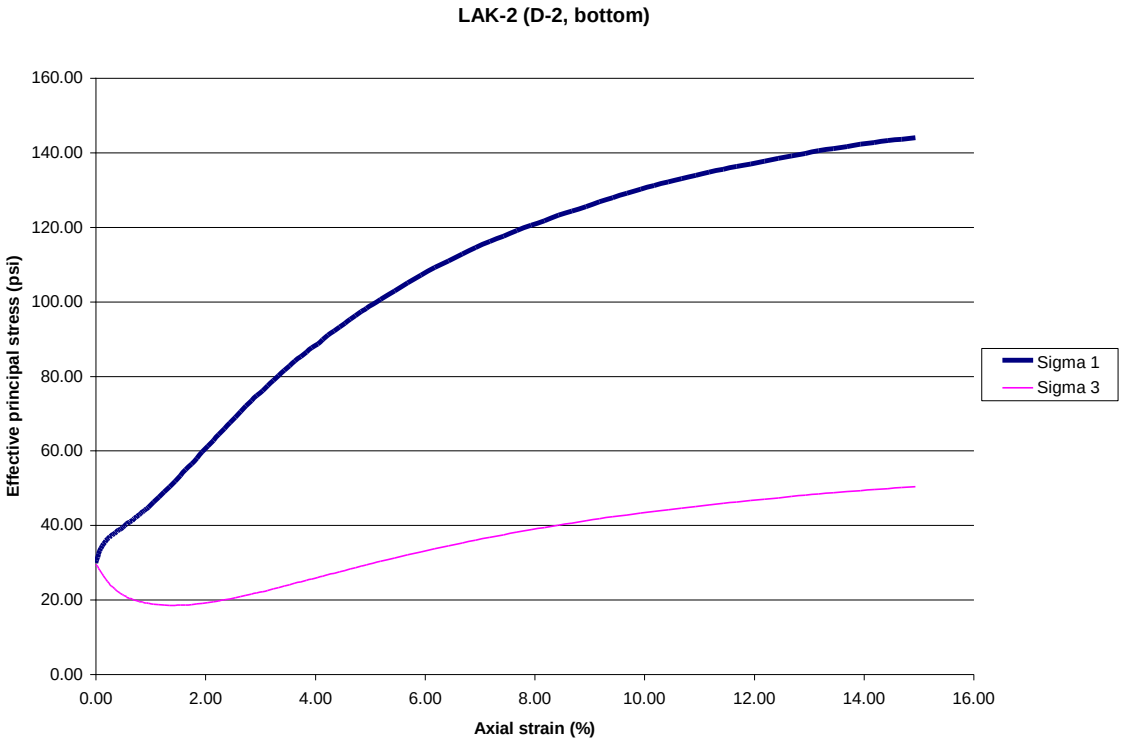


**Figure C.35:** Specimen D-2 (4.7' – 5.2' Depth) – Site No. 3

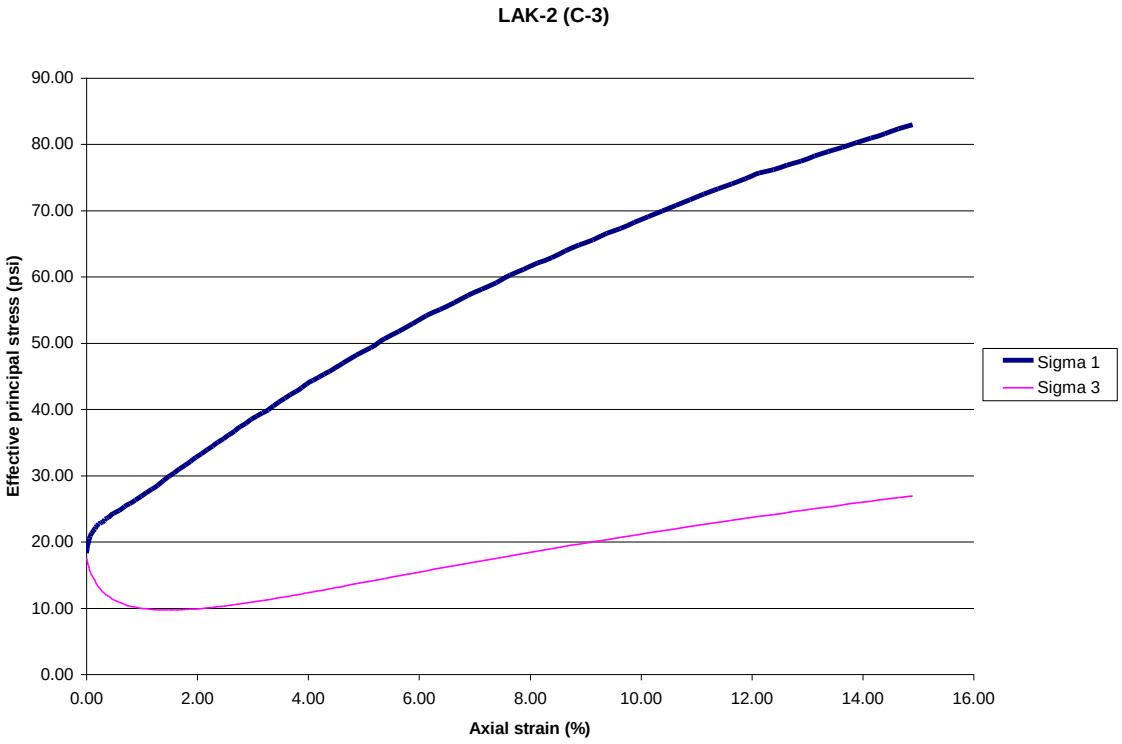


**Figure C.36:** Specimen C-3 (14.7' – 15.2' Depth) – Site No. 3

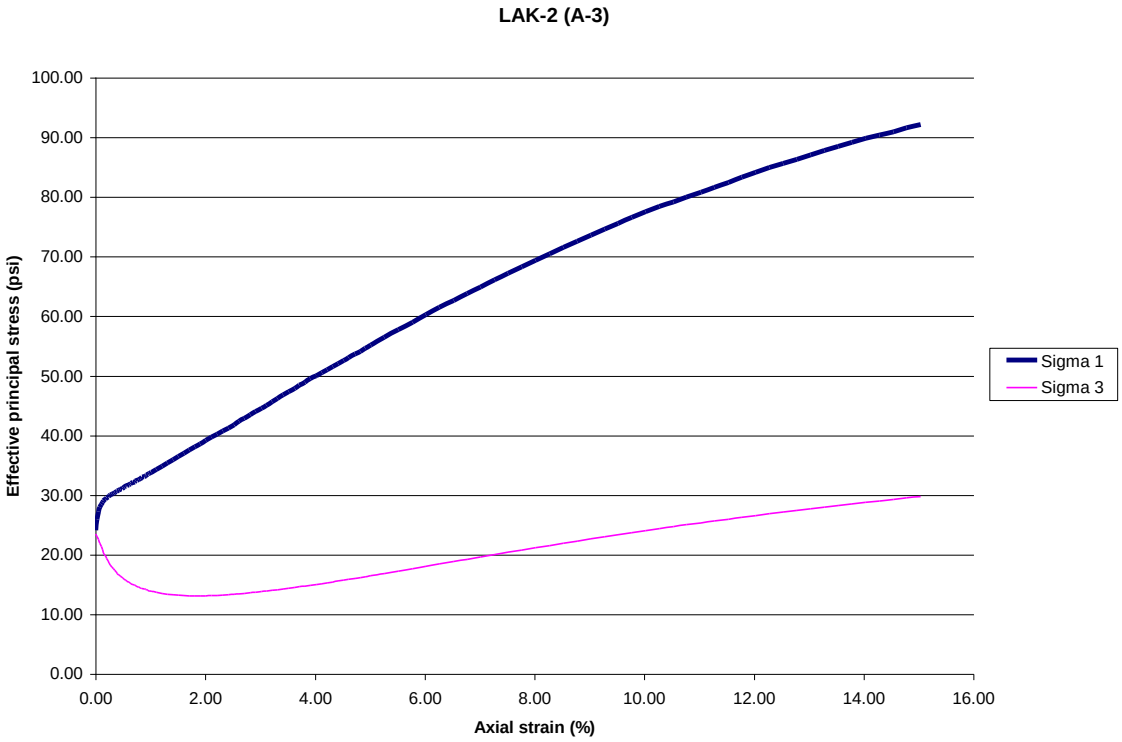


**Figure C.37:** Specimen A-3 (14.6' – 15.1' Depth) – Site No. 3

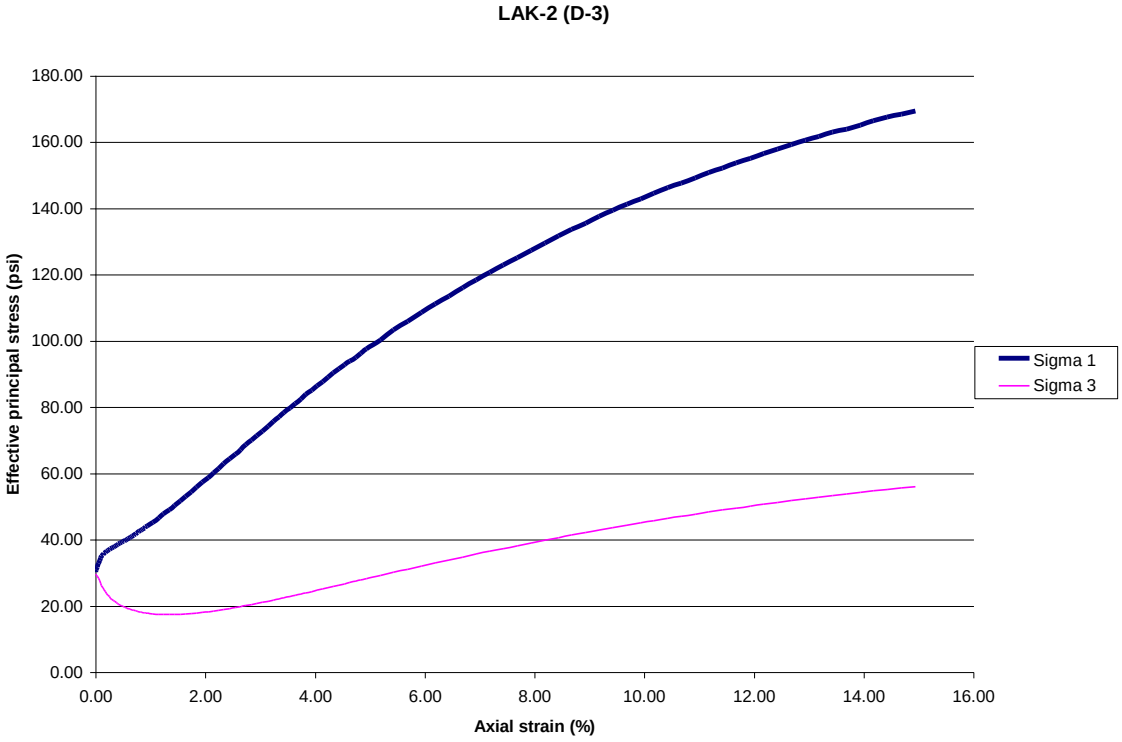


**Figure C.38:** Specimen D-3 (14.6' – 15.1' Depth) – Site No. 3

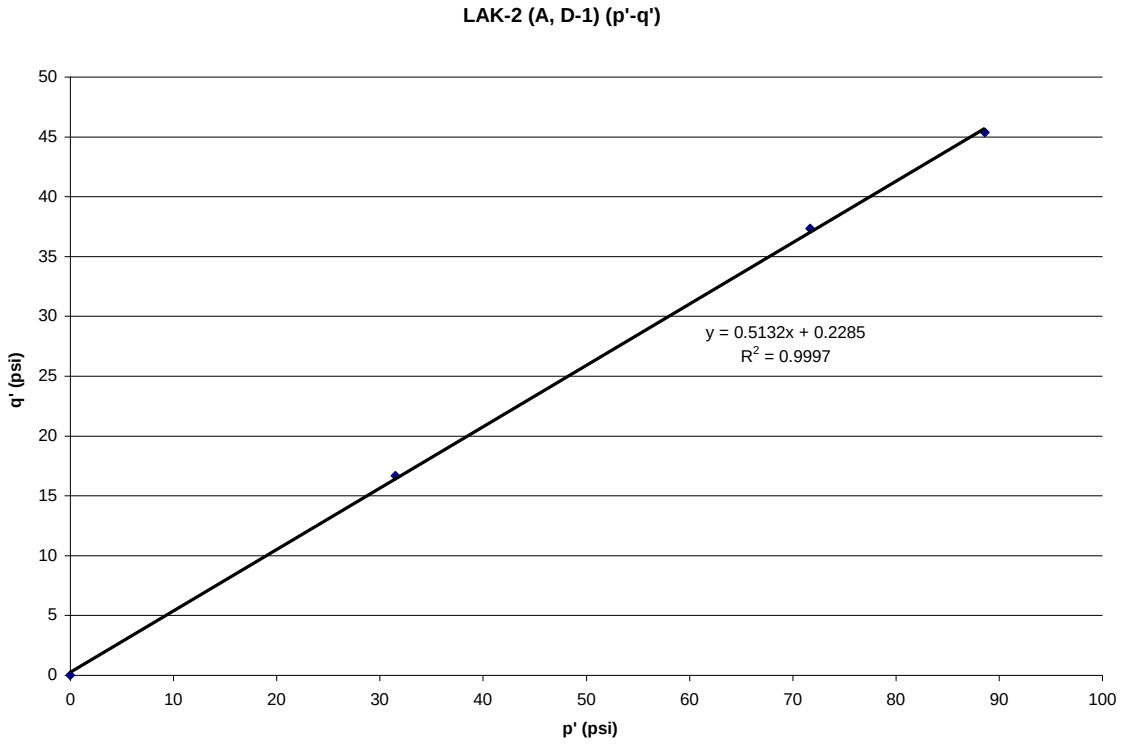


**Figure C.39:** p'-q' Diagram for the Highest Depth Range – Site No. 3

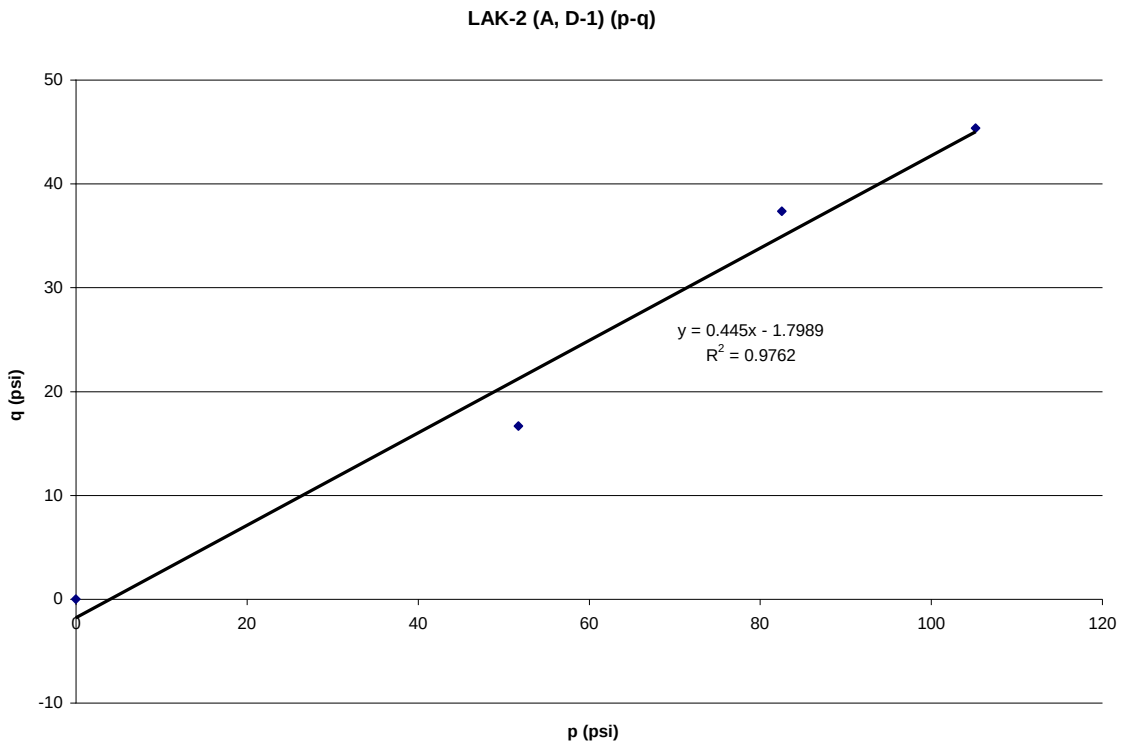


**Figure C.40:** p-q Diagram for the Highest Depth Range – Site No. 3

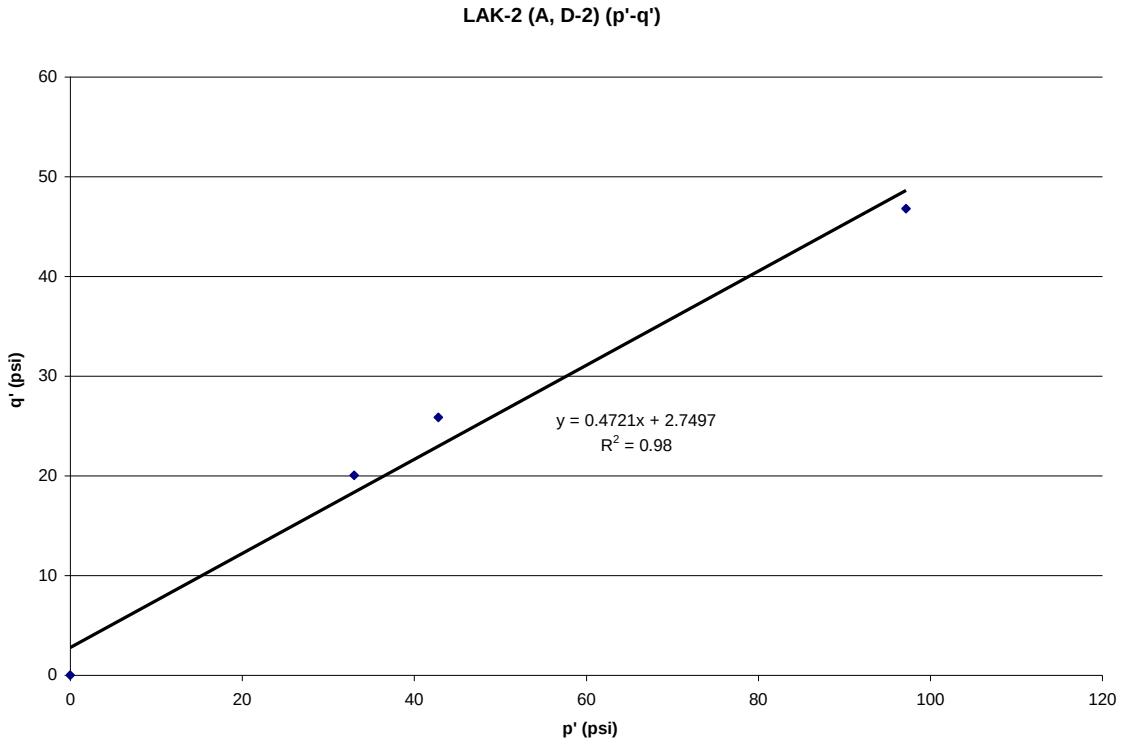


**Figure C.41.** p'-q' Diagram for the Middle Depth Range – Site No. 3

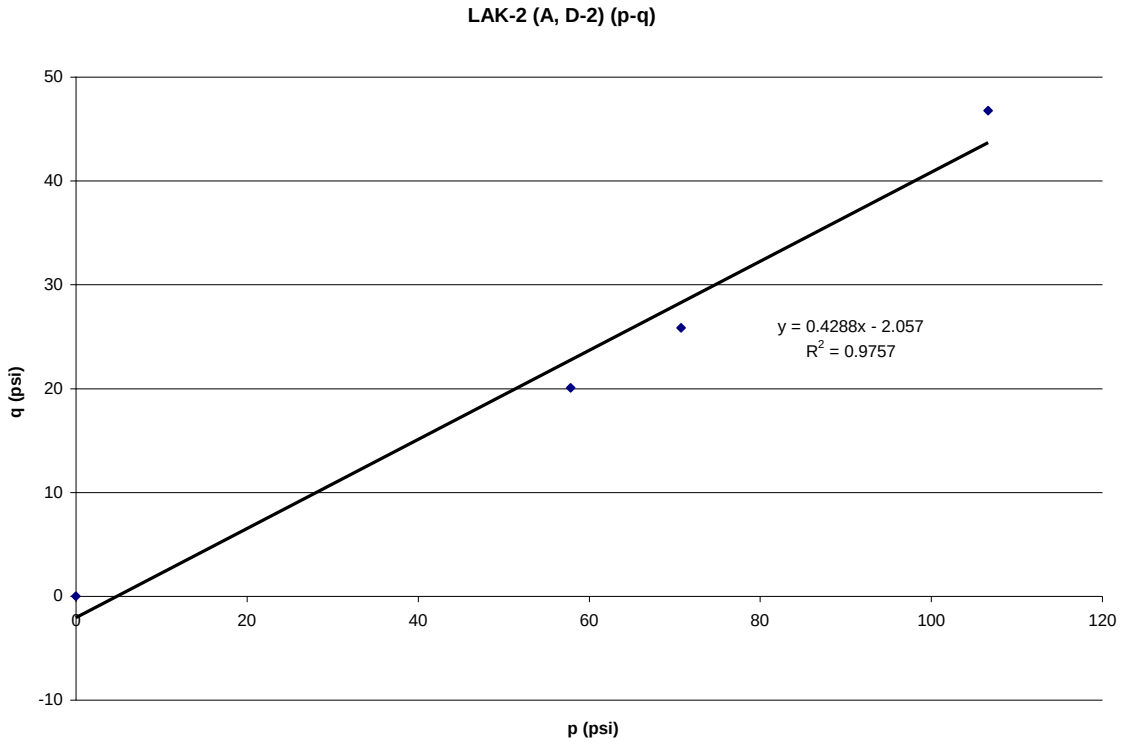


**Figure C.42:** p-q Diagram for Middle Depth Range – Site No. 3

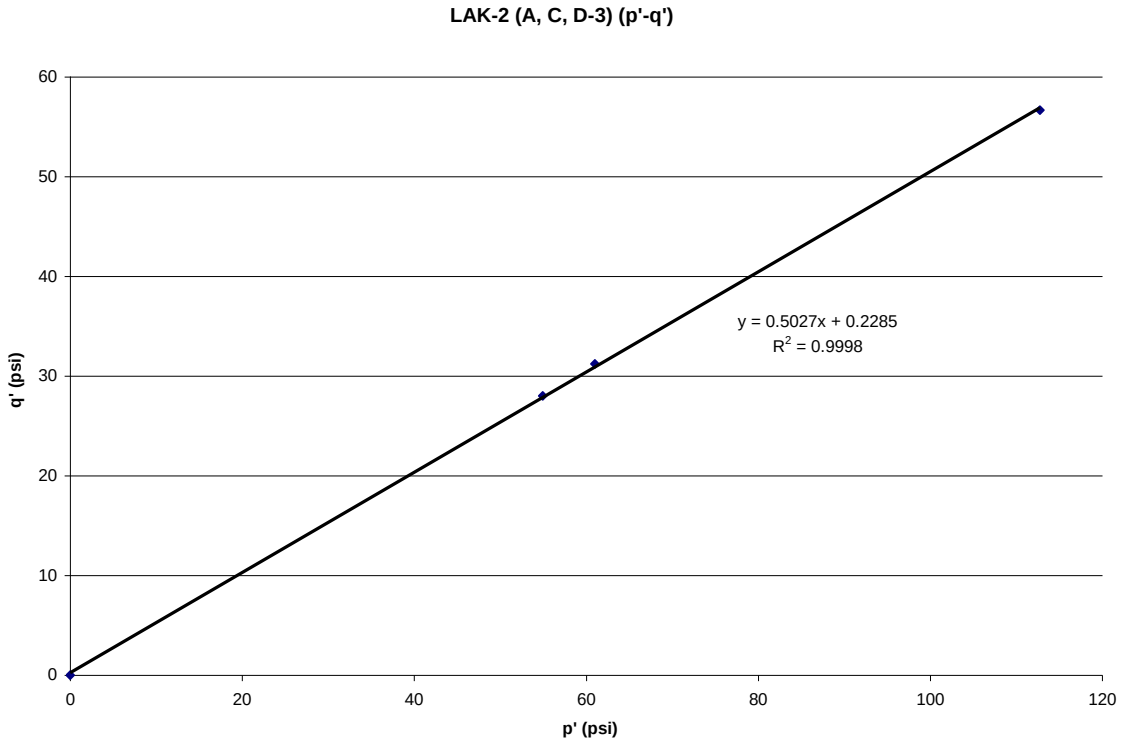


**Figure C.43:** p'-q' Diagram for the Lowest Depth Range – Site No. 3

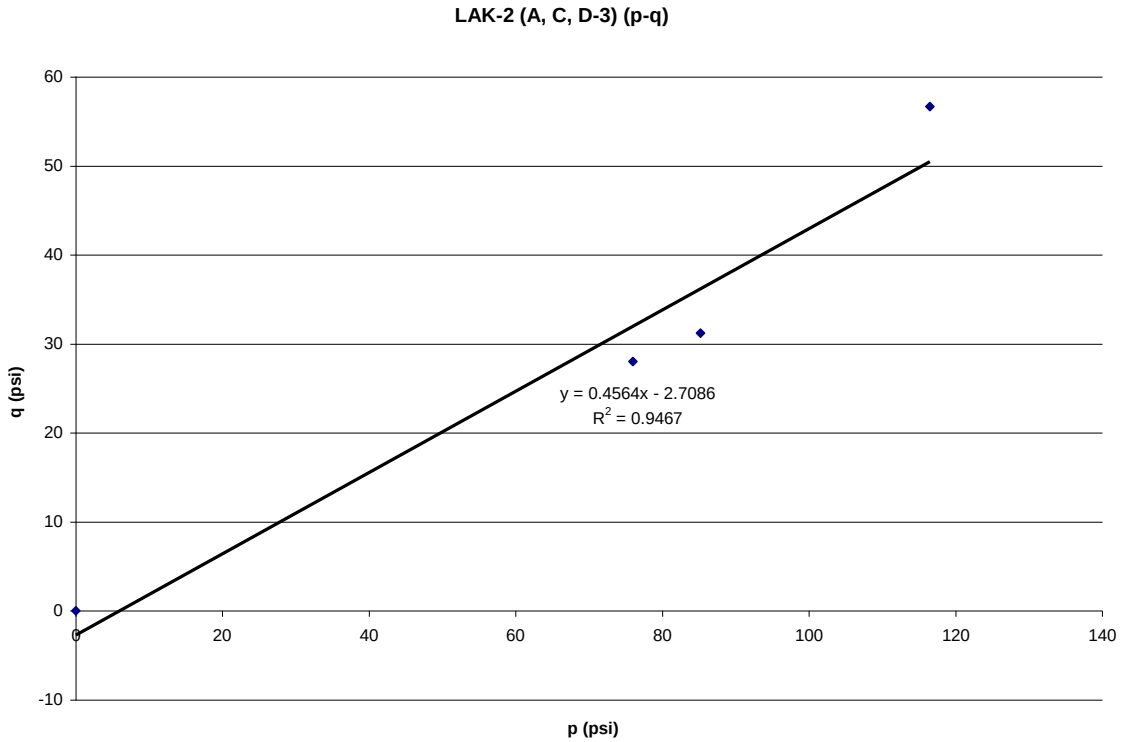


**Figure C.44:** p-q Diagram for the Lowest Depth Range – Site No. 3

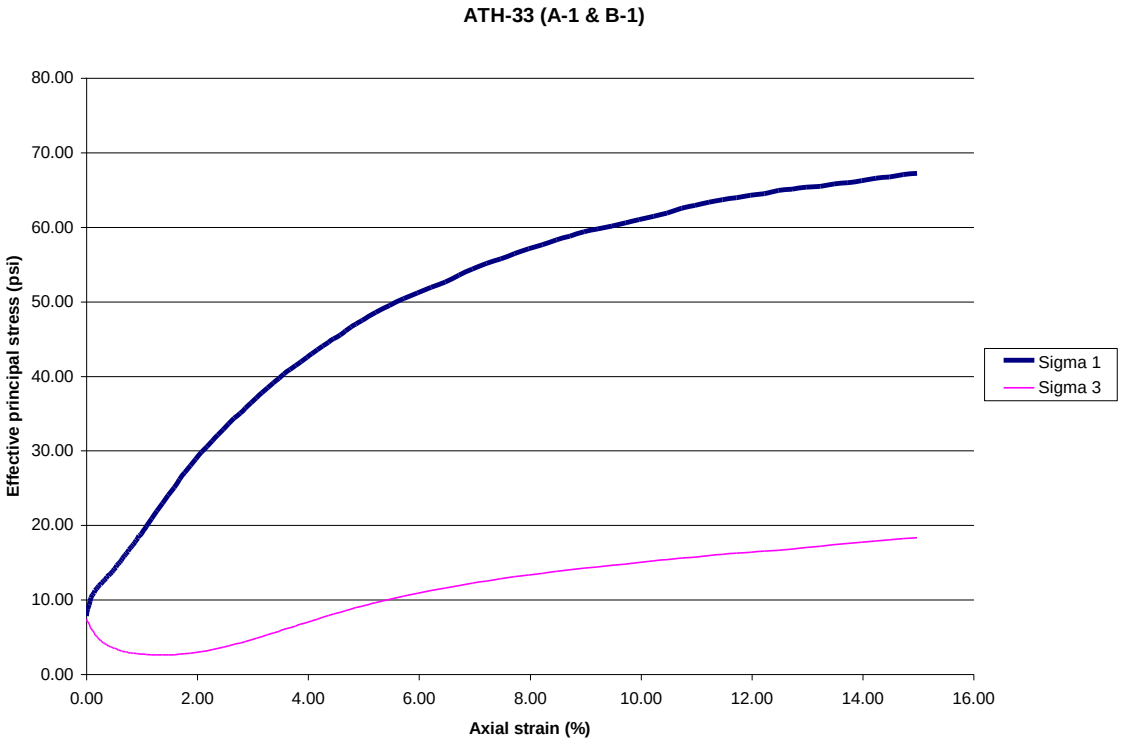


**Figure C.45:** Specimens A-1 (5.9' – 6.1' Depth) & B-1 (6.1' – 6.4' Depth) - Site No. 4

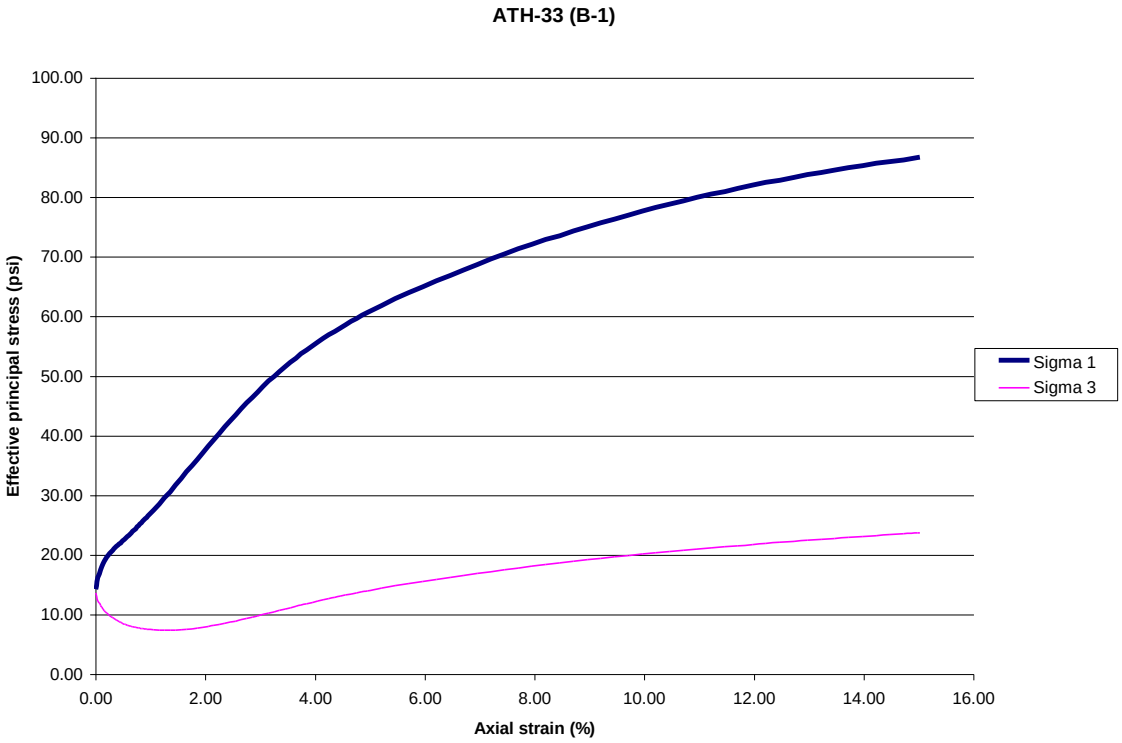


**Figure C.46:** Specimen B-1 (5.5' – 6.0' Depth) – Site No. 4

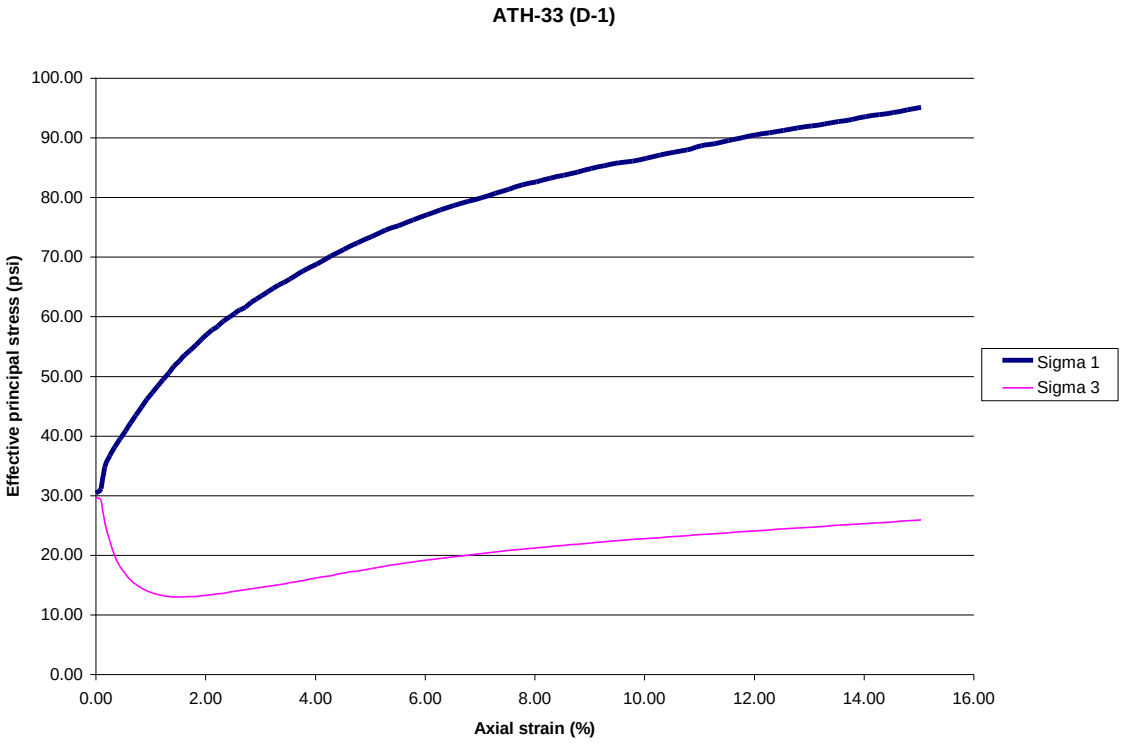


**Figure C.47:** Specimen D-1 (5.3' – 5.7' Depth) – Site No. 4

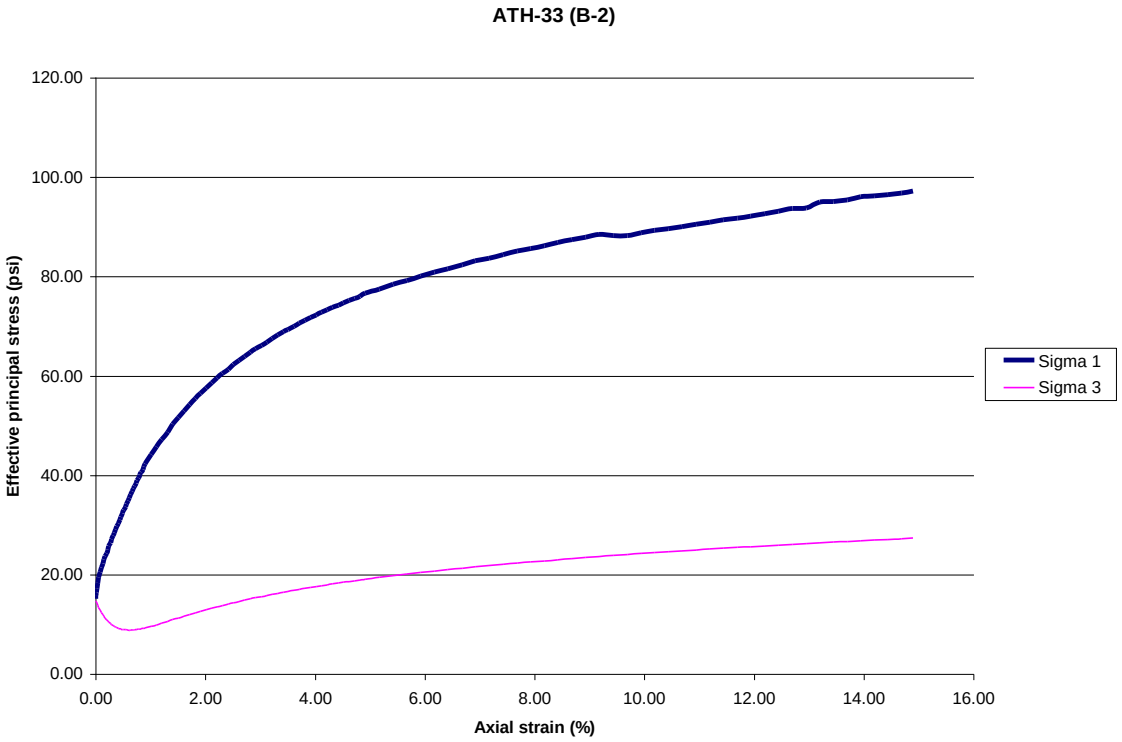


**Figure C.48:** Specimen B-2 (8.8' – 9.3' Depth) – Site No. 4

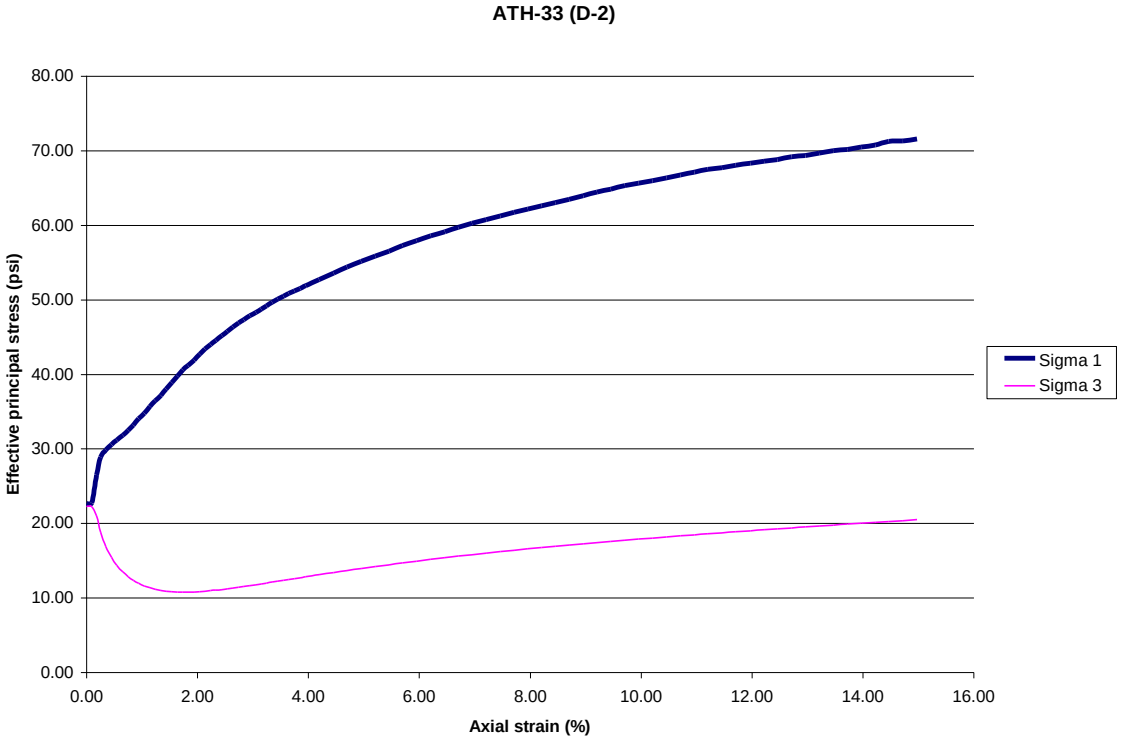


**Figure C.49:** Specimen D-2 (9.0' – 9.5' Depth) – Site No. 4

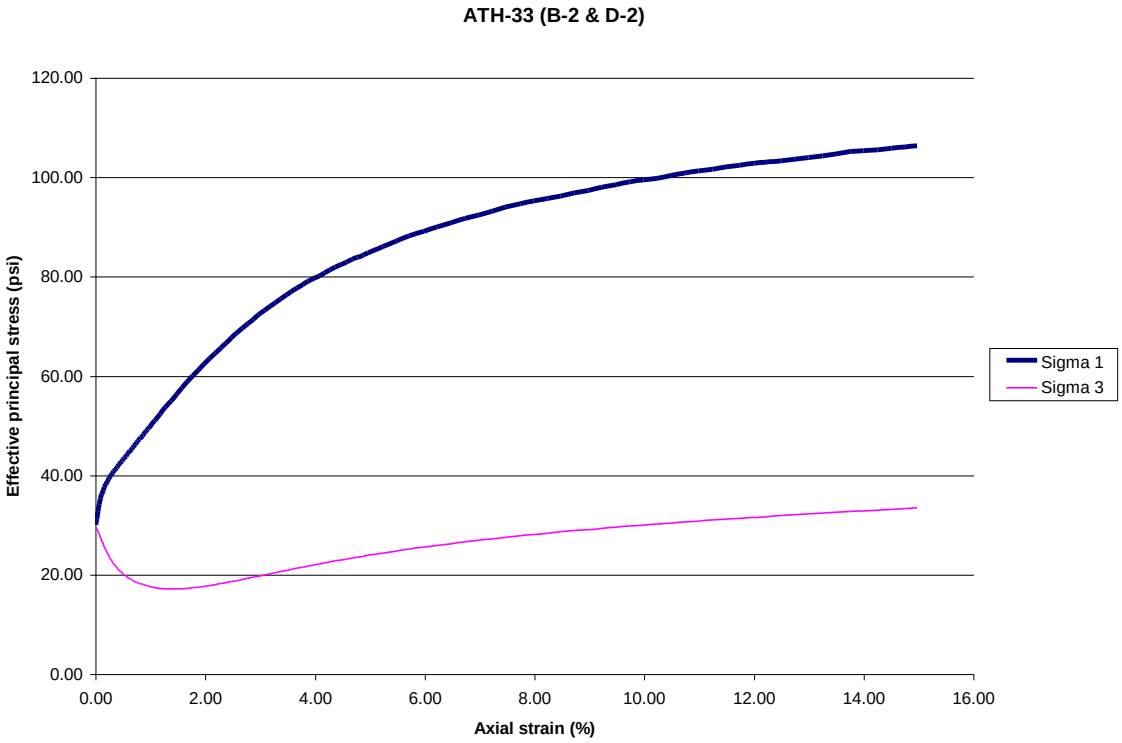


**Figure C.50:** Specimens B-2 (9.4' – 9.5' Depth) & D-2 (9.6' – 10.0' Depth) – Site No. 4

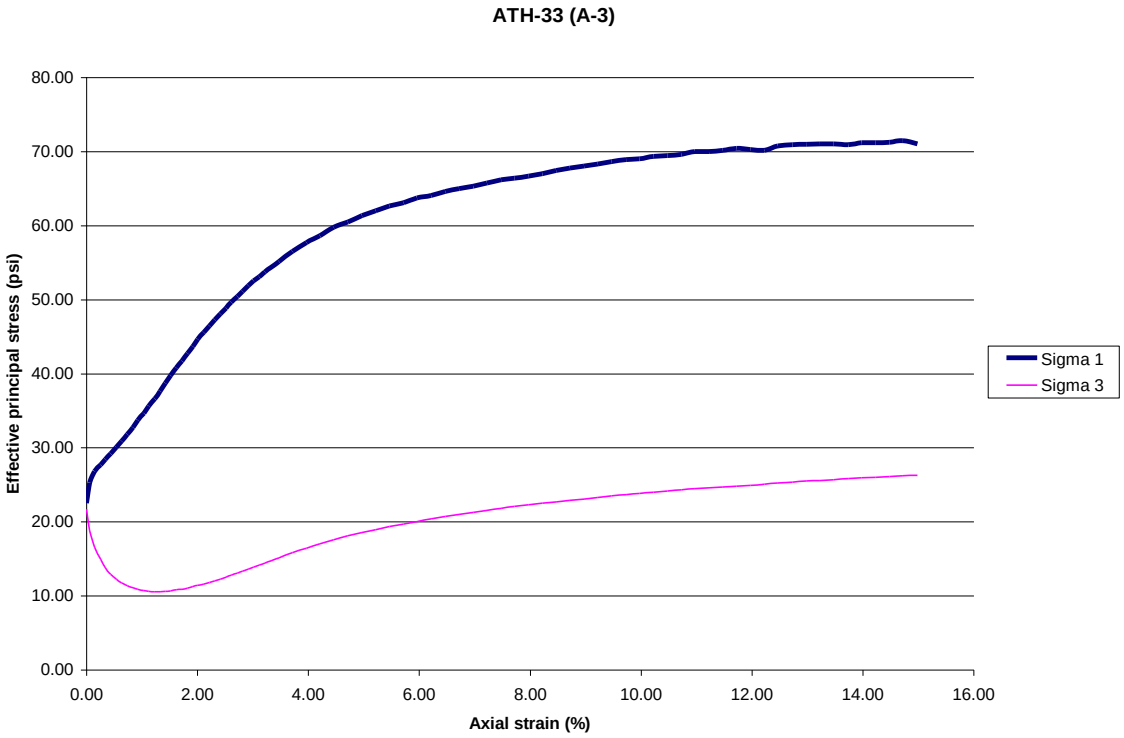


**Figure C.51:** Specimen A-3 (20.0' – 20.5' Depth) – Site No. 4

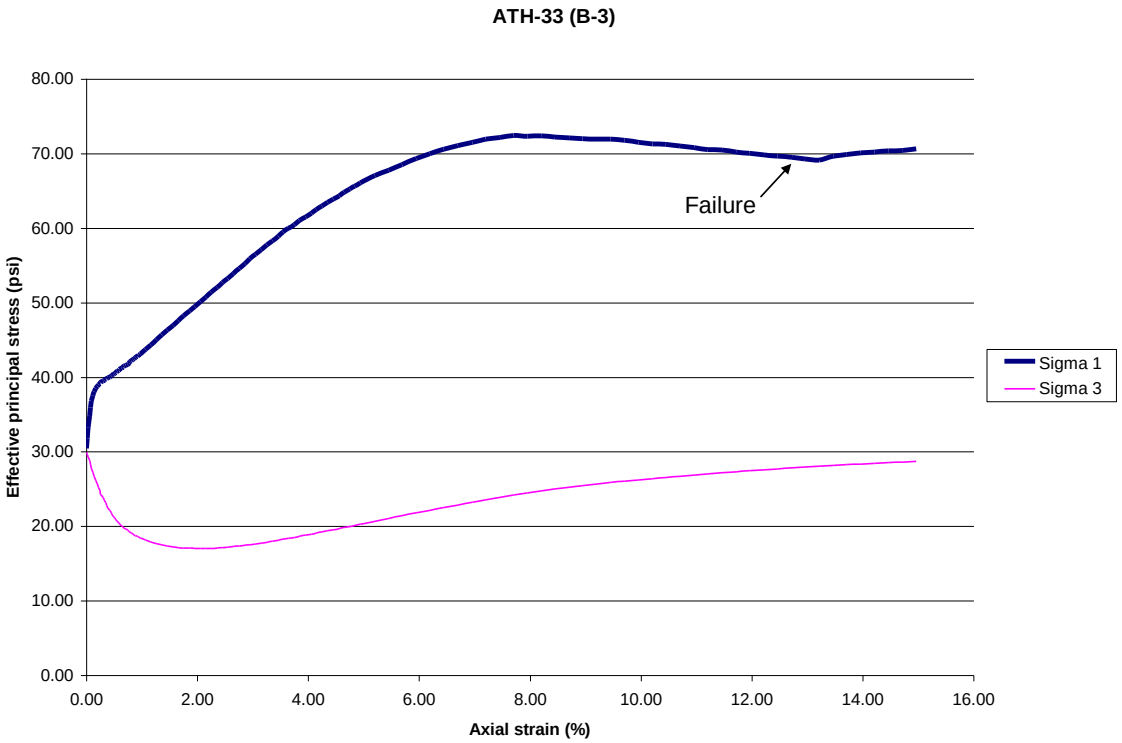


**Figure C.52:** Specimen B-3 (20.0' – 20.5' Depth) – Site No. 4

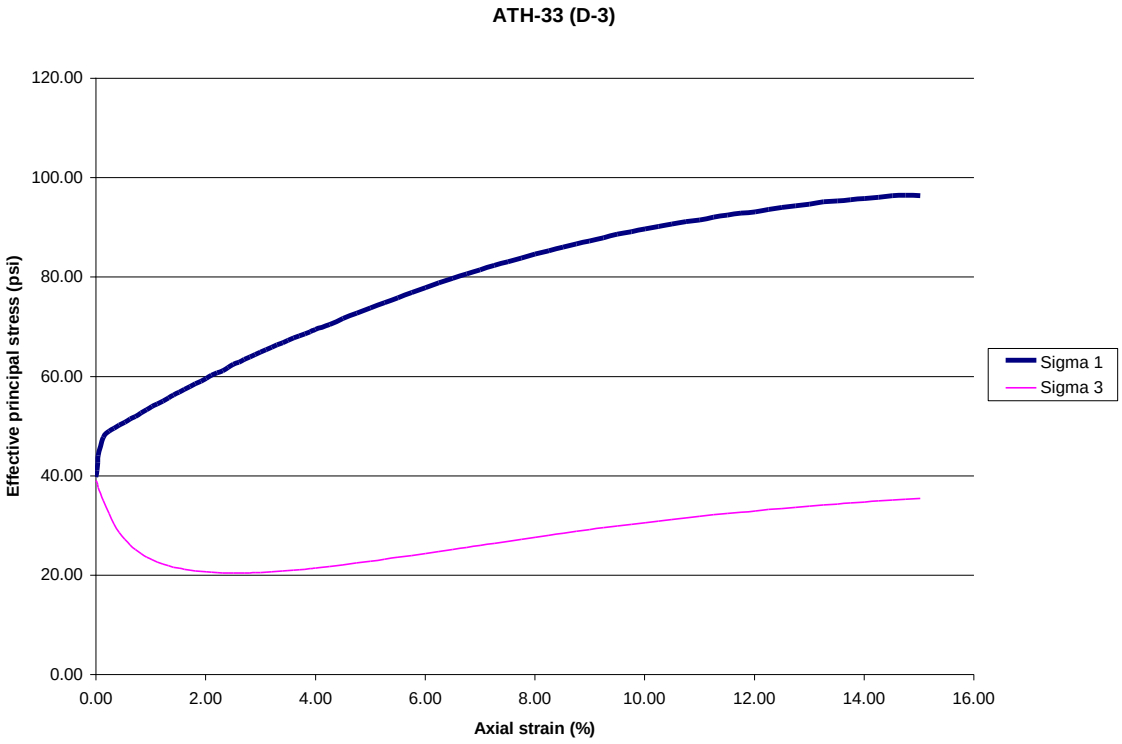


**Figure C.53:** Specimen D-3 (20.0' – 20.5' Depth) – Site No. 4

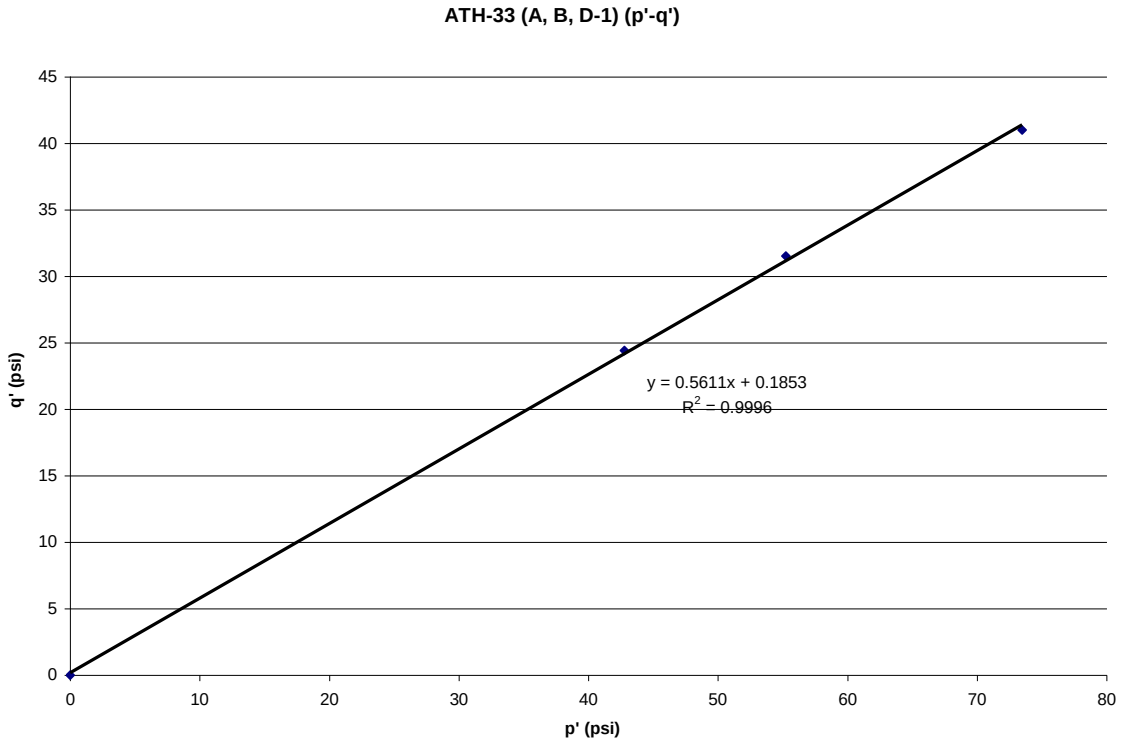


**Figure C.54:** p'-q' Diagram for the Highest Depth Range – Site No. 4

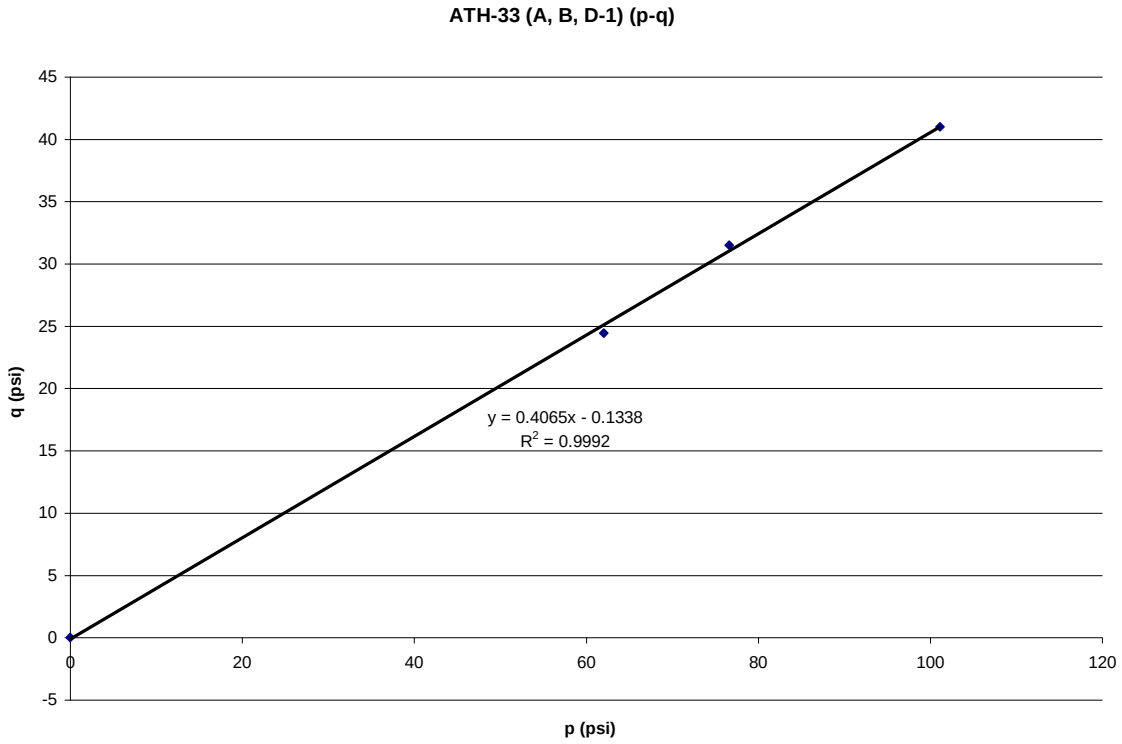


**Figure C.55:** p-q Diagram for the Highest Depth Range – Site No. 4

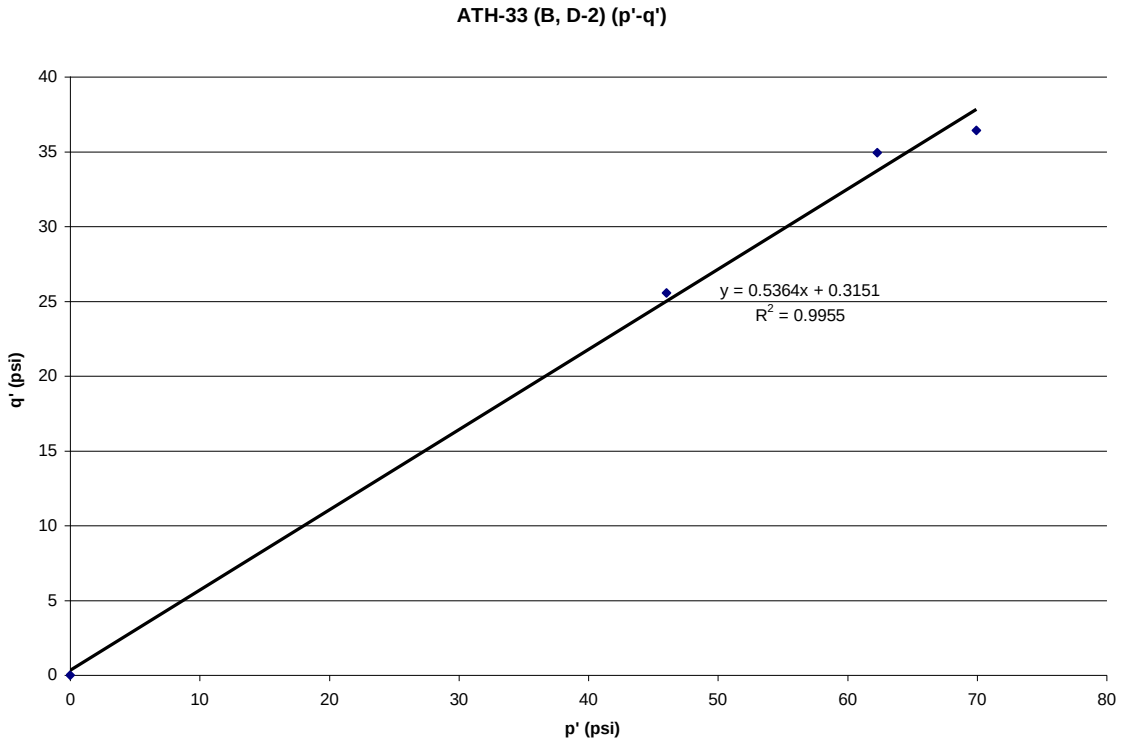


**Figure C.56:** p'-q' Diagram for the Middle Depth Range – Site No. 4

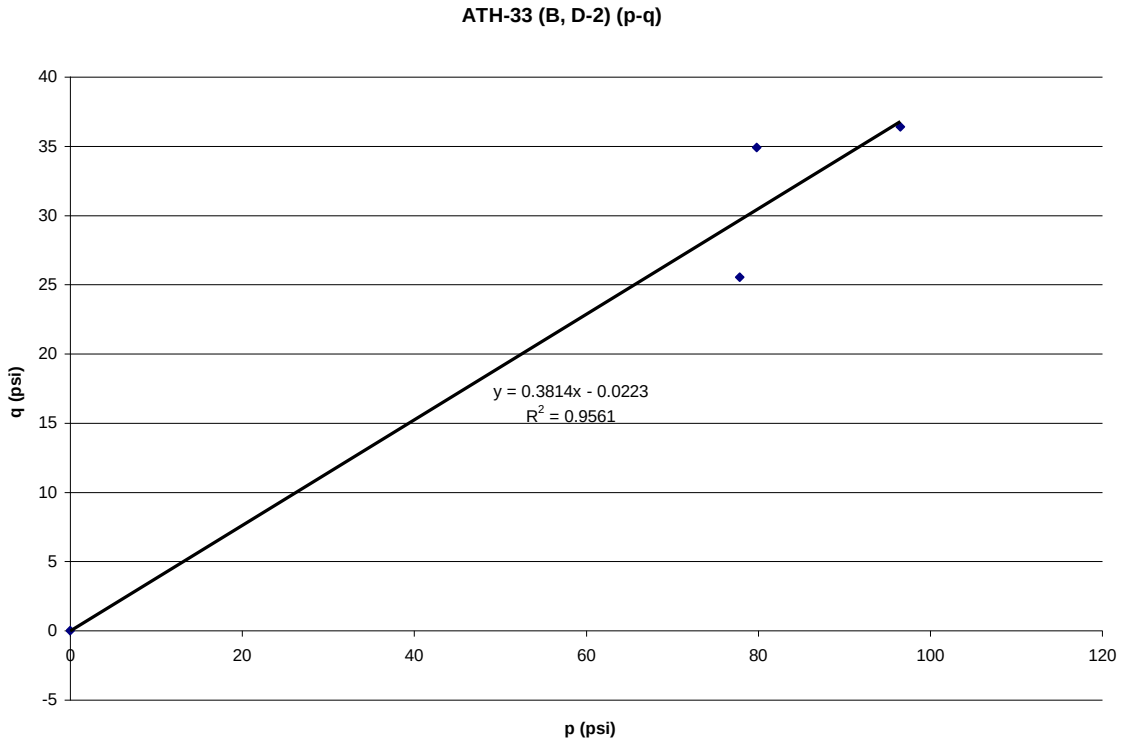


**Figure C.57:** p-q Diagram for the Middle Depth Range – Site No. 4

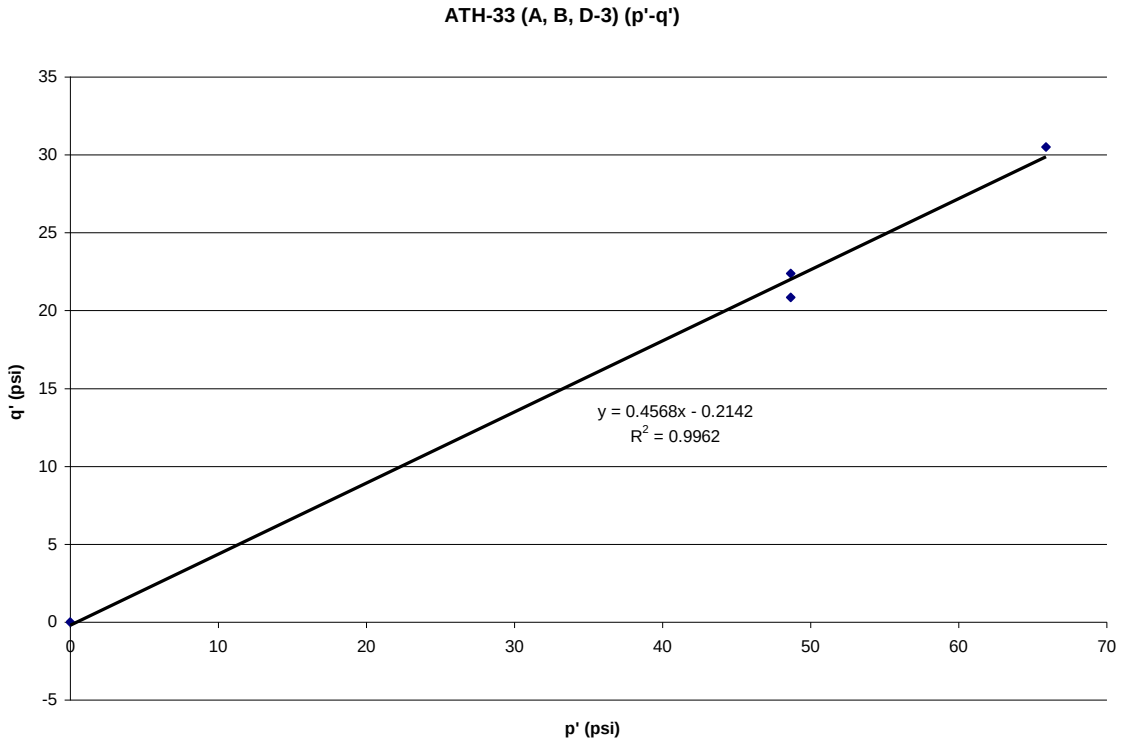


**Figure C.58:** p'-q' Diagram for the Lowest Depth Range – Site No. 4

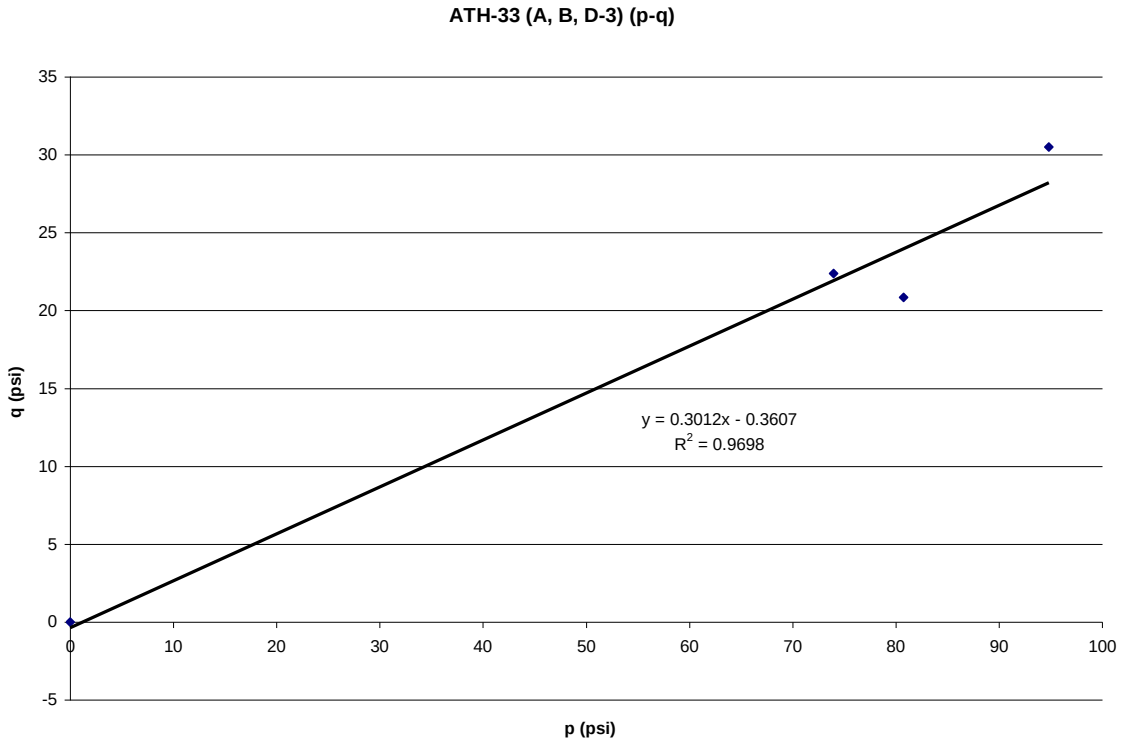


**Figure C.59:** p-q Diagram for the Lowest Depth Range – Site No. 4

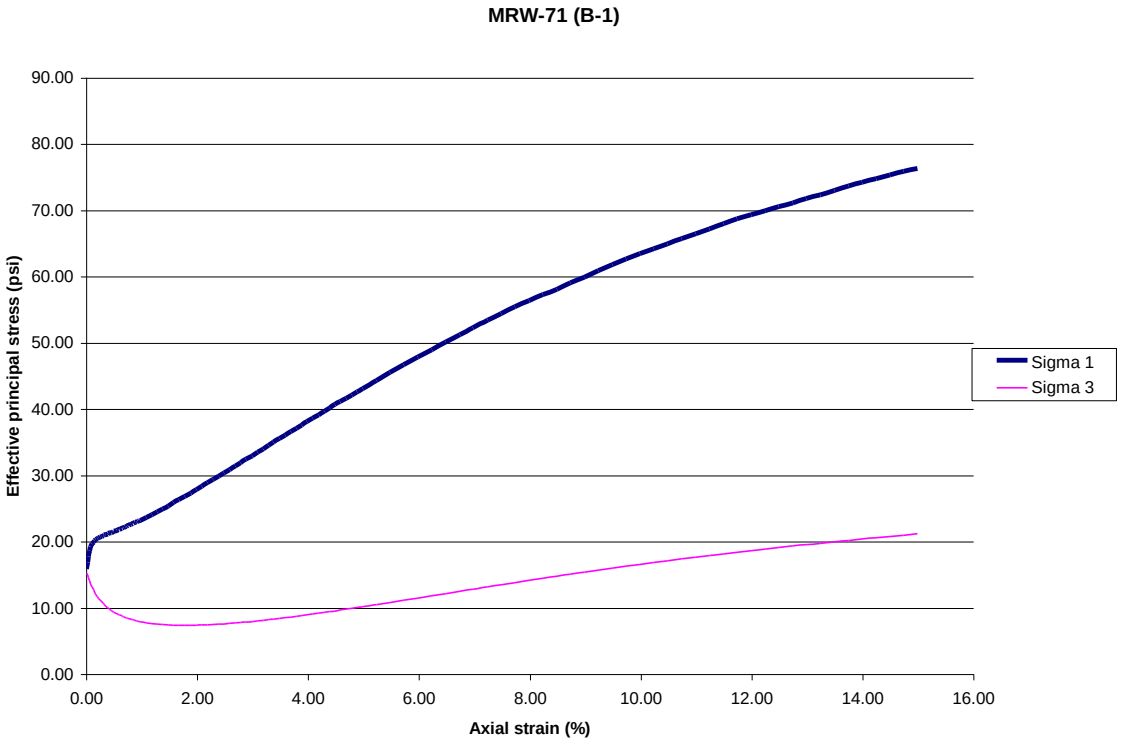


**Figure C.60:** Specimen B-1 (10.5' – 11.0' Depth) – Site No. 5

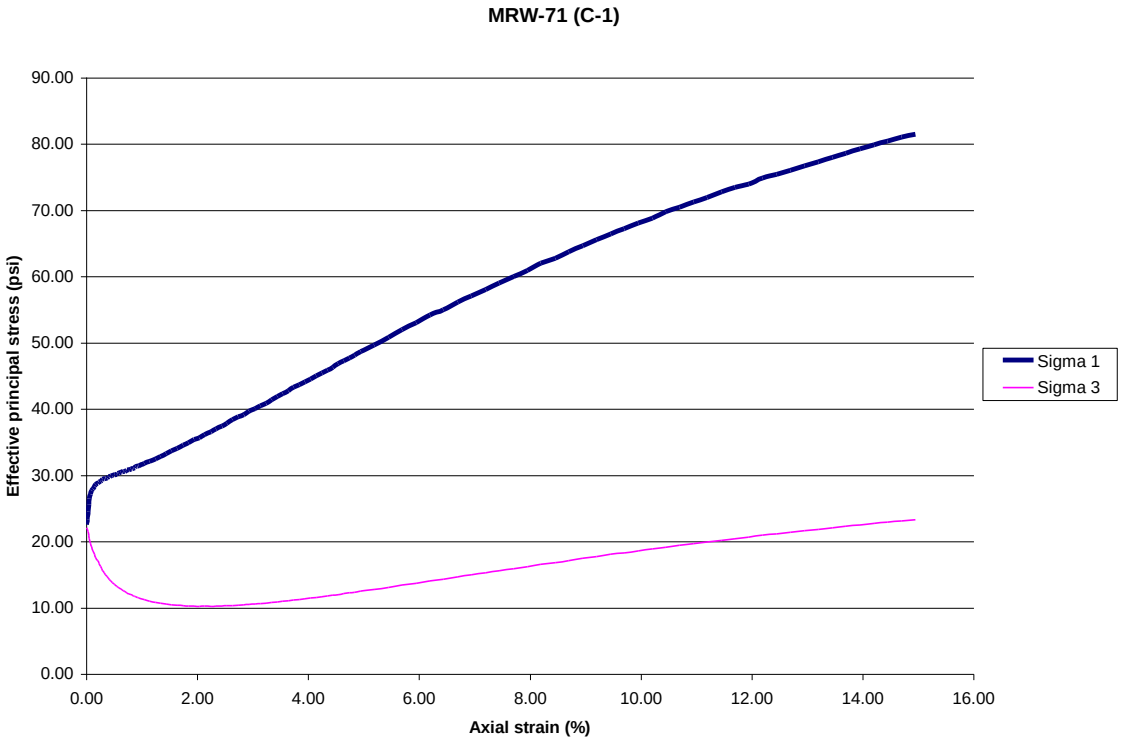


**Figure C.61:** Specimen C-1 (10.5' – 11.0' Depth) – Site No. 5

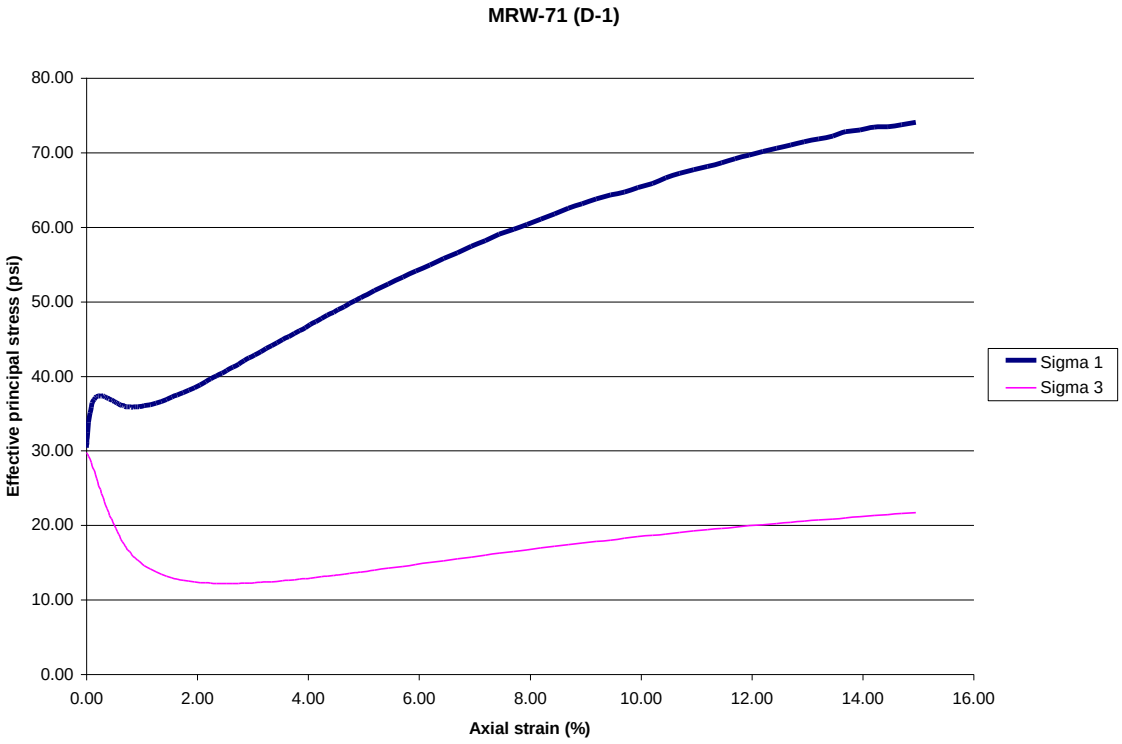


**Figure C.62:** Specimen D-1 (10.5' – 11.0' Depth) – Site No. 5

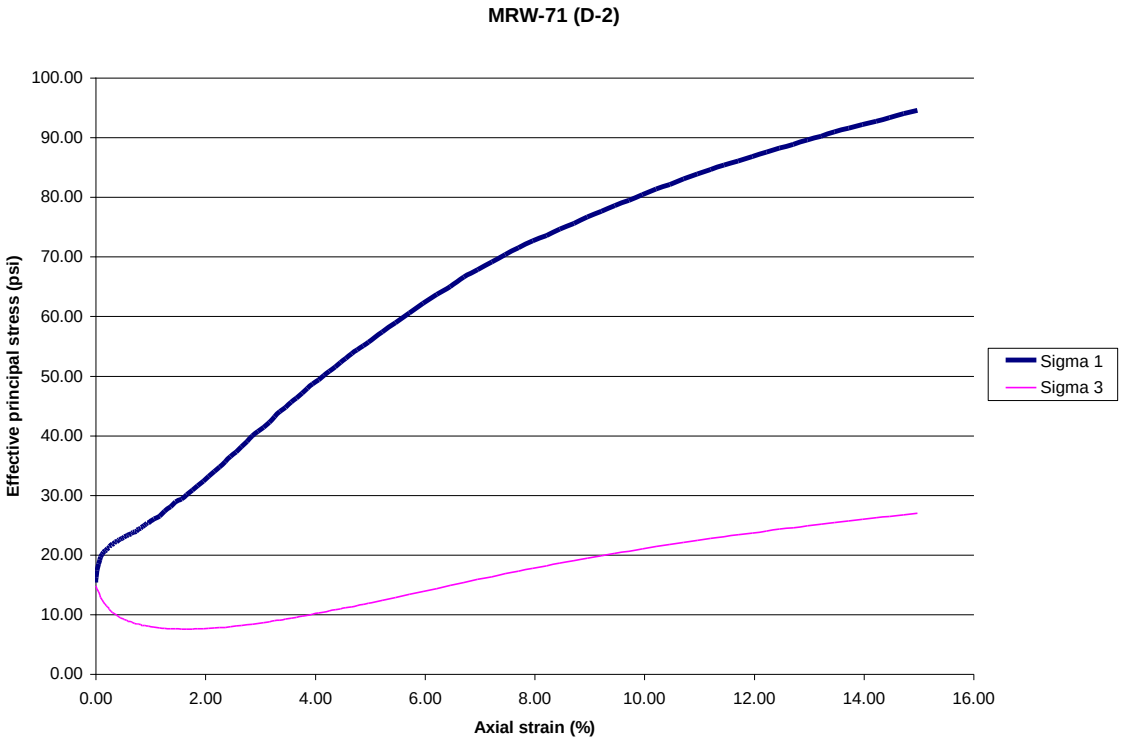


**Figure C.63:** Specimen D-2 (13.3' – 13.8' Depth) – Site No. 5

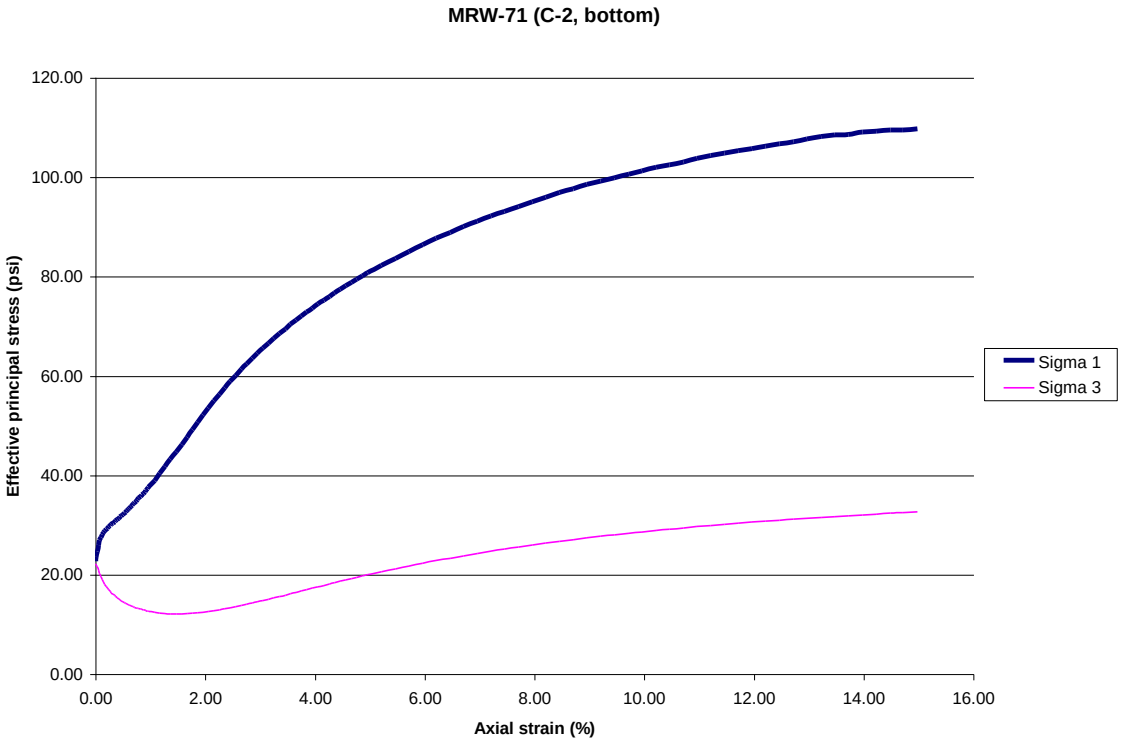


**Figure C.64:** Specimen C-2 (13.8' – 14.3' Depth) – Site No. 5

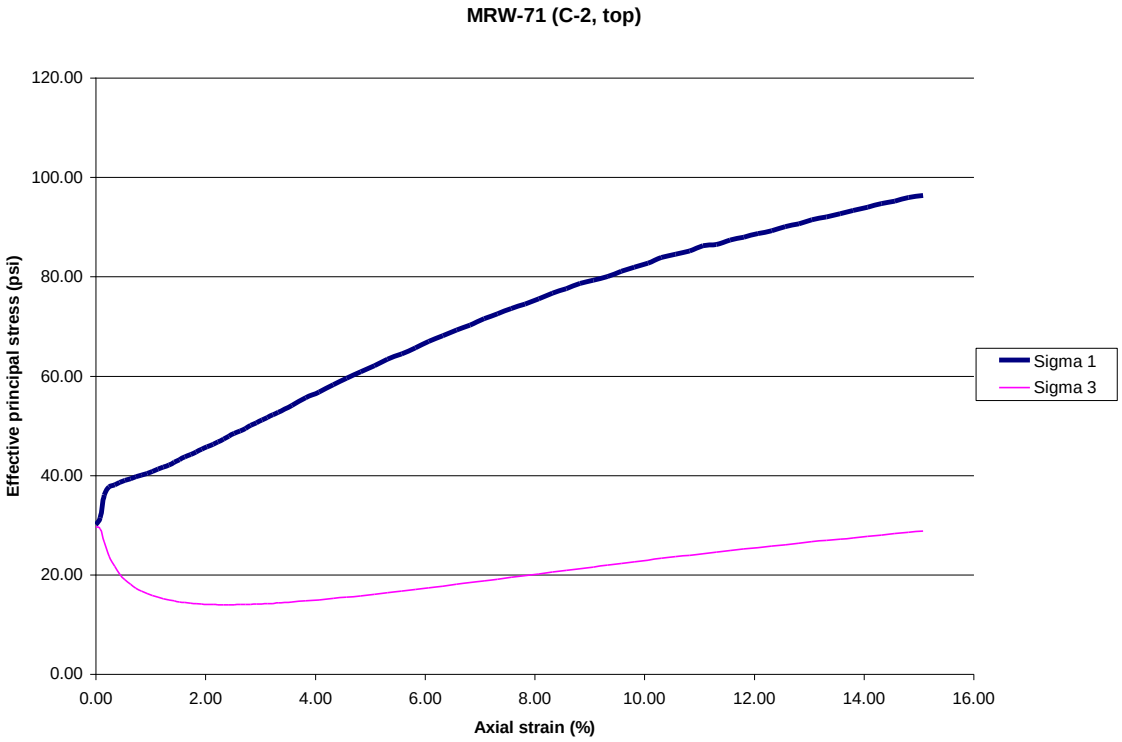


**Figure C.65:** Specimen C-2 (13.3' – 13.7' Depth) – Site No. 5

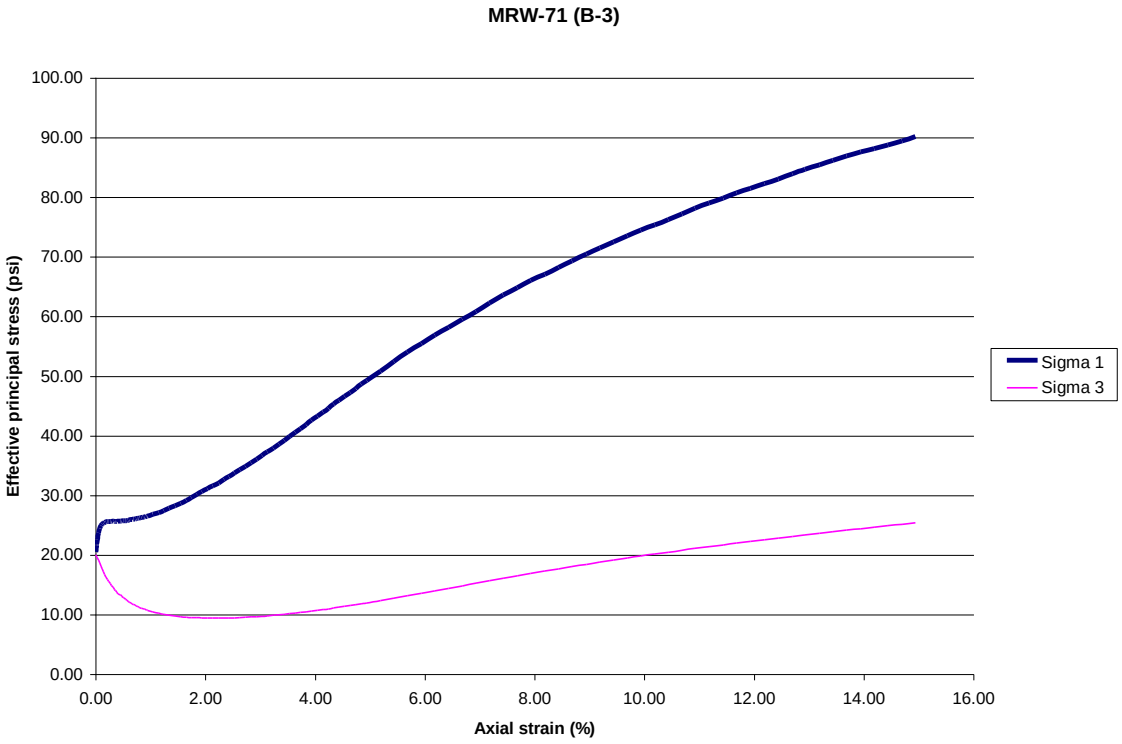


**Figure C.66:** Specimen B-3 (17.9' – 18.4' Depth) – Site No. 5

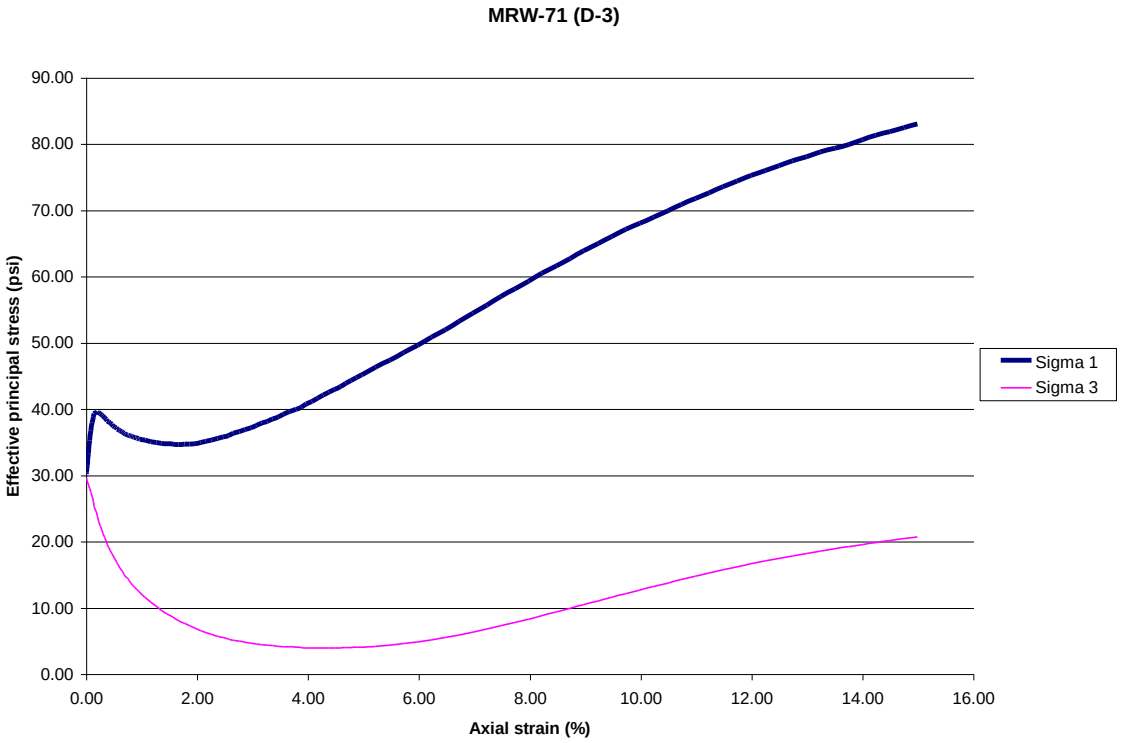


**Figure C.67:** Specimen D-3 (18.2' – 18.6' Depth) – Site No. 5

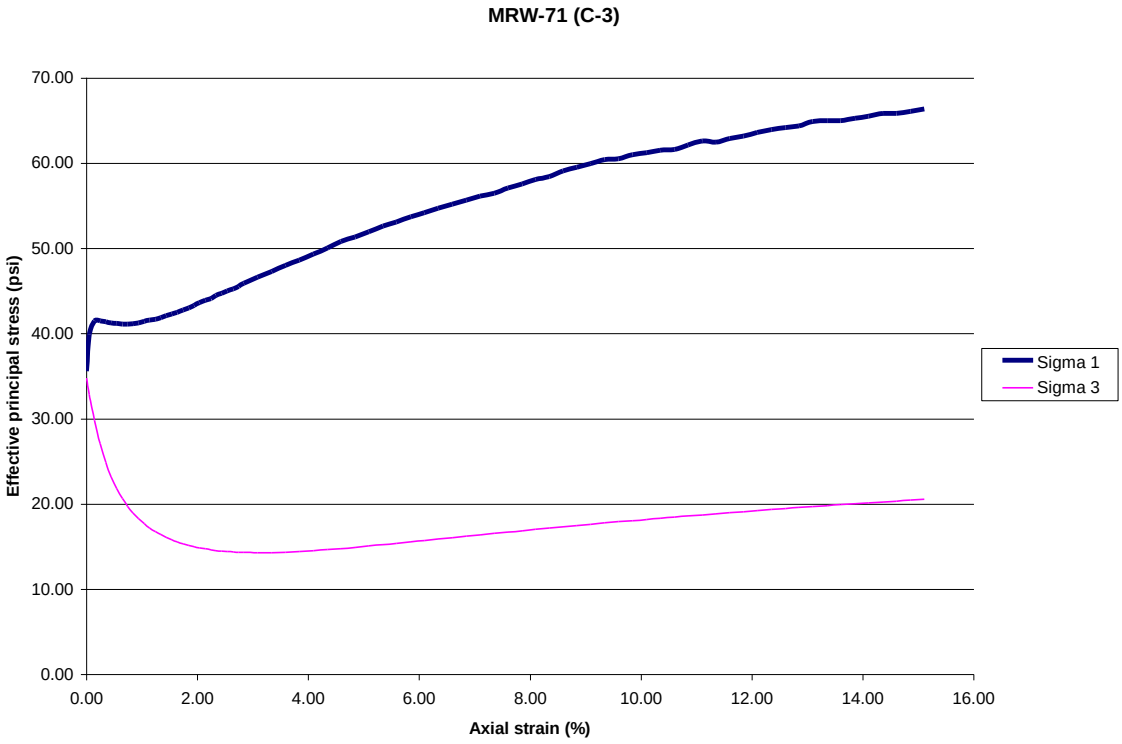


**Figure C.68:** Specimen C-3 (17.6' – 18.1' Depth) – Site No. 5

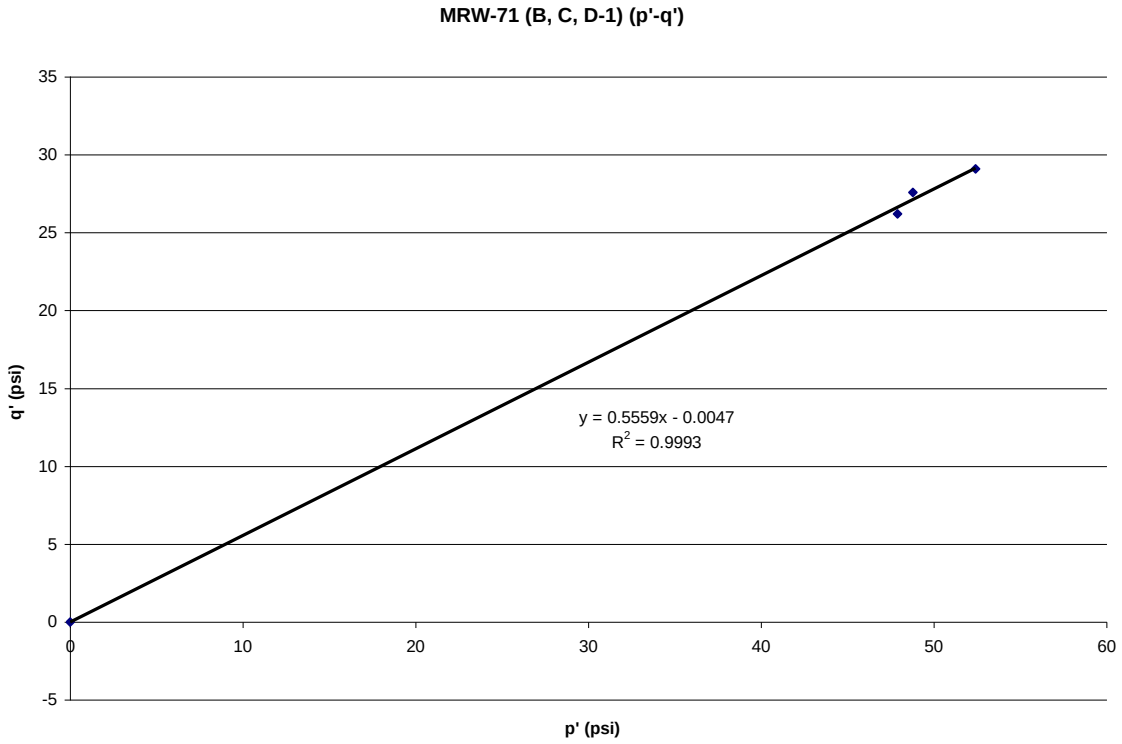


**Figure C.69:** p'-q' Diagram for the Highest Depth Range – Site No. 5

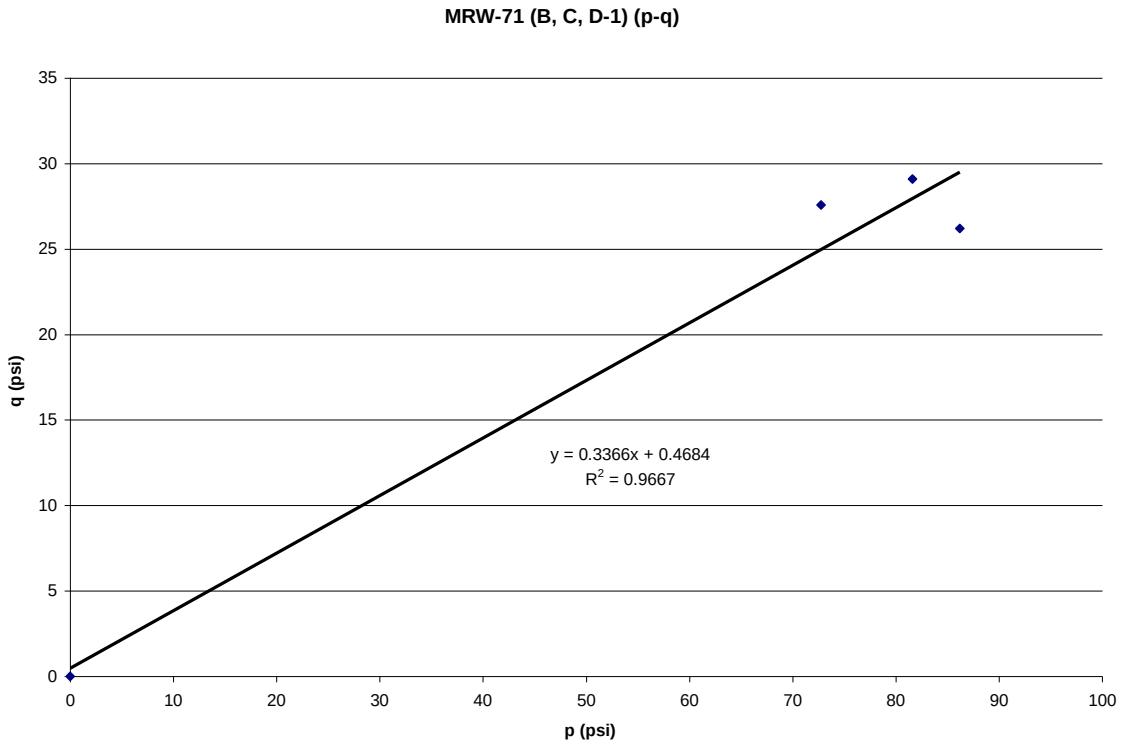


**Figure C.70:** p-q Diagram for the Highest Depth Range – Site No. 5

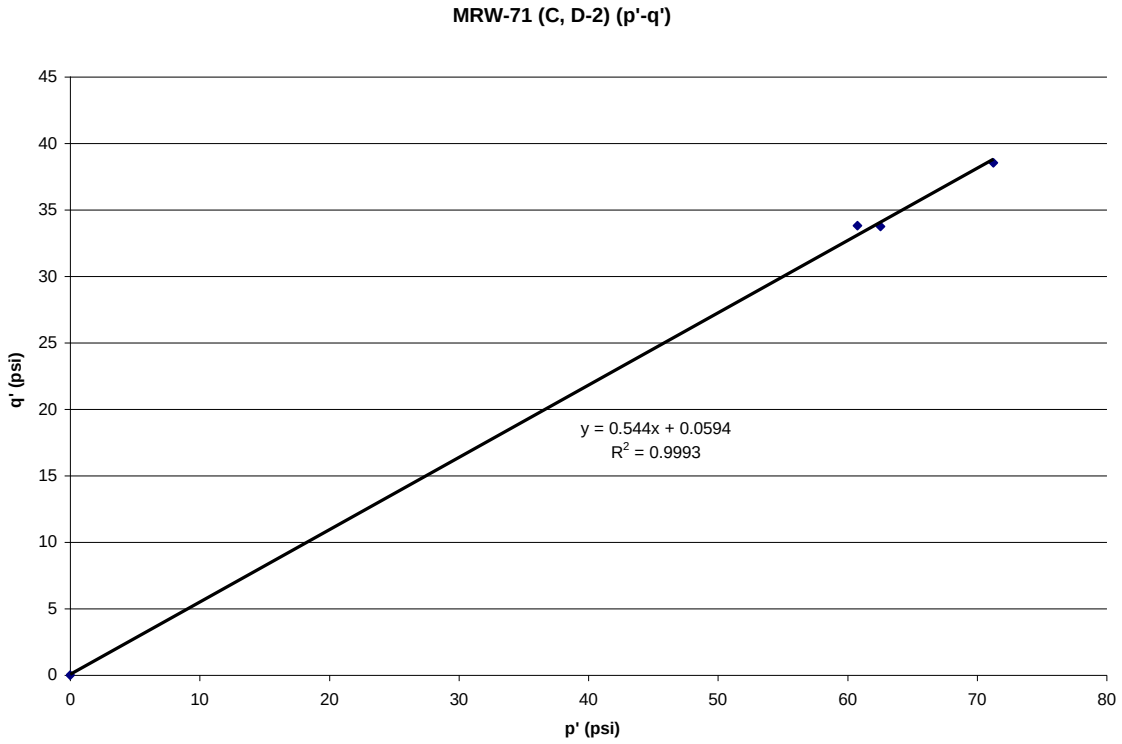


**Figure C.71:** p'-q' Diagram for the Middle Depth Range – Site No. 5

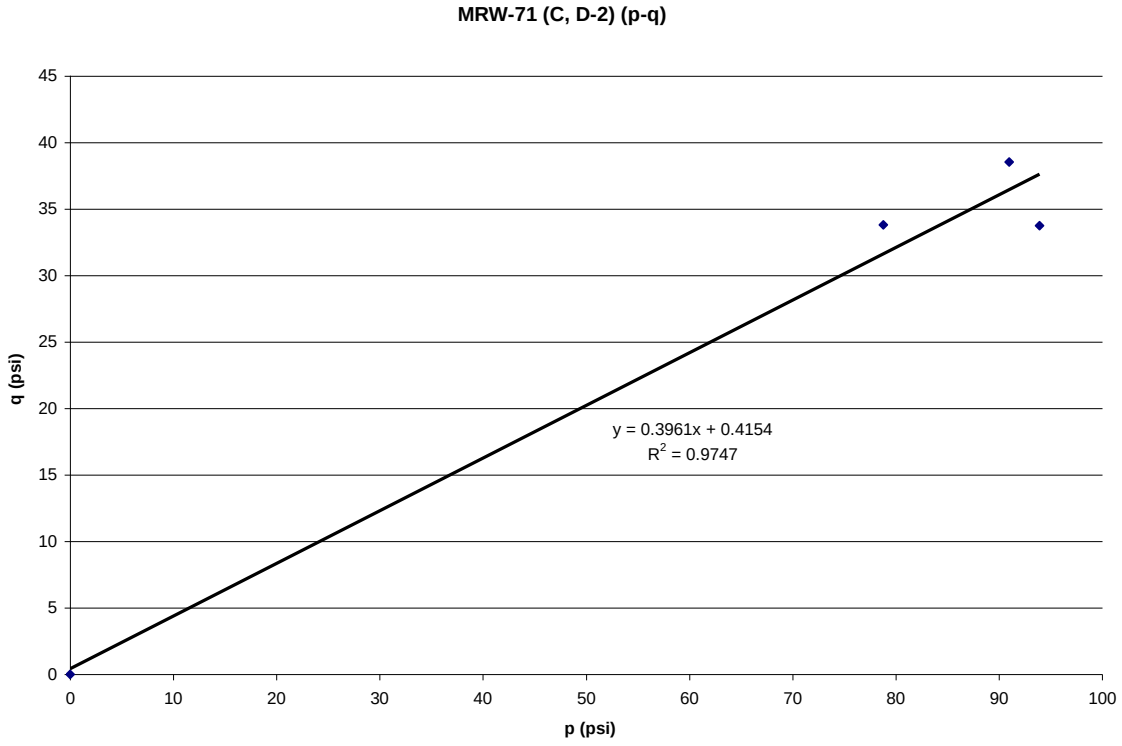


**Figure C.72:** p-q Diagram for the Middle Depth Range – Site No. 5

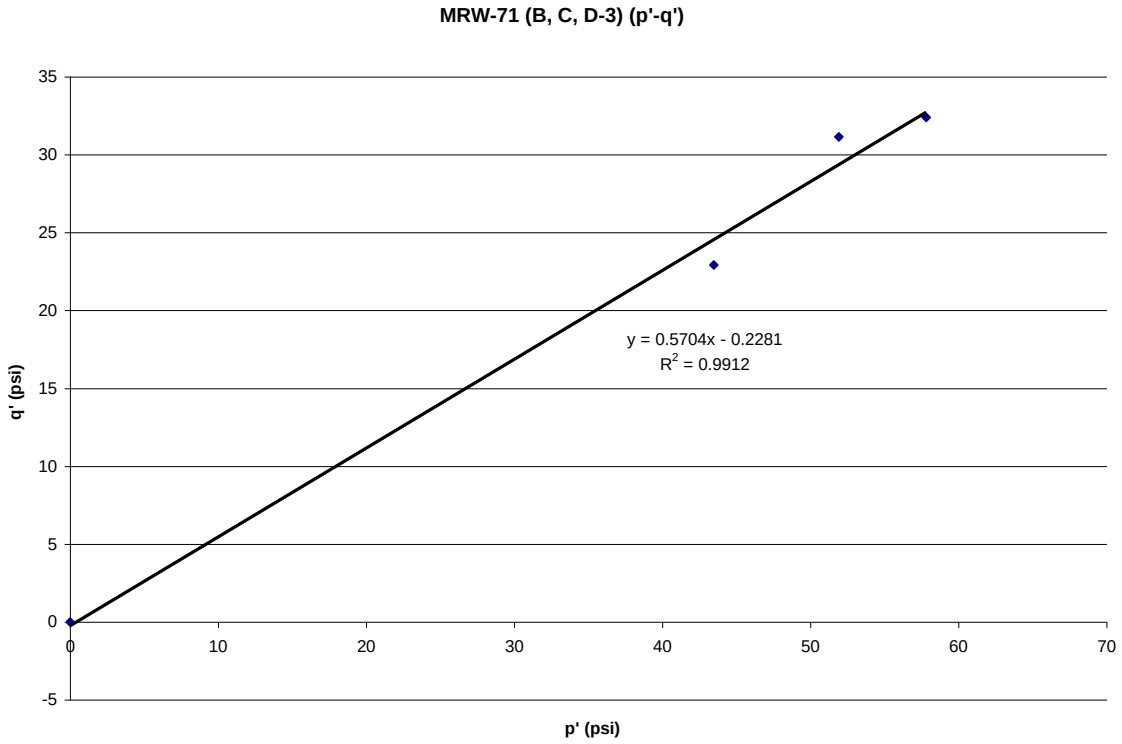


**Figure C.73:** p'-q' Diagram for the Lowest Depth Range – Site No. 5

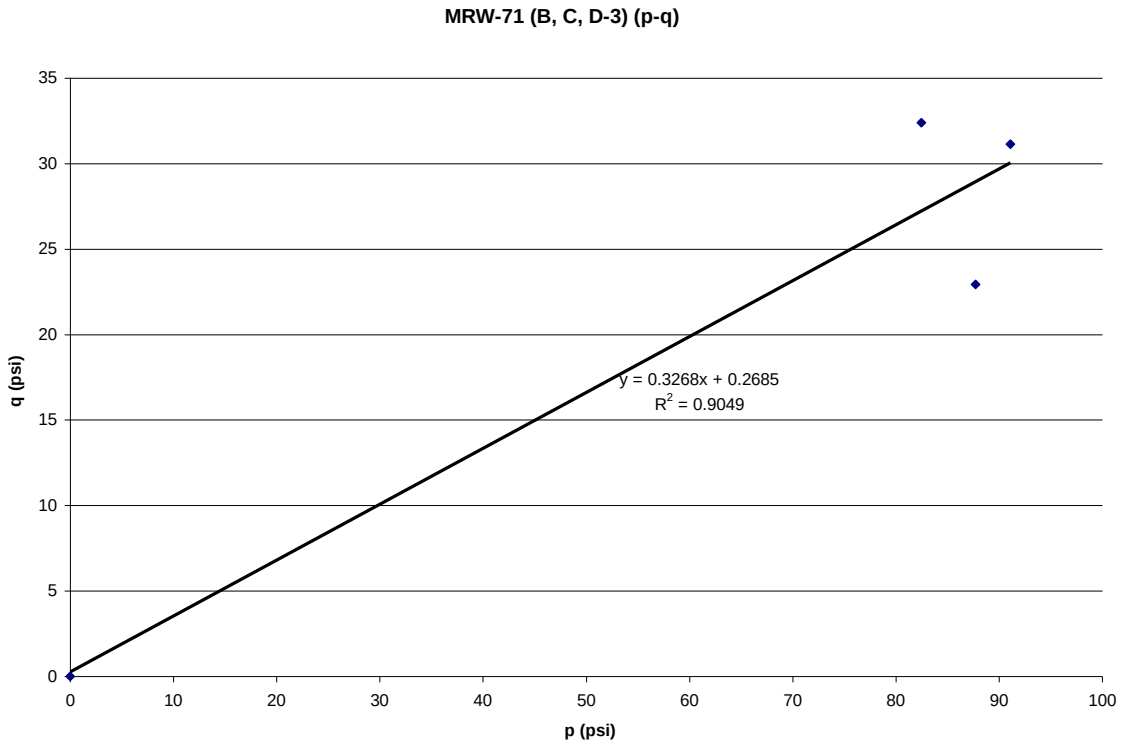


**Figure C.74:** p-q Diagram for the Lowest Depth Range – Site No. 5

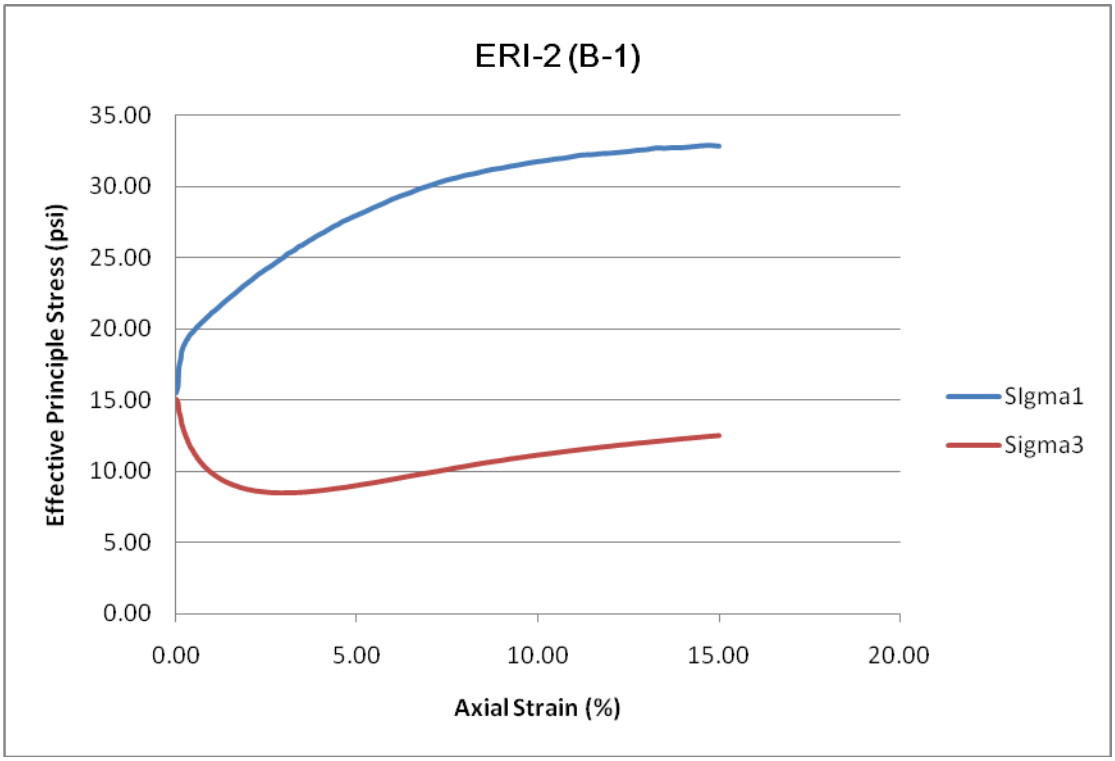


**Figure C.75:** Specimen B-1 (3.0' – 3.5' Depth) – Site No. 6

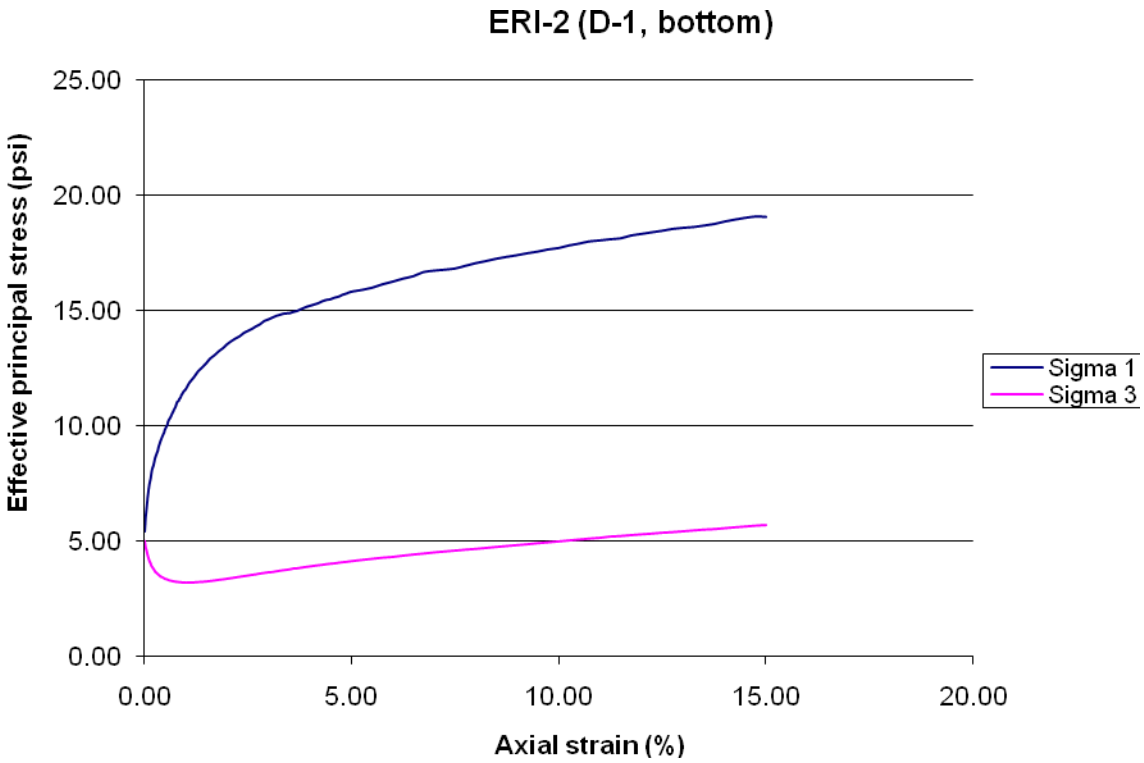


**Figure C.76:** Specimen D-1 (3.3' – 3.8' Depth) – Site No. 6

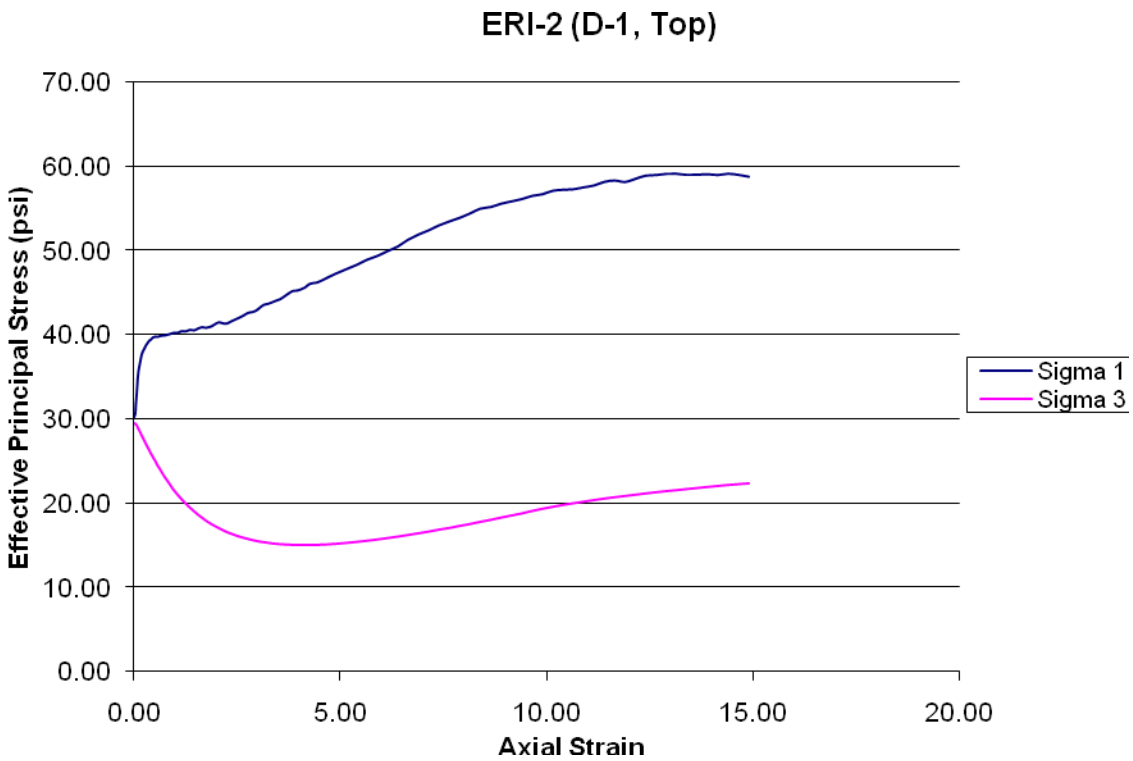


**Figure C.77:** Specimen D-1 (2.7' – 3.2' Depth) – Site No. 6

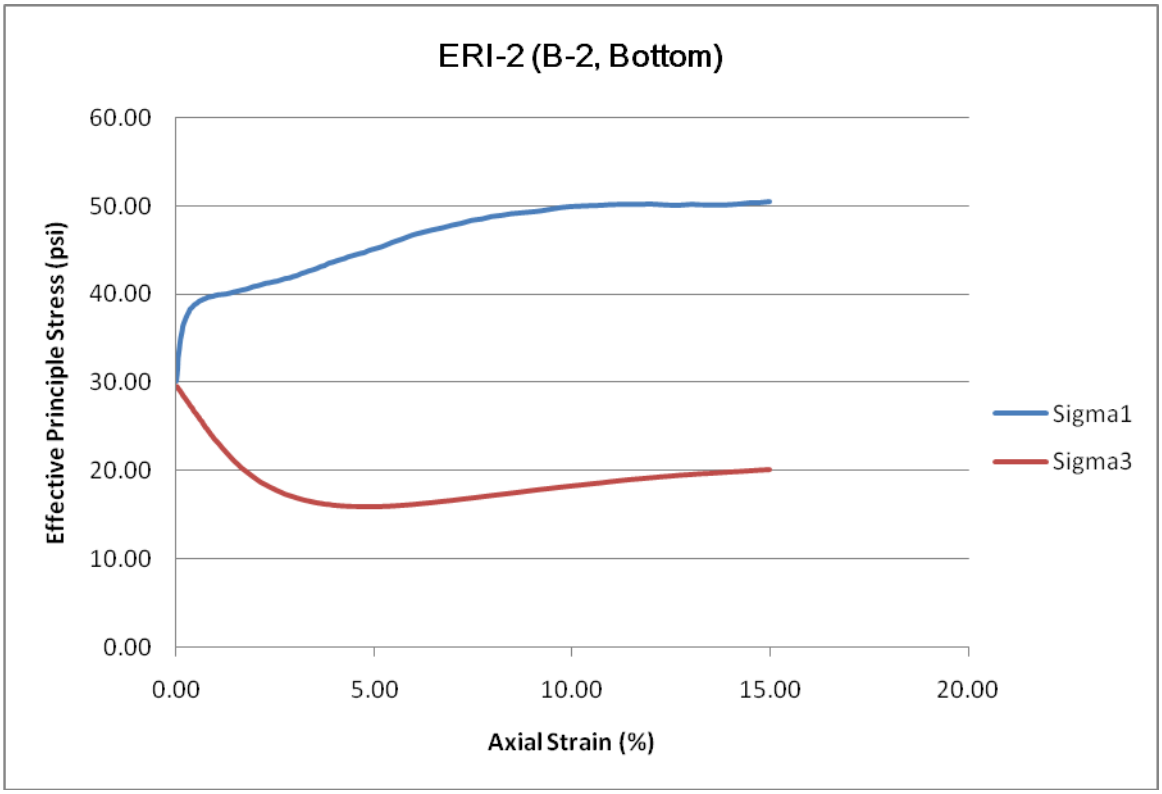


**Figure C.78:** Specimen B-2 (7.0' – 7.5' Depth) – Site No. 6

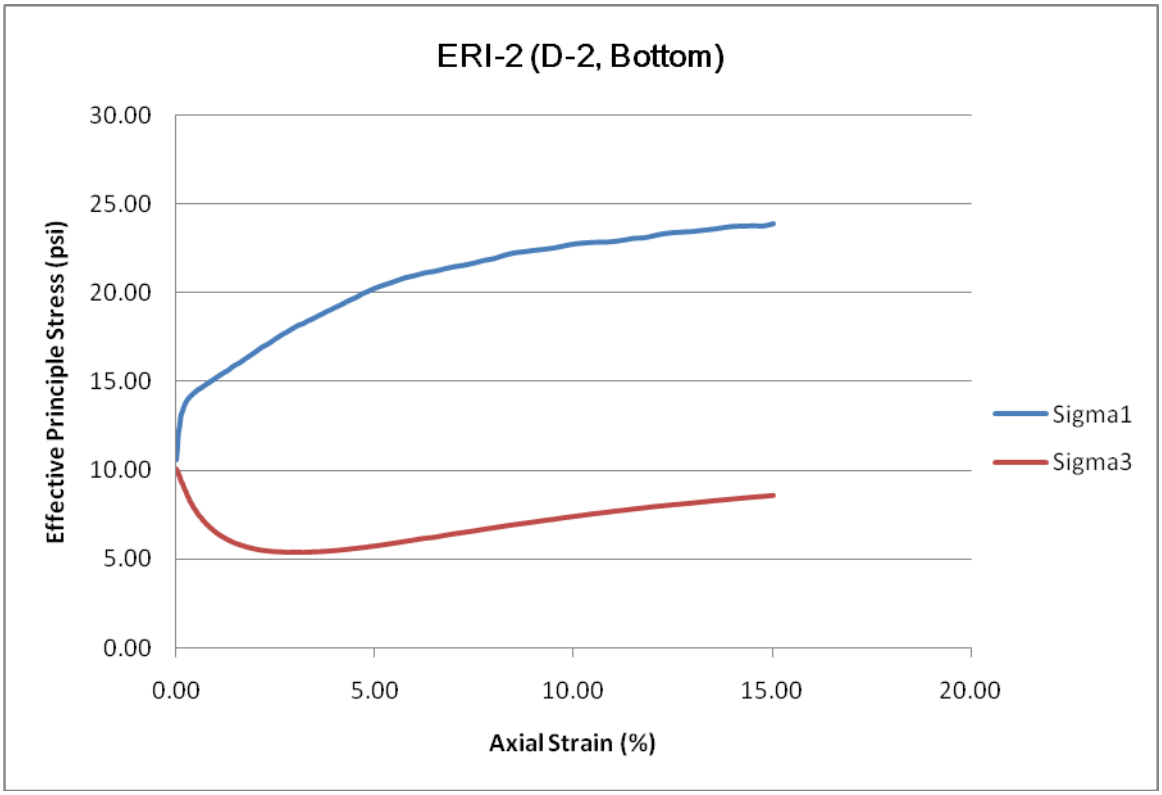


**Figure C.79:** Specimen D-2 (6.9' – 7.4' Depth) – Site No. 6

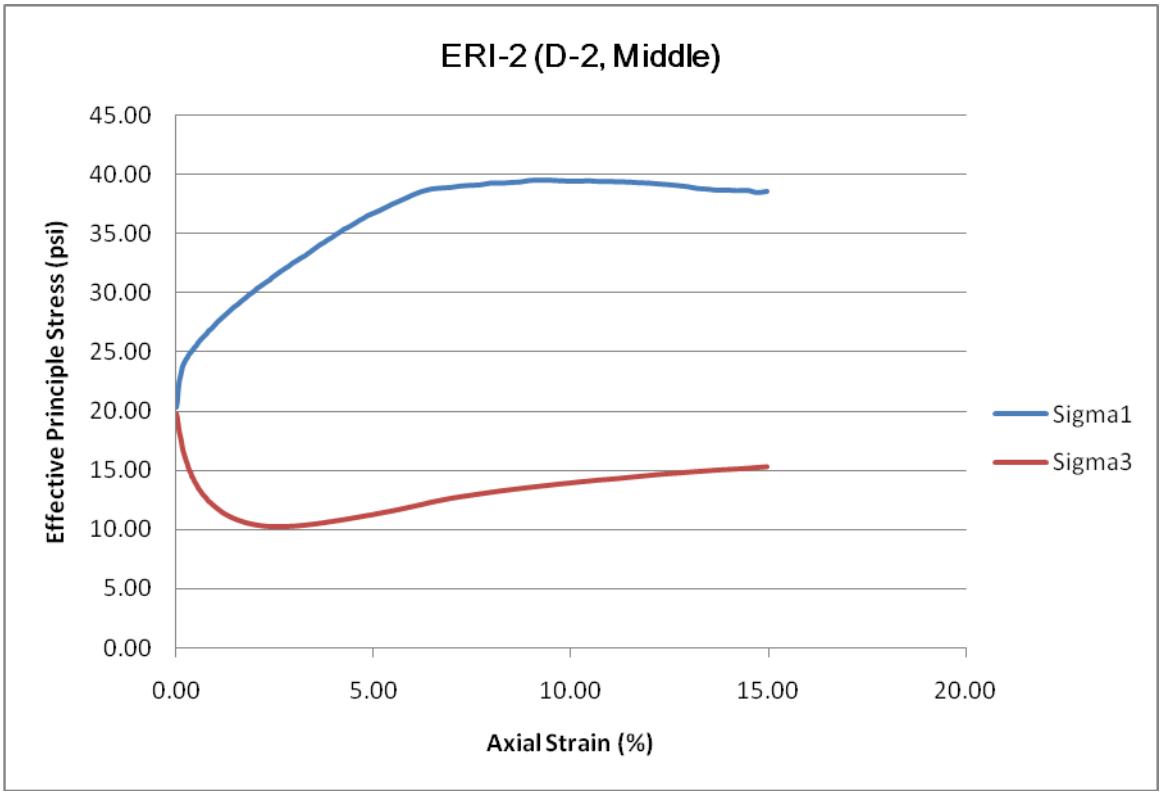


**Figure C.80:** Specimen D-2 (6.3' – 6.8' Depth) – Site No. 6

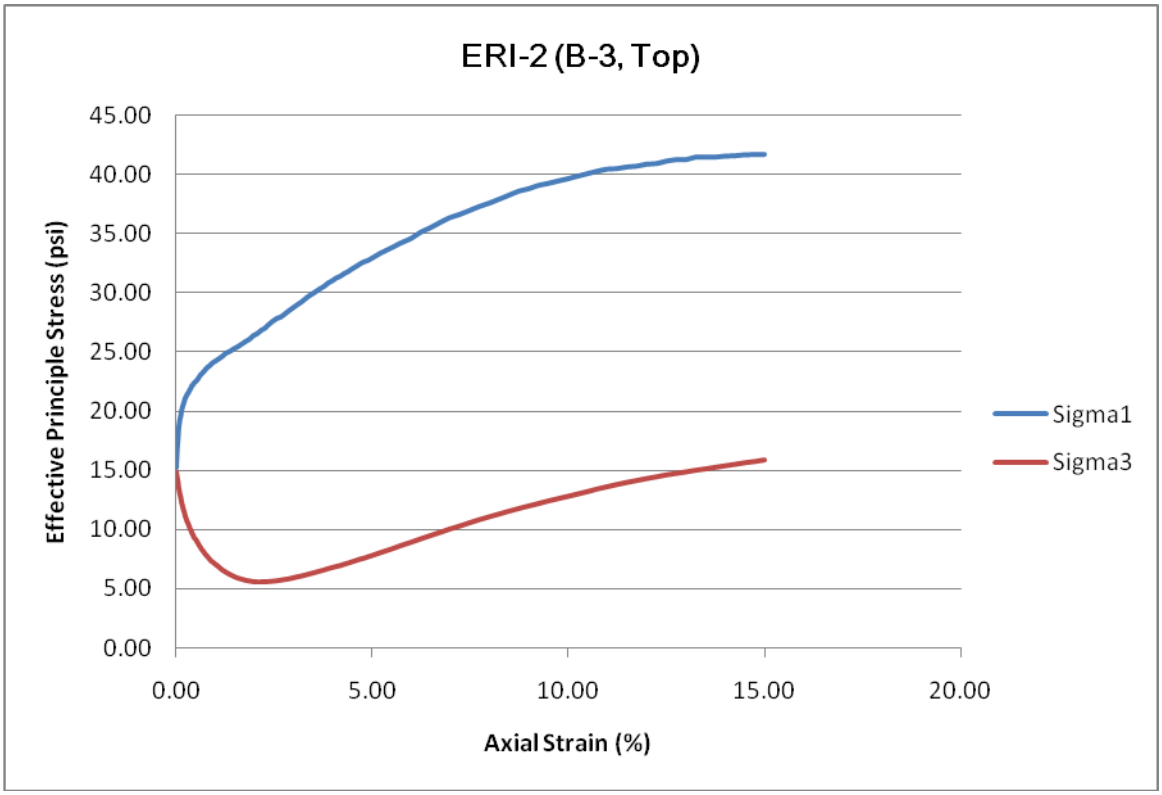


**Figure C.81:** Specimen B-3 (11.6' – 12.1' Depth) – Site No. 6

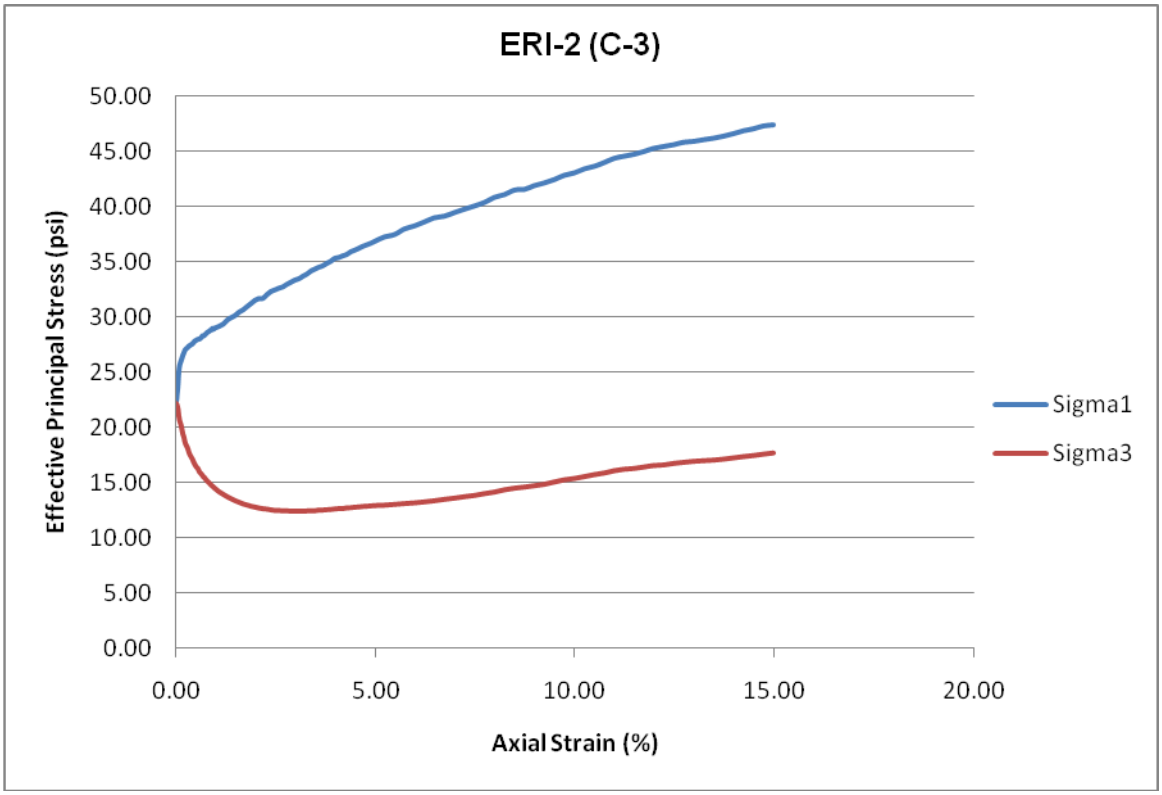


**Figure C.82:** Specimen C-3 (11.7' – 12.2' Depth) – Site No. 6

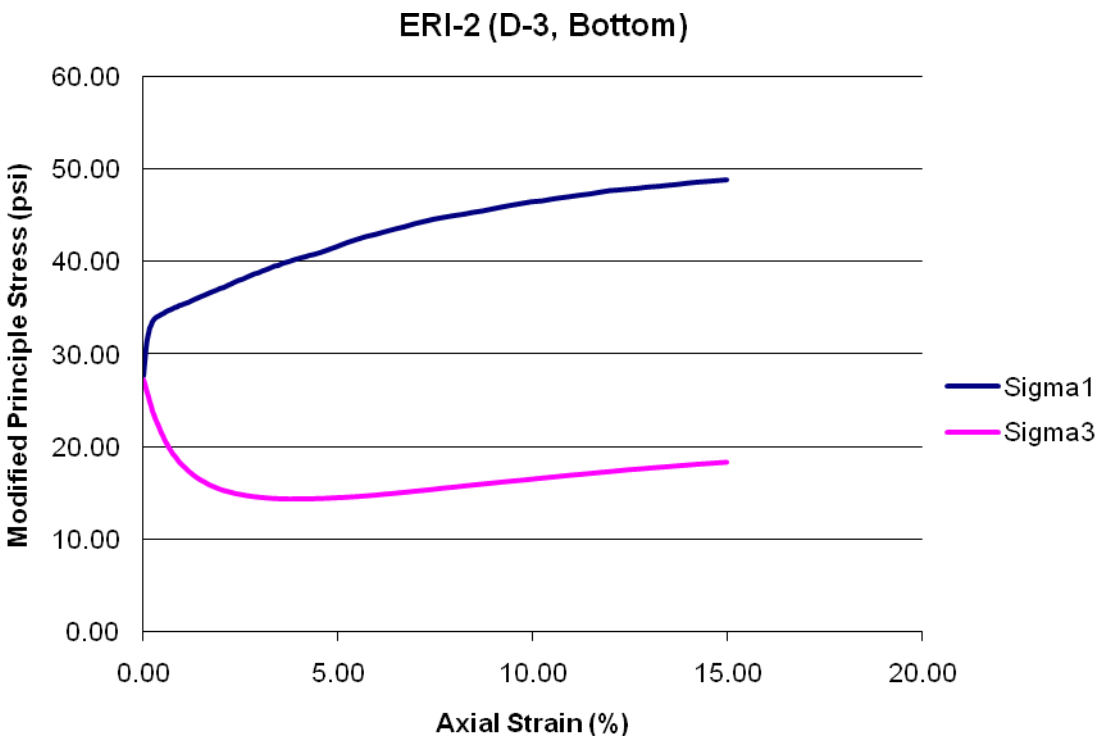


**Figure C.83:** Specimen D-3 (13.0' – 13.5' Depth) – Site No. 6

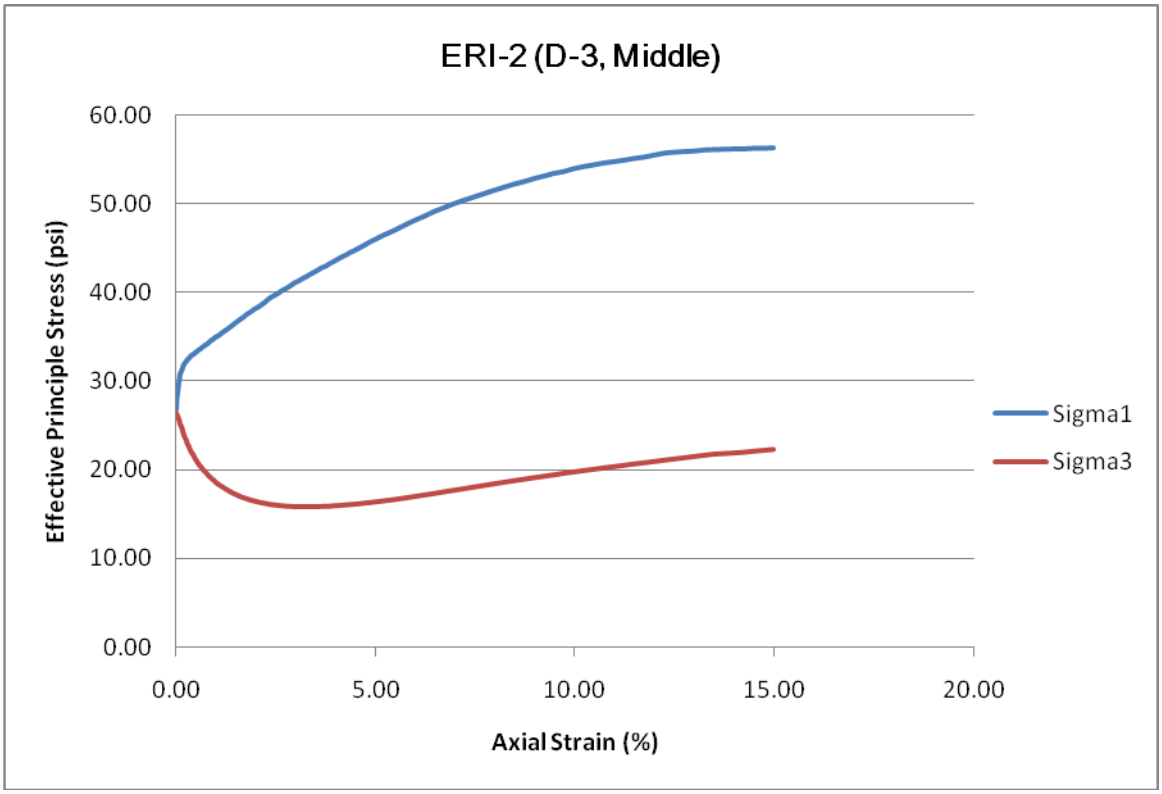


**Figure C.84:** Specimen D-3 (12.3' – 12.8' Depth) – Site No. 6

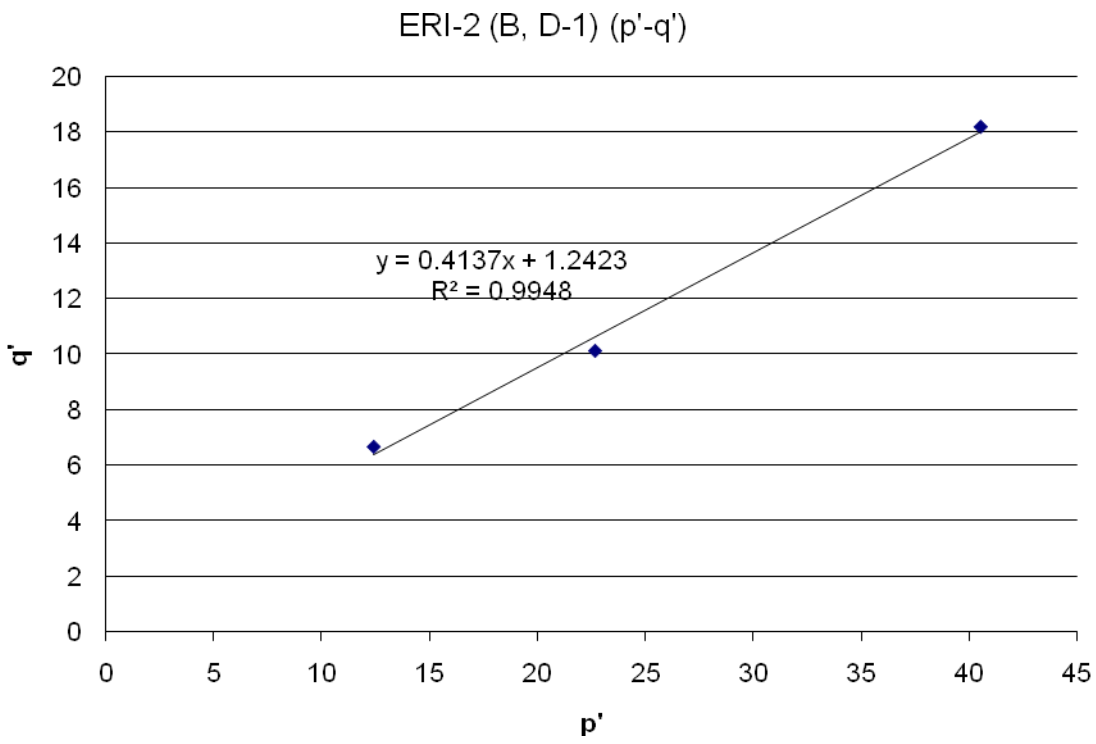


**Figure C.85:** p'-q' Diagram for the Highest Depth Range – Site No. 6

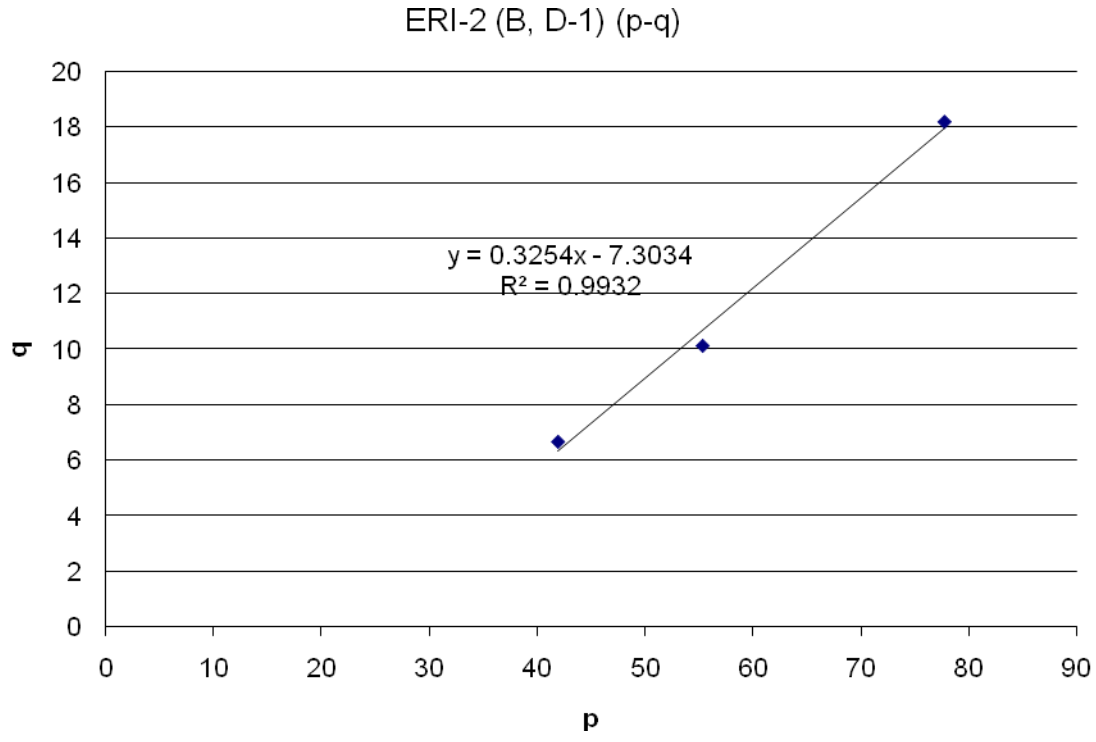


**Figure C.86:** p-q Diagram for the Highest Depth Range – Site No. 6

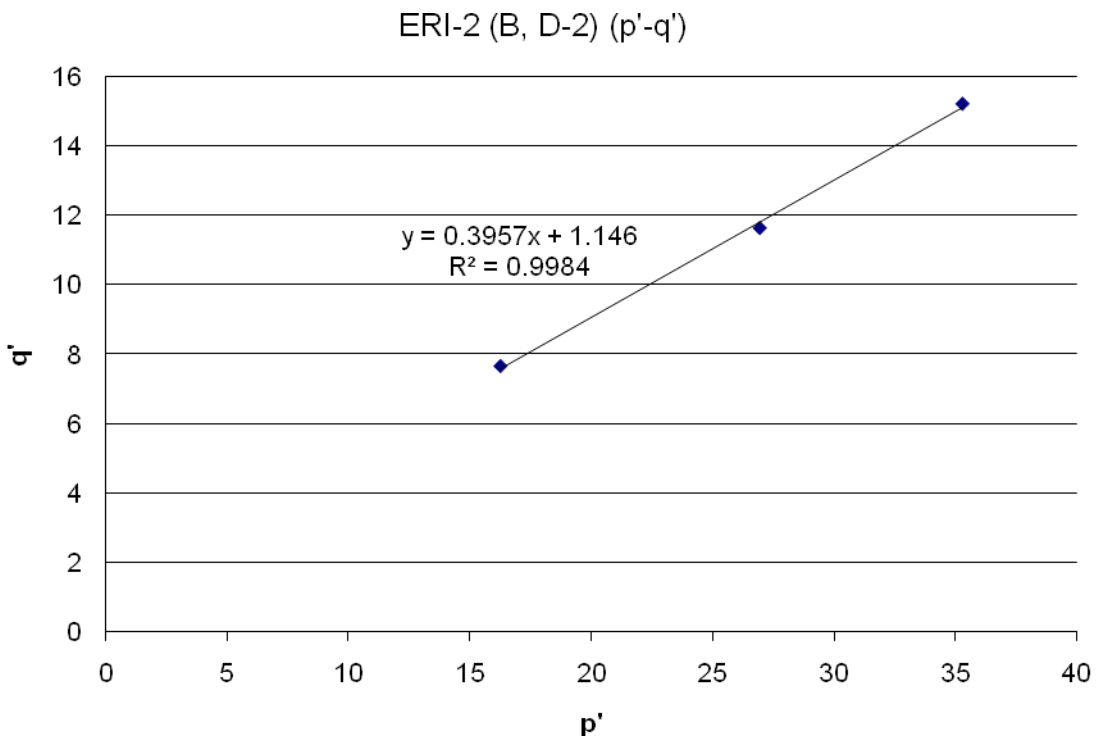


**Figure C.87:** p'-q' Diagram for the Middle Depth Range – Site No. 6

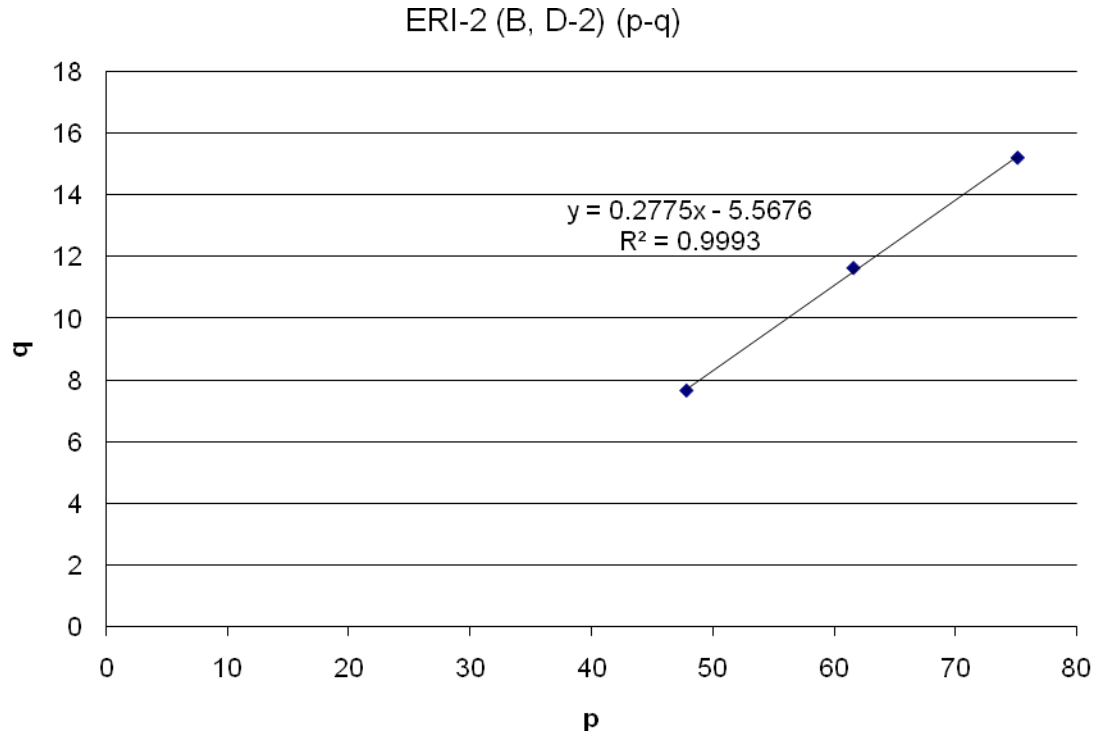


**Figure C.88:** p-q Diagram for the Middle Depth Range – Site No. 6

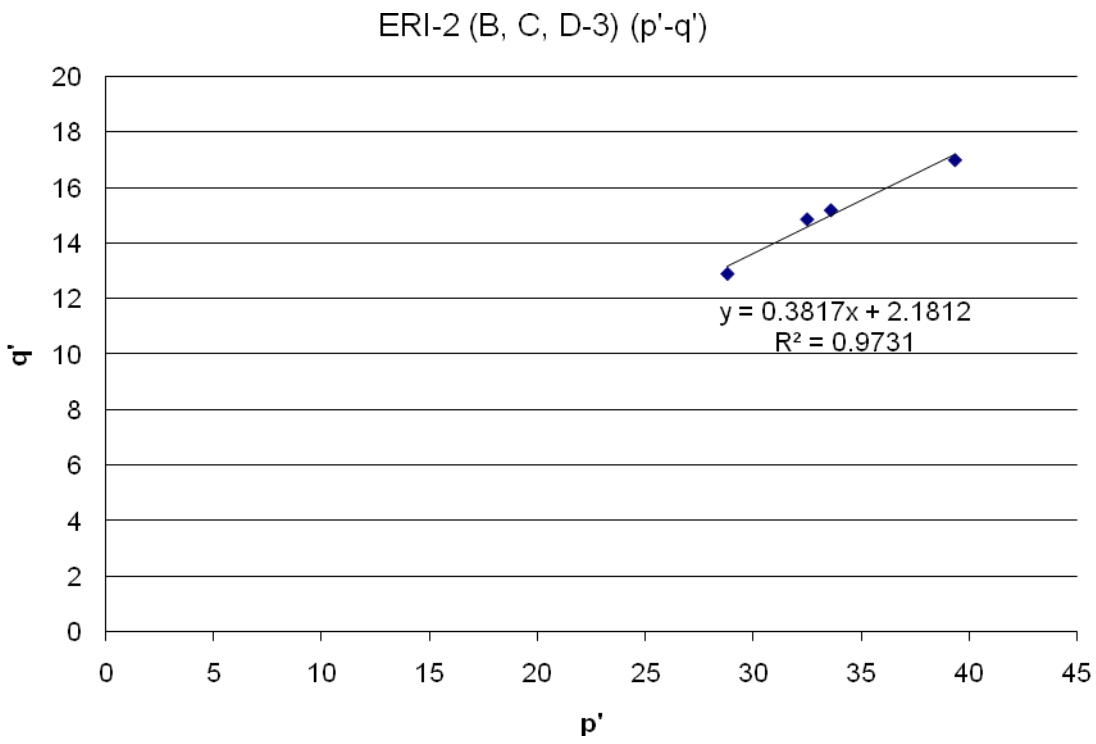


**Figure C.89:** p'-q' Diagram for the Deepest Depth Range – Site No. 6

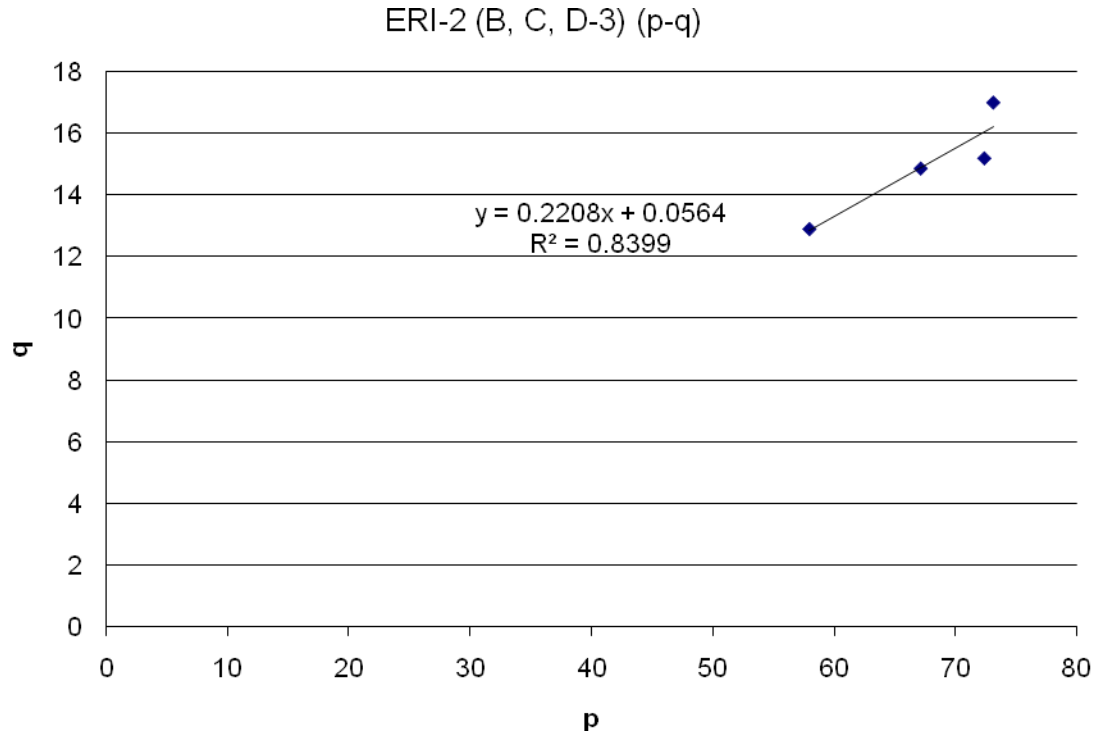


**Figure C.90:** p-q Diagram for the Deepest Depth Range – Site No. 6

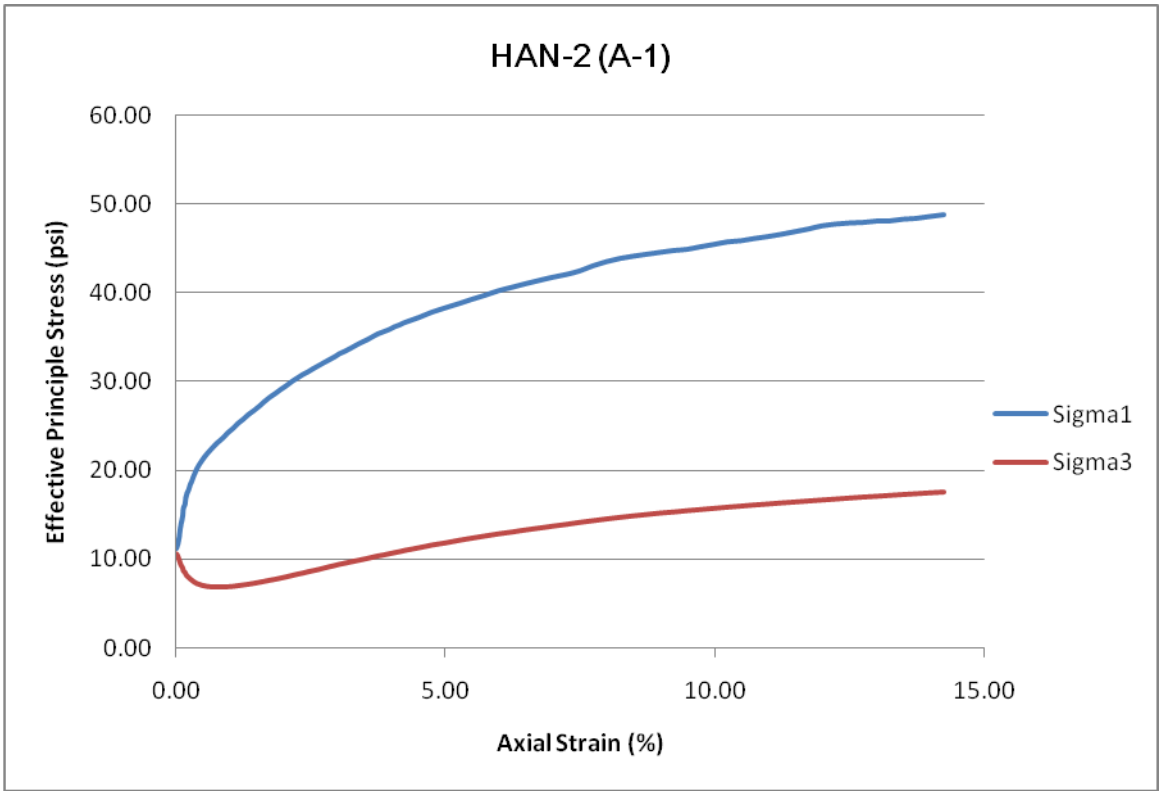


**Figure C.91:** Specimen A-1 (6.8' – 7.3' Depth) – Site No. 7

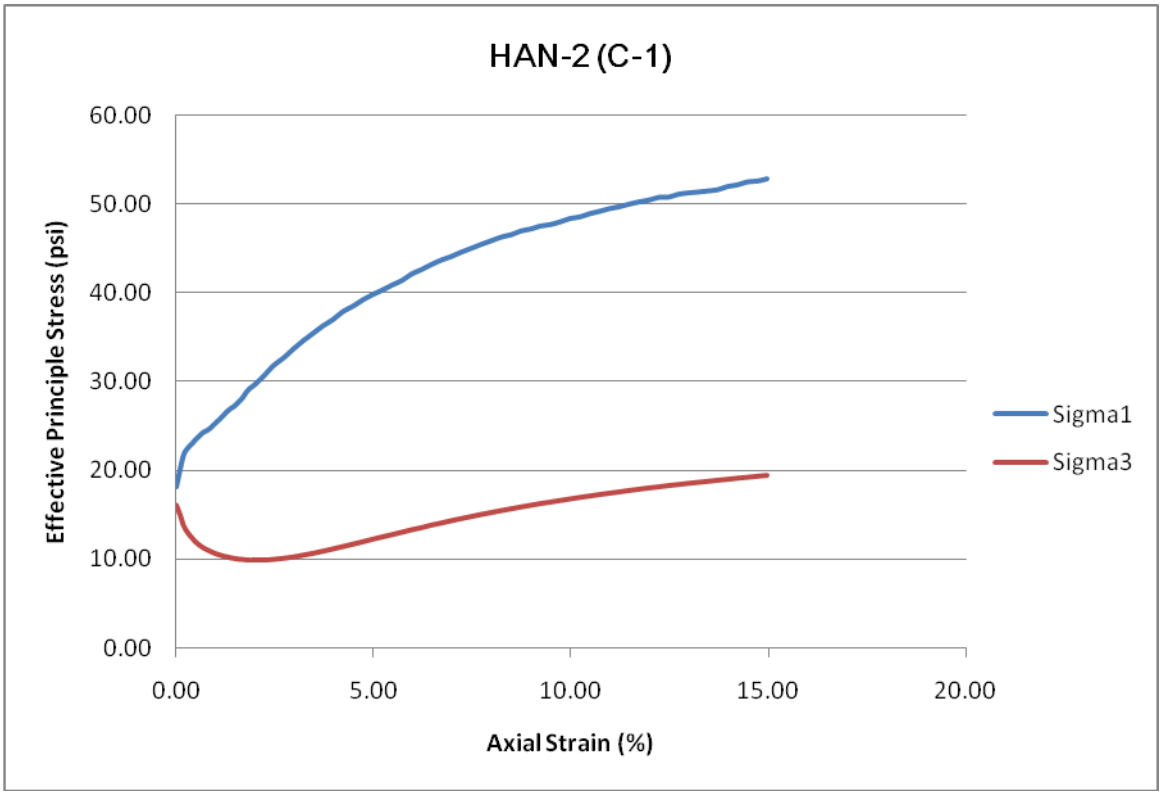


**Figure C.92:** Specimen C-1 (6.6' – 7.1' Depth) – Site No. 7

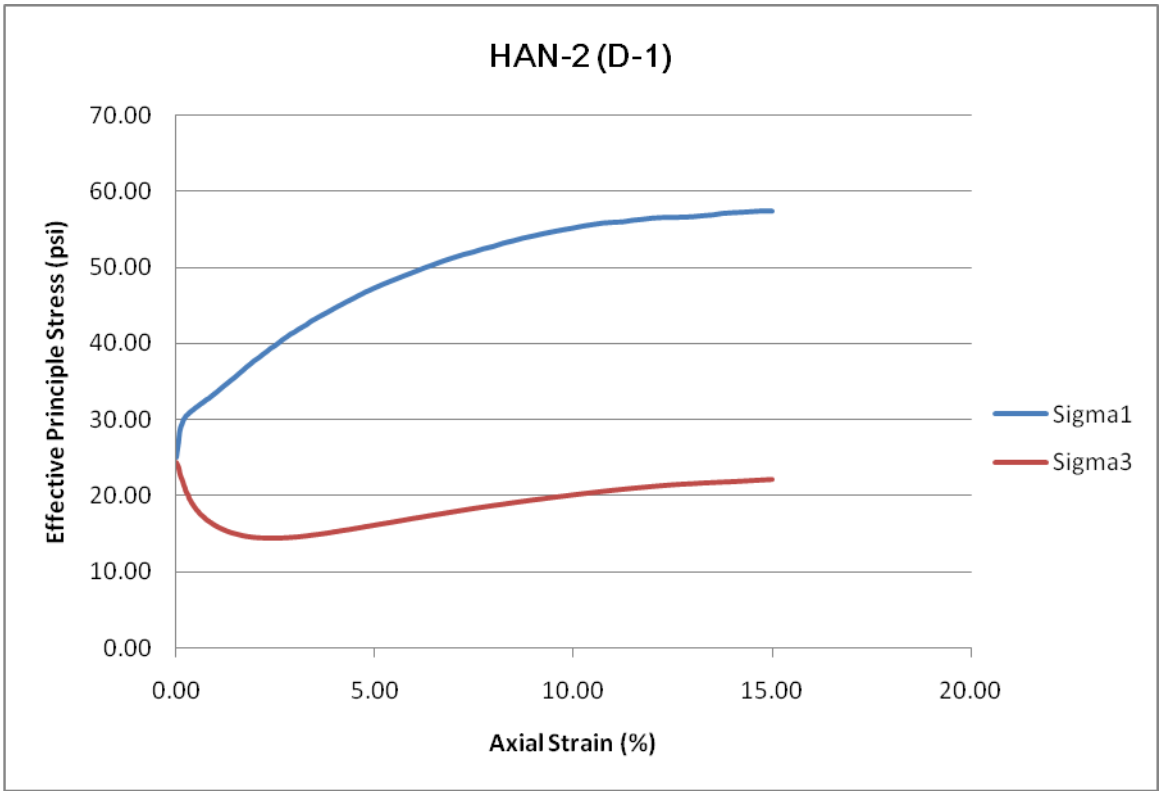


**Figure C.93:** Specimen D-1 (6.4' – 6.9' Depth) – Site No. 7

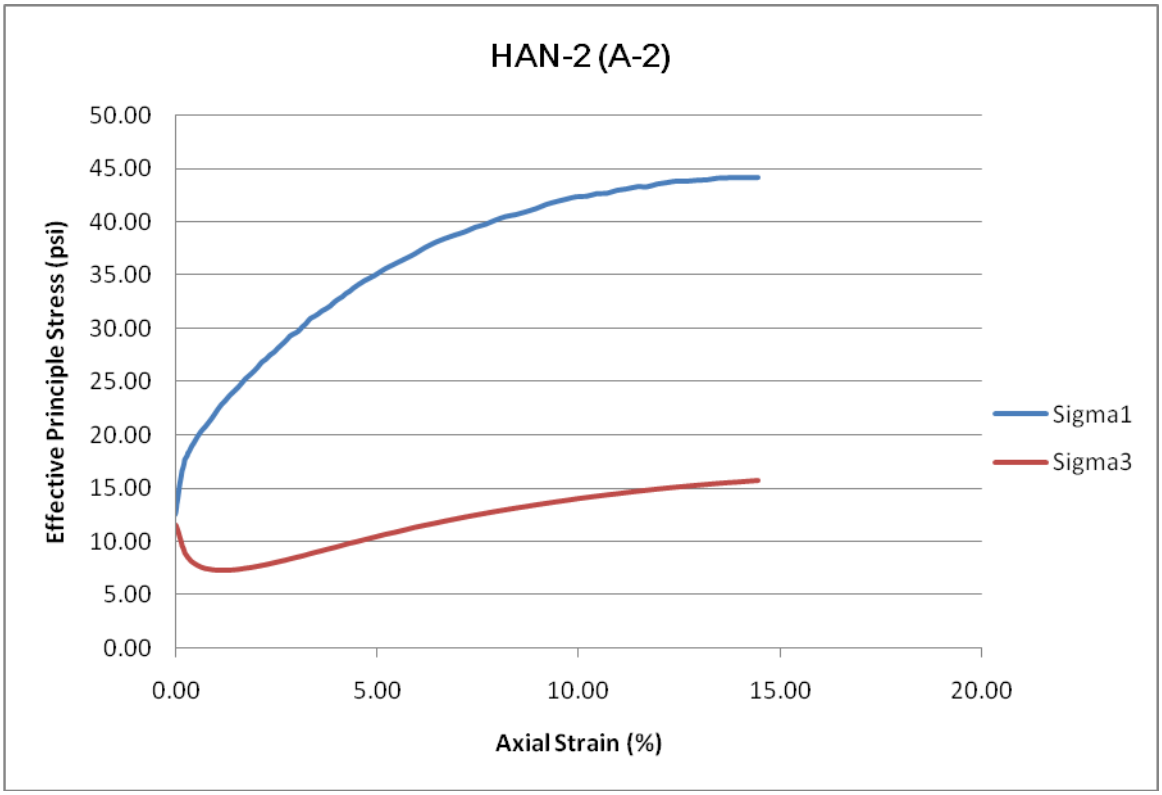


**Figure C.94:** Specimen A-2 (10.8' – 11.3' Depth) – Site No. 7

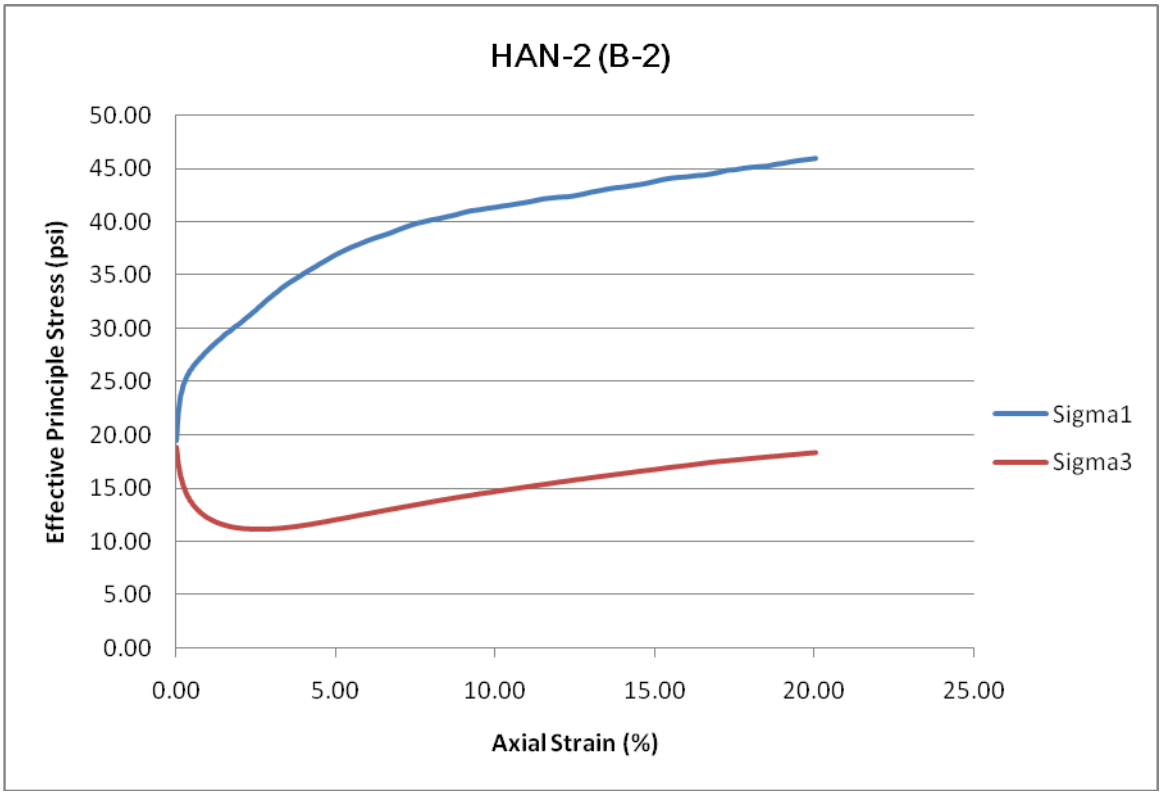


**Figure C.95:** Specimen B-2 (10.8' – 11.3' Depth) – Site No. 7

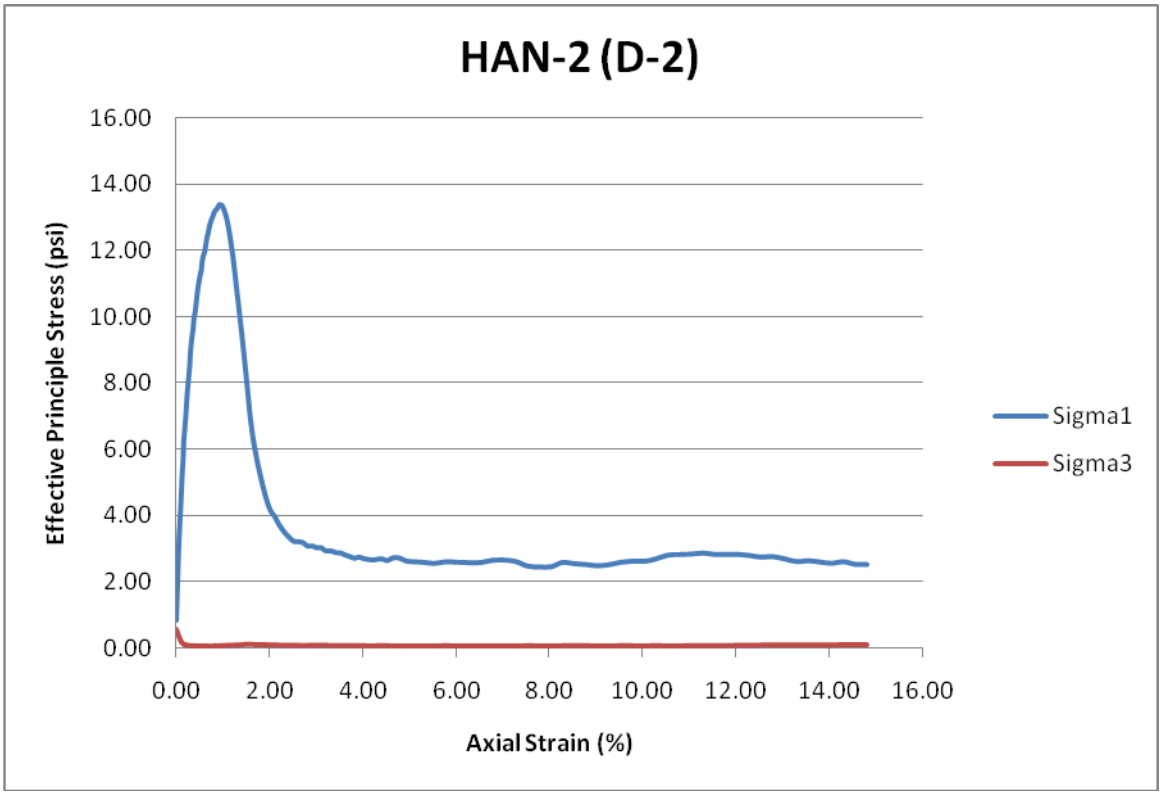


**Figure C.96:** Specimen D-2 (10.9' – 11.4' Depth) – Site No. 7

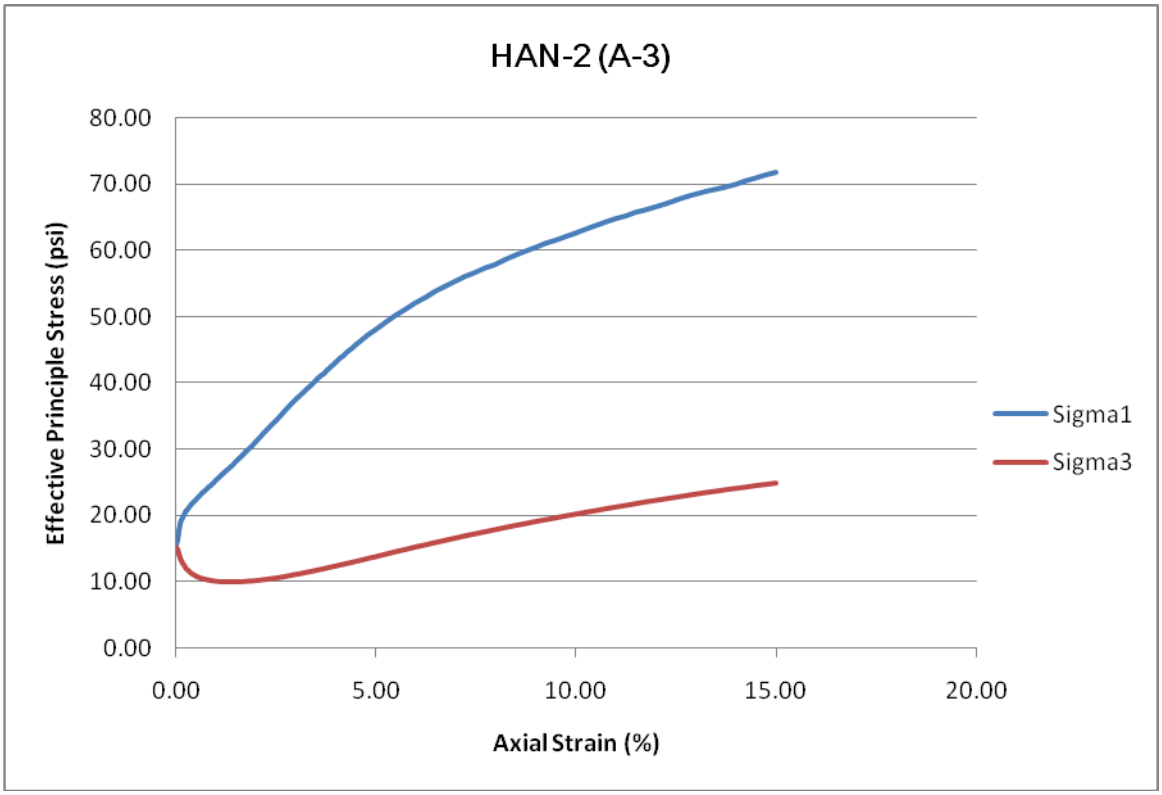


**Figure C.97:** Specimen A-3 (17.3' – 17.8' Depth) – Site No. 7

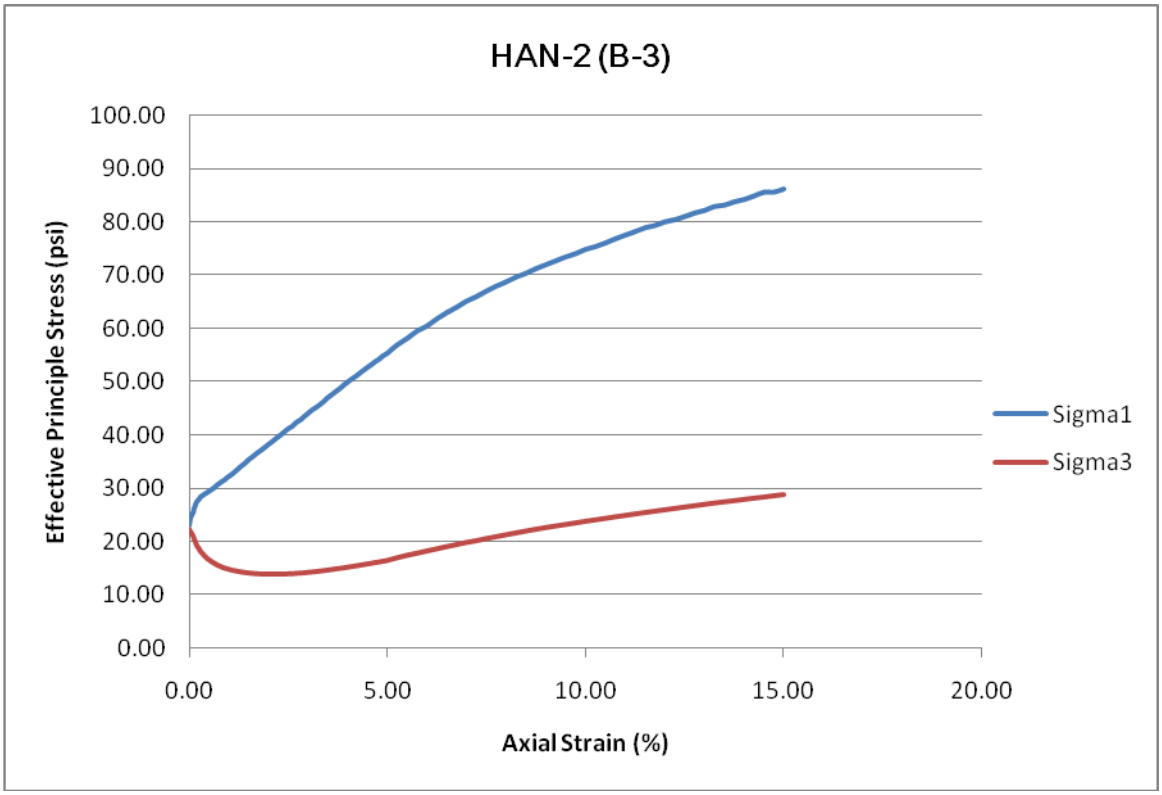


**Figure C.98:** Specimen B-3 (17.3' – 17.8' Depth) – Site No. 7

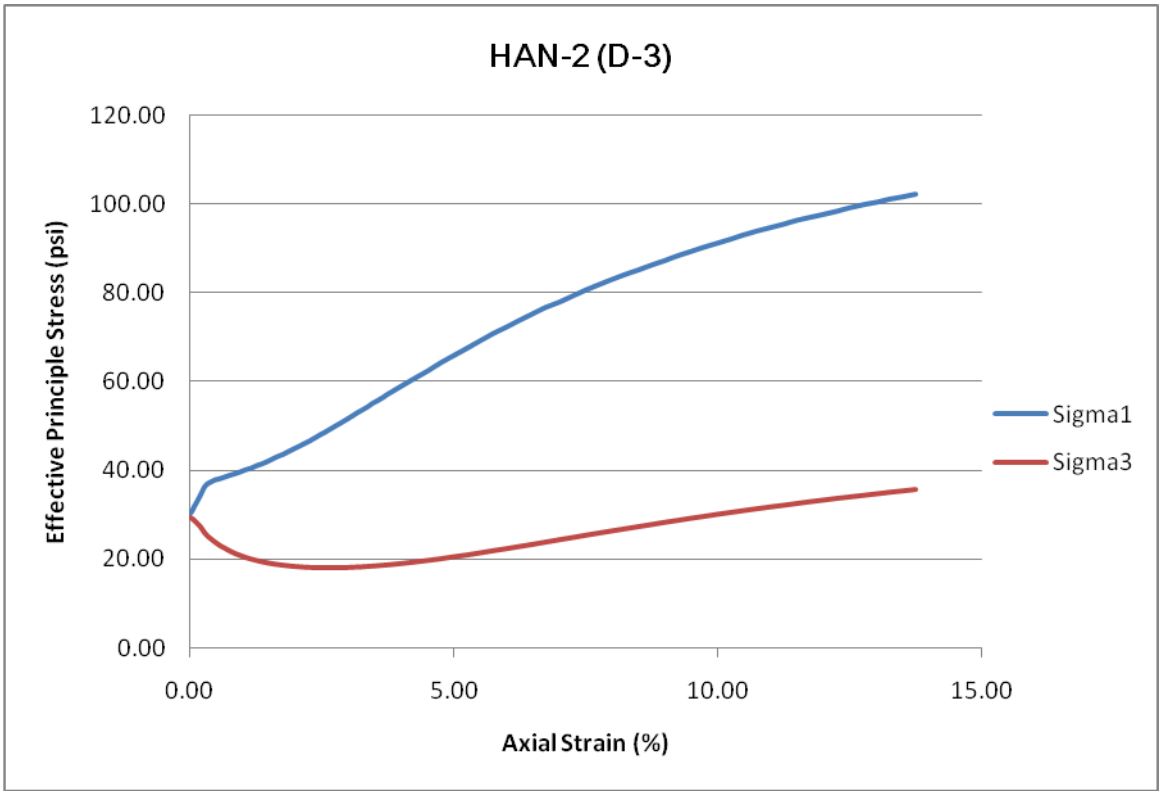


**Figure C.99:** Specimen D-3 (17.3' – 17.8' Depth) – Site No. 7

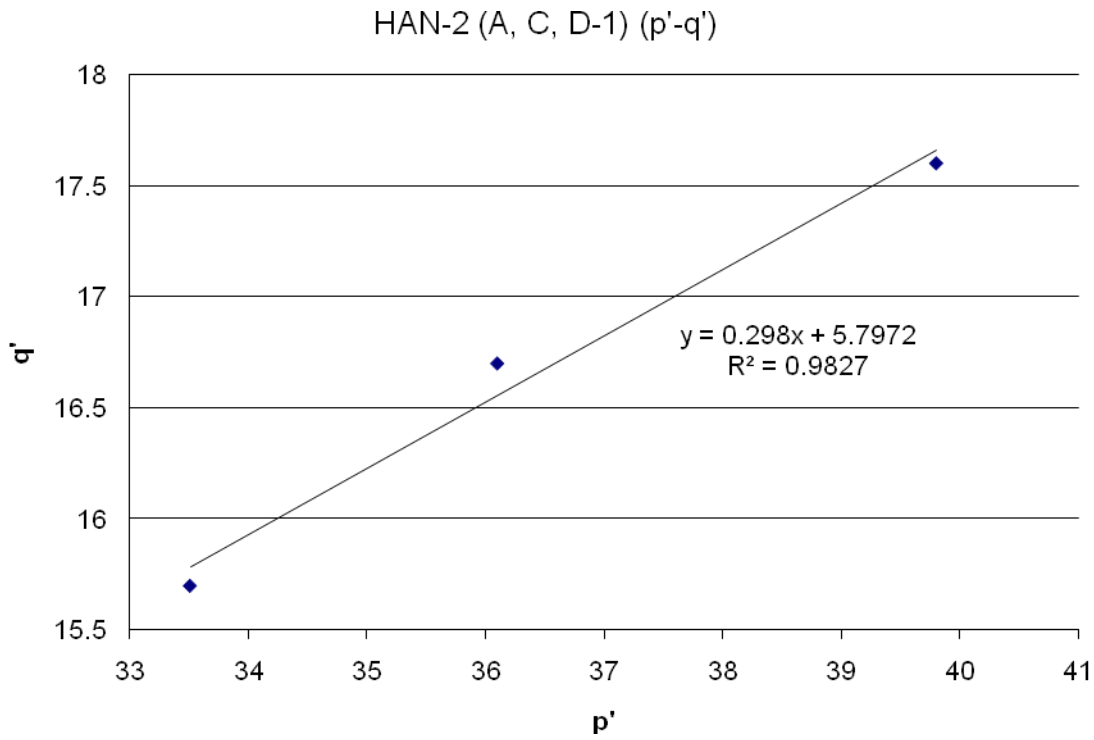


**Figure C.100:** p'-q' Diagram for the Highest Depth Range – Site No. 7

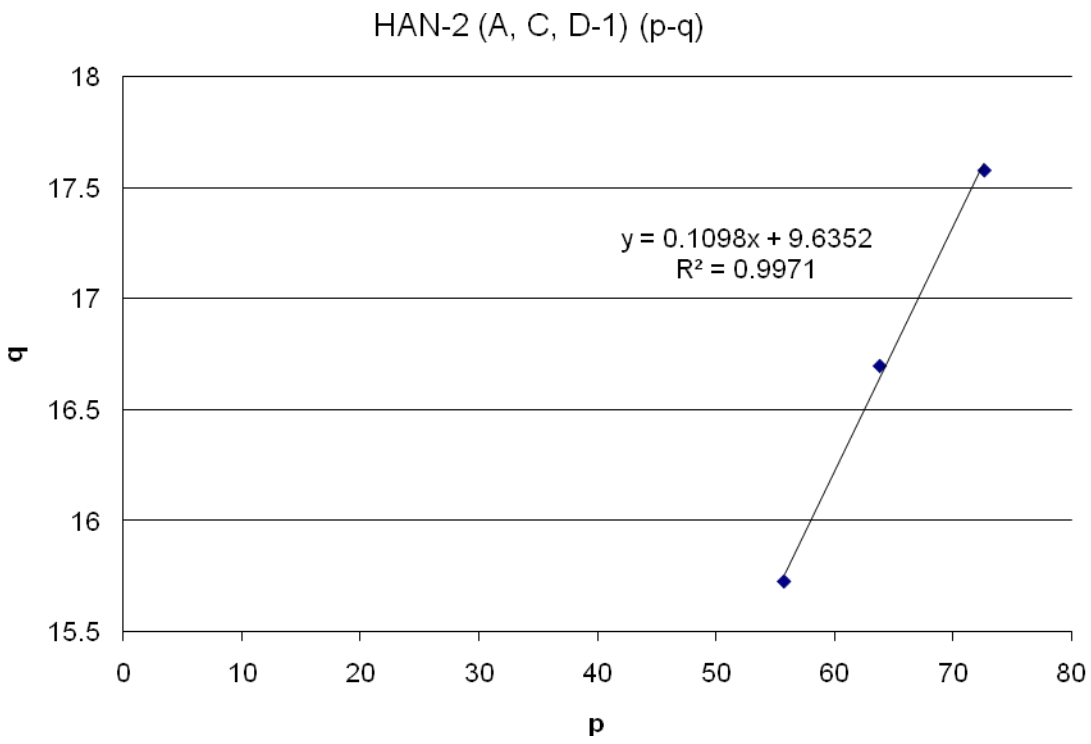


**Figure C.101:** p-q Diagram for the Highest Depth Range – Site No. 7

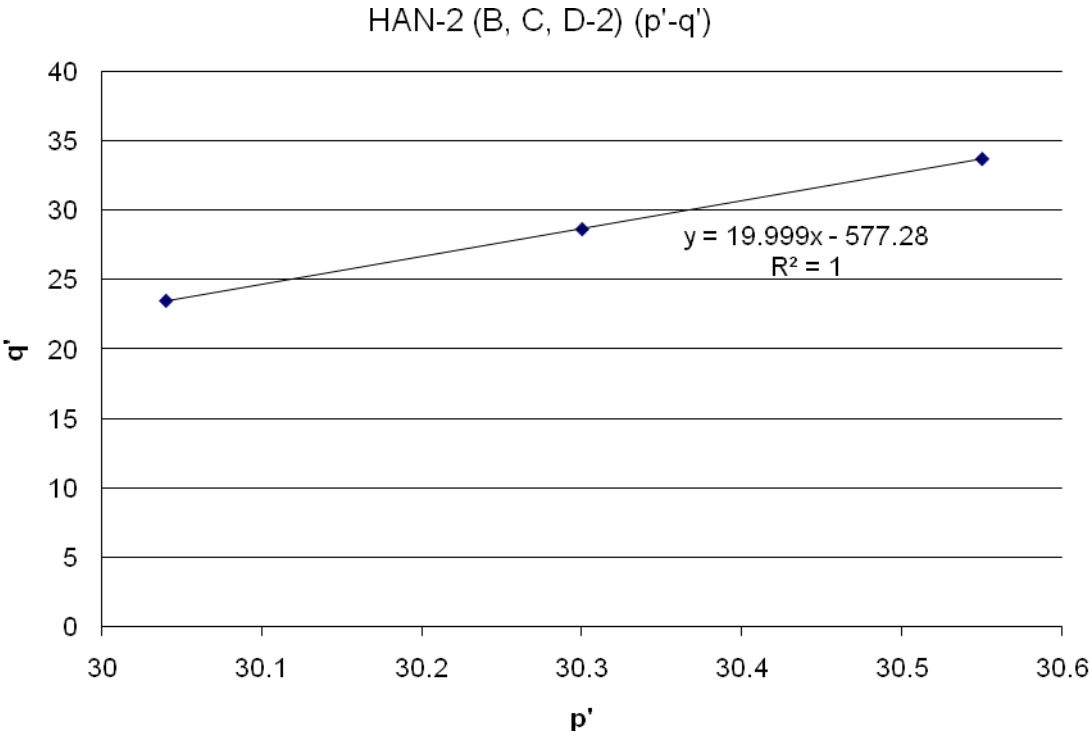


**Figure C.102:** p'-q' Diagram for the Middle Depth Range – Site No. 7

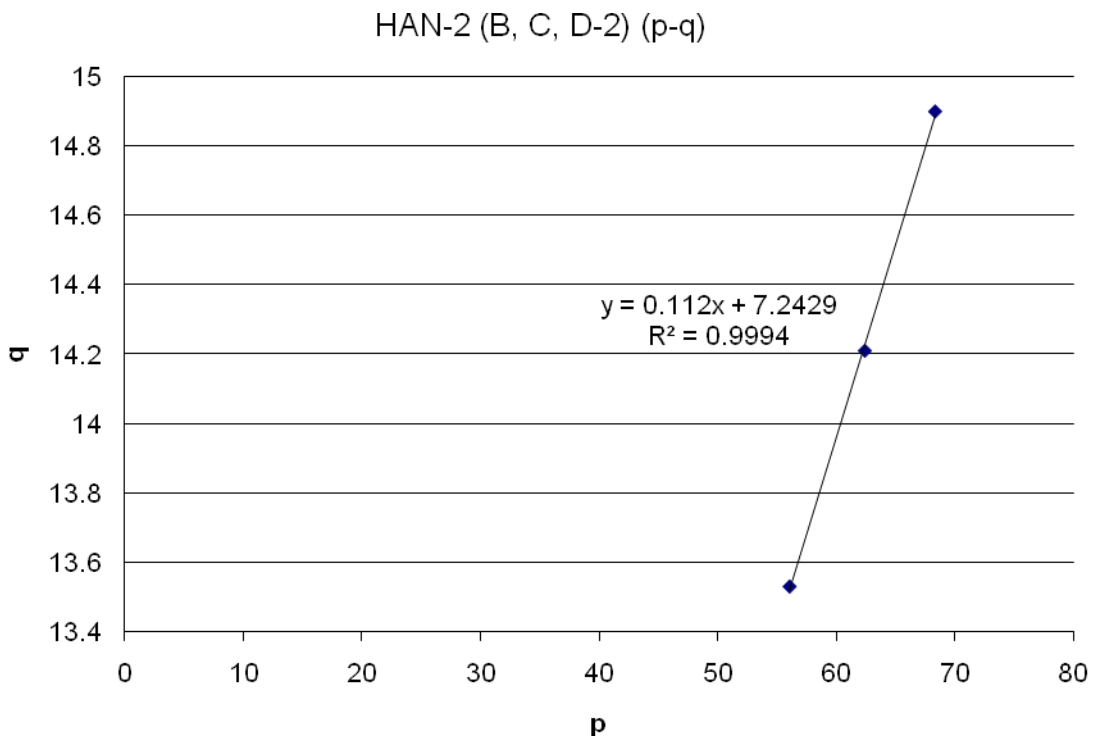


**Figure C.103:** p-q Diagram for the Middle Depth Range – Site No. 7

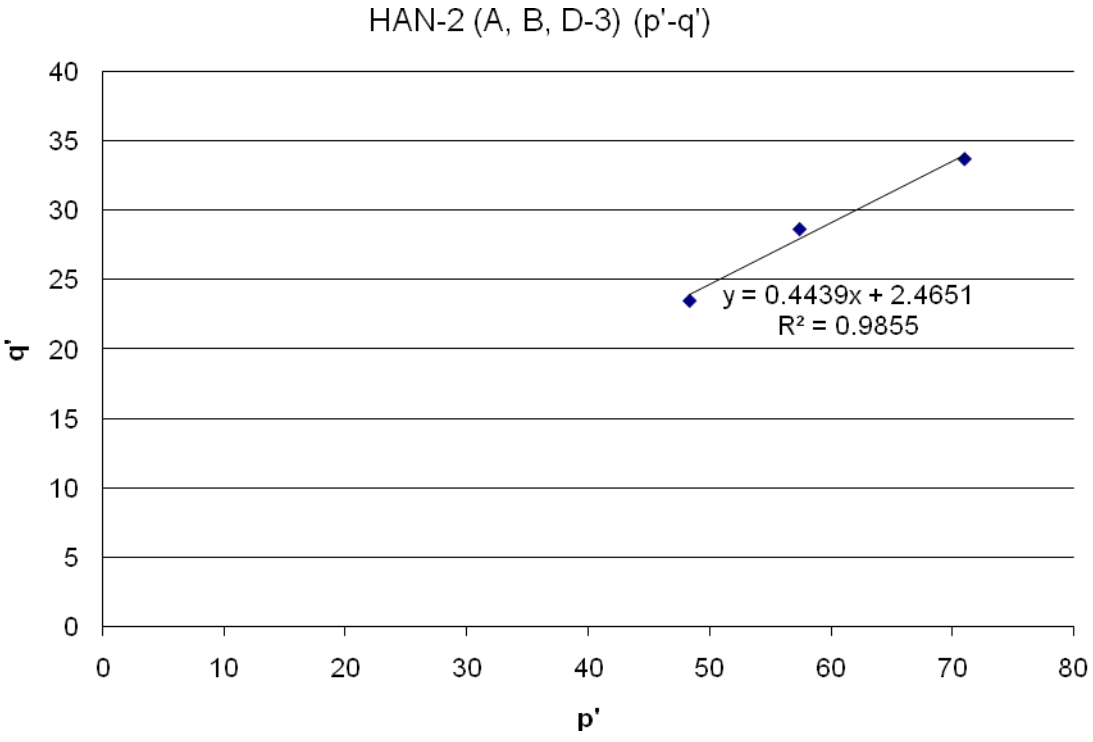


**Figure C.104:** p'-q' Diagram for the Lowest Depth Range – Site No. 7

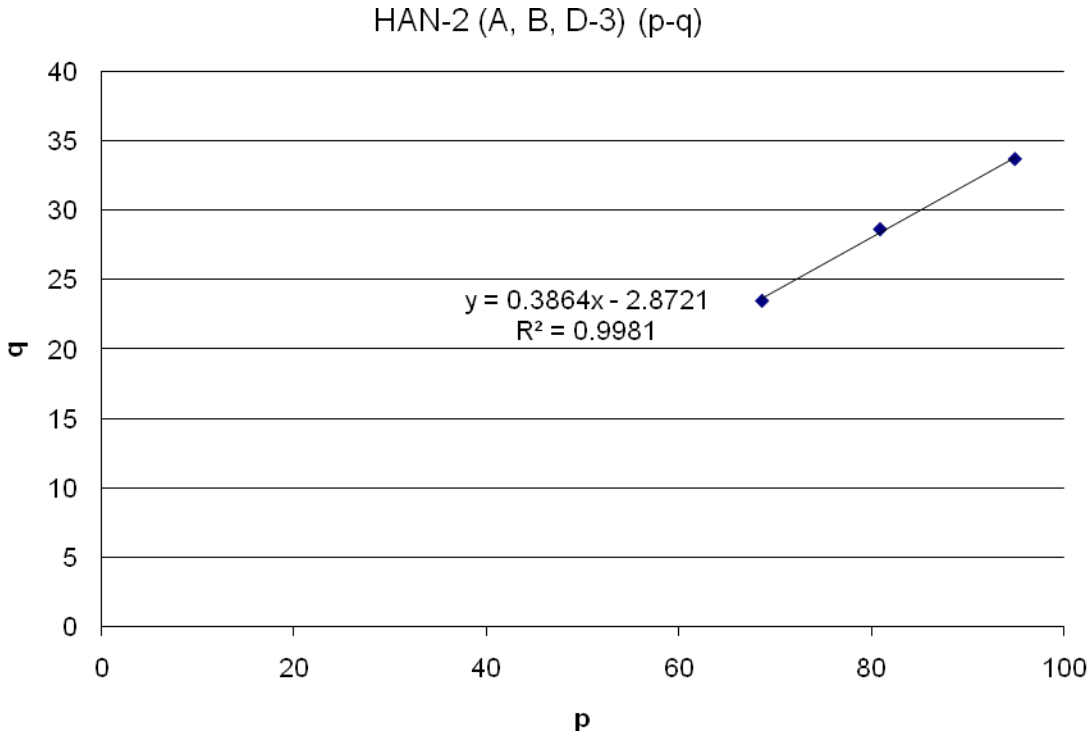


**Figure C.105:** p-q Diagram for the Lowest Depth Range – Site No. 7

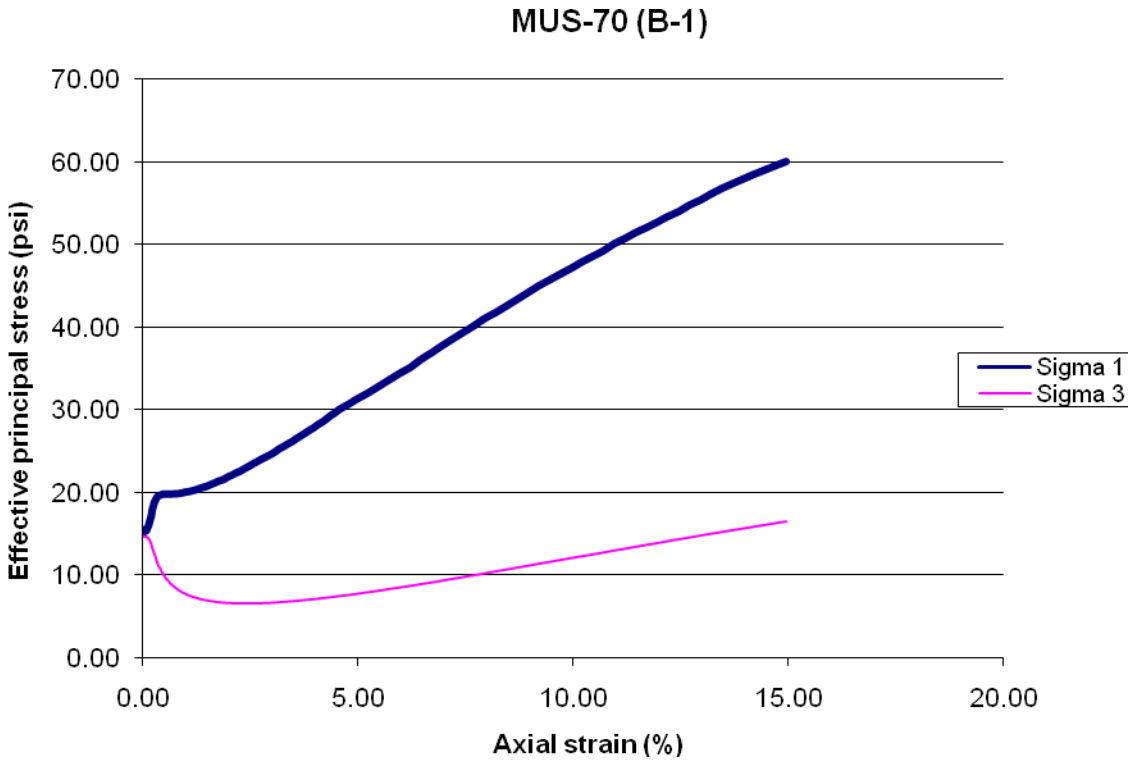


**Figure C.106:** Specimen B-1 (9.5' – 10.0' Depth) – Site No. 8

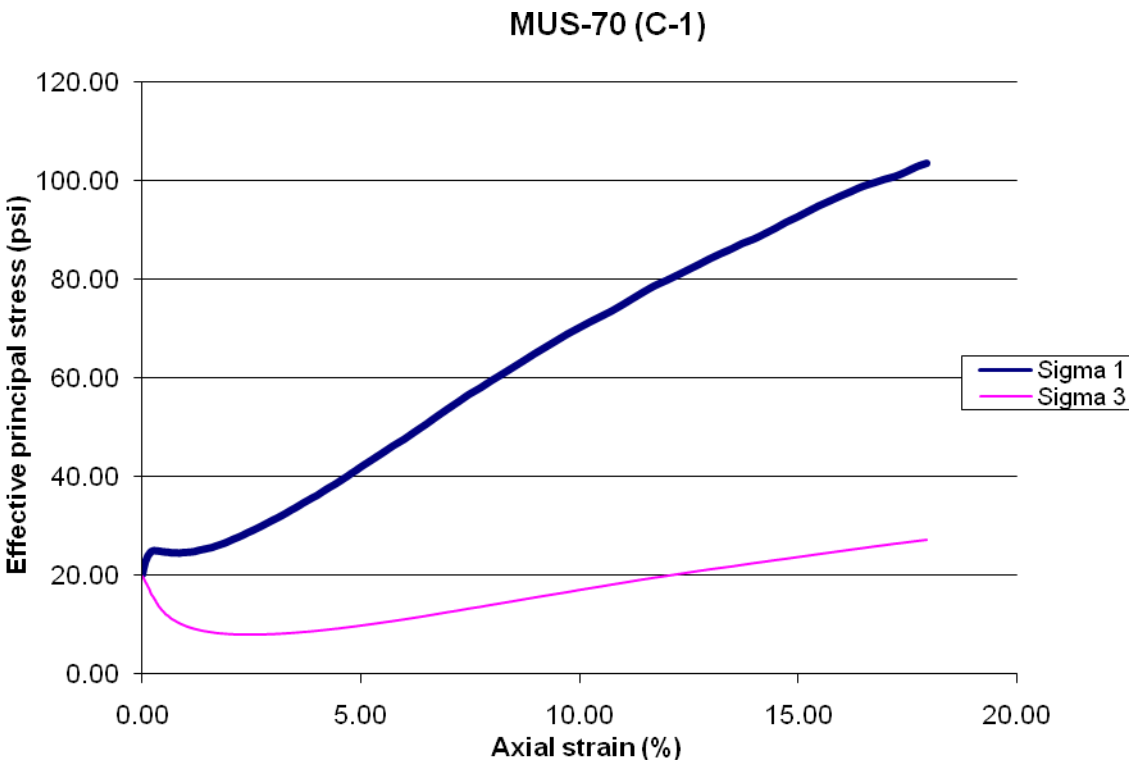


**Figure C.107:** Specimen C-1 (9.5' – 10.0' Depth) – Site No. 8

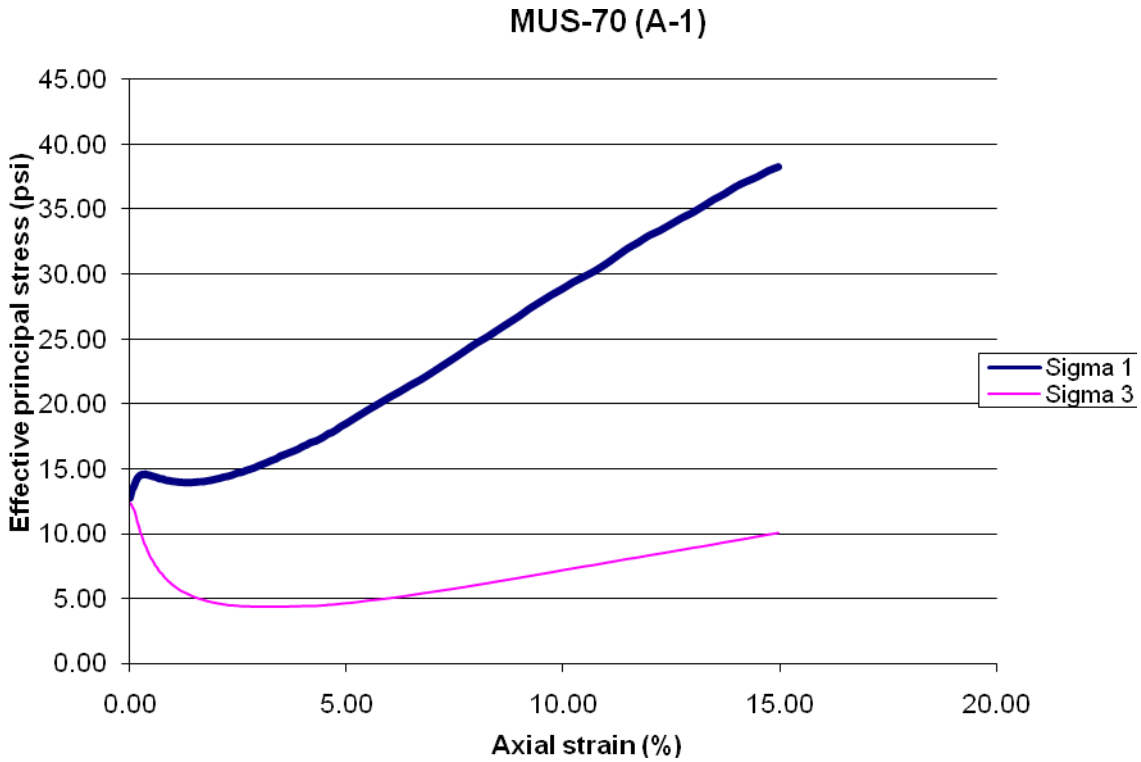


**Figure C.108:** Specimen A-1 (10.1' – 10.6' Depth) – Site No. 8

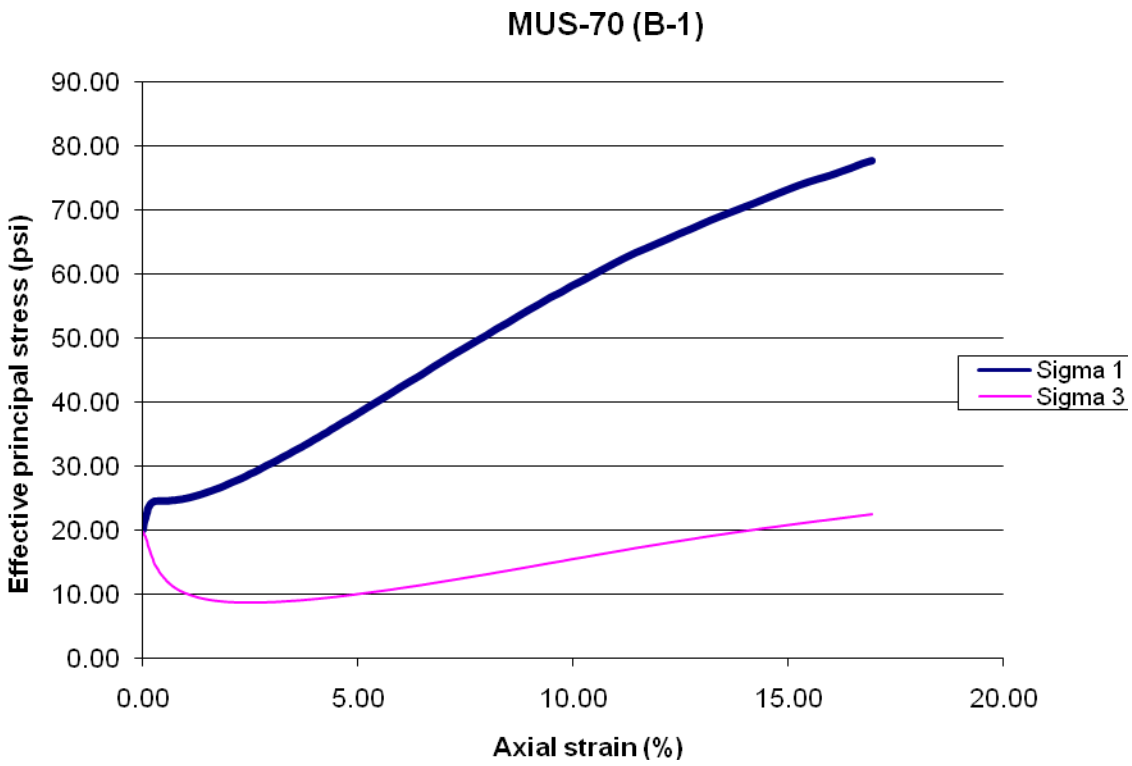


**Figure C.109:** Specimen B-1 (10.1' – 10.6' Depth) – Site No. 8

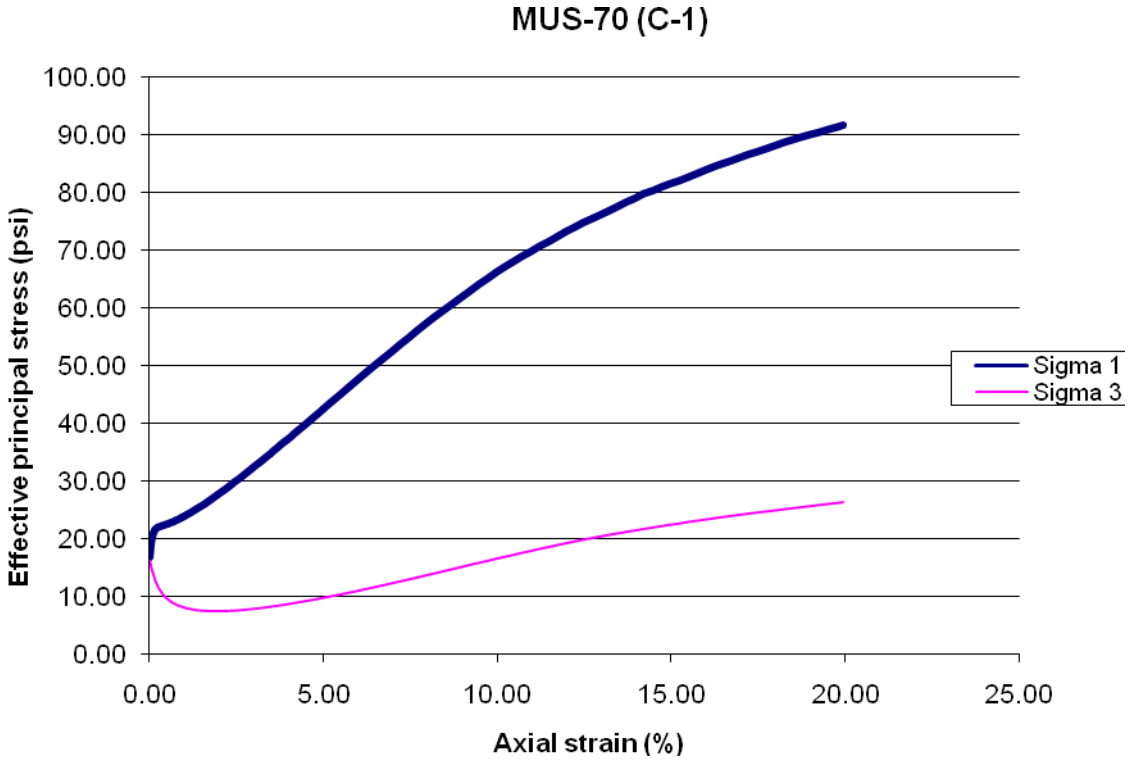


**Figure C.110:** Specimen C-1 (10.1' – 10.6' Depth) – Site No. 8

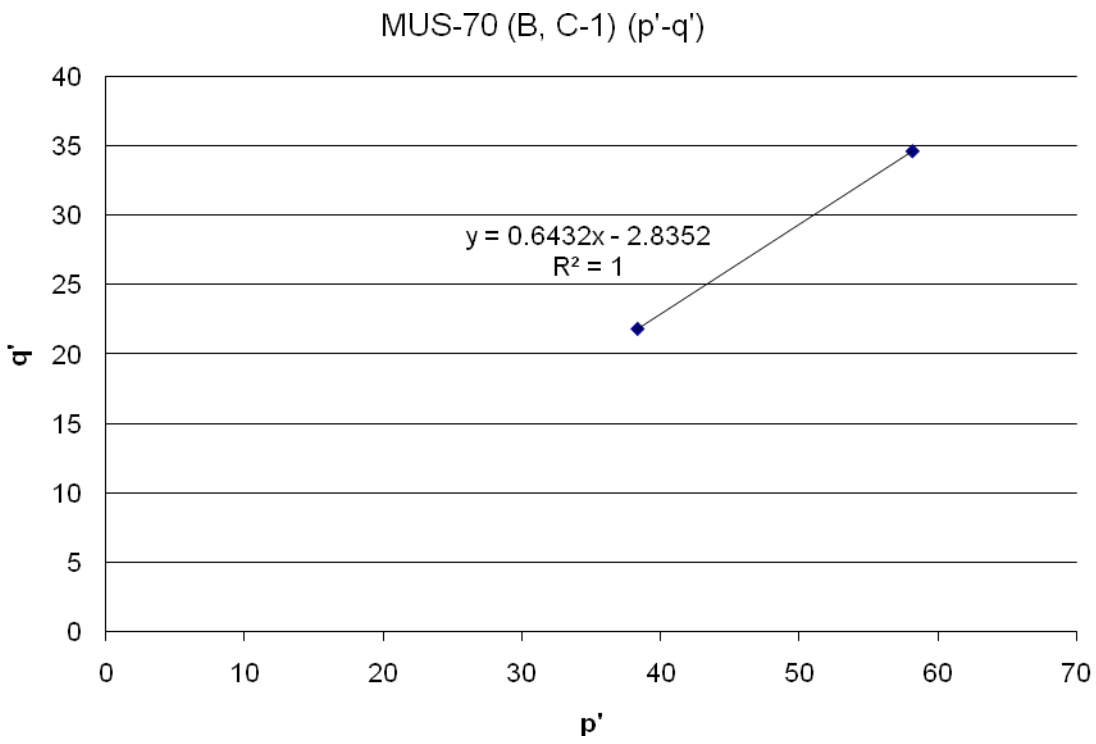


**Figure C.111:** p'-q' Diagram for the Highest Depth Range – Site No. 8

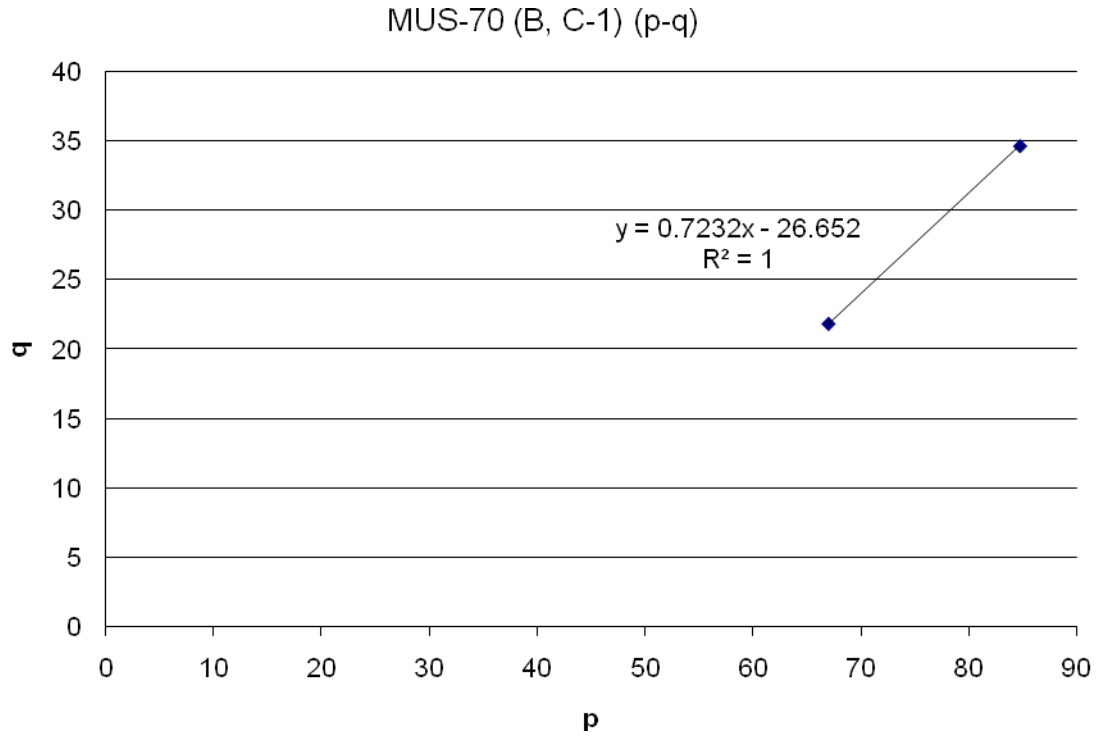


**Figure C.112:** p-q Diagram for the Highest Depth Range – Site No. 8

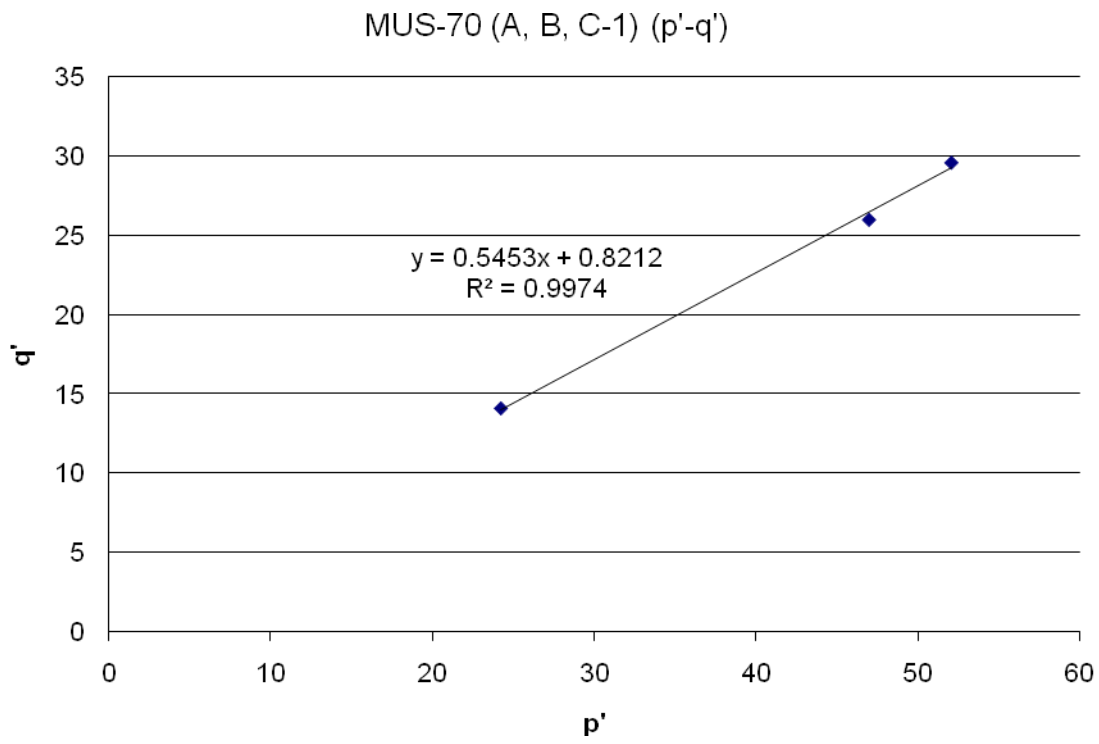


**Figure C.113:** p'-q' Diagram for the Lowest Depth Range – Site No. 8

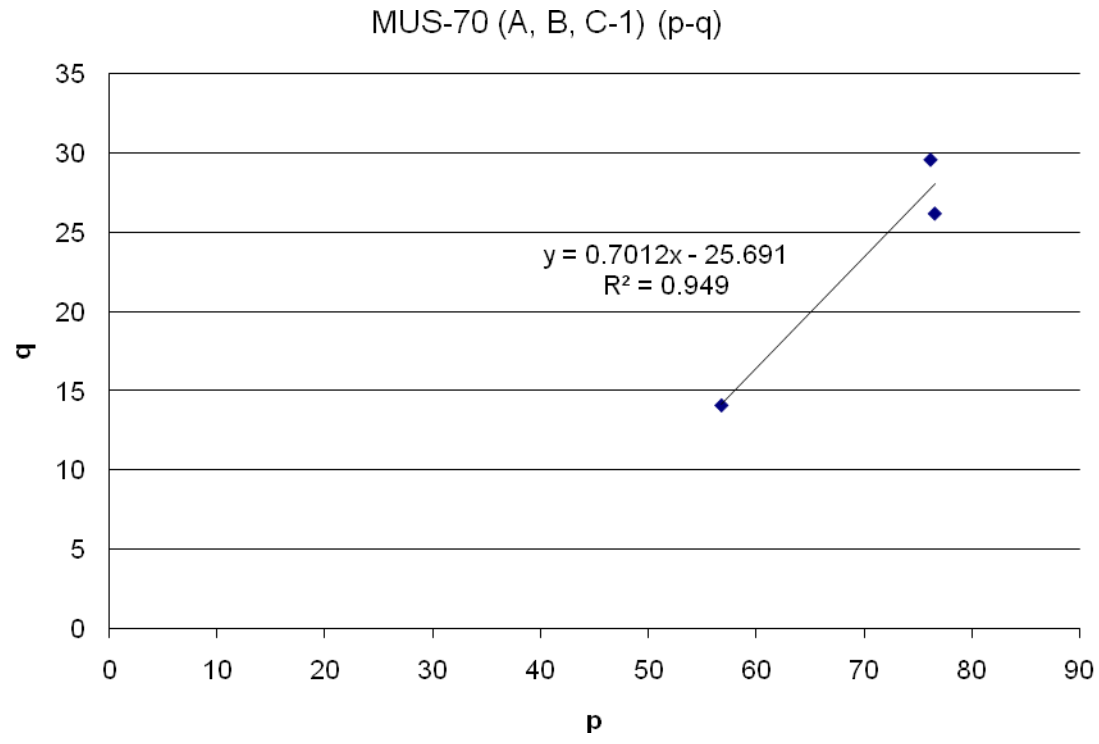


**Figure C.114:** p-q Diagram for the Lowest Depth Range – Site No. 8

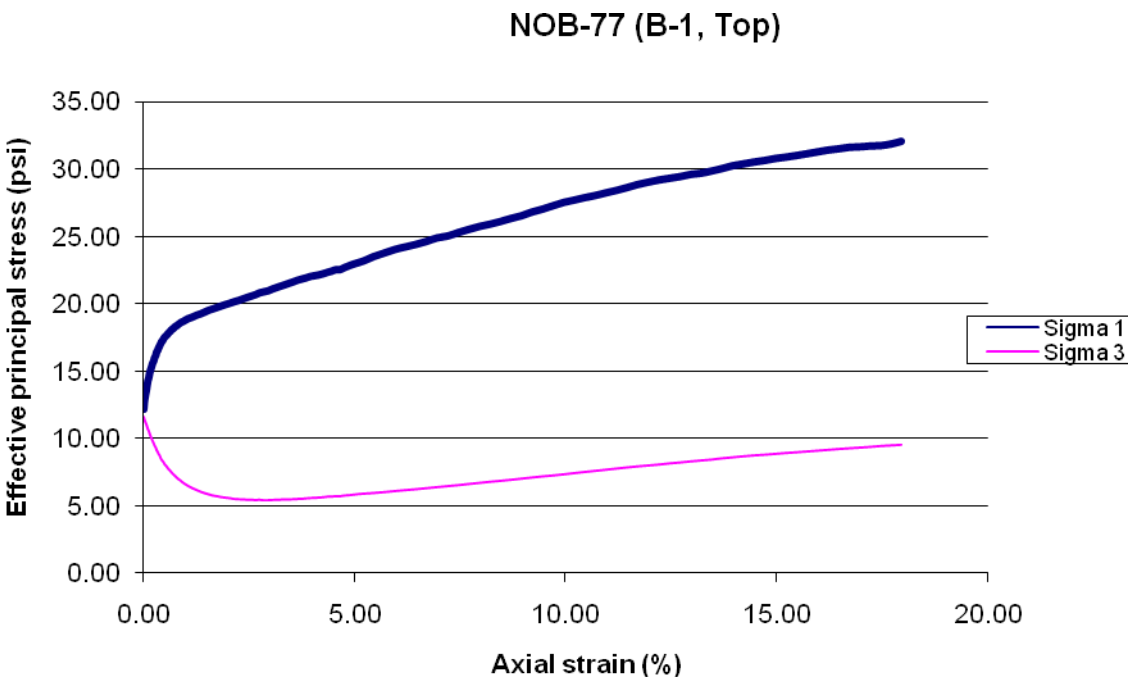


**Figure C.115:** Specimen B-1 (4.0' – 4.5' Depth) – Site No. 9

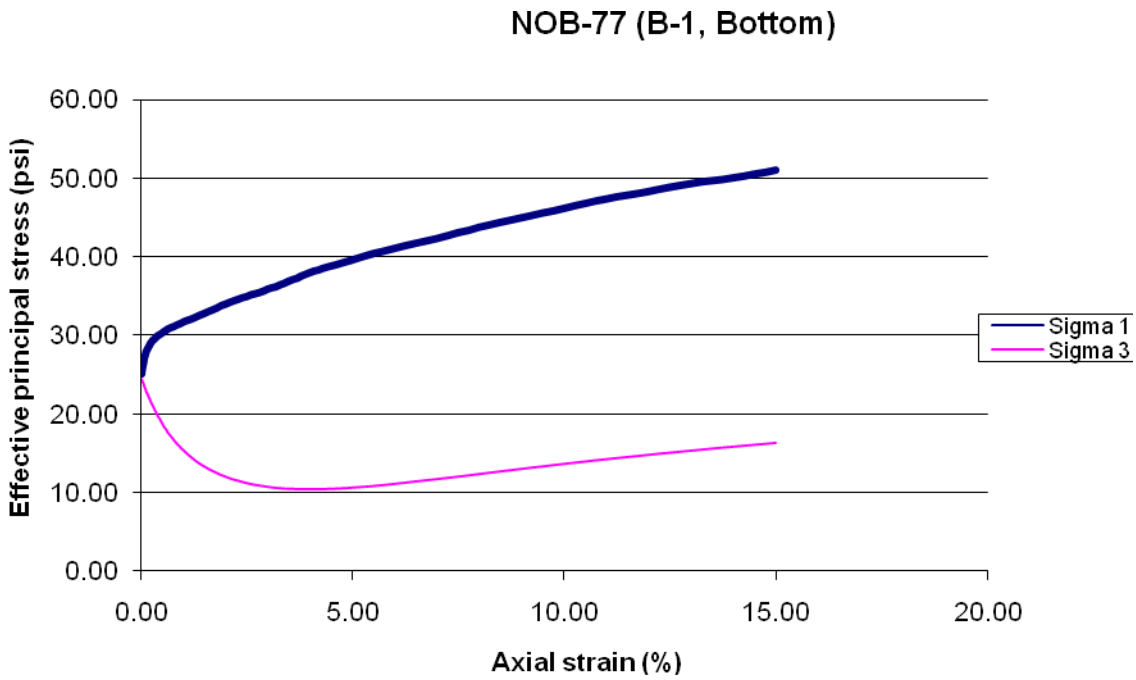


**Figure C.116:** Specimen B-1 (4.6' – 5.1' Depth) – Site No. 9

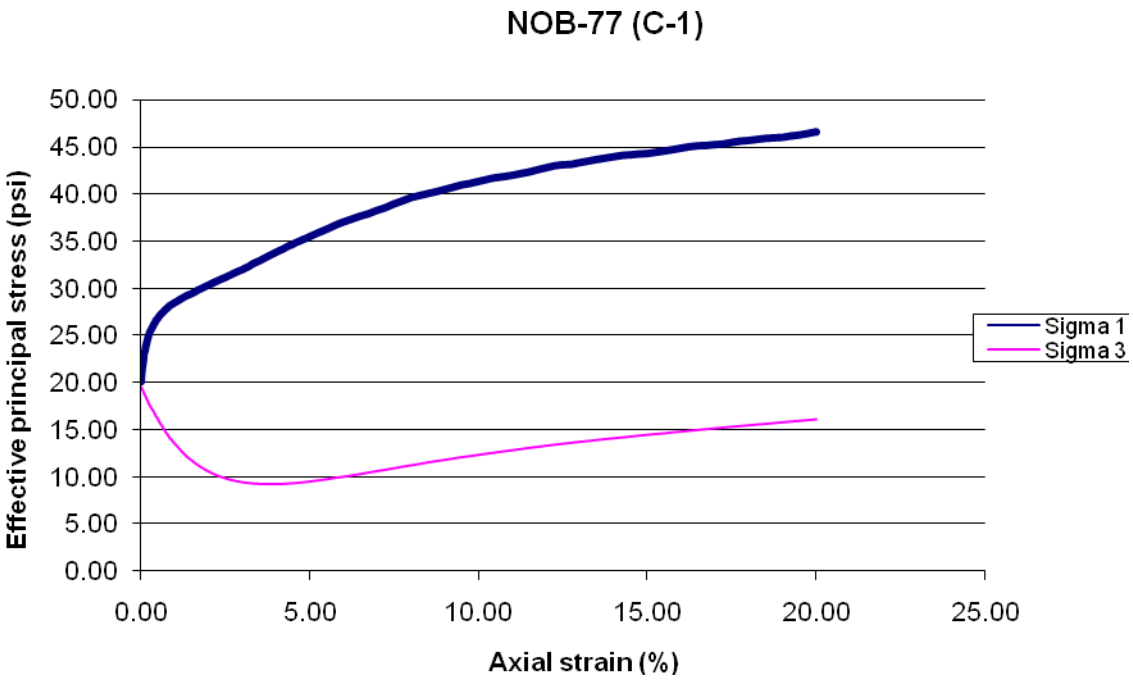


**Figure C.117:** Specimen C-1 (4.0' – 4.5' Depth) – Site No. 9

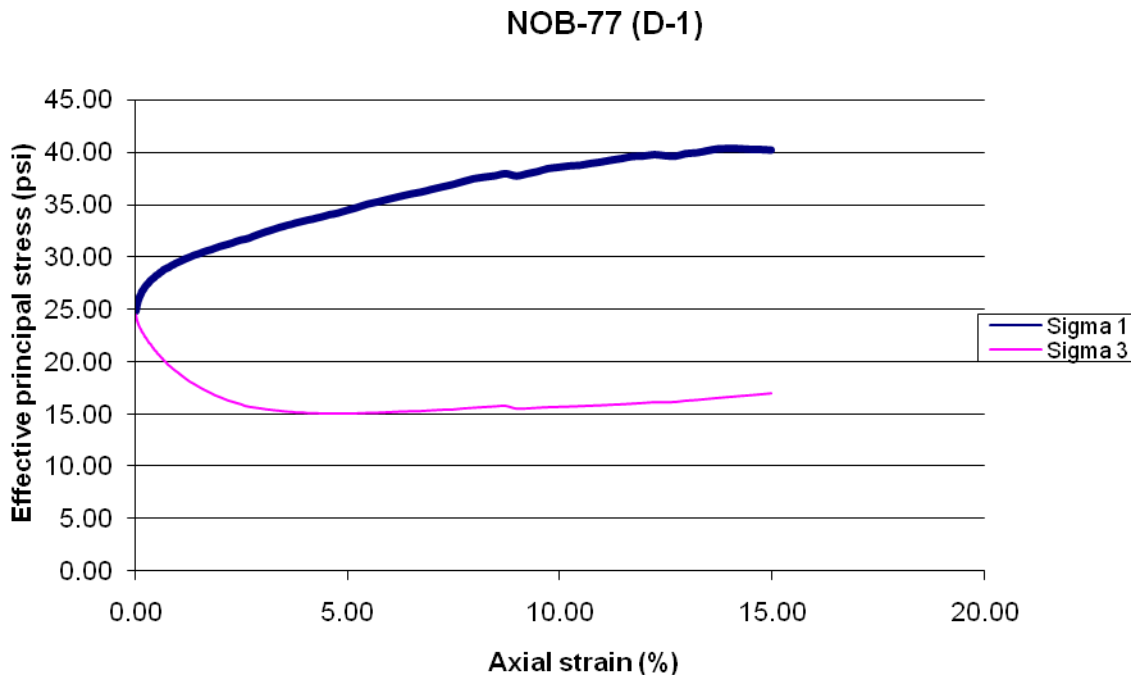


**Figure C.118:** Specimen D-1 (4.0' – 4.5' Depth) – Site No. 9

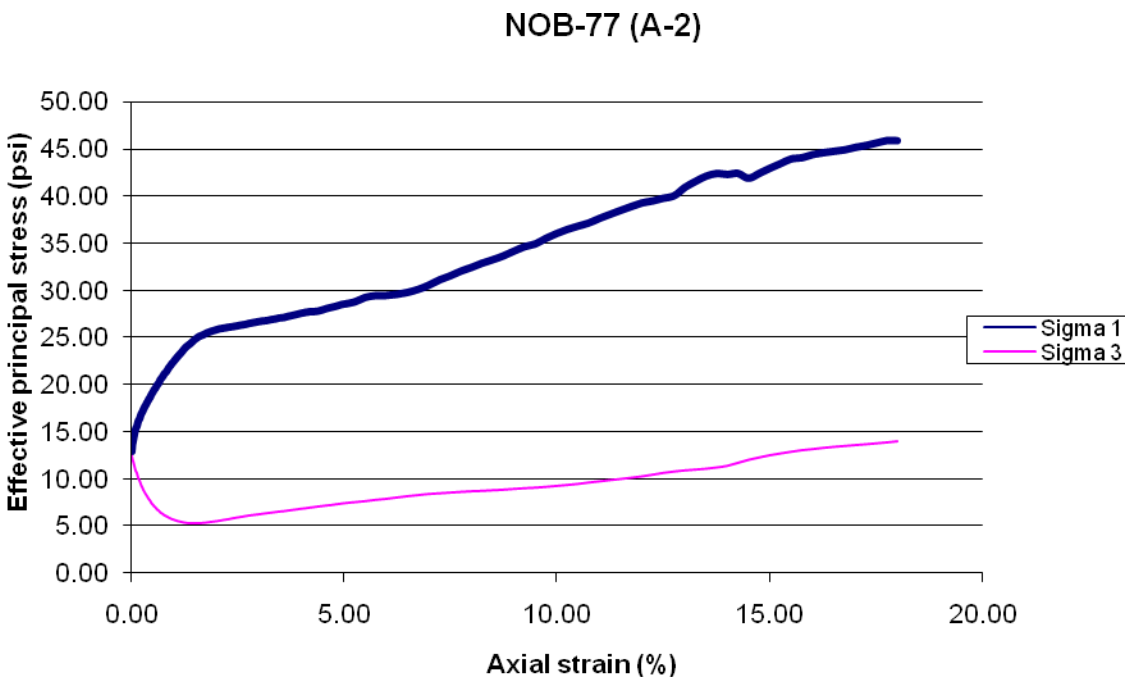


**Figure C.119:** Specimen A-2 (7.0' – 7.5' Depth) – Site No. 9

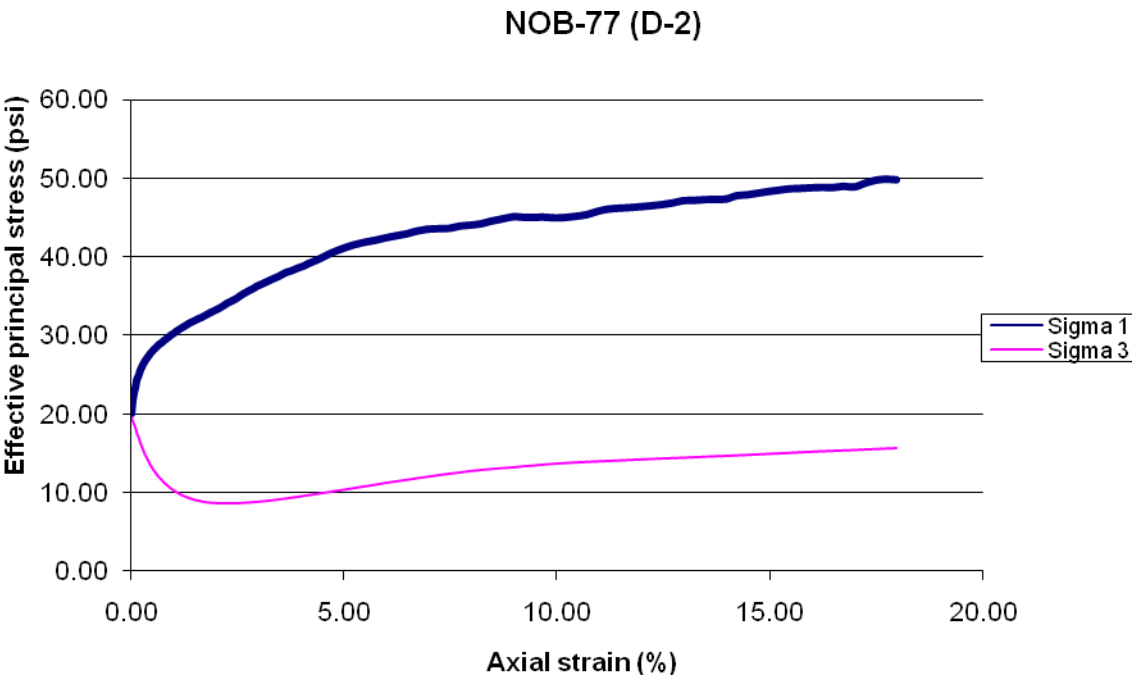


**Figure C.120:** Specimen D-2 (7.0' – 7.5' Depth) – Site No. 9

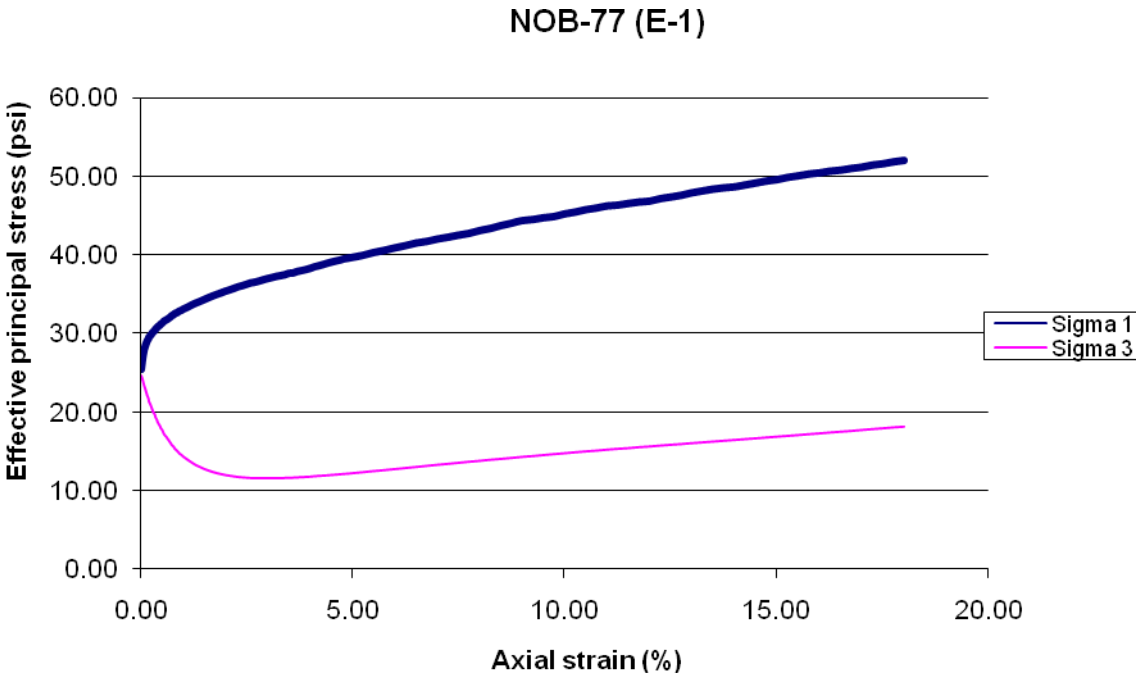


**Figure C.121:** Specimen E-1 (7.0' – 7.5' Depth) – Site No. 9

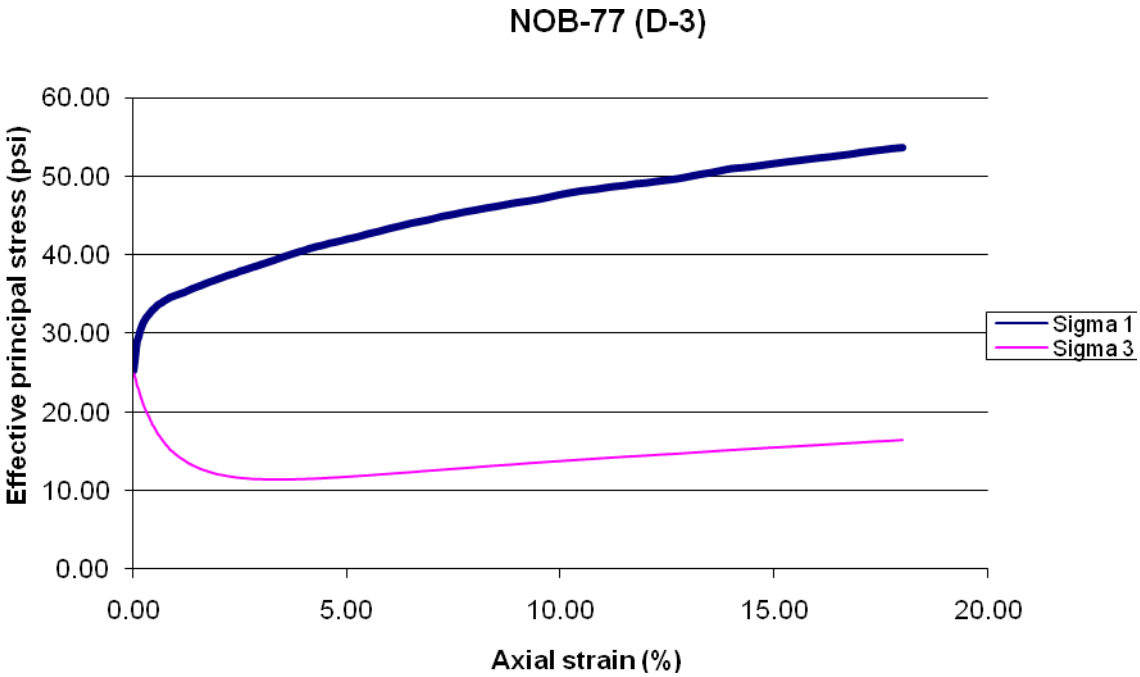


**Figure C.122:** Specimen D-3 (10.0' – 10.5' Depth) – Site No. 9

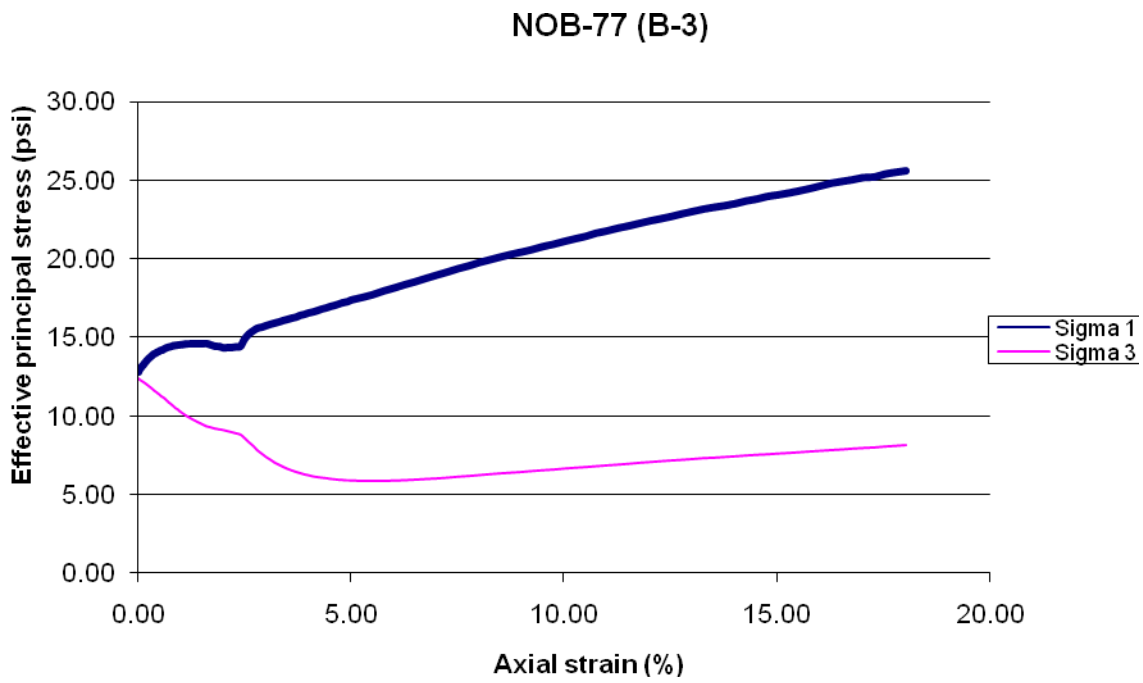


**Figure C.123:** Specimen B-3 (10.0' – 10.5' Depth) – Site No. 9

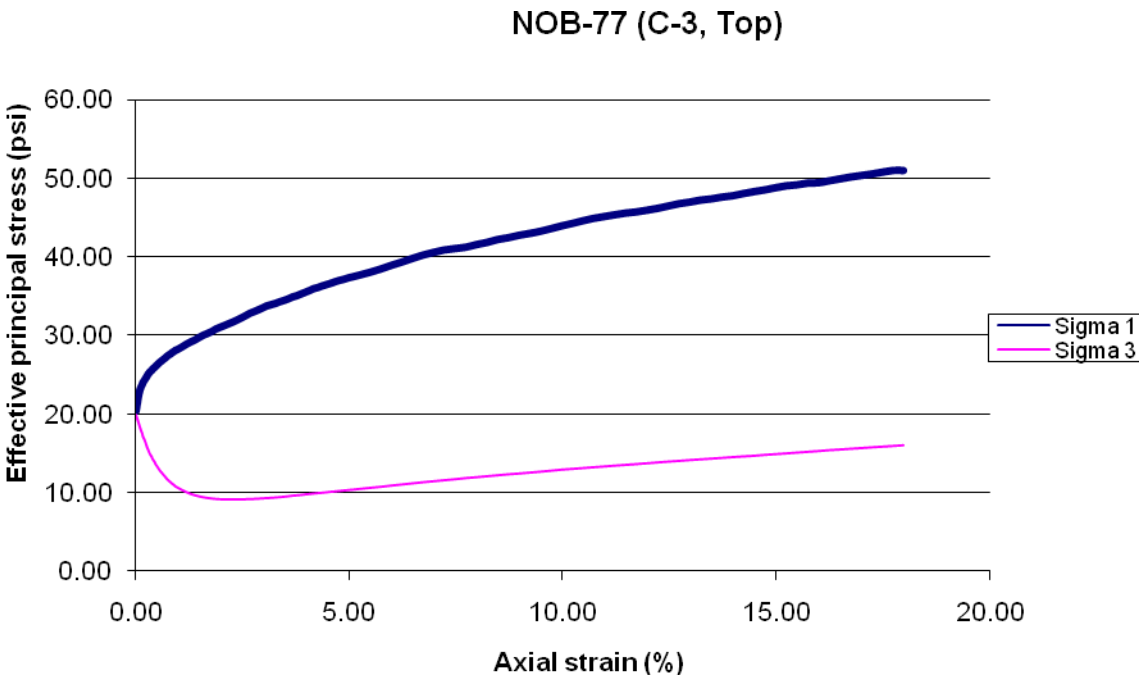


**Figure C.124:** Specimen C-3 (10.0' – 10.5' Depth) – Site No. 9

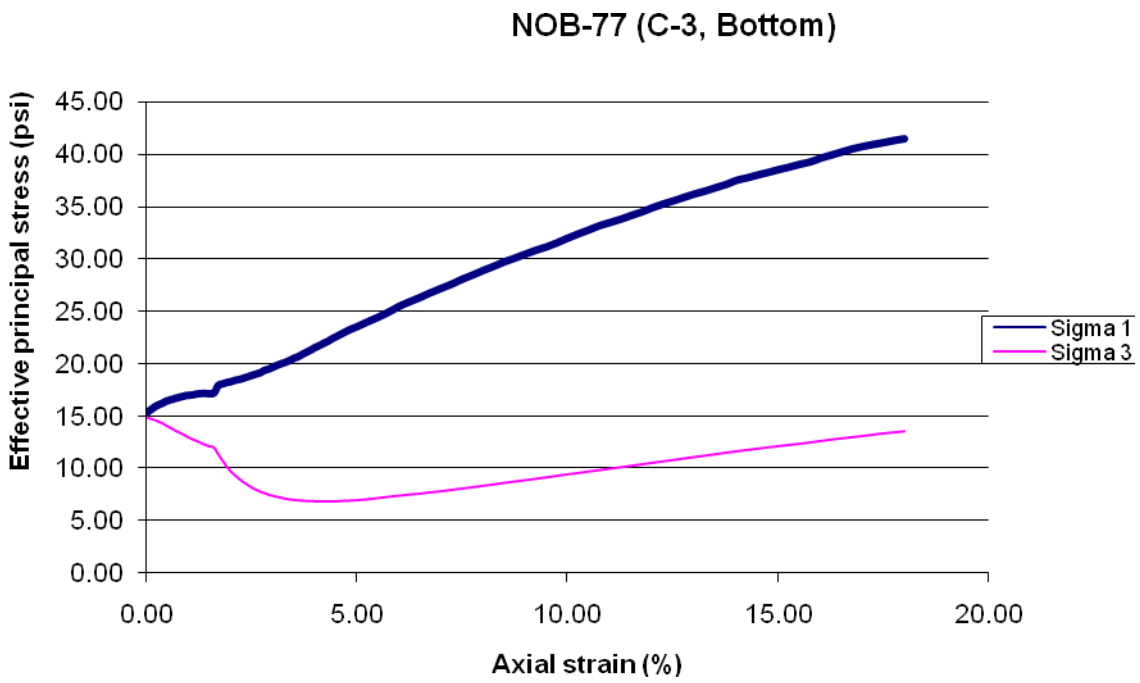


**Figure C.125:** Specimen C-3 (10.6' – 11.1' Depth) – Site No. 9

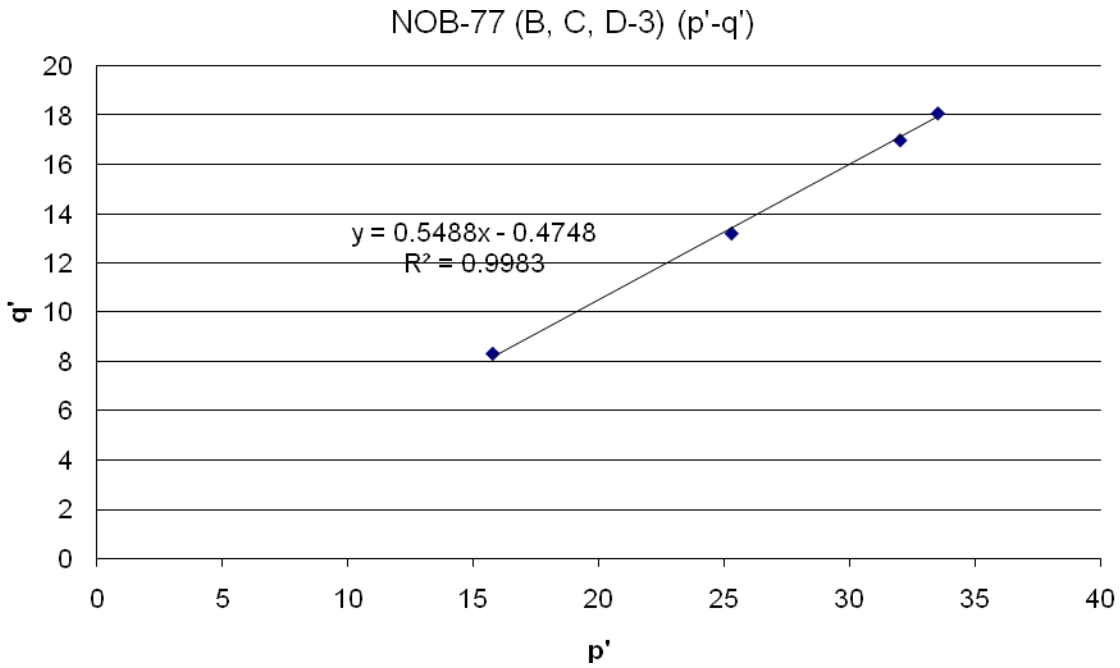


**Figure C.126:** p'-q' Diagram for the Lowest Depth Range – Site No. 9

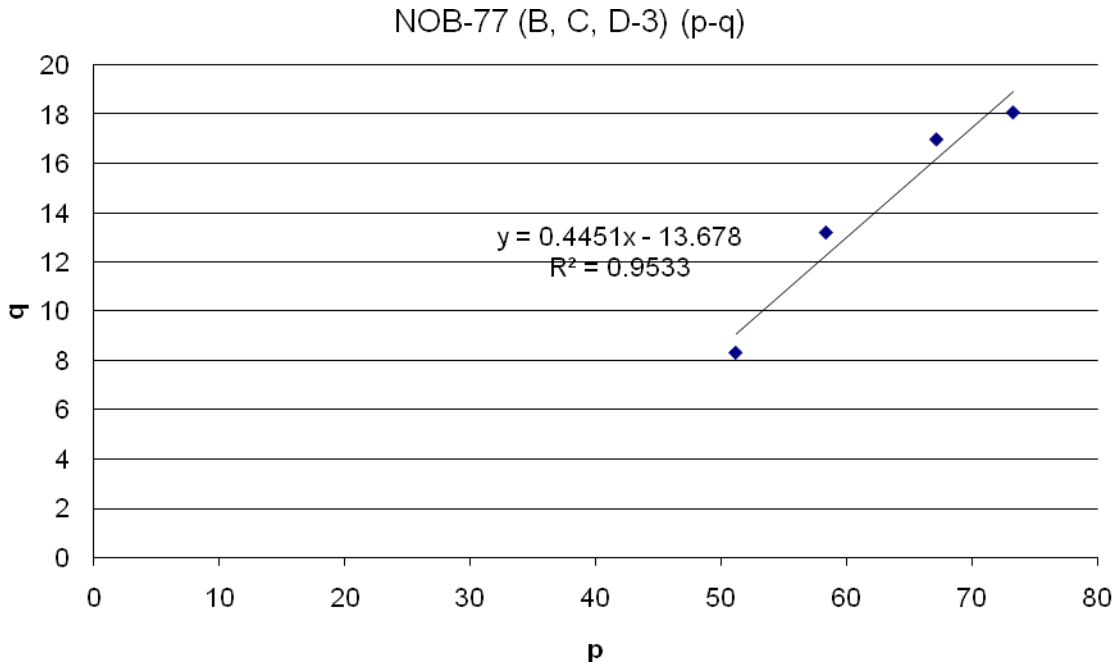


**Figure C.127:** p-q Diagram for the Lowest Depth Range – Site No. 9

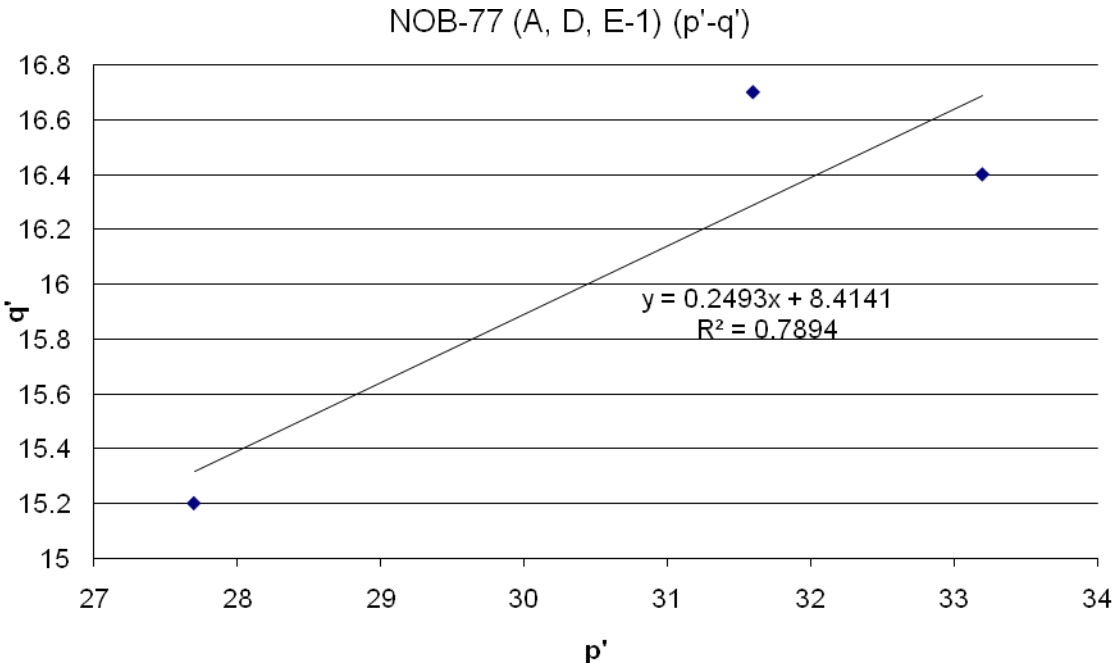


**Figure C.128:** p'-q' Diagram for the Middle Depth Range – Site No. 9

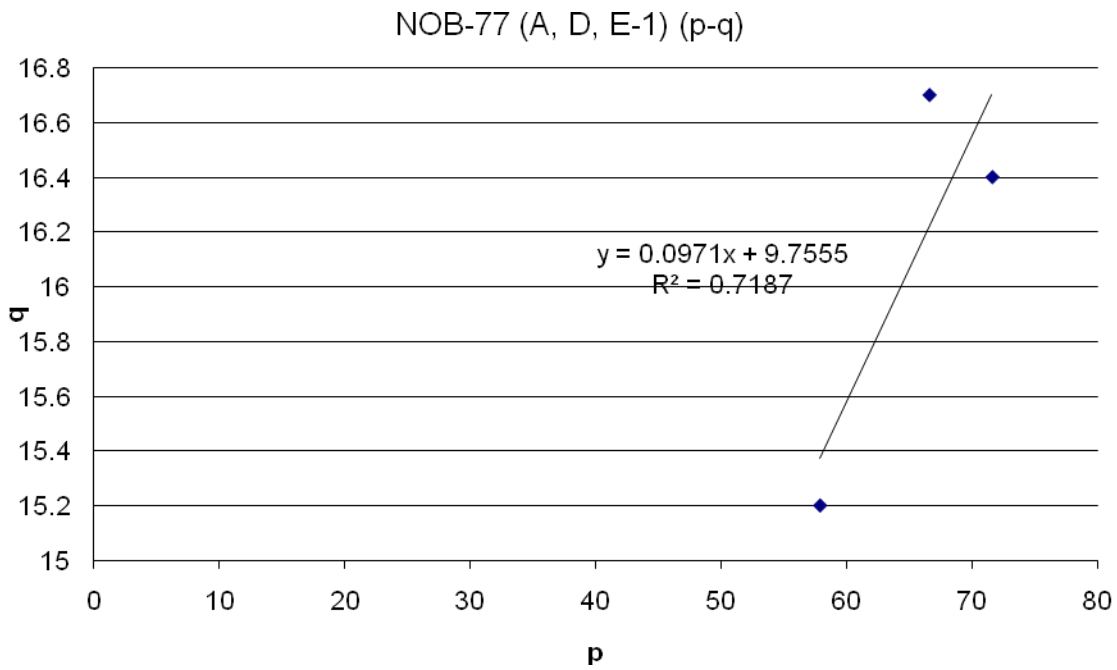


**Figure C.129:** p-q Diagram for the Middle Depth Range – Site No. 9

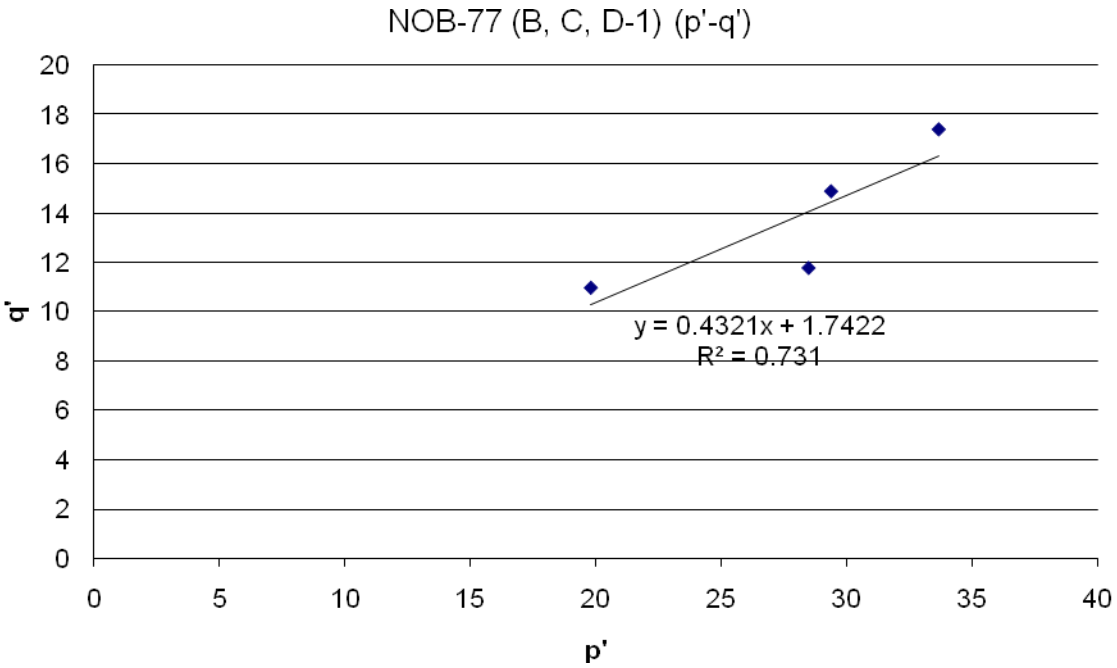


**Figure C.130:** p'-q' Diagram for the Highest Depth Range – Site No. 9

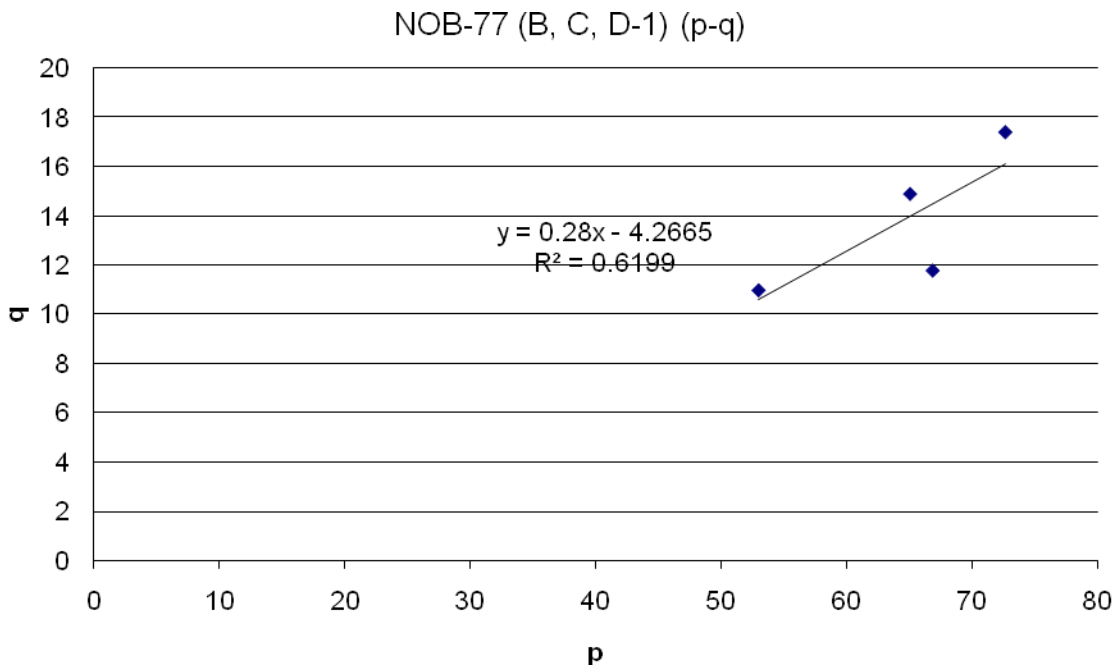


**Figure C.131:** p-q Diagram for the Highest Depth Range – Site No. 9

## APPENDIX D: PLOTS FOR SOIL COHESION DETERMINATIONS

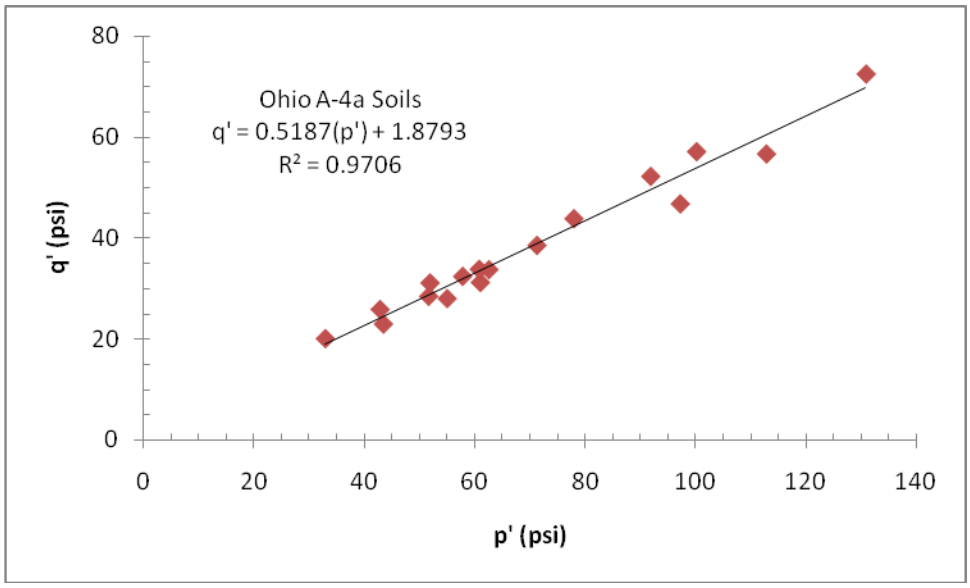


**Figure D.1:** Combined p'-q' Diagram for All A-4a Soils

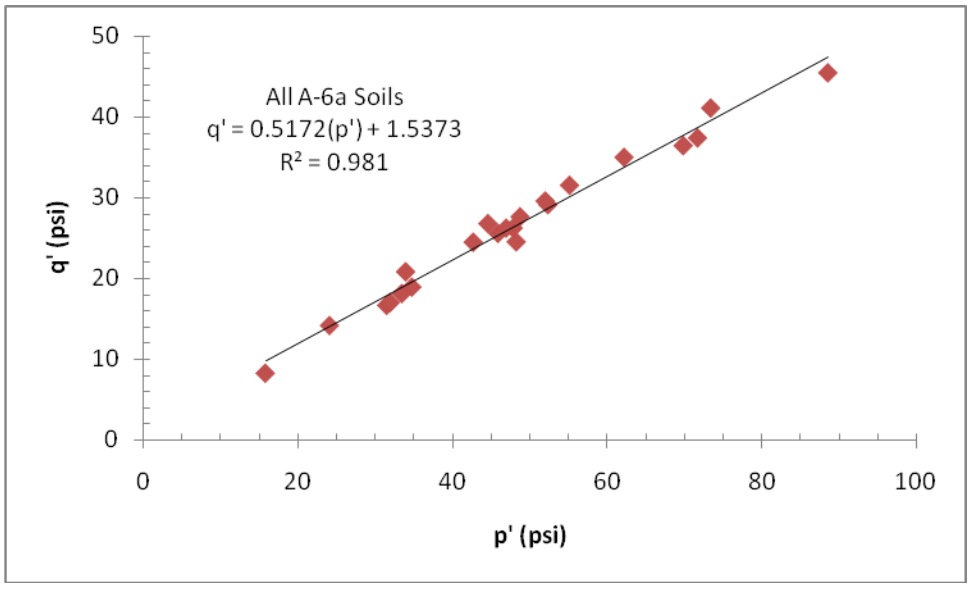


**Figure D.2:** Combined p'-q' Diagram for All A-6a Soils

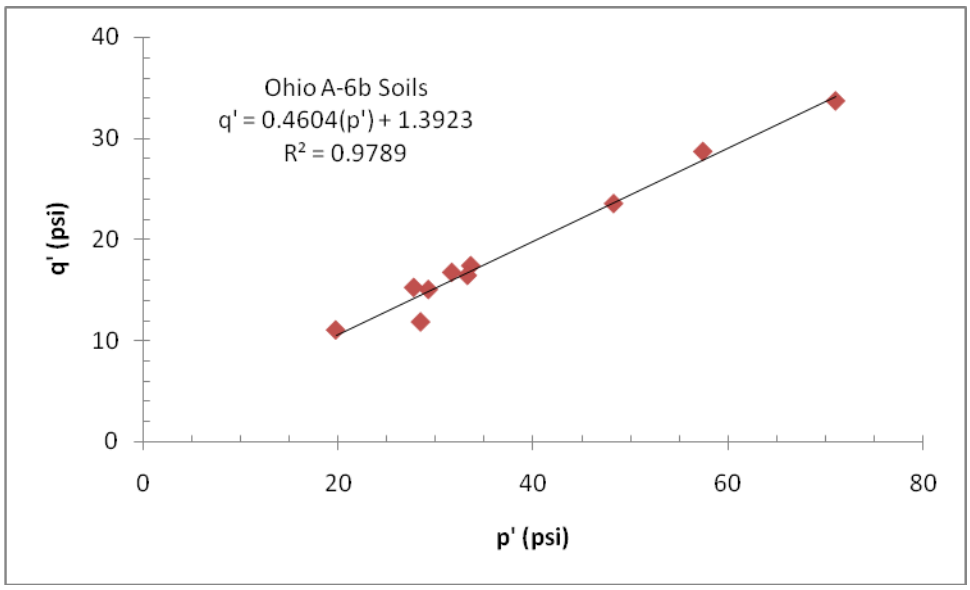


**Figure D.3:** Combined p'-q' Diagram for All A-6b Soils

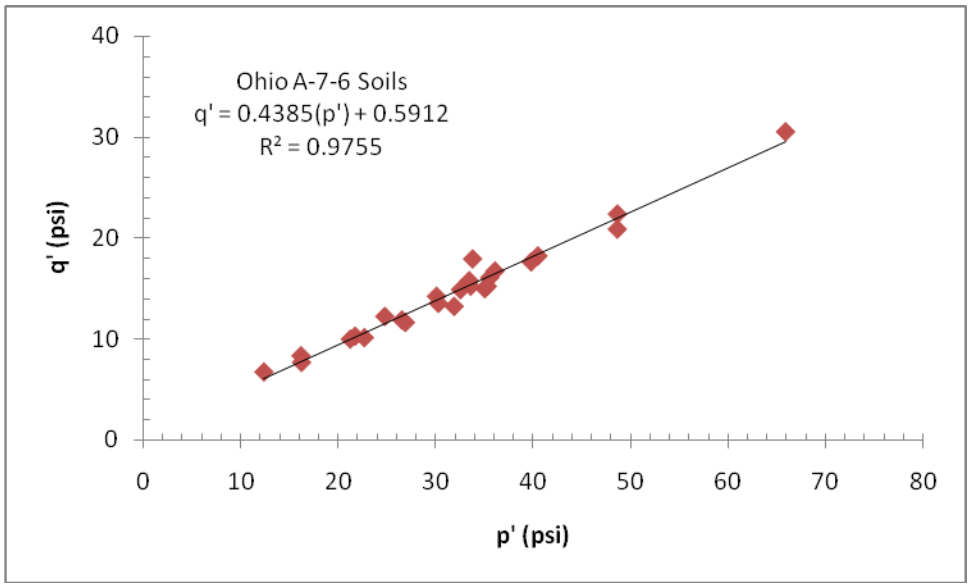


**Figure D.4:** Combined p'-q' Diagram for All A-7-6 Soils

## APPENDIX E: STATISTICAL CORRELATION PLOTS

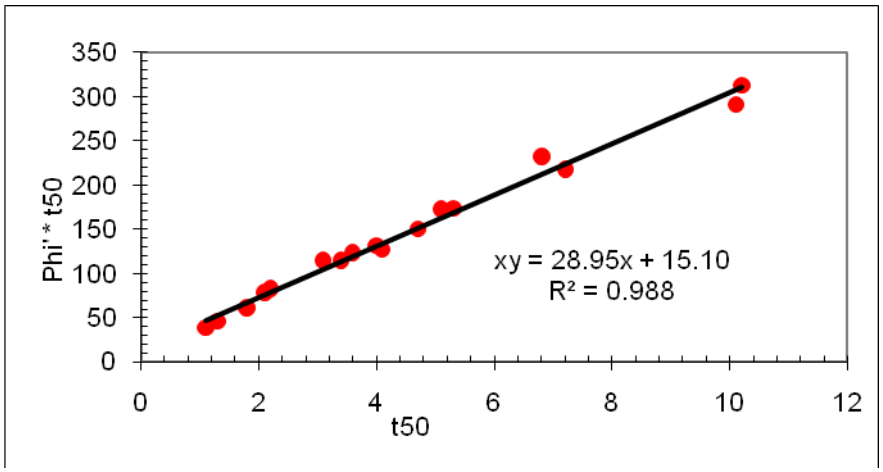


**Figure E.1:** $\phi'$ vs. $t_{50}$ (Hyperbolic Function) – A-4a Soil Type

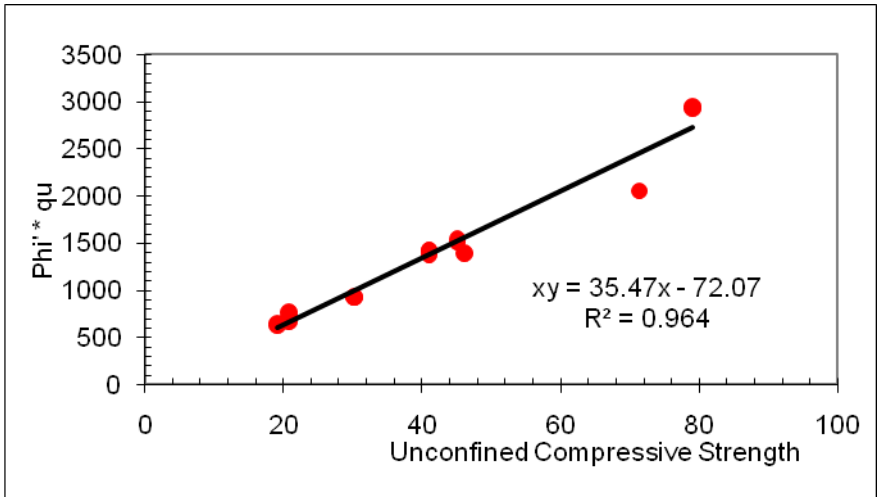


**Figure E.2:** $\phi'$ vs. $q_u$ (Hyperbolic Function) – A-4a Soil Type

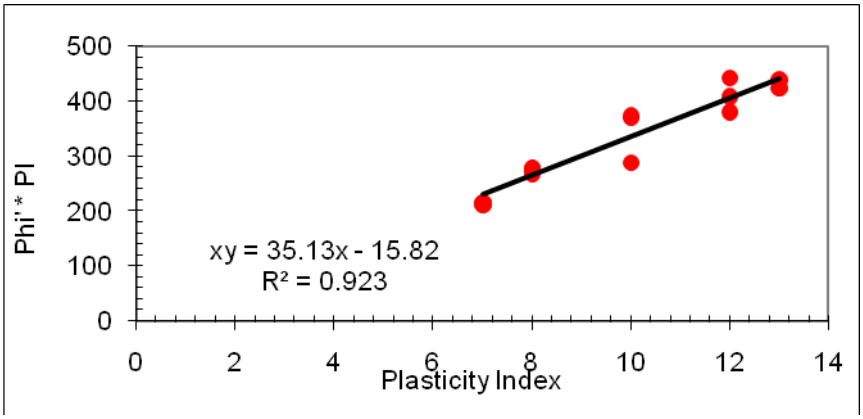


**Figure E.3:** $\phi'$ vs. PI (Hyperbolic Function) – A-4a Soil Type

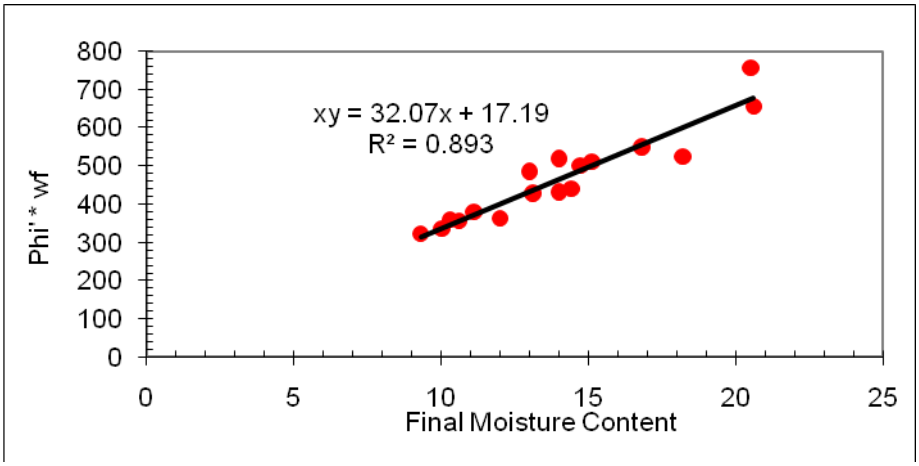


**Figure E.4:** $\phi'$ vs. $w_f$ (Hyperbolic Function) – A-4a Soil Type
where $w_f$ = final saturated moisture content (measured during C-U triaxial test)

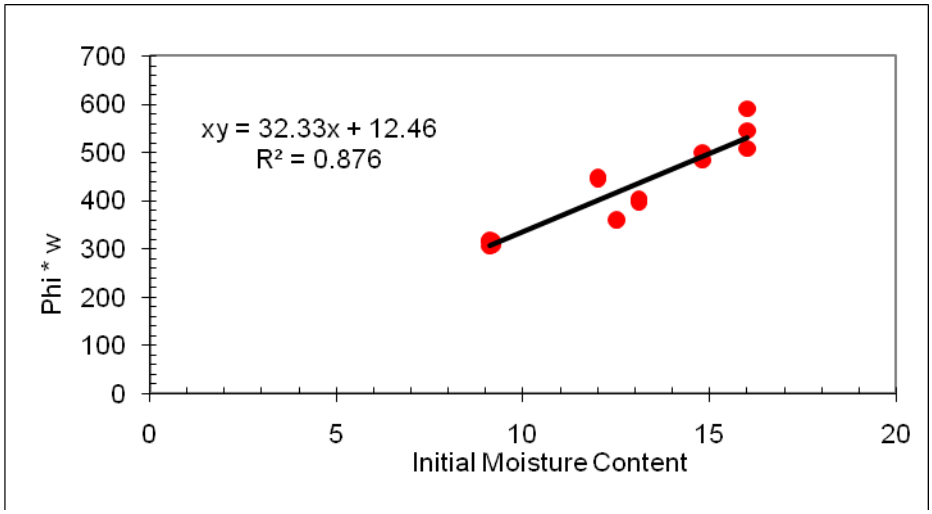


**Figure E.5:** $\phi'$ vs. w (Hyperbolic Function) – A-4a Soil Type

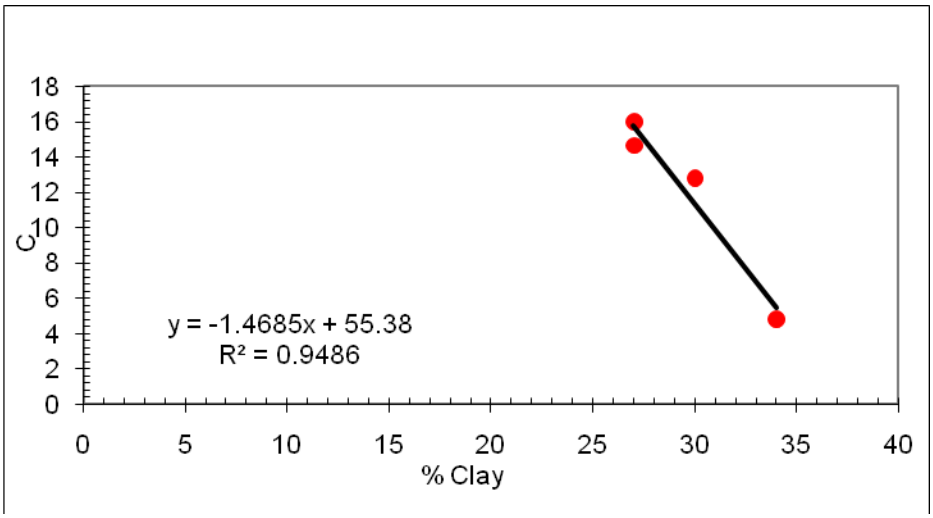


**Figure E.6:** C vs. %Clay (Linear Function) – A-4a Soil Type

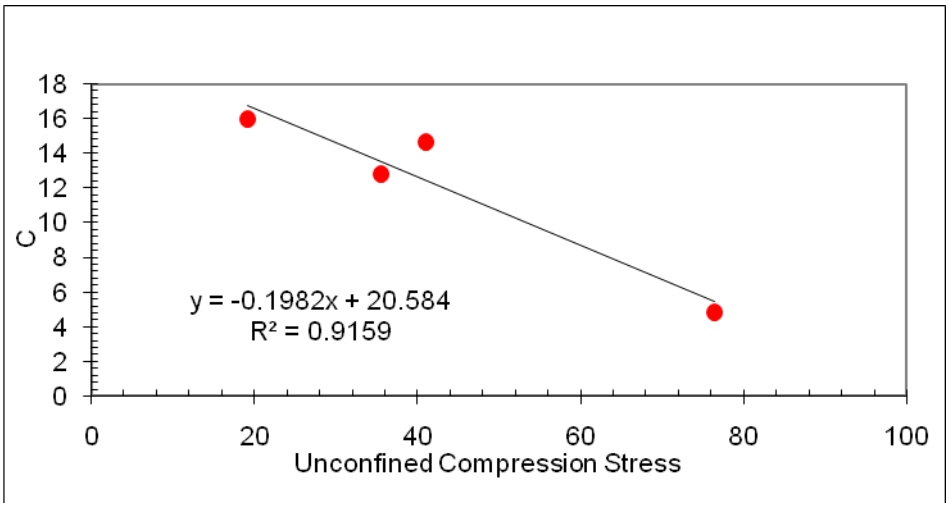


**Figure E.7:** C vs. $q_u$ (Linear Function) – A-4a Soil Type

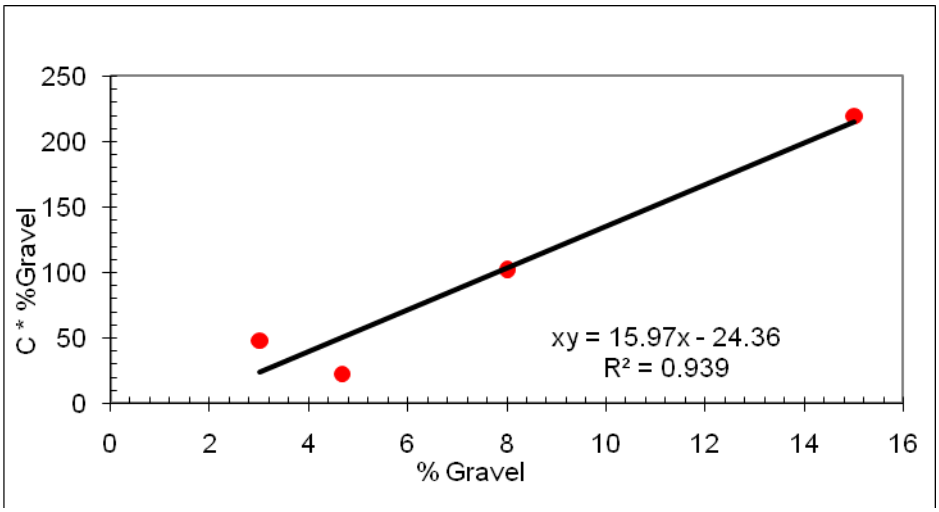


**Figure E.8:** C vs. %Gravel (Hyperbolic Function) – A-4a Soil Type

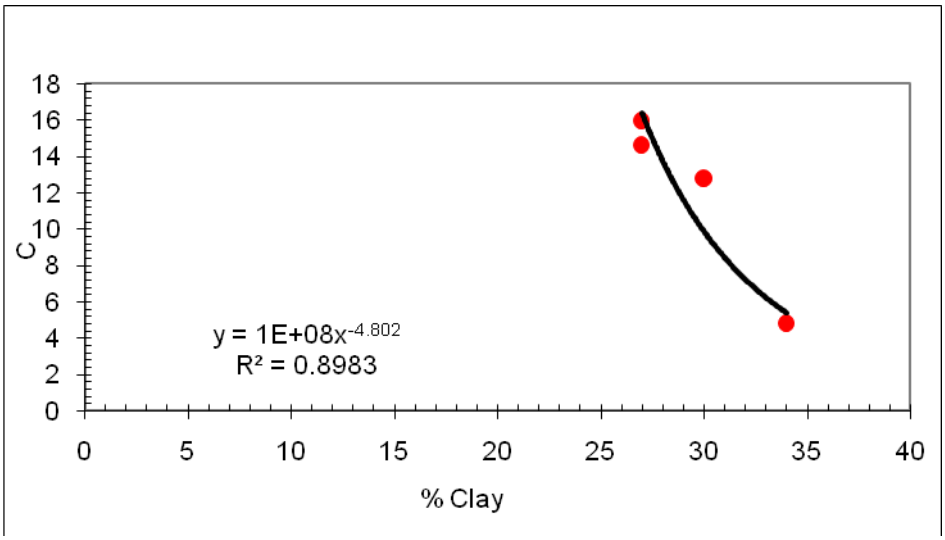


**Figure E.9:** C vs. %Clay (Power Function) – A-4a Soil Type

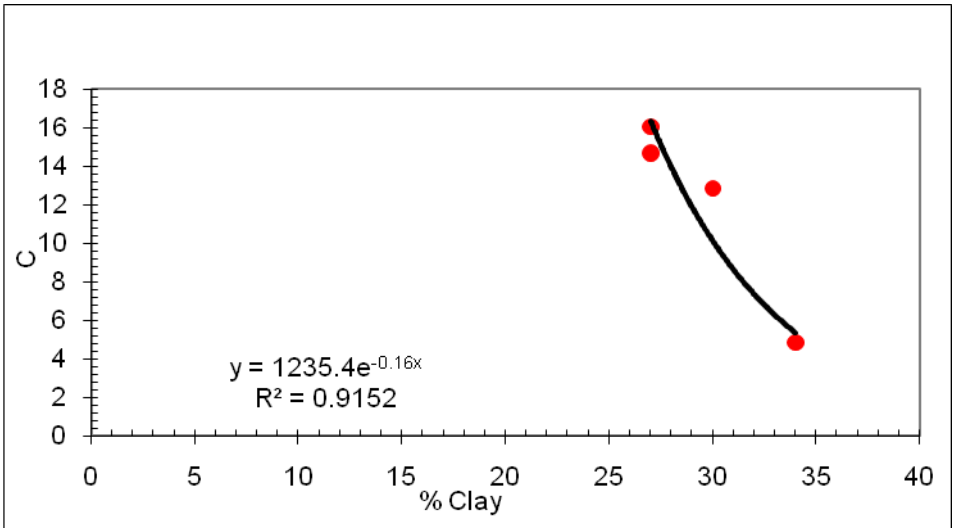


**Figure E.10:** C vs. %Clay (Exponential Function) – A-4a Soil Type

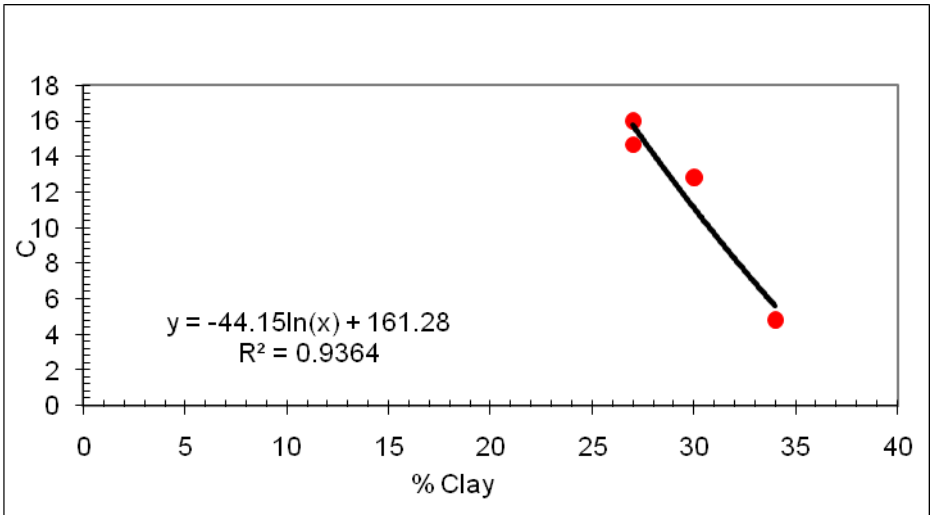


**Figure E.11:** C vs. %Clay (Logarithmic Function) – A-4a Soil Type

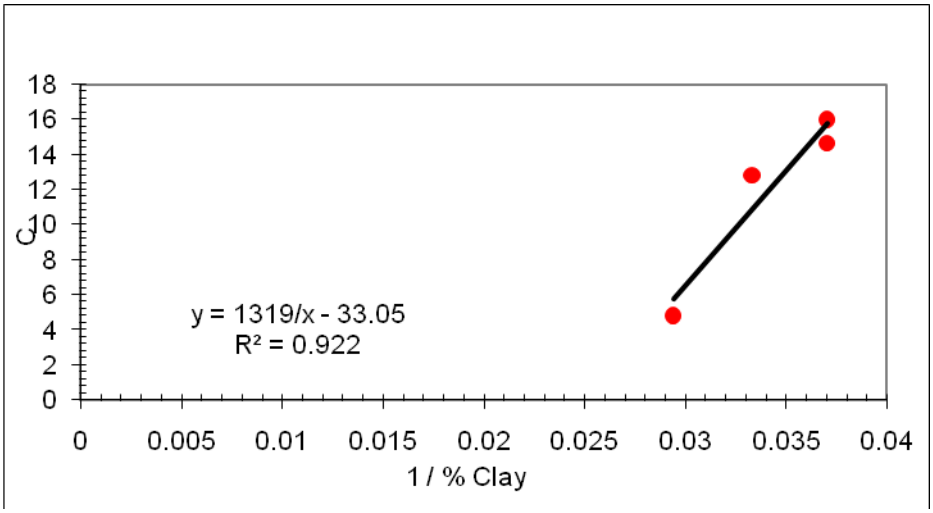


**Figure E.12:** C vs. %Clay (Reciprocal Function) – A-4a Soil Type

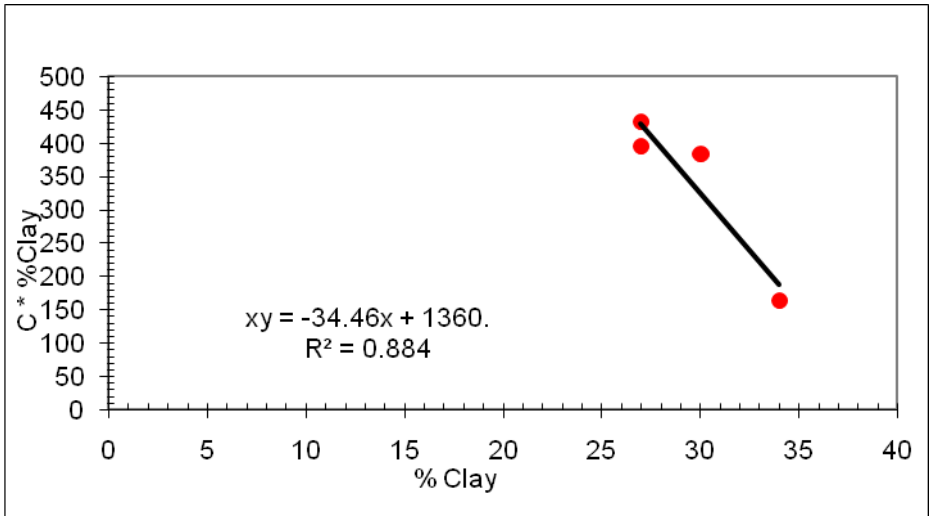


**Figure E.13:** C vs. %Clay (Hyperbolic Function) – A-4a Soil Type

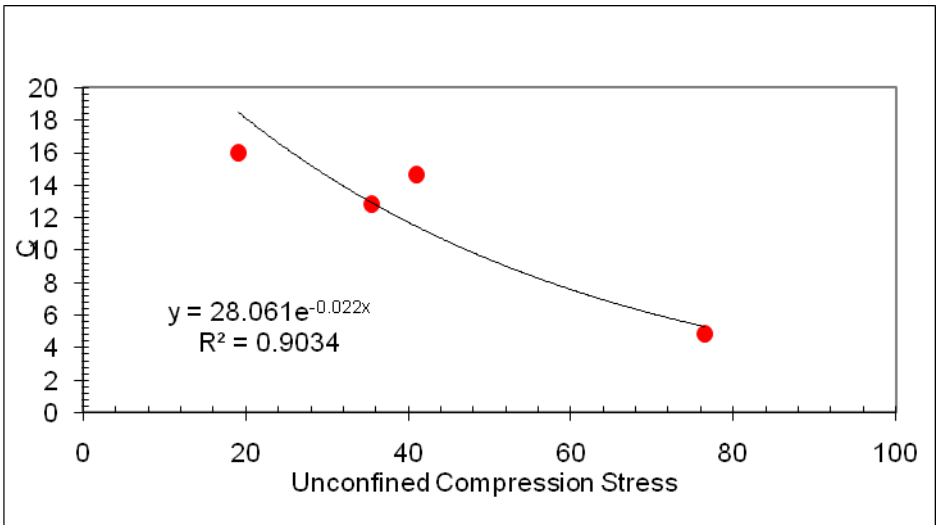


**Figure E.14:** C vs. $q_u$ (Exponential Function) – A-4a Soil Type

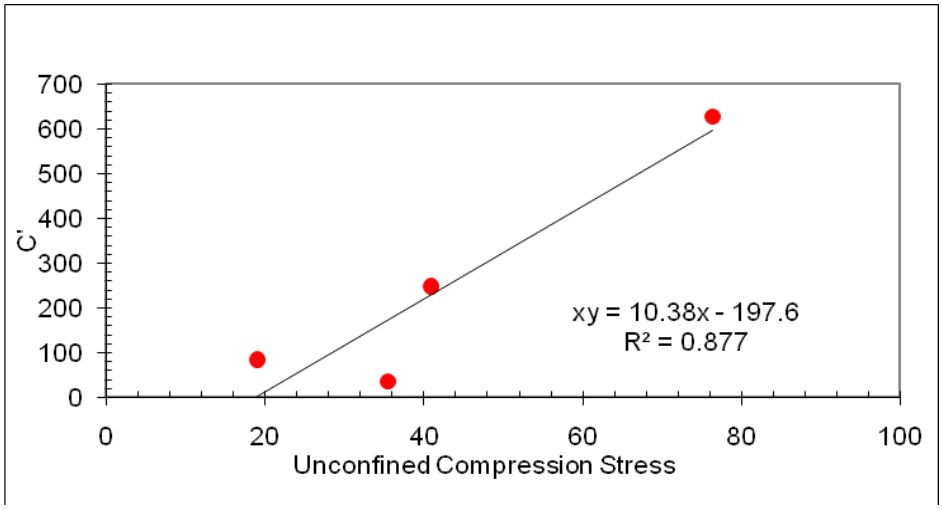


**Figure E.15:** C' vs. $q_u$ (Hyperbolic Function) – A-4a Soil Type

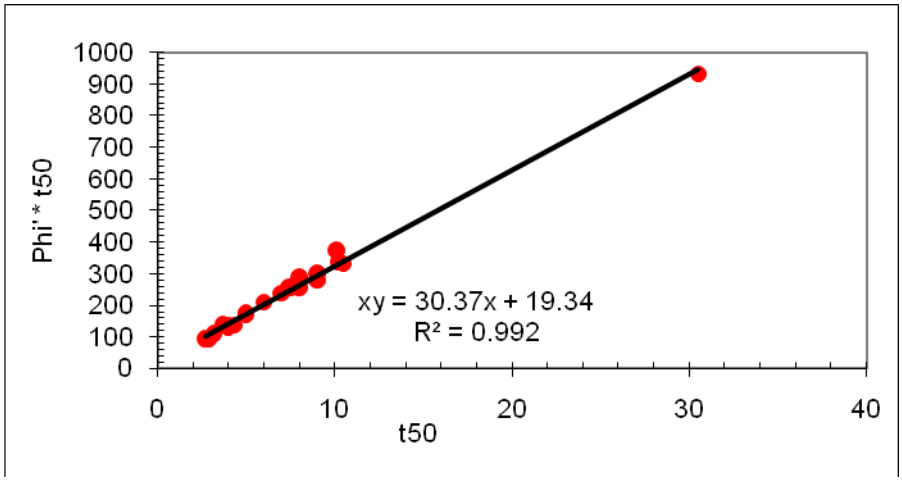


***Figure E.16:*** *$\phi'$ vs. $t_{50}$ (Hyperbolic Function) – A-6a Soil Type*

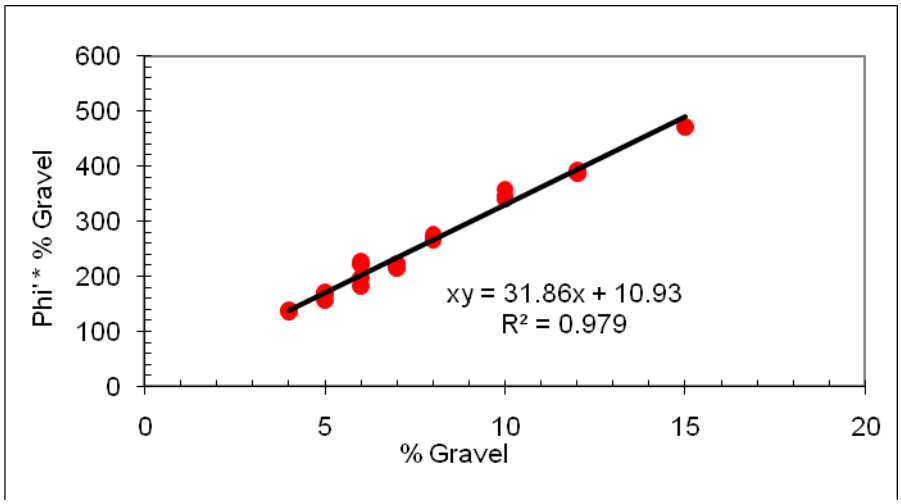


***Figure E.17:*** *$\phi'$ vs. %Gravel (Hyperbolic Function) – A-6a Soil Type*

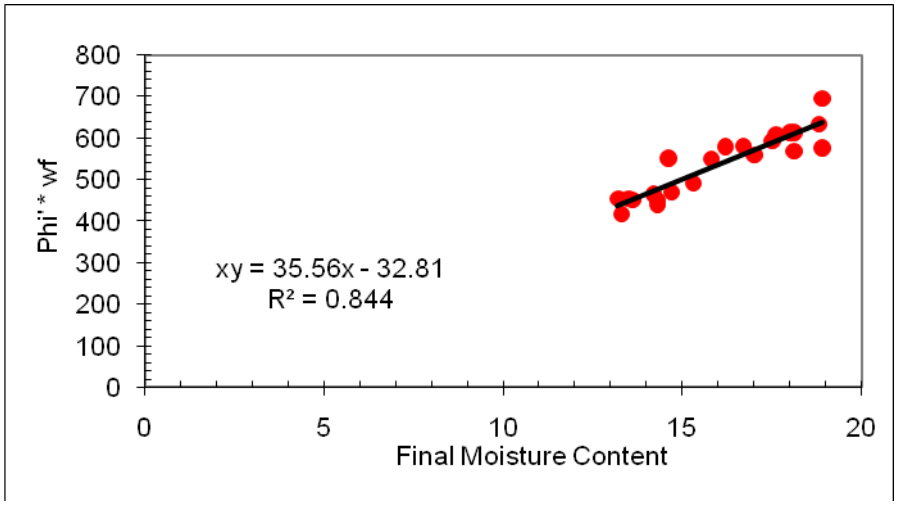


***Figure E.18:*** *$\phi'$ vs. $w_f$ (Hyperbolic Function) – A-6a Soil Type*

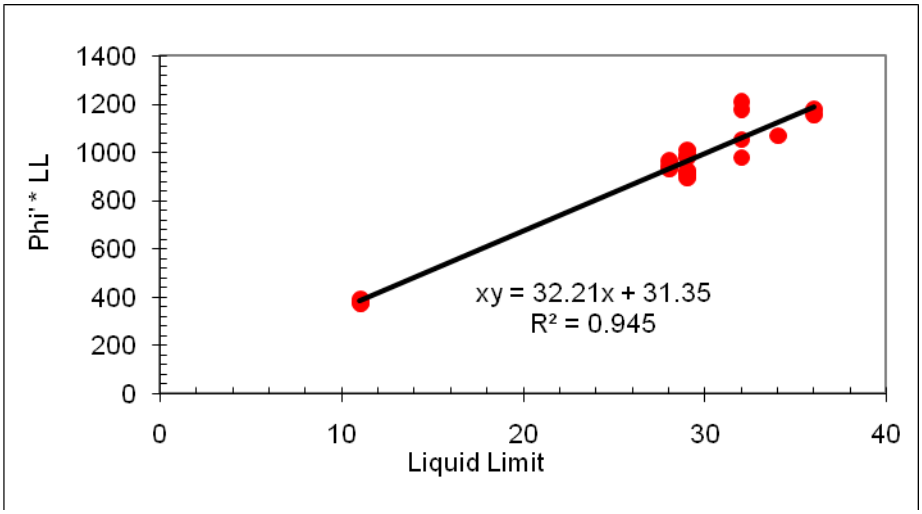


***Figure E.19:*** *ϕ′ vs. LL (Hyperbolic Function) – A-6a Soil Type*

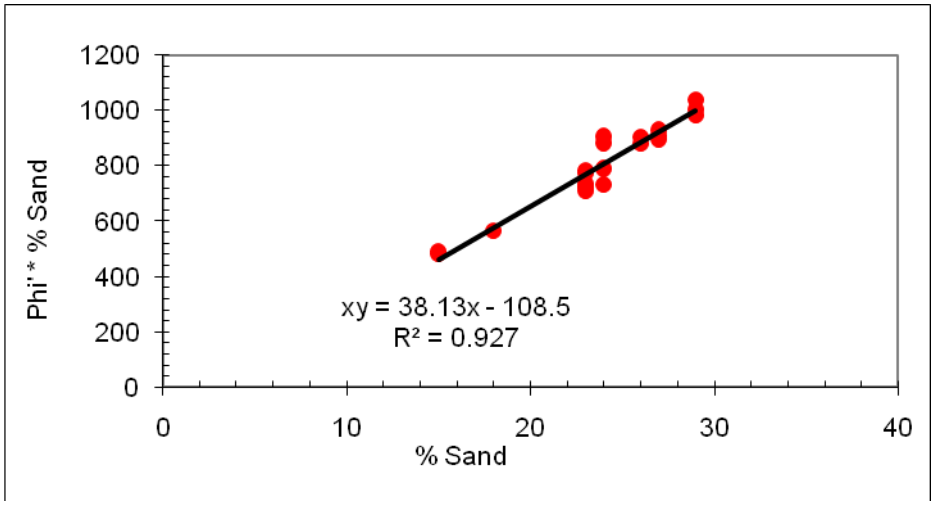


***Figure E.20:*** *ϕ′ vs. %Sand (Hyperbolic Function) – A-6a Soil Type*

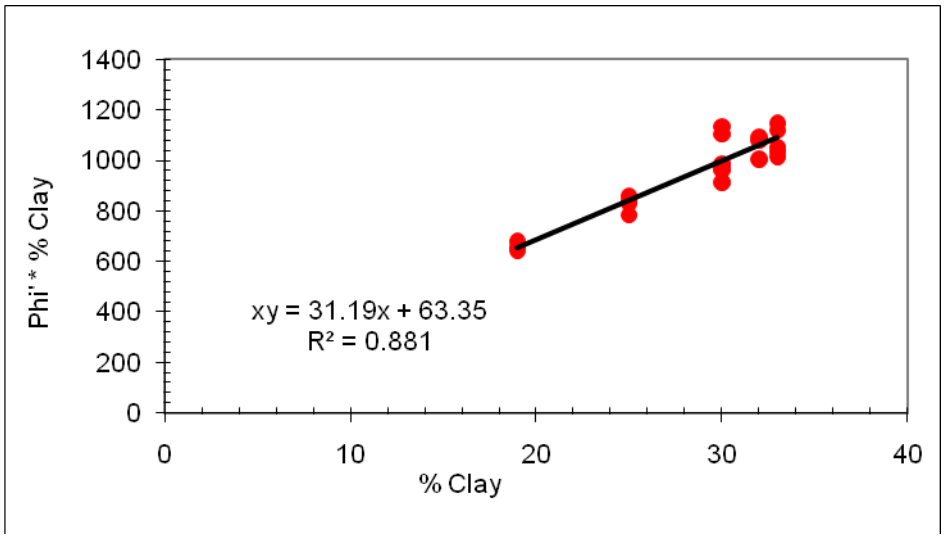


***Figure E.21:*** *ϕ′ vs. %Clay (Hyperbolic Function) – A-6a Soil Type*

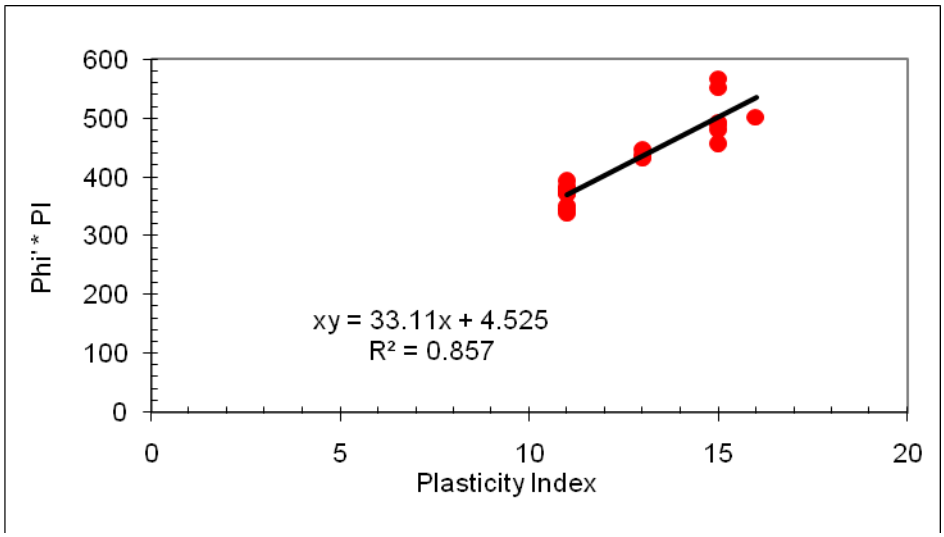


***Figure E.22:*** *ϕ′ vs. PI (Hyperbolic Function) – A-6a Soil Type*

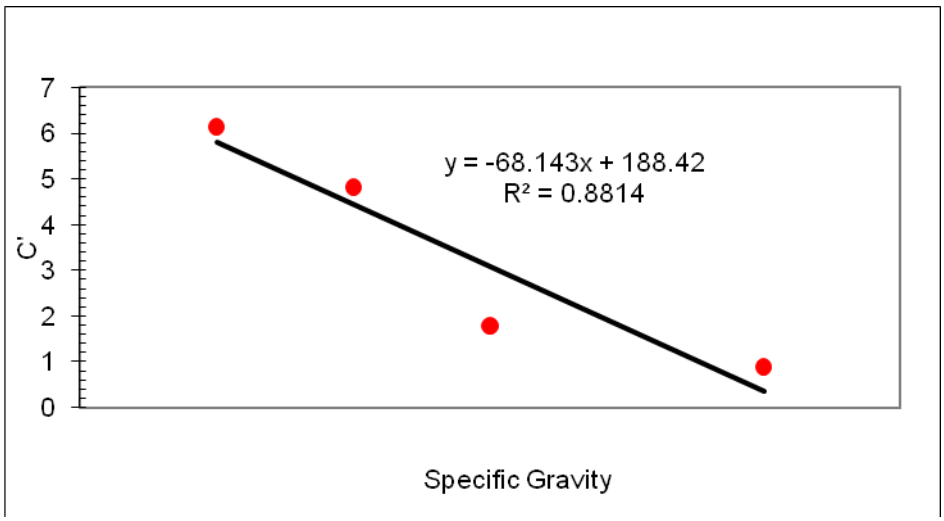


***Figure E.23:*** *C' vs. Gs (Linear Function) – A-6a Soil Type*

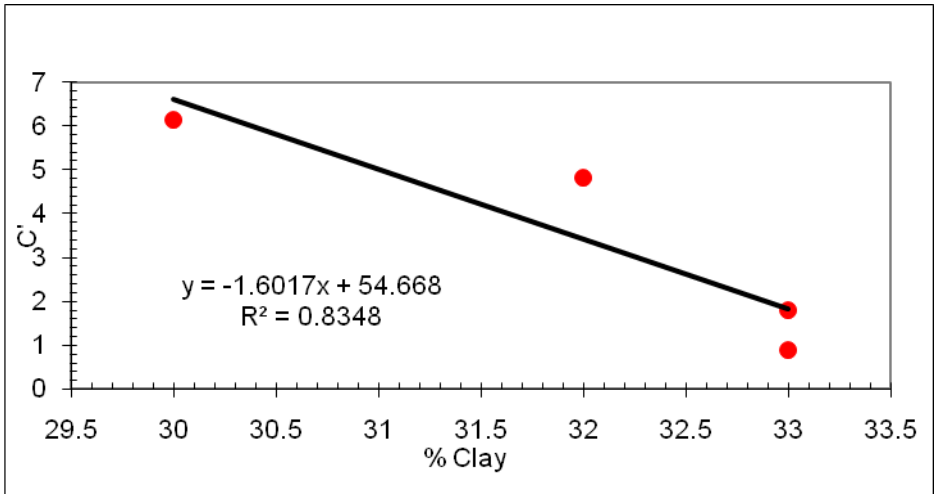


***Figure E.24:*** *C' vs. %Clay (Linear Function) – A-6a Soil Type*

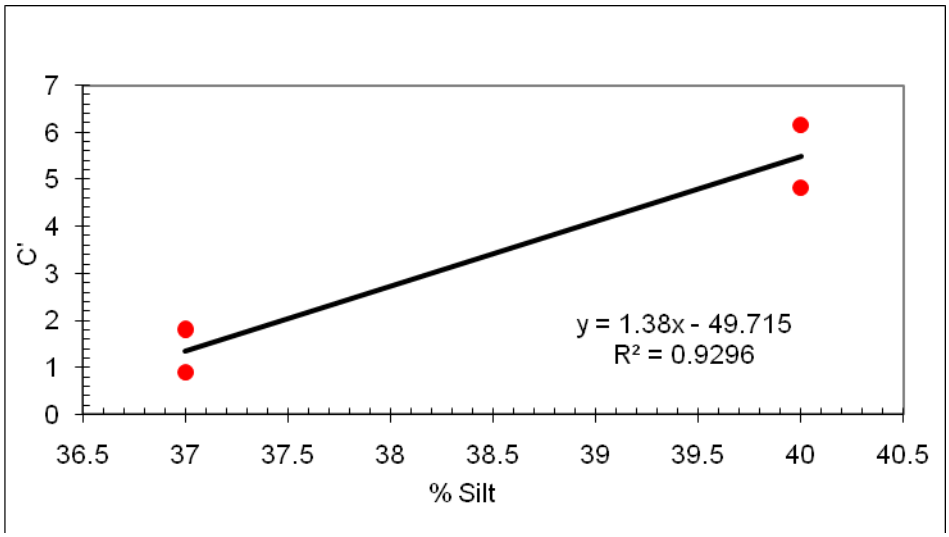


***Figure E.25:*** *C' vs. %Silt (Linear Function) – A-6a Soil Type*

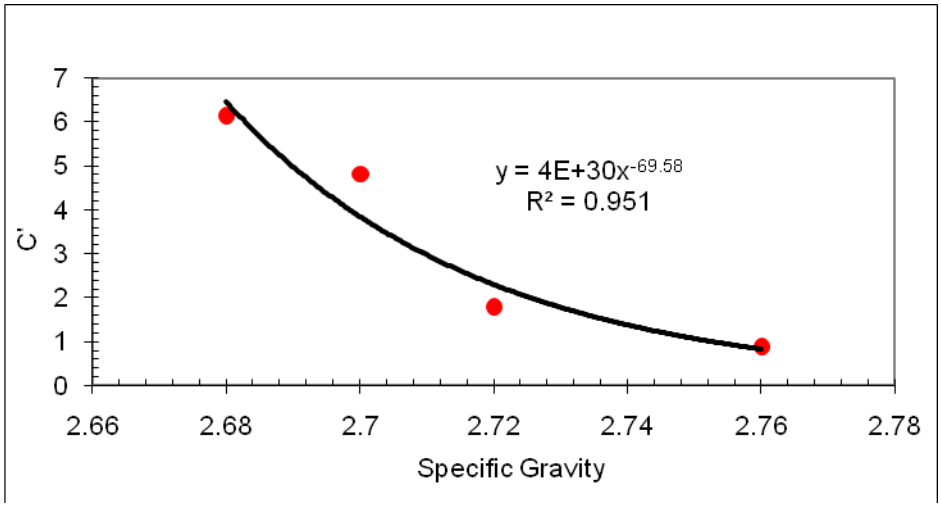


***Figure E.26:*** *C' vs. Gs (Exponential Function) – A-6a Soil Type*

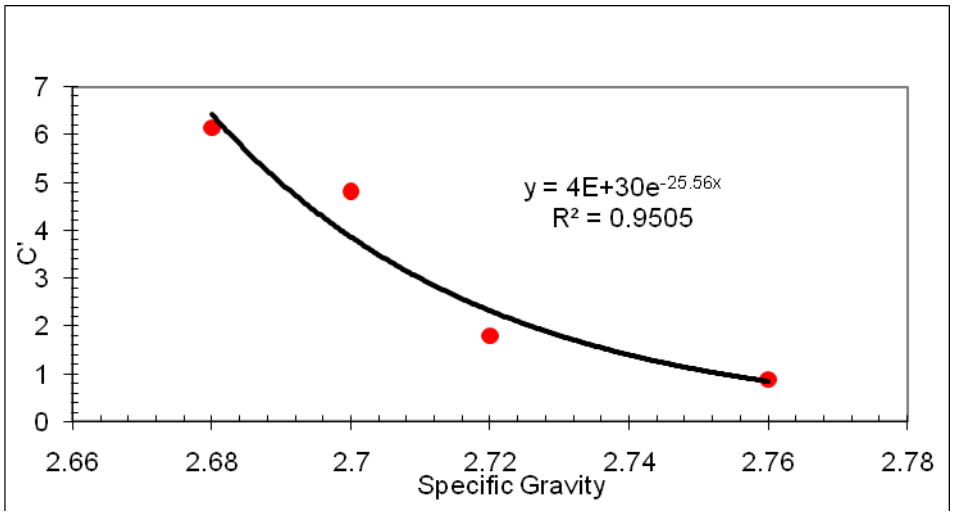


***Figure E.27:*** *C' vs. Gs (Exponential Function) – A-6a Soil Type*

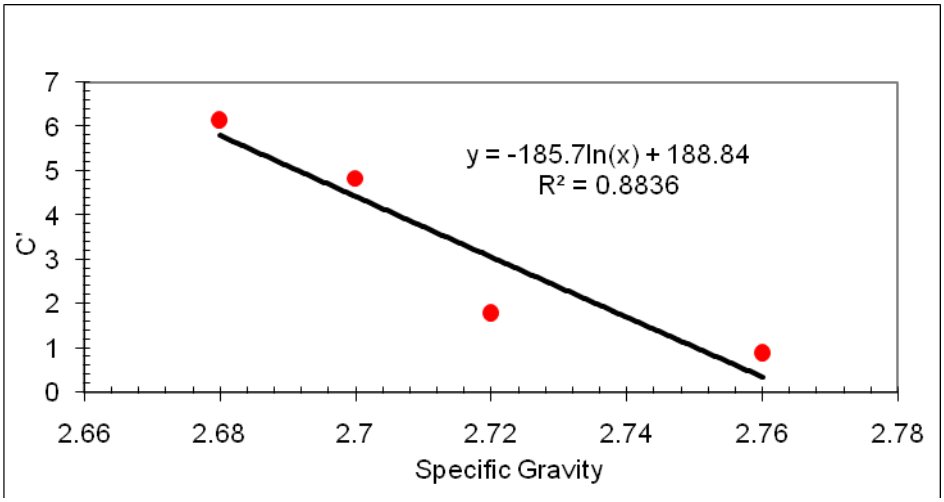


***Figure E.28:*** *C' vs. Gs (Logarithmic Function) – A-6a Soil Type*

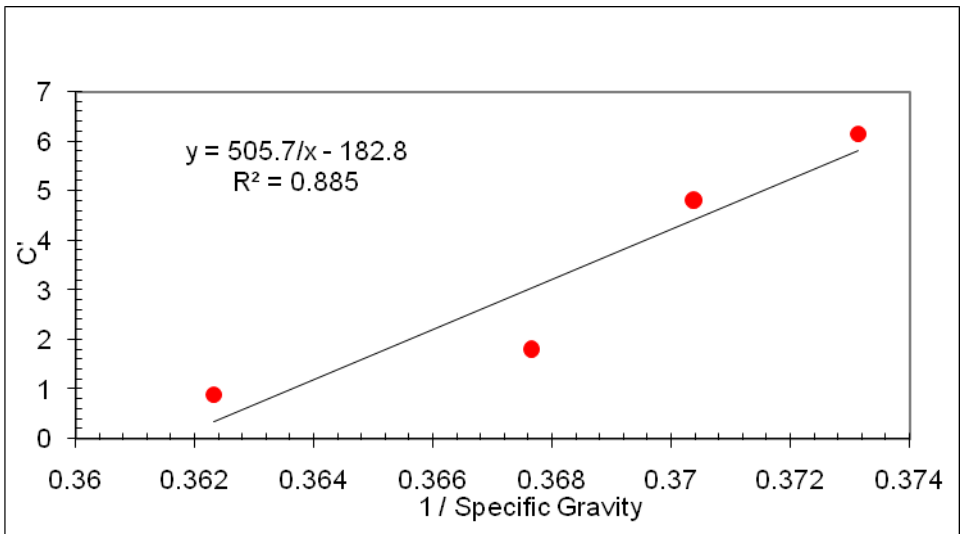


***Figure E.29:*** *C' vs. Gs (Reciprocal Function) – A-6a Soil Type*

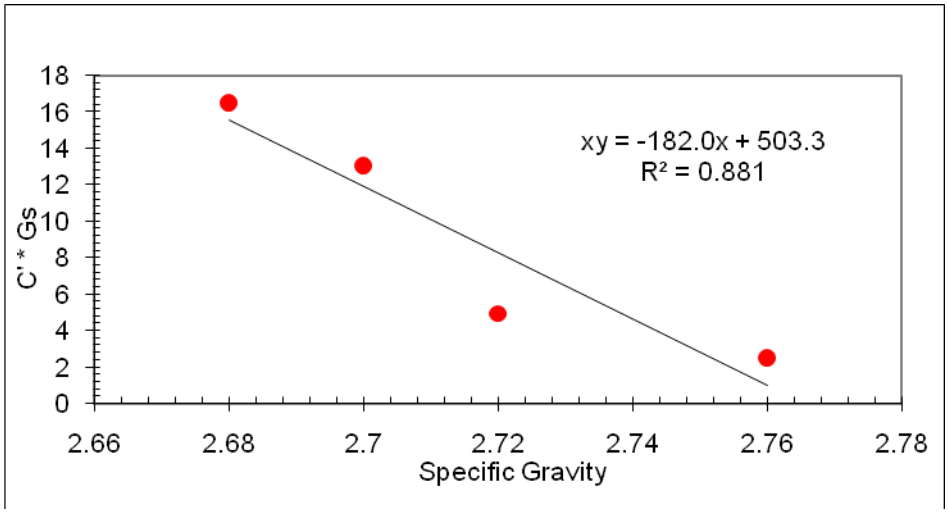


***Figure E.30:*** *C' vs. Gs (Hyperbolic Function) – A-6a Soil Type*

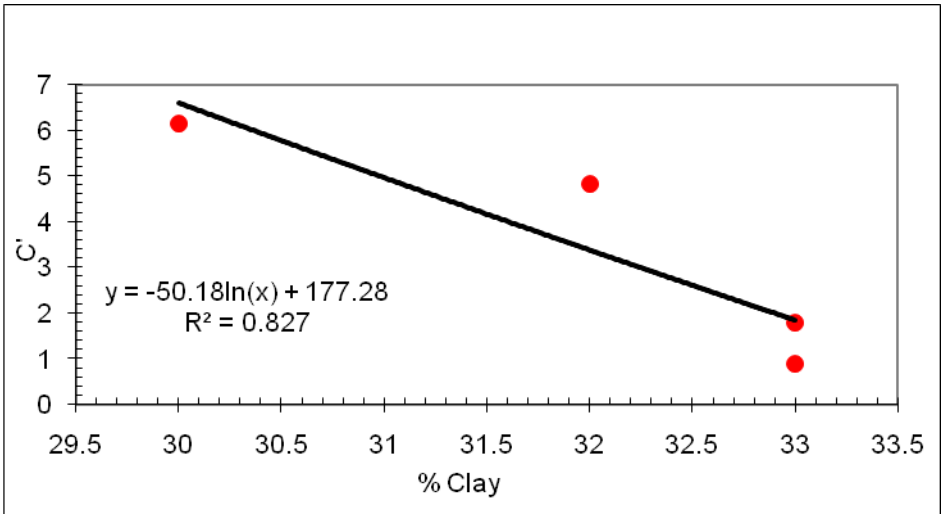


***Figure E.31:*** *C' vs. %Clay (Logarithmic Function) – A-6a Soil Type*

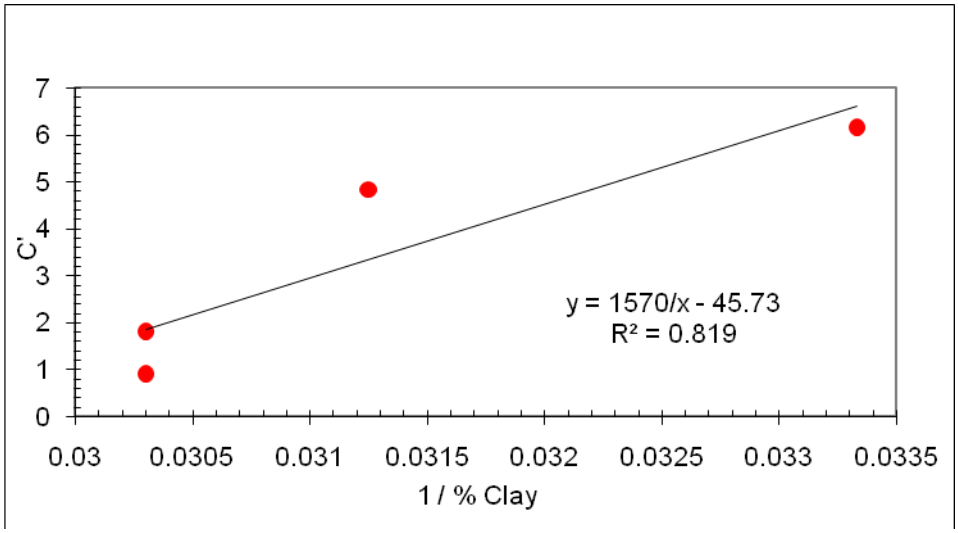


***Figure E.32:*** *C' vs. %Clay (Reciprocal Function) – A-6a Soil Type*

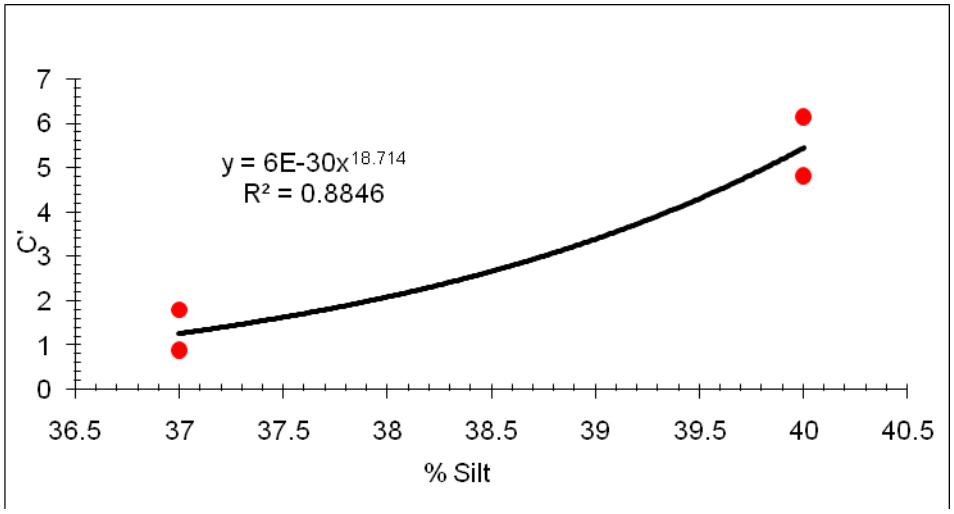


***Figure E.33:*** *C' vs. %Silt (Power Function) – A-6a Soil Type*

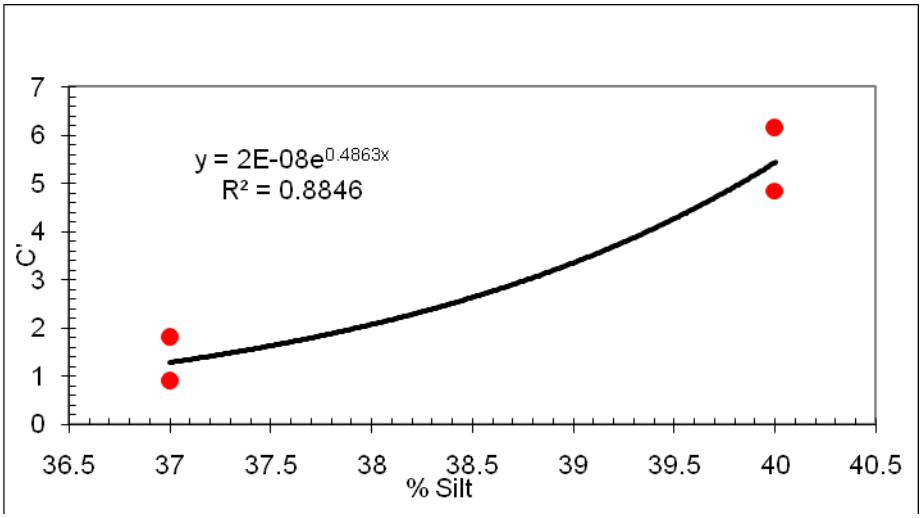


***Figure E.34:*** *C' vs. %Silt (Exponential Function) – A-6a Soil Type*

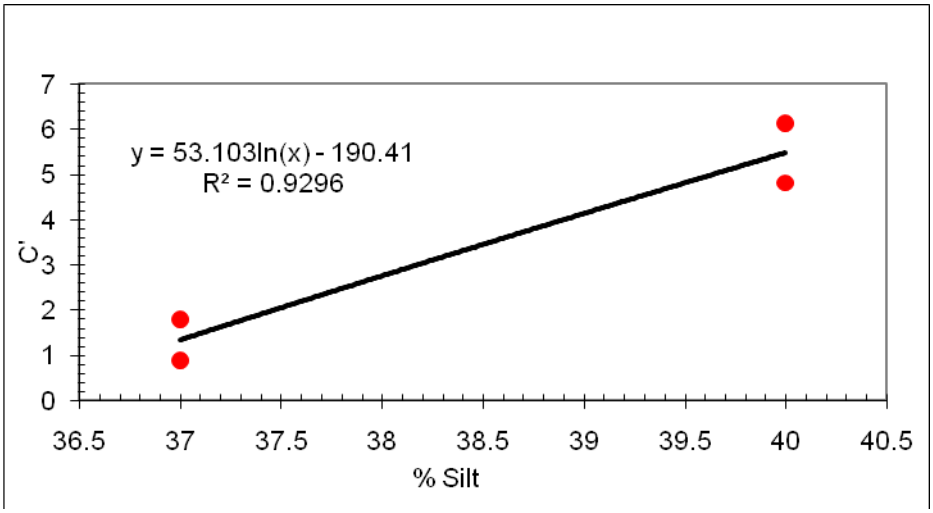


***Figure E.35:*** *C' vs. %Silt (Logarithmic Function) – A-6a Soil Type*

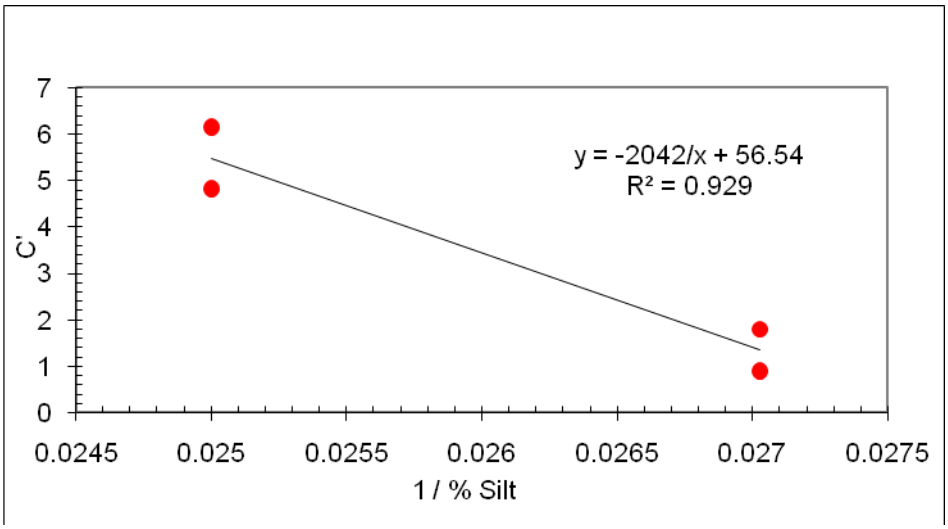


***Figure E.36:*** *C' vs. %Silt (Reciprocal Function) – A-6a Soil Type*

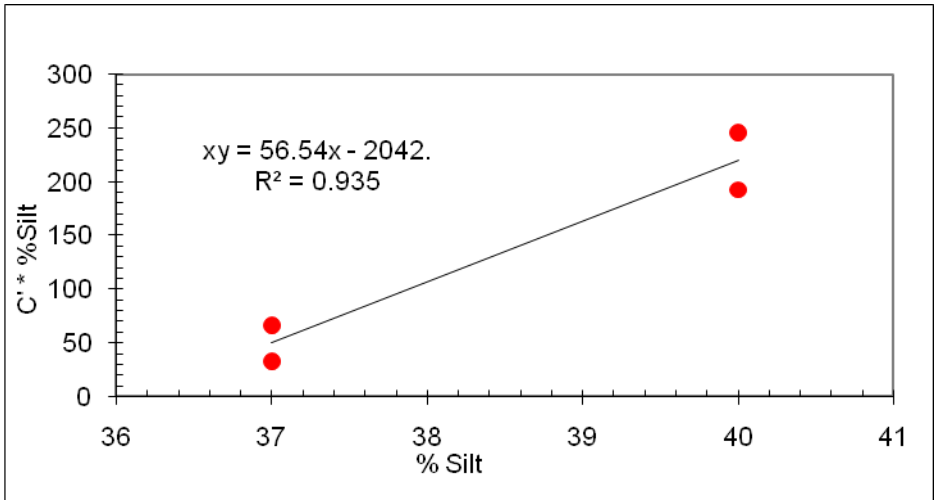


***Figure E.37:*** *C' vs. %Silt (Hyperbolic Function) – A-6a Soil Type*

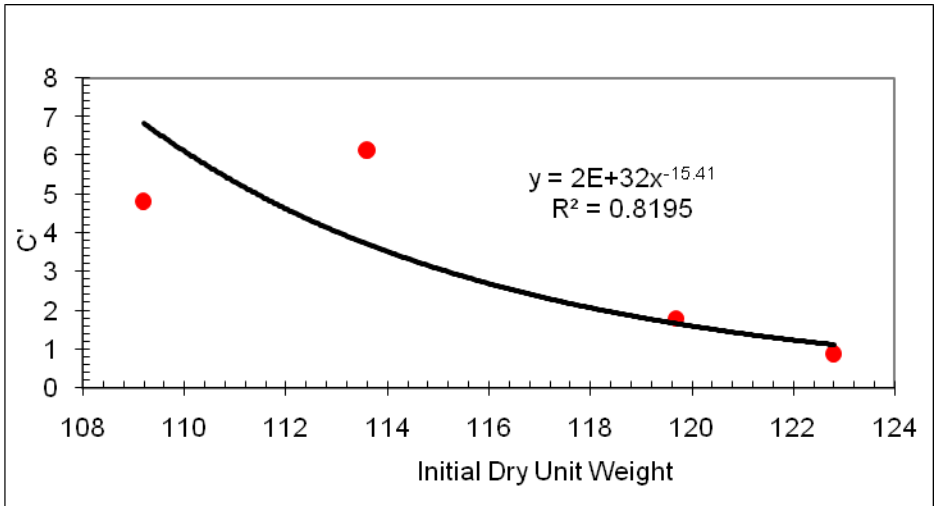


***Figure E.38:*** *C' vs. $\gamma_d$-uc (Power Function) – A-6a Soil Type*
*where $\gamma_d$-uc = Initial dry unit weight (measured during unconfined compression test)*

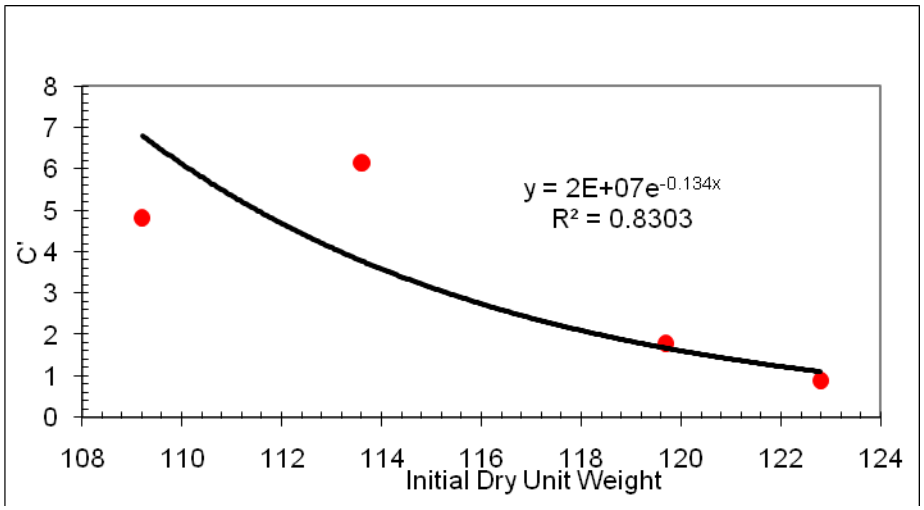


***Figure E.39:*** *C' vs. $\gamma_d$-uc (Exponential Function) – A-6a Soil Type*

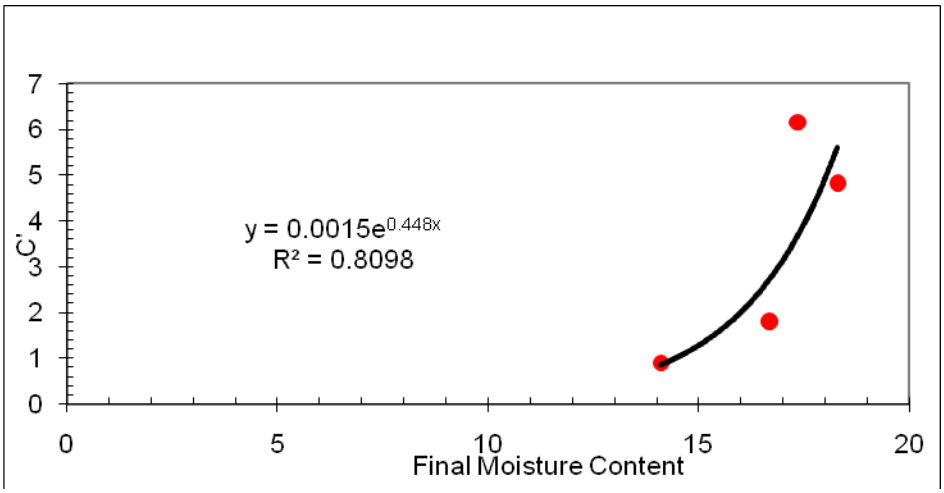


***Figure E.40:*** *C' vs. $w_f$-cu (Exponential Function) – A-6a Soil Type*

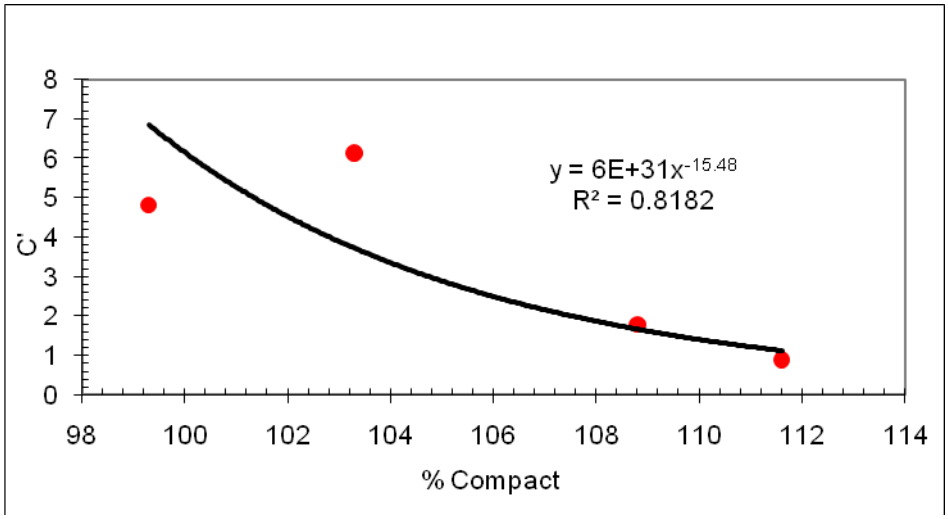


***Figure E.41:*** *C' vs. %Compact (Power Function) – A-6a Soil Type*

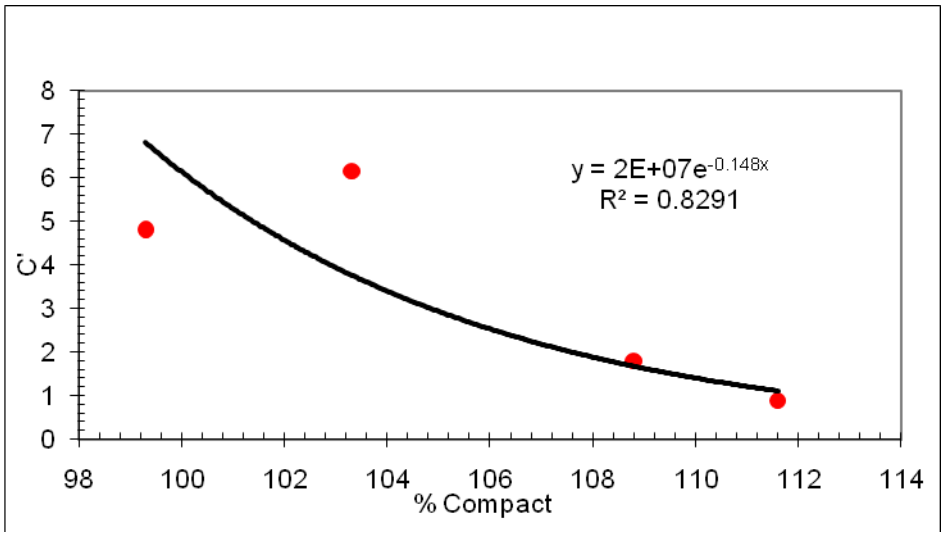


***Figure E.42:*** *C' vs. %Compact (Exponential Function) – A-6a Soil Type*

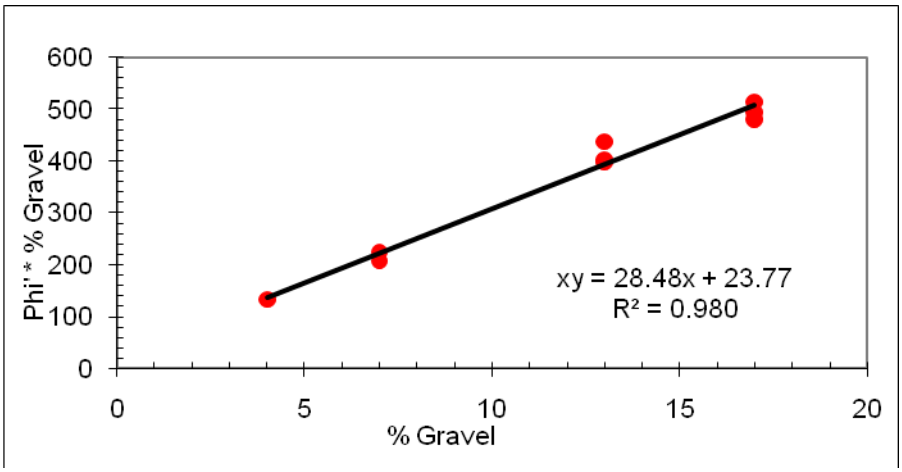


***Figure E.43:*** *ϕ′ vs. %Gravel (Hyperbolic Function) – A-6b Soil Type*

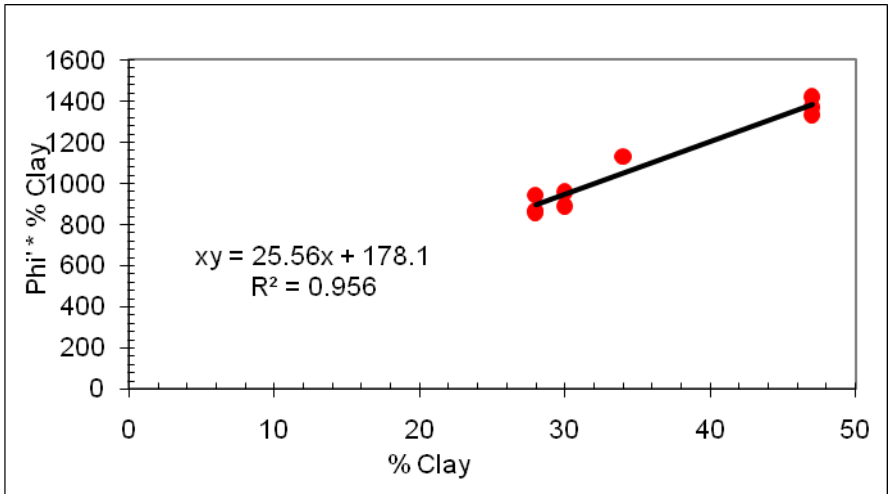


***Figure E.44:*** *ϕ′ vs. %Clay (Hyperbolic Function) – A-6b Soil Type*

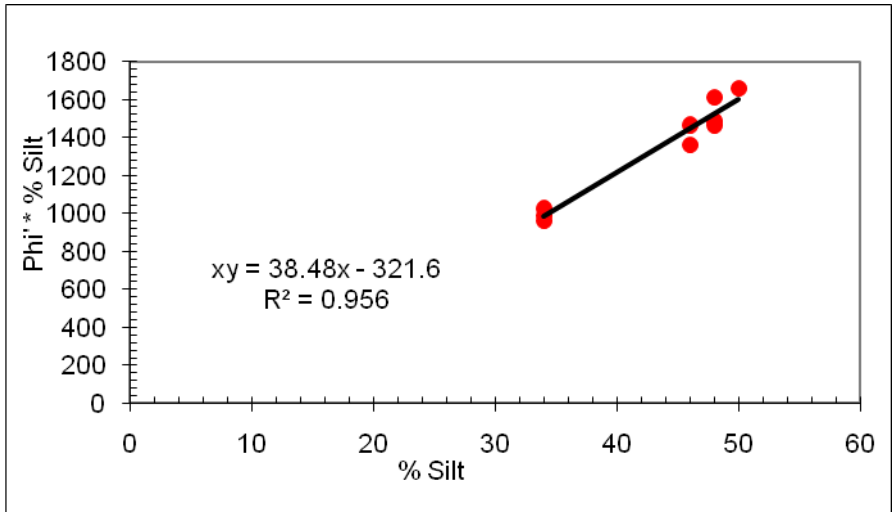


***Figure E.45:*** *ϕ′ vs. %Silt (Hyperbolic Function) – A-6b Soil Type*

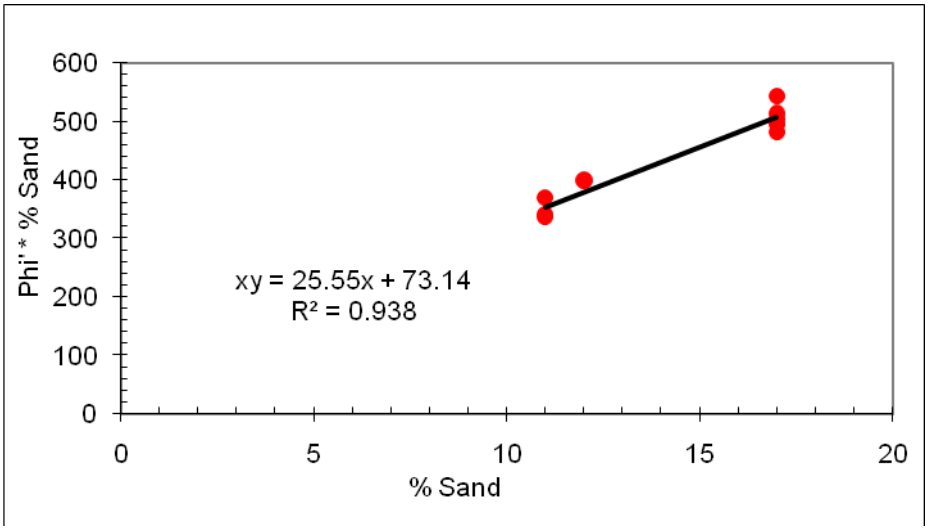


***Figure E.46:*** *ϕ′ vs. %Sand (Hyperbolic Function) – A-6b Soil Type*

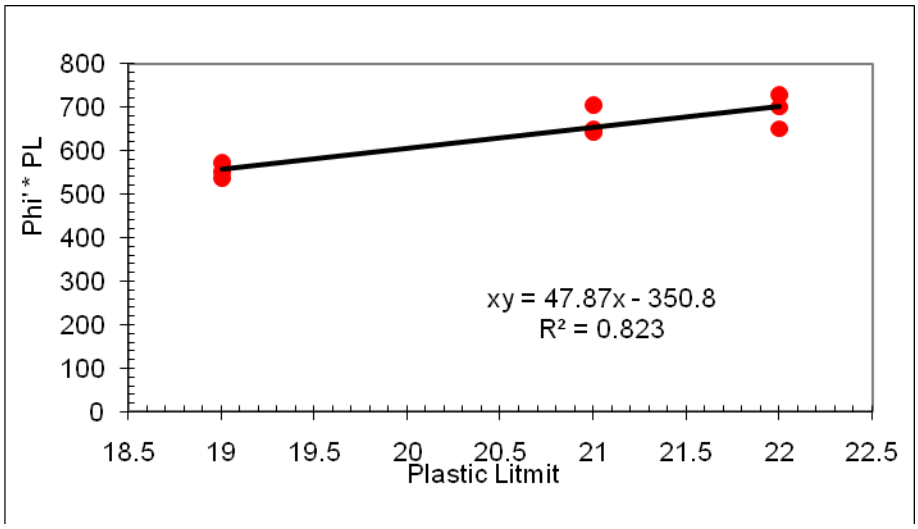


***Figure E.47:*** *ϕ′ vs. PL (Hyperbolic Function) – A-6b Soil Type*

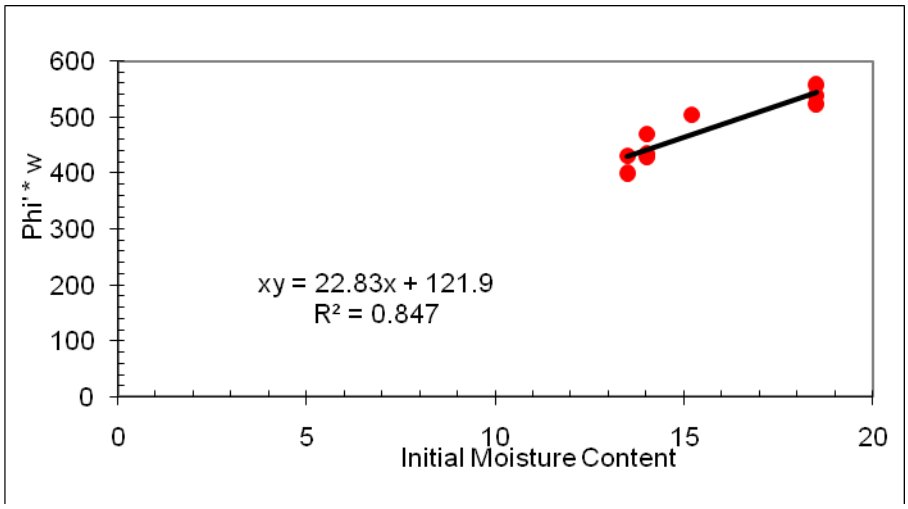


***Figure E.48:*** *ϕ′ vs. w (Hyperbolic Function) – A-6b Soil Type*

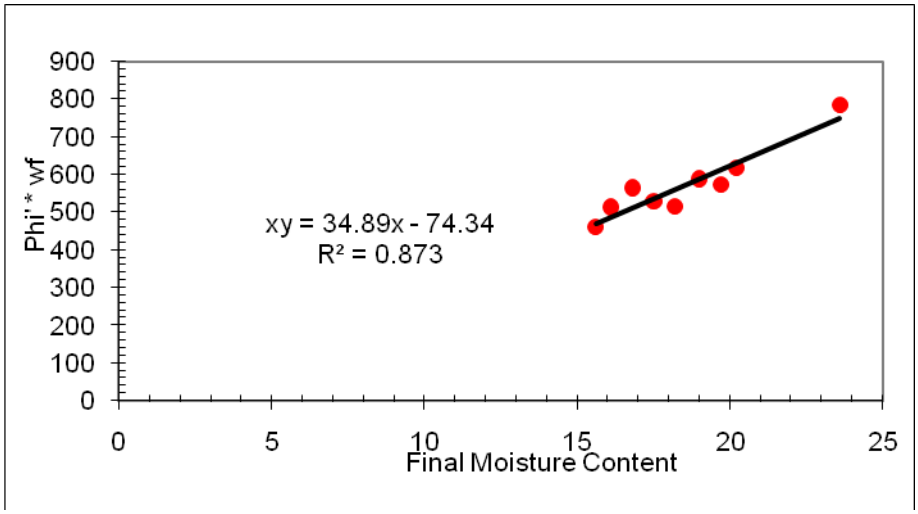


***Figure E.49:*** *$\phi'$ vs. $w_f$-cu (Hyperbolic Function) – A-6b Soil Type*

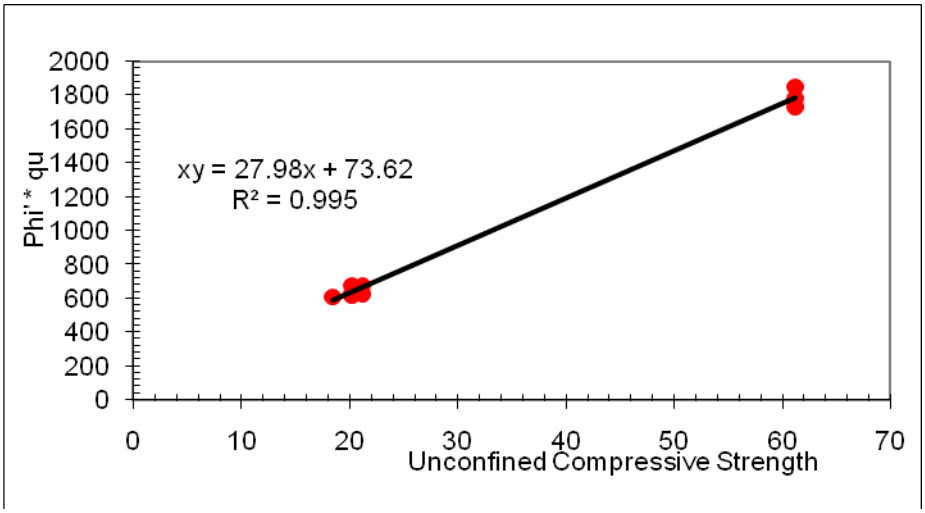


***Figure E.50:*** *$\phi'$ vs. $q_u$ (Hyperbolic Function) – A-6b Soil Type*

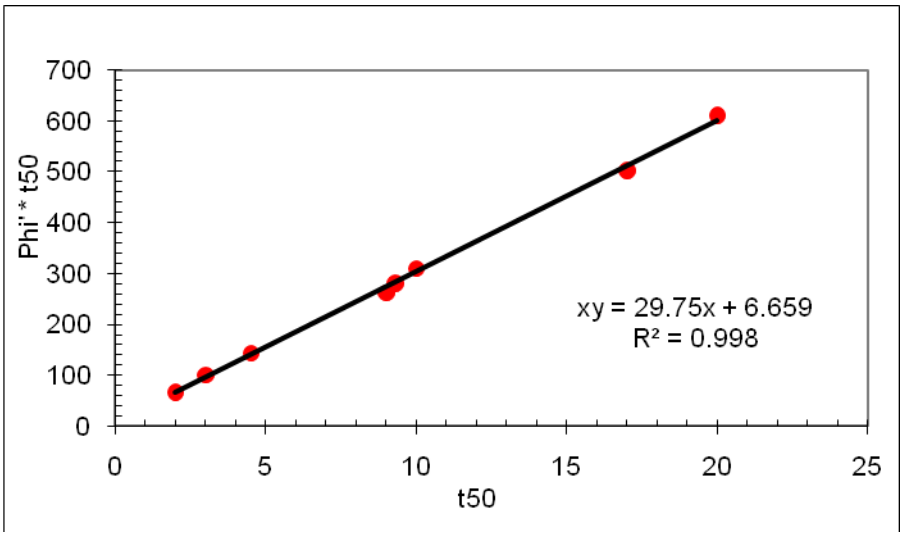


***Figure E.51:*** *$\phi'$ vs. $t_{50}$ (Hyperbolic Function) – A-6b Soil Type*

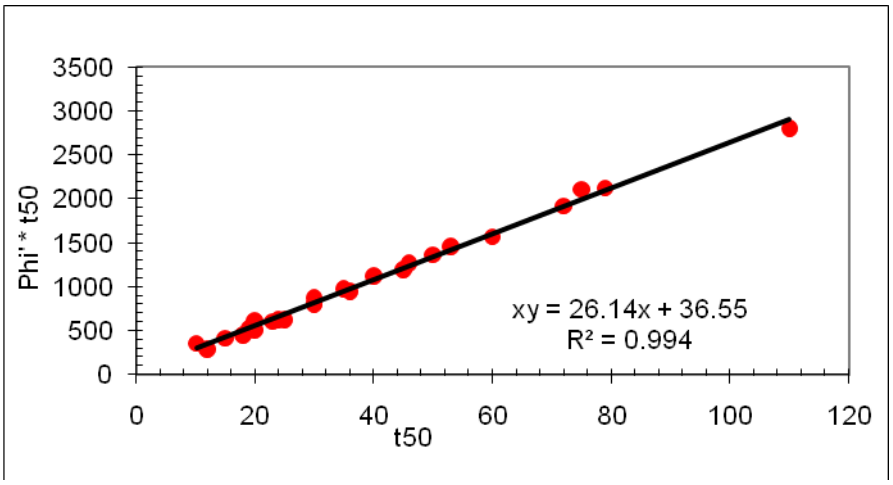


***Figure E.52:*** *$\phi'$ vs. $t_{50}$ (Hyperbolic Function) – A-7-6 Soil Type*

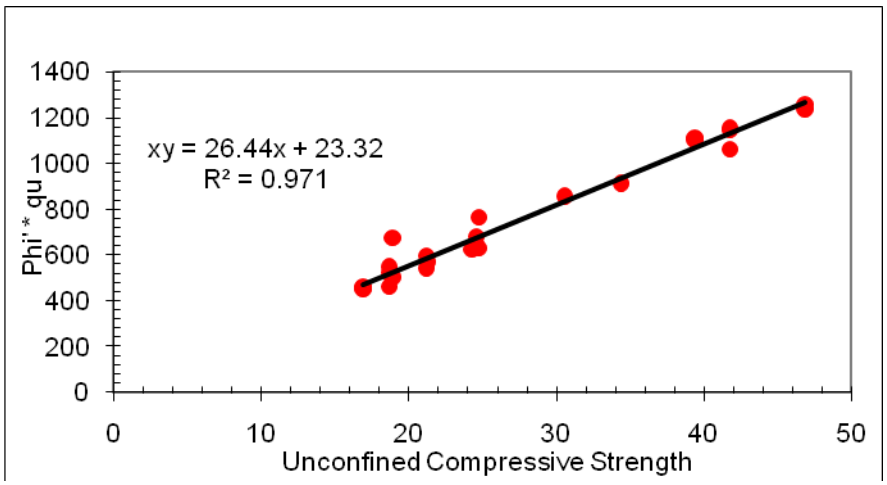


***Figure E.53:*** *$\phi'$ vs. $q_u$ (Hyperbolic Function) – A-7-6 Soil Type*

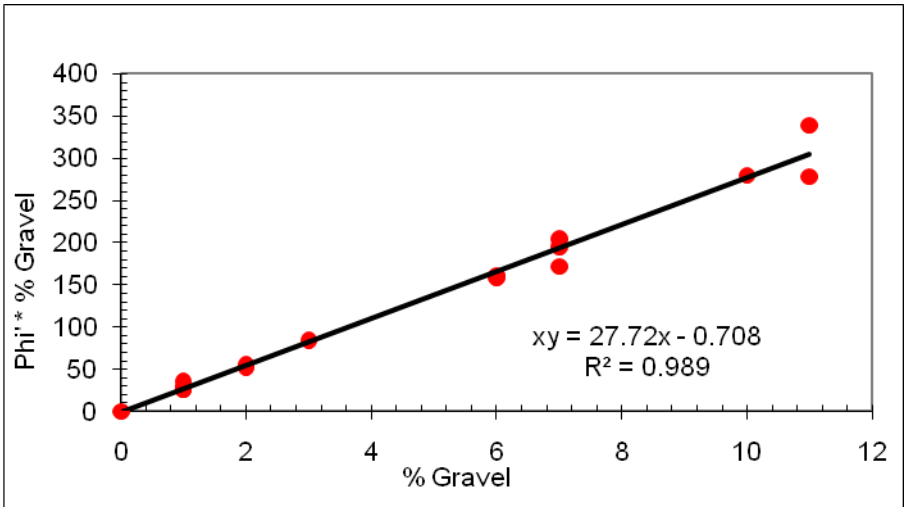


***Figure E.54:*** *$\phi'$ vs. %Gravel (Hyperbolic Function) – A-7-6 Soil Type*

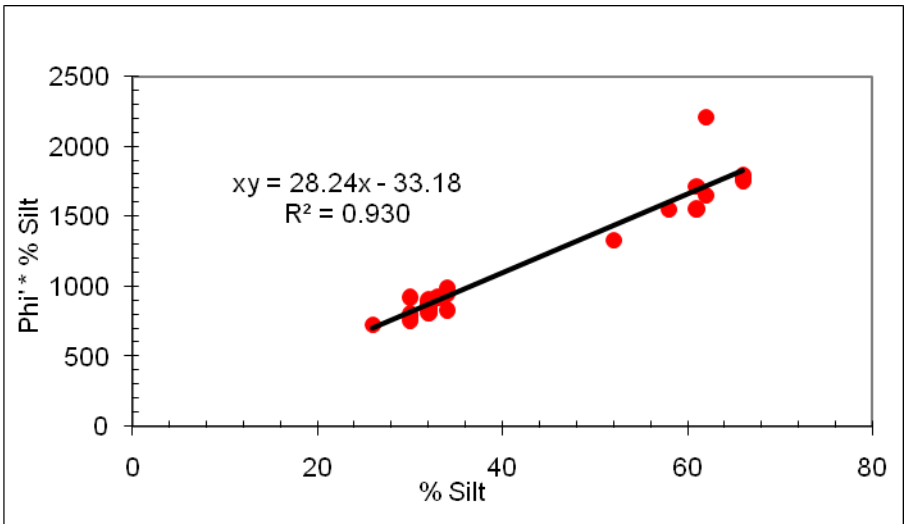


***Figure E.55:*** *ϕ′ vs. %Silt (Hyperbolic Function) – A-7-6 Soil Type*

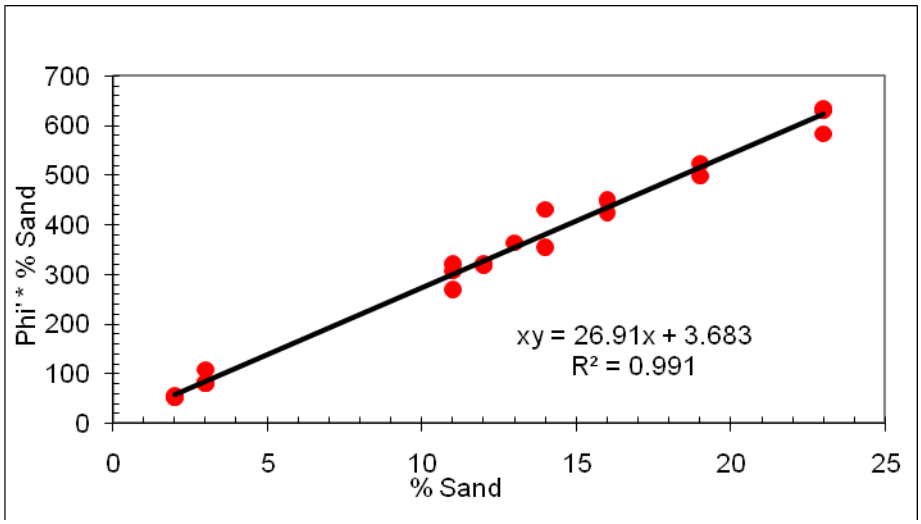


***Figure E.56:*** *ϕ′ vs. %Sand (Hyperbolic Function) – A-7-6 Soil Type*

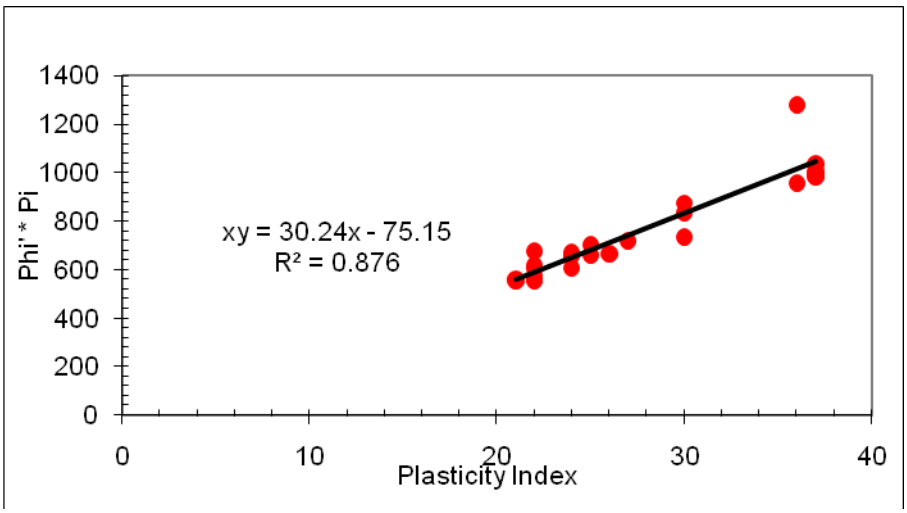


***Figure E.57:*** *ϕ′ vs. PI (Hyperbolic Function) – A-7-6 Soil Type*

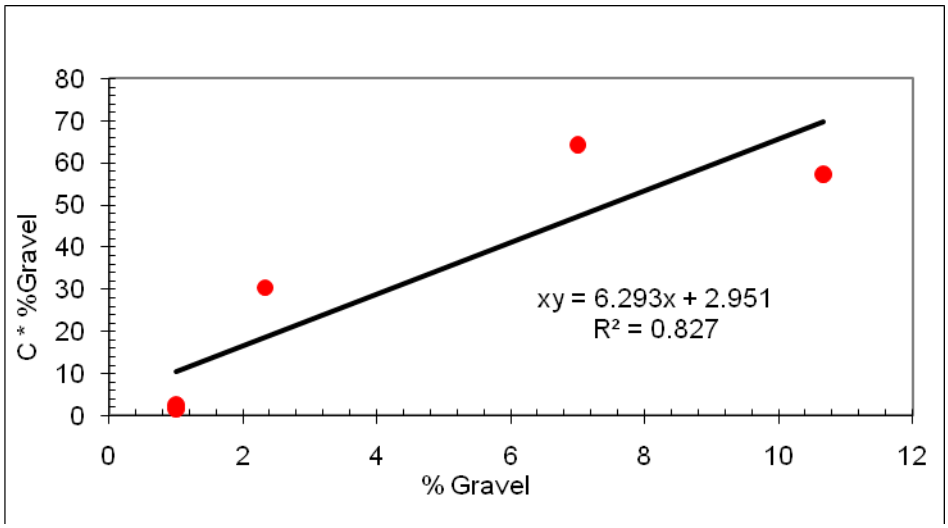


***Figure E.58:*** *C vs. %Gravel (Hyperbolic Function) – A-7-6 Soil Type*

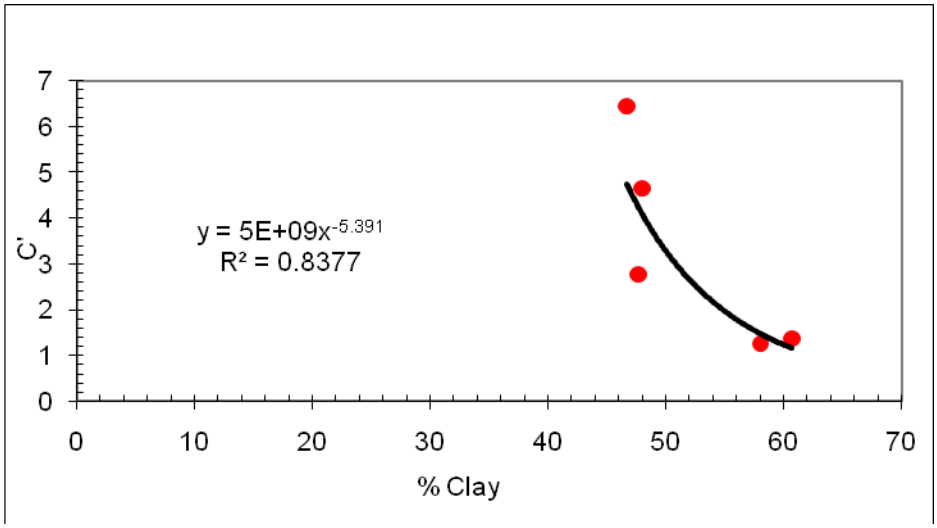


***Figure E.59:*** *C' vs. %Clay (Power Function) – A-7-6 Soil Type*

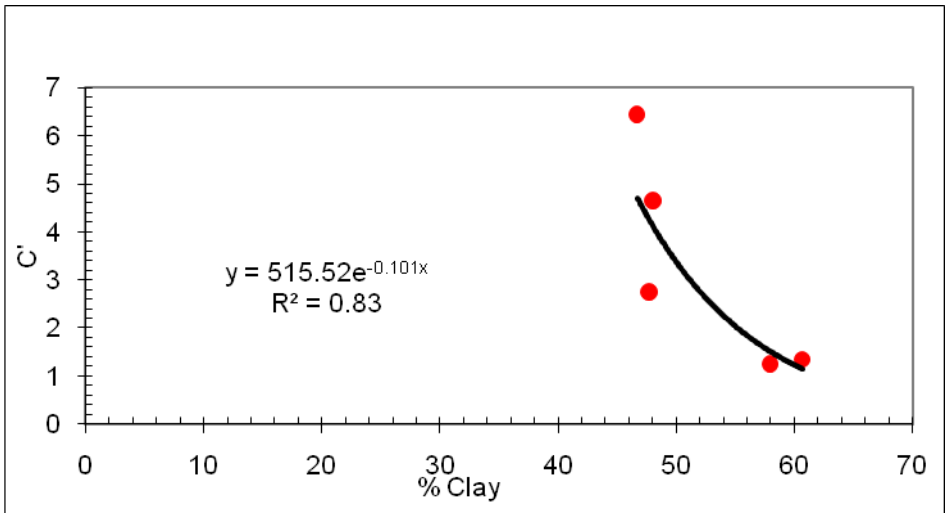


***Figure E.60:*** *C' vs. %Clay (Exponential Function) – A-7-6 Soil Type*

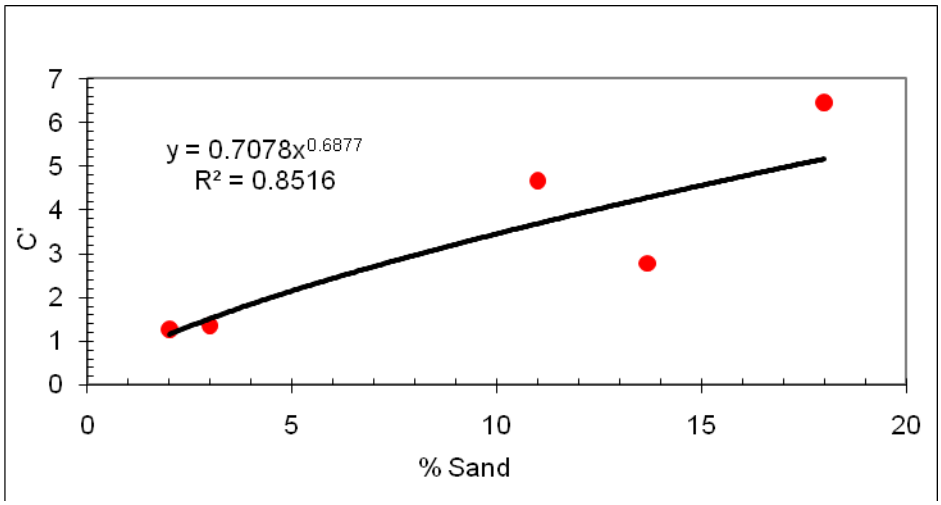


***Figure E.61:*** *C' vs. %Sand (Power Function) – A-7-6 Soil Type*

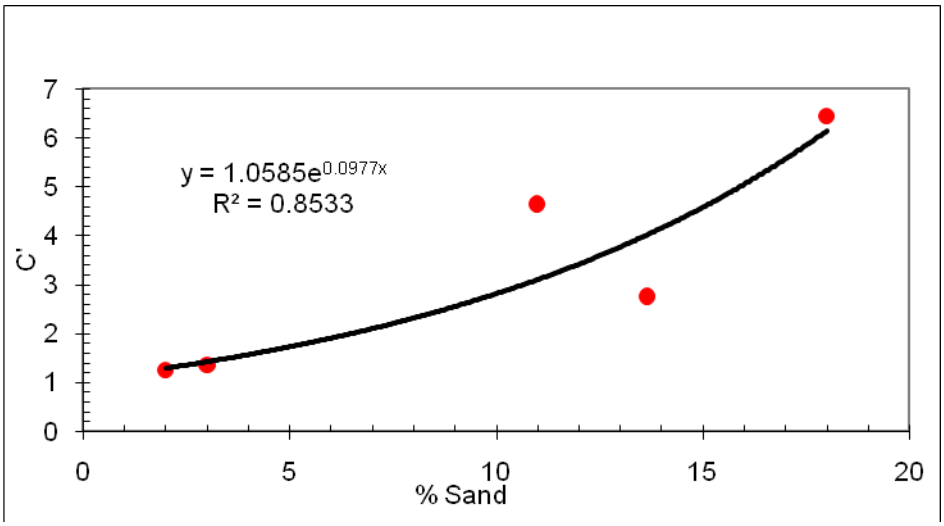


***Figure E.62:*** *C' vs. %Sand (Exponential Function) – A-7-6 Soil Type*

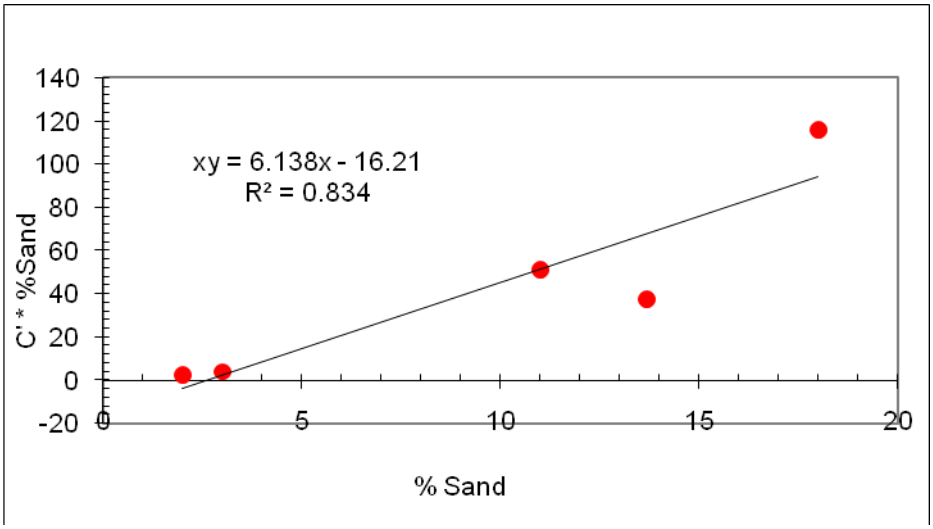


***Figure E.63:*** *C' vs. %Sand (Hyperbolic Function) – A-7-6 Soil Type*

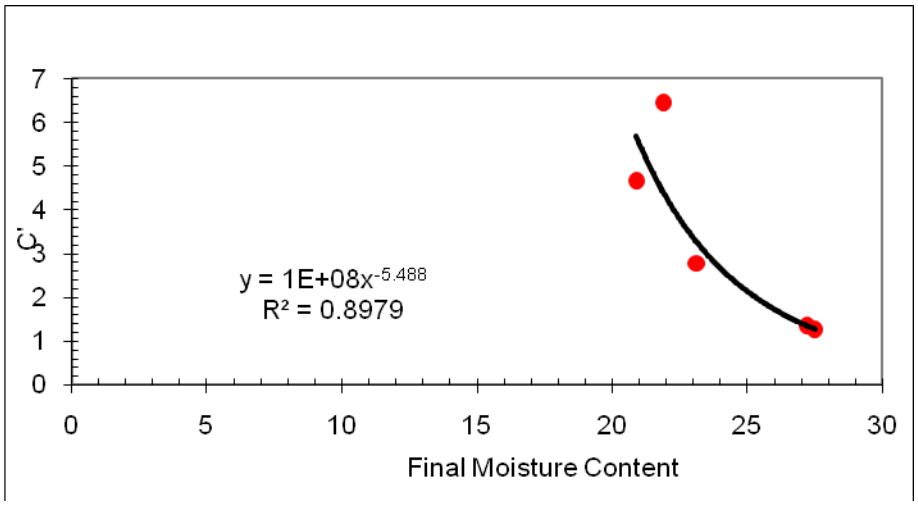


***Figure E.64:*** *C' vs. $w_f$ (Power Function) – A-7-6 Soil Type*

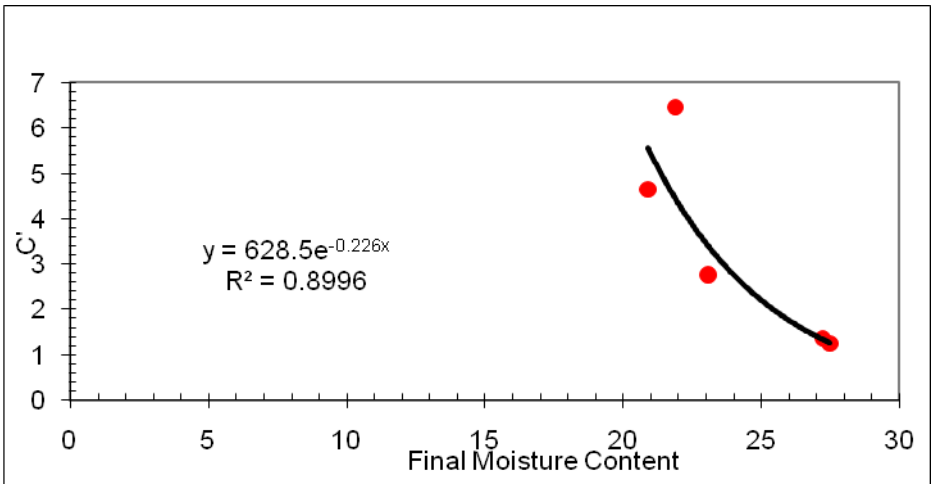


***Figure E.65:*** *C' vs. $w_f$ (Exponential Function) – A-7-6 Soil Type*

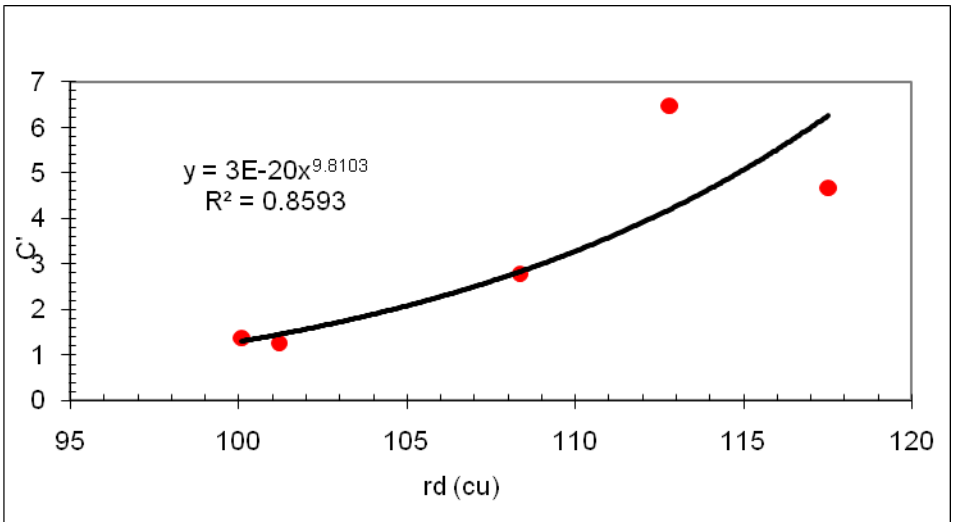


***Figure E.66:*** *C' vs. $\gamma_d$-cu (Power Function) – A-7-6 Soil Type*
*where $\gamma_d$-cu = Initial dry unit weight (measured during C-U triaxial test)*

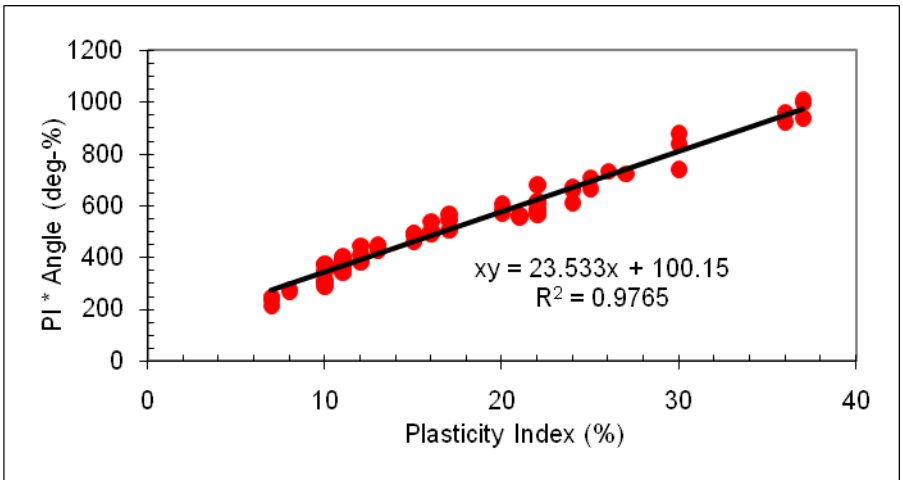


***Figure E.67:*** *ϕ′ vs. PI (Hyperbolic Function) – All Cohesive Soil Types Combined*

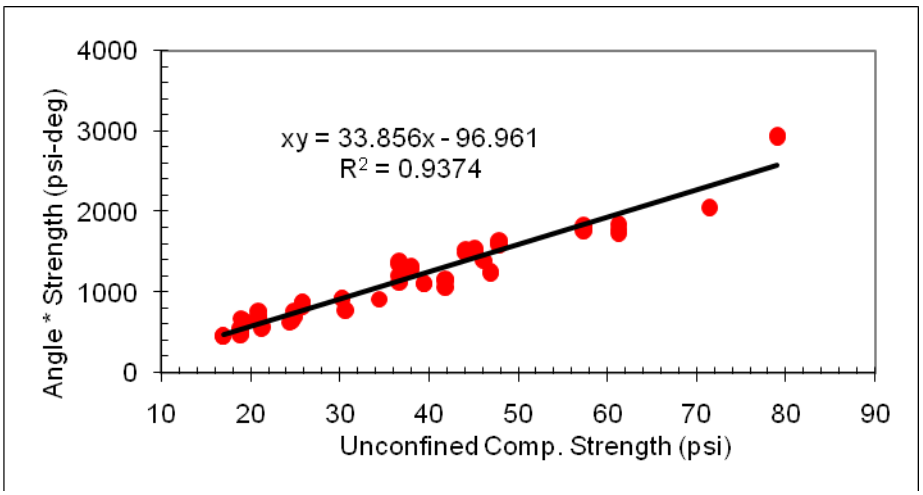


***Figure E.68:*** *ϕ′ vs. $q_u$ (Hyperbolic Function) – All Cohesive Soil Types Combined*

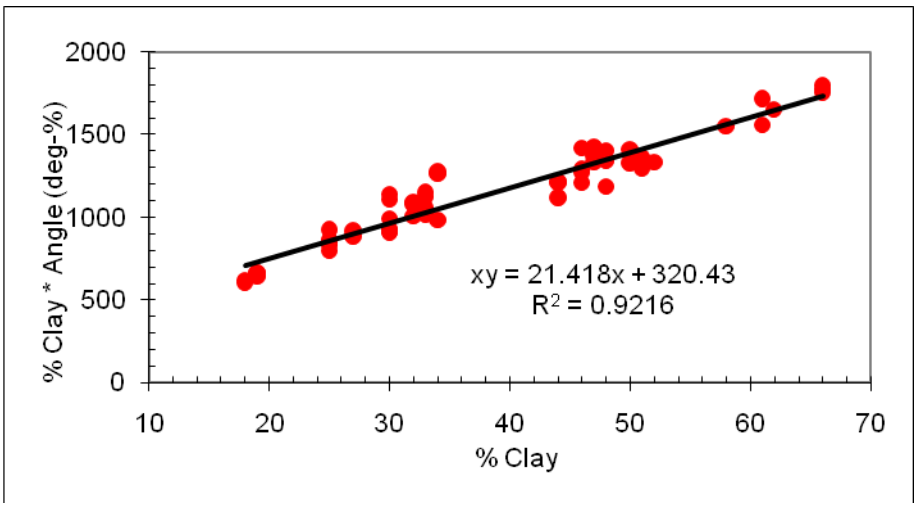


***Figure E.69:*** *ϕ′ vs. % Clay (Hyperbolic Function) – All Cohesive Soil Types Combined*

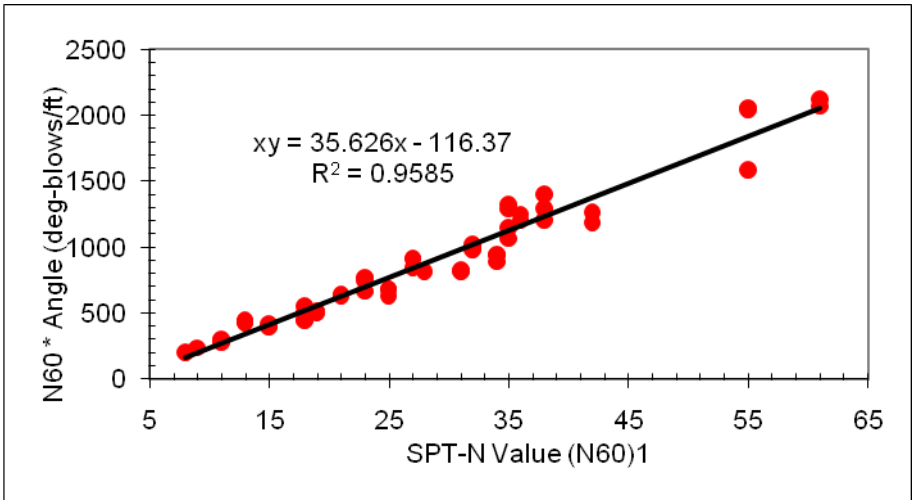


***Figure E.70:*** *$\phi'$ vs. SPT-$(N_{60})_1$ (Hyperbolic Function) – All Cohesive Soil Types Combined*

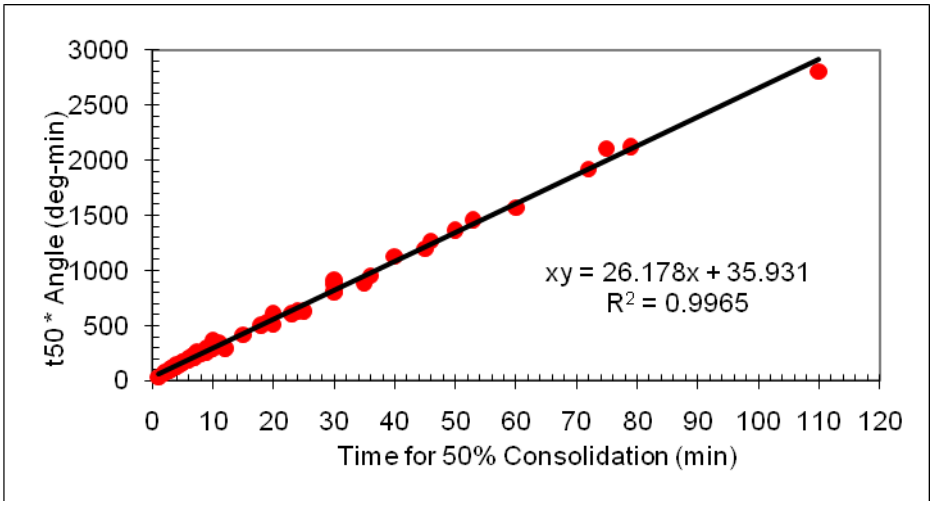


***Figure E.71:*** *$\phi'$ vs. $t_{50}$ (Hyperbolic Function) – All Cohesive Soil Types Combined*

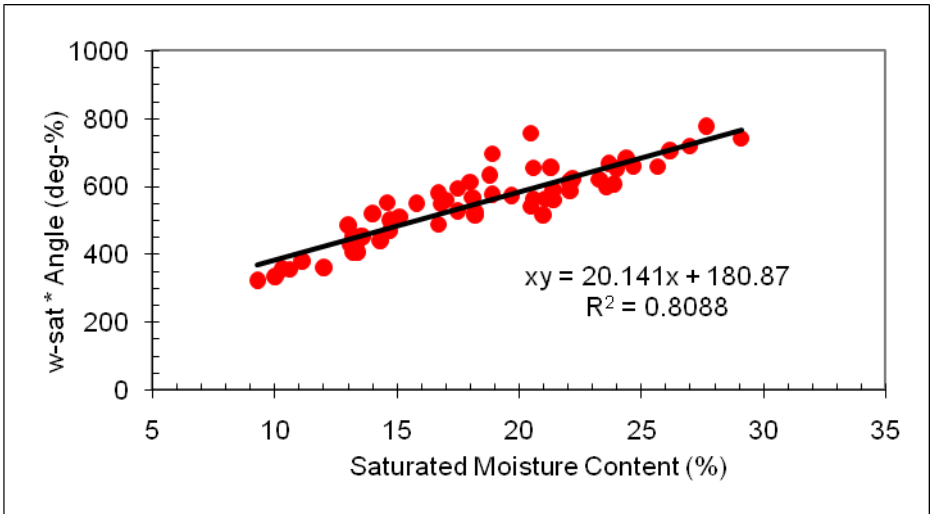


***Figure E.72:*** *$\phi'$ vs. $w_f$ (Hyperbolic Function) – All Cohesive Soil Types Combined*

## *APPENDIX F: LIST OF SYMBOLS*

*$A$ = pore water pressure parameter*
*$c$ = cohesion*
*$c_u$ = undrained cohesion*
*$c'$ = effective-stress cohesion*
*CD = consolidated drained*
*CU = consolidated undrained*
*$C_1$ , $C_2$ = dimensionless constants*
*$d_i$ = inside diameter of the sampler*
*$d_o$ = outside diameter of the sampler*
*EMX = maximum energy transferred to the rods*
*ETR = energy transfer ratio*
*$\varepsilon$ = axial strain*
*$f$ = the unit frictional force on the sampler*
*$f_c$ = side friction stress (associated with the cone penetration test)*
*$F$ = the force transferred from the hammer to the sampler*
*$F_{avg}$ = the average force used through the six inch interval*
*$F_e$ = the reaction force given by the ground onto the bottom surface to the sampler*
*$F_i$ = the frictional reaction force on the inside of the sampler*
*$F_o$ = the frictional reaction force on the outside of the sampler*
*$F(t)$ = force measured at time t*
*$G_s$ = specific gravity*
*$L$ = the depth of the sampler into the ground.*
*LL = liquid limit*
*$n_1$ = number of samples in population 1*
*$N_{60}$ = standard penetration N value at 60% free-fall energy delivery*
*$(N_{60})_1$ = standard penetration N value corrected for energy delivery and depth effects*
*PI = plasticity index*
*PL = plastic limit*
*$p_a$ = atmospheric pressure = 14.7 psig (101 kPa)*
*$p$, $q$ = stress path parameters (in total stresses)*
*$q$ = the unit bearing pressure on the bottom of the sampler*
*$q_c$ = tip resistance stress (associated with the cone penetration test)*
*$q_u$ = unconfined compression strength*
*$p'$, $q'$ = stress path parameters (in effective stresses)*
*$r^2$ or $R^2$ = coefficient of determination*
*$R_f$ = friction ratio*
*$s_p^2$ = pooled variance*
*$s_1^2$ = variance in population 1*
*SPT = standard penetration test*
*$t$ = student t-statistics*
*$t_{50}$ = time for 50% consolidation*
*$u$ = pore water pressure*
*$u_a$ = pore air pressure*

*UC = unconfined compression*
*$u_f$ = pore water pressure at failure*
*$u_w$ = pore water pressure.*
*UU = unconsolidated and undrained*
*V(t) = velocity measured at time t*
*w = soil moisture content*
*$w_f$ = final soil moisture content (measured during triaxial compression test)*
*W' = the weight of the rods and sampler*
*$\bar{x}_1$ = the mean in population 1*
*%C = percent clay (in mass)*
*%Comp = percent compaction*
*%G = percent gravel (in mass)*
*%M = percent silt (in mass)*
*%S = percent sand (in mass)*
*$\alpha$ = level of statistical significance*
*$\Delta L$ = the length of sample pushed into the ground*
*$\Delta N$ = an increase in blow count*
*$\Delta u$ = increase in pore pressure*
*$\Delta\sigma_3$ = increase in confining pressure.*
*$\phi$ = angle of internal friction*
*$\phi'$ = effective-stress angle of internal friction*
*$\gamma$ = moist unit weight*
*$\gamma_d$ = dry unit weight*
*$\sigma$ = total normal stress applied*
*$\sigma_d$ = deviatoric stress*
*$\sigma_1$ = major principal stress = $\sigma_d + \sigma_3$*
*$\sigma_{1f}$ = major principal stress at failure = $(\sigma_d)_f + \sigma_3$*
*$\sigma_3$ = minor principal stress = confining pressure or chamber pressure*
*$\sigma'$ = effective overburden stress*
*$\sigma_c'$ = the highest past effective overburden stress*
*$\sigma_0'$ = effective overburden stress*
*$\tau_f$ = shear strength*
*$\chi$ = degree of saturation*

ORITE • 141 Stocker Center • Athens, Ohio 45701-2979 • 740-593-2476
Fax: 740-593-0625 | • orite@bobcat.ent.ohiou.edu | • http://webce.ent.ohiou.edu//orite/